CRANFIELD UNIVERSITY
LIBRARY

Cranfield University

C J A Lawson

Refrigeration Appliances:
Performance enhancements via novel
Thermal – Energy Storage

School of Mechanical Engineering

Ph.D. Thesis

CRANFIELD UNIVERSITY
LIBRARY

Cranfield University

School of Mechanical
Engineering

Thermal Processes Group

Department of Automotive, Combustion and
Energy Engineering

PhD Thesis

Academic Year 1999/00

Chukwuemeka Jonathan Adeolu Lawson

Refrigeration Appliances: Performance enhancements via novel Thermal – Energy Storage

---

Supervisors

M. Newborough *D. J. Highgate*

October 1999

Submitted in partial fulfilment of the requirements for the award of the degree of
Doctor of Philosophy

Acknowledgements

The decision to undertake doctoral research for the first time is seldom undertaken with a full appreciation of the magnitudes and diversity of the tasks which lie ahead. From personal experience, and observing my colleagues, the process almost invariably exposes hitherto hidden character traits as it brings about intellectual and character changes. These changes not only remain part and parcel of the individual through life, but also form part of the foundation blocks for later life. I for one have found it an especially arduous and harrowing time; particularly the 24 months leading up to May 1999 which must be (and I pray will be) the worst in my entire life.

In that time certain individuals succumbed to the divine unction to offer invaluable assistance to me as I stumbled through different (temporal and spiritual) phases at various periods. Usually, assistance has been from most unlikely quarter (which will serve as a lasting lesson in faith); this made me all the more grateful and thus will like to seize this opportunity to mention, in no particular order, a handful of these individuals.

I will like to extend my gratitude to my two academic supervisors Dr.'s Marcus Newborough and Donald Highgate; who were always ready to point to some issue in the literature, shed light on some technical aspect, correct some written script and offer words of encouragement. I am deeply in their debt, for times when I appeared almost visionary was when I occasioned to stand on (one or the other of) their shoulders and when the contrary was true, I had ill–advisédly elected to stand in a footprint of either. I am particularly grateful to Dr. Newborough who a–times went as far as to offer counsel regarding non–academic issues which arose from time to time, many of which presenting on scales which were potentially detrimental to my academic progress.

I will also like to thank the various sources of industrial/technical support which were invaluable to the precession of this project. Many of whom provided, gratis, what would have otherwise been prohibitively expensively services (usually without the knowledge of 'senior management'). I in particular I would like to thank Messrs. Imran Shah and Philip Mayhew (Quest Refrigeration UK Ltd.), Mr. Andy Dahabal (Isotron PLC), the gentlemen of Flectalon Ltd. (Wales), Dr. Giuseppe Persano–Adorno (Institutio Giordano, Italy), Messrs. Sergio Bubani and Giacomo Bartolini (Indel B srl, Italy), Mr. Norman Bagshaw (NEB Consultants UK), Mr. Mike Olive (Bartoli UK Ltd.), Dr. Gunter Claus (FGHLK Stuttgart mbH) , Mr. Tim Robbins (3M UK Ltd.), Mr. Tim Stonebanks (Biodata UK Ltd.), Mr. Robert Crowe (NatWest Cranfield University branch), Martin (Babs's Landlord), and most notably Mr. Phil Bacon (Europus UK Ltd.)

As with projects of this nature, (theoretical, computational and experimental) it

was imperative to draw on various sources of expertise whilst addresing the different aspects. The extent of the computational assistance I received is illustrated by the fact that prior to the commencement of this research undertaking the scope of my computer programming exposure was a two page heat transfer program! I am thus grateful to Mrs. Ruth Fuller (ccref) Messrs. Jonathan Haynes (ccjh), Kenneth Caines (cckrc) and Jeffrey Goldberg (cc047) of the Cranfield Computer Centre, Dr. 'Pat'. Leazeau (**AMAC**) and a multiplicity of individuals on the **Internet** who were always ready to respond to one question or the other which I would regularly post to some mailing list on the net.

In the gathering of experimental data, ofttimes the rig building/proving process can pose the greatest obstacles; something which is only ever realised by those actively involved in the entire experimentation process (from conceptualisation to data presentation). Looking back at the setting up of the experimental phase of this work, it amuses and amazes me to realise the amount of equipment which was 'borrowed' or scrounged of some, usually hitherto unknown, gracious individuals from across the different colleges/schools across the Cranfield campus. Principally, I will like to extend my sincerest gratitude to Mr. 'Charlie' Knight of the Applied Energy Labs., who seemed to know where anything that could be possibly be had, was and could always be relied on to come up with some suggestion to cross some impasse or the other. Also my thanks go out to (the two ladies at the end of the **AE** corridor) Mrs. 'Binnie' Hunt and Mrs. 'Barbara' McGowan, Messrs. 'John' Dawe, Barry Philips, Pat. Healey, Dr.'s David Mba, 'Bill' Batty and 'Marcus' Newborough (**SME**); Messrs. Barry Walker, Morris Crook, Malcolm Goodridge (**CoA**); Dr. 'Babs' Ogunbiyi and a host of technicians (**SIMS**), Mr. Stephen Lovell (and several of the operators) in the Computer Centre.

I would also like to seize this opportunity to thank Dr.'s Newborough, Welch and Highgate for taking the time to proof–read much of my dissertation; which for several reasons must have been a particularly difficult process. That said, I take responsibility for any errors or omissions which are contained herein, for on occasion I have either elected to leave things unchanged or due to some oversight omitted some vital correction.

I would also like to express an appreciation to the various individuals who, in distinguishing themselves amongst others have contributed in a diverse number of ways to the successful completion of this project. Many of these contributions took one or the other forms of: references to the literature (including photocopied articles), offers of (usually unspecified) assistance, words of encouragement, open office doors, meals, financial support (refundable and non–refundable), Christian Fellowship and most importantly prayer. In the years since it all began many such favours would have slipped to the recesses of my minds to resurface only when I am occasioned to meet or remember the individual concerned. As such, I admit

that in drawing up this list, several omissions will inadvertently be made and I duely apologise for this. At this time, foremost (in no particular order) in my mind are: Mrs. M. Lawson, Dr. M. Lawson, Mr. Adebowale Lawson. Prof. S. Ogunyemi, Dr. 'Lola' Ogunyemi, Dr.'s Iman Mansouri, Babatunde Ogunbiyi, Nicholas Harle, Robert Attuh, Emmanuel Okoroafor, Paul Augood, David Mba, Marcus Newborough, Miss. Christina Oniah, Mr.'s and Mrs.'s Peta and Robert Stanton, Daphne and Graham Stephens, Kay and Philip Petty, Graham and Phyllis Woodland, Louise and Stephen Woodland, Sarah and Nick Angel, several other folk of the Wooton Baptist Church, Members of the: Basketball club, Cranfield Christian Union (1993–1999), Applied Energy discussion Forum (1996–1998), Mr. Alan Pibworth, Mr. and Mrs. Mark and Angela Knight, Prof. John fielding, Mrs. Ruth Fuller, Dr. Caleb Ekundayo, Dr. Antony Juwah, Mr Sola Balogun ... The list is virtually endless, once again to those whose names are omitted from this list, I extend both my deepest apologies and my heartfelt gratitude.

I would also like to seize this opportunity to express my profound gratitude to my mother, for everything and above all to thank the Almighty, Who despite everything continues in His love for me.

Abstract

In recent years there has been increasing concern for the environmental impacts of economic and technological development. This (principally socio–political) concern has led to the well–known series of environmentally motivated (global and local) conventions, agreements and legislation put forward in a bid to manage these environmental impacts, which in turn has led to research and commercial activity on environmental issues. One of the major activities identified as adversely impacting the environment is the manner in which energy is currently harnessed, inter–converted and utilised.

Within developed world economies, refrigeration has long been identified as one of the two greatest energy consumption activities, a trend which is uniform across the industrial and domestic sectors[1]. Thus the potential energy and environmental benefits realisable in improving the energy performance of the refrigeration process/appliances is of considerable importance.

Currently no commercially acceptable controllable technology for energy–demand management in refrigeration appliances is known to exist. A non–toxic, biodegradable and economically cheap pseudo–eutectic thermal–energy store is herein proposed as the basis of such a controllable technology. The research here presented looks into this energy–demand management issue within the 'demand side management' context of resource (available energy or exergy) conservation, in a *demand side* implementation *viz* a domestic refrigerator. The work amalgamates some of the best available technologies[2] and employs several phenomena intrinsic to the refrigeration process in seeking to minimise the energy consumption of such appliances; whilst, at the same time, providing sufficient latitude for the exploitation of whatever other economic opportunities which may be accessible in the utilisation locale.

Within the (domestic) context, the work identifies energy management strategies which may be applied on the basis of (a) minimising energy consumption, (b) energy availability, (c) minimising operating cost, depending on prevailing billing criteria or (d) demand load profile. The identified technologies permit the ability to design optimally for a particular criterion, a subset or the ensemble of the energy management criteria listed. In addition, the technologies afford (a) the 'designing in' of thermal–performance robustness to both energy supply and appliance utilisa-

[1] Within the OECD, the yearly domestic energy consumption alone amounts to between four and five hundred of terrawatt hours.

[2] Working within the framework of the Best Available Technologies Not Entailing Excessive Cost (BATNEEC) protocol.

tion profiles, (b) the downsizing of the prime–mover, (c) more uniform appliance temperatures and (d) possibly longer prime–mover life.

Preliminary modelling, performed on the basis of energy consumption, indicated that the designed appliance will fare better when compared to a similar, basic, appliance *i.e.* one with neither the controllable technology nor the allied energy management strategy. These results were validated by the findings of subsequent experiments. The experimental results indicate that (depending on the control strategy employed) up to 65% and 52% improvements in prime–mover coefficient of performance and appliance energy consumption, respectively, may be achieved. Other measured improvements include up to a 20% reduction in the mean power demand of the prime–mover, an eight–fold reduction in prime–mover cycling, a 16% reduction in running time and observed greater stability in appliance temperatures. Importantly, the experimental results demonstrated the effectiveness in the technology to enable the intelligent control of an appliances energy–demand profile.

The (economic) cost benefit of these performance improvements may well exceede 50% of the initial running cost of the appliance depending on use and energy tariffs prevailing during operation. The additional cost of implementation (not retrofitting) will depend on the extent to which the technologies are to be applied. However, it is estimated that substantial improvements in prime–mover performance may be obtained for as little as (3–15)% of the basic appliance (retail) cost, depending on size, utilising only the core energy management facilitating technology.

On the one hand, this research has far–reaching environmental conservation implications, particularly in terms of green house effects (power generation) and ozone layer depletion (refrigerant use); on the other, it has industrial/process implications for (a) processes with rigorous temperature control requirements, (b) environments where there are cost and/or availability restrictions on energy use, (c) applications where there is a need for transient high coolth energy transfer in regions of low, but constant, energy supply densities and (d) applications where there is the need to ensure uninterrupted coolth delivery during periods of power interruption or during systems maintenance.

Preface

The main thesis of this work is that, energy use and thermal performance, domestic (and similar) refrigeration systems may be improved by the incorporation of appropriate energy storage devices.

This thesis has been written up as follows:

A summary of the current state of the literature, which was principally undertaken at the commencement of the project and updated periodically forms, along with rationale for the research, the substance of Chapter One.

Chapter Two considers several of the various concepts which were useful in the research undertaking. Consisting of an assessment of the various parts of the basic (vapour compression) refrigeration cycle, a discussion on the problems experienced during utilisation and the conceptualisation of energy storage (particular thermal storage) as a means for improving the energy performance of domestic refrigeration systems.

Chapter Three consider thermal energy storage in greater detail and highlights the problems hitherto associated with thermal energy storage. In considering the various thermal energy storage technologies, it identifies an appropriate technology and proposes the use of a novel thermal energy storage medium for the current research exercise.

Chapters Four and Five are a formal presentation of the energy requirements for different identified appliance control regimes which may be of importance in assessing the comparative feasibility (in terms of energy use) of such refrigeration systems fitted with passive (Chapter Four) and active (Chapter Five) thermal energy storage systems.

The equations thus derived formed the basis of an assessment–prediction computer–based model which is described in Chapter Six along with the results of computer–based experiments about an identified base–case set of design parameters. Based on the results obtained for a *passive* thermal energy storage system, the construction parameters for a small appliance were specified and subsequently built.

Chapter Seven describes the experimental rig along with modifications made to the initial specifications. The experimental procedure and results thereof are subsequently presented and form the main essence of the chapter.

Chapter Eight concludes the work and makes recommendations regarding further activity into the research area.

Contents

Nomenclature xx
Abbreviations . . . xx
List of symbols . . . xxii
Subscripts . . . xxiii
Non–dimensional quantities . . . xxv
Greek letters . . . xxvi

I The Context 1
1.1 Proem . . . 2
1.2 The Energy Consequences . . . 3
1.2.1 The Developed World . . . 3
1.2.2 The Developing World . . . 8
1.3 The Environmental Consequences . . . 18
1.4 Economic Considerations . . . 20
1.5 Socio–Political Considerations . . . 22
1.6 Regulatory Activities . . . 24
1.6.1 Legislation . . . 25
1.6.2 Programmes . . . 27
1.6.3 Information Dissemination . . . 29
1.7 Utilisation Considerations . . . 31
1.8 Aims and Objectives . . . 34
1.9 Closure . . . 35

II Concepts 38
2.1 Demand Side Management . . . 39
2.1.1 Demand Side Management in Perspective . . . 43
2.2 Load Management in Domestic Refrigeration Appliances . . . 44
2.2.1 Load Management . . . 44
2.2.2 Load Management in the Domestic Refrigeration Appliance Context . . . 46

2.3 Objective Statement 48
2.3.1 Project Methodology 49
2.4 Energy Transfer Considerations 50
2.4.1 The Prime Mover 50
2.4.2 Other Heat Transfer Considerations 59
2.5 Heat Ingress Inhibition 61
2.5.1 Critical Thickness 63
2.5.2 Composite Insulant Distribution 64
2.5.3 Temperature–Time Lag 66
2.6 Closure 72

III Thermal Storage as an Attribute to Thermal Management 74
3.1 Introduction 75
3.2 Energy Storage 76
3.3 Applications, Benefits and Requirements 77
3.4 Thermal Energy Storage 82
3.5 Thermal Energy Store Types 84
3.5.1 Thermo–Chemical Energy Storage 85
3.5.2 Sensible Heat Storage 86
3.5.3 Latent Heat Storage 87
3.5.4 Latent Heat Media Selection Criteria 90
3.6 Application to Domestic Refrigeration Appliances 99
3.7 Thermal Energy Store Media selection 101
3.8 Closure 103

IV The Thermal Engineering Design Analysis of a Storage Refrigerator 104
4.1 Proem 105
4.2 Design Specification 106
4.3 Design Philosophy 109
4.3.1 Design Concepts 109
4.4 Systems Design 111
4.4.1 The General Layout 111
4.4.2 System Configurations 112
4.4.3 General discussion on conceptual design 115
4.4.4 Comparative Systems Design Analysis 118
4.5 Parameter Design 134
4.5.1 General Discussion On Parameter Design 135
4.5.2 Load Analysis 136
4.5.3 The Compartment 136

4.5.4 Evaporator Design 145
4.5.5 Food Load 147
4.5.6 Thermal Energy Storage analysis 147
4.5.7 Solar Cell Sizing 150

IV Active Thermal Storage Systems **104**
4.1 General Discussion on the Application 106
4.1.1 Brief Description 106
4.1.2 Flow Characterisation 108
4.2 Design Parameters 110
4.2.1 Basic Assumptions 110
4.2.2 Physical Property Estimates 113
4.3 Energy Requirement Assessment 116
4.3.1 Slurry Bulk Velocity 117
4.3.2 Head–Loss Assessment 120
4.3.3 Bend Losses 121
4.3.4 Reservoir agitation requirements 125
4.3.5 Heat Gains 129
4.3.6 Conductive Heat Gains 129
4.3.7 Viscous Dissipation 130
4.3.8 Summary 131
4.4 Thermal Energy Store Sizing 132
4.5 Closure 133

V Model Results **135**
5.1 Introduction 136
5.2 A Brief Description of the Application 137
5.3 Model Findings 138
5.3.1 Base Case Results 139
5.3.2 Passive–TES 143
5.3.3 Active Storage 148
5.4 Parametric Study 154
5.4.1 Load Dependence 154
5.5 Discussion 161
5.5.1 Further Parametric Analysis 169
5.5.2 General Discussion 171
5.5.3 Closure 179

VI Experimental Results 180
6.1 The Experimental Apparatus . . . 183
6.1.1 Rig Description . . . 183
6.1.2 Thermocouples . . . 187
6.1.3 General Observations . . . 189
6.1.4 The Compressor . . . 195
6.1.5 Other Observations . . . 196
6.2 The experimental procedure . . . 199
6.3 The Pull–Down and Charge–Discharge Times . . . 200
6.3.1 The Pull–Down Times . . . 201
6.3.2 The Thermal Store Charge Time . . . 203
6.3.3 The Thermal Store Discharge Time . . . 206
6.4 Response to Thermal Cycling . . . 210
6.5 Energy Consumption Tests . . . 214
6.5.1 Night–Time Only Prime–Mover Operation . . . 216
6.5.2 Day–time only Prime–Mover Operation . . . 219
6.5.3 Normal Prime–Mover Operation . . . 221
6.5.4 Conformance to the Regulatory Standards . . . 225
6.6 Discussion . . . 225
6.7 Closure . . . 229

VII Conclusions and Recommendations 230
7.1 Introduction . . . 231
7.2 Research Rationale . . . 231
7.3 Results . . . 232
7.4 Recommendations For Further Research . . . 234
7.5 Opportunities for Commercial Exploitation . . . 236
7.6 Closure . . . 237

– Appendices –

Appendix A
The calibration of the instrumentation . . . A 240
A.1 General Procedure . . . A 240
A.2 The Calibration of the Thermocouples . . . A 241
A.3 The Calibration of Voltage and Current measurement devices A 244

A.4 General discussion A-251

Appendix B

Determination of the *in situ* thermal resistance of the composite insulant B-301
B.1 Aim B-301
B.2 Apparatus and Set up B-301
B.3 The setup B-303
B.4 Procedure B-305
B.5 Theory B-306
B.6 Experimental Results B-309
B.7 Discussions B-310
B.8 The sources of errors B-311
B.9 Summary B-312

Appendix C

The Production of Hydrophilic PVA LHTES Samples C-313
C.1 Aim C-314
C.2 Apparatus C-314
C.3 Procedure C-315
C.4 Other tests C-316
C.5 Basic calculations and observations C-318
C.6 Discussions C-318

Appendix D

Computer Code Listing D-322

List of Figures

1.1 Electricity consumption (Domestic and Total) in the OECD world . . . 5
1.2 Electricity consumption (Domestic and Total) in the UK 5
1.3 Changes in the predominant DRA requirement in the UK 7
1.4 Total electricity consumption and distribution losses in the UK 7
1.5 Current and projected data and estimates of demographic trends . . . 10
1.6 Seasonal variation (1994–1995) in fridge–freezer electricity consumption, in low–income households 13
1.7 Mean monthly distribution of global irradiance on the earths surface averaged over the duration of the sunshine. 14
1.8 Annual mean Global irradiance on a horizontal place at the surface of the earth (W/m² averaged over 24 hours.) source UK-ISES (1976). . . . 15
1.9 Seasonal dependence of electricity demand in England and Wales . . 16
1.10 Changes in 'modal' DRA requirements in the UK 27
1.11 Effect of energy labelling on DRA's 29
1.12 The relation between price and performance in DRA's (Larder Refrigerators) 30
1.13 The relation between capacity and performance in Fridge Freezers . . 31

2.1 Schematic T–S diagram for the basic Carnot refrigeration cycle . . . 51
2.2 Schematic T–S diagram for basic refrigeration cycle 53
2.3 The effect of $\mathcal{R}_{\mathrm{DRA}(T)}$ on changes in *in situ* COP vs. Q_{load} 56
2.4 The effect of compartment $\mathcal{R}_{(T)}$ on changes in *in situ* COP vs. Q_{load} . . 56
2.5 The effect of Temperature on changes in *in situ* vs. COP 57
2.6 The relationship between the thermal conductance and insulant thickness in a cubic compartment. 62
2.7 Computational data (modelled) for the annual electricity consumption versus insulation thickness for a 200 litre 63
2.8 Diagram indicating two instances of different distributions of thermal insulation 64
2.9 Variation of thermal resistance ($\mathcal{R}_{(T)}$) for a cylinder of composite insulation 67

2.10 Variation of thermal resistance ($\mathcal{R}_{(T)}$) for a hollow sphere of composite insulation 67

3.1 Schematic diagram of TES charge–discharge cycle 88

4.1 Comparison of single and multiple prime–mover arrangements. 113
4.2 Schematic diagram of the electric–battery configuration. 114
4.3 Schematic diagram of the TES configuration. 114
4.4 Schematic diagram of the hybrid (electric–battery and TES) configuration. 114
4.5 Schematic diagram of two evaporator–TES arrangement options. . . . 116
4.6 Schematic (battery only system) diagram of the battery energy content and heat pump output during one daily cycle. 122
4.7 Schematic (TES only system) diagram of the TES energy content and heat pump output during one daily cycle. 123
4.8 Schematic (HES system) energy and heat pump output profiles for a night only prime–mover operation control regime 125
4.9 Schematic (HES system) energy and heat pump output profiles for a continuous prime–mover operation control regime 125
4.10 Illustration of the differing time periods (t_{D}, t_{N}, t_{sol}, t_{overlap}, $t_{\mathrm{top\,up}}$) within a 24–hour day. 126
4.11 Schematic diagram of the inclement period 129
4.12 Support figure for eqn (4.48) 139
4.13 The effect of temperature difference on the buoyancy–driven heat transfer coefficient for horizontal and vertical surfaces 141
4.14 The effect of temperature difference on the buoyancy–driven heat transfer coefficient within a vertical enclosure. 142
4.15 The effect of temperature difference on the buoyancy–driven heat transfer coefficient within a horizontal enclosure. 144
4.16 Initial evaporator–TES design sketch. 146
4.17 Revised (concertina) evaporator–TES design sketch. 146
4.18 Schematic diagram of the actual TES layout 148
4.19 Schematic diagram of the TES charge–discharge process. 149

4.1 Schematic diagram of integrated TES's 106
4.2 Schematic diagram of ES–DRA compartment 109
4.3 Schematic diagram of ES–DRA compartment 109
4.4 Schematic diagram of external storage TES. 109
4.5 Schematic diagram of integrated TES's 134

5.1 Plot of the solar–cell specifications against utilisation ratio 164

5.2 Plot of the battery and TES capacities against utilisation ratios 165

6.1 Schematic plan–view illustration of the entire experimental 'rig' indicating the main component parts. 186
6.2 Diagrammatic representation of experimental circuit. 187
6.3 Location of thermocouples on the ES–DRA rig exterior. 188
6.4 Location of thermocouples in the ES–DRA rig interior. 189
6.5 Images indicating the location of the TES's within the DRA 191
6.6 Diagrammatic representation of the velocity flow (m/s) across the condenser; air intake (left) and air exit (right) 194
6.7 End view of the DRA indicating the condenser (air intake, left) and compressor (right). 194
6.8 Graph indicating the effect of compressor cycling on DRA (*with* TES) interior heat transfer inventory. 197
6.9 Graphs indicating the effect of compressor cycling on DRA (*without* TES) interior heat transfer inventory. 198
6.10 Pull–down Temperature–Time history of the DRA with the TES in place in a *circa* 25 °C ambient. 201
6.11 Pull–down Temperature–Time history of the DRA with the TES in place in a *circa* 32 °C ambient 202
6.12 Pull–down Temperature–Time history of the DRA without the TES in place (25 °C environment). 203
6.13 Characteristic Temperature–Time history of different locations about the ES–DRA in a 25 °C environment during the charge process. 204
6.14 Temperatures, power and energy consumption and COP attending the TES charge process in a 25 °C ambient 205
6.15 Temperature–Time history of the TES charging in a 35 °C ambient. . . 206
6.16 Enlargements of indicated portions of Figure 7.15. 207
6.17 Temperature–Time history of the TES discharging in a 25 °C ambient. 208
6.18 Temperature–Time history of the TES discharging in a 32 °C ambient. 209
6.19 Temperatures across the TES mid–plane during discharge at 25 °C. . . 211
6.20 Temperatures across the TES mid–plane during discharge at 32 °C. . . 211
6.21 Graphical representation of the results from the experimental determination of the thermal lag of the ES–DRA cabinet 212
6.22 Enlargements of various portions of Figure 7.21 on page 260. 213
6.23 Instantaneous and mean coefficient of performance COP (top), condenser heat ejected, $Q_{condenser}$ ($kWh_{(T)}$), and compressor energy consumption, E_{HP} ($kWh_{(e)}$, bottom), during compressor 'on' periods for the night time control regime. 217

6.24 Compressor Temperature profile T_{HP} (top), Voltage V_{HP} and Current drawn (bottom) during compressor 'on' periods for the night–time control regime. 218
6.25 Mean temperature profile at various locations on the experimental rig (bottom) during compressor 'on' periods for the night–time control regime. 218
6.26 Instantaneous and mean coefficient of performance COP (top), condenser heat ejected, $Q_{condenser}$ ($kWh_{(T)}$), and compressor energy consumption, E_{HP} ($kWh_{(e)}$, bottom), during compressor 'on' periods for the day–time control regime. 220
6.27 Compressor Temperature profile T_{HP} (top), Voltage V_{HP} and Current drawn (bottom) during compressor 'on' periods for the day–time control regime. 220
6.28 Mean temperature profile at various locations on the experimental rig (bottom) during compressor 'on' periods for the day–time control regime. 221
6.29 Instantaneous and mean coefficient of performance COP (top), condenser heat ejected, $Q_{condenser}$ ($kWh_{(T)}$) and compressor energy consumption, E_{HP} ($kWh_{(e)}$, bottom), during compressor 'on' periods for the normal–operation mode scenario. 222
6.30 Compressor temperature profile T_{HP} (top), Voltage V_{HP} and Current drawn (bottom) during compressor 'on' periods for the normal–operation mode scenario. 223
6.31 Mean temperature profile at various locations on the experimental rig (bottom) during compressor 'on' periods for the normal operation mode scenario. 223

A.1 Thermocouple calibration data (low end). A–243
A.2 Thermocouple calibration data (high end). A–244
A.3 Thermometer in dewar flask A–245
A.4 Circuit diagram for the voltage divider and shuts calibration. A–246
A.5 Voltage and current calibration data (open circuit). A–248
A.6 Current and voltage calibration data (full load). A–249
B.1 Plan view of (open) experimental rig used for composite insulant conductivity determination. B–302
B.2 End view of experimental rig used for composite insulant conductivity determination. B–302
B.3 Cut–away sketch of insulated compartment indicating dimensions. . . B–303
B.4 Diagrammatic location of thermocouples. B–304
B.5 Circuit diagram of experimental control layout B–305

B.6 Supporting figure for eqn (B.I) B–307
B.7 Thermal conductance charts B–309
B.8 Temperature difference charts B–310
B.9 Graphs indicating thermal lag during experiment. B–312
C.1 Temperature–time history of the TES charging and discharging −25 and +20 °C ambients respectively. C–319
C.2 PVA (cross–linked *circa* 95% w/w) *above* the phase–change temperature (T_{LH}) of water. C–319
C.3 PVA (cross–linked *circa* 95% w/w) *below* the phase–change temperature (T_{LH}) of water. C–319
C.4 PVA (cross–linked *circa* 95% w/w) with fungal growth. C–321

List of Tables

1.1 Thermal efficiencies (%) of electricity generating plants in the UK . . . 6
1.2 World's ten most populous countries 9
1.3 Estimates of the heat gain into a DRA 12
1.4 Ownership of Appliances in the UK 1970–1975 by % of households. . . 32

2.1 Break–down of the boundary conditions (a–c) given in eqn (2.30) . . 70

3.1 TES classification by associated energy transfer mechanism 84
3.2 Comparative (minimum) generated entropy for the charge–discharge process 90
3.3 Desirable properties for candidate PCM–LHTES media 95
3.4 Problems and possible solutions facing LHTES implementations. 98

4.1 Some typical applications indicating the relative weights of different requirements. 107

4.1 Comparative characterisation of two–phase solid–liquid flow. 111

5.1 Model input data 140
5.2 Application characteristics. 141
5.3 Thermal energy store/carrier data. 142
5.4 Base–case dimensions, heat energy burden and heat exchange requirements for 39, 85 and 110 litre ES–DRA's. 143
5.5 Single–day requirements 60% (day–load) utilisation capacity (night–time cooled). 144
5.6 Three–day inclement period 60% (day–load) utilisation capacity (night–time cooled). 146
5.7 Five–day inclement period 60% (day–load) utilisation capacity (night–time cooled). 147
5.8 DRA compartment properties. 148
5.9 Active–TES layout description. 149
5.10 Slurry pump and agitator description. 149

5.11 Active–TES ES–DRA additional requirements/modifications, 60% (day–load) utilisation capacity. 150
5.12 Active–TES ES–DRA energy requirements, 60% utilisation capacity. . . 151
5.13 Active–TES ES–DRA additional system requirements, 0% utilisation capacity. 152
5.14 Active–TES ES–DRA energy requirements, 0% utilisation capacity. . . . 153
5.15 Base–case dimensions, heat energy burden and heat exchange requirements for a 39 litre ES–DRA under different utilisation patterns. 154
5.16 39 litre DRA requirements for no–utilisation capacity. 155
5.17 39 litre DRA requirements for 50% night–time and 50% day–time utilisation capacity. 156
5.18 39 litre DRA requirements for 40% night–time and 20% day–time utilisation capacity. 157
5.19 39 litre DRA requirements for 30% night–time and 30% day–time utilisation capacity. 158
5.20 39 litre DRA requirements for 20% night–time and 40% day–time utilisation capacity. 159
5.21 39 litre DRA requirements for a 60% night–time utilisation capacity (day–time cooled). 160
5.22 39 litre DRA requirements for 60% day–time utilisation capacity and 100% (electrical) energy transfer efficiency. 162
5.23 39 litre DRA requirements for no–utilisation capacity and 100% (electrical) energy transfer efficiency. 163

6.2 Table of non–dimensional parameters Bi and Fo for the TES using the properties of H_2O. 193
6.3 Thermal lag estimates across a polyurethane foam wall based on eqn (2.31). 214
6.4 Daily ambient–temperature set–points used during the experiments. . 215
6.5 Summary of experimental results for the night–time prime–mover control regime. TES control temperature $(-2 - -1)\,°C$. 217
6.6 Summary of experimental results for the night–time prime–mover control regime with TES control temperature $(-3.0 - -2.5)\,°C$. 219
6.7 Summary of experimental results for the day–time prime–mover control regime. 219
6.8 Summary of experimental results for the 'normal mode' prime–mover control regime. 222
6.9 Summary of the experimental results for all regimes of prime–mover control. 224

6.10 Comparion of the energy consumption of the ES–DRA with different standards and projected estimates. 225

7.1 Cost of various addended components to the basic DRA. 237
A.1 . . . . . A–249
B.1 Distribution of composite insulation around compartment. B–308
B.2 Computed values for the thermal conductances and apparent conductivity B–308
C.1 Estimation of water content in the cross–linked PVA data C–318
C.2 Chart of the latent heat energy storage capacity in relation to the degree of hydration of the PVA. C–320

Nomenclature

Abbreviations

ac *Alternating current.*

ACEEE *American Council for an Energy Efficient Economy* (USA).

ADEME *Agence de l'Environnement et de la Maîtrise de l'Energie (France)*: The French Agency for the Environment and Energy Management, formerly AFME.

AFME *see* ADEME *qv.*

AHAM *Association of Home Appliance Manufacturers* (USA).

AMEDEA *Association of Manufacturers of Domestic Electric Appliances* (UK).

ANSI *American National Standards Institute.*

ASHRAE *American Society of Heat, Refrigeration and Air Conditioning Engineers.*

ASME *American Society of Mechanical Engineers.*

BATNEEC *Best Available Technology Not Entailing Excesive Cost.*

BHRA *British Hydromechanics Research Association.*

CADDET *Center for Analysis and Dissemenation of Demonstrated Energy Technologies* (USA).

CCGT *Combined Cycle Gas Turbine.*

CECED *European Committee of Manufacturers of Electrical Equipment.*

CFC *Chloro–Floro–Carbon.*

COP *Coeficient of Performance*: An index of merit for heat pumps which characterises the relative benefit obtained (in energy terms) from an appliance to the energy consumed.

CPU *Central processing unit*: The main computational engine of a computer.

dc *Direct current.*

DECADE *Domestic Electricity and CArbon Di-oxide Emissions*: The Environmental Change Unit, Oxford University (UK).

DGXII *Directorate General 12*: The science directorate of the (EU).

DGXVII *Directorate Generate 17*: The energy directorate of the Commision of European Comminuties.

DoE *Department of Energy (USA) or the defunct UK's department of the Environment; superseeded by the DETR.*

DRA *Domestic Refrigeration Appliance*: Principally, appliances used for domestic (non-freezing) refrigeration. The definition is loosely extended to like appliances used in small industry, mobile leisure and medical activities *etc.*

DSC *Differential Scanning Calorimetory*: A scientific investigative process of monitoring constant rate heating/cooling for the accurate observation of property behaviour of a substance in a changing thermal environment.

DSM *Demand Side Management*: An (incentive based) electrical energy management tool devised by utility companies in the bid to effect a change in the demand profile of electrical energy.

DTI *Department of Trade and Industry, UK.*

EC *European Community.* see **EU** *qv.*

emf *Electro–Motive Force.*

EPA *Environmental Protection Agency (US).*

EPI *The WHO/UNICEF's (qv.) Expanded Programme on Immunisation.*

ES *Energy Store/Storage*: A repository, or the stockpiling process, of an energy resource for strategic use. The inferred meaning will be context dependent.

ES–DRA The designed **DRA** *qv.* with **TES** *qv.* facilities.

EU *European Union*: An alliance of member states within Europe, working together to foster mutual soci–economic growth. The **EU** supeseded the earlier (now defunct) **EC**, *qv.*

GEA *Group for Efficient Appliances*: An energy–efficiency analysis and pressure group within the **EU**.

GWP *Global warming potential*: The relative ability (usually with reference to carbon–dioxide) of a substance to act as a greenhouse gas.

HES *Hybrid Energy Store/Storage*: This refers to an energy store/storage system employing more than one energy storage mechanism, see section 4.4 on page 114. The acronym is used interchangeably for store and storage.

HVAC *Heating Ventilation and Air Conditioning.*

IEA *International Energy Agency.*

ISES *International Solar Energy Society.*

ISO *International Standards Organisation.*

LCO *Least Cost Option.*

LCUP *Least Cost Utility Planning*: A kernel of energy managerial strategies/decision making tools for planning utility expenditure to ensure minimum expenditure and maximum plant usage.

LH *Latent Heat.*

LHTES *Latent Heat Thermal Energy Store/Storage*: The acronymn is used interchangeably for both storage and store. The implied meaning will be clear within the context.

LOLP *Loss of Load Probability.*

OECD *Organisation for Economic Co–operation and Development.*

PBP *Pay Back Period*: The period required for an investment to recoup its capital expenditure. As to whether monetary indexes (inflation, value in other investment) are to be taken into account should be stated along side its computation.

PCM *Phase Change Material.*

PSU *Power Supply Unit.*

PV *Photo–Voltaic.*

PVA *Poly Vinyl Alchol*: A polymer with the chemical formula $-(CH_2.CH.OH)_{p(\sim 40-88)}-$

SAP *Structural Adjustment Programme*: An austere economic agenda for curtailing national expenditure, typically issued by creditors to debtor nations, as a prerequisite to further borrowing.

SAVE *Specific Action for Vigourous Energy efficiency.*

SEC *Specific Energy Consupmtion*: An unfortunate term denoting the index of the energy consumed per unit volume in a DRA *qv.*

SI *System International.*

SPV *Solar Photo Voltaic.*

TES *Thermal Energy Store/Storage*: The implied meaning will be clear from the context.

UK *United Kingdom.*

UN *United Nations.*

UNICEF *The* UN*'s (qv.) International Childrens Emergency Fund.*

US *see* USA.

USA *United States of America.*

VPSI *Vacuum Panel Super Insulation.*

WHO *World Health Organisation.*

List of symbols

A *Area*: m^2

D *Diameter*:m

E *Energy*: J

H *Enthalpy*: J
S *Entropy*: $\mathrm{J\,K^{-1}}$
g *Acceleration due to gravity*: $\mathrm{m\,s^{-2}}$
H *Head*: m
Q *Heat*: J
q *heat transfer per unit area*: $\mathrm{J\,m^{-2}}$
$\dot{Q}$ *Heat transfer rate*: W
$\dot{q}$ *Heat transfer rate per unit area*: $\mathrm{W\,m^{-2}}$
H *Height*: m
h *Hours.*
h *Heat transfer coeficient*: $\mathrm{W\,m^{-2}\ ^{\circ}C^{-1}}$
k *Conductivity*: $\mathrm{W\,m^{-1}\ ^{\circ}C^{-1}}$
K *Conductance*: $\mathrm{W, ^{\circ}C^{-1}}$
L *Length*: m
m *Mass*: kg
$\dot{\mathrm{m}}$ *Mass flow rate (mass velocity)*: $\mathrm{kg\,s^{-1}}$
N *Molarity.*
P *Power*: W
P *Pressure*: Pa
r *Radius*:m
$\mathcal{R}$ *Resistance*: $\mathrm{^{\circ}C\,W^{-1}}$
s *Seconds.*
C *Specific Heat capacity*: ($\mathrm{J\,kg^{-1}\ ^{\circ}C^{-1}}$) Whether this be with respect to constant pressure or constant volume is indicated by the subscript.
T *Temperature*: °C, K
t *time*: s
U *Overall heat transfer coeficient*: $\mathrm{W\,m^{-2}\,^{\circ}C^{-1}}$
v *Velocity*: $\mathrm{m\,s^{-1}}$
V *Volume*: $\mathrm{m^3}$
$\dot{\mathrm{V}}$ *Volume flow rate*: $\mathrm{m^3\,s^{-1}}$
W *Work*: J

Subscripts

amb. *ambient.*
Bat. *Battery.*
r *Bends*: This particularly refers to the various elbows within the slurry conveying conduit.

$_{C}$ *Carnot.*

$_{\Delta+}$ *charge.*

$_{l}$ *Cold.*

$_{\text{evap.}}$ *Cold (Carnot) end.*

$_{\text{HP}}$ *Compressor (Heat Pump).*

$_{\succ}$ *Sudden contraction.*

$_{\text{D}}$ *Day.*

$_{\Delta-}$ *Discharge.*

$_{\text{DRA}}$ *Domestic Refrigeration Appliance.*

$_{\text{end}}$ *This denotes the totality of the effects of sudden contraction and sudden expansion.*

$_{(e)}$ *Electricity.*

$_{\prec}$ *Sudden expansion.*

$_{\text{ext.}}$ *External.*

$_{f}$ *Fluid.*

$_{food}$ *food.*

$_{\rightarrow}$ *Flow in the horizontal.*

$_{h}$ *Hot.*

$_{\text{cond.}}$ *Hot (carnot) end.*

$_{i}$ *Ingress.*

$_{\text{insul.}}$ *Insulation.*

$_{\text{int.}}$ *Internal.*

$_{L}$ *Length.*

$_{\text{LH}}$ *Latent Heat.*

$_{(l)}$ *Liquid.*

$_{load}$ *Load.*

$_{\text{LM}}$ *Logarithimic Mean.*

$_{\text{mech.}}$ *Mechanical.*

$_{\text{max}}$ *Maximum.*

$_{\text{min}}$ *Minumum.*

$_{\text{N}}$ *Night.*

$_{\text{overlap}}$ *Overlap*: That fraction (with respect to the day–time length) of the time difference between the day–time length and the solar insolation period during which the night–time cooling regime effectively begins.

$_{\text{pipe}}$ *Slurry conveying conduit.*

$_{\text{pump}}$ *Fluid pump.*

$_{\text{PVA}}$ *Poly Vinyl Alchol.*

$_{res.}$ *Resultant.*

$_{SH}$ *Sensible Heat.*

$_{slur.}$ *Slurry.*

$_{sol}$ *Solar.*

$_{solD}$ *Solar Day.*

$_{SPV}$ *Solar Cell.*

$_{(s)}$ *Solid.*

$_{,}$ *between.*

$_{TES}$ *Thermal Energy Store/Storage.*

$_{(T)}$ *Temperature.*

$_{top\ up}$ *Top up*: That fraction (with respect to the total day–time heat gains) of the day–time heat loads which are catered for by direct prime mover action irrespective of the (compressor) control regime in effect.

$_{tot.}$ *Total.*

$_{\uparrow}$ *Flow in the vertical.*

$_{[H_2O]}$ *Water.*

Non–dimensional quantities

Bi *Biot Number.*

De *Flow Dean Number.*

C_D *Drag Coeficient.*

Fo *Fourier Number.*

f *Non–dimensional friction Coefficient*: This specifically refers to the friction factor for the head–losses in single phase pipe flow.

Gr *Grashof Number.*

Nu *Nusselt Number.*

Po_N *Flow Power Number.*

Pr *Prandtl Number.*

Ra *Rayleigh Number.*

Re *Reynolds Number.*

Ste *Stefan Number.*

Greek letters

ω *Stirrer (angular) speed*, rev/s.
α *Thermal diffusivity*, $\mathtt{m}^2\,\mathtt{s}^{-1}$.
η_i *First Law efficiency*, %.
η_{ii} *Second Law efficiency*, %.
μ *Electro Chemical potential*, molar fraction.
Φ *Non-dimensional excess head–loss.*
ϱ *Resistivity*, $\Omega\,\mathtt{m}$.
σ *Standard deviation (with respect to the entire sample size).*
μ *Viscosity*, $\mathtt{kg\,m\,s}^{-1}$.

Chapter One

The Context

Domestic Refrigeration Appliances

1.1 Proem

The progress of any civilisation is inextricably linked to its ability to reduce the time required to satisfy basic needs *e.g.* thirst, hunger, clothing, shelter *etc.* The ability to store basic amenities is intrinsic to this requirement, as it reduces the number of times certain tasks (such as foraging for food, fetching water, cooking *etc.*) are performed, permitting the allocation of human resources to the building of society. This is suggestive of a critical, 'minimum living standard' necessary for the onset and perpetuation of development. The rate of this development would depend, to some extent[1], on a society's proximity from this basic living standard and the states of development of other mutually–interacting societies. Thus, there is a natural interest and requirement throughout the world to improve the living standards and overall health of communities, particularly in developing countries. At the same time, there are enormous economic advantages to be gained in an awareness, and possible exploitation, of the commercial potentials inherent in the supply

[1] As with all things, the laws of diminishing returns would apply.

of provisions (goods, services, utilities *etc.*) necessary to facilitate this development.

The role of refrigeration is invaluable within most preservation/storage contexts. The proliferation of domestic and small–scale commercial refrigerating (cold/coolth) devices (appliances), hereinafter referred to as DRA's[1], began in the 1920's–1930's [Bianchi and Forlai, 1988; Atwood, 1991; Nagengast, 1998]. Currently in many countries of the developed world, there is a saturation (or near saturation) of DRA's [FICHTNER, 1988; Sillanpää et al., 1996]. In the UK, for instance, the 'average' household owns between *circa* 1.4 [Boardman et al., 1997] and *circa* 1.8 [Mansouri-Azar, 1996] coolth appliances.

Among domestic appliances, the energy utilised by refrigeration appliances represents the fastest growing portion of household energy consumption [Boardman, 1995a]. Electricity statistics [Hardcastle, 1984; Frachet, 1995; IEA (for OECD), 1996; Ward, 1997] indicate that, within the OECD, domestic electricity consumption constitutes the greatest, or second greatest[2], portion of national electricity consumption when compared with electricity usage from the other major sectors: *viz* the iron and steel industry; industrial (excluding iron and steel); transport; and other commercial users (Figures 1.1 and 1.2, *qv.* pages 5 and 5 respectively). The developing world is also requiring dramatically increasing numbers of coolth appliances [Waide, 1993] as integral to its development, with attendant energy consumption implications [Anon., 1995]. The results from one survey [Sathaye, 1988] indicate that, in Beijing China, prevalence of DRA's grew from a few percent in 1981 to more than 60% in 1989. A similar trend was observed in the UK between 1973 and 1983 with domestic freezers, where the ownership level rose from 3% to 32% over the same period [Mansouri-Azar, 1996].

1.2 The Energy Consequences

1.2.1 The Developed World

Domestic refrigeration (coolth) appliances are almost invariably 'mains' electricity driven. The very nature of the application and the concomitant stringent performance requirements, mandate continual operation all year round. Notwithstanding the relatively low power consumption (50–150) W normally associated with their operation, DRA's are, as a group, a significant contributor to the electricity

[1] Collectively, larder refrigerators, fridge–freezers and freezers. In this case excluding air conditioners but inclusive of small–scale non–domestic refrigeration applications such as in public houses, corner shops *etc.*

[2] Depending on whether iron and steel consumption is accounted for along with the other industries or not.

consumption of typical domestic dwellings[1], as a consequence of their virtually 'all year round' operation [UK Consumers' Association, 1982; Smith and Porter, 1990; Boardman, 1995b]. This has attendant implications on national electricity consumption, especially for countries with a high level of DRA saturation *i.e.* much of Western Europe, Canada and North America [FICHTNER, 1988; Mansouri-Azar, 1996].

Nørgård (1989) estimated that between 30 and 50% of an industrialised nation's total electricity consumption is used to run domestic appliances; for Denmark, in 1988, the author quotes a value of 45%. In the US in 1989, 20% of all the residentially–consumed electricity (7% of the nations total) was put to DRA–use alone [Turiel and Levine, 1989]. More recent statistics, [Frachet, 1995; IEA (for OECD), 1996; Ward, 1997], tend to indicate that, within the OECD, the proportion of national electricity used for domestic purposes is in the region of 20 to 40%. In 1990 the ACEEE released a document [Burke, 1990] cataloguing the ten most energy–efficient appliances. In the introduction, the authors state that in the US prior to 1990, *refrigerators alone* accounted for about 5% of the nation's total electricity consumption. According to one CADDET study [CADDET, 1994], in 1993 the US DRA electricity consumption was an estimated 293 TWh, a 9.2% increase relative to 1990.

In the EC in 1993, DRA's were the most dominant of all domestic appliances in terms of energy consumption, accounting for an estimated 24% (111.2 TWh) of all domestically–consumed electricity (6% of the total electricity consumption in that year) [Waide, 1993]. In another DECADE report, the authors state that in 1996, domestic coolth appliances accounted for 6% of the total electricity consumption in the UK, a staggering 17 TWh [Boardman et al., 1997], apparently more than all the electricity consumed in offices in the UK in the same year. Sillanpää et al. (1996) claim that in the preceding year *circa* 30% of the Finnish domestic electricity consumption was used for DRA's, some 2.215 GWh, the general proportion being in the region of 20 to 30%.

The specific energy consumption (SEC)[2] over time have been affected by several factors including:

- Trends in efficiency, size and features in appliances, reflecting a change in consumption under test conditions.
- Demographic factors, [Boardman et al., 1997, (Chapter 5)], such as reduced family size or greater number of working single person homes (including students).
- Changes in the usage patterns of appliances (*e.g.* buying more frozen food and freezing more foods *etc.*) which may, in part, be a reflection of changes in the

[1] More so, when air conditioning is taken into account.
[2] Energy consumption per unit litre, typically $kWh_{(e)}$/litre

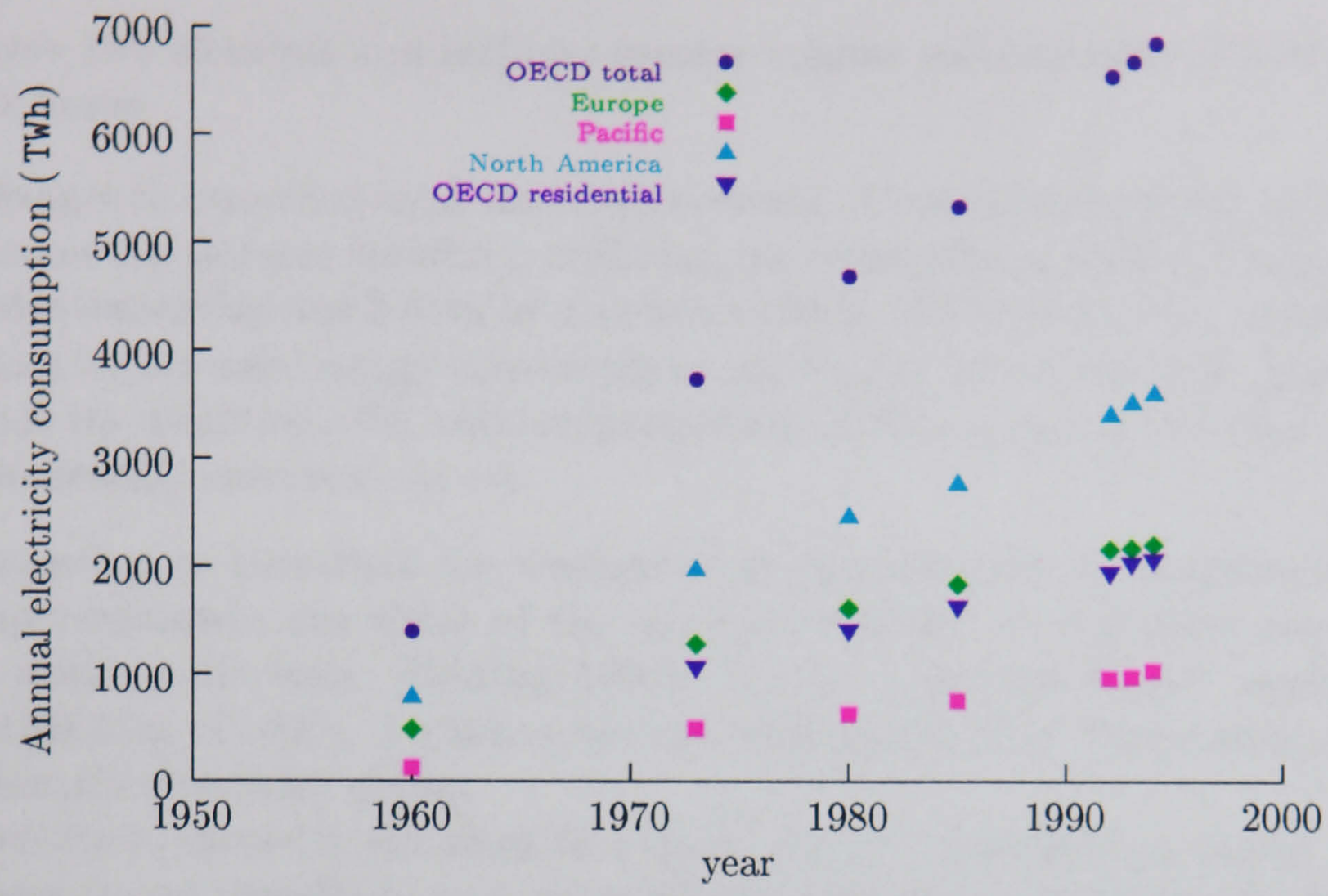


Figure 1.1: Electricity Consumption (Domestic and Total) in the OECD world (1960–1995) source [IEA (for OECD), 1996]

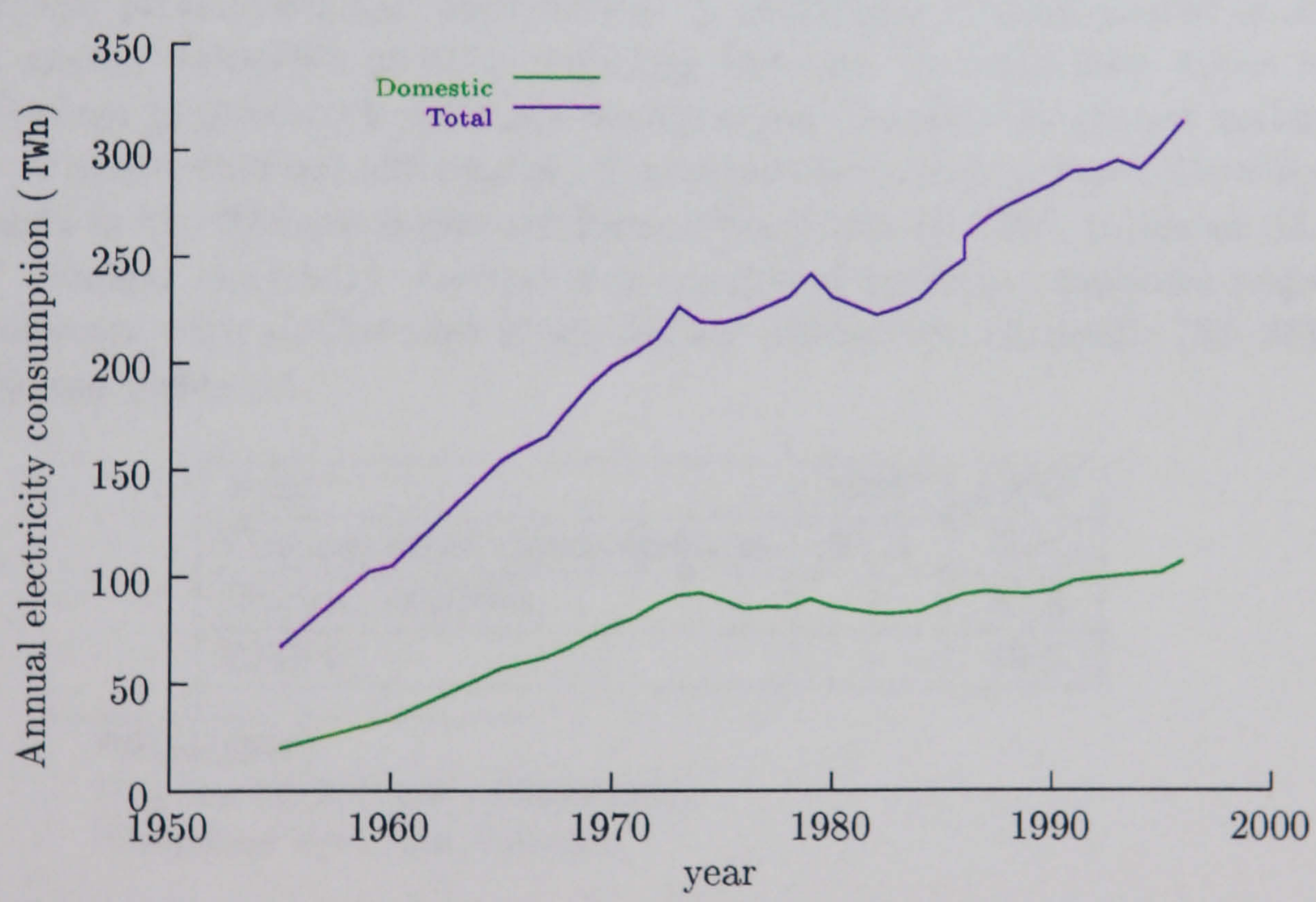


Figure 1.2: Electricity Consumption (Domestic and Total) in the UK (1955–1996) source [Ward, 1997]

(a). Only from 1990 does the data indicate that combined cycles were used (see also Table 1.1 on the following page).

above two elements and includes greater volume requirements of frozen space per home.

- Changes in 'standard appliance requirements'. Over time the fridge–freezer has become the *de facto* standard, replacing the conventional fridge. The growth of fridge ownership was halted by a switch to fridge–freezers *loc. cit.*, which have a much higher unit energy consumption, see Figure 1.3 on the next page. Also, since its inception, the volume/proportion of frozen space in fridge–freezers has steadily increased *op. cit.*

It is interesting to note that the amount of energy required to manufacture each DRA is approximately one third of the amount of energy it consumes over a 12–15 year working life span, [Herring, 1994]. In discussing the energy implications of the utilisation of DRA's, it cannot be over–emphasised that these appliances are predominantly electricity driven.

Electricity is currently the most convenient form of transporting energy and, in many cases it can contribute to a more efficient conversion of energy at the point of use *e.g.* the electric kettle. For these reasons, it serves an increasing number of applications and thus the demand for electricity has continued to increase steadily. However, the production and distribution of electricity in most countries is an inefficient, energy–intensive process requiring between two and four times as much primary energy (expressed in primary energy units) per unit generated energy. Over the past 40 years, thermal efficiencies of conventional steam power electricity generating plants in the UK have improved from *circa* 24.2% in 1955, to about 33 to 36% in 1996. Nuclear electricity stations and combined cycle gas turbines respectively tend to operate with similar and much higher efficiencies, currently (35–36)%, and (43–47)%, see Table 1.1.

Year	1965[a]	1996[b]
Conventional steam stations	27.4	36.6
Nuclear stations	–	35.8
CCGT's[c]	–	46.8

[a] Ward (1997)
[b] IEA (for OECD) (1996), Ward (1997)
[c] Combined Cycle Gas Turbines

Table 1.1: Thermal efficiencies (%) of electricity generating plants in the UK

In addition to this, a considerable amount of energy is 'lost' between generation and delivery. In the UK for instance, between four and seven percent of the electricity generated is lost in distribution, *i.e.* the difference between the *net* generated and

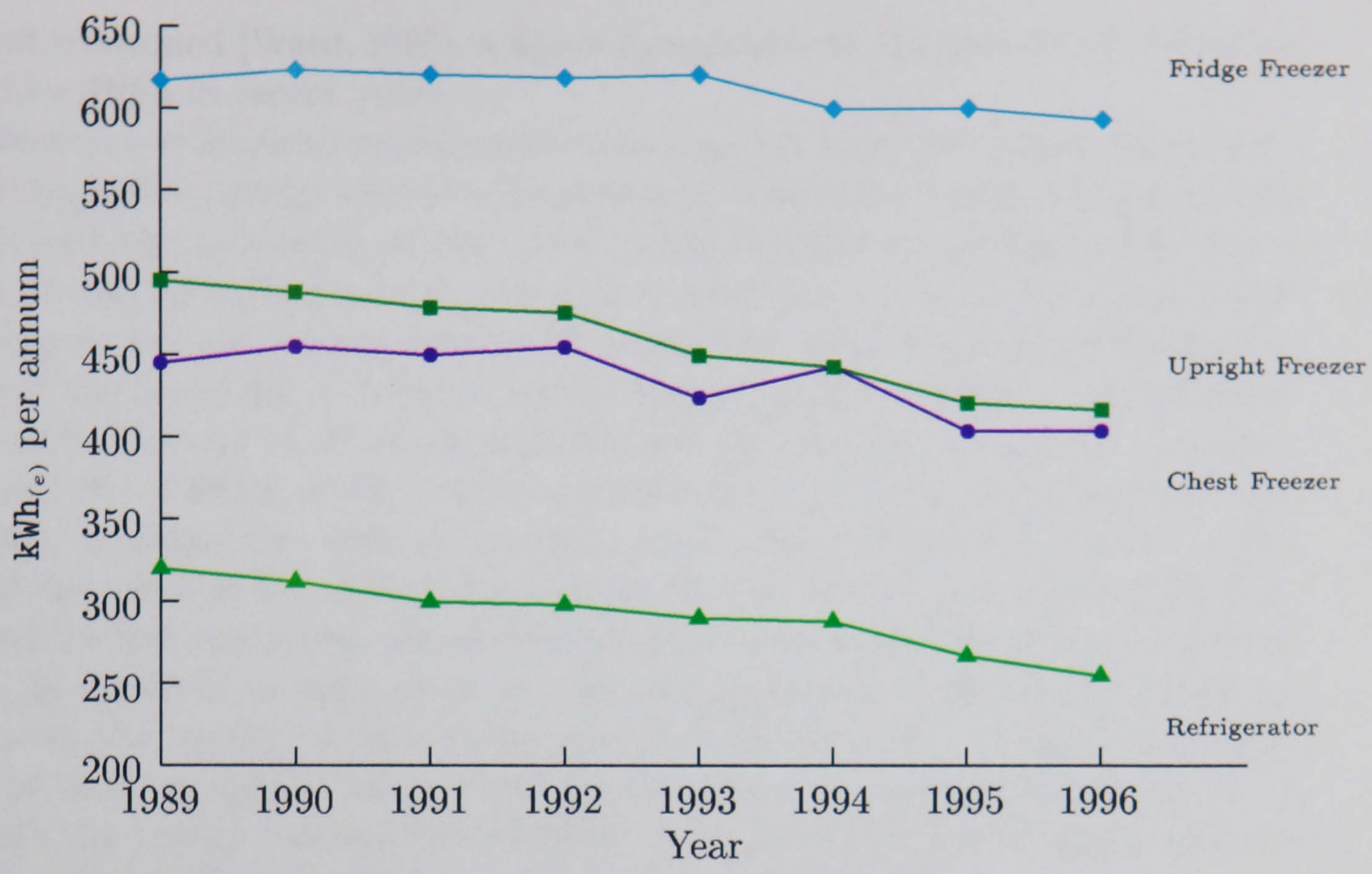


Figure 1.3: Changes in the predominant DRA requirement in the UK source [Boardman et al., 1997]

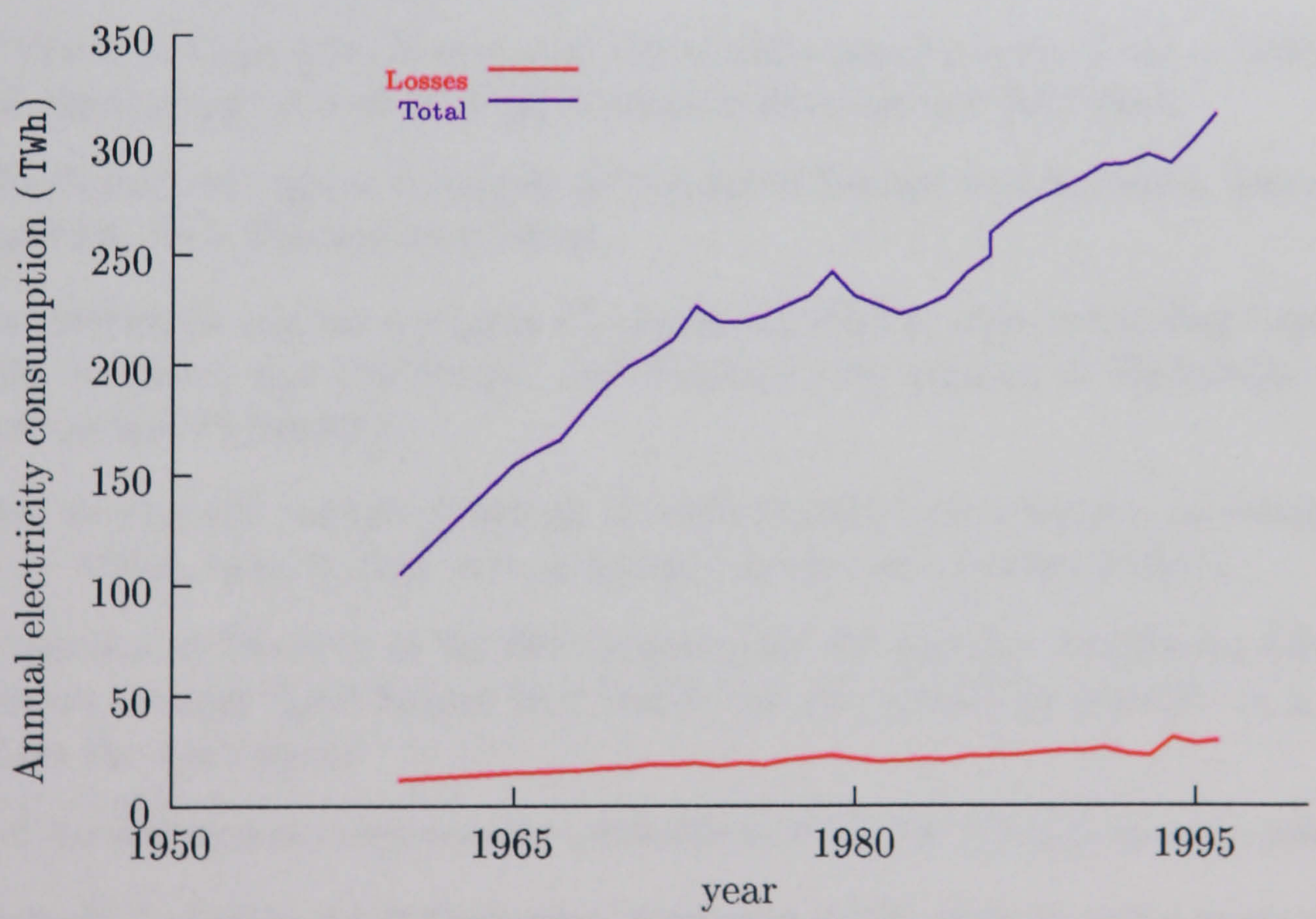


Figure 1.4: Total electricity consumption and distribution losses in the UK (1960–1996) [Ward, 1997]

the amount consumed [Ward, 1997], a figure comparable to the amount of electricity consumed by DRA's in recent years.

Therefore any reductions in electricity consumption will have a high (*circa* two–three fold) impact on energy resource conservation. The scale of energy consumption associated with the utilisation of DRA's, even when the manufacturing energy cost is neglected, is such as to have salient economic implications on most economies where such appliances are extensively used (with attendant environmental ramifications).

Much of the foregoing is deferred to the energy and/or economic cost of DRA's, without much reference to the environmental implications associated with the manufacture and use of DRA's. If the environmental impact of the halocarbons, typically used in DRA manufacture, were to be taken into consideration along with similar impacts of the combustion of fossil fuel during the production of the necessary electricity used for DRA operation, the environmental consequences become a prominent concern[1]. In addition to this, there are (techno–economic) logistical problems associated with the supply of such large quantities of electricity. In all but a small minority of limiting special cases, there are beneficial environmental effects in reducing both the energy consumption of DRA's[2] and, the quantities of energy and raw materials (particularly halocarbons) used in their manufacture.

1.2.2 The Developing World

The United Nations (UN) demarcates the world's population into three different categories, depending on level of socio–economic development [UN, 1996].

- More developed regions comprise all regions of Europe and Northern America, Australia, New Zealand and Japan.
- Less developed regions comprise all regions of Africa, Asia (excluding Japan), Latin America, the Caribbean, and Oceania (the regions of Melanesia, Micronesia and Polynesia).
- Least developed[3] regions which as of 1995 included 48 countries, of which 33 are in Africa, nine in Asia, one in Latin America and five in Oceania.

The Populations Division of the UN's Department of Economic and Social Affairs, also publishes demographic figures and trends for the world, by country (*e.g.* see Table 1.2 on the next page).

[1]Much of the awareness of this prominence, desirable as it may be, is largely for socio–political concerns.

[2]One such case is given by the UK Consumers' Association (1982) where the prime–mover waste heat was used also as a means of providing space heating.

[3]Also included in the list of 'less developed' regions.

Rank	Country	Year		
		1950	1996	2050
		Population (million)		
1	China	555		
	China		1,232	
	India			1,533
2	India	358		
	India		945	
	China			1,517
3	United States of America	158		
	United States of America		269	
	Pakistan			357
4	Russian Federation	102		
	Indonesia		200	
	United States of America			348
5	Japan	84		
	Brazil		161	
	Nigeria			339
6	Indonesia	80		
	Russian Federation		148	
	Indonesia			318
7	Germany	68		
	Pakistan		140	
	Brazil			243
8	Brazil	54		
	Japan		125	
	Bangladesh			218
9	United Kingdom	51		
	Bangladesh		120	
	Ethiopia			213
10	Italy	47		
	Nigeria		115	
	Iran (Islamic Republic of)			170

Table 1.2: Worlds ten largest countries ranked by year and order of decreasing population.Source [UN, 1996]

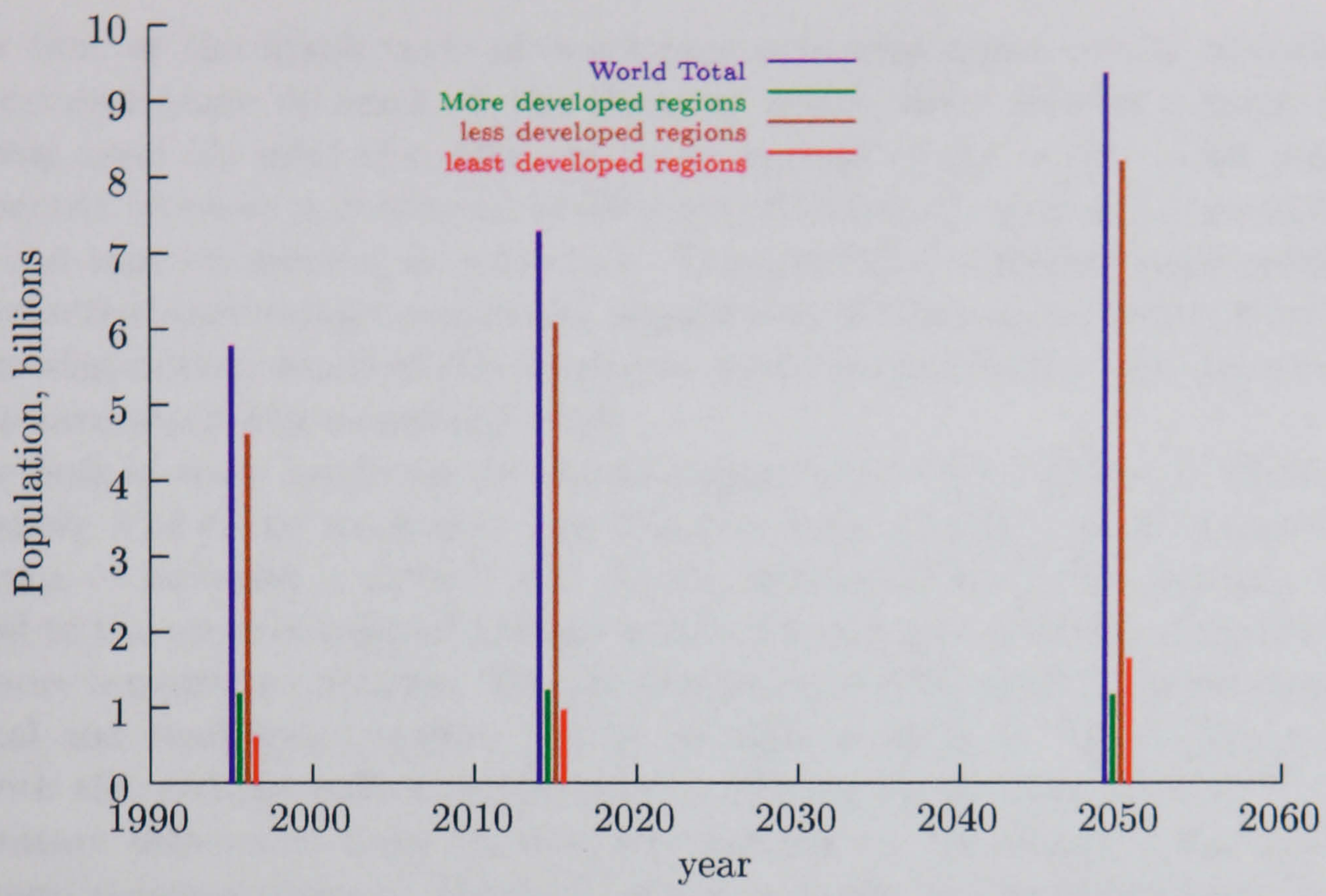


Figure 1.5: Current and projected data and estimates of demographic trends (1996, 2015, 2050) categorised by development Source [UN, 1996]

With the exceptions of the USA, Japan and the Russian Federation, the majority (accounting for *circa* 3 billion people) of the world's ten most populous nations are categorised as, 'less or least developed'. The demographic data projections for year 2050 is weighted in favour of the less developed regions of the world, when about eight of the ten most populous countries in the world will then be classified as 'less developed'. The current ratio of the population of the lesser developed nations to the more developed nations is *circa* 5:1 (and increasing), with a current world population of about 5.9 billion people. The year 2050 estimates represent a 50.8% increase[1] on the current population. It is against this population–development distribution that the following discourse on DRA ownership, location and subsequently the energy consequences is undertaken.

Whereas appliance utilisation/ownership data (or estimates) exist for much of the developed world, there is a paucity of similar data for much of the under–developed (or developing)[2] world. For such regions, in the light of the absence of data (and thus analysis), the impacts of DRA's cannot be estimated accurately. However, it

[1]The UN Population Information Network (http://www.popin.org) publish an estimate of a total world human population of 8.9 billion by the year 2050.

[2]This is used interchangeably for the collective of the less and least developed regions of the world.

is clear that as the inhabitants of developing countries aspire to the standards of living commonplace in much of the Western world, there will be a surge in the ownership level of, *inter alia*, DRA's in those regions of the world. This potential for dramatic increase is evidenced in the case of China *cf:* section 1.1 on page 2, if that trend may be deemed as indicative. This potential is further compounded by the (projected) increasing trend in the populations of these underdeveloped regions. In contradistinction, much of the developed world is characterised by saturated (or close to saturated) DRA ownership levels.

The bulk of these less/least developed regions are within continents which lie at least partly within the tropical or sun belt (*i.e.* between the tropics of Cancer and Capricorn — latitudes $\pm$ 23½°) *viz*: Africa, much of Asia, South America *etc.* as opposed to the more developed nations within Europe, and in North America which have more temperate climates. The air temperature differences between these two (tropical and temperate) regions can be as high as 30 °C at certain times of the year with the average *indoor* temperatures differing by between (5–10) °C[1]. These temperature differences have considerable bearing on the energy consumption of DRA's used comparatively (a likelihood which is small, as illustrated later) in both regions.

One implication of this difference in air temperature, is that there will be a greater energy requirement to operate an otherwise similar DRA in the tropics, for the following reasons.

- The first is in consequence of the increased temperature difference between the refrigerator interior and the ambient temperature. The current consensus is that, the heat gain through the DRA compartment constitutes upwards of 80% of the energy requirements of a standard fridge, not including air infiltration (which constitutes a further 8% or thereabouts) [Guldbrandsen et al., 1986; Nørgård, 1989; March Consulting Group, 1990; Boardman, 1995b]. ASHRAE (1994)[2] gives a detailed breakdown of the heat gain distribution, see Table 1.3 on the next page. According to Nørgård (1989), the operating environment temperature is very important; a 5 °C increase in ambient temperature could affect the energy consumption by as much as 30%[3]. Similar results were observed by Malin et al. (1993) and Boardman

[1]This is after steps have been taken to regulate these temperatures to within the (location dependent) human comfort zone. In places like garages and garden sheds the differences can be as much as five times as much (25 to 50 °C) particularly, when the hot dry season in the tropics coincides with winter in the temperate regions.

[2]Chapter 48.

[3]As a consequence of increased thermal loading and a reduction of prime–mover performance. The ambient temperature during the tests was the standard (*EN 153*) 25 °C. By way of a very basic example, not considering changes in prime mover performance and on the estimates given in Table

et al. (1997). Figure 1.6 on the following page illustrates the effect of seasonal temperature changes in low income households in Edinburgh, UK. Of immediate interest is the difference in the variation of the fortnightly energy consumption from 20 $\mathbf{kWh}_{(e)}$ to 33 $\mathbf{kWh}_{(e)}$ (between summer and winter), an increase of 60%. With much of the developing world having ambient and indoor temperatures higher than those of the bulk of the more developed world (*circa* (10–20) °C and (5–10) °C respectively), the magnitude of the 'compartment associated' gains would be significantly greater in the developing regions.

Heat ingress avenue	Percentage of total (%)
Wall insulation	52
Door gasket region[a]	30
External heater	6
Defrost heater	6
Fan motor	6

Table 1.3: Estimates of the heat gain into a DRA. Source [ASHRAE, 1994, *pp.* 48.3]

[a]Conduction associated.

- The second is related to climate–dependent DRA utilisation. Whilst in some instances in more temperate climates, some foods can be left unrefrigerated[1], in regions of the world where the average outdoor temperatures are, say, in excess of 32 °C (and indoor temperatures are *circa* 25 °C), the preservation of say, vegetables, milk, meat *etc.* depends more on the use of refrigerating appliances. Thus, increased per capita cold storage volume requirements and use can be envisaged. It is expedient to ensure that DRA's are fully laden from an operating standpoint[2], however this has to be traded against the increased internal cooling load associated with the increased storage volume requirement and higher load input temperatures.

Increased solar insolation within the the sun–belt is the reason for increased air temperature within this region as compared to the more northernly and southernly

1.3, the heat gain may be represented as $82 \times (0.22+1) \times U \cdot \Delta T$ and $82 \times \left(0.22 + 1 + \frac{5}{\Delta T}\right) \times U \cdot \Delta T$ before and after the 5 °C ambient temperature increase respectively. The inverse ratio of which reduces to $1 + \frac{4.09}{\Delta T}$ or a 20% change for an initial 20 °C temperature difference.

[1]Possibly on a window sill or on a table.

[2]The increased thermal mass would reduce compressor cycling and thus has a propensity to improve use–associated efficiency, see Guldbrandsen and Nørgård (1986), particularly in situations where a high number of interactions with the DRA are expected per unit time.

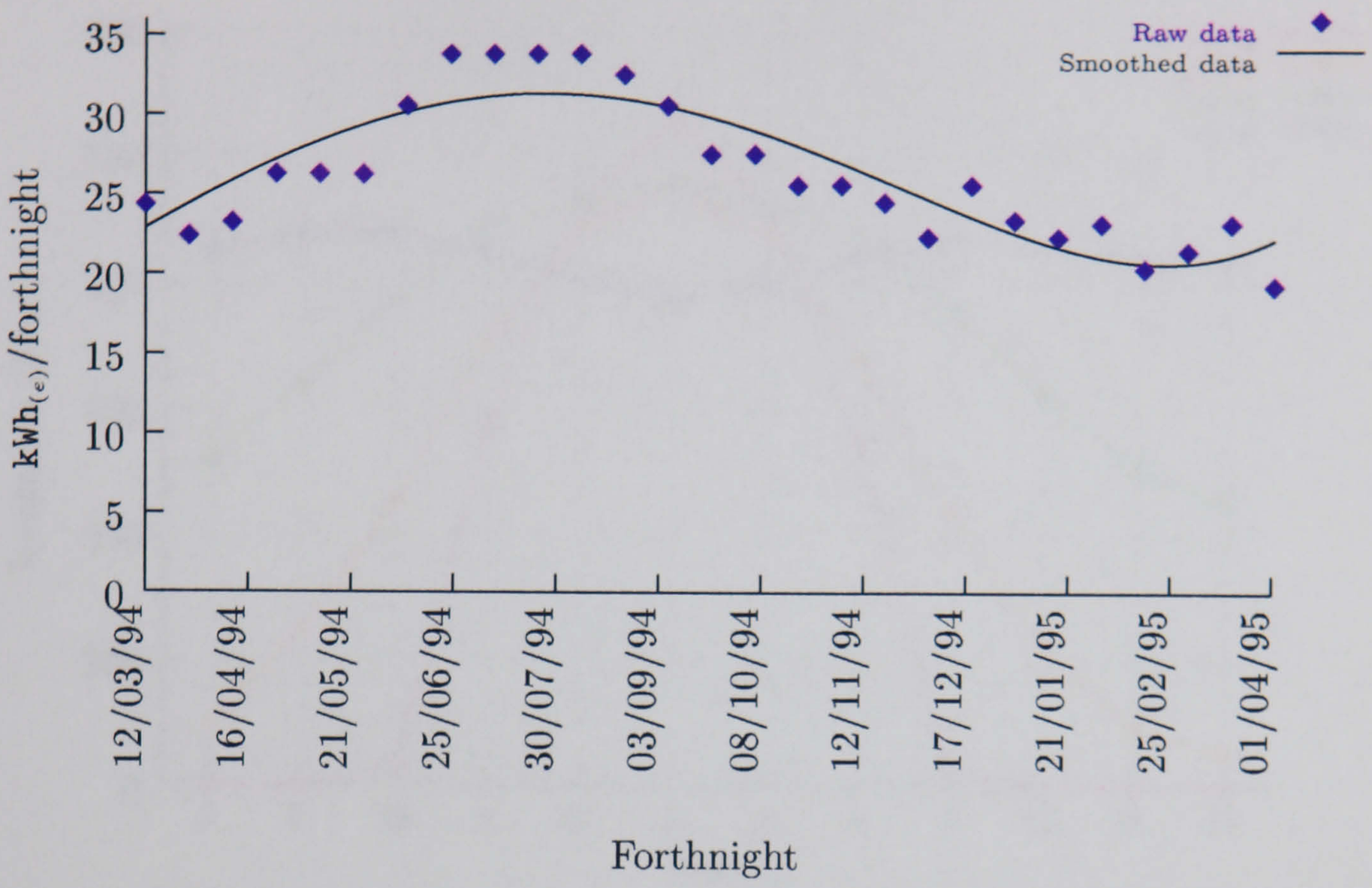


Figure 1.6: Seasonal variation (1994–1995) in fridge–freezer electricity consumption (measured on a fortnightly basis), in low–income households, source [Boardman et al., 1997]; originally Bill–Savers Project

latitudes. This increased solar insolation may have another less obvious implication on comparative energy consumption of DRA's within and without this sun–belt. Consider Figure 1.7 on the next page, which is an estimate of the mean global solar irradiation at different longitudes and Figure 1.8 on page 15, the yearly (24 hour) mean distribution of global insolation. These indicate (a) that the solar absorption, within and around the sun–belt, is fairly equitable over the year in stark contrast to regions outside the sun–belt and (b) the solar radiosity is comparatively greater over and around the sun–belt. While the relative ambient air temperature may give a comparative indication of the heat ingress into a DRA within and without the sun–belt; it fails to take cognisance of any direct solar irradiation such appliances may be subjected to as a result of user practices, and/or habitat design[1]. Thus it is possible to conceive a scenario where a DRA is (wholly or partly) exposed to direct solar irradiation during some period of the day, this will further increase the

[1]For example in Saharan and sub–Saharan Africa houses are built with large windows to facilitate cross–ventilation. This has the unfortunate effect of letting larger proportions of direct solar irradiation into the building were it built otherwise.

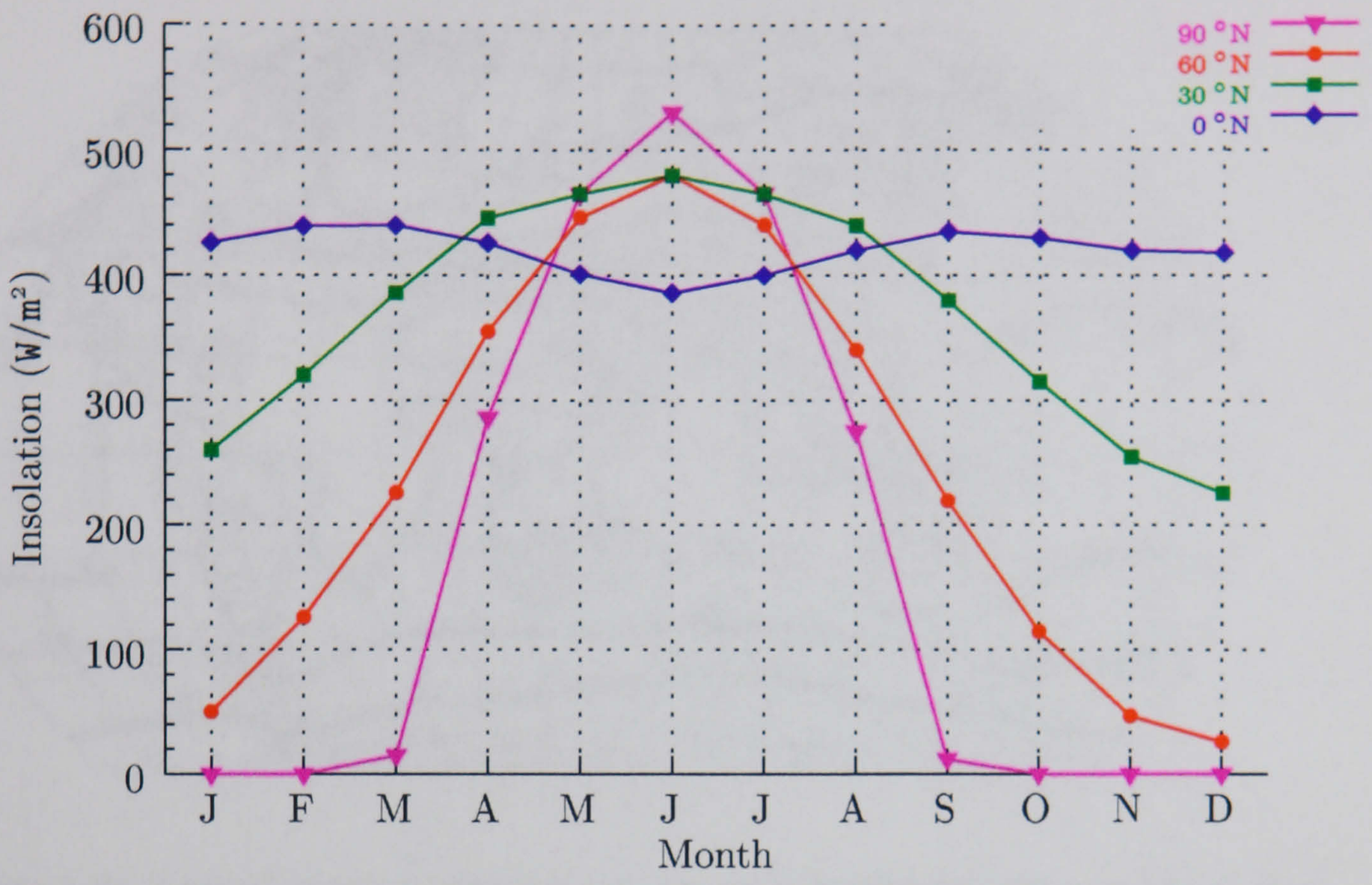


Figure 1.7: Mean monthly distribution of global irradiance on the earths surface averaged over the duration of the sunshine.

thermal–loading on the appliance and consequently its energy consumption[1].

When these greater energy requirements (estimated to be 30–60%, based on 30% per 5 °C air temperature increase[2] [Nørgård, 1989; Malin et al., 1993; Boardman et al., 1997]) for DRA operation in and around the tropics are combined with the number of inhabitants in the developing world aspiring to acquire such devices (estimated at *circa* four times the current number, see section 1.2.2 on page 8), the total annual energy utilised for operating these devices could potentially increase by an estimated (400–800)%[3].

[1]For example at a solar radiosity of 200 W/m² a 33 cm square portion of an appliance will be subjected to an additional 14–15W heat gains for the duration of the irradiation, assuming a surface absorptivity of, say, 0.7–0.8 (even for some white paints, see Incropera and DeWitt (1990), *pp.* 735).

[2]This estimate is conservative, as (a) the relationship between prime mover performance or compartment heat gain is not linear, (b) the defining tests do not attempt to simulate the utilisation (*food*) loading and (c) the estimate does not consider the possibility of the appliance being in receipt of direct solar irradiation

[3]This does not take into account air–conditioning requirements.

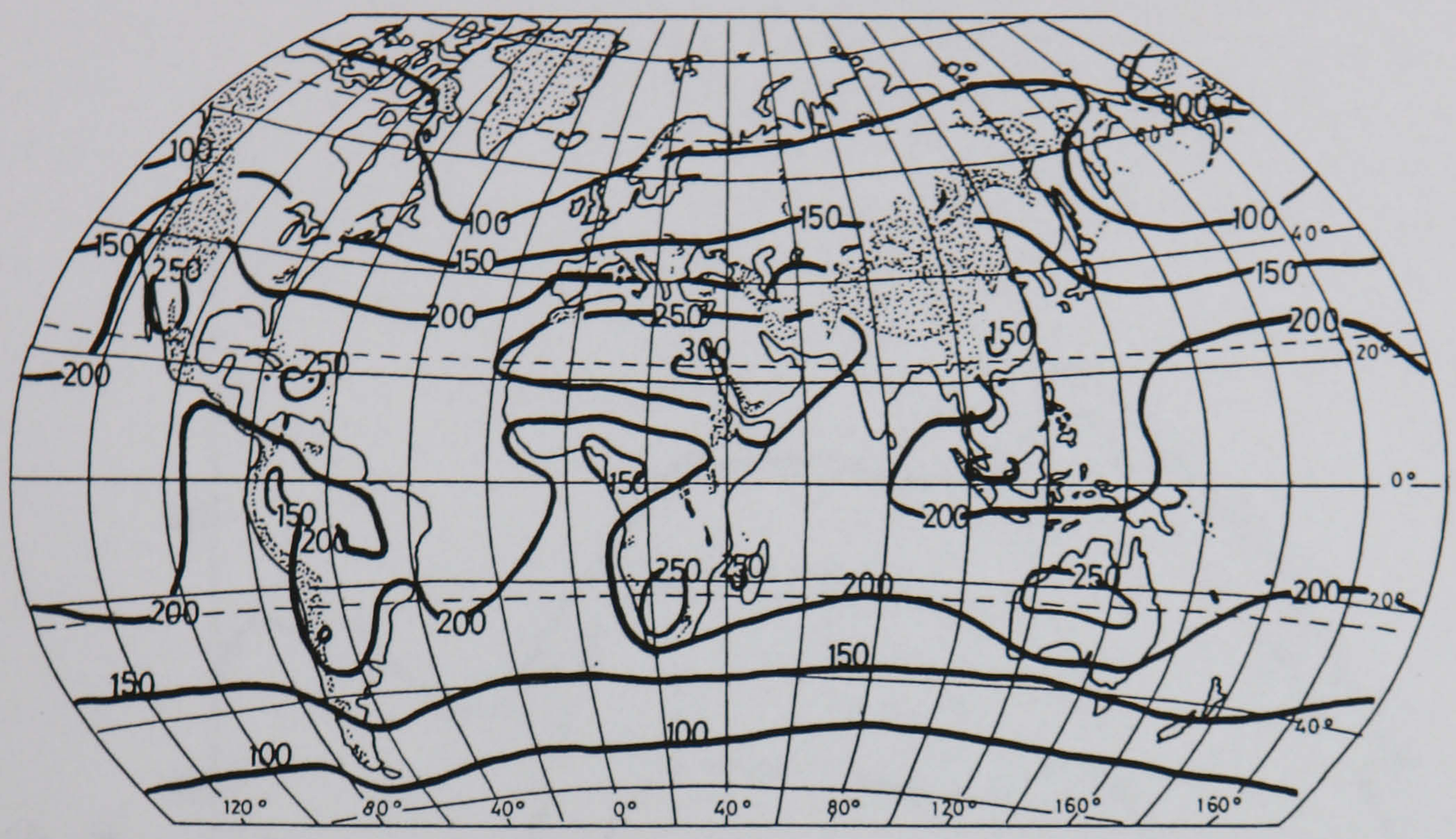


Figure 1.8: Annual mean Global irradiance on a horizontal place at the surface of the earth (W/m² averaged over 24 hours.) source UK-ISES (1976).

The OECD residential electricity consumption for 1994 was *circa* 2077 TWh, with an estimated 19% (*circa* 411 TWh) of this being used for DRA's. Not considering the effect of the disparity in population (which as noted earlier, will serve to increase the electricity consumption values even further), the estimates for the DRA energy consumption would scale to *circa* (1644–3288) TWh/p.a. in a similarly–sized developed region. If the current UK trend in distribution and transmission losses is deemed representative of expectable losses of similar type[1] in the distribution of electricity, this would add another 6% (see Figure 1.4 on page 7) to this value. Figure 1.9 on the next page indicates the effect the ambient temperature can have on daily electricity demand.

These projected increases in energy consumption have, *inter alia*, economic and environmental implications. In much of the developing/underdeveloped world, money is typically *very* scarce and financial economics dominates most other considerations[2]. Unduly large refrigerating bills would place an unwarranted burden on the individuals in those regions, with the knock–on effect of making refrigeration in

[1] Again another conservative estimate, as the transmission distances, ambient temperatures and the gradient of the load curve (which all bear upon these losses) are probably on average less than can be expected in the larger tropical region.

[2] Probably with the exception of religious and cultural taboo's.

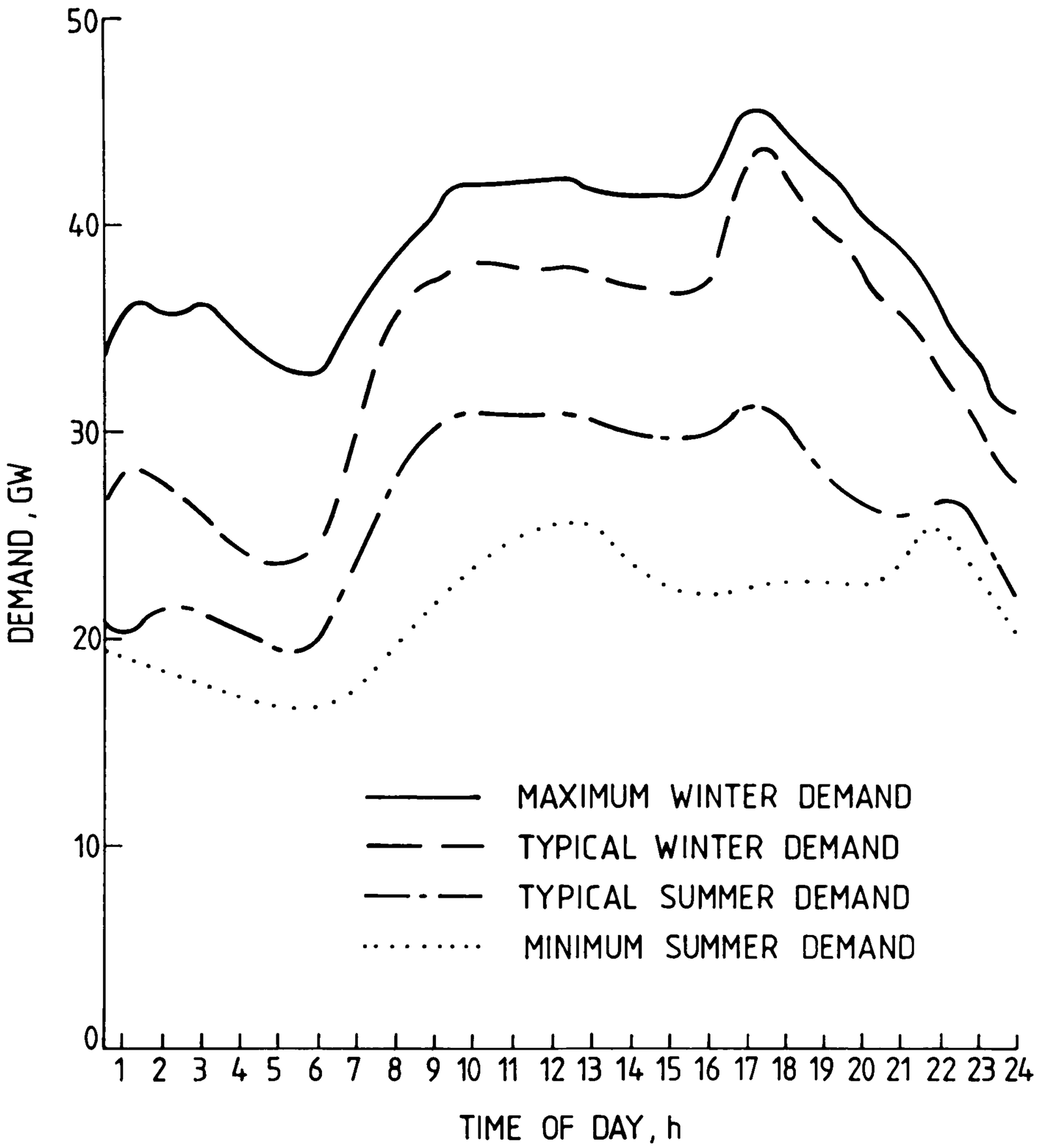


Figure 1.9: Seasonal dependence of electricity demand in England and Wales from [Lumb, 1996]

those areas prohibitively expensive to the greater proportion of the population.

In addition to the 'local' or domestic economics, national economic considerations also play a role in the acquisition and effectiveness of refrigeration in the developing world. At present, in many developing/developed countries, energy is heavily subsidised (either as fuel or as electricity). Many governments of such countries have huge financial debts and are under increasing pressure from their creditors and loan organisations to adopt 'Structural Adjustment Programmes' (SAP) before any further debt reschedulement can be effected or further loans procured. One criteria inherent in such SAP schemes is the requirement to reduce the amount of subsidy on energy (numbered amongst other non–essentials). This would further exacerbate the cost implications of appliance use.

Even if the costs could be met by the appliance user, the requirement remains for the governments (typically responsible for power generation) to supply sufficient electricity to run such appliances. As the demand for electricity increases, so does the cost of subsidy *and* the need for capital expenditure on generating plants, thus tending to worsen the government's already weak financial position. It is not untypical for electricity to be rationed (on whatever basis) when such situations arise (for whatever reason *i.e.* lack of funds and/or components to effect immediate repairs to broken–down generating sets, excessive demand *etc.*). In some instances, several days may go by with some regions cut off from an electricity supply. Whilst this may, at worst, be a nuisance when one wants to watch television or to read, this is mild by comparison when the implications for food preservation are considered.

- From the perspective of the developing world, there is economic expediency in manufacturers ensuring from the outset, that DRA's are as efficient as possible to curtail energy consumption and thus running costs.

- Sillanpää et al. (1996) note that the DRA's which are being pressed into service under a diversity of social and climatic conditions are increasingly similar. DRA's manufactured for temperate environments are currently routinely being exported to tropical (usually developing) countries for use. As such it is potentially of considerable benefit, to both manufacturer and consumer alike, to manufacture DRA's which are robust and relatively unaffected by lapses in energy input (or energetic penury).

The benefits to the appliance user and governments are obvious; somewhat less obvious is the benefit to the manufacturer. However, the economic implications of these two criteria to manufacturers cannot be over–emphasised. Whereas DRA's have a life span of between 14 and 20 years [Burke, 1990; Boardman et al., 1997] in the developed world, similar appliances in the developing world would be kept in service for periods approaching twice as long. As such the tendency is to purchase, from

the outset, a reliable appliance. Typically, most individuals would ask around for what is considered to be the 'best buy' in the market. Considering the potential number of appliances that are to be sold, manufacturers cannot afford to have their brand names associated with high running costs and/or unreliability.

1.3 The Environmental Consequences

During the early 1950's, in the UK[1], for several winters, cities were continually en–shrouded in thick smog[2] resulting in *inter alia*, the loss of life as a direct consequence of environmental pollution. Environmental concern has, to varying extents, been close to the fore of government and individual agenda alike. In the US, since the late 1960's[3] [De Nevers, N., 1994] there has also been increasing concern about the detrimental effect of man's impact on the environment. However, prior to the 1980's the problem was conceived largely as local and efforts were concentrated on pollutants that were seen to have a direct bearing on the local environment. In the 1980's three phenomena relating to the remote effects of longer–lived pollutants came into prominence. Their perceived consequences were sufficiently serious as to alter the general perception of pollution and the manner in which it is dealt with.

Ozone Layer Depletion In the late 1980's scientists discovered sharp discrepancies from the expected levels of ozone in the Ozonosphere[4] at various locations of the earth (notably, Antarctica). The evidence tended to suggest that in some areas there was a continuing cyclic depletion of the 'ozone layer', a phenomenon which has since come to be known as 'ozone layer depletion' and manifests as an increase in the intensity of (solar originating) electro–magnetic radiation reaching the earth's surface. The increasing levels of certain frequencies of this radiation, UV–A in particular [O'Neil, 1993], have been indicated in the increased incidence of malignant melanoma and ocular cataracts in regions of the world with marked ozone layer depletion [Thompson, 1984]. Another consequence of these increased levels of short–wave electromagnetic radiation is the formation of low–level ozone (*i.e.* within *circa* 8 km of the atmosphere, technically known as the troposphere). This low–level ozone is toxic in volume

[1]The period from the late 1940's to the early 1950's was about the worst. Regulatory action by the UK government brought the era to an end.

[2]The cumulative effect of naturally occurring fog and a high density of particulates, typically soot, in the air.

[3]Prior to 1945, the major concern was in the control of industrial air pollution which was in response to nuisance damage suits (or threats of such). Between the mid 1940's and the late 1960's awareness of air pollution problems gradually increased.

[4]An expanse 15 to 30 kilometres in altitude, within the region known as the stratosphere.

quantities as small a 1 part per million (1 ppm–V)[1] [O'Neil, 1993, *pp.* 34]. Currently, two main causative agents associated with this phenomenon have been identified as: Halocarbons, a principal raw material used in the manufacture of, *inter alia*, DRA's, and Nitrous Oxide, a byproduct from the combustion of fossil fuels for the production of electricity.

Acid Rain First noticed in the 1950's, acid rain occurs when high levels of Oxides of Sulphur and Nitrogen are present in the atmosphere and are subsequently precipitated (as an aqueous solution) during rainfall [Harvey, 1980]. Acid rain has the propensity to devastate entire ecosystems, characteristically stripping vegetation[2], leading subsequently to acute soil erosion and making it impossible for areas so affected to support animal life. Aquatic organisms are unlikely to survive for long in strongly acidic environments resulting from sustained acid rainfall. Indicated as perpetrating this phenomenon are oxides of Nitrogen and Sulphur *inter alia*. These are byproducts of the combustion of fossilised fuels for the production of electricity.

The Green–House Effect The third phenomenon, which came to prominence in the 1980's, was the greenhouse effect[3]. This relates to the increasing temperature of the atmosphere, due to the alteration of the thermal energy balance between the earth and the solar system. The phenomenon is so–named as its workings are very much the same as that of a green–house, whereby short–wave radiation (from the far infra–red through the visible and beyond) is admitted through a 'window' and the subsequent re–radiation of longer infrared radiation in inhibited by the same 'window'. Water vapour, carbon–dioxide, nitrous oxide and methane are listed amongst the principal green house gases (characterised by an index known as the Global Warming Potential GWP). Of the proportion of these gases that are released into the atmosphere daily, a significant amount can be associated with either the collection or combustion of fossil fuels.

From the foregoing, it is clear that the increasing production of electricity from the combustion of fossil fuels plays a major role in exacerbating the aforementioned conditions. In addition to this is the problem of 'localised thermal pollution', caused by the dumping of waste heat from power stations into surrounding lakes, streams *etc.* and from exhaust gases expelled into the atmosphere. Thermal pollution may have the effect of: increasing local summer–time temperatures (with local thermal

---

[1]Human beings experience breathing difficulties at concentrations as low as 120 ppb–V.

[2]More commonly referred to as "deforestation"; however the effects are not strictly confined to forests.

[3]More commonly known as "global warming".

effects exacerbating things further), producing shorter winters and giving rise to the increased incidence of floods.

If one primary function of DRA's is to improve the quality of life, then any perceived improvement (in the quality of life) in consequence of the use of these appliances should be placed in context within its overall impact. This must entail the environmental (and economic) impacts associated with the manufacture and use of such equipment[1]. From an environmental standpoint, it is clearly expedient to reduce (if not totally eliminate) the efflux of agents causal to these phenomena. One manner in which this may be done is to alter or constrain processes which engender these agents. The reduction in electrical energy consumption could be beneficial, as would any reduction in the use of halocarbons.

Research tends to indicate that the DRA sector provides one of the greatest avenues for energy conservation when compared with other appliances in the domestic category [Boardman, 1995b; Geller, 1988; March Consulting Group, 1990]. This may be as much in consequence of the control regime under which these appliances typically operate (frequent on–off cycling) as the design and construction of the appliance and its constituent parts.

1.4 Economic Considerations

There is much to be said for the argument that an environmental impetus as a basis for curtailing energy consumption is the prerogative of the affluent [De Nevers, N., 1994], and that folk living on the poverty line, or thereabouts, are less likely to have environmental issues (or even the efficient operation of owned appliances [Boardman et al., 1997][2]) in the fore of their minds. Indeed, research done by Boardman (1995a) indicates that there are several other reasons which might influence attitudes towards environmental issues, where the authors claim ... "Recent anthropological research comparing cultural groups (in the West) which have strikingly different environmental relationships, suggests that it is possible to pinpoint some of the most influential factors in the formation of differing levels of environmental concern. In very general terms, these include factors such as:

- Process socialisation (sources of environmental knowledge and values).
- Type/stability of tenure and continuity of residence.
- Level of commitment to the local environment.

[1]This is the essence of the so–called Taguchi definition of quality *viz* the 'cradle–to–grave' losses a product causes society [Sudhakar, 1995].

[2]The mentality being, *so long as it 'works'* ...

- Local community involvement.
- Religious or moral beliefs, concepts of environmental responsibility.
- World views and concepts of nature.
- Personal values and aspirations.
- General knowledge and perception of environmental issues.
- Understanding of technical and cost–related aspects of energy use.
- Household decision–making and social dynamics.

... There is no saying which would prove to be the most influential". They further go on to stress that the list is "not in any particular order". However there are also salient economic/fiscal reasons for doing so (*i.e.* curtailing appliance energy consumption), which may be broadly categorised into the following perspectives:

Consumer This refers to the additional cost to the consumer for the use of inefficient DRA's. It may be argued that to the consumer the saved cost represents too small a saving. That, however, has to be placed in the context of the particular circumstances of the consumer[1] and to real estate managers/owners the difference might be considerable taken over blocks of apartments, or on housing estates.

Utilities Supplier This is the cost to the utilities supplier, in transmission losses, fuel costs, early project commission, logistics *etc.* for the consumers' use of inefficient equipment. Analysis has shown that, as a result of the framework of the current legislation in the US, the most profitable (techno–economic) approach to supply may not necessarily be increased sales. In the light of that analysis, a certain method was developed by the utilities, known as 'Demand Side Management' (DSM), purposely for the examination of the logistics of differing energy distribution scenario's and to provide the capacity to inform profitably as to the 'Least Cost Option' (LCO) on decision–making in energy supply management. Some precepts of which are brought to bear in the present work, see Chapter 2 on page 39.

National This cost is associated with either the purchase of fuel or the loss of potential revenue by the consumption of otherwise salable fuel. In some instances as much as 6% (section 1.2.1 on page 3) of the total energy consumption is

[1] To one for whom every penny counts, no saving is insignificant.

expended on domestic refrigeration appliances. If this proportion is reduced by 1%, irrespective of increasing appliance purchase, the monetary, amongst other, savings would be considerable. In fact it is, economically, most expedient on a national level to cut back on energy consumption for reasons of energy security/stability. This need for energy resource conservation is as true for energy–export dependent countries (generating revenue from energy/fuel sales), as it is for energy–import dependent nations, particularly in the light of the energy crises of the 1970's.

1.5 Socio–Political Considerations

There is increasing pressure on governments (from within and without) to effect regulatory instruments to 'manage the environmental impacts' of *inter alia* energy consumption within their jurisdictions. In recent years, induced by the possible imminence of a global ecological crisis, countries the world over have reached a common consent regarding the need to control the processes which directly, or indirectly, negatively impact on the environment. As a result of this, there has been much governmental activity in several countries in a bid to concur with standards set internationally (and in some cases internally *e.g.* California, Florida, Massachusetts *etc.* in the US [Mansouri-Azar, 1996; Geller, 1995] and more recently within the EU, the 'Dutch Notification' [Waide, 1993]) for the control of processes and the efflux of substances which 'adversely affect the environment'.

It is difficult to reach and regularly revise such inter–community agreements and very often impasses are reached. In order for potential signatories to reach a common consent there is a need to fulfil the following requirements:

1. Agree on the imminence, existence or persistence of a problem.

2. Be informed of the *facts* about the causative factors (primary and secondary) of the problem, in this case pollution.

3. Determine the level of each activity which engenders or constitutes pollution to the environment and their interrelation to each other.

4. Determine how best to curtail the agents of the pollutant in the light of:

   - The economic impact of the aforesaid changes.
   - The social impact of same changes.

5. Determine the best instruments by which to institute regulatory mechanisms; this typically comes under two categories:

- Economic/fiscal instruments:
  The relevant governing/legislative body attaches some punitive economic cost to the efflux of pollutants *e.g.* carbon taxes or pollution licenses. Another variation on this theme is the so–called LCO, where initial licenses are issued (possibly *gratis*) on the understanding that prior to any increase in quota there is a requirement to demonstrate that all other economic avenues have been exhausted.
- Regulatory instruments:
  The relevant governing/legislative body stipulates maximum levels of pollutant discharge. This is subject to the feasibility of the current scientific/technical know–how to satisfy said constraints. In situations where the technology is mutative, it may be expedient to motivate the industry to set standards.

6. Determine a manner by which to enforce whatever regulations are passed into law in effecting the change.

7. Determine a manner in which to address breaches.

8. Determine a review protocol by which to revise the standards.

The nett effect of this is that the legislation, where reached, may be late and/or considered inadequate (compromised so as to foster group consensus) by participating parties or obsolescent in view of advances in the various technologies [Waide, 1993]. In spite of this, progress was made as far back as 1968–1970 in America, when the National Environmental Policy and the Clean air Acts were respectively passed into law. Since *circa* 1973, the European Council (the then EC, currently the European Union EU) has pursued an energy efficiency programme. It currently categorises its activities into [Mansouri-Azar, 1996]: (i) support for basic Research and Development (R & D) in energy efficiency through the JOULE programme, (ii) support for demonstration of energy efficient technologies through the THERMIE programme, (iii) improving the efficiency of electricity use through the PACE programme (1989) and (iv) an energy efficiency policy programme, SAVE which espouses legislative, pilot project and disseminative instruments. Other national laws and inter–national/continental acts and treaties have also been ratified, for instance the 1987 Montreal Protocol, which committed signatories to a 50% reduction of the 1986 production of CFC's by the year 1998 [Pickering and Owen, 1994; Her Majesty's Government, 1990] and *Agenda 21* of the Rio conference on sustainable development [Anon, 1992; UN, 1993; Grubb, 1993]. More recently, there has been the Tokyo and Kyoto conferences which further pressed for targets on carbon dioxide emissions and vegetation conservation amongst others.

Enforcement is typically by the imposition of punitive fines and/or taxes and, there are constant efforts to continually revise the standards with stringency[1]. Many of these standards stipulate minimum emissions levels for perceived pollutants such as Carbon–dioxide, and also to maximise energy use (particularly electricity generation), much of which are relevant (directly or indirectly) to DRA's.

1.6 Regulatory Activities

Prior to 1975 there was very little by way of R&D or 'policy initiatives' to promote energy efficiency improvements for domestic appliances, particularly in the UK. This is evident when comparing the energy consumption per unit volume of models available in the UK with that of models available elsewhere in Europe [March Consulting Group, 1990]. As part of an energy review series, the UK Department of Energy (UK–DoE) commissioned work (*op. cit.*) into the energy efficiency of appliances. The results suggest that the energy utilisation efficiency of the average appliance has improved since 1975. One major UK manufacturer interviewed for the purpose of that review claimed it had achieved a 15% and 30% improvement in the energy efficiencies of its refrigerators and freezers respectively. The UK Association of Manufacturers of Domestic Electric Appliances, AMEDEA, catalogue a table of improvements for freezing/refrigerating appliances *ibid.* However, these modest improvements pale in the face of those claimed elsewhere. The UK–DoE (*op. cit.*), by way of comparison, stated that the specific energy consumption of larder refrigerators has improved by 57% in Denmark and by 70% in Germany, respective to the 14 and 13 years leading up to 1989. Geller (1995) reports a 62% decrease in appliance energy consumption in the 12 years running up to 1994 in US appliances (about 1725 kWh per year in 1972 to about 635 kWh in 1994)[2]. Between 1975 and 1982 the yearly improvement in the US was between 4 and 5% but, between 1982 and 1986 the improvement fell to 2% [Geller, 1988]. While these represent the measured consumption figures based on test standards, due to the diversity in cultures, use practices, climates *etc.*, care must be taken in equating these figures to *in situ* utilisation/consumption figures and using that as a basis for energy consumption comparison between countries [Mansouri-Azar, 1996; Sillanpää et al., 1996]

[1] As the last two conferences have highlighted, it is becoming increasingly difficult to reach agreements.

[2] It is of particular note that the comparative figures given in the study do not appear have a similar basis to facilitate comparison. No indication is given as to whether the figures represent average values, typical values or illustrative ones. Moreover, there is no indication as whether the appliances tested are those tested on–site or if they were stock appliances.

DRA's were developed as technologies became available and, as such, improvements/ upgrades have typically been made as changes to existing models with the basic design remaining largely unaltered[1]. The current DRA technology is relatively mature [March Consulting Group, 1990]. At first glance, one could be excused for assuming that they are all made by the same manufacturer, possessing very similar geometries, colour, with fairly standard shapes and parts located at similar locations within the appliance. The compressors are almost invariably of the hermetic type, there are small variations in the condensing and evaporating heat exchangers across manufacturers, but these are relatively minor. In fact, the similarities are such that the UK Consumers' Association (1982), claimed that greater variations are likely to occur between products of the same manufacturer than between similar products across manufacturers, one consequence of this being that the industry, characteristically oligopolic [Bianchi and Forlai, 1988], is fairly resilient to change.

1.6.1 Legislation

Legislation with respect to energy performance began in California in 1974, with the adoption of the Warren–Alquist Act. Between 1977 and 1979, the state of California imposed initial standards on 15 different domestic appliances. The standards were revised consistently throughout the early 1980's. Other states, Florida, New York, Connecticut and Massachusetts, adopted similar legislation in the same periods. Initial attempts at establishing a national US standard began in the early 1970's and the Energy Policy and Conservation Act of 1975 called for the setting of appliance efficiency targets. The National Energy Policy Act NEPCA of 1978 directed the US–DoE to develop mandatory efficiency standards for 13 classes of DRA's. However, the US–DoE never completed the standards proposition it began in 1980. Finally, standards were adopted by the US federal government in 1987, under the National Appliance Energy Conservation Act (NACECA) establishing minimum efficiency standards for home appliances. The adoption of the standards was consequent to the Montreal Protocol and the move was driven principally by impetus from appliance manufacturers (due to differing legislation across different states), environmental and conservation groups and the electric utilities [Turiel and Levine, 1989; Geller, 1995]. The standards for DRA's came into force on the 1st of January 1990[2]. Typically these standards required a 10–30% reduction in the energy consumption of new appliances over the 1987 average equivalent–capacity appliance. Inherent in these standards are legal requirements and deadlines for updating the initial standards by the US–DoE [Geller, 1995].

[1] See Atwood (1991) and Nagengast (1996, 1997, 1998) for interesting accounts on the history and evolution of the refrigeration systems.

[2] While those for air conditioning equipment took effect from 1st January 1992.

In 1989, the EU adopted the PACE programme, an action plan for the efficient use of energy, which included initiatives such as energy labelling and the introduction of energy efficiency standards for household appliances [Mansouri-Azar, 1996][1]. In 1991, the French Agency for the Environment and Energy Management (ADEME, formerly AFME) performed an analysis for the Directorate General for Energy (DGXVII) of the commission of the European Community. The study estimated the electricity savings that would result from the energy efficiency standard for five residential appliances and concluded that the greatest savings would result from implementing the standards for cold appliances. Consequently, ADEME and the EU focused on developing standards for these equipments [Lebot and Szabo, 1992].

The initial draft standards for cold appliances were published in 1993 and they came into force in 1997. The proposed standards were intended to reduce the electricity consumed by the stock of new models by 10% from the average consumption of all models sold in 1992. The standard further stipulated a figure of 15% within three years of adoption. In the light of severe criticism of the standards and the need to have them tightened [Waide, 1993; Mansouri-Azar, 1996], the European parliament voted in a plenary session of the 26th of October 1995 to tighten the energy standards for DRA's to 20% within the two years immediately subsequent to the adoption of the standard. Pursuant to that, the Parliament voted that 'phase II' should be *within the current directive*, stipulating a 40% target within 5 years. The final position, adopted on March the 11th 1996 [EU, 1996], stipulates that the energy consumption of DRA's should be expressed in kWh/24hrs. It recognises some factors upon which this consumption would depend and, as such, categorises DRA's into 10 different types[2]. Based on a series of appliance criteria (geographic location, volume, evaporator operation, design temperature) it also explicitly defines equations to compute the maximum permissible energy consumption over 24 hour periods [Waide, 1993]. Other forms of legislation also exist which have an indirect bearing on DRA production such as those to do with CFC emissions *etc.*

Mandatory standards have faced opposition from, in Europe, the European Committee of Manufacturers of Electrical Equipment (CECED) [Service, 1996] and in America, initially by the Reagan administration and then by appliance manufacturers [Mansouri-Azar, 1996; Geller, 1995]. More recently however, the utilities have increasingly begun to embrace the idea, notably in Germany [Herring, 1994] and largely due to these standards, there have been major improvements in the energy efficiency of DRA's in the USA and in the EC over the past twenty years. In addition to these standards, there have been policy initiatives to induce appliance

[1] Awareness of the need for an effective energy labelling goes as far back as (1979) there were calls within the EC for a voluntary appliance labelling scheme which went as far as indicating what appliances to label see EC (1979).

[2] 9 actually, the 10th refers to appliances that do not fall into any of the other 9 categories.

manufacturers to increase their R&D activities. Typically, these have included, the keeping of databases of appliance data (including energy consumptions), and making the information public via advertisements, competitions [Mansouri-Azar, 1996] and government research contracts *etc.*

1.6.2 Programmes

In 1986 the Directorate–General Science, Research and Development (DGXII) of the Commission of European Communities (EC) issued a contract into the research and development of Energy Efficient Electrical Household Appliances[1]. The first stage of the contract was to build a prototype of a 200 litre, low–energy refrigerator utilising 20% of the electricity of a similar 1975 model [Guldbrandsen et al., 1986]. The result was, the so called LER, a 200 litre 102 kWh p.a. (279.5 Wh per day) refrigerator;[2] even now a decade later, fridge–freezer (adjusted) standards do not require that level of performance.

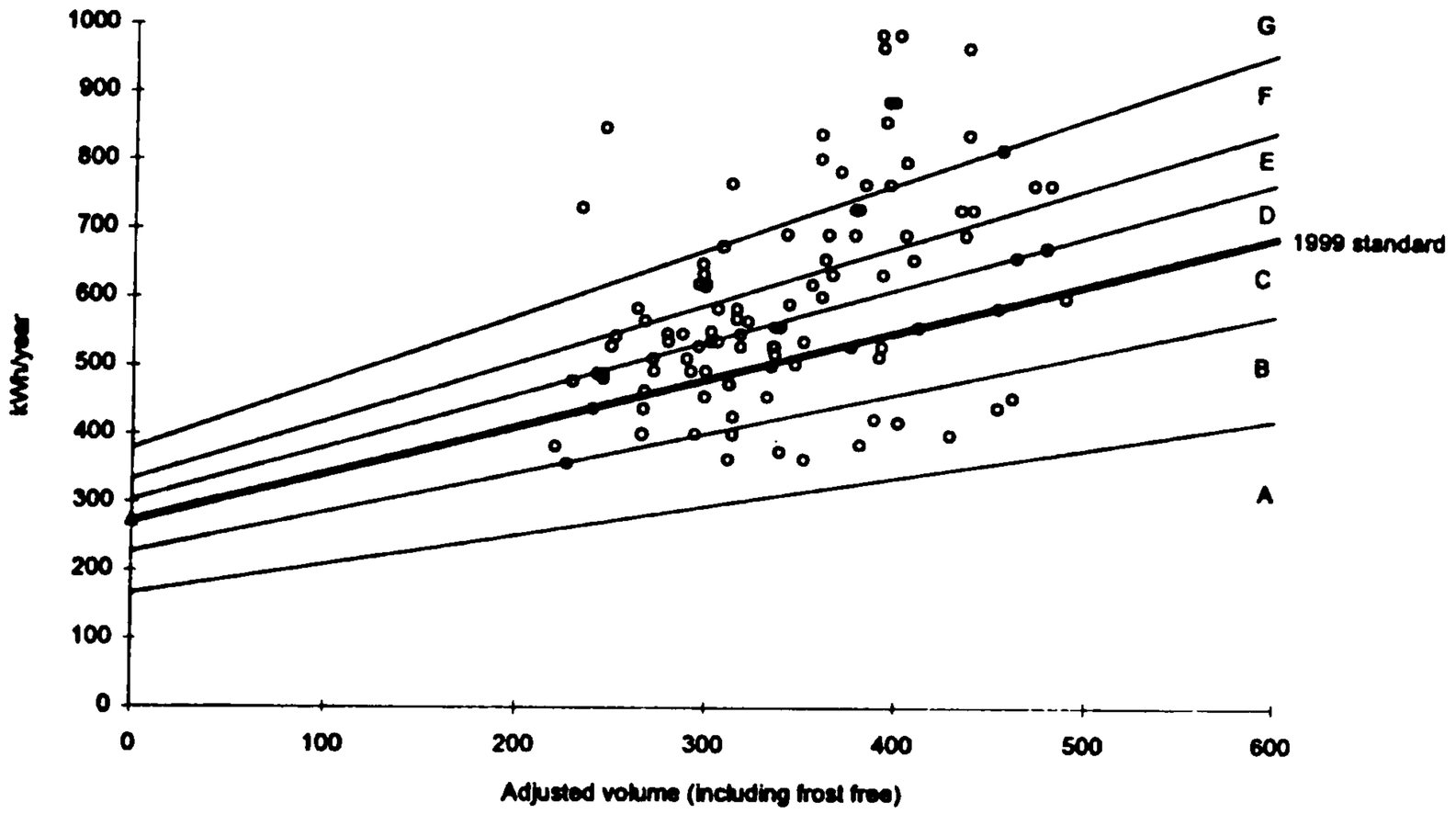


Figure 1.10: Changes in 'modal' DRA requirements in the UK taken from [Boardman et al., 1997]

[1]The contract, in three stages, was issued to the Technical University of Denmark.

[2]This can be adjusted to 137.7 kWh and 377 Wh to conform to the US (AHAM–HRF–1), Canadian (CAN/CSA–C300–M89) and the Australian/New Zealand (AS 2575.2–1989) standards, as the tests were performed in Europe in a 25 °C environment (internal temperature 5 °C) according to the ISO/R 824 (19), DIN 8950 (8) standards, as opposed to the 32 °C environment (internal temperature 3.3 °C) stipulated by those standards; see [Buhl-Pedersen et al., 1993, *pp.* 20–22] for a synopsis and critique of the current (EN–153) EU–recommended standard procedure.

In the USA, some programmes targeted incentives to spur the development and market acceptance of equipment substantially more efficient than the best units presently on the market. One such programme, the Super Efficient Refrigeration Program, SERP, was jointly developed by a group of electric utilities, public interest organisations and government agencies [Nadel, 1994]. Based on the research completed by the United States Department of Energy US–DoE, in 1989 and the United States Environmental Protection Agency, US–EPA, in 1992, the consortium was of the belief that refrigerators/freezers could be developed that used at least 25% less energy than the 1993 Federal Government minimum efficiency standards. In July 1992, manufacturers were invited to compete in a US$30 million prize[1] (raised from 24 participating utilities), to develop such a unit. Limitations were placed on the CFC use. According to the submitted bids, in October 1992, these savings were to be achieved through use of high–efficiency compressors, better insulation, an improved condenser fan motor and adaptive defrost control [Waide, 1993; Nadel, 1994][2].

Particularly in the US, several utility–initiated schemes have arisen to stimulate energy efficiency on the part of their customers, the so–called "Utilities Incentive Programmes". These have included rebates and low–interest loans for the purchase or implementation of more energy–efficient appliances or measures. While these programs inadvertently complement the minimum efficiency standards, their *rasion d'être* has little environmental basis: they were initiated to reduce peak demand (and transmission) losses and consequently the need for new generating capacity, curtailing or delaying new capital project expenditure [Geller, 1988]. Currently in the UK the "price setting formula" for the supply of electricity permits only the *cost* of electricity supplied to be passed on to the customer. This does not provide any real incentives to the utilities to effect such 'Utilities Incentive Schemes'. One 1986 survey indicates more than 50% of US households were served by utilities offering such schemes. While the extent to which these utility programmes affect appliance manufacturers is uncertain, there is evidence to suggest that in regions where such programs are in effect, higher efficiency appliances tend to dominate the markets *ibid.* The basic idea of utilities being responsible for inducing energy–efficiency improvements has further been extended to what is now known as Least Cost Utility Planning (LCUP). This integrates demand side and supply side planning into a framework seeking to provide resources at the lowest possible price, consistent with lower consumption. Other such utility schemes which place the onus on their customers to limit their energy consumption exist in Europe. Such schemes include, imposing punitive peak–time tariffs on consumption and/or limiting consumption

[1] Also known as the golden carrot scheme.

[2] The competition was won by Electrolux and payment continent upon a (market) delivery milestone basis. Since then not much has taken place in the same manner or scale.

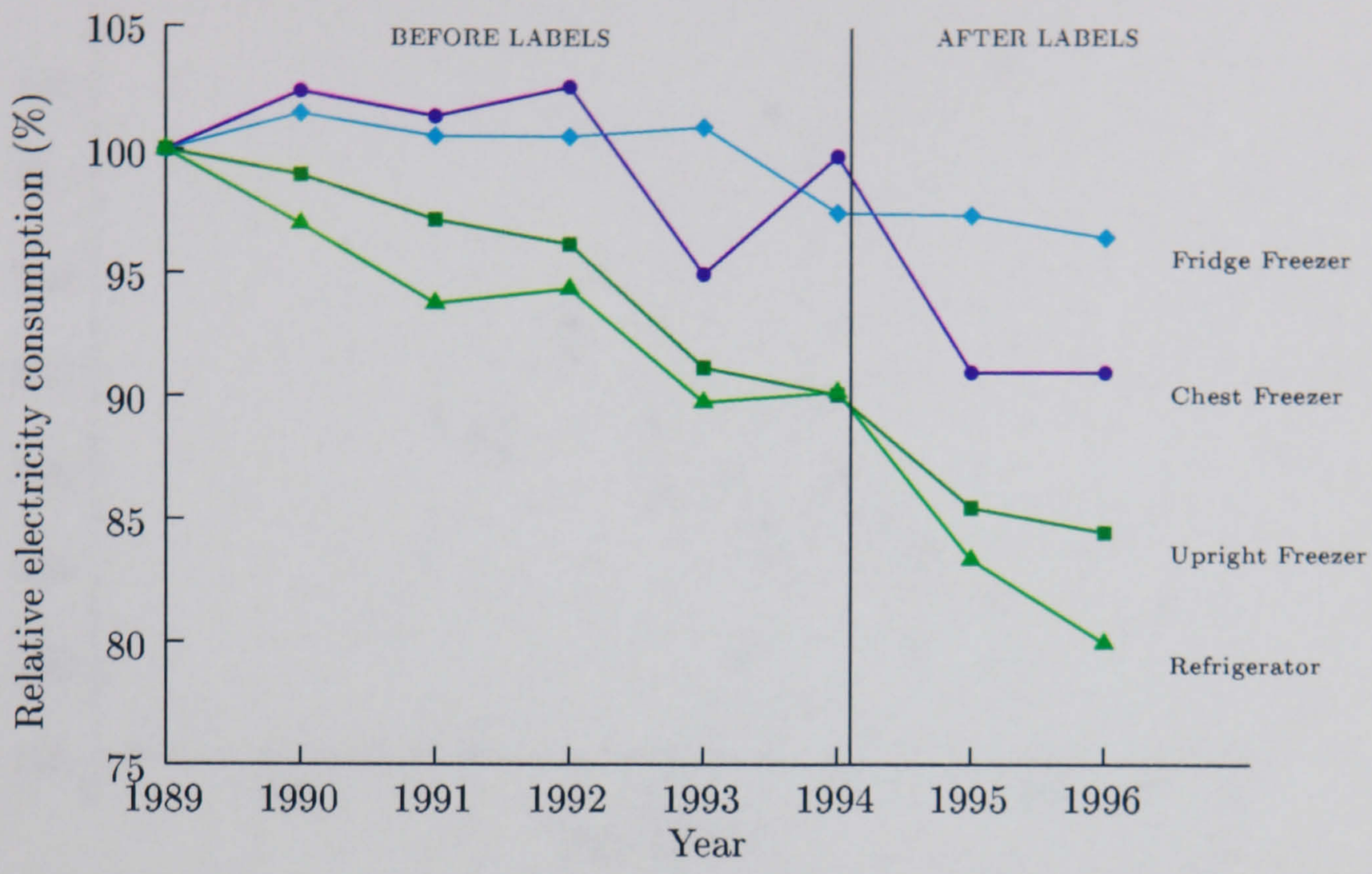


Figure 1.11: Effect of energy labelling on DRA's source [Boardman et al., 1997]

to a fixed prearranged quota.

1.6.3 Information Dissemination

Another strategy, arguably the most efficient, for effecting a conscientious energy conservation policy is to educate and inform the general public as to the economic and environmental implications of their decisions. It is with this in mind that the EU energy labelling scheme for DRA's has been implemented.

This has met with varying degrees of success [Mansouri-Azar, 1996; Boardman et al., 1997] depending on the energy/ environmental/ economic consciousness of the country in question. In some countries, for instance Germany, there is the additional industrial impetus, apart from legislature and policies, of market share economics to improve standards so as to woo buyers. The situation is not quite so everywhere. Herring (1994) claimed " ... *that the lack of an effective labelling scheme in the* UK *leads to the 'dumping' of overseas inefficient models.* ... " and that there was no consistent correlation between cost and efficiency (see Figure 1.12 on the following page), a point made elsewhere in the literature [Mansouri-Azar, 1996; Boardman et al., 1997].

Usually, more efficient models do not cost more than their inefficient counterparts but, in instances where they do, the pay–back period is in the region of (2–4) years

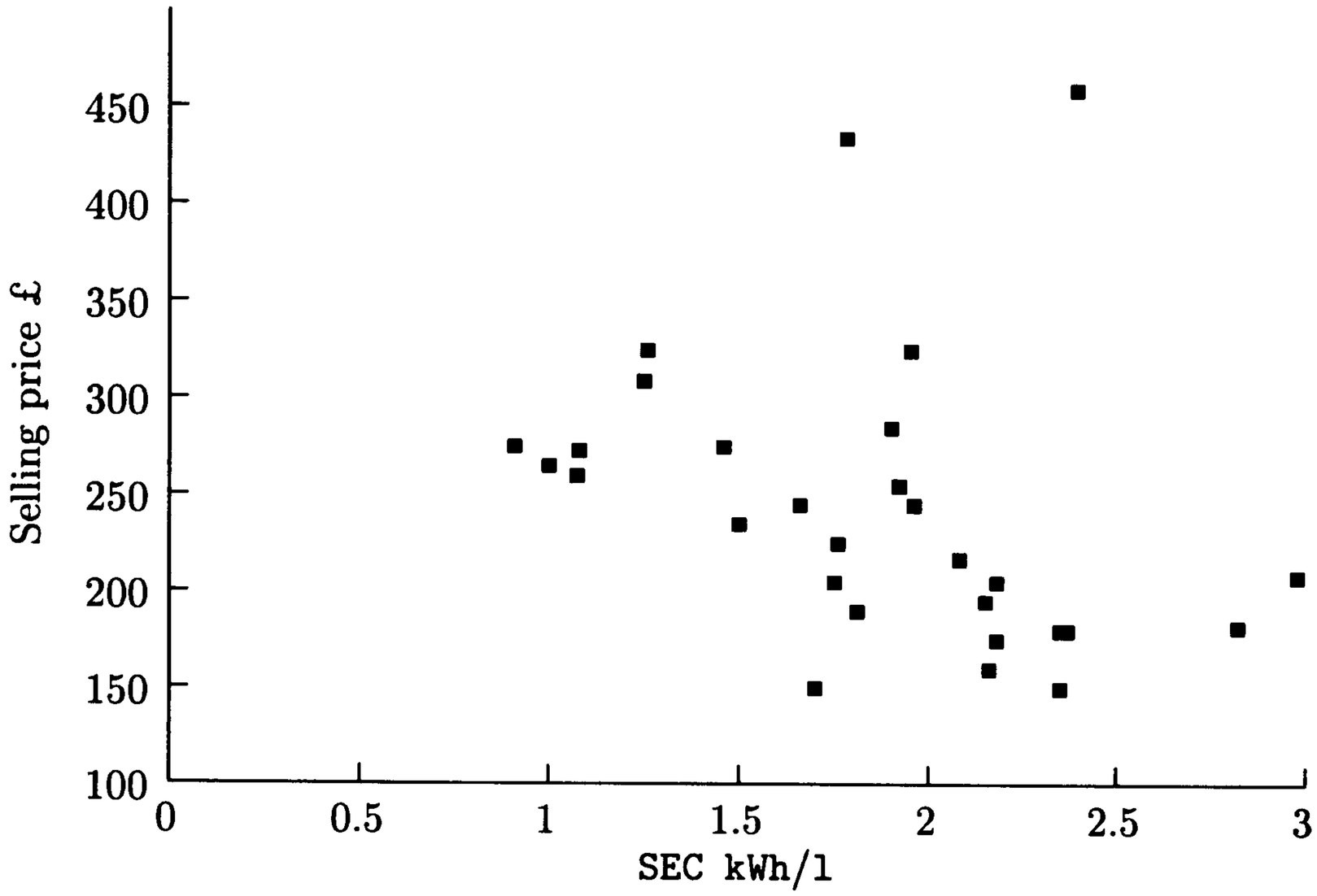


Figure 1.12: The relation between price and performance in Larder Refrigerators [Herring, 1994]

[Burke, 1990; Mansouri-Azar, 1996]. This is as a consequence of the least efficient models consuming about twice as much energy as the most efficient models, in all categories. In most cases the consumer need not pay more (and if not so, then only marginally[1] more) to reap substantial savings[2]. Thus, consumers can obtain the cost benefits of the lower energy consumption, 'for free', through the judicious use of energy labels. The role of retail staff is important as many cold appliances are 'distress' purchases, bought when the old machine has broken down [Boardman et al. *op. cit.*].

In a paper published by the ACEEE [Burke, 1990], the authors highlight the false economy of purchasing energy–inefficient devices, contrasting the overall cost of ownership of energy–efficient devices with that of the less energy conscious ones. They hold that the cost of running a DRA for the 15–20 years it is typically owned, is in the region of three times the capital outlay.

Herring (1994), tabulates and compares a list of refrigerators on sale in Germany and in the UK. In all cases, the Specific Energy Consumptions, SEC, for the German fridges were lower than those of their UK counterparts (even in cases where the UK

[1] Less than 10%.

[2] Sufficient to recover any expense over the cost of less efficient machines (if any) and a percentage saving on the 'normal' bill depending on the model.

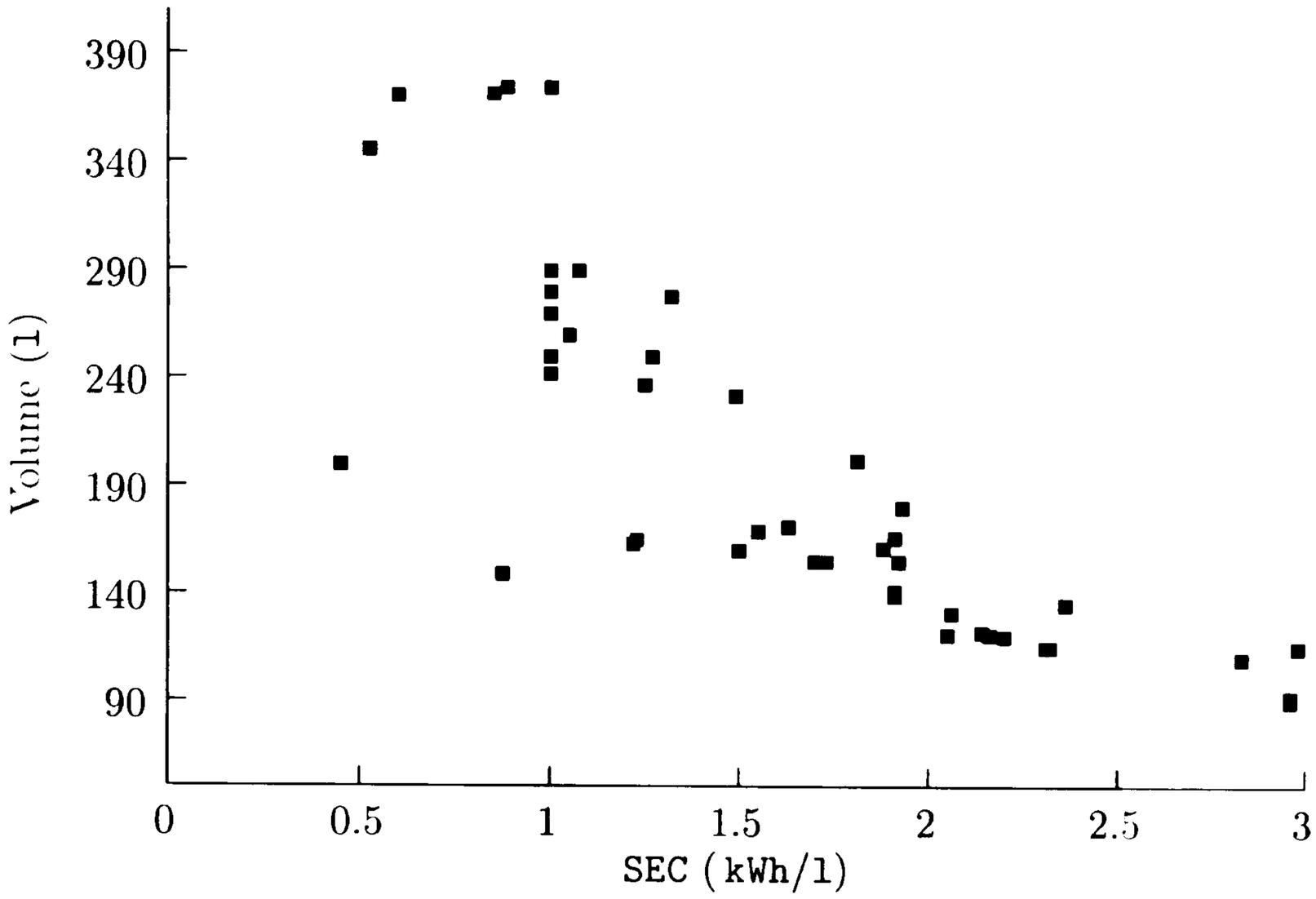


Figure 1.13: The relation between capacity and performance in Fridge Freezers, [Herring, 1994]

appliances were larger and hence should be more energy efficient per unit volume, see Figure 1.12 on the page before). The author cites the willingness of the populace to buy more efficient appliance models (even at a slightly higher cost) and the ready availability of the information to facilitate their doing so, as the reason for the higher efficiencies in German DRA models. Attesting to this, he claims, is that there were simply no UK brands available in Germany for these reasons at the time.

1.7 Utilisation Considerations

Customer attitude influences the 'quality' of the products on sale, as manufacturers have to be well attuned to consumer preferences. If consumers do not consider energy, environmental or running costs to be as important, then manufacturers will pay little attention to these issues. If, conversely, these issues are seen as a priority, they will become a priority in product development [Boardman, 1995b]. Two illustrative cases will serve the point:

- The first is the change in the *status quo* with regard to the dominant type of DRA on the market. For most of the 1970's larder refrigerators were preponderant. If a freezing facility was required, a separate freezer was purchased. In the

1980's fridge–freezers began to increase in popularity, mainly because of the convenience they afforded at a much smaller price and space requirement, when compared with (two) separate fridge and freezer units. By the 1990's fridge–freezers were the fastest–selling DRA's on the market.

	1970	1980	1990	1995
Fridge–freezers	0	19	51	58
Refrigerators	58	72	52	46
Chest Freezers	3	16	16	16
Upright Freezers	0.5	11	21	22

Table 1.4: Ownership of Appliances in the UK 1970–1975 by % of house holds. Source [Boardman, 1995b]

Initially, freezing compartments in fridge–freezers were small (which was the initial selling point, 'Why buy a large freezer when you only need very little freezing space each week?') and with the increasing demand for larger frozen space storage, the size of the freezing compartment increased. Today, it is not uncommon to see models with fridge and freezer compartments of similar sizes. Whereas, for aesthetic, space, economic *etc.* reasons the concept seems very appealing (a two in one at half the price and utilising only half the floor space!) the energy implications are less so. From a thermodynamic standpoint, it is inefficient to create a +5 °C environment from a cycle reaching -20 °C or lower. From a thermal design perspective, it is a near disaster[1]:

1. If one evaporator serves both fridge and freezer the evaporator will be subject to moisture from both. Since the refrigerator door is opened more frequently than the door in the freezer, the frost built–up on the evaporating surface (designed to cater for the freezer load) will typically be more than 10 times thicker than for a dedicated freezer [Nørgård, 1989].
2. Defrosting a refrigerator requires very little or no extra energy input, normally occurring spontaneously between prime–mover runs; the freezer on the other hand is a different matter. What would be required would be to have two different cycles, which would defeat the cost–reduction objective. A single compressor can be used if it is specially wound for different speeds; however, the lubricating mechanisms may also have to be redesigned [Guldbrandsen et al., 1986].

[1]More recent research into temperature–glide refrigerants (*i.e.* the technique of blending immiscible refrigerants to obtain a refrigerant with more than one phase transition temperature.) may offer a more efficient way of designing such systems.

3. Well–designed freezers require much more insulation than similarly–sized refrigerators. In hybrid (fridge–freezer) designs, due to the disparity in the respective compartment temperatures and thus insulation requirements, the insulation thickness for *both* adjoining compartments should be the minimum required for the coldest compartment. However, implementing this would reduce the amount of refrigerator space for given external dimensions (and increase the cost) which serves to in some way defeat the space–saving objective and, therefore, some compromise is invariably reached. The nett result is that fridge–freezers consume more energy than either fridges *or* freezers of similar capacity [Nørgård, 1989; Boardman et al., 1997], see also Figure 1.3 on page 7.

- The second case is to do with the number of features added to DRA's[1]. Examples of such are different temperature cabinets, automatic defrosting mechanisms (typically utilising heaters) *etc.* Many of these features actually place an extra energy overhead on the system and the resultant effect is that appliances boasting these features are less energy efficient (with respect to the basic task) than their non–sophisticated counterparts. Also, along with the greater multiplicity (and usually complexity) comes a higher risk of breakdown/malfunctioning due to component failure [Malin et al., 1993]

Space and the way it is perceived would always play a key role in determining the manner in which DRA's evolve. As noted earlier, it affects the design of these appliances. Space considerations can seriously affect the manner in which DRA's operate *in situ*. According to a paper published on the basis of feasibility research carried out by the Work Efficiency Institute (TTS) in Finland [Sillanpää et al., 1996], the manner in which a DRA is located during utilisation can significantly compromise its performance when compared to results obtained under test conditions. Often during standard tests, the laboratory environment is carefully controlled. In reality, however, the manner and location in which a device is used can significantly differ from the control or intended. The authors cite three cases:

- The design of the casing around a DRA in a fitted kitchen, can increase energy consumption by up to 90% due to air flow restriction [Malin et al., 1993; Sillanpää et al., 1996].

- Where the external air circulation path around a refrigerator[2] is blocked (wholly or partially), a 10–160% increase in the energy consumption of the appliance results (in one case, *circa* 60–950 kWh/p.a.) *op. cit.*

[1] 'Features' here refers to any addition to the basic DRA design which is not necessary for proper operation, including devices that are perceived to enhance the performance of the system.

[2] Particularly around the prime–mover.

- The location of a heat dissipating device (*e.g.* a cooker or dishwasher) immediately adjacent to a refrigerator. This caused an increase of between 12 and 22% in the energy consumption of the refrigerator when the devices were operating simultaneously *op. cit.*

According to Sillanpää (1997) such practices are rife in many Scandinavian countries where space is at a premium. As there are no standards, or even guidelines in many cases, to the location of these appliances during installation, they are simply located contingent on space availability, aesthetics *e.g.* in some cases the nearest work top is not in the immediate vicinity of the DRA and hence the doors are left open while items are ferried across to a convenient place. Nørgård (1989) states that " 'future use–behavioural patterns' will play a key role in determining the energy trends in DRA's". The phrase 'future use–behavioural patterns' not only encompasses customers attitudes' to each new feature (on whatever basis it is assessed) but, also includes the way in which the appliances are installed and used. Apart from the energy implications of poor practices in appliance usage there may also be a possible decrease in appliance life.

1.8 Aims and Objectives

From the foregoing it is clear that if the current spate of environmental concerns, legislation and energy consequences are to be addressed in the light of an expanding world population and rapidly increasing DRA use, research should be undertaken into these appliances. According to Guldbrandsen et al. (1986), even taking cognisance of the usual discrepancies that exist between theoretical[1] and techno–economic limits, in terms of energy efficiency there is, as yet, no indication that this techno–economic limit has been reached. The average annual consumption (for a 200 litre DRA) now in the EU lies between 280–301 kWh/p.a. but a low energy prototype constructed at the Technical University of Denmark [Guldbrandsen et al., 1986] consumed only 82 kWh/p.a., while prototypes in the USA have reached 50 kWh/p.a. [Boardman, 1995b]. However, according to Geller (1988), most of the major improvements have been made, and what may be needed in the near future is a more radical approach to appliance design.

The research presented herein focuses on DRA's, and in bringing a radical approach to appliance design has three principal objectives:

1. The utilisation of energy storage to provide an effective method for decoupling energy demand from supply in DRA's.

[1]The author states that this is *circa* 13 kWh/p.a., but does not specify for what kind of refrigerator this applies or, how these values came about.

2. The utilisation of thermal energy storage to enhance temperature stability within working DRA's.

3. To investigate the influence of such storage (particularly thermal energy storage) on the energy consumption of DRA's and thus devise a method of effecting the reduction of said consumption, utilising of energy storage technologies to enable the management of the prime mover energy conversion regimes.

The main advantages of doing this are to:

- Provide an avenue for achieving *sustained* performance and thermal stability in DRA's, particularly in regions of the world where the electricity supply is infrequent (or dependent on a diurnal weather resource *e.g.* the sun), also taking into account the possibility of periods of inclement weather and thus energy dearths. This is of importance in, *inter alia*, food preservation and health care delivery to remote areas in the *developing* world, where there is a need to maintain closely controlled temperatures *e.g.* for vaccines, cultures *etc.*

- Facilitate economic utilisation of DRA's in regions of the *developed* world where there are temporal and/or capacity tariff dependencies, particularly with the existence of punitive peak–time electricity tariffs.

- Utilise prime–mover dependence on diurnal ambient air temperature changes in order to maximise effective energy use in DRA's.

This research aims to provide a technical instrument to facilitate the intelligent control of DRA's on an economic and/or energetic basis and in conjunction, to evolve a strategy for the optimal use of energy in DRA's, irrespective of appliance design or constituent component efficiencies.

1.9 Closure

Currently, in the UK, the purchase of domestic electricity can be made optionally from a single or dual, '*Economy* 7' tier–tariff system. The 1989 Electricity Act [Her Majesty's Government, 1990; Mansouri-Azar, 1996] paved the way for deregulation of the Electricity Supply Industry (ESI) due to come into effect in 1998/9. With deregulation, it is envisaged that much more complex billing arrangements will become available with utilities vying for larger market shares and at the same time seeking avenues for minimising their aggregate peak demands. One manner by which the latter may be addressed is, from current experience, to associate higher tariffs

with peak demand periods. At present there are several commercially–available gadgets for harnessing the cost benefit of the lower night–time tariff on the '*economy* 7' scheme for central heating. However, currently there is no corresponding (commonplace) tool for load control (load spreading, shifting *etc.*) in DRA's[1]. Whilst the loss of this benefit (which may well increase with deregulation), due to a lack of effective load spreading, is a nuisance in the developed world, such a mechanism is an absolute necessity in developing countries with infrequent energy/electricity supply or in applications where energy is not constantly available.

The consensus in the literature is that the greatest proportion of the DRA load is due to heat gains through the compartment walls. The rate of heat ingress is a strong function of the ambient temperature. There is evidence to suggest that an energy–consumption efficiency[2] change of as much as a 30% can be attributed to a 5 °C change in ambient temperatures, *cf:* section 1.2.2 on page 8. The implication of this for temperate regions of the world is the existence of higher summer–time DRA electricity consumption and thus bills, *cf:* Figure 1.6 on page 13, a situation which may well be exacerbated with increased global warming, see Figure 1.9 on page 16.

In countries where storage heaters are used during the winter, *e.g.* the UK, there is a dip in the summer night–time demand due to the absence of storage heating requirements. The use of a similar load control mechanism in DRA's could afford 'storage cooling' whenever appropriate. Used during the summer night–time, such a mechanism could assist in redressing the imbalance in the summer day– and night–time energy consumption, as well as provide a means for more energy–efficient cooling, given that DRA prime–movers perform better in the cooler night–time temperatures.

As the the bulk of DRA manufacture is increasingly targeted for the non–saturated markets of the developing world, where compared to the saturated markets of the developed world higher ambient temperatures exist and electricity supply is infrequent; these two criteria will become *major* design factors for future research. The current work is set out in a bid to initiate this new (load and energy–availability orientated) approach to DRA design and to address the issue of load spreading; concomitantly revisiting energy conservation in DRA's. Thus, it is relevant to, the tightening EC legislation [EU, 1996, article 8] on DRA's and the possible implications of impending electricity deregulation in the UK. With reference to these issues, it is also timely, occurring within three years of both events.

The research also has important implications:

---

[1]Extensible to include of air conditioners and generalised to be irrespective of scale.

[2]Here, the term efficiency applies to that fraction of the energy consumption which is used specifically for load–cooling purposes.

1. In applications with rigorous thermal control requirements.

2. Where the concern for thermal control within meagre/modest energy budgets, dictate expedient energy consumption.

3. In areas where intermittent energy supplies threaten to compromise thermal energy applications *e.g.* DRA's in developing countries, WHO rural area immunisation programmes, mobile and recreational applications *etc.*

4. In areas where temporal phase–shifts exists between thermal (coolth) energy requirements and energy supply *e.g.* in solar or wind applications.

5. In environments where the economic or other incentives/penalties are in place for the consumption of electricity at given periods of the daily energy demand cycle.

Chapter Two

Concepts

Whatever you do will be insignificant; however it is important that you do it

–Mahatma Ghandi

Introduction

This chapter deals with concepts central to the current research. It begins with the more general theme of energy management and goes on to address the particular case of DRA's. The chapter also deals with different heat transfer phenomena which may be exploited in the quest for better efficiency in DRA's. Where possible, theoretical bases for assertions made in this regard are presented and/or discussed.

2.1 Demand Side Management

In order to effectively address the problem of improving energy use performance[1] in DRA's, the issue must be set against the wider picture of the totality of energy use in domestic appliances. This entails technical, social, environmental, economic and

[1]The issue of service delivery will be addressed later.

psychological aspects which can be categorised within supply/supplier (utilities and manufacturers) and demand (end–user) contexts. In reality the 'coupling' between these factors is tight, each one bearing upon the other. In tackling the problem of energy–use optimisation it is necessary to assess, characterise and thus understand these interdependencies within the general picture.

A managerial technique, known as Demand Side Management (DSM), was developed in the USA in the 1970's [Duguid and Mee, 1994] for assessing and optimising the use of energy. It was developed primarily for economic reasons but, of recent, it is being implemented more frequently for environmental ones [Redford and Fry, 1993].

DSM was developed in order to cope with the increasing disparity between the daily maximum and minimum electricity demand. Historically the variability in the electricity–demand cycle became a major concern to the utility companies (in the US) in the 1960's and 1970's with the proliferation of, *inter alia*, heat pumps for air conditioning and food preservation in society. The response to the increasing variation between peak and off–peak electricity demand had been the procurement of greater generating capacity[1] simply to cater for the peak demand. This resulted in an excess in generating capacity for long periods of the daily energy demand cycle. The economic ramifications of this were becoming more and more unsatisfactory as the maximum daily demand increased, demanding greater capital expenditure for plant expansion. With increasing pressure (from shareholders *etc.*) to recoup capital expenditure over the shortest possible time (*i.e.* Pay Back Period, PBP) and for maximum profitability, the utilities were faced with two principal options:

1. To increase the unit price of electricity. This would have a detrimental economic effect, particularly in regions where several operators compete within the same market and/or, possible legal implications where electricity prices are set by some government regulatory body.

2. To seek avenues by which the end–users may be cajoled or compelled to alter their energy–use habits in a manner as to alter their energy demand profiles.

The second alternative was considered the better option and it was in the search for an effective method to implement the strategy that the concept of DSM emerged. DSM, as a concept, was first implemented within the (USA) Electric Power Research Institute (EPRI), where it was defined as: 'The planning, implementation and monitoring of utility activities designed to influence customer use of electricity in ways that will produce desired changes in load–shape' [Redford and Fry, 1993]. It can be used as the major tool in a Least Cost Utility Planning (LCUP) strategy for determining the Least Cost Option (LCO), for the supply of utilities, in general. It is

[1] More and larger plants.

important to note that the emphasis is on *altering* the load–shape and not necessarily on total demand reduction[1].

The basic idea is to maximise the utilisation (and hence profits) of the existing (generating) capacity before further capacity expansion is undertaken. The underlying motif in such programmes is: for the utilities, is it 'cheaper to save *or* generate a kWh of electricity?' (where in this case, 'cheaper' translates indirectly to 'more profitable'). The *excess* generation (or generating capacity) avoided is measured in 'Nega–Watts' [Lovins 1988, 1990, 1996]. The initial impetus, primarily techno–economic, soon began to be superseded by socio–political, environmental and more recently legislative considerations. Due to the broad nature of it's (DSM's) foundation, different applications tend to focus on different aspects and as such DSM can mean several things. For instance, according to Nilsson (1994):

1. It can have a strictly technical meaning by describing the technical outcomes in the electricity system when applied.

2. It can be regarded from it's impact on resource allocation when described by its economic rationality.

However, all DSM definitions (reflecting a diverse range of objectives and perspectives) have as a central theme, the need to modify the end–use of (electricity–related) supplies to 'shape' demand in some beneficial manner [Redford, 1994]. Generally speaking a flat demand load curve is advantageous to most forms of supply[2]. DSM is a broad dynamic concept and may be approached from several different perspectives (and consequently different ensuing outcomes) depending on the initial reason for its implementation, see Nilsson, *loc. cit.*, for a more detailed account. However it is mainly a demand–side implementation alternative to new capacity on the supply side which means that the benefit is the 'avoided cost' for that capacity [Formby, 1994]. These avoided costs include generation, as well as distribution (hot–wire) costs. The effects of a properly implemented DSM program are several: (a) to the end–users it *should* manifest as lower energy procurement costs[3], (b) within industry it is felt in an increased manufacturing/production efficiency, (c) to the utilities suppliers it manifests as delayed capital expenditure and (d) on a global scale it serves to limit environmental damage associated with increases in utilities production.

The actual method of influencing end–user electricity demand is dependent on application and DSM implementation. As an example, in some instances, financial

[1]The utilities *are* in business to make money; however increased sales may only marginally improve profitability.

[2]Many a marketing goal aims for just that.

[3]As yet there is no indication that the utilities pass on the full benefits of the avoided costs unto their customers.

incentives such as loans and grants are given to encourage a move to more energy–efficient devices, while in some others, a time and/or capacity–oriented multi–tariff billing system is instituted, with punitive tariffs being associated with, say, either resource consumption, or exceeding an agreed demand capacity at pre–stipulated times [Formby, 1994]. Usually, both may be instituted in conjunction with each other (probably depending on the nominal demand of the user). The implementation can be scheduled in a manner as to offset the costs and losses in revenue incurred, by the utilities, in promoting measures of energy efficiency and any consequent reduction in sales. In the future, other strategies like, reduced cost per unit utility consumed dependent of consumption *pattern* and generation cost reflective pricing, may become options [Redford, 1994]. Characteristically, there are at least five main objective categories around which these programs are designed [Redford and Fry, 1993; Nilsson, 1994; Redford, 1994; Augood, 1997] *viz*:

Peak clipping Demand reduction by voltage reduction, supply interruption or other focused energy–efficiency programs.

Valley filling Demand re–scheduling, by the promotion of utility consumption particularly at periods of low demand, to maximise utilisation of generation and network assets.

Load Shifting Demand relocation is essentially an extension of peak clipping, *qv.*, effected by use of accumulators.

Strategic conservation Overall reduction of demand through energy efficiency is typically a societal issue, with most activities geared towards environmental goals, (although, sometimes it may be used as a means of capital expenditure control).

Strategic load growth This is a variation of the Valley filling theme, with the primary objective of increasing overall consumption.

In any DSM program, cost recovery plays a major part. In some instances, the recovery of cost may not necessarily be financial but may take other forms such as: a raised company profile *etc.* According to Nilsson, *loc. cit.*, in instances when financial[1] economics are involved, utility companies and end–users tend to have different economic perspectives and time–scales. This leads to a systematic bias in their economics. Suppliers tend to calculate and act based on lower rates of return than the end–user, typically precipitating an over–spend on the supply side and a neglect of opportunities on the demand side. The difference in the respective

[1] As opposed to energy.

maximum investments for the supplier and his client (end–user) is known as the 'payback gap' and the discount rate the end–user adopts, the 'implicit' discount rate[1]. These differences exist in spite of pricing, but can only be felt in terms of pricing. With the privatisation and deregulation of the UK electricity industry there is the increasing probability that utilities would seek avenues to 'pass on' the 'avoided cost' to the demand side in an attempt to increase market share through pricing.

2.1.1 Demand Side Management in Perspective

The main precept of DSM, *i.e.* the modification of the electricity demand profile to some desired, predetermined shape, to some purpose or advantage, can also be implemented by equipment manufacturers[2], given a suitable enabling mechanism. Such a mechanism, which must intrinsically consist of, *both*, (a) a control *philosophy* and (b) a *controllable technology*, can be incorporated as an intelligent part of the resource management strategy for an appliance[3]. DSM concepts can be applied within the basic design–control regimen of *any* device exhibiting a temporal dependence on resource consumption. In this sense DSM cannot be viewed as the *ex-parté* preserve of the utilities[4], nor is it to be restricted to techno–economic issues. Socio–psychological research effort has been expended on identifying the societal impacts of these programs (*cf:* section 1.4 on page 20 and section 1.5 on page 22). If the motif of the utilities bears directly on whether it is 'cheaper to save a kWh or generate a kWh of electricity', then that of the end–user is increasingly sympathetic to the environment in addition to cost. From the end–users perspective, what is wanted is *seldom* just the purchase of cheaper kWh of electricity but, an effective, reliable service (*e.g.* effective lighting, cooling, heating *etc.*) at an affordable price [Boardman et al., 1997], and preferably at little or no *perceived*[5] environmental cost.

---

[1]The utilities tend to borrow comparatively larger amounts of money and thus are in a better position to bargain for lower return rates from the banks. In making a comparison the maximum investment per unit profit expected is used as indicative.

[2]To the advantage that the appliances can be marketed as being able to take advantage of whatever utility–side DSM strategy is in place.

[3]This is precisely what has been devised and validated for DRA's in this work.

[4]In fact there is no reason why the technique cannot, suitably modified, be applied to the delivery of other fluctuating resources. This is manifest herein, in the application of the principle to coolth demand in DRA's.

[5]A perception not necessarily based on correct or 'perfect' information, much to the disgust of the nuclear electricity companies. In discussions with colleagues researching into the socio–psychological aspects of energy use, what became increasingly apparent is that many individuals, even energy–conscious ones, generally do not consider the use of DRA's as adversely impacting the environment. Probably because most advertisements on the television and radio are geared towards heating and lighting *etc.*

Currently, this translates loosely into more energy–efficient devices run at a lower energy costs (although there is some evidence that some consumers would pay more for 'cleaner' energy). The translation is loose, as there are many other socio–psychological factors which bear up on the consumer's final choice. Availability appears to be singularly the most constricting (you simply cannot buy what isn't available). Affordability is another major factor[1]. Beyond these, other considerations are (a) number of available features, (b) need for (and ease of) maintenance, (c) design aesthetics/ergonomics, (d) economic savings due to differences in energy consumption, (e) environmental impact and (f) *perceived* compromise or change in living standard *etc.* between different product options (not necessarily in that order). In the design of any appliance or scheme to influence the *use* of energy, these must also be taken into account.

2.2 Load Management in DRA's

Introduction

This section briefly discusses aspects of load demand management. In converging on the load management in DRA's, it tries to highlight sources of appliance thermal instability and goes on to propose a single measure which may be used to address the problem.

2.2.1 Load Management

The demand for the supply of energy is a constantly varying time–dependent function, as is the production of suitable forms of energy from primary sources. The satisfaction of such demands from a stored fuel requires the matching of conversion to the load variation. However, the two tend to exhibit different patterns of temporal variations for fundamental and practical reasons.

To ensure a continual and reliable energy supply service, conversion equipment must be able to provide the maximum power ever required, *i.e.*, its rated power must equal or surpass the peak load. In practice, if the conversion equipment consists of several units operating in parallel, there must be a sufficient surplus capacity such that: given the probability distribution of equipment failure, the likelihood of not being able to meet demand can be kept acceptably low.

When the load demand is characterised by a time distribution which is not completely predictable *e.g.* determined largely by individual choices, then the probability

[1]To each, his coat according to his cloth, the old adage goes.

of supply insufficiency takes on, in addition to (a) equipment failure, a second dimension *viz* (b) load uncertainty. The later probability is also referred to as the 'loss of load probability' (LOLP). The surplus capacity necessary for meeting a given LOLP requirement is termed the 'reserve capacity', which usually decreases inversely as the multiplicity of conversion units.

Traditional energy supply chains all involve the storage of fuel (or primary energy) typically,

Mining/Extraction ➡ Fuel Storage ➡ Conversion ➡ Energy Use

However, in situations where the cost[1] of conversion equipment is considered high relative to the cost of 'driving fuel'[2], then the addition of a (secondary) energy storage facility *after* [3] the conversion may be considered. Such a storage must hold the energy in the form required or one easily and efficiently converted into the 'load energy form'. Otherwise a new conversion step will be present, and the system may exhibit the same shortcomings as the original one. With 'secondary storage', it may be possible to operate the conversion equipment at a constant or moderately varying level of power output. In such a scenario, surplus energy (produced in excess of demand) is fed into the secondary energy store, and energy deficits (demand exceeding momentary production levels) are drawn from the store; two examples of this are thermal energy and mechanical energy (pumped water) storage.

The match between a given system of conversion equipment and the load structure may be described in terms of a time 'duration curve' of the instantaneous power capacity (P_{supply}) minus the corresponding instantaneous load (P_{load}).

$$\text{'Over capacity'} = P_{supply} - P_{load} = \text{'Reserve Capacity'}$$

This can be useful in assessing the need for implementing storage, as opposed to procuring extra capacity. This curve is unique to each implementation and the specification of storage systems may vary greatly with respect to the storage capacity requirement, the storage duration, access time, extraction time, charge time *etc.* One of the most important features is the uncontrollable variability of the load. In many cases the variation is known only to a first approximation and thereon modelled as

[1]Here in the broader sense which includes, in addition to financial, other aspects like space *etc.*

[2]Driving fuel is used *here* in the sense that it feeds off the conversion equipment. It might be anything from unrefined crude to electricity.

[3]The connotation here is for immediately prior to use as opposed to (primary) storage *before* conversion. Whether a given 'fuel' is classed as primary or secondary will depend on the application. For instance, raised steam (a fuel) may be used to provide mechanical work as an end product (*e.g.* in steam trains) or as fuel for one of the energy conversion processes in the production of electricity, which is also a fuel.

stochastic [Jensen and Sørenden, 1984]. The intrinsic ability of a 'load energy form' (secondary) energy storage facility to smooth out these power/load phase differences can be extremely advantageous.

2.2.2 Load Management in the DRA Context

One major problem associated with DRA's is that of maintaining thermal stability within the compartment. Current ISO test procedures stipulate methods for determining the length of time required for the appliance interior to reach temperature, the so called pull–down time (the corresponding tests known as the pull–down tests), see [ASHRAE, 1998], for a brief exposition on the subject. However, the current (EU) legislation only categorises the four star (★★★★) domestic freezer in this regard [Waide, 1993; Buhl-Pedersen et al., 1993; EU, 1996]. The net effect of this latitude is made patent by one pilot study conducted in the UK, where the mean temperature in 85% of a sample of 21 randomly selected domestic refrigerators was, on the average, above the recommended 5 °C [James and Evans, 1990]. In fact, only in one case was the temperature *consistently* below the recommended 5 °C. The authors cite another Chinese study where only 2.8% of the appliances sampled operated consistently below 6 °C and highlight the need for more thermally–stable devices. Noting that, because the ISO (and other such) standards *e.g.* ISO/R 824 (19), DIN 8950 (8); [ANSI/AHAM, 1988; CAN/CSA, 1991; UL and CAN/CSA, 1998] only pertain to the average of the maximum and minimum temperatures in any one thermal cycle[1], these standards ignore the differences that may exist therein (in some cases 12 °C) which can be detrimental to stored products. This is despite the fact that very strict guidelines exist under which foods may be handled (storage temperatures, cooling down times, storage times *etc.* see [ASHRAE, 1998, Chapters (16–28) and (47–51)] for pointers to more detailed food preservation information). It appears that very little notice is taken of this when appliances are legislated upon. Glaring evidence of this is that the current EU standard test procedure is based on an *empty* appliance (see Waide (1993)), with the principal objective being the determination of (24–hourly) energy consumption figures, see also EU (1996). In examining the literature, it was evident that:

1. It is imperative to differentiate between energy consumption and energy efficiency. This distinction is necessitated by the fact that it is possible to have a low energy consumption DRA with poor prime–mover efficiency[2].

[1] The time between two successive prime–mover duty cycles during normal operation.
[2] As a consequence of insulant performance.

2. In the same vein, a clear distinction must be made between energy performance and cooling performance[3].

3. Any comprehensive definition of DRA performance[4] has to reflect, in addition to the usual energy consumption indicators ($\mathtt{kWh}_{(e)}$/24 hours *etc.*), prime–mover COP's, heat exchanger effectiveness, heat ingress inhibition capability ($\mathtt{kWh}_{(T)}$/24 hours) and pull–down times, as well as some indication of thermal stability[1] about a stipulated internal temperature (referred to loading conditions).

Thermal stability in an operational DRA can be broadly classified under two categories. The preceding discussion hinted at the thermal excursions which may result from the insertion of some 'thermal load' into the DRA. A second category results as a consequence of the continual heat ingress into the system across the cabinet (containment) walls. As with all thermal response systems, low thermal inertia DRA's are prone to respond more readily to changes in the ambient temperature. The manifest effect of this being that the prime–mover, in such low inertia systems, would tend to cycle (on/off) more rapidly than a higher inertia DRA, *ceteris parabus*, in an attempt to effect compartment temperature regulation[2]. As with virtually all inertial machines, power requirements at start up are in excess of those for normal operation, in order to overcome inertial loads. Furthermore, during each off cycle, the pressure across the prime–mover equilibrates. Arguably, this equilibration of pressure helps reduce the inertial loads (due to pressure) at start up. However, the energy utilised in the restoration of this pressure differential (prerequisite to normal operation) is extraneous to the primary purpose of the device, and so amounts to a hiatus in the resulting process efficiency. This is not to mention the heat injected *into* the system during the restoration of normal working pressures. Clearly, this incipient lavish energy consumption predicament is aggravated with increased prime–mover cycling. Thus for the same changes in ambiance, lower thermal inertia DRA's will consume more energy in total as a consequence of this, in comparison to their counterparts of higher thermal inertia.

Problems with thermal stability within a working DRA can be addressed utilising a suitable 'buffer' (or thermal–energy store, 'TES'). This can (under the right set of circumstances) augment the restoration of the thermal balance within the appliance after some destabilising interaction (*e.g.* the door opened for a protracted length of time or the insertion of a large thermal mass at a temperature greater than the

[3]This distinction, while subtle, is a very significant one and is evident in the difference between solely standards–oriented designs, and the more robust contingency–based designs.

[4]An Efficient Energy Consumption Indicator.

[1]Possibly as a temporally–weighted, central temperature tendency indicator.

[2]This can lead to systems control problems due to over sensitivity.

DRA control temperature.). In both cases (changes in ambiance and utilisation), it can serve to limit the frequency of prime–mover cycling as well as lead to increased appliance robustness. This is in addition to the provision of a mechanism by which stricter thermal regulation can be imposed.

As noted later in section 1.3.1 on page 12, one of the central ideas behind this research is to demonstrate that the use of certain heat transfer techniques may be beneficial in DRA design. In this regard the focus is on energy consumption (see item 1 on page 9) in relation to the cost (not necessarily monetary) of energy consumed by the appliance. As the instantaneous COP of the prime–mover is dependent on the ambient temperature, there may be some benefit obtained by avoiding the use of the prime–mover during comparatively less (thermodynamically) expedient times. The loads incurred during these times may then be offset by the use of thermal (coolth) storage, stockpiled during some other profitable period.

This strategy may also be brought to bear (possibly with the inclusion of a different pertinent form of energy storage) in situations where there are variations (and probable periods of dearth) in energy supply, enabling sustained appliance operation (or in one sense, robustness to supply variation).

2.3 Objective Statement

It is within the foregoing context that the current research (*i.e.* the design of an energy–efficient, power–supply and use–profile independent DRA) is set. The central tenet of this research (*cf:* section 1.8 on page 34) is the concept that energy storage, *in particular* thermal energy storage, can be instrumental in the delivery of sustained and reliable thermal performance in, as well as the reduction of energy consumption of, DRA's. The prime objective of this research is the validation of this thesis (which is invaluable an DSM mechanism), giving specific address to measures for:

(a) Increasing energy consumption efficiency.

(b) Reducing average energy consumption (and thereby running cost).

(c) Reducing the power variability ratio[1].

(d) Exploiting the concept of time–dependent tariffs to further reduce appliance energy consumption cost whilst, at the same time, ensuring robustness to energy supply fluctuations and user habits.

[1]The ratio of the difference, over a relevant cycle, between the maximum and minimum power demands to one or the other of (i) the maximum power demand, (ii) the minimum power demand or (iii) the time–averaged mean power demand. Irrespective of the definition used it is clear that this value will approach zero for less 'peaky' demand profiles.

(e) Ensuring that no changes are admissible which may (or may be perceived to) amount to a decline in living standards[2].

2.3.1 Project Methodology

The method by which this is to be achieved is by careful thermal design, amalgamating established, available technologies (notably thermal accumulation[1] and vacuum insulation[2]) optimised for inculcation into small–scale/domestic refrigeration systems. This is in addition to attempting to exploit certain thermodynamic phenomena inherent within the basic DRA design. These choices (thermal accumulation and vacuum insulation) were made as they present, *prima facie*, appropriate and effective enabling technologies with the potential to make the most economic or best technical use of the available energy. This could be achieved by facilitating the: (a) reduction of 'non–utilisation' associated appliance heat gains (and thus energy consumption), (b) decoupling energy demand and supply, (c) reducing the frequency of prime–mover (on–off) cycling [Guldbrandsen and Nørgård, 1986] and (d) increase of the prime–mover index of performance[3].

The underpinning rationale in all this is that reductions in the energy consumption of a DRA (or any non–trivial energy conversion system for that matter) is best achieved by addressing in greater detail the *process* layout and efficiency, rather than the individual component energy conversion efficiencies. In this regard much of the analysis will be undertaken comparatively, with the view to specifying what an optimal configuration of a DRA should approach, irrespective of component efficiencies.

The basic DRA consists of an insulated cabinet, two heat exchangers and one heat pump (prime–mover). The principles behind its operation were understood well over a century ago [Bianchi and Forlai, 1988; Atwood, 1991; Nagengast, 1996; Nagengast, 1997; Nagengast, 1998]. Over time, the design of such systems has been modified as new technologies came to the fore. The following discussions on the

---

[2]This is highly subjective; however some criteria are fairly standard *i.e.* maximised internal/external volume *etc.*

[1]See section 1.2.2 on page 9 for the rationale behind this.

[2]As the greater proportion of the heat gain into DRA's is through the walls, the best available type of insulation is to be employed in the specification. Typical resistance values for polyurethane foam are 'R–5' (per inch) while the VPSI intended for this application has an 'R–75' (per inch) rating. Other manufacturers produce vacuum–based insulants with 'R' ratings of less than 75 but, in the region of an order of magnitude greater than for conventional insulants, see McElroy et al. (1984), Potter and Benson (1990), Smith and Porter (1990), Benson and Potter (1992), Owens Coring (1994), Babyak (1994), Owens Coring (1994).

[3]As the cold end of the prime–mover can operate from a fixed (accumulator) temperature rather than at several degrees below this, see section 1.4.1 on page 13 for pertinent arguments.

various considerations given in this research exercise is restricted to the ubiquitous vapour compression cycle[4].

2.4 Energy Transfer Considerations

Introduction

This sections deals with the dynamics of energy transfer and conversion within a DRA. It attempts to highlight the different aspects of the energy conversion process indicating the influence different systems parameters have on the entire process. The section also presents relations for the prime–mover index of merit with the underlying derivative analysis. In doing so it also attempts to discuss the manner in which real systems deviate from the theoretical predictions.

2.4.1 The Prime Mover

The prime–mover index of merit is called the Coefficient Of Performance, (hereinafter COP) and is defined as the average ratio of the *useful* heat (Q_l) removed from a system to the (thermodynamic) work (W) required to effect this removal. *viz*[1]

$$\mathtt{COP} = \frac{Q_l}{W} = \frac{\dot{Q}_l}{\dot{W}} \tag{2.1}$$

For an ideal process, such a heat pump is assumed to be operating isothermally between two infinite reversible heat reservoirs (one sink and one source) and with all the expansion and work transfer processes being reversibly adiabatic (isentropic). This ideal cycle's index of merit is the so–called Carnot[2] cycle *C*oefficient *O*f *P*erformance[3], hereinafter referred to as the ideal or Carnot cycle COP *viz* $(\mathtt{COP})_C$. If one considers

[4] As this is most commonly encountered device of its type and boasts superiority in one or more terms of cost, efficiency or proven reliability over other major heat pumps as applied to DRA's, see [ASHRAE, 1994, Chapter 48].

[1] The dots indicate unit time quantities. Strictly speaking the $\dot{W}$ is defined as the instantaneous (in this case electrical) power; however, the basic assumption here is that these 'rates' are steady.

[2] **Carnot, Sadi** *(1796–1832).* French mathematician and pioneering thermo-dynamist *(son of Lazare Carnot). He made important contributions to the Mathematical theory of heat and engineering thermodynamics where he devised the Carnot cycle.*

[3] The reader is referred to standard texts *e.g.* Callen (1960) for introductory and detailed discussions on the subject of heat pumps and their performance.

the high and low temperature heat sinks to be at temperatures[1] T_h and T_l, with respective heat transfer rates $\dot{Q}_h$ and $\dot{Q}_l$ (see Figure 1.1 on page 14) then from the basic Carnot cycle analysis:

$$\begin{aligned}(\mathtt{COP})_C &= \frac{T_l}{T_h - T_l} \\ &= \frac{T_l}{\Delta T_{hl}} = (\tau_C - 1)^{-1}\end{aligned} \tag{2.2}$$

where the cycle temperature ratio is defined as $\tau_C = \frac{T_h}{T_l}$

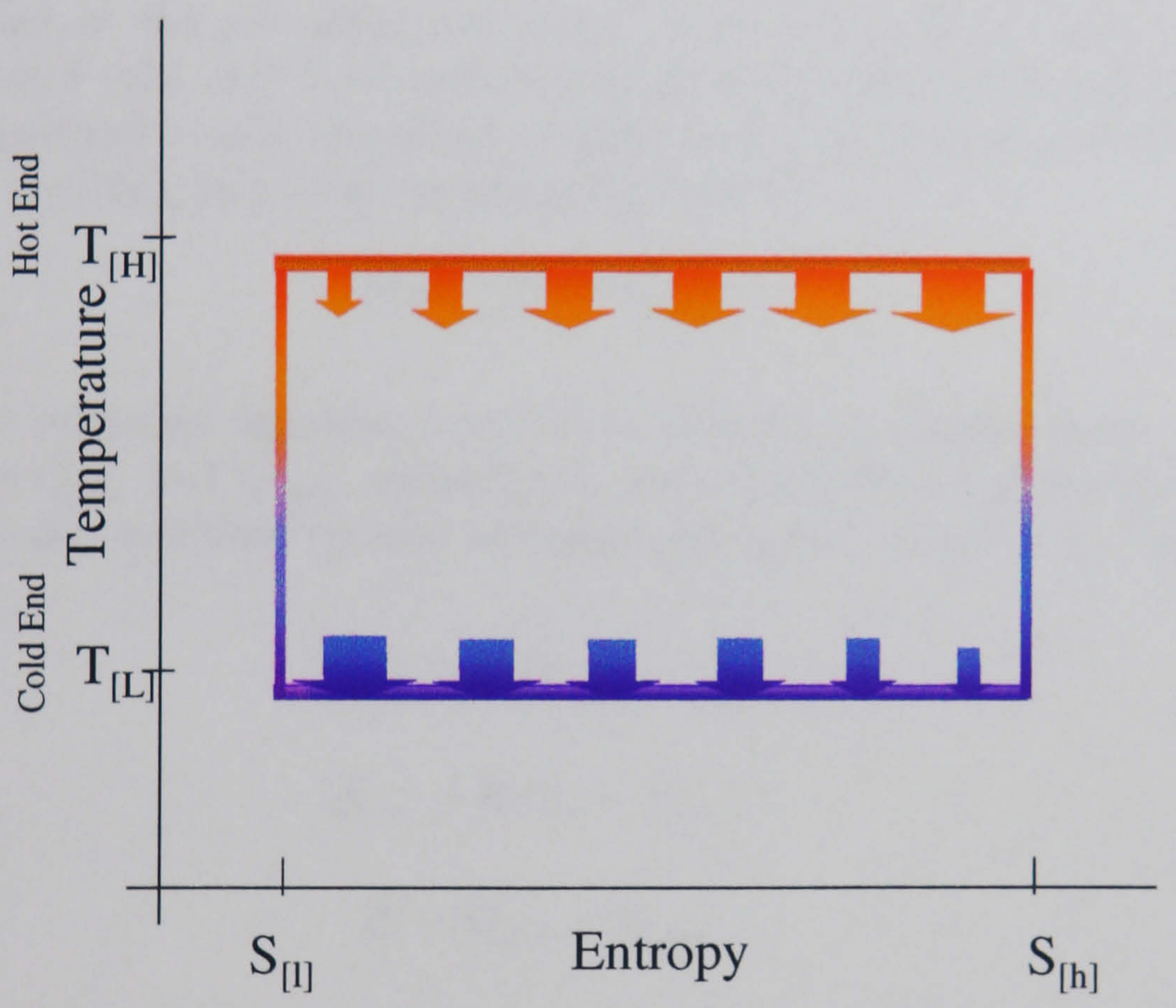


Figure 2.1: Schematic T–S diagram for the basic Carnot refrigeration cycle indicating the context of the different symbols used in the text.

The arrowwidths are to give an indication of the relative proportion of the heat transfer as the fluid traverses the exchanger.

The COP values of real prime–movers are much less than this ideal $(\mathtt{COP})_C$, compromised by departures from the theoretical assumed isentropic and isothermal behaviours, see Figure 1.1 on page 14. These are particularly, (a) that the heat transfers across the heat exchangers *must* take place across a finite thermal gradient

[1] More rigorously, thermodynamic temperatures or thermal potentials.

(*i.e.* that $T_{\text{cond.}} \gtrneqq T_h$ and $T_{\text{evap.}} \lneqq T_l$) and, (b) there is direct heat transfer into the system due to the nature of the design (principally, due to heat transmission across the system's boundary from the ambient, but also from other sources *e.g.* the hot end, fixtures *etc.*). In keeping with the literature [Bejan, 1988; Bejan, 1989], the ratio of these two indices of merit (real and Carnot COP's) is here defined as the *second law* efficiency of the real system *viz*[1]

$$\eta_{ii} = \frac{\text{COP}}{(\text{COP})_C} \tag{2.3}$$

If in consequence of the isentropic behaviour alluded to and the irreversibilities inherent in (a) in the preceding paragraph, it is assumed that heat exchange at both the hot and cold 'end' heat exchangers are with equivalent temperatures $T_{\text{cond.}}$ and $T_{\text{evap.}}$ respectively; also, the effect of (b) above can be characterised by a heat ingress ($\dot{Q}_i$), resulting in a total refrigerating load *i.e.*

$$\dot{Q}_{\text{evap.}} = \dot{Q}_i + \dot{Q}_{load} \tag{2.4}$$

Using the subscript notation *l* and *h* to demarcate conductances (K) for the heat transfers $\dot{Q}_{\text{evap.}}$ and $\dot{Q}_{\text{cond.}}$, respectively, then the following basic definitions are illustrated in the modified Carnot refrigeration cycle[2] diagram in Figure 1.2 on page 16

$$\dot{Q}_{\text{cond.}} = \mathsf{K}_h(T_{\text{cond.}} - T_h) \tag{2.5}$$

$$\dot{Q}_{\text{evap.}} = \mathsf{K}_l(T_l - T_{\text{evap.}}) \tag{2.6}$$

$$\dot{W} = \dot{Q}_{\text{cond.}} - \dot{Q}_{\text{evap.}} \tag{2.7}$$

Also, noting the relevant *system's (boundary)* second law condition[3]

$$\frac{\dot{Q}_{\text{cond.}}}{T_{\text{cond.}}} - \frac{\dot{Q}_{\text{evap.}}}{T_{\text{evap.}}} \geq 0 \tag{2.8}$$

[1]Deducible from the so–called Gouy–Stodola theorem: $\Delta\dot{W}_{available.} = T_0\Delta\dot{S}$, see Bejan (1982b), *pp.* 24.

[2]In many a sense, this is still an idealised schematic diagram, depicting isentropic and isothermal processes.

[3]Again, another idealisation. The reality is that the process has inherent irreversibilities, due to prime–mover inertia *etc.* In fact for this reason, the tendency is for larger devices to possess better COPs than smaller devices, due to a lesser proportion of the total energy consumed being deployed to overcome these inertial forces.

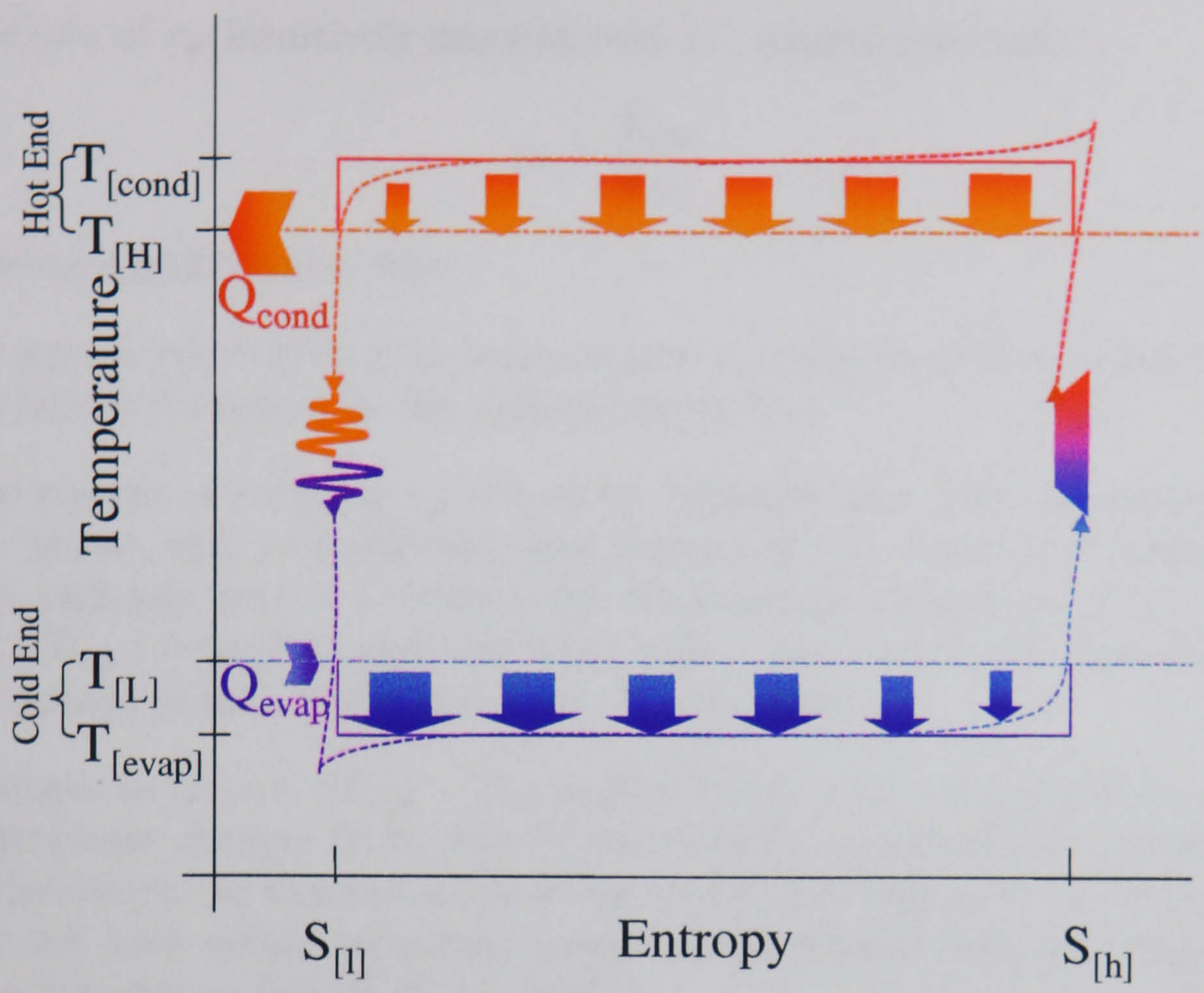


Figure 2.2: Schematic T–S diagram for a modified basic (Carnot) refrigeration cycle indicating the context of the further symbols used in the text.

Using eqn (1.1), eqn (1.4), eqn (1.7) and observing the limiting equality (reversibility) condition of eqn (1.8).

$$\begin{aligned} \mathtt{COP} &= \frac{\dot{Q}_{load}}{\dot{W}} \\ &= \frac{(\dot{Q}_{\mathsf{evap.}} - \dot{Q}_i)}{(\dot{Q}_{\mathsf{cond.}} - \dot{Q}_{\mathsf{evap.}})} \end{aligned} \tag{2.9}$$

$$= \frac{1 - \dot{Q}_i/\dot{Q}_{\mathsf{evap.}}}{T_{\mathsf{cond.}}/T_{\mathsf{evap.}} - 1} \tag{2.10}$$

Based on the definitions of $\mathtt{COP}_C$ and η_{ii}, this yields [Bejan, 1989]

$$\eta_{ii} = \frac{\tau_C - 1}{\tau_{\mathtt{HP}} - 1}\left(1 + \frac{Q_i}{Q_l}\right)^{-1} \tag{2.11}$$

the definition of τ_{HP} intuitively carrying over *i.e.* temperature ratio

$$\tau_{HP} = \frac{T_{cond.}}{T_{evap.}}$$

The foregoing illustrates that:

1. For a given ratio of reservoir temperatures τ_C, reductions in τ_{HP} would maximise the service furnished by the system (eqn (1.11)).

2. The process of reducing τ_{HP} should be achieved, preferably, by reducing both the hotter end temperatures *and* increasing the lower end temperatures. The rationale here is to reduce the temperature differences ($T_{cond.}$ - T_h) and (T_l - $T_{evap.}$) (eqn (1.5) and eqn (1.6)) which characterise the irreversibility of the system (eqn (1.8)) [Bejan, 1989; Bejan, 1982a].

3. Changes in $\dot{Q}_h$ *i.e.* ($T_{cond.}$ - T_h) and/or $\dot{Q}_l$ *i.e.* (T_l - $T_{evap.}$) can be offset by appropriate changes in K_h and K_l respectively to maintain the same systems performance. In thermal engineering terms, this translates to increasing the relevant heat exchanger areas, increasing the relevant heat exchanger overall heat transfer coefficient (U) or both.

It is noted in passing that the extent to which these can be achieved in practice will be restricted by economic as well as other technical considerations.

The truth is that the idealised COP relation eqn (1.1) cannot be deemed to sufficiently represent DRA reality. In considering the implementation of the measure stated in point 2 above, it is important to bring to bear some aspects of the actual utilisation dynamics of DRA's. In the light of this, the following is presented as a better representation of the COP in relation to the systems parameters. In what follows, the definition of COP is relaxed to embrace the actual performance of the prime–mover *in situ* and addresses the issue of the Efficient Energy Consumption indicator raised in item 3 on page 9. Again, beginning from the basic COP definition: eqn (1.9)

$$\begin{aligned} \mathrm{COP} &= \frac{\dot{Q}_{load}}{\dot{W}} \\ &= \frac{(\dot{Q}_{evap.} - \dot{Q}_i)}{(\dot{Q}_{cond.} - \dot{Q}_{evap.})} \end{aligned}$$

and again observing the limiting equality condition of eqn (1.8)

$$T_{cond.} = \frac{\dot{Q}_{cond.} \times T_{evap.}}{\dot{Q}_{evap.}} \tag{2.12}$$

which, with $T_{\text{evap.}}$ as the subject of eqn (1.6), in eqn (1.5) yields

$$\dot{Q}_{\text{cond.}} = -\frac{\mathsf{K}_h \mathsf{K}_l \dot{Q}_l T_h}{\dot{Q}_{\text{evap.}}(\mathsf{K}_h + \mathsf{K}_l) - \mathsf{K}_h \mathsf{K}_l T_{\text{evap.}}} \tag{2.13}$$

If this is substituted into eqn (1.9) the following results

$$\begin{aligned} \mathtt{COP} &= \frac{(\dot{Q}_{\text{evap.}}(\mathsf{K}_h + \mathsf{K}_l) - \mathsf{K}_h \mathsf{K}_l T_l) \times (\dot{Q}_{\text{evap.}} - \dot{Q}_i)}{\dot{Q}_{\text{evap.}}(-(\mathsf{K}_h + \mathsf{K}_l)\dot{Q}_{\text{evap.}} - \mathsf{K}_h \mathsf{K}_l (T_h - T_l))} \\ &= \frac{(T_l - \mathcal{R}_{\mathtt{DRA}(T)} \dot{Q}_{\text{evap.}}) \times \dot{Q}_{load}}{\dot{Q}_{\text{evap.}}(\mathcal{R}_{\mathtt{DRA}(T)} \dot{Q}_{\text{evap.}} + \Delta T_{hl})} \end{aligned} \tag{2.14}$$

where

$$\mathcal{R}_{\mathtt{DRA}(T)} = \frac{(\mathsf{K}_h + \mathsf{K}_l)}{\mathsf{K}_h \mathsf{K}_l}$$

and

$$\Delta T_{hl} = (T_h - T_l)$$

Note that as the conductances (K_h and K_l) become infinitely large $\mathcal{R}_{\mathtt{DRA}(T)}$ vanishes, with $T_h \rightarrow T_{\text{cond.}}$ and $T_l \rightarrow T_{\text{evap.}}$. Also, as the heat ingressing into the system diminishes, $\dot{Q}_{load} \rightarrow \dot{Q}_{\text{evap.}}$ and the conditions effectively tend towards the ideal *i.e.*, eqn (1.14), the equation for the measured COP of the DRA approaches eqn (1.2), the Carnot relation for the prime–mover.

Using base parameters $\mathcal{R}_{\mathtt{DRA}(T)} = 0.8\,^{\circ}\mathrm{C/W}$, (compartment) $\mathcal{R}_{(T)} = 0.5\,^{\circ}\mathrm{C/W}$, $T_l = 4\,^{\circ}\mathrm{C}$, $T_h = 25\,^{\circ}\mathrm{C}$ a simple parametric study of eqn (1.14) was undertaken for varying Q_{load}.

Figure 1.3 on page 19 is a parametric display of the effect of load demand with changing $\mathcal{R}_{\mathtt{DRA}(T)}$ on the profile of eqn (1.14) (the measurable *in situ* prime–mover performance COP). Of particular interest is the dependency of loading conditions on machine performance.

Figure 1.4 on page 19 is another parametric plot (apparent $\mathtt{COP}_{\mathtt{DRA}}$ vs. Q_{load}) indicating the effect of changing compartment thermal resistance $\mathcal{R}_{(T)}$. Notice the strong dependence on the relative proportions of $\dot{Q}_{load} : \dot{Q}_i$, or in other words the systems' insulative properties. The measured *in situ* COP in this case increases markédly as the compartment thermal resistance $\mathcal{R}_{(T)}$, the implication being, the better the insulation the greater the benefit obtained from the prime–mover.

Likewise parametric displays Figure 1.5 on page 20, indicate the effect of changes in the apparent COP with T_l and T_h respectively. These illustrate the expected increases in $\mathtt{COP}_{\mathtt{DRA}}$ with decreasing T_h and increasing T_l. The charts also take into account the changes in Q_i as a result of these variations.

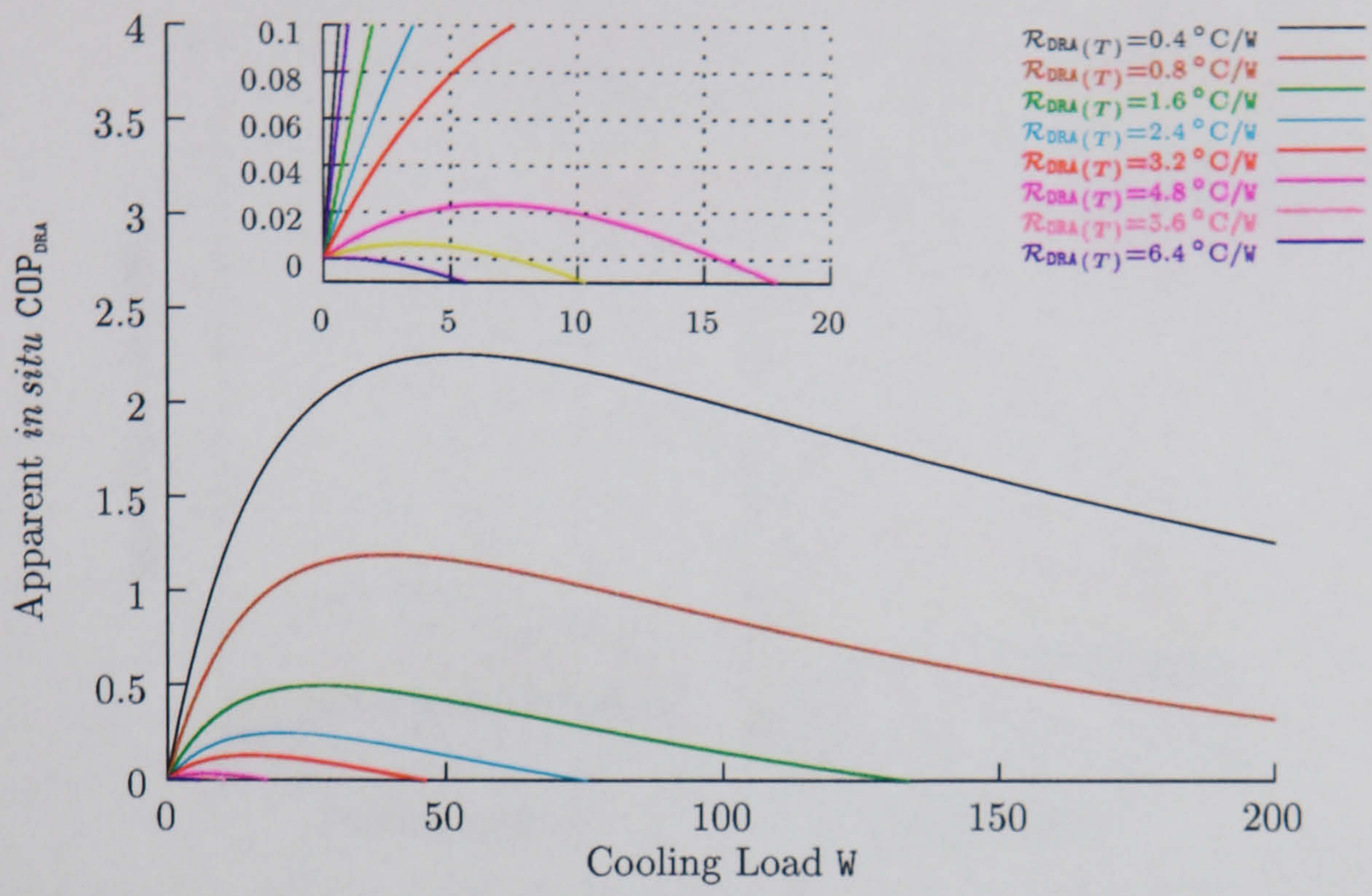


Figure 2.3: The effect of $\mathcal{R}_{\text{DRA}(T)}$ on changes in*in situ* COP vs. Q_{load} eqn (1.14)

Base parameters $\mathcal{R}_{\text{DRA}(T)}$ =0.8 °C/W, (compartment) $\mathcal{R}_{(T)}$ = 0.5 °C/W, T_l = 4 °C,T_h = 25 °C.

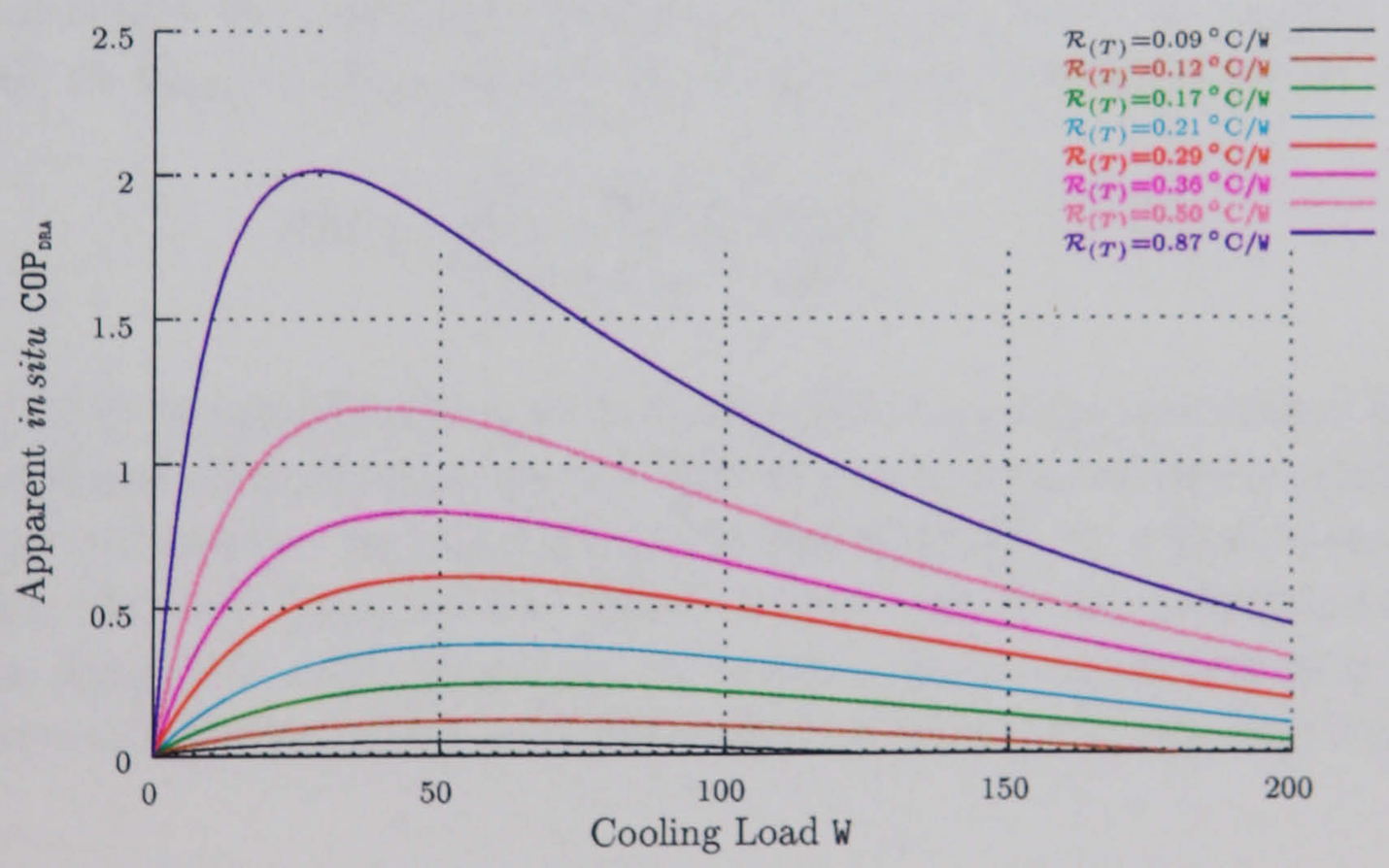


Figure 2.4: The effect of compartment $\mathcal{R}_{(T)}$ on changes in *in situ* COP vs. Q_{load} eqn (1.14)

Base parameters $\mathcal{R}_{\text{DRA}(T)}$ = 0.8 °C/W, (compartment) $\mathcal{R}_{(T)}$ = 0.5 °C/W, T_l =4 °C, T_h = 25 °C.

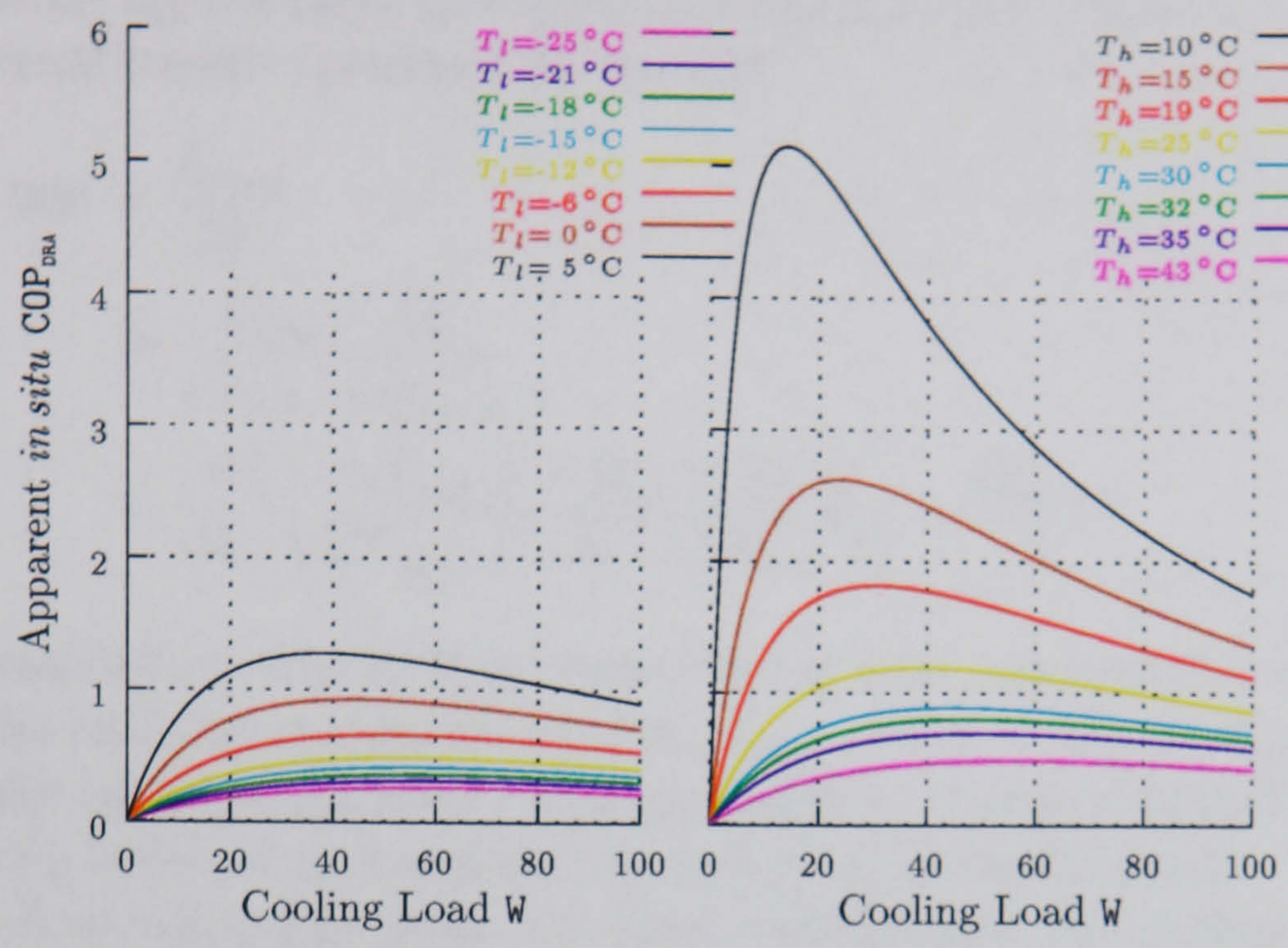


Figure 2.5: The effect of changes in T_l (left) and T_h (right) on *in situ* COP eqn (1.14)

Base parameters $\mathcal{R}_{\text{DRA}(T)}$= 0.8 °C/W, (compartment) $\mathcal{R}_{(T)}$ = 0.5 °C/W, T_l = 4 °C,T_h = 25 °C.

In situations where the appliance load greatly exceeds the heat ingress *i.e.* $Q_{load} >> Q_i \Rightarrow Q_{load} \rightarrow Q_{\text{evap.}}$, eqn (1.14) would be somewhat modified *viz*:

$$\text{COP} = \frac{(T_l - \mathcal{R}_{\text{DRA}(T)}\dot{Q}_{\text{evap.}})}{\mathcal{R}_{\text{DRA}(T)}\dot{Q}_{\text{evap.}} + \Delta T_{hl}} \tag{2.15}$$

While eqn (1.14) and eqn (1.15) may well represent *in situ* prime–mover COP sufficiently for theoretical characterisation, the COP of real systems differ markédly from their theoretical estimates. In order for pertinent analysis of a real system to be undertaken, the characteristics of the prime–mover has to be determined experimentally[1]. The data is usually presented in discrete form, consisting of a range of internal and external temperatures as well as the experimentally–observed estimates for the COP.

[1]This is routinely done by DRA manufacturers and the ISO standard recommends a rather complicated procedure for this. This procedure is probably followed by the prime–mover manufacturers; however a more common practice in the DRA industry is to measure the electrical energy required to cool a given load and find the quotient of these figures in different environments.

As before modifying the basic COP definition eqn (1.1) (see Figure 1.1 on page 14) to reflect the actual benefit furnished by the DRA

$$\begin{aligned} \mathtt{COP} &= \frac{\dot{Q}_{load}}{\dot{W}} \\ &= \frac{\dot{Q}_{evap.} - \dot{Q}_{i}}{(\dot{Q}_{cond.} - \dot{Q}_{evap.})} \\ &= \frac{(\mathsf{K}_{l} \cdot |\Delta T_{evap.,l}| - \mathsf{K}_{i} \cdot |\Delta T_{h,l}|)}{(\mathsf{K}_{h} \cdot |\Delta T_{cond.,h}| - \mathsf{K}_{l} \cdot |\Delta T_{evap.,l}|)} = \frac{\dot{Q}_{heater}}{\dot{W}} \end{aligned} \tag{2.16}$$

On the understanding that K_i is an approximate heat transmission conductance characterising the heat ingress into the system, $T_{cond.} > T_{amb.} > T_{DRA} > T_{evap.}$, Q_{heater} is an experimentally (arbitrarily) fixed constant quantity of heat supplied by a heater and $\dot{W}$ the energy required to maintain the system at a steady–state.

For a given heat exchanger area, the heat conductance (K) is dependent only on the mean heat transfer coefficient of the heat exchanger (h). This coefficient is usually defined with respect to the physical properties of the convecting fluid at the mean temperature between the exchange surface and the fluid, see Chapman (1984). For a given fluid and over moderate temperature ranges about this mean, the h may be approximated by the form:

$$h \approx a_0 + a_1 \overline{T}^{\,\varsigma} \tag{2.17}$$

$\overline{T}$ being the mean of the bulk fluid and exchanger surface temperatures[1] and the a's and ζ being constants. The effect of the area can be absorbed in the constants a_0 and a_1 thus, eqn (1.16) may be represented as:

$$\mathtt{COP} = \frac{(a_0 + a_1 \overline{T}_{evap.}{}^{\varsigma}) \cdot \Delta T_{evap.} - \text{`}(\mathsf{K} \cdot \Delta T)_i)}{(b_0 + b_1 \overline{T}_{cond.}{}^{\varsigma}) \cdot \Delta T_{cond.} - (a_0 + a_1 \overline{T}_{evap.}{}^{\varsigma}) \cdot \Delta T_{evap.}} \tag{2.18}$$

The values of the a's (evaporator), b's (condenser), K_i and ζ particularise eqn (1.18) to a given system based on the data available and

$$\begin{aligned} \Delta T_{cond.} &= (T_{cond.} - T_{h}) \\ \Delta T_{evap.} &= (T_{l} - T_{evap.}) \\ \Delta T_{i} &= (T_{h} - T_{l}) \\ \overline{T}_{cond.} &= (T_{cond.} + T_{h})/2 \\ \overline{T}_{evap.} &= (T_{l} + T_{evap.})/2 \end{aligned}$$

[1] Admittedly some other authors use ΔT rather than $\overline{T}$, *e.g.* see Sparrow (1970); however the practice seems harder to justify on the basis of correlations considered for the purpose.

During service, DRA's tend to go through several transient stages where the ambient air is suddenly raised in consequence of some human interaction (*e.g.* a 'door opening' or the insertion of a thermal 'load'). Significant changes in air temperature have an effect on the *short term* COP of the prime–mover. In order to circumvent this, a 'thermal storage buffer' may be placed on the evaporator surface acting as a thermal interface between the prime–mover heat exchanger and the DRA interior air. Depending on the operating temperature of the 'buffer' this can help to define and regulate $T_{evap.}$ within other confines of the system. Importantly, this 'buffer' can also influence the COP of the prime–mover by ensuring its operation at a strictly controlled evaporating temperature and consequently.

2.4.2 Other Heat Transfer Considerations

Some modern DRA manufacturers install fans to enhance circulation in an attempt to increase the overall heat transfer coefficient (U) of the heat exchanger by increasing the heat transfer coefficient (h) rather than, say, increasing exchanger surface areas. The following analysis examines the validity of this practice in terms of its usefulness in improving DRA performance; considering only the simplest of effects and on the understanding that the effect of the associated component efficiencies and friction coefficients (both < 1) serve to further *diminish* the energy consumption efficiency of the system, the analysis, neglecting both these considerations, is laid out as indicative of an upper bound on 'performance'.

Mass flow

For such an implementation, the fan power requirement is proportional to the cube of its mass flow requirement *i.e.* assuming constant densities

$$\begin{aligned} \dot{W} &\geqslant \frac{Force \times distance}{time} = Pressure \times Area \times velocity \\ &\geqslant \frac{\mathsf{P} \times \dot{\mathsf{m}}}{\rho_{\mathsf{m}}} \\ &\geqslant \frac{\dot{\mathsf{m}}^3}{2.(\rho_{\mathsf{m}}.A)^2} \end{aligned} \tag{2.19}$$

A in this case being the fan cross–sectional flow area[1].

The heat transfer coefficient

The flow Nusselt[2] number (Nu), and by definition h, is proportional to the

[1] Also, see any standard text on the subject *e.g.* Duncan et al. (1981).

[2] **Nusselt, Enerst Kraft Wilhelm** *(1882–1957).* German engineering scientist. He was the first to apply the principles of dimensional analysis to the mathematical formulations of heat and then mass transfer; the concept of

Reynolds[1] number (Re) raised to some exponent m, say; this may be represented by a general convection coefficient correlation:

$$\begin{aligned} \mathrm{Nu} &\propto C\mathrm{Re}^{\mathrm{m}} \\ &\approx C \cdot \left(\frac{\dot{\mathrm{m}} \cdot L}{\mu \cdot A}\right)^{\mathrm{m}} \end{aligned} \tag{2.20}$$

A in this case being the fan cross–section area and L some characteristic dimension.
Typically $(\mathrm{m} < 1)$[2], see Chapman (1984) and Incropera and DeWitt (1990) for some correlations for flat plates[3].

From eqn (1.19) and eqn (1.20) the following conclusions may be drawn:

- Mass flow can only be doubled at the expense of an eight–fold power requirement ($\dot{W} \propto \dot{\mathrm{m}}^3$).
- Doubling the mass flow will increase h, but by a factor of less than two *viz* 2^m as $h \propto \dot{\mathrm{m}}^{\mathrm{m}}$.

Combining these two results yields

$$\dot{W} \propto \dot{Q}^{\left(\frac{3}{m}\right)} \propto h^{\left(\frac{3}{m}\right)} \tag{2.21}$$

If the heat transfer coefficient, h, on account of increasing the power to the fan, is designated as $h + \triangle h \equiv \epsilon h$, then the changes in the power requirements $(\dot{W} + \triangle\dot{W})$ are:

$$\dot{W} + \triangle\dot{W} \propto \epsilon^{\left(\frac{3}{m}\right)} h^{\left(\frac{3}{m}\right)} \tag{2.22}$$

With these definitions, the ratio of the 'new' COP to the 'old' COP can then be seen to be:

$$\begin{aligned} \frac{\mathrm{COP}_{new}}{\mathrm{COP}_{old}} &= \frac{(h + \triangle h)\triangle T}{\triangle\dot{W} + \dot{W}} \times \frac{\dot{W}}{h\triangle T} \\ &= \epsilon^{\left(1 - \frac{3}{m}\right)} \end{aligned} \tag{2.23}$$

---

dimensionless *e.g.* Prandtl (Pr), Nusselt (Nu), Reynolds (Re) *etc.* numbers are his brainchild. He made numerous other contributions in several areas of convective (heat and mass) transport.

[1] **Reynolds, Osborne** *(1842–1912)*. English engineering scientist. Worked principally in hydraulics and hydrodynamics. He formulated a theory of lubrication and developed the standard mathematical framework used in the study of turbulence.

[2] This is true even for the most severe case of jet impingement.

[3] Some other relevant correlations are given in Guyer and Brownell (1988).

The situation can be much worse as fans placed within the DRA cooling compartment dissipate heat equivalent to the fan power consumption ($\equiv \dot{W}$), thus reducing the effective cooling capacity of the DRA. From thermal performance considerations, fan installations may be necessary (for instance for convection control, where either the heat exchangers are located in regions where the air flow is restricted or would otherwise have regions of stagnation in their ducting *e.g.* horizontal cross–flow heat exchangers). However, it is clear that the practice has severe limitations from the standpoint of increasing systems energy efficiency. As a result of this, before the addition of any gadget (and thereby increased level of complexity) is addended to the basic DRA design, all options for maximising the benefit of the basic device should be explored. Placing this within the context of increasing exchanger conductance, an increased surface area should be considered as a better alternative to fan inclusion[1], *after* due consideration has been given to the basic exchanger design and geometry.

2.5 Heat Ingress Inhibition

Introduction

This section briefly covers the role thermal insulants have to play in the design of DRA's and outlines the various options which may bear upon DRA design, see also Smith and Porter (1990). Arguably, the most important aspect of an energy-conscious, DRA design is the inhibition of heat ingress into the system, the rationale being, 'if the heat can not get into the system, there will be no need to get it out'. Of more than the 80% of the current DRA energy consumption[2] attributed to heat ingress into the system [ASHRAE, 1994, Chapter 48], some 52% entrains through the system's insulative shell. There are several criteria for the optimisation of the thickness and type of insulation used on such systems [Bejan, 1979; Malloy, 1969; Bar-Cohen and Rohsenow, 1984; Sciubba and Bejan, 1992; Bejan, 1993]. Cost usually plays a major role in the specifications (see Malloy (1969), Wells (1971), Barnhart (1974)), alongside considerations of aesthetics and practicality (*e.g.* toxicity, fluid impermeability, physical strength *etc.* [Probert, 1967; Merler, 1968]). These factors tend to override the technical ones as in *theory*, the amount of heat ingress into the system can be reduced without limit as the amount of insulation is increased in similar manner. However, the economic and even technical rationale of this is called into question beyond some finite limit see Probert and Giani (1976). Figure 1.6 on page 25 is

[1] That said, whilst increasing the evaporator surface area has its merits, the limitations of this in the guise of the current DRA design will become clear later, see section 6.3.3 on page 220.

[2] Not including user–associated heat loads.

a graph of the relationship between the thickness of the applied insulant and the thermal conductance for a 200 litre (cubic) compartment based on correlations given in the literature (see Appendix B on page B-264); also, Figure 1.7 on page 26 is a computational prediction of the relation between energy use and insulation thickness for a 200 litre refrigerator with a constant COP = 1 (culled from Guldbrandsen et al. (1986)). The diminishing benefit of simply increasing insulant thickness is apparent and indicative of the need for further research into higher quality insulants. Within the aforementioned economic limit though, technical considerations as to how the insulation can be optimally placed and proportionally distributed have been arrived at [Lim et al., 1992; Bejan, 1993]. Lim and Bejan (1994), have also applied the concept to the theoretical design of insulant distribution in DRA's of the fridge–freezer type.

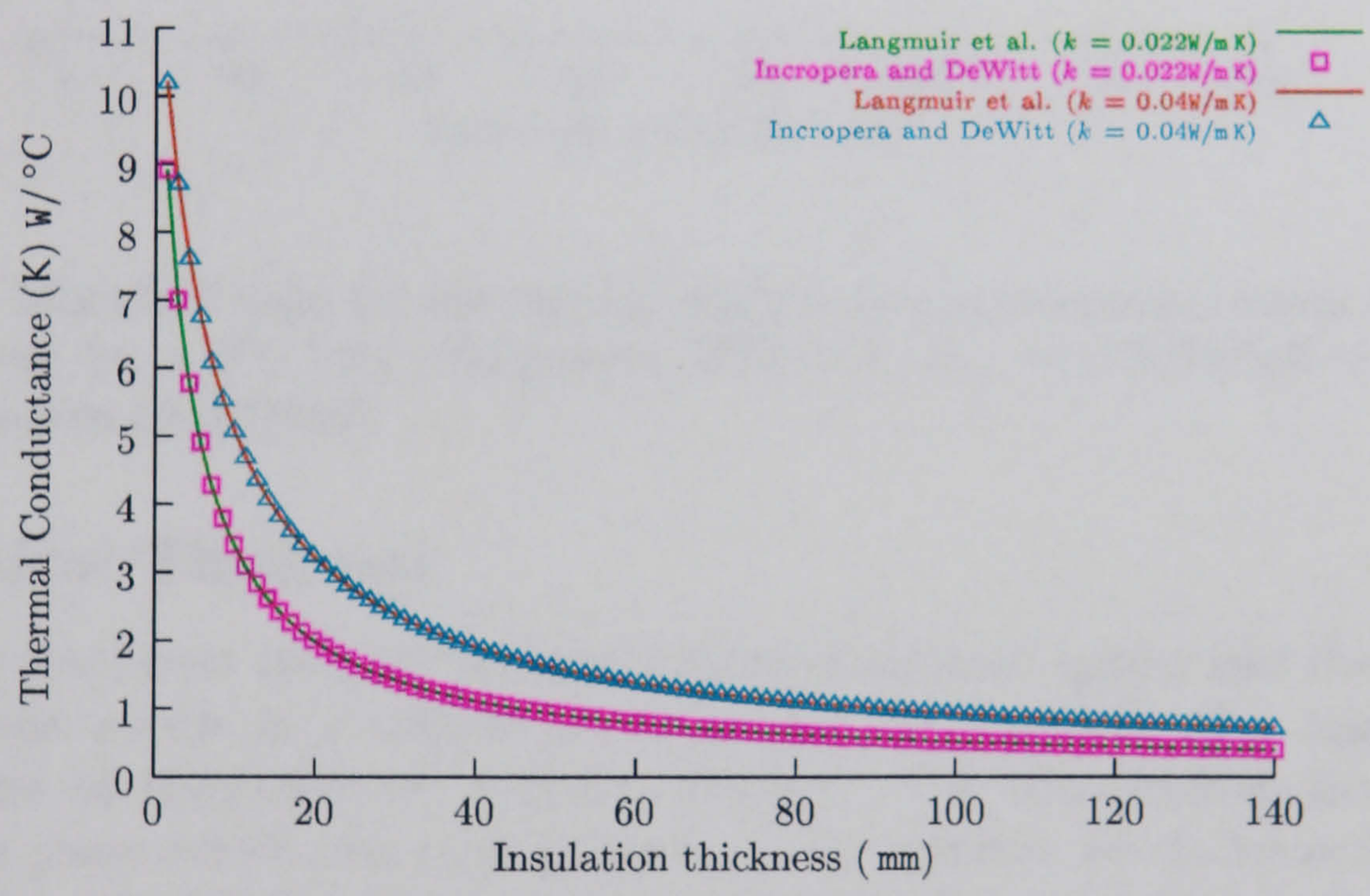


Figure 2.6: The relationship between the thermal conductance and insulant thickness in a (200 litre) cubical compartment; exterior heat transfer coefficient (h) 6W/m² °C, based on Langmuir et al. (1913) and correlations given on *pp.* 88 of Incropera and DeWitt (1990).

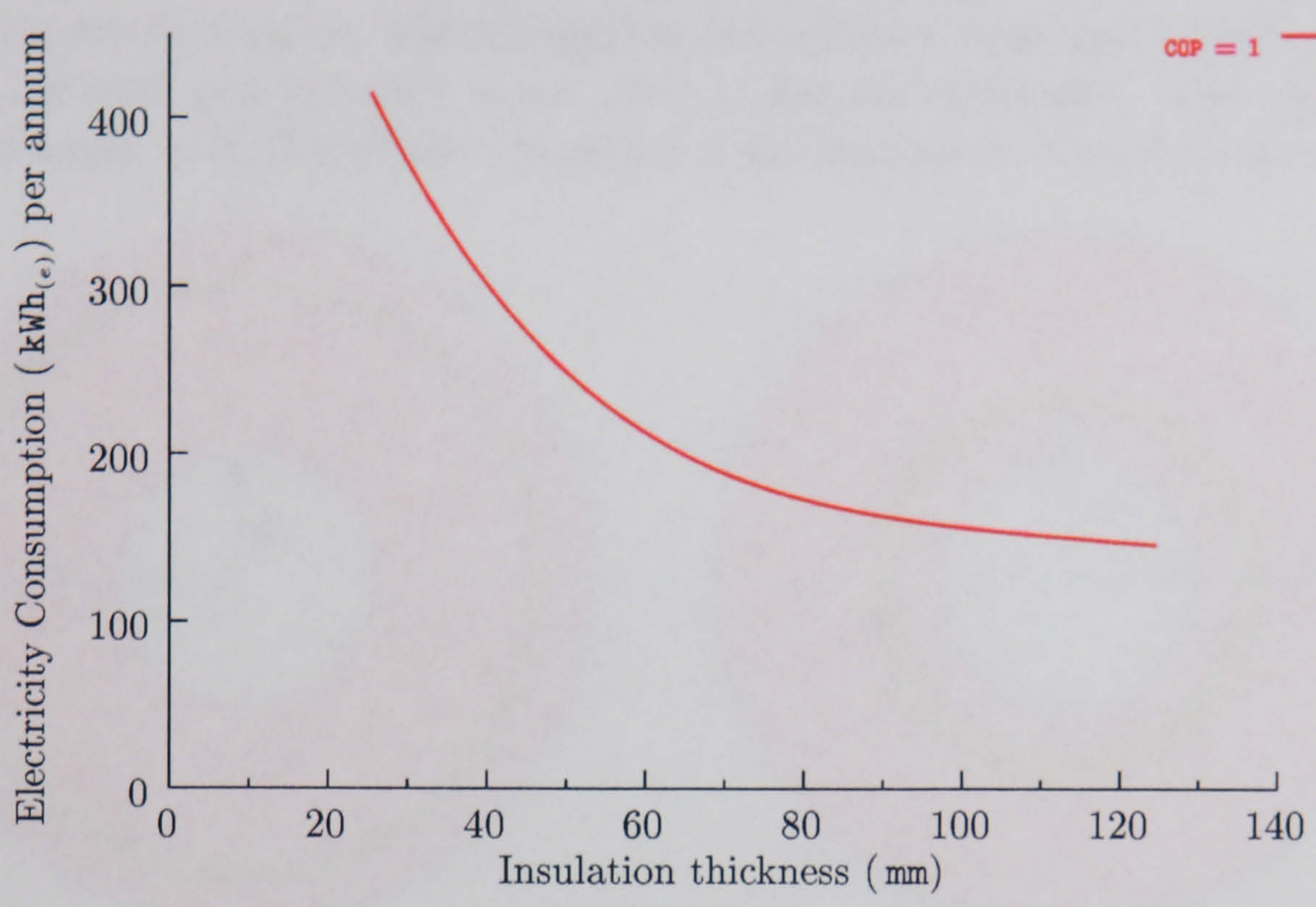


Figure 2.7: Modelled data for the annual electricity consumption versus insulation thickness for a 200 litre refrigerator (COP = 1, $k_{(T)} = 0.029\mathrm{W/m\,K}$) culled from Guldbrandsen et al. (1986).

2.5.1 Critical Thickness

The *steady–state* heat transfer between insulated enclosed spaces and their surrounding ambient occurs in a manner as to permit the definition of a minimum critical thickness of insulation for a given insulant. The phenomenon has been well defined for some curvilinear type geometries, for instance see Sparrow (1970), Chapman (1984), Aziz (1997). Comparatively more recently, some authors have attempted to deduce similar correlations for prismatic [Balcerzak and Raynor, 1961] and square [Hsieh, 1980; Aziz, 1983] exterior sections[1] and to state a formal theory for the phenomenon [Hsieh and Yang, 1984]. As yet, the case for insulation on rectangularly hollow, cuboidal geometries remains undetermined. In general, the applicability of this principle is limited to small geometries and for any appreciable enclosed volume, the value of the critical thickness would be small. Aziz (1997) attempts to pool all the available information into one document which contains a number of solved examples.

[1]The internal sections are usually assumed to be of circular or ellipsoidal cross–section.

2.5.2 Composite Insulant Distribution

Also of interest is the bearing of the relative location of the thermal insulants (of differing conductivities, which together constitute a composite insulant) on the resultant insulant conductance when used to lag an enclosure. The value of the insulant changes with the relative location of the insulants. This may be illustrated

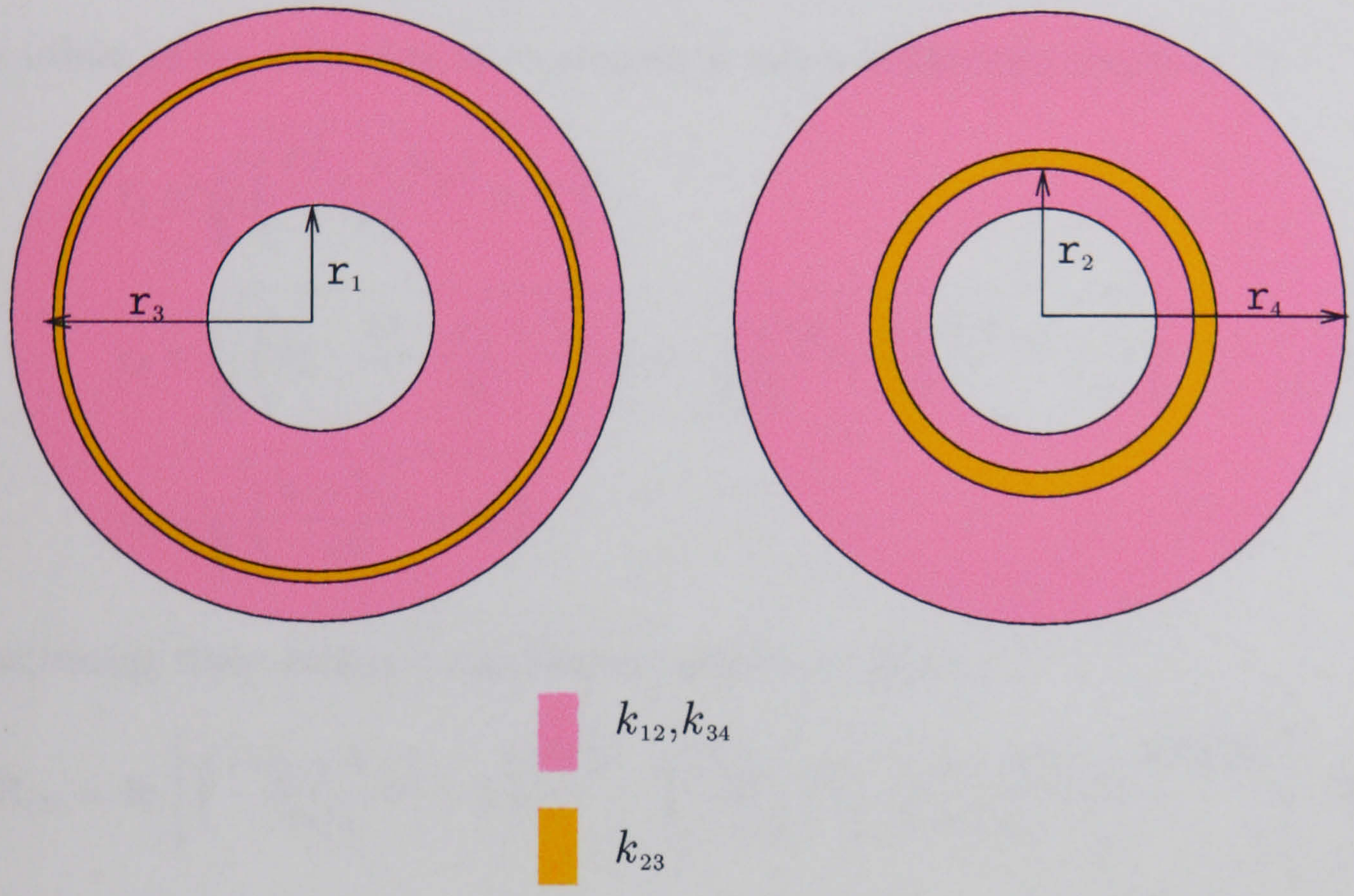


Figure 2.8: Diagram indicating two instances of different distributions of thermal insulation within a two component insulation system.

with the case of a steady–state pipe of uniform cross–section and infinite length (L), lagged in three tiers with two different insulants (with volumes $\mathsf{a}\cdot V_{12}$, V_{23} and $V_{34} = \mathsf{b}\cdot V_{12}$, such that $\mathsf{a}+\mathsf{b} = 1$), see Figure 1.8 on page 27. The pertinent quantity is the resultant thermal resistance which may be represented as:

$$\mathcal{R}_{(T)} = \frac{\ln \frac{r_4}{r_3}}{2\pi L k_{12}} + \frac{\ln \frac{r_3}{r_2}}{2\pi L k_{23}} + \frac{\ln \frac{r_2}{r_1}}{2\pi L k_{12}}$$

$$= \ln \left(\frac{r_4}{r_3}\right)^{\frac{1}{2\pi L k_{12}}} + \ln \left(\frac{r_3}{r_2}\right)^{\frac{1}{2\pi L k_{23}}} + \ln \left(\frac{r_2}{r_1}\right)^{\frac{1}{2\pi L k_{12}}} \tag{2.24}$$

$$= \ln \left[\left(\frac{r_4}{r_1}\right)^{\frac{1}{2\pi L k_{12}}} \cdot \left(\frac{r_3}{r_2}\right)^{\frac{k_{12}-k_{23}}{2\pi L k_{12} k_{23}}} \right]$$

From the basic relations

$$V_{23} = \pi\left(r_3^2 - r_2^2\right)$$
$$(a+b)V_{12} = V_{12} = \pi\left[\left(r_2^2 - r_1^2\right) + \left(r_4^2 - r_3^2\right)\right]$$
$$(aV_{12} + V_{23}) = \pi\left(r_3^2 - r_1^2\right)$$

The values of the radii may be expressed in terms of the base radius r_1 *i.e.*

$$r_4 = \sqrt[2]{\left(\frac{(V_{12}+V_{23})}{\pi L} + r_1^2\right)}$$

$$r_3 = \sqrt[2]{\left(r_4^2 - \frac{(1-a)\times V_{12}}{\pi L}\right)} = \sqrt[2]{\left(\frac{(a\times V_{12}+V_{23})}{\pi L} + r_1^2\right)} \qquad (2.25)$$

$$r_2 = \sqrt[2]{\left(\frac{a\times V_{12}}{\pi L} + r_1^2\right)}$$

Substituting these values in the thermal resistance gives

$$\mathcal{R}_{(T)} = \ln\left[\left(\frac{(V_{23}+V_{12})}{\pi r_1^2 L}+1\right)^{\frac{1}{4\pi L k_{12}}} \cdot \left(\frac{(V_{23}+a\times V_{12}+\pi r_1^2 L)}{(a\times V_{12}+\pi r_1^2 L)}\right)^{\frac{k_{12}-k_{23}}{4\pi L k_{12}k_{23}}}\right] \qquad (2.26)$$

Equation (1.26) represents the resultant thermal resistance of the composite insulant in terms of constants for a given setup and variable a. Importantly, depending on the magnitude of a ($0 < a < 1$) the *location* of the central insulant will *vary*, as would the *value* of the thermal resistance $\mathcal{R}_{(T)}$. The actual manner would depend on the relative magnitudes of the thermal resistivities and volumes of the insulants involved. The same analysis may be carried out for a sphere with similar observations. In such a case the pertinent equation is

$$\mathcal{R}_{(T)} = \frac{1}{a\pi}\left[\frac{1}{k_{12}}\left(\frac{1}{r_1}-\frac{1}{r_4}\right) + \left(\frac{k_{12}-k_{23}}{k_{12}k_{23}}\right)\cdot\left(\frac{1}{r_2}-\frac{1}{r_3}\right)\right] \qquad (2.27)$$

with the necessary relational changes being:

$$r_4 = \sqrt[3]{\left(\frac{3\cdot(V_{12}+V_{23})}{4\pi L}+r_3^2\right)}$$

$$r_3 = \sqrt[3]{\left(\frac{3\cdot(aV_{12}+V_{23})}{4\pi L}+r_1^3\right)} \qquad (2.28)$$

$$r_2 = \sqrt[3]{\left(\frac{3aV_{12}}{4\pi L}+r_1^3\right)}$$

The conclusion in both cases is: in instances where V_{23} is (presumably) smaller than V_{12}, typically where k_{23} is a higher quality and costlier insulant, it is generally more expedient to place this lower conductivity insulant on the inside of the enclosing composite insulation.

Also of interest is the question as to whether the results remain the same if the thickness (as opposed to the volume) of each individual type of insulation were kept constant. In such a case eqn (1.24), for the cylinder, and eqn (1.27), for the sphere, would remain unchanged. However there would be changes to the radii definitions *viz*:

$$\begin{aligned} r_4 &= \triangle r_{12} + \triangle r_{34} + \triangle r_{23} + r_1 \\ r_3 &= \triangle r_{12} + \triangle r_{23} + r_1 \\ r_2 &= \triangle r_{12} + r_1 \end{aligned} \qquad (2.29)$$

with $(\triangle r_{12} + \triangle r_{34})$ and $\triangle r_{23}$ being constants and, $\triangle r_{12} = a\cdot(\triangle r_{12} + \triangle r_{34})$

The conclusion is again the same: for the most effective and economic (in terms of both material and energy cost) use of composite, enclosing insulation, the better insulant is best placed internal to the lower quality insulant. Hence, this is true irrespective of whether the insulant volumes or thicknesses are kept constant. Figures 1.9 and 1.10, *qv.* pages 30 and 30 respectively are plots indicating this for a cylinder and a sphere respectively (in steady–state).

2.5.3 Temperature–Time Lag

One of the most fundamental behavioural characteristics of the response of real systems to perturbations is the existence of a delay between the initial disturbance and the response of the system. This delay, or lag, is function of the magnitude of the pertinent inertial quantity. The knowledge of these response delay characteristics can aid systems understanding and facilitate design. With respect to thermal

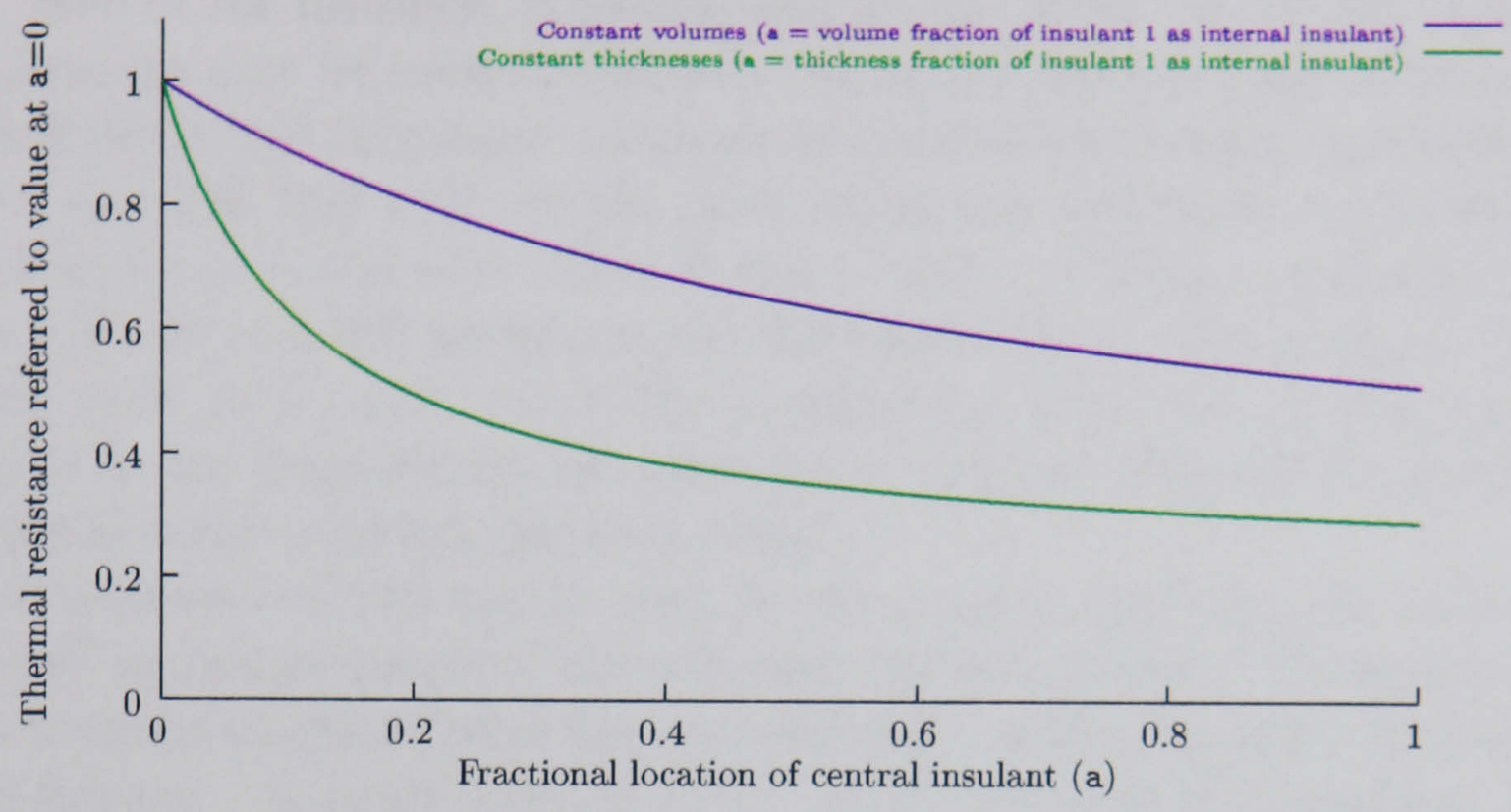


Figure 2.9: Variation of thermal resistance ratio $\left(\frac{\mathcal{R}_{(T)}(0<=a<=1)}{\mathcal{R}_{(T)}(a=0)}\right)$ for a cylinder of composite insulation with the location of low conductivity insulant.

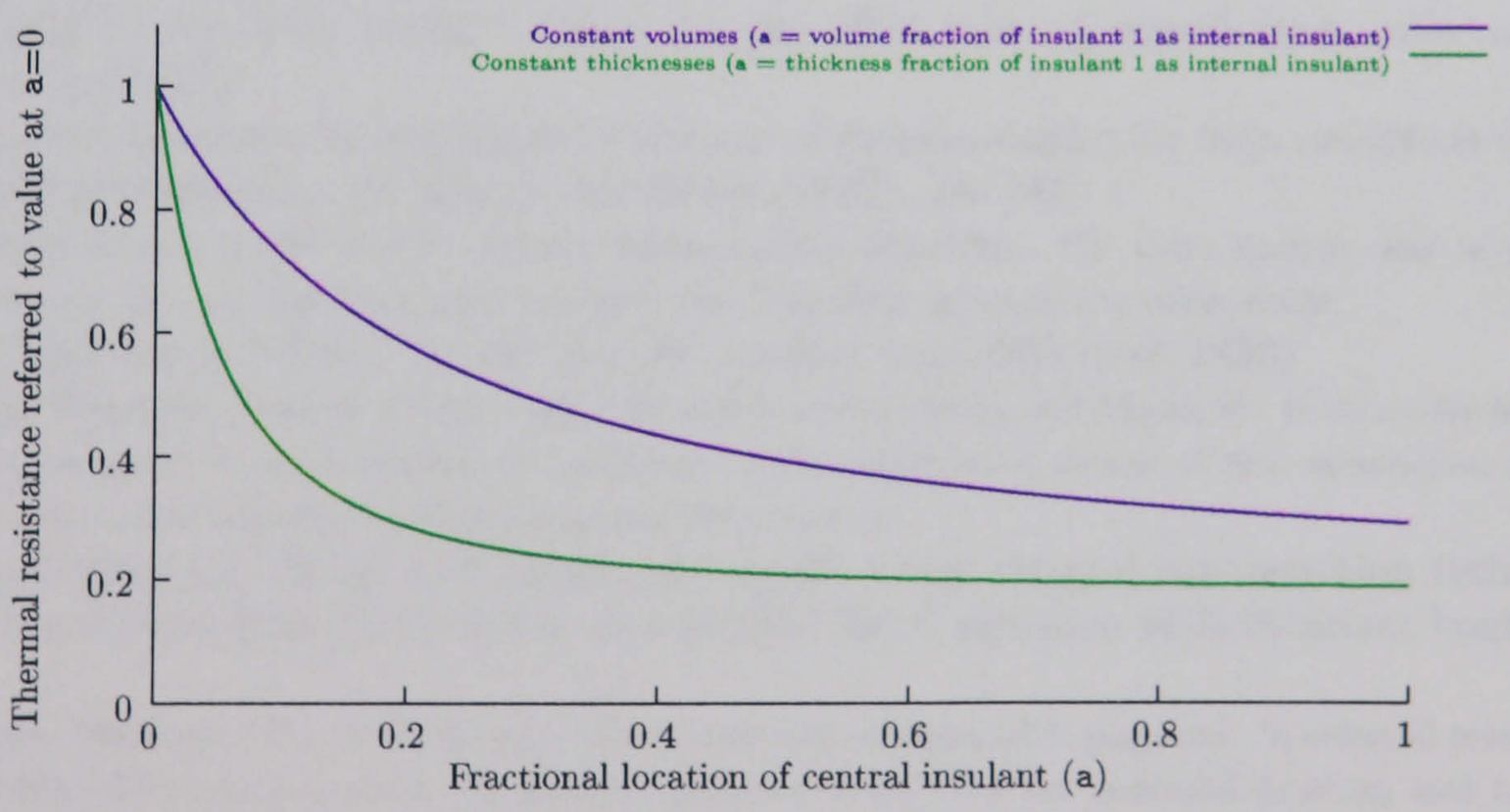


Figure 2.10: Variation of thermal resistance ratio $\left(\frac{\mathcal{R}_{(T)}(0<=a<=1)}{\mathcal{R}_{(T)}(a=0)}\right)$ for a hollow sphere of composite insulation with the location of low conductivity insulant.

systems the existence of this lag forms the basis of several heat transfer methodologies. The phenomenon has been exploited to advantage in different aspects of heat transmission. Kelvin for instance, [Carslaw and Jaeger, 1959, on *pp.* 84] indicates how the phenomenon may be used to estimate the age of the earth and it forms the basis of the Ångström and Neumann methods of estimating thermal conductivities [Carslaw, 1945, *pp.* 136 and 146]. It has been utilised in optimising the design of building structures *e.g.* in the root cellar [Keener, 1988, *pp.* 380] and the so–called Norman church [Probert, 1993] problems *etc.* All these fall into the general class of so–called 'thick wall' problems[1], where the requirement is to deduce the time lag between changes in the temperature on some plane and the corresponding changes on a parallel plane some specified distance away[1].

Solutions to problems of this nature may be obtained by applying the Duhamel[2] integral theorem[3] to the solutions of the relevant classical Fourier[4] [Freeman, 1955] transient heat transfer problem (with time invariant boundary conditions) to obtain the required solutions[5]. Another method is the use of the Laplace[6] transform, [Eckert and Drake, *op. cit.* (Chapter 4); Carslaw and Jaeger, *op. cit.* (Chapters XIII and XV); Carslaw, *op. cit.*]. Solutions thereof may be represented in terms of the temperature 'in excess' of the mean value of the fluctuating boundary condition(s) and indicate the extent of the delay between a thermal disturbance and associated response, as well as the degree of attenuation at some remote depth.

DRA's are utilised in environments where there are diurnal differences in the ambient temperature[7], where it can be envisaged that the heat ingress profile with

---

[1]'Thick', strictly in the heat transfer sense, *i.e.* the Biot lumped capacitance criterion *viz*: Bi $>$ 0.1, see Heisler (1947).

[1]The phenomenon is extremely important in the use of thermocouples for data collection within transient thermal environments, see Eckert and Drake (1972), *pp.* 141.

[2]**Duhamel, Jean–Marie** *(1797–1872).* French Mathematical Physicist. His main interest was in partial differential equations; he then applied his results (notably the 'Duhamel principle') to other fields.

[3]See Carslaw and Jaeger (1959), *op. cit. pp.* 30, original work Duhamel (1833)

[4]**Fourier, Jean Baptiste Joseph** *(1768–1830).* French Mathematician and Physicist. Famous for his pioneering work in trigonometric series expansion of functions. His mathematical theory of heat conduction ([Freeman, 1955]) is one of the most important published in the 19th century.

[5]Boelter et al. (1965), *pp.* 244 *ff.* and 252 *ff.*, give another non–integral superposition technique of obtaining such solutions from the solution to a similar 'heat' equation with invariant boundary conditions.

[6]**Laplace, Pierre–Simon** *(1749–1827).* French astronomer and mathematical physicist. In celestial mechanics he proved the stability of the solar system. In analysis, Laplace introduced the potential function and Laplace coefficients; he also put the theory of mathematical probability on a sound footing, contributing to the foundations of the mathematical science of electricity and magnetism.

[7]Even in thermally regulated dwellings, it is not atypical to have temperature regulators turned off during certain periods of the day.

time, $\dot{Q}_i$[8], into the system will vary accordingly. The central idea here is to exploit the phase difference (thermal lag) between ambient temperature variations and their resulting effect on the interior of DRA's; offsetting this against the dependence of prime–mover COP on ambient temperature, thus ensuring that the worst ambient effects 'occur' at, thermodynamically, the most expedient cooling periods.

By way of simplification, it is here assumed that the behaviour of a single wall may suffice to characterise the response of the DRA *i.e.* that the problem is one dimensional. Lending credence to this assumption is the observation that:

- Typically the length–to–thickness ratios of the walls of conventional DRA's result in aspect ratios which would justify this assumption. From experience, this ratio is usually in excess of five.

Thus, one may mathematically represent the thermal circumstance of the DRA wall with a one (x) dimensional Fourier equation as:

$$(\nabla_t - \alpha \nabla_x^2)\, T_{wall} = 0 \tag{2.30}$$

and the boundary conditions

$$\begin{aligned} (-k \cdot \nabla_x + h) \cdot (T_{wall}(x=0) - T_{\text{DRA}}) &= 0 \\ h\left(T_{wall}(x=L) - T_{\text{amb.}}\right) + k \cdot \nabla_x T_{wall}(x=L) &= 0 \end{aligned} \tag{1.30-a}$$

$$T_{wall}(x,t) = \zeta(x) \quad \forall t \le 0 \tag{1.30-b}$$

$$T_{\text{DRA}}(x<0 : \forall t) = T_{\text{DRA}} \quad ; \quad T_{\text{amb.}}(x>L : \forall t) = \psi(t) \tag{1.30-c}$$

L being the wall thickness; where the boundary temperatures are: for the DRA interior environment T_{DRA} (presumed constant) and $T_{\text{amb.}}$ the DRA exterior (periodically varying with time) *i.e.* @ x = L, $T_{\text{amb.}} = \psi(t)$. To facilitate solution, the linearity of the governing equation and boundary conditions may be exploited thus[1]: T_{wall} may be further broken up into the sum of two functions, $T_I(\ldots)$ and $T_{II}(\ldots)$, each being the solution of the same differential equation with (differing) simpler boundary conditions[2]. These together, constitute the boundary conditions of the original problem. In the present case, these boundary conditions may be expressed as represented in Table 1.1 on page 32:

Barring differences in orientation and in the temporal variation of one of the 'ambient' temperature conditions, these boundary conditions are in essence the same. The T_{II} solution to eqn (1.30) is the more complex of the two and may be obtained

[8]Excluding utilisation associated impacts *e.g.* effect of door openings *etc.*
[1]See Gröber et al. (1961) and Boelter et al. (1965), *pp.* 244 *ff.* and 252 *ff.*
[2]See Carslaw and Jaeger (1959), *loc. cit. pp.* 29-30.

Boundary Conditions	$T_I(\ldots)$	$T_{II}(\ldots)$
$x = 0$	$k \cdot \nabla_x T_{wall} = 0$	$(-k \cdot \nabla_x + h) \cdot (T_{wall} - T_{DRA}) = 0$
$x = L$	$(h + k \cdot \nabla_x) \cdot T_{wall} + h \cdot T_{amb.}$	$k \cdot \nabla_x T_{wall} = 0$
Initial condition	$T_{wall}(x, t \leq 0) = \zeta(x)$	$T_{wall}(x, t \leq 0) = 0$

Table 2.1: Break–down of the boundary conditions (a–c) given in eqn (1.30)

from the T_I solution by a simple affine transformation and the application of the Duhamel integral theorem. The solution to T_I may be obtained by one of the standard techniques. Though the procedures are quite straightforward, the classical solutions (orthogonal series expansions), can be cumbersome both to obtain and to use further. This may be partly reduced by observing that in the event that the pertinent Fourier number exceeds a certain critical value (0.2), the classical solutions of eqn (1.30) may be reduced to the leading term of the expansion, see Incropera and DeWitt (1990), *pp.* 239 *ff.*

Other 'approximate' techniques exist, for instance Goodman (1958, 1961, 1964) adapted the integral boundary layer technique to the solution of the 'heat' equation. The method gives 'approximate' results, the accuracy of which may be arbitrarily defined depending on the chosen equation profile and the extent[1] to which the method is applied [Goodman, 1964]. The method has been demonstrated to be sufficiently reliable to apply to most engineering problems, particularly if the solution profile is known *a priori* or can be estimated from solution of similar problems; see also Gröber et al. (1961) and Boelter et al. (1965).

For the current application, analysis based on that given in Gröber et al., *loc. cit.*, has been used and as such would not be repeated here. It will be sufficient to present just that part of the solution which characterises the thermal lag constant of the DRA wall.

T_I

The T_I solution consists of an exponentially–decaying transient part and a steady–state part (solution to $\nabla_x^2 T = 0$ with the relevant parts of the same boundary conditions) which would reduce to a constant (the steady–state part) as time traverses. The effect this will have on the sum $T_I + T_{II}$ will be simply to add a constant term to alter the solution of T_{II} and as such, in the quest for the thermal lag constant for the wall, may be safely omitted from the ensuing analysis.

[1] Two methods for refining initial solutions are given by Chambré (1959) and Abarbanel (1960).

T_{11}

For convenience defining (a) a new temperature variable, θ, to be the relative temperature *in excess* of the average of the maximum and minimum diurnal temperatures $\overline{T}_{amb.}$ and (b) ω, the fundamental frequency of the components of the Fourier series expansion of the ambient temperature profile[2]. Also by way of information suppression, defining:

$$f_c(u) = \cosh u \cos u$$
$$f_c'(u) = \sinh u \cos u - \cosh u \sin u$$
$$f_s(u) = \sinh u \sin u$$
$$f_s'(u) = \cosh u \sin u + \sinh u \cos u$$
$$\theta_{max} = T_{amb.\ max} - \overline{T}_{amb.}$$

and the non–dimensional parameters :

$$\mathrm{Bi}_L = \frac{h_L}{k}$$
$$\mathrm{Fo}_{\omega,L} = \frac{\alpha}{\omega \times L^2}$$
$$X = \frac{x}{L}$$

L being the DRA wall thickness.

Using the referred principal part of the expansion $\psi(t)$ *i.e.* $\theta_{max}\cos(\omega t)$ as representing the ambient fluctuations, and following the analysis in Gröber et al. (1961), *pp.* 89 *ff.* it is possible to arrive at a solution of the form:

$$\theta_{DRA}(X, \mathrm{Bi}_L, \mathrm{Fo}_{\omega,L}, \omega, t) = \theta_{max} \times \mathrm{Bi}_L \times \sqrt{\frac{A}{B^2 + C^2}} \times \cos(\omega t + \phi(X)) \quad (2.31)$$

[2]According to Carslaw (1945), this is the most important part as the others tend to 'fall off' rapidly with harmonic and wall depth.

with the following definitions in operation

$$A = \left[f_c \left(\sqrt{\frac{\mathrm{Fo}_L}{2}} \cdot X \right) \right]^2 + \left[f_s \left(\sqrt{\frac{\mathrm{Fo}_L}{2}} \cdot X \right) \right]^2$$

$$B = \mathrm{Bi}_L \times f_c \left(\sqrt{\frac{1}{\mathrm{Fo}_{\omega,L} \cdot 2}} \right) + \sqrt{\frac{\mathrm{Fo}_{\omega,L}}{2}} \times f_c' \left(\sqrt{\frac{1}{\mathrm{Fo}_{\omega,L} \cdot 2}} \right)$$

$$C = \mathrm{Bi}_L \times f_s \left(\sqrt{\frac{1}{\mathrm{Fo}_{\omega,L} \cdot 2}} \right) + \sqrt{\frac{\mathrm{Fo}_{\omega,L}}{2}} \times f_s' \left(\sqrt{\frac{1}{\mathrm{Fo}_{\omega,L} \cdot 2}} \right)$$

$$\phi(X) = \arctan \left(\frac{B \times f_s \left(\sqrt{\frac{1}{\mathrm{Fo}_{\omega,L} \cdot 2}} \cdot X \right) - C \times f_c \left(\sqrt{\frac{1}{\mathrm{Fo}_{\omega,L} \cdot 2}} \cdot X \right)}{C \times f_s \left(\sqrt{\frac{1}{\mathrm{Fo}_{\omega,L} \cdot 2}} \cdot X \right) + B \times f_c \left(\sqrt{\frac{1}{\mathrm{Fo}_{\omega,L} \cdot 2}} \cdot X \right)} \right)$$

From the definition of $\phi(X)$ it is possible to deduce the thermal time lag ($\phi(0)$ *i.e.* $x = 0$) for a given DRA wall thickness, given the relevant physical properties. Note that ϕ is a function of, amongst other parameters, $\mathrm{Fo}_{\omega,L}$, which in turn depends on the effective conductivity of the insulating material. The analysis given in section 1.5.2 on page 26 demonstrates a mechanism whereby for a multi–tier, composite insulative compartment, ϕ may be 'tuned' slightly[1]. Note that the value of the total thermal mass of the composite system would remain constant. Within the DRA context, the combination of these mechanisms might be utilised in effectively 'moving' the time ambient heat effects which are manifest within the DRA cabinet[1] to a period whereby it is either economic and/or more energy efficient to operate the prime–mover.

2.6 Closure

In this chapter, some of the main precepts of DSM were looked at in an attempt to apply the basic ideas of DSM *on the demand side*. Intrinsic to the success of this undertaking is the availability of a safe, reliable and controllable technology *and* a control philosophy; which will enable the (temporal) dissociation of demand–side energy requirements from supply availability. To date, neither does such a suitable technology exist nor has the required the appliance–management strategy been developed for DRA's, which are ostensibly an ideal platform on which to benefit from

[1] This thermal lag effect has been experimentally observed see Appendix B on page B–264. However, due to insufficiencies in the basic DRA design (see see section 6.4 on page 221), no appreciable thermal lag in the appliance response to ambient temperature fluctuations can be achieved.

[1] *i.e.* altering the heat ingress aspect of the load–shape.

the concept. This work seeks to uniquely provide, both, this technology and management rationale for the *feasible* implementation of the DSM concept in DRA's; thus, for the first time, providing a means whereby appliance users may either capitalise on whatever DSM scheme may be available to them or regulate the appliances' energy demand profile depending on energy availability or to some other advantage.

The chapter also discusses (internal DRA temperature) thermal stability arising from human interactions during normal use and the slow rate of recovery attending DRA's after an internal temperature excursion. Thermal energy storage (TES) is proffered as one possible means of addressing this problem. Highlighting the need to minimise the temperature gradient across the prime–mover and reduce the frequency of thermal–cycling the prime–mover undergoes, it indicates the COP improvements which may result from the presence of a TES adjacent to the DRA evaporator.

In the light of the nature of the application, the chapter goes on to stresses the need for the best possible means of thermal insulation and proffers the use of vacuum panel super insulation (VPSI), the best currently commercially available insulation, for this application. The chapter further discusses some of the underlying principles of DRA operation. In considering the energy transfer mechanisms inherent in the application, the prime–mover (and allied inventory) is initially considered and performance relations to assist in a load–centred DRA design are developed. The discussion then precesses through to weighing the effect of the changes in the different parameters on the performance of the prime–mover within a working DRA.

One of the major precepts of the research is decoupling the energy demand from supply and, as such, mechanisms of load control (and relocation) have been borne in mind. Thus, the issue of thermal insulation is revisited, considering the merits of the insulation design. Finally the the time–temperature lag due to the DRA compartment insulation has been investigated as an avenue for altering the appliance's load (and thus energy) demand profile.

Chapter Three

Thermal Storage as an Attribute to Thermal Management

And that food shall be for store to the land against the seven years of famine, which shall be in the land of Egypt; that the land perish not through the famine.

–Genesis 41.36 (KJV)

3.1 Introduction

Earlier on in section 1.2.2 on page 9, inference was as to the possible role thermal energy storage (TES) could play in addressing the issue of increasing energy consumption efficiency in DRA's. This chapter takes a deeper look into the technology of energy storage (ES), focusing on thermal energy storage with a particular slant towards the intended (DRA) implementation. The pros and cons are examined, as well as the necessity of ES in general, highlighting why TES is suited to this application and discussing the various facets to implementation of a workable scheme.

There is a huge interest in *secondary* energy storage for economic and technological reasons, amongst others. Even after several decades of research, the subject still has a huge following and the enormous bibliography on the subject is ever increasing. Perhaps the reason for this pedigree lies, on the one hand, in that it grapples

with the optimisation of predictions of several transient (and in some cases stochastic) quantities *e.g.* energy availability, energy supply and energy demand and on the other, that nagging at potential solutions are issues that are not easily quantified *e.g.* nuisance value, toxicity, acceptability, reliability *etc.* The following attempts a brief overview of the available (secondary storage) technologies with the view to highlighting the salient points pertinent to this work[1].

3.2 Energy Storage

Energy storage (ES) is intrinsic in almost every process contingent of some kind of energy inter–conversion. Sometimes the energy inadvertently stored within a system, on account of the system's nature or design, can constitute major causes of energy inefficiencies *e.g.* heat exchangers, regenerators *etc.* [Weston, 1983]. However, in many cases, particularly in those where there are periodic variations in either the system's input or the output demand, the process energy–utilisation efficiencies can be enhanced by the inclusion of the appropriate kind of energy storage[2]. However, in doing so, there must be an awareness of the implications and limitations of ES.

Energy storage can in no wise be considered an energy panacea. Energy stores do not 'save' energy in their own right [Wood et al., 1983], nor is storage a substitute for efficiency[3]. In fact the processes attending energy storage (charge, hold, discharge) are sources of energy losses[4]. In the pertinent case of thermal energy storage (TES), energy and thermodynamic availability are *always* lost during the storage and recovery processes.

Resolution of this apparent contradiction (that it is undesirable yet, expedient) is to be realised in understanding that: (a) ES can facilitate energy–cost savings when utilised as an *aid* to energy management[5] of complex thermal systems and (b) in *some* instances expedient use of energy storage technologies may serve to enhance the energy conversion efficiencies of other components within such complex systems[6]. Most proponents will agree that there is no single solution to the 'energy' problem and that technical, technological, demographic, cultural and social factors

[1] For a fuller treatment see either Lane (1983) or Jensen and Sørenden (1984).

[2] Essentially, ES permits better phasing of supply and demand.

[3] However, while it is true that energy conversion efficiency may not be enhanced by ES, the energy *utilisation* efficiency may be improved.

[4] Typically, associated with energy conversion and transfer processes are irreversibilities, so from a thermodynamic perspective ES's are undesirable [Bell, 1991].

[5] Usually for waste recovery and/or control; here ES will be deployed as a DSM facilitating mechanism.

[6] The particular case of a TES acting as a thermodynamic reservoir for a (Carnot–type) refrigeration cycle is one of the central ideas of this research.

will have to be brought to play [Bell, 1991]. However the ensemble of ES technologies form a potentially important subset of the kernel of available enabling technologies. These may be used for maximising both cost effectiveness and energy conservation potential of existing capital equipment.

3.3 Applications, Benefits and Requirements

As energy demand (and/or supply) can vary hourly, daily, seasonally *etc.*, appropriate solutions to energy storage problems will depend largely on local circumstances. It is important to differentiate between the real variation in energy demand and that which is apparent or artificially induced [Weston, 1983]. Thus, the decision as to the required scale and when to employ ES can be a difficult one. As ES is a load–smoothing device, the load factor (the ratio fraction of the peak load to the base load) can be indicative of the effectiveness of the use of the capital resources intended for an implementation[1]. ES technology is indicated in situations where:

- Temporal (preferably periodic) imbalances occur between the supply and demand for energy (more exactly, power) [Soderstrom and Johansson, 1983][2] or, a constant low power density supply is to cater for periodic higher–powered demand rates [Nissen, 1979].

- There exists a recoverable surplus of energy at a sufficiently high potential, after the application of all cost–effective conservation measures, *i.e.* energy is a waste product [Bell, 1991; Soderstrom and Johansson, 1983].

ES may also be considered in situations where it is desired to:

- Reduce the requirement for (transiently) high potentials [Bell, 1991].

- Reduce the frequency of equipment cycling [Bell, *loc. cit.*].

- When the requirement exists for a crucial backup against down–line supply failure or, for enhanced/rapid 'power' production [Edwards, 1984].

Effective ES applications have to be carefully researched and designed for an application. In several instances there is the residual impression that ES technologies are retro–fitted in 'last ditch' attempts at exergy conservation or to salvage an ailing energy management strategy. Indeed several seemingly valid ES schemes

[1]The aim being to decrease the load factor, equivalently, to reduce the 'worst case' maximum power rating.

[2]Traditionally, these have been handled by the storage of fuel rather than energy [Lane, 1983].

have floundered on some apparently ancillary issue. Edwards (1984), identifies several such 'essential secondary' issues which must be taken into consideration when considering an intended ES strategy; these include:

- Aesthetics and practical applicability within a realistic environment.
- Economic competitiveness.
- Environmental impacts.
- Nuisance.
- Reliability.
- Safety.

As with all commercial products, investors will want quick return on their investment and ES can be capital intensive [Wilson and Glendenning, 1976]. Economic feasibility of energy storage is roughly dictated by three parameters [Zegers, 1983] *viz*:

- The number of storage cycles per year. The Pay Back Period (PBP) varies inversely as the yearly frequency of store charge–discharge cycles [Douglass, 1980].
- Capital investment cost.
- Energy cost and running cost.

Energy and therefore financial savings are directly proportional to the number of cycles per year, short cycle periods being potentially more cost effective than comparatively longer cycle periods. Clearly an economic constraint on the cycle period can be determined to suit a particular application. However, as the process cycling periods reduce, it becomes necessary to charge the store at increasingly higher powers. Thus a further technical constraint, in addition to the above economic constraint, must be applied to the data to exclude those processes where the required 'transfer' power density exceeds that which is feasible for a particular storage technology, see Wood et al. (1983). Apart from the economic PBP, another important issue is the expected lifetime of the storage system which ideally, should be as long, if not longer than that of the device of which it is a part[1]. The lifetime of such systems is therefore defined by the number of (charge and discharge) cycles that can be obtained before the energy storage density falls off to a certain percentage of the original value[2]. The life cycle of secondary energy storage systems may also impose

[1]Failing that, the ES should be quickly and easily replaceable. A bad and good example of this is the car battery.

[2]This lifetime, called the 'life cycle', has to be distinguished from the non–operational shelf life.

technical limitations for certain applications and may become a decisive economic factor.

In the light of these and the hitherto mentioned thermodynamic shortcomings of the technology it is advantageous to ensure that, irrespective of the genre of the storage intended to an application, the size[1] of the store should be the minimum permissible. The preference is to options with high energy storage densities[2] (the reversibly recoverable stored energy content per unit volume) and high specific energies (the energy content per unit storage mass) [Zegers, 1983].

In considering the efficacy of any given storage option, it is necessary to consider the number of additional energy transformations, inter–conversions and transfers that will be incurred as a result of the inclusion of such a system in the energy flow process. Each transitory process/stage would introduce its own unique set of irreversibilities and hence further compromise storage process efficiency. As such, the exact storage mechanism(s) employed should be as few and as relevant[3] to the end use energy type as possible, to limit the number of transitory stages necessary. Similar conclusions can also be reached from considerations for limiting complexity, weight and cost. In addition to this, systems which minimise their total energy loss (transfer losses, transformation losses and storage losses) are generally sought and in many cases size tends to play a significant role such that the preference is for storage media with high energy storage densities. However, this has to be weighed against the energy quality durability within the storage medium/mechanism[4], as energy stockpiled in some stores/forms tends to degrade faster than others (principally due to problems with containment). Thus associated with every ES implementation is a unique energy storage efficiency:

$$\eta_{ES} = \frac{\mathsf{E}_{retrievable}}{\text{Theoretical Storage Capacity (TSC)}} = \frac{\rho_{\mathsf{E}}}{\rho_P \times \tau} \tag{3.1}$$

[1] In terms of both physical size and energy content; for reasons of space conservation and energy loss (degradation, leakage *etc.*) during storage, respectively.

[2] The distinction between the notions of energy storage density and the energy density, however subtle in appearance, must be recognised. The latter, without the storage qualification, implies the total amount of energy inherent in the medium *cf:* mass density [Lane, 1983]. Throughout this work the dealing is, unless otherwise stated, solely with regard to the energy storage density ρ_{E}.

[3] In the sense of limiting the entropy changes that attend energy inter–conversions and/or transfers.

[4] In general, it is not the case that energy stored will remain immutable in quantity and quality. There are losses associated with the transmission of energy to and from storage, and the energy stored within the medium itself may alter depreciatively during storage.

where

$$\tau = \frac{\mathrm{TSC}}{\overline{P}}$$

In most ES implementations, the charge and discharge powers tend to vary exponentially with time (as does the store energy content) *e.g.* the discharge power $P_{\Delta^-} = \mathtt{A} \cdot \exp(-\mathtt{m}\,t)$, (where $\mathtt{A}, \mathtt{m}$ are modulation and time constants respectively). As a result of this, some cut off point is usually defined (particularly in the case of the discharging) to (a) limit the cycling time to within some reasonable length and (b) ensure that the retrieved (or charge) power density meets a given requirement. Typical discharge cut–off times are[1] (i) the time for the power density falls to half its (initial) maximum value $t_{1/2} = \ln\left(\sqrt[n]{2}\right)$ and (ii) the time corresponding to the inverse of the time constant *i.e.* when the power density, P, falls to $\exp(-1)$ of its maximum value $t_{\exp(-1)} = \mathtt{m}^{-1}$. Thus the mean power, $\overline{P}$ defines as:

$$\overline{P} = \frac{\int_0^{t_{\text{cut off}}} \exp(-\mathtt{m}\,t)}{t_{\text{cut off}} - 0}$$

Aside from the notions of energy storage density and energy storage efficiency are the relevant notions of energy quality and energy availability. Energy quality derives from the thermodynamic description of energy in terms of the so–called extensive parameters (S, V, N, *etc.*) *i.e.* the fundamental equation. Inherent in these are the magnitude–independent, intensive parameters (T, P, μ, *etc.*) or energy potentials, which together determine accessibility between thermodynamic states, see Callen (1960), Chapters 1, 2 and 14. These energy potentials characterise energy quality, a distinguishing concept which determines relative admissibility of equi–energetic quanta among end uses. Depending on this quality, equal amounts of energy (even of identical forms) may be restricted in end–use applicability.

Energy availability (or exergy) is described, thermodynamically, as the 'free energy' (usable) fraction of a given amount of energy *i.e.* the work (mechanical, electrical *etc.*) equivalent of energy. It defines the second law (process/entropy) efficiency (see also section 1.4.1 on page 13) of the storage system[2] and is defined in terms of the so–called thermodynamic potentials[3] see Callen (1960), Chapter 5 and Tiza (1977), *pp.* 53 *ff.*

The flexibility of an energy system is therefore highest when storage possibilities for high quality energy are available. Decreases in energy quality occur during

[1] For the case of charging, cut–off is usually defined when the input power is within a few percent (usually less than 10%) of zero.

[2] As opposed to the first law (task/device/energy) efficiency which defines the maximum efficiency of a task, the second law can differentiate, in terms of efficiencies, between different alternate *admissible* processes for a given task.

[3] Helmholtz potential $\mathtt{F} = \mathtt{U}(T)$, Gibbs function $\mathtt{G} = \mathtt{U}(T, \mathrm{P})$, *etc.*

the transfer of energy to and from an energy store. The transfer of energy may involve some degree of energy conversion, and usually the related fraction of low quality energy is called loss or waste. It is called so because it is not used, and not because that part of the total energy has disappeared. After Cohen et al. (1983), the effectiveness of a store/storage process may be defined:

$$\begin{aligned}
\epsilon_{ES} &= \frac{E_{retrievable}}{E_{delivered}} \\
\epsilon_{ES} &= \frac{E_{out}}{E_{in}} \\
&= \frac{E_{out}}{E_{stored}} \frac{E_{stored}}{E_{out}} \\
&= \epsilon_{in} \epsilon_{out}
\end{aligned} \tag{3.2}$$

In the event that there are several transmission and or conversion processes, each with a unique ϵ stage, the resultant is:

$$\epsilon ES = \prod_{j}^{n} \epsilon j \tag{3.3}$$

Conversion may be one or more of several types:

- Conversion of high quality energy to a lower form (degradation).
- Conversion of low or medium quality energy to energy of higher quality[1] (upgrading).
- Conversion of one high form of energy to another high form of energy (transmutation).

For an energy storage system to qualify as a good system, it must possess the potential to supply (a) *useful* energy of the desired form, in (b) the desired amount, at (c) the desired rate with, (d) minimum loss. The aim is to replace a certain amount of (primary) energy, by an equivalent, more convenient, readily accessible, (secondary) energy form exhibiting better or equally good storage capabilities [Jensen and Sørenden, 1984]. Ideally, 'good' storage capabilities include:

1. A high energy storage density.
2. A high energy transfer efficiency.

[1] Requiring some sort of energy transformer.

3. A high energy transfer rate or power transfer density (supply and removal).

4. Stability of the store/storage material under energy charge/discharge cycling.

5. A potentially long and depreciation–free (in terms of quantity and quality), storage dwell (or holdover) time.

6. Modest containment and transmission requirements[2].

It is also important to bear in mind that the maximum power density available from a given application bears significantly on whether such an implementation will be suited to that application. Very few systems meet all these requirements, but fortunately all are not simultaneously required. Manning (1985), identifies several types of storage, a compendium of which is:

- Electro–magnetic (Super-conducting magnets).
- Mechanical storage (Flywheels,Compressed fluids, Hydraulic storage).
- Electro–chemical storage (Batteries, Fuel cells).
- Chemical storage[1] (Fuel generators).
- Thermal storage (Sensible heat, Latent heat).
- Thermo–chemical storage (Heat of reaction stores, Heats of dissolution).
- Thermo–physical storage (Heats of absorption stores).

Most of the discussion here presented will, relevantly, focus on thermal/temperature–related storage.

3.4 Thermal Energy Storage

Of all the modes of ES, Thermal Energy Storage (TES) appears to be the most relevant to the intended DRA application, the end–use energy type being thermal energy. There are also effectiveness benefits to be obtained from decreasing the frequency of cycling the appliance prime–mover and limiting the maximum load demand thereon (see section 1.4.1 on page 13).

[2]These last two (5 and 6) appear to pose the severest requirements on ES systems [Jensen and Sørenden, *loc. cit.*].

[1]Usually for longer–term storage.

Thermal energy is probably the most abundant of the easily harnessable energy types available. Problems with its utilisation arise due to its quality or exergetic potential [Cohen, 1986]. TES research is both cost– and labour–intensive because it necessarily involves a broad blend of theoretical, computational and experimental work applied recursively. As such, the field tends to be intensively knowledge–based. Judging from the literature, it is very easy to create a disaster, especially for longer–term applications. The number of variables to consider in any TES implementation is surprisingly large and the tendency is for different researchers to attach different weights to different properties, making different aspects the focus of their research. This has, at times, led to a failure to give sufficient attention to some important aspect of an implementation before full–scale experiments are embarked upon, with inevitable results. Lane (1983), details some examples of this, along with the lessons that are to be learnt from the various experiences.

Despite the vast amount of work which has gone into TES research, there still exists the requirement for economic, reliable, efficient, compact, isothermal TES's to provide a management tool for shifting energy conversion to higher revenue periods [Eissenberg and Wyman, 1980; Dinter et al., 1991]. While indeed, technically–sophisticated TES's have been be built, tested and issues of systems optimisation and cost minimisation addressed, many of these have never left the laboratory/research stage. Excepting a few cases Telkes (1949), Freedman and Dudley (1974), Lorsch et al. (1976), Telkes (1977), Sousa (1989), Augood (1997) these have tended to be for applications operating around or above ambient. Given the current state of the technology, a surprisingly small number of applications are *designed* with TES as an *inherent* part of the energy management strategy, the tendency being to have applications retro–fitted with TES.

Whereas store charging with, and/or to, higher potentials than needed can severely limit the usefulness of the store[1], low charge/store potentials tend to engender greater proportional transmission losses (on account of the increased time available for losses during transfer) [Fearon, 1984], incur excessive transfer times and provide meager energy transfer (on account of the low store potential), thus hampering any associated energy management process[2]. Methods for optimising between these two criteria are dealt with by Bejan (1982b). In most cases degradation during storage has to be taken into account; due to problems of containment (insulation and isolation), there are difficulties in storing thermal energy over long time–scales *i.e.* seasons. This suggests the adoption of a short–term 'load–centred' approach to TES design whenever feasible. In the event that longer–term energy storage is re-

[1] Higher *charge* potentials will cause an increased loss in thermodynamic availability; also higher *storage* potentials increase the propensity for store/storage associated losses.

[2] A TES charged to, or with, an insufficient thermal potential is virtually useless.

quired, such requirements may be more advantageously met by other storage means, see Wilson and Glendenning (1976).

3.5 Thermal Energy Store Types

TES devices may be classified in several categories. For instance, a broad classification may be based on the mechanism(s) attending the energy transfer process[3].

Passive storage	Active storage	
No working fluid. Typically used within the intended application as a stabiliser	Direct Storage: Working (heat transfer) fluid is the storage medium. Used in applications where thermal imbalances within the system are over longer distances.	Indirect Storage: An auxiliary thermal store is employed. Typically requiring greater heat exchange inventory (cost). Usually located extraneous to the application, can be quite large.

Table 3.1: TES classification by associated energy transfer mechanism

Another important criterion for classification is the dynamics of the storage mechanism. This section highlights the kinetic differences of different thermal storage regimes as they bear upon the choice of a TES medium.

Thermal energy storage entails the storage of thermal energy[1] utilising either the physical or chemical properties of some storage medium. Basically there are three types of TES (in increasing order of implementation complexity) *viz*: sensible, latent (LH) and thermo–chemical heat storage. They differ in (a) the amount of heat that can be stored per unit weight or volume of storage media, (b) the temperature–time history of the medium during heat storage and retrieval, (c) the relative values of the different process efficiencies and (d) the degree of complexity and the relative state of development of storage technology at the present time [Lane, 1983].

Just as 'Phase Change Material Latent Heat Thermal Energy Storage' (PCM–LHTES) offers an order of magnitude markup in heat storage capability when compared with sensible heat media, thermo–chemical heat storage technology has the *potential* of an order of magnitude markup over LH storage. In deciding on an implementation it is important to bear in mind what would constitute an acceptable level of complexity

[3]Which in effect determines the limit of applicability of the TES application.

[1]In this case, *i.e.* applied to DRA's, the pertinent form is coolth for direct use within the refrigerator (no other energy conversion processes).

for the TES system, alongside other issues like cost. In some cases it is possible to combine one or more of these technologies to greater effect, see Scarinage (1979). This can be effected by employing series or parallel thermal store arrangements or in some cases by a combination of both. The following goes on to briefly consider the various technologies in increasing order of relevance to the present.

3.5.1 Thermo–Chemical Energy Storage

This consists of TES utilising non–physical processes *i.e.* in a strict sense those involving some chemical interaction within the storage medium. A less rigorous definition would include all those processes in which the evolution of heat is incidental to the phenomenon. A few examples of these are Heats of concentration, absorption, adsorption, reaction, osmosis [Bell, 1991; Kauffman et al., 1977] and solution (saturation/re–saturation) [Nissen, 1979]. Such systems rely on the energy absorbed and released in breaking and reforming molecular bonds in a completely reversible chemical reaction. In this case, the heat stored depends on the quantity of storage material, the endothermic (or exothermic) heat of reaction[1] and the *extent* of the reaction *i.e.* conversion. Potential thermo–chemical heat applications are diverse (encompassing heat pumps, heat pipes, thermal transformers *etc.*) as in some cases the mechanism can exhibit very high efficiencies [Nissen, 1979; Lane, 1983]. However this is not true in all cases *e.g.* osmosis, where the reversal of the process requires more energy than can be obtained from the process. The systems tend to be more compact than sensible or latent heat applications and suffer less energy degradation over time. However TES systems based on this principle also have several drawbacks which makes their implementation difficult, requiring a comparatively greater level of technological sophistication and as a result the level of implementation lags behind. Two examples of this are:

- Usually the attendant chemical processes require reactants that are difficult to contain because of their corrosive nature and in cases where adequate containment is achieved, the mechanisms by which heat can be transfered to and from such storage media are greatly compromised.

- One general mandatory characteristic of any storage medium is the ability to rapidly cycle the systems. Many chemical reactions have their equilibrium biased in one direction such that the reverse reaction is either impossible or may require several energy–intensive intermediary stages to recover the reactants of the initial reaction. Such systems although conceptually possible are difficult

[1] These can be paired up for the purpose of charging and discharging.

to realise in practice due to the necessary equipment and the several stages involved.

These are in addition to these other implementation–specific problems like monitoring and control [Cohen, 1986], fouling and re–solubility [Nissen, 1979]. The technology is summarised in detail elsewhere in the literature, see Lane, *loc. cit.*

Physical Process Heat Storage

In the last section, the consideration was on energy storage processes which utilise non–physical processes. This section (and most of all that will follow) will deal with thermal storage systems that use physical processes. This, as noted earlier, can be broadly categorised into two groups *viz*: sensible and latent heat storage.

3.5.2 Sensible Heat Storage

In this case thermal energy is stored as sensible heat *i.e.* changes in the energy content of the storage medium are perceptible as changes in the bulk mean temperature of the store (*i.e.* its thermal potential). The amount of heat stored depends on the heat capacity of the storage medium, the temperature change undergone by the medium and the quantity of storage material. This kind of storage is apparently the most common type of TES application, as seen in domestic hot water tanks, regenerators *etc.* [Lane, 1983; Jensen and Sørenden, 1984]. Implementation of this type of storage process is relatively straightforward; however, there are also several drawbacks to it which limits its usefulness.

- In general the achievable energy (storage) densities and specific energy contents in sensible heat thermal stores are much smaller in comparison to those that can be achieved with other methods of thermal energy storage.

- The thermal exchange takes place over a range of temperatures; thus the transfer of energy will vary over time. In such cases the energy exchange effectiveness worsens as the temperature difference between the thermal store and its discharging medium approach the same temperature.

- There are irreversibilities associated with temperature changes in both the thermal store and the discharging medium (see the analysis commencing on page 50). This poses *severe* restrictions on the cost and efficiency of the storage process. It is with these types of stores that the notions of energy availability and quality are most readily associated. In that regard (*i.e.* second–law efficiencies), sensible heat systems are inherently inefficient [Bejan, 1978, 1982a, 1982b; Adebiyi and Russell 1987].

The effectiveness of TES's of this type can be enhanced if stratification considerations (in liquids) are borne in mind [Al-Muslahi, 1979].

3.5.3 Latent Heat Storage

In latent heat storage systems, the thermal energy is stored by utilising the reversible thermal energy change associated with a *first–order*[1] phase transition.

Solid–liquid transformations are the most widely used, although solid–solid (typically, second–order) transitions have been [Benson et al., 1985] and are still being investigated [Lloyd, 1998]. These single–state phase transitions tend to produce only *circa* 30% of the enthalpy changes of comparable multi–state phase transitions [Zegers, 1983]. Solid–solid LHTES tend to be for higher temperature applications[1] (comparison to the ambient) and, in contrast to multi–phase transition materials, they are easier to handle. Liquid–gas and solid–gas phase changes involve, increasingly in that order, the most energy of the possible latent storage methods. However, the gas phase is bulky and difficult to store [Lane, *loc. cit.*]. In fact problems of the fluid phase containment pose a major consideration in TES installations, introducing further restrictions (rigidity, isolation *etc.*) on the container design.

Phase change material (PCM) TES systems may be thought of as second generation subsystems, in the context that (fluid and solid) sensible heat systems might be considered as first generation energy storage systems. In general these latent heat thermal energy stores (LHTES) do not suffer (or do so to a lesser degree) the drawbacks that attend sensible heat thermal storage. Generally, compared to sensible heat TES's, LHTES's potentially offer the following advantages, [Manley and Smith, 1983]:

- Permit smaller store sizes as the energy storage density is higher.
- Permit the use of lower temperature differences between storage and intended use. This has ramifications with respect to availability losses during energy transfer and hold–over storage, typically exhibiting substantially better overall process efficiencies [Adebiyi and Russell, 1987].
- Substantially isothermal charge–discharge operation. This permits better overall process control, particularly in cases where one fundamental function of the TES is to ensure thermal stability.

[1] Apparently, there are several orders of phase transitions, characterised loosely by the severity of discontinuities the physical properties undergo, the stability of the ensuring states *etc.* Good examples can be seen in the Carbon–Iron phase equilibrium diagram where several solid 'phases' exist at different temperatures; expositions on the subject is given in Callen (1960) and in Tiza (1977).

[1] Although, eutectic cold–storage applications are increasingly being developed.

- Afford higher energy exchange rates to and from storage [Rarid et al., 1990].

There are also thermodynamic arguments which may be adduced as to the superiority of latent heat storage over sensible heat storage. The following is a simplified sketch of one such argument with a few auxiliary notes.

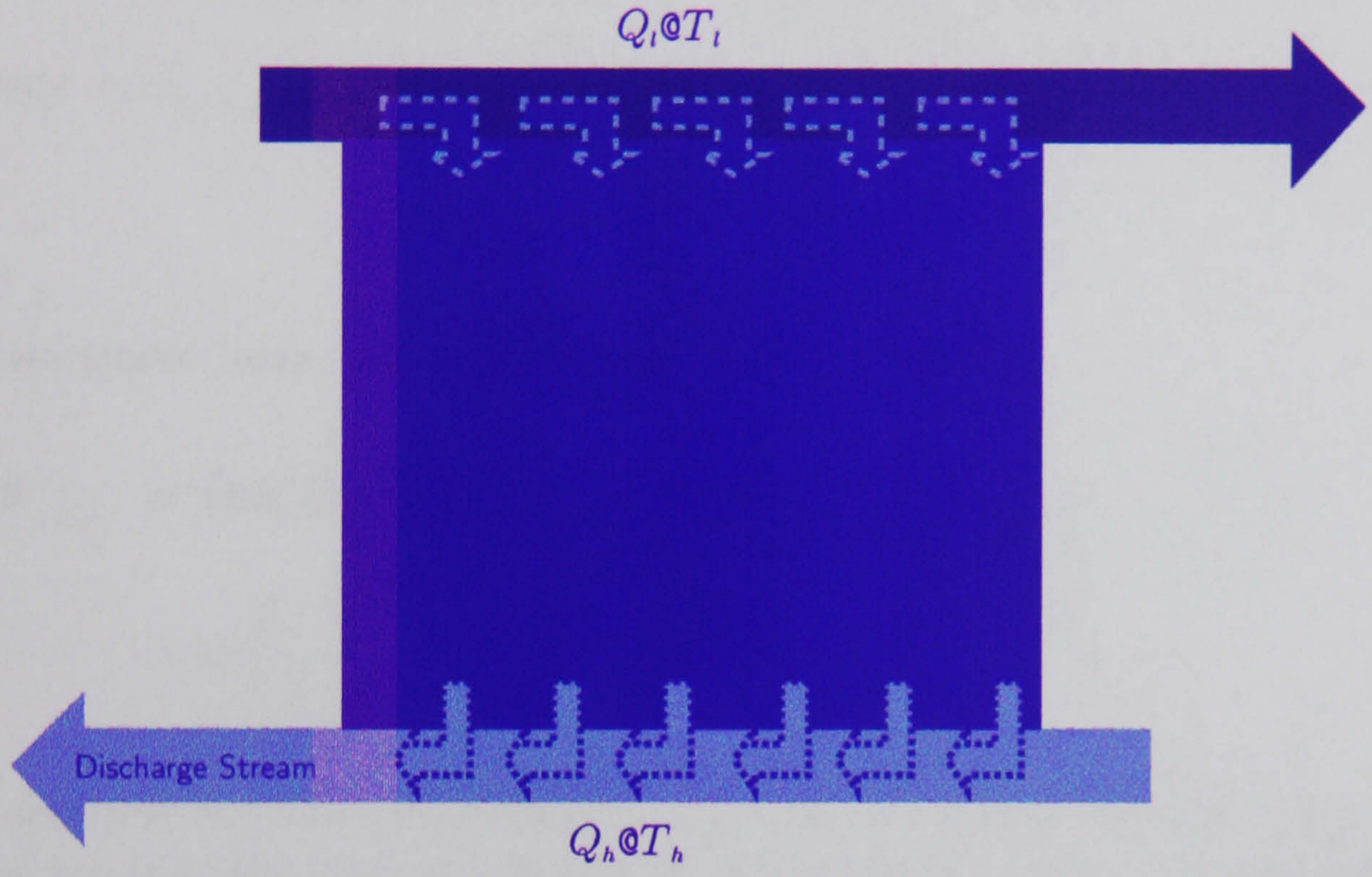


Figure 3.1: Schematic diagram of TES charge–discharge cycle

Consider the Figure 2.1 on page 51 which is a schematic diagram of a thermal store and the allied charge (at $T_{\Delta+}$) and recovery (at $T_{\Delta-}$) temperature streams. Neglecting the losses from the store and the allied transfer processes and assuming:

1. Q to be the amount of *working* heat the store is to cater for.
2. $(mC_P)_{SH}$ the thermal mass of a (sensible heat) store.
3. $(\Delta T_{LM})_{min}$ is the minimum logarithmic mean temperature difference for process–admissible heat transfer.
4. $(mQ)_{LH}$, is the latent heat storage equivalent of the heat storage requirement *qv.* 1.

In the case that the storage is of the sensible heat type then:

$$\begin{aligned} Q &= (mC_P)_{SH}\left(T_{\Delta-} - T_{\Delta+} - 2\cdot(\Delta T_{LM})_{min}\right) \\ &= (mC_P)_{SH}\left(\Delta T_{\Delta-,\Delta+} - 2\cdot(\Delta T_{LM})_{min}\right) \end{aligned}$$

and for a latent heat store:

$$Q = (mQ)_{LH}$$

Thus for equivalent storage capacities:

$$mQ_{LH} = (mC_p)_{SH}\left(\Delta T_{\Delta-,\Delta+} - 2\cdot(\Delta T_{LM})_{min}\right)$$

The entropy ($\Delta S_{\Delta+\Delta-}$) generated in one storage (charge–discharge) cycle is thus:

$$\Delta S_{\Delta+\Delta-} = \frac{Q_{out}}{T_{\Delta-}} - \frac{Q_{in}}{T_{\Delta+}} \geq 0$$

In this case where losses are neglected $Q_{in} = Q_{out}$[1] and thus

$$\begin{aligned}\Delta S_{\Delta+\Delta-} &= (mC_p)_{SH}\left(\Delta T_{\Delta-\Delta+} - 2\cdot(\Delta T_{LM})_{min}\right)\cdot\left(\frac{1}{T_{\Delta+}} - \frac{1}{T_{\Delta-}}\right) \\ &= Q\left(\frac{1}{T_{\Delta+}} - \frac{1}{T_{\Delta-}}\right)\end{aligned} \tag{3.4}$$

This equation, eqn (2.4), is invariant (under the current set of assumptions) irrespective of whether the storage type be latent or sensible. However, the definitions of $T_{\Delta-}$ and $T_{\Delta+}$ would vary depending on the storage type, for the following reason: the amount of heat stored in the sensible heat store is dependent on the temperature range $\left(\frac{Q}{mC_p}\right)$ over which it operates. For latent heat storage however, there is no need for this thermal gradient for energy storage. The implication of this is that while, in the sensible heat case, the minimum temperature difference between the charge and recovery streams and the sensible heat store operating temperature range must be at least $(\Delta T_{LM})_{min}$, in the latent heat storage case this (charge–discharge stream) temperature difference is simply $2\cdot(\Delta T_{LM})_{min}$.

- From Table 2.2 on page 52, it is clear that more entropy is generated as a result of the sensible heat storage process. This entropy is proportional to the loss in exergetic potential from the energy stream. The implication is that more thermodynamic work (W) is required to produce the same amount of cooling in the recovery stream[1]. This is evident in the requirement for a greater charge potential ($T_{\Delta+}$).

[1]In this case (coolth storage). Also note that Q is negative, reversing the order of the subtraction.

[1]Were this a heat engine, the logic would be the converse where more heat would be required to produce more work.

Storage process type	Sensible heat	Latent heat
Recovery temperature	$T_{\Delta-}$	$T_{\Delta-}$
Charge temperature	$T_{\Delta-} - \left(2 \cdot (\Delta T_{LM})_{min} + \frac{Q}{(mC_p)_{SH}}\right)$	$T_{\Delta-} - 2 \cdot (\Delta T_{LM})_{min}$
Entropy generated (minimum)	$Q \cdot \left(\frac{2 \cdot (\Delta T_{LM})_{min} + \frac{Q}{(mC_p)_{SH}}}{T_{\Delta-} \cdot \left(T_{\Delta-} - \left[2 \cdot (\Delta T_{LM})_{min} + \left(\frac{Q}{(mC_p)_{SH}}\right)\right]\right)}\right)$	$Q \cdot \left(\frac{2 \cdot (\Delta T_{LM})_{min}}{T_{\Delta-} \cdot \left(T_{\Delta-} - 2 \cdot (\Delta T_{LM})_{min}\right)}\right)$

Table 3.2: Comparative (minimum) generated entropy for the charge–discharge process

- The situation is much worse when one considers comparatively the losses each storage type engenders. If one assumes a similar heat transfer coefficient for both stores, then the heat loss from the sensible store will be greater than that from the latent heat store on account of the higher mean store temperature which the former operates at.

- Sensible heat stores tend to require a larger amount of technology to produce constant temperature output streams when compared with latent heat stores. This is because of the storage temperature gradients which must accompany sensible heat storage.

- Latent heat stores on the other hand require considerably larger heat exchange inventories to transfer similar proportions of heat when compared to similar sensible heat stores. This is because of the small temperature gradients which are available for energy transfer[2].

- Another down side is that a substantially higher level of technology is required to bring (PCM) LHTES to fruition. According to Telkes (1949, 1975, 1977), several applications failed because of problems with corrosion of the containment vessel, phase segregation and incongruent melting, and success in application has not been uniform, nor economic competitiveness conclusively demonstrated.

3.5.4 Latent Heat Media Selection Criteria

Although there exists an incalculable number of crystalline compounds and mixtures that might suffice as candidates for LH storage materials, most can be rejected

[2]For this reason, in (PCM) LHTES applications, some degree of sub/super cooling is sought.

on the basis of economics, safety and general (physical, chemical and thermal) properties. While it is true that a wide range of candidate materials and configurations have been identified (certainly more than there are applications to put them to) [Hale et al., 1971; Humphries and Griggs, 1977], less than 20% of the vast number which remain have received detailed experimental attention. It is thus inappropriate to identify a single system as having the greatest potential for near–term acceptability because there are too many candidate materials on which the requisite data and experience have not been obtained yet. The knowledge–based nature of the research indicates the strong need for a compendium of carefully standardised experimentally–determined properties and relevant phase diagrams of candidate materials. The data should include detailed information as to the precise descriptions of the compositions employed *e.g.* eutectics **vs**. non–eutectics, temperature(s) of phase change, thermo–physical data, transport properties, thermodynamic properties, observed chemical reactions, other pertinent kinetic information *e.g.* congruence, ease of nucleation, rates of phase change *etc.* as well as information regarding safety *e.g.* toxicity, inflammability *etc.* and the various potentials *e.g.* electrochemical (galvanic) *etc.* which would given indications as to material compatibility.

LHTES systems, like all other types of storage systems, have their own set of unique problems. From considerations of storage efficiency the rate of heat removal should not exceed that dictated by the maximum velocity of the thermal front which would sustain an isothermal phase on either side of the phase front. This is to prevent excessive temperature excursions within the storage medium, effectively making it a sensible heat storage process. LHTES's are limited by the thermal diffusivities of the storage material medium, a problem which worsens with growth in the solid phase [Marshall, 1981]. This limits the maximum *unaided* power density at which store charging and discharging can take place. The (energy transfer) situation is slightly better in the liquid phase, as convective vortices are set up within the liquid which aid the heat transfer [Peube and Hewitt, 1976]. However this tends to exacerbate the overall situation somewhat, in consequence of the differential in the maximum rates of heat transfer between both phases giving rise to a hysteresis in the heating and cooling curves as observed with DSC [Priestnall, 1985; Bahar, 1980]. This hysteresis can make energy–regulation difficult [Marshall, 1981]. In order to circumvent this problem many different devices have been employed, principally in the form of extended surfaces, the most common (from the literature) being PCM encapsulation. The technology (encapsulation) is also important in the control of phase segregation (in multi–component systems); however, its soundness is yet to be demonstrated and there are reports of the technology inhibiting nucleation, see Gladwell (1979).

Thus there still remains the requirement for an efficient, reliable and controllable mechanism by which energy transfer to and from the LHTES can be effected. Table 2.3 on page 58 attempts to categorise a few of the important parameters in LHTES, while Table 2.4 on page 61 lists a few known problems and the current methods being investigated as solutions. Lane (1983), *op. cit.*, gives a history of LHTES applications and a brief synopsis of applications where they have been pressed into service; the work highlights a number of interesting patents.

Desirable properties for candidate PCM–LHTES media

Properties	Phenomena	Comment
1. Thermal properties.	Suitable phase transition temperature	The temperature at which phase transition takes place *must* suffice to ensure the minimum (thermal) potential difference for the required energy transfer rates.
	High latent heat of fusion	The unit mass latent heat (LH) of fusion in effect defines the size (volume and mass) of the TES. High LH values ensure high energy storage densities (ρ_E).
	Good heat transfer properties	These include high (I) specific heat capacities, (II) heats of fusion, (III) thermal conductivity. In general, inorganics tend to have better heat transfer characteristics than organics; however it may be difficult to find a suitable inorganic PCM compound. Organic compounds, although they can possess high heats of fusion, tend to be lower in thermal conductivity, inflammable with low flash points, exhibit low temperature instability and have varying levels of toxicity[a].
2. Physical Properties.	Favourable[b] phase equilibria	Congruence (in composition and transition temperature) is a real necessity. Materials having lower heat of fusion are to be preferred above higher heat of fusion materials on the basis of possessing more favourable melting characteristics[c], also see *qv. (3)*.

... continued on next page

... continued from previous page

Properties	Phenomena	Comment
	Low vapour pressure	Low vapour pressure materials are preferred as these tend to be less influenced by changes in temperature. This is especially important as the induced pressure changes can damage the containing vessel and/or alter the phase–transition temperature of the PCM.
	Geometric stability during thermal cycling (*i.e.* across phase change(s))	Volumetric (and hence mass density) changes can be a real hindrance to effective implementation of PCM–TES's. Notable is gap formation, as a result of medium contraction, impairing heat transfer and/or stress damage to heat transfer inventory on expansion[d]. One manner in which this can be handled is to use snug–fitting deformable enclosures *e.g.* thin plastics may be used within permissible environments.
	High mass density	This will help to ensure higher (I) energy density (ρ_E) and, (II) volumetric thermal capacity (mC_p) storage, essential to limit TES size[e].
3. Chemical properties	Long term chemical stability	With respect to chemical stability and compatibility, longer term instabilities may be a problem (*e.g.* accelerated aging [f]); oxidation, thermal decomposition, hydrolysis *etc.* may well rule out an otherwise favourable PCM. In such cases, the longer term consequence of not using an inert material may make an initially economic and ostensibly technically acceptable implementation untenable[g].

... continued on next page

... continued from previous page

Properties	Phenomena	Comment
	Compatibility with materials of construction	As noted earlier, different research groups attach different weights to each of these properties. However the bulk of the literature tends to suggest that the failure to rate phase equilibria, in particular, segregation (and the formation of meta–stable states), and the particularly high tendency for the occurrence of *corrosion*, high in the ordering of priorities will most likely ensure that an implementation fails[h].
	Low/non-toxicity Low flammability potential No nuisance factor	Safety is an important issue, hazardous (toxicity, corrodibility, flammability, nuisance) and ultimate disposal considerations should be addressed early on in the PCM evaluation. Howbeit, it is also important to bear in mind that, with the exception of a few cases (*e.g.* water), the notion of absolute safety is a deception[i].
4. Kinetic Properties	Little or no super–cooling	If super–cooling does not exist, the rate of heat extraction *can* be slow. Typically a PCM is selected with *circa* 5–10 °C temperature latitude, to provide a sufficiently high temperature difference for good heat transfer. Excessive super–cooling (> 5–10 °C) will interfere (if not totally inhibit) heat exchange with the store[j].
	Sufficient crystallisation rate	Incomplete nucleation (especially in very hydrated salts with several hydrides) can be a problem, reducing the efficiency of the storage process[k].

... continued on next page

... continued from previous page

Properties	Phenomena	Comment
5. Economics	Abundant	In considering economics, the cheapest material may not necessarily be the cheapest to produce; the processes involved in making the raw PCM acceptable as a TES may involve costs which make the final product prohibitively expensive as a commercial application[l].
	Available at low cost	
	Cost effective	

Table 3.3: Desirable properties for candidate PCM–LHTES media

Notes in Table 2.3

[a][Rochester, 1981; Lane, 1983].

[b]This appears to be singularly the most frequent source of failure and the need to pay close attention to phase diagrams cannot be overemphasised [Al-Muslahi, 1979]. The literature is awash with examples of partial success where the technology has not been properly conceived, usually on this account.

[c][Telkes, 1949; Telkes and Kondo, 1980; Rochester, 1981].

[d][Elliott and Stephens, 1976; Peube and Hewitt, 1976; Rochester, 1981].

[e][Cohen, 1986].

[f][Priestnall, 1985].

[g][Telkes, 1949; Rochester, 1981; Telkes and Kondo, 1980].

[h][Telkes, 1949; Telkes and Kondo, 1980; Elliott and Stephens, 1976; Cohen, 1986].

[i][Telkes, 1949; Cohen, 1986; Elliott and Stephens, 1976; Telkes and Kondo, 1980].

[j][Telkes, 1949; Telkes and Kondo, 1980; Lane, 1983].

[k][Cohen, 1986].

[l][Telkes, 1949; Telkes and Kondo, 1980; Cohen, 1986].

PCM–LHTES pitfalls and possible solutions

Problem	Possible Solution	Comment on effectiveness
Heat transfer Limitations	Typically thermal–diffusivity limited (irrespective of the phase); more severe with growth in the solid phase (partially due to the loss of the convective component of the heat transfer)[a]. Solutions include the use of extended surfaces *e.g.* encapsulation, honeycomb structures *etc.*. More recently[b], fluidised pseudo–eutectic particles have been used to overcome this limitation.	This is probably one of the greatest limitations on the use of TES, as the cost of suitable honeycomb structures and other surfaces can significantly increase the cost of the heat transfer inventory. The use of encapsulation provides a 'potentially cheap' method for increasing surface areas for heat transfer and decreasing the propensity for phase segregation[c]. Its applicability is somewhat limited however, as it tends to inhibit nucleation and the consequent release of latent heat[d]. Fluidised pseudo–eutectic particles appear to present a mechanism for overcoming the inhibition of nucleation experienced by encapsulation; as the particle sizes may be reduced to ensure thermal 'lumped capacitance' behaviour and no encasing material is required. The technique can be invaluable in overcoming the thermal conduction limitation inherent in most TES applications and results in (orders of magnitude) higher rates of heat transfer to and from storage, than could otherwise be achieved in non–mobile LHTES's. The technology (as with most LHTES technologies) is subject to the availability of suitable materials, this has already been addressed to some extent[e].

... continued on next page

... continued from previous page

Problem	Possible Solution	Comment on effectives
		These tend to alter other characteristics of the medium and the determination of an appropriate agent can be the source of extensive investigation in itself. From the outset, it is imperative to bear in mind that both phases *have* to be managed and close attention paid to phase diagrams. There is little benefit in looking at either phase in isolation, or giving sole consideration to the amount of energy recoverable[g].
Phase segregation and formation of meta–stable states	Use thickening/gelling agent to suspend crystals[f].	
Super/sub–cooling	Use nucleating agent; suggested methods of nucleation include the use of Borax, activated charcoal, Ultrasonic insonation, Ultraviolet radiation, high–energy spark discharge, injection of cold free metal surfaces[h].	There are reports, in the literature, of sub–cooling to ambient temperature without the release of the stored Latent heat[i]. In such cases the need to nucleate becomes paramount. Lower rates of cooling do appear to increase the propensity for sub–cooling into (surprisingly stable) meta–stable states. Several methods for dealing with this have also been proposed. However, few of the suggested methods are suitable or even effective, the use of 'cold surface insertion' being the most consistently successful[j].

... continued on next page

... continued from previous page

Problem	Possible Solution	Comment on effectives
Chemical Corrosion	Use inhibitors *e.g.* additives, oxide films[k]	Many of the feasible salts are so chemically aggressive that even high alloy steels cannot withstand the process for any appreciable time[l]. It is important that this is one of the first considerations in PCM selection.
Changes in volume $(\Delta V) \gg (5-10)\%$	Use high–wetting PCM[m]; introduce a conducting gas into the system[n]; use flexible containment and/or 'thin' stores.	For high–temperature applications, this may not be a serious problem, thermal radiation compensating for the presence of the gap. At lower temperatures, the gas may be necessary; this would institute high pressure problems on re–melting (possibly engendering sub–cooling), especially if the melt does not absorb the gas. Flexible containment may not always be expedient, if available, as this tends to impair heat transfer.

Table 3.4: Problems and possible solutions facing LHTES implementations.

Notes in Table 2.4

[a] [Rochester, 1981; Lane, 1983].

[b] This appears to be singularly the most frequent source of failure and the need to pay close attention to phase diagrams cannot be overemphasised [Al-Muslahi, 1979]. The literature is awash with examples of partial success where the technology has not been properly conceived, usually on this account.

[c] [Telkes, 1949; Telkes and Kondo, 1980; Rochester, 1981].

[d] [Elliott and Stephens, 1976; Peube and Hewitt, 1976; Rochester, 1981].

[e] [Cohen, 1986].

[f] [Priestnall, 1985].

[g] [Telkes, 1949; Rochester, 1981; Telkes and Kondo, 1980].

[h] [Telkes, 1949; Telkes and Kondo, 1980; Elliott and Stephens, 1976; Cohen, 1986].

[i][Telkes, 1949; Cohen, 1986; Elliott and Stephens, 1976; Telkes and Kondo, 1980].
[j][Telkes, 1949; Telkes and Kondo, 1980; Lane, 1983].
[k][Cohen, 1986].
[l][Telkes, 1949; Telkes and Kondo, 1980; Cohen, 1986].

3.6 Application to Domestic Refrigeration Appliances

Cold storage was practised before refrigeration machines were developed. In times past, blocks of ice used to be harvested from lakes during the winter and kept in sawdust insulated ice houses/barns to last the summer. Coolth storage has been employed for a relatively long time and has been used in some air–conditioning systems [Freedman and Dudley, 1974; Golibersuch, 1977; Sousa, 1989; Hersh, 1994; Lorsch et al., 1976; Al-Hinai, 1992]. More recently, cold accumulators, ice packs, cold packaging *et hoc.* have been designed from PCM's for the preservation, usually during transport, of heat–sensitive products, see Lane (1983).

DRA's, by the nature of the manner in which they are used, are prone to varying thermal loading conditions and thus exhibit variations in energy demand to follow this load pattern, see Soderstrom and Johansson (1983). The implications of this on the prime–mover are that during periods where there are a considerable number of human interactions, they tend to cycle fairly rapidly to control/curtail the temperatures within the cabinet. As noted earlier, there is much, by way of energy thrift, to be gained from minimising the frequency of cycling of the prime–mover [Guldbrandsen and Nørgård, 1986]. Also, the diurnal nature of the ambient temperature tends to create a situation where there is a greater energy/power demand during certain periods of the (daily) day/night cycle than at others.

Thus, from most of the foregoing, it is clear that these two characteristics may be adduced in proffering TES as a natural part of an overall management strategy for DRA's. The initial indication of this is the old wives tale that, stuffing refrigerators with old newspapers tended to 'make them work better', a fact that the results of one study seems to bear out. James and Evans (1990), make the observation that DRA's are frequently opened in use and the loading conditions range from near empty to crammed full. However in all cases (box evaporator, planar evaporator, larder fridge, fridge freezer *etc.*), the incremental insertion of (*appliance temperature*) thermal masses *i.e.* food, into the appliance, not only *decreased* the mean temperatures of the appliance[1], but also *increased* the length of the refrigeration cycle (*i.e.* decreases the frequency of prime–mover cycling). In addition to this, the

[1]Measured at five points within the DRA.

magnitude of the temperature cycle was also substantially reduced. The lesson here is that *the* judicious *increase of the internal thermal mass of a* DRA *may be used to enhance its performance.* The fact that this (thermal) form of storage requires no further conversion lends greater credence to TES as the first choice of the candidate energy storage types. A TES in a DRA can be a valuable aid to:

- The dissociation of user's habits (temporal energy demand) from both the energy supply characteristics and appliance operation, thus enabling the exploitation of any temporal–tariff advantages which may be in implementation under utilities DSM programs.
- The down–sizing of prime–mover equipment and thus equipment cost.
- Instigating better temperature stability within the DRA *i.e.* appliance performance.
- A reduction in the frequency of prime–mover (compressor) cycling and thus the energy consumption associated with these phases of operation.
- Regulating the 'cold–end' (*i.e.* the prime–mover evaporating) temperature, thus providing a means by which the *in situ* COP of the prime–mover might be increased.

Judging from the potential advantages of the process dynamics, it seems strange that only very few efforts have been made to investigate this option see Michael and Yang (1991), Mithal and Yang (1994).

Much of the foregone has looked briefly into energy storage; for most implementations (typically within the thermal range of −25–150 °C) the best approach appears to be latent heat storage, due to its: (a) high energy densities (ρ_E), (b) constant temperature energy storage and delivery, (c) stability over protracted dwell times (practically no degradation) *etc.* [Telkes, 1980; Chen, 1981; Gladwell, 1979; Lane, 1983; Zegers, 1983]. With few exceptions, however, the bulk of the R&D effort has been to applications at temperatures above the ice point [Marshall, 1981]. Methods of cold storage considered in the past have failed for a number of reasons, ice storage receiving limited success in air conditioning applications. The following section attempts to identify a possible candidate PCM for inculcation into a DRA in the region of (0 – 4) °C[1].

[1]This temperature range would provide a sufficient thermal potential relative to the desired DRA compartment temperature for substantive heat transfer.

3.7 Thermal Energy Store Media selection

Perusing the various material handbooks *e.g.* Hale et al. (1971), Humphries and Griggs (1977) and from other sources of literature, water appears, *prima facie*, to be the most appropriate LHTES candidate material. It possesses: (a) one of the highest heat capacities of any substance known, (b) one of the highest heats of fusion per unit weight (and volume) of any of the conventional phase–change materials and (c) a thermal conductivity which is higher than for most liquids. In addition to these physical properties, water is: (a) kinetically stable, (b) chemically inert, (c) non toxic and (d) non flammable. It meets virtually all the practical requirements for a PCM intended for a TES application. What must be the most attractive of its features as an energy storage medium are its abundance and low economic cost. Other low temperature PCM's find it difficult to compete with water on economic grounds as a TES medium, see also Rochester (1981).

That said, there are problems which have to be worked around in the use of water as the PCM of a LHTES. Notably these include: (a) its irregular expansion characteristics[1] and (b) the differential expansion between the different phases and the containing vessel[2]. While the thermal conductivity of water may be comparatively high, compared to other liquids, it is relatively low in the spectrum of thermal conductivities and, as with most LHTES implementations, some mechanism to compensate for this thermo-conduction limitation has to be devised. Water also suffers the same problem all multi–phase PCM's have *viz*: the containment of its fluid phase. One manner in which this can be addressed is to absorb the water with a rigid non–intervening matrix, which would effectively bind the water molecules within its structure. This essentially transforms the liquid–solid phase transition to a solid–solid phase transition whilst preserving the higher enthalpies of transformation associated with the (first–order) liquid–solid phase transition.

The technology to do this has long been available, developed by a UK scientist as far back as the 1970's [Kent and Page, 1980a, 1980b]. The original method involved the gelling of incongruent–melt phase–change materials within polymeric hydro–gels. Cross–linked polymers as PCM's have since been used in the development of 'solid–solid' LHTES's [Highgate, 1977; Kaelble et al., 1975]; in some instances the process is characterised by improved material properties on cross–linking[3] as reported by Rochester (1981) here at Cranfield. More recently, polymeric hydro–gels (also known as hydro–polymers) have been employed by Augood (1997) for thermal stor-

[1]This can be worked around if the temperatures within which the TES operates are carefully controlled.

[2]This may be addressed by careful choice of the containment *e.g.* the use of elastic materials (polymers *etc.*) and/or the use of the least possible thickness of the PCM.

[3]Polyethene (125–135 °C) and Isotactic polypropylene (155–165 °C)

age using water as the sole PCM. Hydro–gel preparation can be achieved by one of chemical, thermal or irradiative means. Non–irradiative manufacturing methods currently tend to be very costly and usually require toxic reagents (typically monomers), making the range of readily available degrees of water uptake hydro–polymers limited[4]. Saler (1979) and more recently Leguay (1994) have investigated irradiative production methods and found them wholly satisfactory. Two major advantages of the irradiative method are: (a) the use of polymers (less toxic, by virtue of their longer molecular chains) as the primary reagents, and (b) commercially available doses of radiation (sterilisation doses) can be used for processing, drastically reducing the cost of manufacture. Further extension of the technology could be the possible impregnation with clathrates, to potentially deal with the problems of phase segregation (after the manner of Kent and Page (1980a, 1980b)). This would, however, require a concerted and sustained research effort if the technology is to be brought to fruition.

Hydro–polymers, though, do have their own brand of problems. For instance, high water–content hydro–polymers tend to be fragile and susceptible to fungal attack, with attendant degradation of their hydration/hydro–retentive properties[1]. This problem may be addressed by the utilisation of gamma (γ) radiation cross–linking of vacuum–packed reagents for the production of the polymeric hydro–gels and ensuring the hydro–polymers are kept isolated post irradiation, effectively sterilising the material. Another problem is the existence of a (temperature–time history) hysteresis in the behaviour of modest water–uptake polymers on initial thermal cycling, see Highgate et al. (1989), Okoroafor et al. (998b, 998a); if high water–content polymers are used, the aforementioned problems are not apt to occur. Based on the work of Leguay (1994), cross–linked Poly Vinyl Alcohol (PVA) *i.e.*, $-(CH_2 \cdot CH \cdot OH)_p -$[2], in the proportions of 5–10% PVA w/w was chosen to be the base hydro–polymer for the current implementation. Pritchard (1970), reviews and discuses the chemical, physical and thermo–mechanical properties of PVA; the monograph includes a discussion as to its uses and technology (*loc. cit.* Chapter 6). Argana (1962), *pp.* 88-109, also contains a discussion on PVA for the interested reader, who may also wish to see Buchholz and Peppas (1994).

In the past methods of cold storage have been considered in the past and have achieved limited success (the reasons for this have been discussed in section 2.4 on page 61). The bulk of the problems which have been previously encountered will be circumvented utilising the proposed polymerised hydro–gel. One problem which would still remain unresolved is the poor coolth transmission to and from the TES on

[4]Dictated by commercial economics. Incidentally, hydro–polymers are also used as the principal manufacturing raw material in the production of contact lenses.

[1]This has been observed in the laboratories, see Figure C.4 on page C–285.

account of the limitations of the PCM's thermal conductivity. This would be debilitating to the effective functioning of the DRA in applications where large heat fluxes are required; especially where prospects for extending the relevant heat transmission areas are non–existent. In such situations, the aforementioned fluidisation process may be used to obtain the required heat transmission; the fluidised bed consisting of granulated hydrophilic material.

3.8 Closure

The previous chapter highlighted some of the benefits of ES mechanisms as part of an appliances' energy management strategy; particularly in instances where there may be some benefit in altering the energy demand profile. This chapter, in seeking to identify such an ES mechanisms, looks into ES technologies and consequently confirms TES as a relevant and appropriate storage technology for DRA's. It then goes on to highlight the different types of TES's and via a brief elimination process selects 'phase change material, latent heat, thermal energy storage' (PCM–LHTES) as the most appropriate form of storage.

LHTES's are consequently examined and various issues regarding their implementation are discussed. Water is subsequently identified as the most logical storage medium, as it doesn't suffer most of the problems which attend other candidate PCM materials. In closing, the chapter highlights the problems to be encountered with the use of water as this medium; mainly to do with heat transfer limitations and containment. It also proposes methods by which these problems can be overcome *i.e.* the use of fluidisation technologies and absorption within a non–intervening matrix respectively.

Chapter Four

The Thermal Engineering Design Analysis of a Storage Refrigerator

In theory, theory and practice are the same ... in practice they are not.
C. 1: The difference between theory and practice is smaller in theory than in practice.

–Anon

4.1 Proem

This chapter documents a 'proof–of–concept' design procedure for a small–scale (solar–powered) energy storage refrigerator. The design considers several possible scenarios which may arise in practice, *e.g.* intermittent power supply, time–dependent differences in energy cost and time–dependent/varying user practices. The possible avenues and methods by which the design may be optimised are discussed. In this analysis, the sun (solar photo–voltaic, SPV) has been chosen as the main energy supply source; this is because it poses one of the severest restrictions on the DRA design. The uncertain and intermittent character of insolation availability (and intensity) represents a generalisation of many other conceivable cases (see also Reis (1975)).

4.2 Design Specification

Introduction

This section charts the various specifications which govern the ensuing design. The aim was to minimise complexity, and at the same time, ensure appliance robustness. The demands on the system (and the resultant specifications) were drawn up from various sources[1] and after lengthy discussions with various component manufacturers.

The objective was to design a non–freezing, refrigerating appliance which is well suited for use in rural equatorial regions, or in environments which may exhibit similar uncertainties in energy supply as well as demand for refrigerated products.

Several categories of applications which fall within the design target criteria are easily identifiable *e.g.* rural commerce, recreation, medicine, space *etc.* In considering any implementation, considerations of cost, weight, energy availability and reliability (SPV in this case), structural strength *etc.* have to be borne in mind. Table 4.1 on page 107 is a short summary of a listing of four of the more likely categories and the different weights attached to each consideration.

Although the technology developed in this research can be applied to virtually any refrigerator in many environments, the original context of this study was to improve the energy efficiency of a solar powered refrigerator for use in tropical countries (*e.g.* possibly for vaccine storage).

This research requirement was suggested by Quest Refrigeration Manufacturing Ltd. who built the trial equipment subsequently used in this research. It is for this application that the following initial design study employs the specific temperatures appropriate to the tropics.

Ambient Environment

- Maximum daily day–time temperature, $43 \pm 1\,^{\circ}C$ (12 hours maximum).
- Minimum daily night–time temperature, $15 \pm 1\,^{\circ}C$ (12 hours maximum).
- Mean day–time temperature, $35\,^{\circ}C$ (assumed sinusoidal, 12 hours).
- Mean night–time temperature, $20\,^{\circ}C$ (assumed sinusoidal, 12 hours).
- Constant temperature test condition $32 \pm 1\,^{\circ}C$[2]. For these (day/night) tests, three hours are stipulated for the ambient temperature to reach the target

[1] *e.g.* [WHO, 1979; WHO, 1986b; WHO, 1986a; WHO, 1988; Silla, 1989]; [Tabassum, 1989; WHO, 1990b; WHO, 1990a]; [Saberi, 1991; WHO/UNICEF, 1992; WHO, 1994; ASHRAE, 1994].

[2] $43 \pm 1\,^{\circ}C$ is given as an alternative worst case (24 hours maximum).

Application	Requirements[a]					
	Low cost	Low weight	Energy supply		Thermal performance	Structural robustness
			availability	reliability		
Rural commerce.	▲▲▲▲	▲	▲▲▲	▲▲	▲▲	▲
Recreational[b].	▲▲	▲▲▲▲	▲▲▲	▲▲	▲▲▲	▲▲▲▲
Medical[c].	▲	▲▲▲	▲▲▲▲	▲▲▲▲	▲▲▲▲	▲▲▲▲
Space[d].	▲	▲▲▲	▲▲▲▲	▲▲▲▲	▲▲▲▲	▲▲▲▲

[a]The ▲'s are used to indicate the estimated importance of the requirement weighted on scale from 1 (least) – 4 (most) important.

[b]Sailing, camping *etc.*

[c]Vaccine storage on (rural) immunisation programmes, organ transportation *etc.*. The WHO actually has one (rather broad) such specification, see pertinent references in Footnote 1.

[d]Such an implementation has been commissioned by NASA, however that implementation did not include TES and is based on a Stirling cycle. see http://powerweb.grc.nasa.gov/stirling/doc/adfreeze.html and OSS (1996)

Table 4.1: Some typical applications indicating the relative weights of different requirements.

temperature, which is then held for nine hours. This commences after initial stabilisation and is carried out for five days. For the 'stable running' tests, in a 32/43 °C ambient, the device is to be loaded and stabilised and then the energy consumption is monitored over 24 hours.

Internal Temperature Requirements

- Control temperature range 5 ± 2 °C when stabilised and fully loaded.
- Maximum permissible internal cabinet temperature 8 °C.
- Minimum permissible internal cabinet temperature 0 °C.

Energy Availability Due to the diurnal and unreliable nature of the energy supply (solar power) an auxiliary energy source is required to provide the required power during periods of solar insufficiency. For the current application rechargeable electric batteries have been chosen to provide this required energy, ensuring that the energy for the system is derived solely from the sun.

- Maximum (harvestable) solar insolation during worst months 3.5–5.2 $\mathtt{kWh/m^2/day}$.
- Maximum (harvestable) solar insolation during best months 5.2–7.0 $\mathtt{kWh/m^2/day}$.

Power Consumption The maximum power consumption[1] shall be less than 0.7 $\mathtt{kWh}_{(e)}$/24 hours for appliances with a gross volume of less than 50 litres and less than 0.1 $\mathtt{kWh}_{(e)}$ per additional 10 litres of gross volume at 43 °C when stabilised and fully loaded.

Photo-voltaic Systems Specification The WHO specifications require that: *The system shall be sized to enable continuous operation of the refrigerator (loaded) during the periods of lowest insolation in the year. The design of the battery–*SPV *system shall be such as to permit a minimum of 120 hours of continuous operation when the battery is fully charged and the* SPV *array is disconnected and the external temperature is 43°C.* This requirement is here extended to include the daily recharging of the appliance during this distress period.

Hold–Over Capacity Longest time (hold–over condition) without solar energy input 72/120 hours (three/five days) @ 32 °C or 10 hours @ 43 °C in addition to 24–hour test period.

[1] Again based on the WHO specifications.

Pull–Down Tests In addition to the test requirements given in section 4.2 on the page before, the system requirements and the limitations of the energy consumption set out in section 4.2, the system is required to undergo the following, so–called, pull–down tests. Initially the appliance is to be allowed to stabilise (with the door open) to the ambient temperature (32 °C) for at least 48 hours. The doors are then closed, the device switched on with its thermostat set to the maximum (7 °C) control setting and left to stabilise. Temperatures should be recorded hourly for 24 hours and the prime–mover duty cycle determined (*i.e.* the percentage on–time over a 24–hour period). The procedure is repeated at the minimum (3 °C) setting after 48 hours have been allowed for stabilisation.

4.3 Design Philosophy

Introduction

The philosophy behind this design is to provide a simple and effective method of improving the energy performance[1] of a DRA using (economically) cheap, reliable and readily available technologies. The ideology espouses what may be viewed as a 'load–centred' approach to DRA design achieved by: (a) minimising the total refrigeration load the system has to cater for (an absolute priority), (b) effectively 'moving' the thermal load, principally by energy storage, to periods where it is demonstrably expedient to do so[2] and (c) spreading this load over the longest available time *i.e.* minimising the maximum *power* requirements for prime–mover operation as well as reducing the frequency of prime–mover cycling.

4.3.1 Design Concepts

This design is based on the following considerations:

- The COP of the prime–mover employed, by virtue of basic thermodynamic considerations, will be dependent upon the temperature difference between the evaporator and the condenser elements (and the ambient temperature obtaining during the operation of the prime–mover).

- The effectiveness of the thermal insulation used in the construction of the refrigerator compartment is of paramount importance, because it possesses

[1] As discussed earlier, the phrase 'energy performance' connotes the totality of internal temperature stability, energy conversion efficiency and energy utilisation effectiveness.

[2] The rationale behind this is somewhat akin to that employed for thermal storage for the heating and air–conditioning of dwellings.

the potential to (a) significantly reduce the load on the system and (b) affect the optimal control strategy for the prime–mover.

- Within this context, a thermal energy store (TES) possesses the following potential functions:

  1. To better stabilise the internal temperature of the refrigerating compartment, thus reducing the necessity of frequent cycling of the heat pump, particularly during periods when there are a lot of human–appliance interactions.

  2. To enable the prime–mover to be operated at normally 'off–line' times *i.e.* (a) when, the external ambient temperature allows the COP of the prime–mover be maximised *e.g.* at night; and (b) when the cost/availability of energy is such as to make it expedient to do so, *e.g.* low tariff times. This has the potential to decrease the size (and likely the cost[1]) of the power input into the system.

  3. To store energy in a form which *may* allow storage at a greater (specific or volumetric) capacity than in conventionally available electro–chemical energy storage[2]. The potential advantage in this case is for the optimisation of the size and cost of the prime–mover.

  4. To assist the distribution of coolth within the system, *i.e.* from the evaporator to the interior of the refrigerator.

- The compartment thermal gains (an estimated 51% of the total, inclusive of ingress through thermal short circuits, but excluding loads associated with human utilisation) lag behind the ambient temperature by a time constant dependent on the properties and quantity of the insulation employed in the construction of the refrigerator cabinet. No such (considerable) lag is experienced by the heat pump. By careful design, periods of high compartment heat gains *may* be made to coincide with periods of maximum prime–mover performance. This would help to reduce thermal store size as well as improve prime–mover utilisation

- The control hierarchy applied to the operation of the prime–mover. This is important as it can be used to dictate the prime–mover operating regime for optimum energy storage and thus utilisation.

---

[1] As the unit cost of energy may be time dependent.

[2] The use of electric batteries are the convention; however it is acknowledged that other types *e.g.* fuel cells are available.

4.4 Systems Design

Introduction

This section deals with the schematic design of the DRA layout. It begins with the general appliance layout, then proceeds to the systems configuration and through to the conceptual designs; consideration is given to a few avenues for maximising the benefits obtained from utilising existing inventory. Some of the inherent characteristics of the individual components are looked at with the view to exploiting their relative location for better systems performance. It specifically does *not* look into individual parameter specifics (prime–mover, insulation, seal *etc.* types) as these are subject to the state of the current available technology. The rationale here is[1] that an inefficiently designed DRA will fare worse, when compared to an efficiently designed appliance *ceteris parabus*. This (poor design) unfortunately is evident, for example, in the trend of locating prime–movers beneath the storage compartment in DRA's, among other things, see Bell (1991). The section goes on to highlight three possible configurations which may be used to satisfy the current design, stating the advantages of each.

4.4.1 The General Layout

Appliance Type Given the current state of the associated technologies and the operating cost implications, in terms of both energy and financial economics (see section 1.7 on page 31), as much as it is possible, DRA designs of either the 'fridge' or 'freezer' type should be preferred over the 'fridge–freezer' type, as this type of appliance tends to be inherently inefficient. In the event that a combined 'fridge–freezer' is necessary, it is more expedient from a heat transfer perspective to place the refrigerator compartment (the hotter of the two) above the freezer compartment. The current design focuses on refrigerators with only passing references to freezers wherever it is deemed appropriate.

Geometry The efficient thermal design of insulating cavities must take into account the optimum geometry for minimum heat loss, *i.e.* the one that provides the greatest volume to surface area ratio. Of all simple geometries, the sphere offers the greatest ratio in this regard. Unfortunately, for practical as well as space utilisation considerations, it is rarely expedient to manufacture a spherical DRA and again the

[1] See also section 2.3.1 on page 49.

next best alternative must be considered. Of the cuboid class of geometrical shapes, the cube offers the greatest volume to surface area ratio. Again, space considerations may restrict the implementation of such designs; however, square bases should be the preferred choice with regard to this.

Access into DRA's is typically through doors located either on the top (chest–type) or one of the sides (larder–type). From a thermal engineering perspective the top access design is preferred. However, this may not always be convenient and in such cases the 'front–loading' option is then indicated. The current (common) practice of using large doors (particularly in 'front–loading' applications) in DRA design is questionable[1] due to its provision of a larger area through which air ingress may occur (or in the case of 'front–loading' appliances cold air falling out) whenever the door is opened.

Location of the Prime–Mover On most DRA's, the prime–mover is usually located beneath or (more rarely) adjacent to the bottom of the appliance, literally the engineering equivalent to placing a stove under an ice box and stoking it at regular intervals! This is due to the fact that any heat generated by the prime–mover and expelled into the ambient air will be transmitted (convectively and radiatively) to the *coldest* part of the device (irrespective of whether or not it is a multi–functional DRA or not). This issue has been addressed in detail elsewhere in the literature *e.g.* Valencia (1991), Bell (1991). Ideally, the prime–mover is better remotely–located from the cooling compartment. For practical and aesthetic reasons, this may not always be feasible and what should be considered as the next best alternative is placing the prime–mover on (or at least closest to) the top of the device. Indeed, some manufacturers are practising both of these options[2].

4.4.2 System Configurations

In the conceptual design of the proposed DRA, apart from the basic requirements for the rudimentary design[3], only a thermal energy store (TES), a solar photo–voltaic (SPV) cell and an electric battery are to be included in the design. The electric battery is included to cater for the absence of solar insolation during periods when it may necessarily be required. The novel design philosophy here developed addresses the unified management of both the electric battery and the TES. The use of multiple

[1]Some shop appliances have doors for each compartment which are opened depending on requirement. Indeed many 'ice cream vans' and 'lolly pop men' use appliances of this nature.

[2]One such manufacturer is INDEL "B" (gruppo Berloni) 61019 S. Agarta Felrita (localitá Ca'. Baldone), Pesaro, Italy.

[3]Inclusive *only* of those components which are expressly required for building a working appliance.

(cascaded) prime–movers can greatly improve the systems energy–use efficiency and offer additional control flexibility (for instance, running one of the prime–movers during high coolth demand times to augment whatever thermal storage facility is available, see Figure 4.1 on page 113). However, in this initial analysis this optional strategy is not considered for reasons of cost and simplicity.

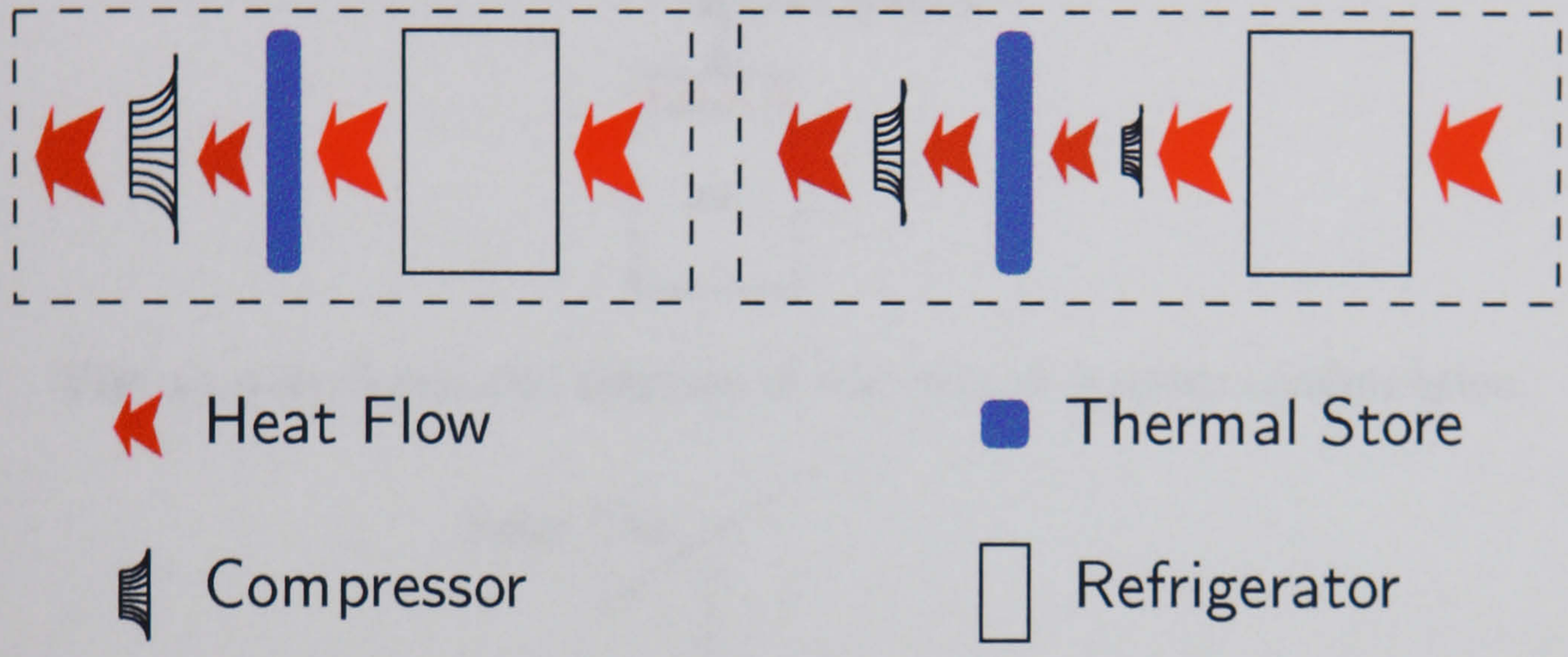


Figure 4.1: Comparison of single and multiple prime–mover arrangements.

Three basic design configurations were considered:

4.4.2.1 Inclusive Only of an Electric Battery

This configuration is a basic rudimentary system with only an electric battery, (see Figure 4.2 on page 114). 'Primary' energy is tapped and stockpiled in the battery whenever it is available and expedient and the stored energy is subsequently used for prime–mover operation whenever energy is costly or unavailable. This design has the benefit of permitting energy to be converted to coolth irrespective of the energy supply (profile or costing). However, limitations to this configuration arise from the necessity to convert energy to coolth as is demanded by the utilisation pattern of the refrigerator. This may not be thermodynamically the most expedient and only partially meets the objective of decoupling appliance energy demand and energy supply profiles (see section 4.3 on page 109).

4.4.2.2 Inclusive Only of a Thermal Energy Store

This is a similar system to that described above with a thermal store in lieu of the electric battery, (see Figure 4.3 on page 114). In this configuration, the 'primary' energy is converted to coolth and stored in a TES. This is then discharged

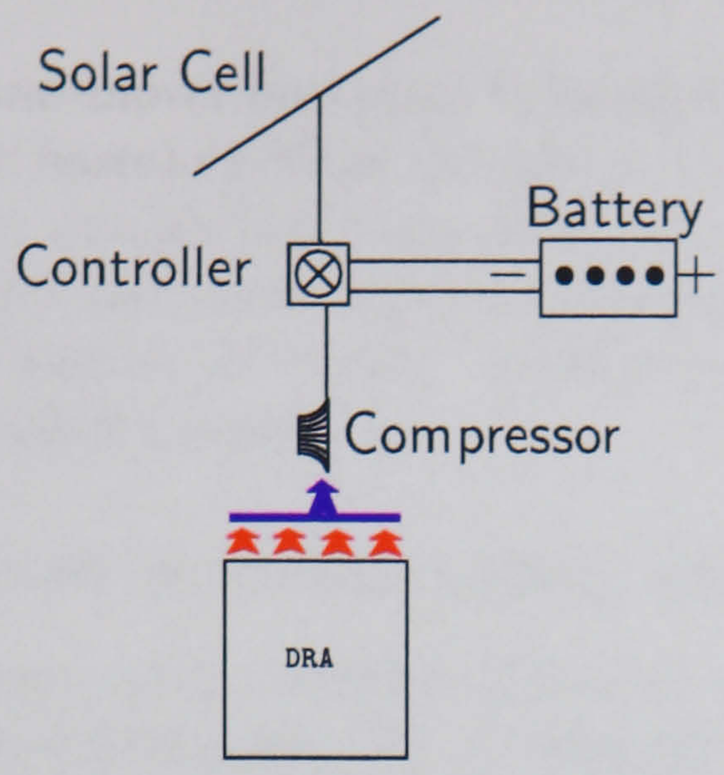


Figure 4.2: Schematic diagram of the electric–battery configuration.

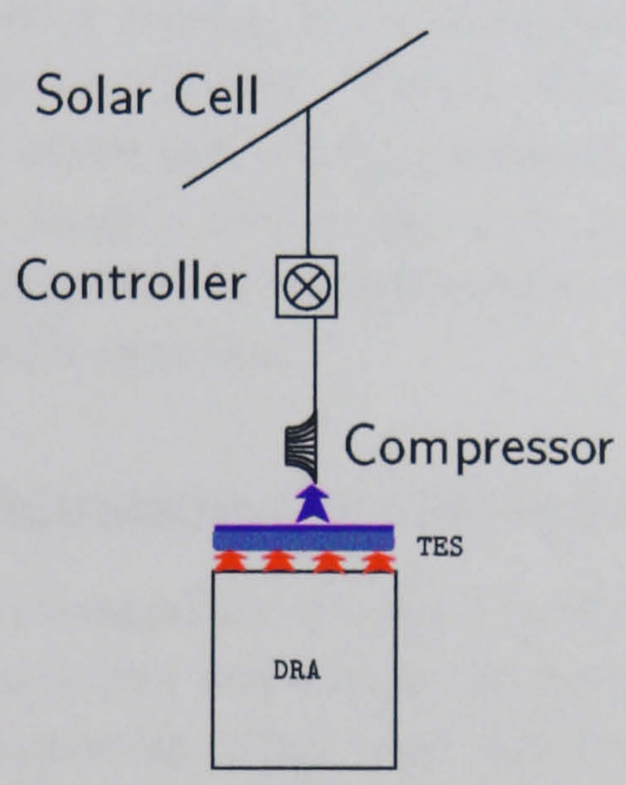


Figure 4.3: Schematic diagram of the TES configuration.

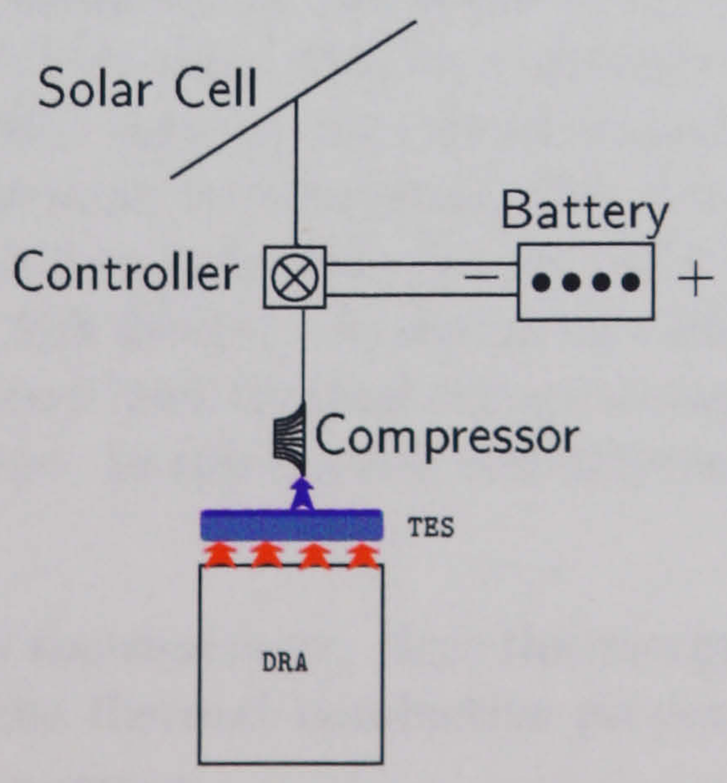


Figure 4.4: Schematic diagram of the hybrid (electric–battery and TES) configuration.

during periods when prime–mover operation is inexpedient (assessed on either economic or thermodynamic bases) or when the prime–mover cannot be operated due to constrictions in energy availability. One advantage of this configuration is that the energy is stored in 'end–use' form. However, it possesses the limitation that the energy conversion is dictated by the energy availability and demand profiles, which may not be thermodynamically expedient.

4.4.2.3 Inclusive of both an electric battery and a thermal energy store

This is a hybrid system with combined thermal and electro–chemical energy storage (HES), (see Figure 4.4 on page 114). In this configuration, 'primary' energy is stored (in a battery) when it is available and is subsequently converted to coolth and stored in a TES during periods when it is thermodynamically advantageous to do so. The store is subsequently discharged independent of the prime–mover operation which may or may not be concurrent. This 'hybrid' configuration possesses within it all the flexibility of the other two configurations, (permitting the storage of cheap, or available, energy from supply and conversion to coolth when it is advantageous to do so) and is better disposed to optimisation. It does however, possess all the complexity inherent in both systems.

4.4.3 General discussion on conceptual design

These designs were motivated by the need to keep any (component) additions to the basic refrigerator design to a minimum. In particular, with regard to the energy storage options, it was borne in mind that the fewer the number of intermediary (energy storage) stages, the lesser the energy losses that will be incurred due to irreversibilities during transfer, conversions and storage hold–over. It is of importance to note that, the likelihood of the application of the 'battery only' system, described in section 4.4.2.1 on page 113, in a domestic setting is small due to the inclusion of a battery which may be seen as an unnecessary addition to the basic DRA design. However, systems incorporating TES, described in section 4.4.2.2 on page 113 and section 4.4.2.3 on page 115, can be easily and relatively unobtrusively incorporated to the basic DRA design[1]. As discussed earlier (section 3.7 on page 101), phase change material–latent heat thermal energy storage (PCM–LHTES) is the chosen medium for thermal storage. In this regard, two different types of configurations are conceptualised *viz*:

1. *A static (or passive) thermal store*: Here the energy transfer (in and out of storage) is limited by the thermal–conductive properties of the storage medium.

[1]The two configurations being essentially the same in such a setting.

This may be conceived of two types (see Figure 4.5 on page 116 which schematically illustrates the choices available in this context):

- a box–type design, where the TES is essentially a solid 'lump' either enclosed within or enclosing the evaporator and,
- a planar–type design, in which the storage medium consists of a thin panel, contacting or enclosing, the evaporator unit and designed to augment the heat transfer process into the interior of the refrigerator compartment.

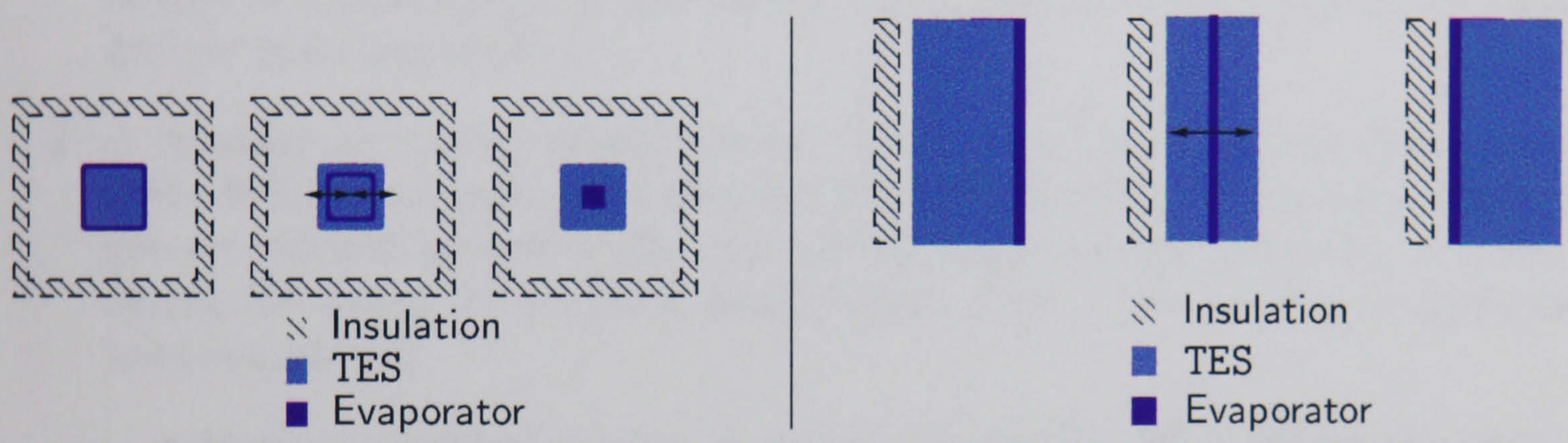


Figure 4.5: Schematic diagram of the two, box (*Left*) and planar (*Right*) – type evaporator–TES arrangements indicating options of possible location of the evaporator within the TES.

In either case (box or planar), whether or not the evaporator is completely enclosed by the thermal store will depend on, amongst other limitations of the design:

- if the quantity of storage material to be used is sufficient for enclosing the evaporator and,
- if the DRA cooling capacity required during the period when the store is being charged can be furnished (due to conduction limitations) via the exposed TES–store surface(s) alone.

In the event that the evaporator is to be completely enclosed within the TES, it cannot necessarily be assumed that the thermal storage medium should be equally distributed on either side of the evaporator. Based on considerations of the ratio of heat ingress into the system (as one side of the evaporator is adjacent to the cabinet wall) to the heat requirements from the use–associated

load, it might be necessary to distribute the quantity of storage material asymmetrically about the evaporator[1], see Figure 4.5 on page 116.

The design of the passive TES within these conceptual designs has to be given careful consideration, to: (a) limit complexity, (b) reduce the necessity for a means of conveying coolth from the evaporator to the TES and, (c) maximise the utilisation of the evaporator for charging the TES. It is clear that the TES should be in pressed contact with the evaporator. However, it must not in any way impair the normal working of the evaporator whilst, at the same time, it must be able to charge and discharge at reasonable rates. This passive storage method is characterised by the lowest capital cost of the two, but is the least flexible and controllable.

2. *A dynamic (or active) thermal store*: In this case the storage medium is actively fluidised to reduce the effective thermal resistance of the store, offering greater thermal control of the store charge and discharge processes and rendering the design of the store shape independent. Two basic arrangements were considered:

   - Internally located storage, similar to the passive TES configuration previously discussed.
   - Externally located storage, where the TES is located exterior to the DRA.

   These options are discussed in more detail in Chapter 4 on page 105. One major difference between these two arrangements is that, for internally–located TES's, store losses need not be accounted as system losses as any store leakage would be internal to the refrigerating compartment. With regard to this the DRA implementation will not suffer one of the major drawbacks that afflict the technology when used in air–conditioning systems *i.e.* energy losses from the energy store.

   In most cases the store (and at least part of its inventory) has to be located exterior to the refrigerating compartment, for size and energy considerations. The method also requires additional inventory (piping, pumps *etc.*) for rendering the storage medium mobile (with attendant energy consumption consequences).

Of the two methods (passive and active storage) a dynamic thermal store possesses the greater level of control flexibility, but it is more complex, costlier and less

[1]This is a consideration which should be borne in mind during the latter stages of any optimisation process.

energy efficient[1]. In the light of the desire to minimise energy losses and the cost constraints imposed by the intended applications, the analysis for these configurations will focus on internal, passive TES. An external, dynamic storage DRA design is discussed later in Chapter 4 on page 105.

4.4.4 Comparative Systems Design Analysis

The purpose of this section is to perform a comparative analysis on the various proposed systems configuration. The following assumptions are made at this stage:

- Henceforth, except where otherwise stated, the rates of any quantities indicated are to be taken as the mean values over the indicated period *e.g.*

$$\dot{Q}_{\mathrm{D}} = \frac{1}{t_{\mathrm{D}}} \int_0^{t_{\mathrm{D}}} Q(\lambda)\, d\lambda$$

- Much of the dynamics of the proposed DRA design are affected by non–linearities attending the different parts of the system. However, to facilitate the initial experimental rig design, the system was considered as passive (steady–state, passive energy storage *etc.*), with linear behavioural characteristics.

- Except where otherwise stated, the efficiencies (η) referred to herein are the product of the first and second law efficiencies *i.e.* $\eta_{\mathrm{i}} \times \eta_{\mathrm{ii}}$.

- The overall energy storage (ES) efficiency of the TES (η_{TES}) is unity *i.e.* the combined effect of the charge ($\eta_{\mathrm{TES}_{\Delta+}}$), hold–over and discharge ($\eta_{\mathrm{TES}_{\Delta-}}$) efficiencies.

- There are charge ($\eta_{\mathrm{Bat.}_{\Delta+}}$) and discharge ($\eta_{\mathrm{Bat.}_{\Delta-}}$) efficiencies associated with the use of the battery and for convenience both may be combined with the representation:

$$\eta_{\mathrm{Bat.}} \equiv \eta_{\mathrm{Bat.}_{\Delta+}} \times \eta_{\mathrm{Bat.}_{\Delta-}}$$

- The hold–over losses in (electro–chemical) battery storage are considered to be negligible for the charge/discharge cycles envisaged in the intended application.

- In an initial analysis, the day– and night–time temperatures may be characterised by representative average values T_{D} and T_{N} respectively.

[1]Inefficient in the sense of the energy recoverable from the store in relation to the total energy input into it (including energy required to operate the store).

- Also as per the specifications laid out in section 4.2 on page 106, day–time temperatures, T_{D}, (as opposed to night–time temperatures, T_{N}) shall persist for no more than a fixed fraction (of *consecutive* hours) of any 24–hour day, a period hereinafter referred to as (t_{D}). The balance of time (over the same 24–hour period) is by default to be allotted to the night–time (t_{N}), the relevant ambient temperature being T_{N}[1].

- The COP of the prime–mover varies with internal and external temperatures and loading conditions. Much of the following analysis depends on the differences in COP of the prime–mover at differing times and ambiances. These have been classified broadly as $\mathrm{COP}_{\mathrm{D}}$ (day–time) and $\mathrm{COP}_{\mathrm{N}}$ (night–time) to characterise the mean COP operating over a given period[2].

- T_l (the mean temperature exchanging heat with the evaporator) has been assumed to have the same constant value throughout[3], for reasons of simplicity. In reality though it varies, and due to the non–linear character of the $\mathrm{COP}(\ldots, T_l, \ldots)$, its dependence on T_l is quite strong, as is evident from the first derivative based on the thermodynamic definition:

$$\frac{\partial \mathrm{COP}(\ldots, T_l, \ldots)}{\partial T_l} = \frac{T_h}{(T_h - T_l)^2}$$

.

- As mentioned earlier in section 3.7 on page 101 the preferred storage medium for TES is hydrated 'cross–linked' Poly Vinyl Alcohol (PVA) of at least 95% $^{\mathrm{w}}/_{\mathrm{w}}$ water content, used as a latent heat thermal storage (LHTES) medium. The properties of the TES medium adopted for this would be computed on that

[1]The occurrence of day– and night–time and their relative lengths is dependent on several factors. For instance a DRA in a 'corner shop' which is closed at 6.00pm in an environment with a high relative humidity would suffer from an additional thermal–lag (to that on account of its insulation) on account of the building's thermal lag. Thus it is conceivable in such a case that the night–time period might well coincide with part of the daily solar insolation period; see also section 2.5.3 on page 66. This issue is indicative of the need for the development of an adaptive controller for DRA's in order to take advantage of such variations due to seasonal changes and between use locations.

[2]However, there are load dependencies on the COP which may have to be accounted for in a more detailed analysis, see eqns (2.15) and (2.18).

[3]This assumption appears justifiable on the grounds that the presence of the immediately adjacent LHTES would ensure a 'constant' T_l. However, in reality, the presence of the TES simply serves to alter the effective conductance of the evaporator surface, T_l remaining as the DRA internal air temperature. That said, it is possible to conceive some time–averaged bulk mean value for T_l sufficiently representative for analysis over different periods of the appliance utilisation cycle.

basis, except however, for the quantity of energy deemed storable and retrievable in the medium which would be reckoned solely on the basis of the latent heat content of the quantity of water in the material.

- Even in the light of the approximation made immediately above (neglecting sensible heats *etc.*) only 95% of the (LHTES) latent heat content available would be deemed recoverable during any charge/discharge cycle, see Appendix C on page C-266. This is to help cope with any irreversibilities arising due to energy transfer and volumetric changes during the freeze–thaw process.

- The sensible heat exchange of the TES has been assumed to be negligible relative to that due to latent heat transfer.

- In line with the specifications given in section 4.2 on page 106, there should be an allowance for an ES capacity equivalent of the energy requirements for an, as yet unspecified minimum period, within the storage facilities of the device *in its fully laden state.* This is to act as a contingency in the event that periods of up to that length occur, when the solar insolation is sub–optimal, referred hereinafter to as the 'inclement period'. By this, it is to be understood that the consideration is for one night–time period more than the number of day periods stipulated; the rationale for this is given in section 4.4.4.2 on page 129.

- Immediately pursuant to any inclement period, there will be a period of equal duration plus an additional fraction thereof in which at least nominal solar insolation is to be expected. This is to ensure the device's storage facilities are replenished by an amount (ψ) of the total storage capacity each 24–hour day.

- During any inclement period, a fixed proportion (ξ)[1] of the normal solar insolation is to be available. This condition may be easily adjusted to cater for circumstances where the energy input into the system is completely cut off for the same period.

- In any 24–hour period, there would be a maximum period, less than the number of day temperature hours, for which nominal solar insolation will be deemed to be available, defined here as the solar duration (t_{sol}).

- The ambient relative humidity can be characterised by two constant values for mean day– and night–time relative humidity.

- The appliance shall be load–charged each day (irrespective of weather clemence) with a fixed 'thermal load' (Q_{load}) at the ambient temperature

[1] Based on discussions with several solar panel manufacturers, 20% was recommended.

which would be expected to cool down over a fixed percentage of the 24–hour period *viz* t_{load}, commencing the start of the night period each day. This is to ensure that the device is capable of reliable performance under load. (see James and Evans (1990) who discuss the problems which can occur when this is not the case, as is usual in practice).

- In any 24–hour period, an as yet unspecified number of volume air changes per hour for the duration of the day (24–hour) period shall be allowed to account for human–appliance interaction[1].

- The maximum size of the TES shall be restricted to the maximum thermal capacity requirement for one 24–hour (day– and night–time) period. This is in order to maximise the cycling of the TES (*i.e.* maximise utilisation) over any given period which improves economic viability and decreases 'hold–over' time losses [Douglass, 1980].

Except where otherwise stated, $\dot{Q}_{\mathrm{N}}$ and $\dot{Q}_{\mathrm{D}}$ correspond to the mean of the totality of the heat loads (use and ingress through the compartment walls) over the indicated period, *i.e.* day–time and night–time. In the interest of clarity, the following notation will be adopted: $\mathtt{COP}\left(\dot{Q}, \triangle T_{hl}\right)$ will be used to denote the relevant COP as defined by eqn (2.15), where the relevant $\dot{Q}$ and $\triangle T_{hl}$ will be explicitly indicated within the formulation.

4.4.4.1 Clement Weather Analysis

The first set of analyses has to do with normal working conditions of the system, where there is sufficient daily insolation and the sole requirement is for the appliance to cater for the basic energy demands day in day out.

Configuration 1 (Battery only system) The minimum battery capacity ($\mathrm{J}_{(e)}$) in this case is given simply as

$$\begin{aligned} \mathsf{E}_{\mathsf{Bat.}} &= \frac{1}{\eta_{\mathsf{Bat.}\,\triangle-}}\left[\frac{Q_{\mathrm{N}}}{\mathtt{COP}_{\mathrm{N}}} + \frac{Q_{\mathrm{D}}\left(t_{\mathrm{D}} - t_{\mathsf{sol}}\right)}{t_{\mathrm{D}} \cdot \mathtt{COP}_{\mathrm{D}}}\right] \\ &= \frac{1}{\eta_{\mathsf{Bat.}\,\triangle-}}\left[\frac{Q_{\mathrm{N}}}{\mathtt{COP}\left(\dot{Q}_{\mathrm{N}}, (\triangle T_{hl})_{\mathrm{N}}\right)} + \frac{\dot{Q}_{\mathrm{D}}(t_{\mathrm{D}} - t_{\mathsf{sol}})}{\mathtt{COP}\left(\dot{Q}_{\mathrm{D}}, (\triangle T_{hl})_{\mathrm{D}}\right)}\right] \end{aligned} \tag{4.1}$$

[1] Sillanpää (1997) suggests 51 door openings per day based on research done in Finland.

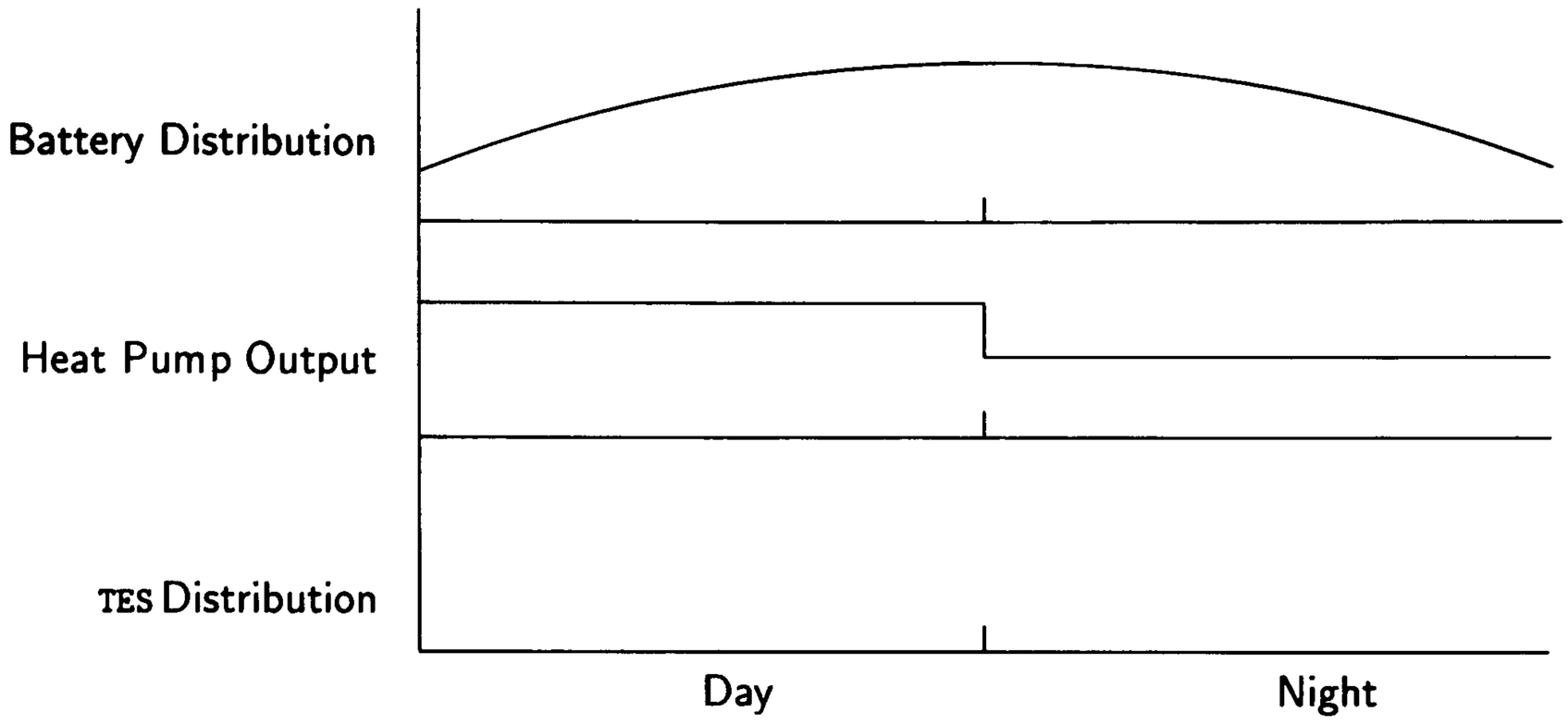


Figure 4.6: Schematic (battery only system) diagram of the battery energy content and heat pump output during one daily cycle.

The battery charge (minimum input) rating ($\mathtt{W}_{(e)}$) is given as

$$P_{\mathsf{Bat.}_{\Delta+}} = \frac{\mathtt{E}_{\mathsf{Bat.}}}{t_{\mathsf{sol}}} \tag{4.2}$$

The battery discharge (minimum output) rating ($\mathtt{W}_{(e)}$) is

$$P_{\mathsf{Bat.}_{\Delta-}} = \frac{\mathtt{E}_{\mathsf{Bat.}}}{(t_{\mathtt{N}} + t_{\mathtt{D}} - t_{\mathsf{sol}})} \times \eta_{\mathsf{Bat.}_{\Delta-}} \tag{4.3}$$

The prime–mover thermal rating ($\mathtt{W}_{(T)}$)[1] is the maximum of

$$P_{\mathtt{HP}(T)} = \max\left(\dot{Q}_{\mathtt{N}}, \dot{Q}_{\mathtt{D}}\right) \tag{4.4}$$

and the prime–mover electrical rating ($\mathtt{W}_{(e)}$) is, the maximum of:

$$P_{\mathtt{HP}(e)} = \max\left(\frac{\dot{Q}_{\mathtt{N}}}{\mathtt{COP}\left(\dot{Q}_{\mathtt{N}}, (\Delta T_{hl})_{\mathtt{N}}\right)}, \frac{\dot{Q}_{\mathtt{D}}}{\mathtt{COP}\left(\dot{Q}_{\mathtt{D}}, (\Delta T_{hl})_{\mathtt{D}}\right)}\right) \tag{4.5}$$

[1] This is in relation to the ambient temperature.

The required electric output rating ($\mathtt{W}_{(e)}$) for the SPV panels is

$$P_{\text{SPV}} = \frac{P_{\text{Bat.}\,\Delta+}}{\eta_{\text{Bat.}\,\Delta+}} + \frac{\dot{Q}_{\text{D}}}{\text{COP}_{\text{D}}}$$

$$= \frac{Q_{\text{N}} \cdot \text{COP}\left(\dot{Q}_{\text{D}}, (\Delta T_{hl})_{\text{D}}\right) + \left[t_{\text{D}} - t_{\text{sol}}\left(1 - \eta_{\text{Bat.}}\right)\right] \cdot \dot{Q}_{\text{D}} \cdot \text{COP}\left(\dot{Q}_{\text{N}}, (\Delta T_{hl})_{\text{N}}\right)}{\eta_{\text{Bat.}} \cdot t_{\text{sol}} \cdot \text{COP}\left(\dot{Q}_{\text{D}}, (\Delta T_{hl})_{\text{D}}\right) \cdot \text{COP}\left(\dot{Q}_{\text{N}}, (\Delta T_{hl})_{\text{N}}\right)} \tag{4.6}$$

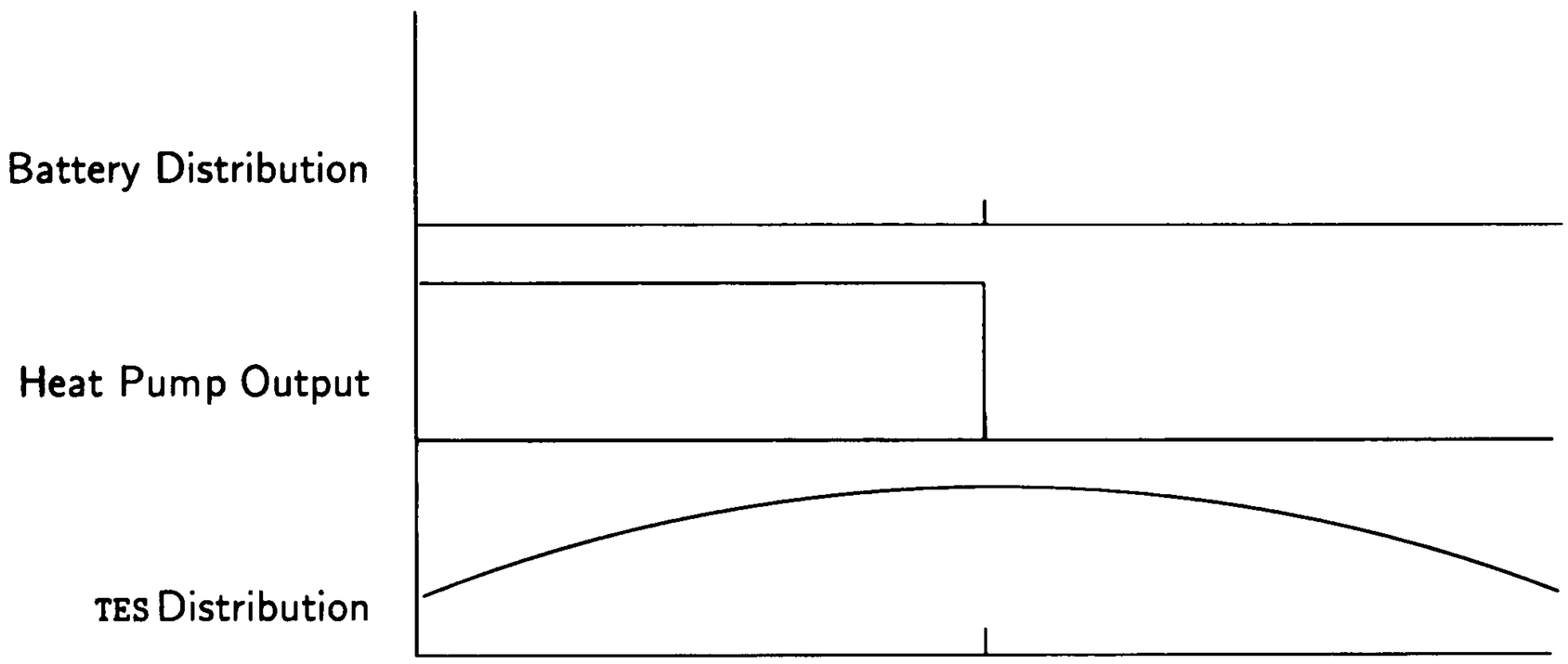


Figure 4.7: Schematic (TES only system) diagram of the TES energy content and heat pump output during one daily cycle.

Configuration 2 (TES only system) In this case the storage type is TES and it is to cater for the periods where there is no solar energy input *i.e.* the period starting from the end of the solar insolation period through the night–time period. Thus the minimum TES capacity ($\mathtt{J}_{(T)}$) is here given simply as

$$\mathtt{E}_{\text{TES}} = \frac{Q_{\text{N}} + Q_{\text{D}}\left(1 - \frac{t_{\text{sol}}}{t_{\text{D}}}\right)}{\eta_{\text{TES}\,\Delta-}}$$

$$= \frac{Q_{\text{N}} + \dot{Q}_{\text{D}}(t_{\text{D}} - t_{\text{sol}})}{\eta_{\text{TES}\,\Delta-}} \tag{4.7}$$

The TES charge rate ($\mathtt{W}_{(T)}$) is given as

$$P_{\text{TES}\,\Delta+} = \frac{\mathtt{E}_{\text{TES}}}{t_{\text{sol}}} \tag{4.8}$$

The TES discharge rate ($\mathtt{W}_{(T)}$) is given as

$$P_{\mathtt{TES}_{\Delta-}} = \frac{\mathtt{E}_{\mathtt{TES}} \times \eta_{\mathtt{TES}_{\Delta-}}}{(t_{\mathtt{N}} + t_{\mathtt{D}} - t_{\mathtt{sol}})} \tag{4.9}$$

The prime–mover thermal rating capacity ($\mathtt{W}_{(T)}$) is

$$\begin{aligned} P_{\mathtt{HP}(T)} &= \dot{Q}_{\mathtt{D}} + \frac{P_{\mathtt{TES}}}{\eta_{\mathtt{TES}_{\Delta+}}} \\ &\dot{Q}_{\mathtt{D}} + \frac{\mathtt{E}_{\mathtt{TES}}}{\eta_{\mathtt{TES}_{\Delta+}} \times t_{\mathtt{sol}}} \end{aligned} \tag{4.10}$$

In this case the relevant COP changes to reflect the larger load and thus the prime–mover electrical output rating ($\mathtt{W}_{(e)}$) is

$$\begin{aligned} P_{\mathtt{HP}(e)} &= \frac{1}{\mathtt{COP}_{\mathtt{D}}} \times \left[\dot{Q}_{\mathtt{D}} + \frac{P_{\mathtt{TES}}}{\eta_{\mathtt{TES}_{\Delta+}}} \right] \\ &= \frac{1}{\mathtt{COP}_{\mathtt{D}}} \times \left[\dot{Q}_{\mathtt{D}} + \frac{\mathtt{E}_{\mathtt{TES}}}{\eta_{\mathtt{TES}_{\Delta+}} \times t_{\mathtt{sol}}} \right] \\ &= \frac{Q_{\mathtt{N}} + \left[t_{\mathtt{D}} - t_{\mathtt{sol}} \left(1 - \eta_{\mathtt{TES}} \right) \right] \dot{Q}_{\mathtt{D}}}{t_{\mathtt{sol}} \times \eta_{\mathtt{TES}} \cdot \mathtt{COP} \left(\frac{Q_{\mathtt{N}} + \left[t_{\mathtt{D}} - t_{\mathtt{sol}} \left(1 - \eta_{\mathtt{TES}} \right) \right] \dot{Q}_{\mathtt{D}}}{t_{\mathtt{sol}} \times \eta_{\mathtt{TES}}}, (\Delta T_{hl})_{\mathtt{D}} \right)} \end{aligned} \tag{4.11}$$

Here the power rating of the SPV panels is simply

$$P_{\mathtt{SPV}} = P_{\mathtt{HP}(e)} \tag{4.12}$$

Configuration 3 (HES system) As mentioned earlier, this configuration is quite flexible and it is possible to conceive of a plethora of quite complex design and control arrangements (see Figures 4.8 and 4.9, *qv.* pages 125 and 125 respectively, for two examples of control options). Here, the restriction is to one of the most basic of such (night–time only prime–mover operation), which it is hoped would serve as illustrative of the available possibilities.

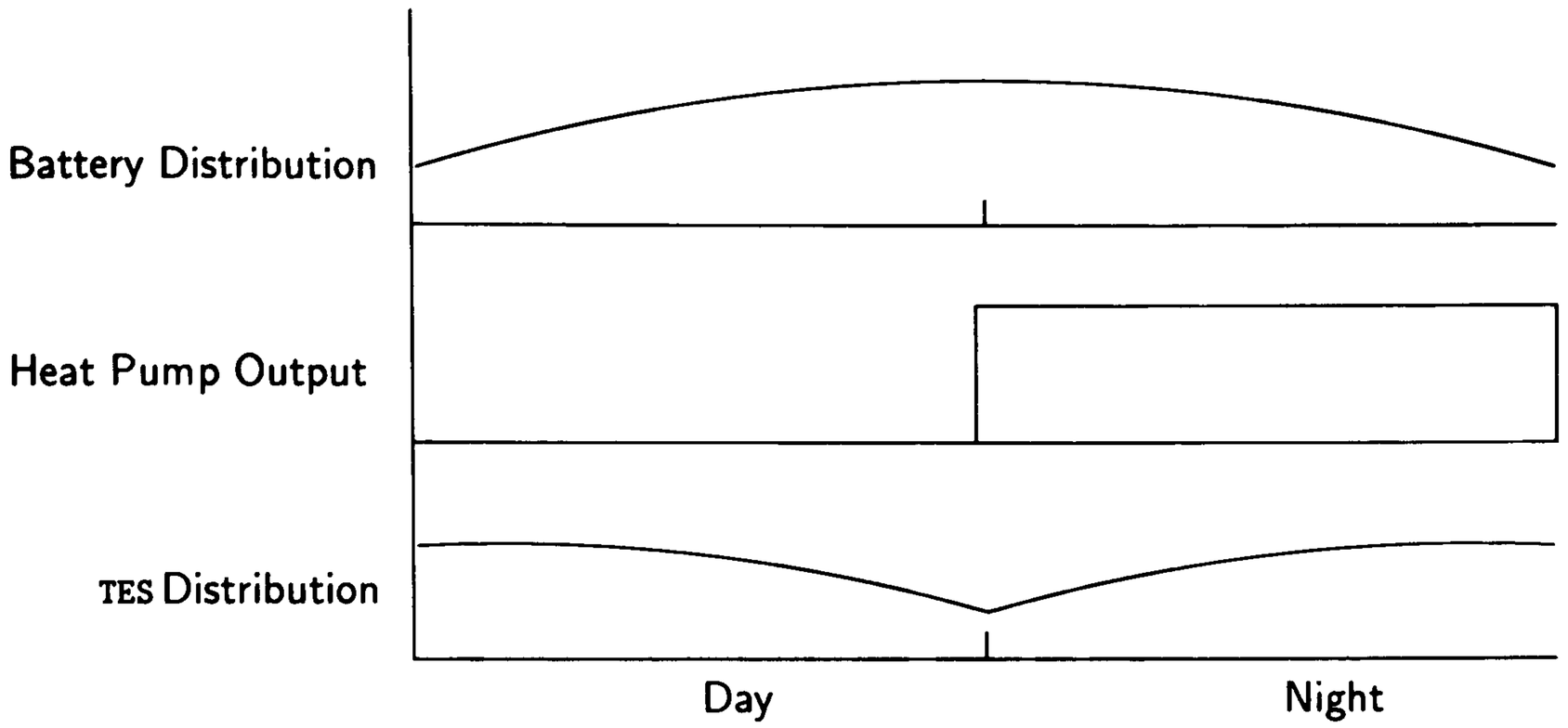


Figure 4.8: Schematic diagram of the battery energy content, TES energy content and heat pump output during one daily cycle for a night–time only prime–mover operation control regime.

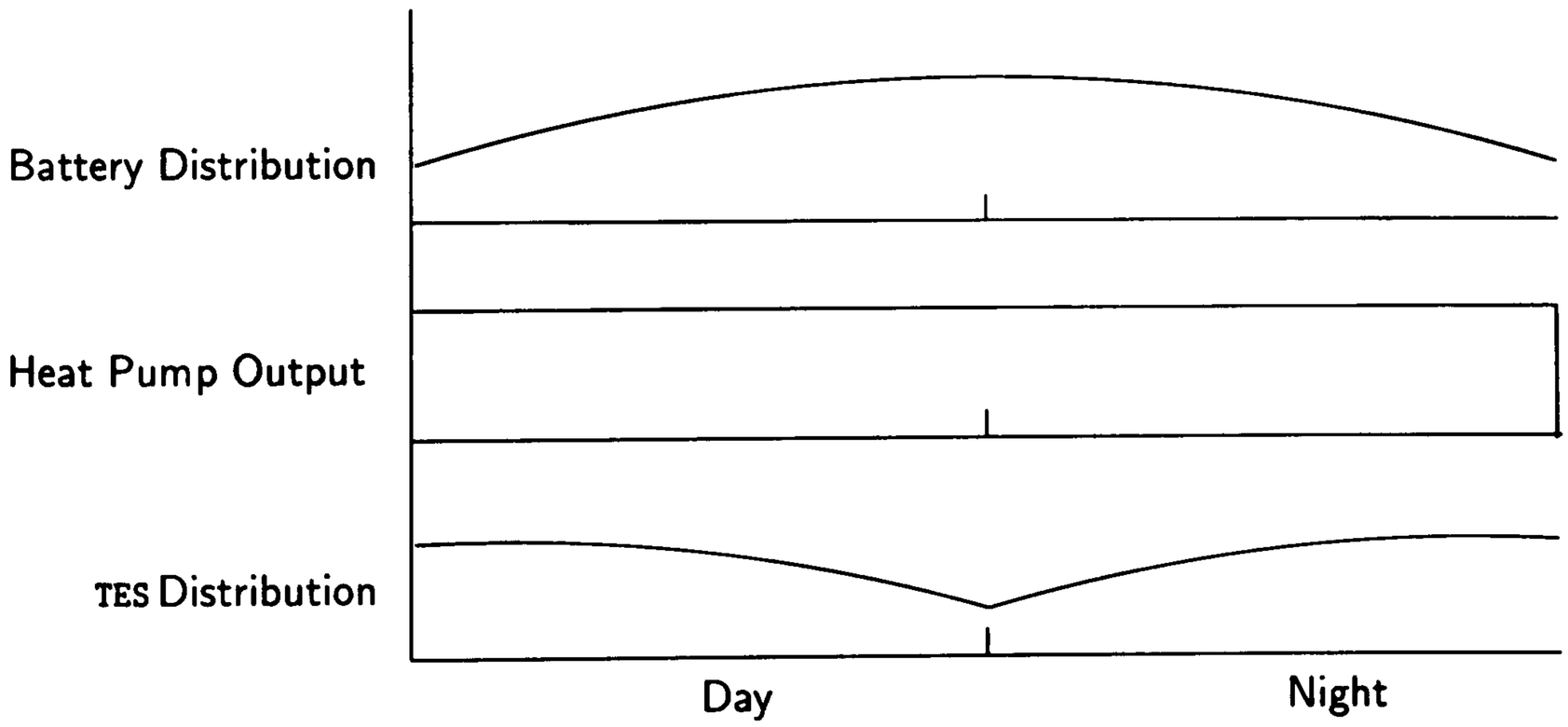


Figure 4.9: Schematic diagram of the battery energy content, TES energy content and heat pump output during one daily cycle for a continuous prime–mover operation control regime.

In line with theoretical observations, a better device COP is to be expected during the night–time than during the day–time (on account of the lower ambient temperatures obtaining over that period), for a given load. In respect of this, the design is based on the initial *premise* that the battery would be charged up during the day–time and the prime–mover run during the night–time, thus catering for any night–time thermal loads, as well as charging the thermal store. This (coolth energy) in turn will be used to cater for the thermal loads of the immediately proceeding day.

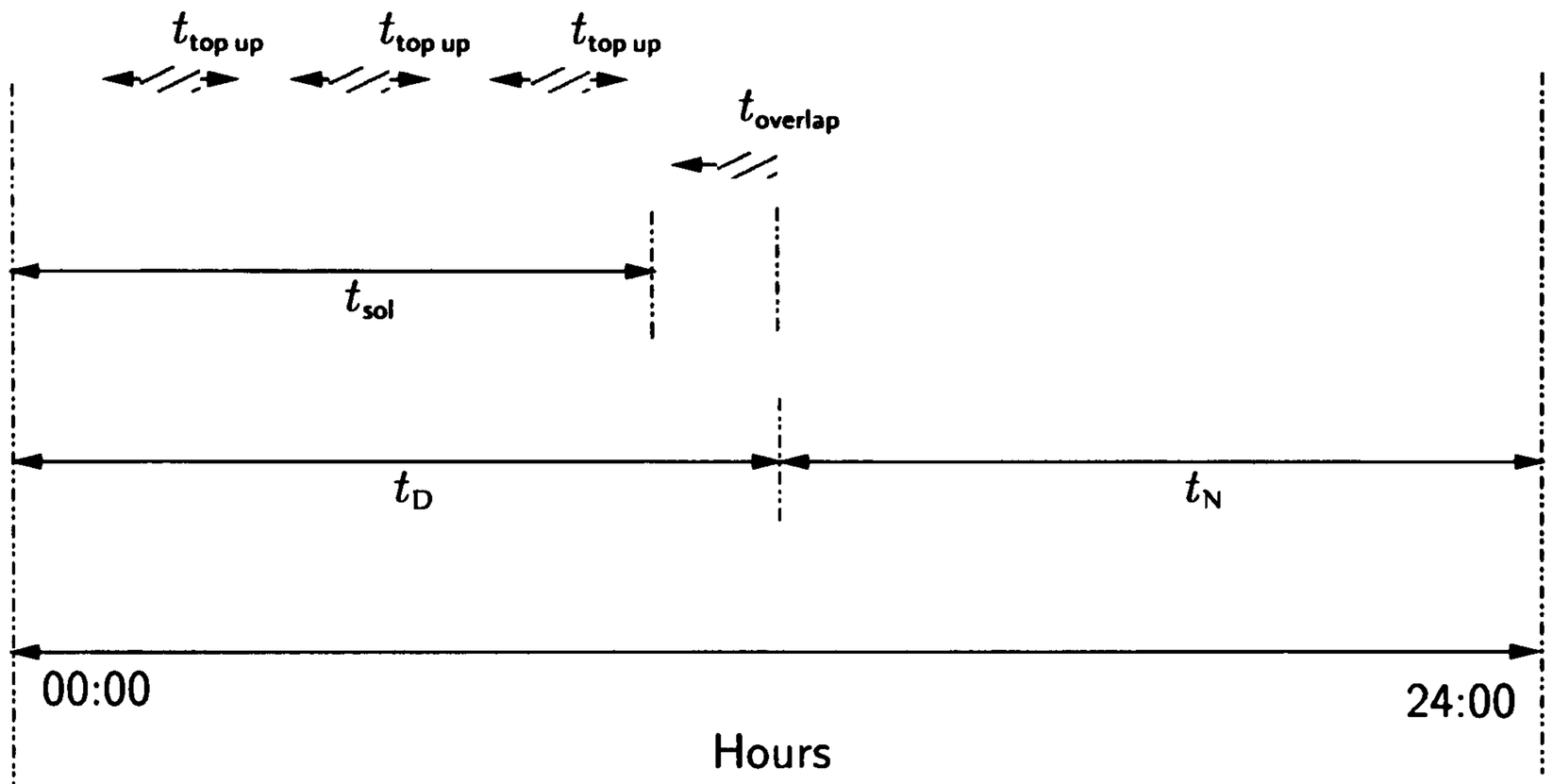


Figure 4.10: Illustration of the differing time periods (t_D, t_N, t_{sol}, $t_{overlap}$, $t_{top\ up}$) within a 24–hour day.

If the thermal requirements of some portion(s) of the day period are to be augmented by the prime–mover directly[1], this can fall into two such categories. These are, *firstly*, a topping–up boost with energy from the solar cell $\zeta_{top\ up} \times Q_D$ (over the period $t_{top\ up}$) to cater for the hotter parts of the day period[2] and, *secondly*, an 'early–start' battery–augmented cooling period, effectively starting the 'night period' at some stage (a fraction $\zeta_{overlap}$, say)[3] of the non–solar active

[1]Possibly for thermal control reasons.

[2]The phrase 'topping–up' is here used in a loose sense, extended to accommodate not only intermittent coolth requirements, but also encompassing the situation where the requirement is for a base/background coolth supply to augment the TES *throughout* the day–time period. Thus, the total amount of energy transfered in consequence of this is $\zeta_{top\ up} Q_D$. It is important to realise the potential of $\zeta_{top\ up}$ for appliance temperature regulation, especially during high heat gain periods of the day.

[3]The cooling at this stage is done under the influence of the day–time temperatures and, as such, no TES charging is assumed to take place; this will *always* be done under the influence of the

period of the day–time (see Figure 4.10 on page 126). In that case the battery capacity can be seen to be:

$$\mathsf{E}_{\mathsf{Bat.}} = \frac{1}{\eta_{\mathsf{Bat.}\,\Delta-}}\left[\frac{\eta_{\mathsf{TES}\,\Delta+} \times Q_{\mathsf{N}} + \mathsf{E}_{\mathsf{TES}}}{\eta_{\mathsf{TES}\,\Delta+} \times \mathsf{COP}_{\mathsf{N}}} + \frac{(\zeta_{\mathsf{overlap}}(t_{\mathsf{D}} - t_{\mathsf{sol}}) + \zeta_{\mathsf{top\,up}}) \times Q_{\mathsf{D}}}{\mathsf{COP}_{\mathsf{D}} \times t_{\mathsf{D}}}\right] \tag{4.13}$$

$$= \frac{(\eta_{\mathsf{TES}} \times Q_{\mathsf{N}} + \mathsf{E}_{\mathsf{TES}}) \cdot \mathsf{COP}_{\mathsf{D}} + (\zeta_{\mathsf{overlap}}(t_{\mathsf{D}} - t_{\mathsf{sol}}) + \zeta_{\mathsf{top\,up}}) \times Q_{\mathsf{D}} \cdot \mathsf{COP}_{\mathsf{N}} \cdot \eta_{\mathsf{TES}\,\Delta+}}{\eta_{\mathsf{Bat.}\,\Delta-}\,\eta_{\mathsf{TES}\,\Delta+} \cdot \mathsf{COP}_{\mathsf{N}} \cdot \mathsf{COP}_{\mathsf{D}}}$$

In this case

$$\mathsf{COP}_{\mathsf{D}} = \mathsf{COP}\left(\dot{Q}_{\mathsf{D}}, (\Delta T_{hl})_{\mathsf{D}}\right) \tag{4.13-a}$$

$$\mathsf{COP}_{\mathsf{N}} = \mathsf{COP}\left(\frac{\eta_{\mathsf{TES}\,\Delta+} \times Q_{\mathsf{N}} + \mathsf{E}_{\mathsf{TES}}}{\eta_{\mathsf{TES}\,\Delta+} \times [t_{\mathsf{N}} + \zeta_{\mathsf{overlap}}(t_{\mathsf{D}} - t_{\mathsf{sol}})]}, (\Delta T_{hl})_{\mathsf{N}}\right) \tag{4.13-b}$$

$\mathsf{E}_{\mathsf{TES}}$ ($\mathsf{J}_{(T)}$) being the TES capacity and is as yet undefined. Note, that due to the non–linear character of eqn (4.13), there are opportunities for minimisation of the battery capacity with respect to the TES capacity and/or the fraction of the non–solar period of the day–load catered for by the battery *i.e.* ζ_{overlap}. The charge rate of the battery is simply:

$$P_{\mathsf{Bat.}\,\Delta+} = \frac{\mathsf{E}_{\mathsf{Bat.}}}{t_{\mathsf{sol}}} \tag{4.14}$$

whilst the battery discharge rate is

$$P_{\mathsf{Bat.}\,\Delta-} = \frac{\mathsf{E}_{\mathsf{Bat.}} \times \eta_{\mathsf{Bat.}\,\Delta-}}{t_{\mathsf{N}} + \zeta_{\mathsf{overlap}}(t_{\mathsf{D}} - t_{\mathsf{sol}})} \tag{4.15}$$

As before, the TES capacity is to be sized for the smallest cycling period. Based on this, and the presumption that the use of the night–time COP is to be most beneficial, it is reasonable to assume, tentatively, the day–load (Q_{D}) as an initial start point. From this, deductions are made for the 'topping–up' input ($\zeta_{\mathsf{top\,up}} Q_{\mathsf{D}}$) and the portion of the day–load accrued between the period t_{sol} and ($t_{\mathsf{sol}} + \zeta_{\mathsf{overlap}} \times (t_{\mathsf{D}} - t_{\mathsf{sol}})$), *i.e.* the non–solar active period which is to be catered

night–time temperature.

for by direct prime–mover action (via the battery). Thus the TES capacity is defined:

$$\mathrm{E}_{\mathrm{TES}} = \frac{Q_{\mathrm{D}} \times \left[1 - \zeta_{\mathrm{overlap}} \left(1 - \frac{t_{\mathrm{sol}}}{t_{\mathrm{D}}}\right) - \zeta_{\mathrm{top\ up}}\right]}{\eta_{\mathrm{TES}_{\Delta-}}} \tag{4.16}$$

The TES charge rate ($\mathrm{W}_{(T)}$) is given as

$$P_{\mathrm{TES}_{\Delta+}} = \frac{\mathrm{E}_{\mathrm{TES}}}{t_{\mathrm{N}}} \tag{4.17}$$

The TES discharge rate ($\mathrm{W}_{(T)}$) is given as

$$P_{\mathrm{TES}_{\Delta-}} = \frac{\mathrm{E}_{\mathrm{TES}} \times \eta_{\mathrm{TES}_{\Delta-}}}{[t_{\mathrm{D}} - \zeta_{\mathrm{overlap}} \times (t_{\mathrm{D}} - t_{\mathrm{sol}})]} \tag{4.18}$$

The prime–mover thermal rating capacity ($\mathrm{W}_{(T)}$) is

$$P_{\mathrm{HP}(T)} = \max\left(\frac{\eta_{\mathrm{TES}_{\Delta+}} \times Q_{\mathrm{N}} + \mathrm{E}_{\mathrm{TES}}}{\eta_{\mathrm{TES}_{\Delta+}} \times t_{\mathrm{N}}}, \dot{Q}_{\mathrm{top\ up}}, \dot{Q}_{\mathrm{overlap}}\right) \tag{4.19}$$

The prime–mover electrical ($\mathrm{W}_{(e)}$) requirement is

$$P_{\mathrm{HP}(e)} = \max\left(\frac{\eta_{\mathrm{TES}_{\Delta+}} \times Q_{\mathrm{N}} + \mathrm{E}_{\mathrm{TES}}}{\eta_{\mathrm{TES}_{\Delta+}} \cdot t_{\mathrm{N}} \times \mathrm{COP}_{\mathrm{N}}}, \frac{\max\left(\dot{Q}_{\mathrm{top\ up}}, \dot{Q}_{\mathrm{overlap}}\right)}{\mathrm{COP}_{\mathrm{D}}}\right)$$

$$\mathrm{COP}_{\mathrm{N}} = \mathrm{COP}\left(\frac{\eta_{\mathrm{TES}_{\Delta+}} \times Q_{\mathrm{N}} + \mathrm{E}_{\mathrm{TES}}}{\eta_{\mathrm{TES}_{\Delta+}} \cdot t_{\mathrm{N}} \times \mathrm{COP}_{\mathrm{N}}, (\Delta T_{hl})_{\mathrm{N}}}\right) \tag{4.20}$$

$$\mathrm{COP}_{\mathrm{D}} = \mathrm{COP}\left(\max\left(\dot{Q}_{\mathrm{top\ up}}, \dot{Q}_{\mathrm{overlap}}\right), (\Delta T_{hl})_{\mathrm{D}}\right)$$

The electric output rating ($\mathrm{W}_{(e)}$) for the SPV panels is

$$P_{\mathrm{SPV}} = P_{\mathrm{Bat.}_{\Delta+}} + Q_{\mathrm{top\ up}} \tag{4.21}$$

Note that, as with the case of the battery capacity, opportunities exist for the minimisation of the TES size, dependent on ζ_{overlap} and the $\zeta_{\mathrm{top\ up}}$. Thus,

the TES may be sized according to one of several criteria *e.g.* (a) from the optimisation of eqn (4.13) for a minimum battery capacity, (b) based on an attempt to equalise the prime–mover output across all the regions eqn (4.19) *i.e.*, for the smallest possible size, (c) for minimum energy consumption (*i.e.* solar cell capacity), eqn (4.21) and (d) for the smallest TES size, eqn (4.16). Whatever consideration is utilised will have a bearing on the actual charge–discharge regime (strategy) adopted in the control of the device and *vice versa*.

4.4.4.2 Inclement Weather Analysis

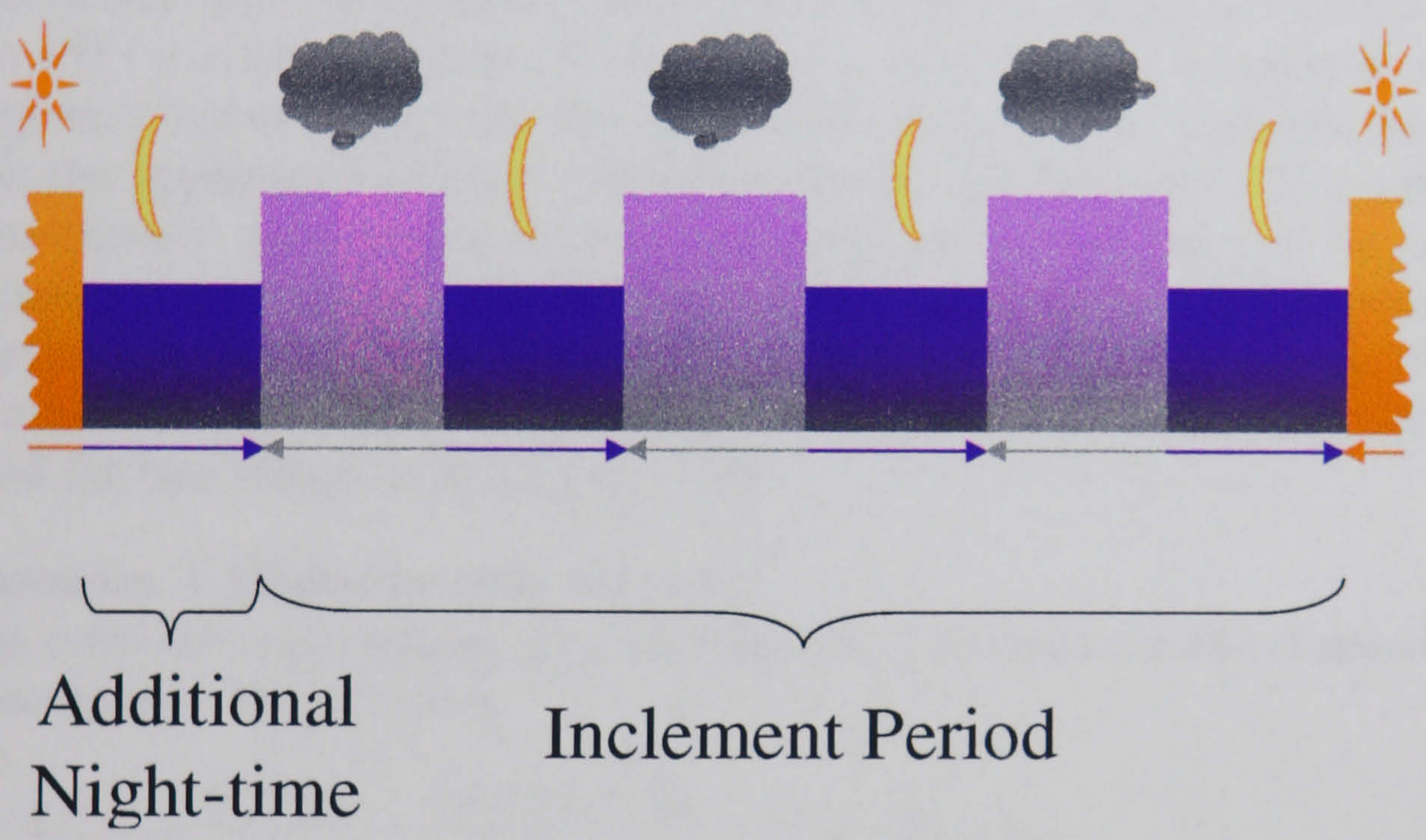


Figure 4.11: Schematic diagram of the inclement period

The second set of analyses has to do with the 'worst' or 'distress' case scenario, where the system is envisaged to sustain performance for a given length of time under some adverse condition. One such scenario occurs in the event when there is insufficient solar insolation for n consecutive days immediately following a period of not less than $(n + 1 = (\psi^{-1}))$ days of normal operation. Such a scenario might arise, within the current context[1], in the event that there is sustained cloud cover over the period, *i.e.* an 'inclement weather' period (see the underlying specifications/assumptions set out in section 4.4.4 on page 118). During this period, it is assumed that the cloud cover will reduce the available power supply ξ of the nominal daily supply. However, the daily temperature variations, humidity and utilisation

[1]In developing, and on occasion in developed, countries this could also simulate a 'power cut'.

pattern will remain essentially the same as those pertaining to normal operating periods.

Prior to any further analysis it is important to be unequivocal about the length of time implied by the stipulated inclement period. Consider three consecutive day–time periods in which only a token amount of solar insolation exists. Within this period, two night–time periods also exist. However, this does not constitute three full days and as such, an additional night–time period will have to be added on to make up the alloted number of full day (inclement) periods. Thus, the system will be expected to fail if there is no solar insulation during the fourth day–time period pursuant to this three (24–hour) day inclement period. However, (a) at the close of any particular day–time period, there is no simple way of predicting whether or not there will be solar insolation on the next day and, (b) the specification clearly states a given number of days (in this case three) capacity which should be catered for above the appliance's normal working capacity. In this regard the night–time loads immediately preceding any such inclement period will have to be added to the required storage capacity, *i.e.* the required storage capacity will be extended by one additional night–time load equivalent. As a result of this, in this example, the thermal loads for four night–time periods and three day–time periods will have to be allowed for (see Figure 4.11 on page 129).

Configuration 1 (Battery only system)

The total electrical energy requirements ($\mathrm{J}_{(e)}$) to cater for the thermal energy demand over the period is

$$\mathrm{E}_{\mathrm{tot.}(e)} = \frac{n \times Q_{\mathrm{D}}}{\mathrm{COP}_{\mathrm{D}}} + \frac{(n+1) \times Q_{\mathrm{N}}}{\mathrm{COP}_{\mathrm{N}}} - n \cdot \xi \cdot P_{\mathrm{SPV}} \cdot t_{\mathrm{sol}}$$

$$\frac{n \times Q_{\mathrm{D}}}{\mathrm{COP}\left(\dot{Q}_{\mathrm{D}}, (\Delta T_{hl})_{\mathrm{D}}\right)} + \frac{(n+1) \times Q_{\mathrm{N}}}{\mathrm{COP}\left(\dot{Q}_{\mathrm{N}}, (\Delta T_{hl})_{\mathrm{N}}\right)} - n \cdot \xi \cdot P_{\mathrm{SPV}} \cdot t_{\mathrm{sol}} \tag{4.22}$$

Thus the battery requirement ($\mathrm{W}_{(e)}$) for this is

$$\mathrm{E}_{\mathrm{Bat.}} = \frac{\mathrm{E}_{\mathrm{tot.}}}{\eta_{\mathrm{Bat.}\,\Delta-}} \tag{4.23}$$

The battery charge (minimum input) rate ($\mathrm{W}_{(e)}$) is given as (*cf:* eqn (4.1))

$$P_{\mathrm{Bat.}\,\Delta+} = \frac{\left[\psi \times \mathrm{E}_{\mathrm{tot.}(e)} + \frac{Q_{\mathrm{N}}}{\mathrm{COP}\left(\dot{Q}_{\mathrm{N}}, (\Delta T_{hl})_{\mathrm{N}}\right)} + \frac{(t_{\mathrm{D}} - t_{\mathrm{sol}}) \times \dot{Q}_{\mathrm{D}}}{\mathrm{COP}\left(\dot{Q}_{\mathrm{D}}, (\Delta T_{hl})_{\mathrm{D}}\right)}\right]}{t_{\mathrm{sol}} \times \eta_{\mathrm{Bat.}\,\Delta-}} \tag{4.24}$$

The battery discharge (minimum output) capacity ($\mathtt{W}_{(e)}$) is

$$P_{\mathtt{Bat.}_{\Delta-}} = \max\left(\frac{\dot{Q}_{\mathtt{N}}}{\mathtt{COP}\left(\dot{Q}_{\mathtt{N}}, (\Delta T_{hl})_{\mathtt{N}}\right)}, \frac{\dot{Q}_{\mathtt{D}}}{\mathtt{COP}\left(\dot{Q}_{\mathtt{D}}, (\Delta T_{hl})_{\mathtt{D}}\right)}\right) \tag{4.25}$$

The prime–mover thermal rating capacity ($\mathtt{W}_{(T)}$) is

$$P_{\mathtt{HP}(T)} = \max\left(\dot{Q}_{\mathtt{N}}, \dot{Q}_{\mathtt{D}}\right) \tag{4.26}$$

Likewise the electrical rating capacity ($\mathtt{W}_{(e)}$) is

$$P_{\mathtt{HP}(e)} = P_{\mathtt{Bat.}_{\Delta-}} \tag{4.27}$$

The power output rating ($\mathtt{W}_{(e)}$) for the SPV panels is

$$\begin{aligned} P_{\mathtt{SPV}} &= \frac{1}{\eta_{\mathtt{Bat.}} \times t_{\mathtt{sol}}}\left[\psi \mathtt{E}_{\mathtt{tot.}(e)} + \frac{Q_{\mathtt{N}}}{\mathtt{COP}_{\mathtt{N}}} + \frac{\dot{Q}_{\mathtt{D}}(t_{\mathtt{D}} - t_{\mathtt{sol}})}{\mathtt{COP}_{\mathtt{D}}}\right] + \frac{\dot{Q}_{\mathtt{D}}}{\mathtt{COP}_{\mathtt{D}}} \\ &= \frac{[t_{\mathtt{D}}(\psi \times n + 1) - t_{\mathtt{sol}}(1 - \eta_{\mathtt{Bat.}})] \cdot \dot{Q}_{\mathtt{D}} \times \mathtt{COP}_{\mathtt{N}} + [\psi(n+1) + 1] \cdot Q_{\mathtt{N}} \times \mathtt{COP}_{\mathtt{D}}}{[t_{\mathtt{sol}} \times \eta_{\mathtt{Bat.}} + n \times \psi \times \xi] \cdot \mathtt{COP}_{\mathtt{D}} \cdot \mathtt{COP}_{\mathtt{N}}} \end{aligned} \tag{4.28}$$

Here $\mathtt{COP}_{\mathtt{D}}$ and $\mathtt{COP}_{\mathtt{N}}$ are defined as per eqn (4.25)

Configuration 2 (TES only system)

The total thermal energy requirements ($\mathtt{J}_{(T)}$) can be seen to be

$$\begin{aligned} \mathtt{E}_{\mathtt{tot.}(T)} &= n \times Q_{\mathtt{D}} + (n+1) \times Q_{\mathtt{N}} - n \cdot \xi \cdot P_{\mathtt{SPV}} \cdot t_{\mathtt{sol}} \cdot \mathtt{COP}_{\mathtt{D}} \\ &= n \times Q_{\mathtt{D}} + (n+1) \times Q_{\mathtt{N}} - n \cdot \xi \cdot P_{\mathtt{SPV}} \cdot t_{\mathtt{sol}} \cdot \mathtt{COP}\left(Q_{\mathtt{D}} + Q_{\mathtt{N}}, (\Delta T_{hl})_{\mathtt{D}}\right) \end{aligned} \tag{4.29}$$

This gives a thermal store capacity of

$$\mathtt{E}_{\mathtt{TES}} = \frac{\mathtt{E}_{\mathtt{tot.}(T)}}{\eta_{\mathtt{TES}_{\Delta-}}} \tag{4.30}$$

The TES charge (minimum input) rate ($\mathtt{W}_{(T)}$) is given as

$$P_{\mathtt{TES}_{\Delta+}} = \frac{\left[Q_{\mathtt{N}} + (t_{\mathtt{D}} - t_{\mathtt{sol}}) \times \dot{Q}_{\mathtt{D}} + \psi \times \mathtt{E}_{\mathtt{tot.}(T)}\right]}{t_{\mathtt{sol}} \eta_{\mathtt{TES}_{\Delta-}}} \tag{4.31}$$

The TES discharge (output capacity) rating ($\mathtt{W}_{(T)}$) is

$$P_{\mathtt{TES}_{\Delta-}} = \max\left(\dot{Q}_{\mathtt{N}}, \dot{Q}_{\mathtt{D}}\right) \tag{4.32}$$

The prime–mover thermal rating capacity ($\mathtt{W}_{(T)}$) is

$$P_{\mathtt{HP}(T)} = \dot{Q}_{\mathtt{D}} + \frac{P_{\mathtt{TES}_{\Delta+}}}{\eta_{\mathtt{TES}_{\Delta+}}} \tag{4.33}$$

Again, making the relevant changes in the COP loading conditions, the prime–mover electrical output rating ($\mathtt{W}_{(e)}$) is

$$\begin{aligned} P_{\mathtt{HP}(e)} &= \frac{P_{\mathtt{HP}(T)}}{\mathtt{COP}_{\mathtt{D}}} \\ &= \frac{\dot{Q}_{\mathtt{D}} \cdot (t_{\mathtt{D}} - t_{\mathtt{sol}}[1 - \eta_{\mathtt{TES}}]) + \psi \times \eta_{\mathtt{TES}_{\Delta-}} \mathtt{E}_{\mathtt{TES}}}{t_{\mathtt{sol}}\eta_{\mathtt{TES}} \cdot \mathtt{COP}\left(\frac{\dot{Q}_{\mathtt{D}} \cdot \left(t_{\mathtt{D}} - t_{\mathtt{sol}}\left[1-\eta_{\mathtt{TES}}\right]\right) + \psi \times \mathtt{E}_{\mathtt{tot.}(T)}}{t_{\mathtt{sol}}\eta_{\mathtt{TES}}}, (\Delta T_{hl})_{\mathtt{D}}\right)} \end{aligned} \tag{4.34}$$

In this case the power rating of the SPV panels is simply

$$P_{\mathtt{SPV}} = P_{\mathtt{HP}(e)} \tag{4.35}$$

Configuration 3 (HES system)

Adopting the observations made in the discussion on page 124 with regard to this system and under the modified assumptions (due to weather inclemence), the total systems energy requirement in this case may be deduced:

$$\mathtt{E}_{\mathtt{tot.}(e)} = \frac{(n+1) \cdot Q_{\mathtt{N}} \cdot \eta_{\mathtt{TES}_{\Delta+}} + n \cdot \mathtt{E}_{\mathtt{TES}}}{\eta_{\mathtt{TES}_{\Delta+}} \mathtt{COP}_{\mathtt{N}}} + n\left[\frac{Q_{\mathtt{D}} - \eta_{\mathtt{TES}_{\Delta-}} \mathtt{E}_{\mathtt{TES}}}{\mathtt{COP}_{\mathtt{D}}} - \xi \cdot P_{\mathtt{SPV}} \cdot t_{\mathtt{sol}}\right]$$

$$\mathtt{COP}_{\mathtt{D}} = \mathtt{COP}\left(\frac{Q_{\mathtt{D}} - \mathtt{E}_{\mathtt{TES}} \cdot \eta_{\mathtt{TES}_{\Delta-}}}{t_{\mathtt{D}} - \zeta_{\mathtt{overlap}}(t_{\mathtt{D}} - t_{\mathtt{sol}})}, (\Delta T_{hl})_{\mathtt{D}}\right) \tag{4.36}$$

$$\mathtt{COP}_{\mathtt{N}} = \mathtt{COP}\left(\frac{\eta_{\mathtt{TES}_{\Delta+}} \cdot Q_{\mathtt{N}} + \mathtt{E}_{\mathtt{TES}}}{\eta_{\mathtt{TES}_{\Delta+}} \cdot t_{\mathtt{N}}}, (\Delta T_{hl})_{\mathtt{N}}\right)$$

E_{TES} ($\mathsf{J}_{(T)}$) being the TES capacity. As before, the TES capacity is to be tentatively sized for the daily cycling period; based on this and the presumption that the use of the night–time COP is to be most beneficial, the day–load (Q_{D}) is used as an initial starting point. From that, deductions are made for the 'top up' input ($\zeta_{\text{top up}} Q_{\mathsf{D}}$) and the portion of the day–load accrued during the fraction of the non–solar period ($\zeta_{\text{overlap}} \times (t_{\mathsf{D}} - t_{\text{sol}})$) which is catered for directly by the prime–mover. Thus the TES capacity is defined[1]:

$$\mathsf{E}_{\text{TES}} = \frac{Q_{\mathsf{D}} \cdot \left[1 - \zeta_{\text{overlap}} \left(1 - \frac{t_{\text{sol}}}{t_{\mathsf{D}}}\right) - \zeta_{\text{top up}}\right]}{\eta_{\text{TES}_{\Delta-}}} \tag{4.37}$$

The battery capacity ($\mathsf{J}_{(e)}$) can be seen to be

$$\mathsf{E}_{\text{Bat.}} = \frac{\mathsf{E}_{\text{tot.}(e)}}{\eta_{\text{Bat.}_{\Delta-}}} \tag{4.38}$$

The charge rate of the battery is simply

$$P_{\text{Bat.}_{\Delta+}} = \frac{Q_{\mathsf{N}} + \mathsf{E}_{\text{TES}} + \eta_{\text{TES}_{\Delta+}} \psi \mathsf{E}_{\text{tot.}(e)} \mathsf{COP}_{\mathsf{N}}}{\mathsf{COP}_{\mathsf{N}} \cdot \eta_{\text{TES}_{\Delta+}} \eta_{\text{Bat.}_{\Delta-}} t_{\text{sol}}} \tag{4.39}$$

whilst the battery discharge (output) rate is

$$P_{\text{Bat.}_{\Delta-}} = \max\left(\frac{Q_{\mathsf{N}} \cdot \eta_{\text{TES}_{\Delta+}} + \mathsf{E}_{\text{TES}}}{\eta_{\text{TES}_{\Delta+}} \cdot \mathsf{COP}_{\mathsf{N}} \cdot t_{\mathsf{N}}}, \frac{Q_{\mathsf{D}} - \eta_{\text{TES}_{\Delta-}} \mathsf{E}_{\text{TES}}}{t_{\mathsf{D}} \cdot \mathsf{COP}_{\mathsf{D}}}\right) \tag{4.40}$$

The TES charge rate ($\mathsf{W}_{(T)}$) is given as

$$P_{\text{TES}_{\Delta+}} = \frac{\mathsf{E}_{\text{TES}}}{t_{\mathsf{N}}} \tag{4.41}$$

The TES discharge rate ($\mathsf{W}_{(T)}$) is given as

$$P_{\text{TES}_{\Delta-}} = \frac{\mathsf{E}_{\text{TES}} \times \eta_{\text{TES}_{\Delta-}}}{[t_{\mathsf{D}} - \zeta_{\text{overlap}} \times (t_{\mathsf{D}} - t_{\text{sol}})]} \tag{4.42}$$

[1]Note that the observations given immediately after eqn (4.13) are also applicable here.

The prime–mover thermal rating capacity ($\mathtt{W}_{(T)}$) is

$$P_{\mathtt{HP}(T)} = \max\left(\frac{\eta_{\mathtt{TES}} \times Q_{\mathtt{N}} + \mathtt{E}_{\mathtt{TES}} \times \eta_{\mathtt{TES}\,\triangle-}}{\eta_{\mathtt{TES}} \times t_{\mathtt{N}}}, \dot{Q}_{\mathtt{top\ up}}\right) \tag{4.43}$$

$$\dot{Q}_{\mathtt{top\ up}} = \frac{Q_{\mathtt{D}} - \eta_{\mathtt{TES}\,\triangle-}\,\mathtt{E}_{\mathtt{TES}}}{t_{\mathtt{top\ up}}}$$

The prime–mover electrical ($\mathtt{W}_{(e)}$) requirement is

$$P_{\mathtt{HP}(e)} = \max\left(\frac{\eta_{\mathtt{TES}} \cdot Q_{\mathtt{N}} + \mathtt{E}_{\mathtt{TES}} \times \eta_{\mathtt{TES}\,\triangle-}}{\eta_{\mathtt{TES}} \times t_{\mathtt{N}} \times \mathtt{COP}\left(\left[\frac{\eta_{\mathtt{TES}} \times Q_{\mathtt{N}} + \mathtt{E}_{\mathtt{TES}} \times \eta_{\mathtt{TES}\,\triangle-}}{\eta_{\mathtt{TES}} \times t_{\mathtt{N}}}\right], (\triangle T_{hl})_{\mathtt{N}}\right)}, \frac{Q_{\mathtt{D}} - \mathtt{E}_{\mathtt{TES}} \cdot \eta_{\mathtt{TES}\,\triangle-}}{t_{\mathtt{top\ up}} \cdot \mathtt{COP}\left(\frac{Q_{\mathtt{D}} - \mathtt{E}_{\mathtt{TES}} \cdot \eta_{\mathtt{TES}\,\triangle-}}{t_{\mathtt{top\ up}}}, (\triangle T_{hl})_{\mathtt{D}}\right)}\right) \tag{4.44}$$

The electric output rating ($\mathtt{W}_{(e)}$) for the SPV panels is

$$P_{\mathtt{SPV}} = \frac{P_{\mathtt{Bat.}\,\triangle+}}{\eta_{\mathtt{Bat.}\,\triangle+}} + \frac{Q_{\mathtt{D}} - \mathtt{E}_{\mathtt{TES}} \cdot \eta_{\mathtt{TES}\,\triangle-}}{\mathtt{COP}_{\mathtt{D}} \cdot t_{\mathtt{sol}}}$$

$$= \frac{\left[\mathtt{COP}_{\mathtt{N}} \cdot \eta_{\mathtt{TES}}(Q_{\mathtt{D}} - \eta_{\mathtt{TES}\,\triangle-}\,\mathtt{E}_{\mathtt{TES}}) \cdot [\eta_{\mathtt{Bat.}} + \psi n]\right]}{\mathtt{COP}_{\mathtt{D}} \cdot \mathtt{COP}_{\mathtt{N}} \cdot \eta_{\mathtt{TES}} \cdot (\eta_{\mathtt{Bat.}} + n \cdot \xi \cdot \psi) \cdot t_{\mathtt{sol}}} + \frac{\left[\mathtt{COP}_{\mathtt{D}} \times \left([Q_{\mathtt{N}} \cdot \eta_{\mathtt{TES}} + \eta_{\mathtt{TES}\,\triangle-}\,\mathtt{E}_{\mathtt{TES}}] \cdot [1 + \psi \cdot (n+1)] - \eta_{\mathtt{TES}\,\triangle-}\,\mathtt{E}_{\mathtt{TES}}\right)\right]}{\mathtt{COP}_{\mathtt{D}} \cdot \mathtt{COP}_{\mathtt{N}} \cdot \eta_{\mathtt{TES}} \cdot (\eta_{\mathtt{Bat.}} + n \cdot \xi \cdot \psi) \cdot t_{\mathtt{sol}}} \tag{4.45}$$

4.5 Parameter Design

Introduction

This section documents the design methods for the main component parameters of the system. These include the DRA compartment, the evaporator temperature and the thermal store. The section also deals with issues of the loading conditions which might arise in practice and other allied heat transfer issues.

4.5.1 General Discussion On Parameter Design

An ideal design specification of the individual components for the DRA should take into consideration not only the static design point specification of the component, but also the interaction between components and the dynamics consequent of that interaction. Such a process would necessarily involve an extensive amount of iteration between the design, prototype and appliance test phases (due to the approximate nature of the modelling process and the ubiquitous presence of non–linearities in the pertinent design equations). For the current exercise, much of the analysis considers the various components in their 'uncoupled' state and in many instances linear approximations have been used to characterise properties and processes.

The design specification of the compartment is subject to: (a) the design point internal temperature (or temperature range) and (b) the prevailing ambience and any effects that the changes in that ambience will have on the 'arrival time' of heat ingressing into the system through the compartment. The design specification should ideally take into consideration the various trade-offs which may occur as a result of the operation of the prime–mover at different periods. However, in this instance the computations are to be based on a quasi steady–state (see also the assumptions in section 4.4.4 on page 118). Of importance is an estimate of an upper bound for the heat transfer coefficients obtaining at different locations within (and without) the compartment. As such, the assessment of this heat transfer coefficient is the main focus of the initial stage of the ensuing analysis.

During periods when the prime–mover is non–functional, the evaporator presents a direct heat transmission path from the inside of the appliance to the ambient environment[1]. Attaching a TES to this surface will cause some proportion of the energy stored within the store to be lost via this heat transmission path. The ramifications of this becomes more punitive with (a) increasing ambient temperature, (b) increasing evaporator surface area and, (c) decreasing TES bulk–temperature. The gravity of (a) is somewhat more severe than would be experienced during conventional DRA operation. This is a consequence of the potential for loss from the TES being relatively greater than from the DRA interior temperature, which would be the case in the absence of the TES (on account of the necessarily lower TES temperature). The second observation (b) of these is an unfortunate fact, as it is precisely this mechanism (increasing the evaporator surface area) which is recommended for the improvement of the performance of the prime–mover (section 2.4.2 on page 59). The effect of the third, (c), serves to compound (a) and (b), as heat gains are to a lower thermal potential than would normally be associated with an 'off–cycle' con-

[1]The effect of this was observed during experimentation see Figures 6.19 and 6.20, *qv.* pages 211 and 211 respectively

ventional DRA evaporator[1]. What is more, any unrejected heat from the condenser during an 'on–cycle' would, at least in part, be dissipated within the store during the immediately proceeding 'off–cycle'.

While this may not affect the charge process too adversely, it is clear that the TES will have to be oversized in order to offset the resulting heat gains, if the (energy storage–retrieval) process is not to be too severely hampered. One manner in which this situation may be ameliorated is to keep the size of the evaporator small. This in turn, would require a lowering of the evaporator temperature for the same rate of heat transfer, compromising the COP of the prime–mover. There is also the consideration of ensuring that the thermal capacities of the condenser and evaporator are of similar size[2]. In addition to this, there may be some benefit in thermally isolating the two ends of the heat transfer inventory (condenser and evaporator), using a thermally–insulating bridge at (at least) two places within the refrigerant circuit[3]. Pertinent to the current design case is the use of a 'plastic' evaporator; the casing (which may be metallic) of the enclosing TES (also a polymer) may then be used to protect such an evaporator housed within the TES. The technology to provide a sufficiently strong, thin polymer for this purpose is available, although the financial cost might be a problem. What is clear though, is the extent to which attention must be paid to each of these factors, and their weighting, in the overall design process.

4.5.2 Load Analysis

4.5.3 The Compartment

A brief discussion on compartment geometry was given in section 4.4.1 on page 111. Given the considerations in that section, the natural choice is to use a cube. As the aim of this exercise is simply to prove a concept, it is not necessary to have a large appliance and thus a 39 litre internal volume was chosen. Also in line with the further discussion given in that section, regarding the location of the

[1]In this regard the dynamic TES may possess an advantage over the passive TES, as the bulk of the stored energy is removed from the evaporator surface. The condition is clearly indicated (in the presence of the TES) in Figures 6.19 and 6.20, *qv.* pages 211 and 211 respectively constructed from data obtained during experimentation.

[2]Done for thermodynamic reasons; Bejan (1989) demonstrates, using eqn (2.5) and eqn (2.6), that the refrigerating capacity is maximised with respect to the internal and external exchanger conductances when the ratio of these two conductances is unity.

[3]This might not be as straightforward as it appears *prima facie*, as there might be heat transmission on account of the (gas–phase) *refrigerant* in the circuit. Further investigation needs to be carried out to assess the proportion of metal–metal (heat exchange inventory) heat conduction to the refrigerant heat transmission effects.

DRA door, the decision was made to adopt a top loading (chest) appliance.

The ASHRAE (1994) handbook details the insulation thicknesses, most often relating to polyurethane foam which is commonplace in DRA's. For polyurethane foam, foamed *in situ*, a thickness of 48 mm is deemed sufficient for -18 °C freezing compartments, while for non–freezing compartments, (at 3 °C) 40 mm is considered appropriate. It is noted that as a point of (best practice) reference that the LER 200 refrigerator referred to in section 1.6.2 on page 27[1] utilised 65 mm. As mentioned in section 2.3.1 on page 49, the intention is to use vacuum panel insulation VPSI as it is the best commercially–available insulation. However, as these are manufactured in panels, it is necessary to provide a (preferably insulative) binding for fixity and the reduction of inter–panel thermal leaks. Thus, a decision was made to use 65 mm walls of composite, polyurethane foam–VPSI insulation. Based on the results of the analysis in section 2.5.2 on page 64, and noting that the preliminary analysis is a passive one[2], the VPSI is to be located interiorly within the enclosing, composite, insulation.

Three principal sources of heat ingress (Q_i) into the system are:

Heat Ingress Through The Door–Cabinet Seal

This is the heat transfer through the appliance door–cabinet seal[3]. Unfortunately, this is difficult to estimate with much accuracy. However, on the assumption that the ingress is only conducted across the seal itself (no air leaks etc) an estimate may be found using the relation

$$Q_i = (L \cdot H)_{seal} \cdot \frac{T_{amb.} - T_{DRA}}{\frac{1}{h_{DRA\,ext.}} + \frac{\text{thickness}_{seal}}{k_{seal}} + \frac{1}{h_{DRA\,int.}}} \tag{4.46}$$

Heat ingress through heat transfer inventory

This is the heat transfer through the inventory (condenser–evaporator circuit) and is, of the three, the most difficult to estimate. The reasons for this stem from difficulties in:

(a) Assessing with certainty the heat transfer area and heat transfer coefficient for the condenser surface.

(b) Determining the relevant cross-sectional flow area for the conductive path between the evaporator and either the condenser or the prime–mover.

[1] [Guldbrandsen et al., 1986]

[2] For the implications of this in the non–passive case see section 2.5.3 on page 66, specifically eqn (2.31) and the ensuing discussion.

[3] See ASHRAE (1994), *pp.* 48.3 *op. cit.* for an indication of the percentage of the total heat gain this can amount to.

(c) Characterising the effects of the on-off prime–mover cycles on the transient temperatures of the evaporator, condenser, heat pump and allied conduits.

The processes involved in arriving at a mathematical expression for this aspect of Q_i, is lengthy, convoluted and fraught with uncertainty. For these reasons, no attempt will be made to provide an expression for this estimate.

Heat Ingress Through Compartment Walls

This relates to the heat transfer through the compartment walls themselves. In assessing this, a knowledge is required of an informative subset[1] of:

(a) The mean heat transfer coefficients exterior and interior to the compartment $(h_{\mathtt{DRA}})_{\mathtt{ext.}}$ and $(h_{\mathtt{DRA}})_{\mathtt{int.}}$ respectively.

(b) A representative characteristic temperature for the ambient temperature $(T_{\mathtt{amb.}})$, the DRA interior air temperature $(T_{\mathtt{DRA}})$, the DRA interior wall temperature and the DRA exterior wall temperature.

(c) A representative value for the apparent (or effective) thermal conductance of the DRA compartment wall(s).

(d) The pertinent internal and external compartment dimensions.

Given such an informative subset, it is possible to apply one of the well know techniques to determine this aspect of Q_i *e.g.*

$$Q_i = \frac{T_{\mathtt{amb.}} - T_{\mathtt{DRA}}}{\frac{1}{(Ah)_{\mathtt{ext.}}} + \frac{1}{(\mathtt{K}_{eff})_{\mathtt{DRA}}} + \frac{1}{(Ah)_{\mathtt{int.}}}} \tag{4.47}$$

Schneider (1985) states the following correlation (originally given by Langmuir et al. (1913)) for the steady state heat transfer *conductance*[2] across a parallelepiped shell:

$$\mathtt{K}_{eff} = k\left[\frac{4ac}{\delta_{si}} + ab\left(\frac{1}{\delta_{fl}} + \frac{1}{\delta_{ce}}\right) + 1.08(a+b) + 2.16(a+c) + 0.4(4\delta_{si} + \delta_{fl} + \delta_{ce})\right] \tag{4.48}$$

$$\forall \quad a, b, c > \frac{\delta_{max}}{5}$$

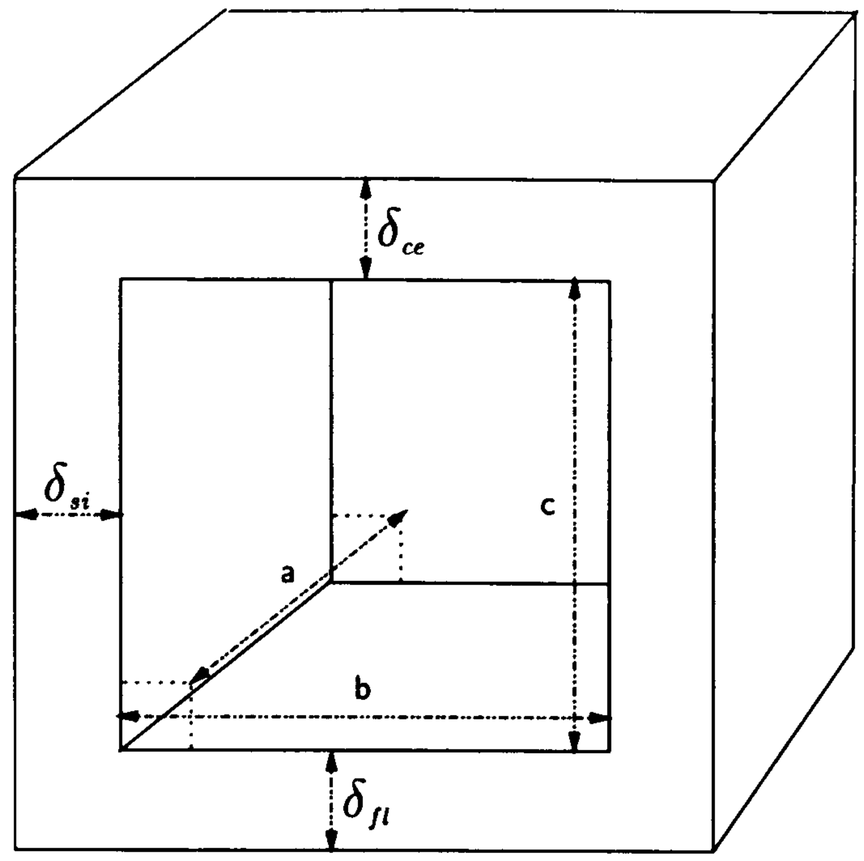


Figure 4.12: Support figure for eqn (4.48)

δ in this case represents the thickness of the enclosing wall, $\{a, b, c\}$ being geometric internal dimensions. The exact representation of {a,b,c} as well as the subscripting notation for δ can be inferred from the Figure 4.12 on page 139.

This relation can be used to estimate the conductance of the DRA wall. In the event that the insulation is composite, then each layer has to be taken account of; an example of an application of this method is given in Appendix B on page B-253.

Heat Transfer Coefficients

As the wall temperatures may not be known with much certainty, it remains to obtain an upper bound[1] on the heat transfer coefficients for the internal and external walls. Considering the DRA compartment the heat transfer is principally buoyancy–driven and there is/are:

1. At least eight[2] surfaces (four internal and four external) where the pertinent heat transfer coefficient is from a vertical surface. For these the following correlation, on the recommendation of Chapman (1984), *pp.* 315 *ff.*, based on

[1] In the sense that it is sufficient to quantify the heat transfer through the DRA wall.

[2] *cf:* $\dot{Q} = \mathsf{K} \cdot \Delta T$

[1] Only the upper bound is here required, for as with most designs, the estimates are to be based on the worst possible cases.

[2] Anticipating the inculcation of the TES, one might include an additional eight more (two from each of the four TES surfaces).

the work of Churchill and Chu (1975) is here used:

$$\mathrm{Nu}_L = 0.68 + 0.670\mathrm{Ra}_L{}^{1/4}\left[1+\left(\frac{0.492}{\mathrm{Pr}}\right)^{9/16}\right]^{-4/9}, \qquad 0 < \mathrm{Ra}_L < 10^9$$

$$\mathrm{Nu}_L = \left\{0.825 + 0.387\mathrm{Ra}_L{}^{1/6}\left[1+\left(\frac{0.492}{\mathrm{Pr}}\right)^{9/16}\right]^{-8/27}\right\}^2, \qquad \mathrm{Ra}_L > 10^9 \tag{4.49}$$

$$\left[\begin{array}{c} 0 < \mathrm{Pr} < \infty \\ \text{Properties except } \beta \text{ at } \overline{T} \\ \beta \text{ at } \overline{T} \text{ for liquids, } T_f \text{ for gases} \\ L \text{ is defined here as } \left(\frac{\text{Plate area}}{\text{Perimeter}}\right) \end{array}\right]$$

2. At least two surfaces for which the heat transfer is either from air to a colder surface facing upwards (DRA external top) or to air from a hotter temperature facing downwards (DRA internal top). For these the correlations based on the works of Goldstein et al. (1973) and Lloyd and Moran (1974)[1] are here considered to be adequate:

$$\mathrm{Nu}_L = 0.54\mathrm{Ra}_L{}^{1/4}, \qquad 2.6\times10^4 < \mathrm{Ra} < 10^7$$
$$\mathrm{Nu}_L = 0.15\mathrm{Ra}_L{}^{1/3}, \qquad 10^7 < \mathrm{Ra} < 3\times10^{10} \tag{4.50}$$
$$\left[\begin{array}{c} \text{Properties except } \beta \text{ at } \overline{T} \\ \beta \text{ at } \overline{T} \text{ for liquids, } T_f \text{ for gases} \\ L \text{ is defined here as } \left(\frac{\text{Plate area}}{\text{Perimeter}}\right) \end{array}\right]$$

3. At least one surface where the heat transfer is to the air from a hotter surface facing upwards (bottom of interior of the DRA). The following correlation, again based on the works of Goldstein et al. (1973) and Lloyd and Moran (1974) is here presented in this regard.

$$\mathrm{Nu}_L = 0.15\mathrm{Ra}_L{}^{1/3}, \qquad 3\times10^5 < \mathrm{Ra} < 3\times10^{10}$$
$$\left[\begin{array}{c} \text{Properties except } \beta \text{ at } \overline{T} \\ \beta \text{ at } \overline{T} \text{ for liquids, } T_f \text{ for gases} \\ L \text{ is defined here as } \left(\frac{\text{Plate area}}{\text{Perimeter}}\right) \end{array}\right] \tag{4.51}$$

4. An argument may be advanced for treating the underside of the DRA (cold surface facing downwards) along with the previous correlation 4.51 *qv*. However, this presumes that the appliance is either not in direct contact with the

[1] Given in Chapman (1984)

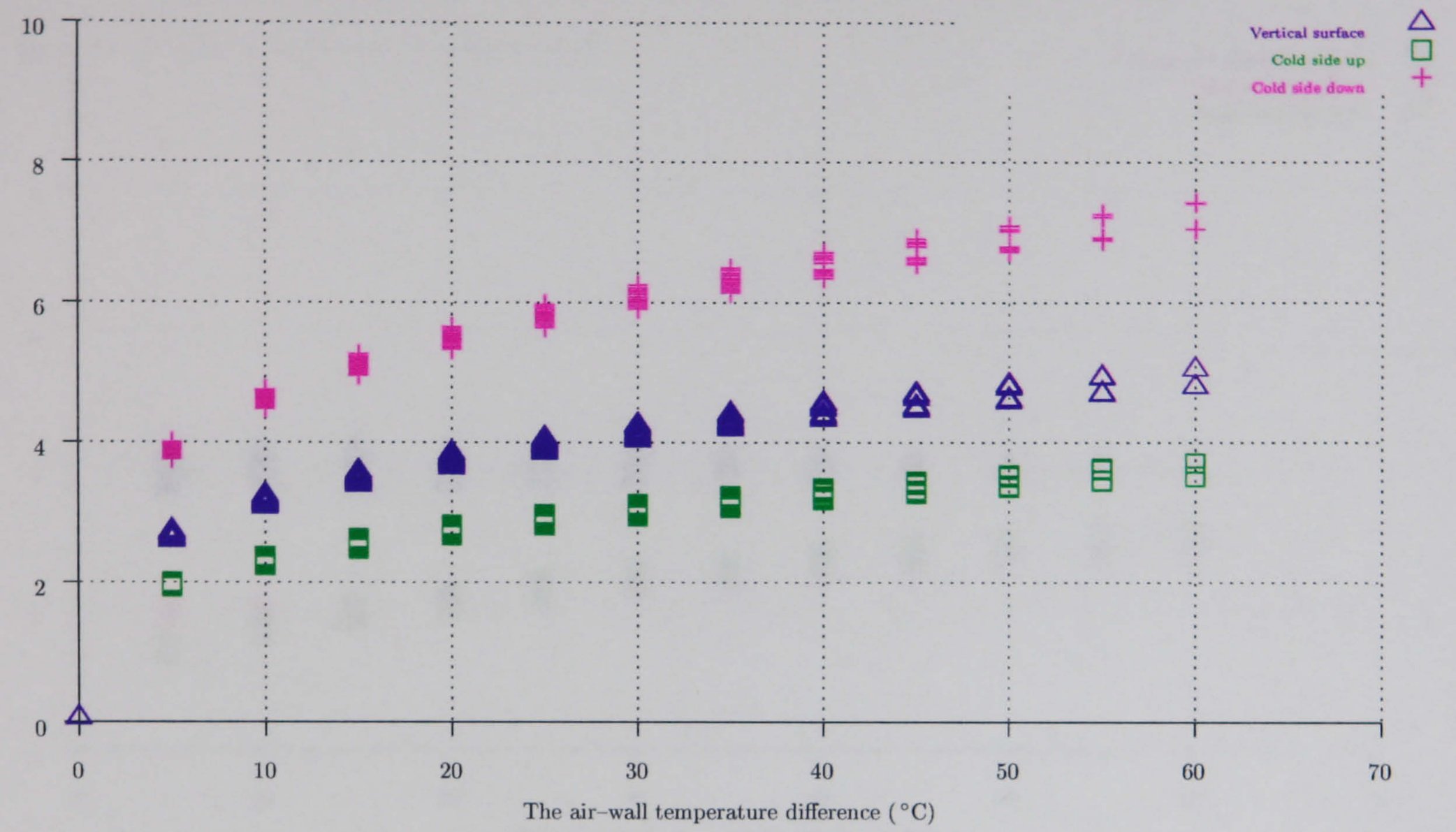


Figure 4.13: The effect of temperature difference on the buoyancy–driven heat transfer coefficient for horizontal and vertical surfaces

The effect of temperature difference ($\triangle T$) on the buoyancy–driven heat transfer coefficient (h) between cold air and (a) a vertical surface [Churchill and Chu, 1975]; (b) a horizontal, downwards-facing, hot surface (upwards-facing, cold surface) and (c) a horizontal, upwards-facing, hot surface (downwards-facing, cold surface) [Goldstein et al., 1973; Lloyd and Moran, 1974]. The data used was computed from equations given by ASHRAE (1976) in the temperature range -10 – 50 °C.

PhD Thesis © 1999 Cranfield University —Refrigeration Appliances: Performance enhancements via novel Thermal - Energy Storage—

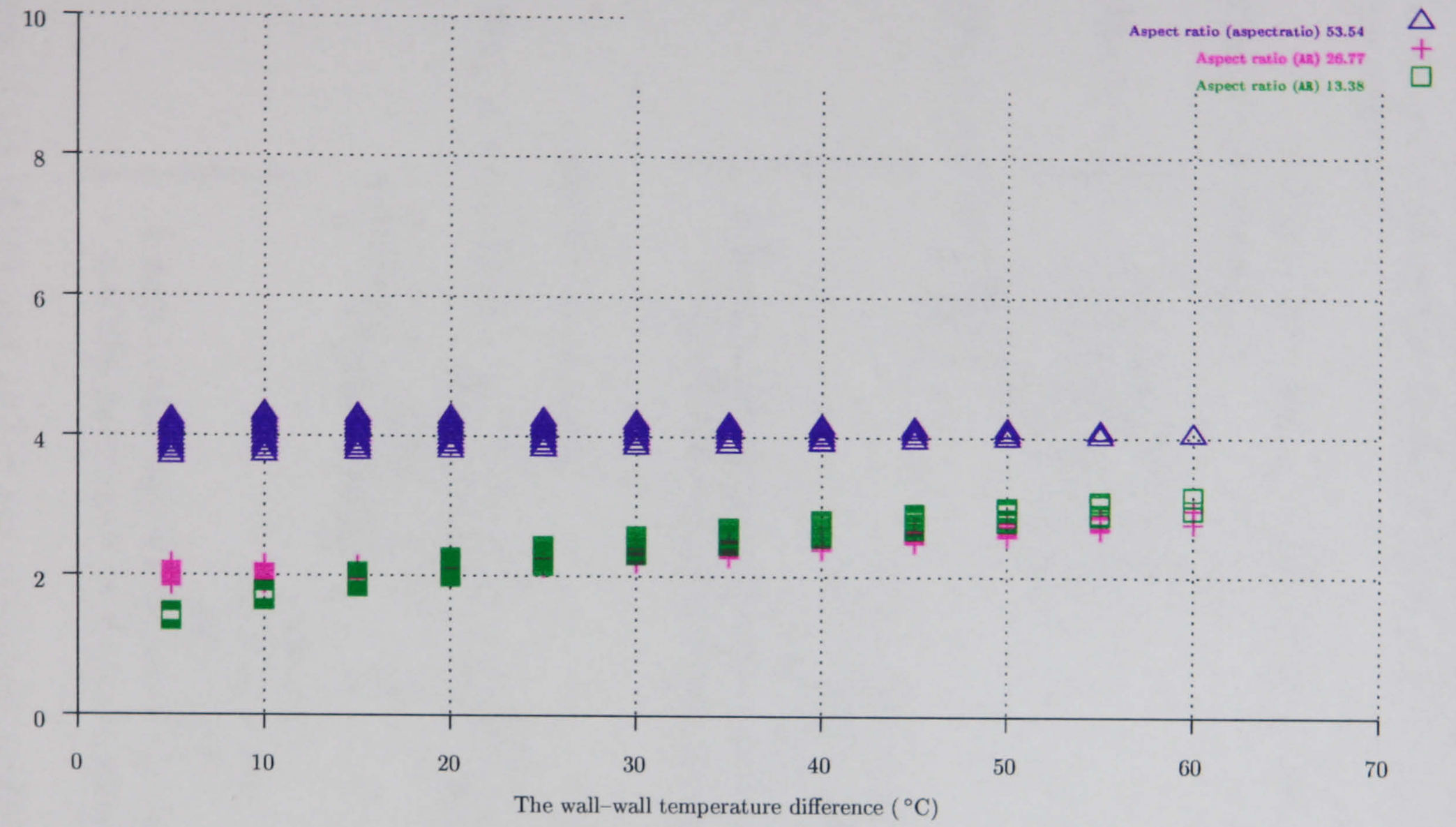


Figure 4.14: The effect of temperature difference on the buoyancy–driven heat transfer coefficient within a vertical enclosure.

The effect of temperature difference ($\triangle T$) on the buoyancy–driven heat transfer coefficient (h) within a vertical enclosure over a range of temperatures (-10 – 50 °C) and aspect ratios [Vliet, 1969; Fuji and Imura, 1972]. The data used is taken from equations given in ASHRAE (1976).

PhD Thesis © 1999 Cranfield University —Refrigeration Appliances: Performance enhancements via novel Thermal - Energy Storage—

ground[1] or, not sufficiently close to the ground for the relevant correlation to be that for an enclosure at 0° to the horizontal *i.e.* it is essentially floating. The latter is more likely; also pre–empting the discussion on the location of the TES's within the device, there will be the need for heat transfer correlations for heat exchange across narrow enclosures. For this reason, the following correlations, based on the works of Vliet (1969) and of Fuji and Imura (1972) is here presented.

$$\text{For } \phi = 90\,^\circ\text{: } \mathrm{Nu}_{L90} = \max\left((\mathrm{Nu}_L)_1, (\mathrm{Nu}_L)_2, (\mathrm{Nu}_L)_3\right)$$

$$(\mathrm{Nu}_L)_1 = 0.0605\mathrm{Ra}_L{}^{1/3}$$

$$(\mathrm{Nu}_L)_2 = \left\{1 + \left[\frac{0.104\mathrm{Ra}_L{}^{0.293}}{1 + \left(\frac{6310}{\mathrm{Ra}_L}\right)^{1.36}}\right]^3\right\}^{1/3}$$

$$(\mathrm{Nu}_L)_3 = 0.242\left(\frac{\mathrm{Ra}_L}{\mathrm{AR}}\right)^{0.272} \tag{4.52}$$

$$\left[\begin{array}{c} 5 < \mathrm{AR} < 110 \\ 10^2 < \mathrm{Ra}_L < 10^7 \\ \mathrm{AR} = \left(\frac{H}{L}\right) \\ L \text{ here is the distance between the two adjacent surfaces and} \\ \phi \text{ is the horizontal inclination angle of the enclosure} \end{array}\right]$$

$$\text{For } 0\,^\circ <= \phi < 60\,^\circ$$

$$\mathrm{Nu}_L = 1 + 1.44\left[1 - \frac{1708}{\mathrm{Ra}_L \cdot \cos\phi}\right]\left[1 - \frac{1708}{\mathrm{Ra}_L \cdot \cos\phi} \cdot (\sin 1.3\,\phi)^{1/6}\right] + \left[0.664\left(\frac{1708}{\mathrm{Ra}_L \cdot \cos\phi}\right)^{-1/3} - 1\right] \tag{4.53}$$

$$\left[\begin{array}{c} \mathrm{AR} > 12 \\ 0 < \mathrm{Ra}_L < 10^5 \\ \mathrm{AR} = \left(\frac{H}{L}\right) \\ L \text{ here is the distance between the to adjacent surfaces} \\ \phi \text{ is the horizontal inclination angle of the enclosure} \end{array}\right]$$

Figures (4.13), (4.14) and (4.15) are graphical renditions of the effect of air–surface buoyancy–driven heat transfer coefficients with temperature difference over

[1]This is unlikely, as usually wheels attached to the device to facilitate moving. Also, there is usually a gap underneath the compartment for housing the prime–mover.

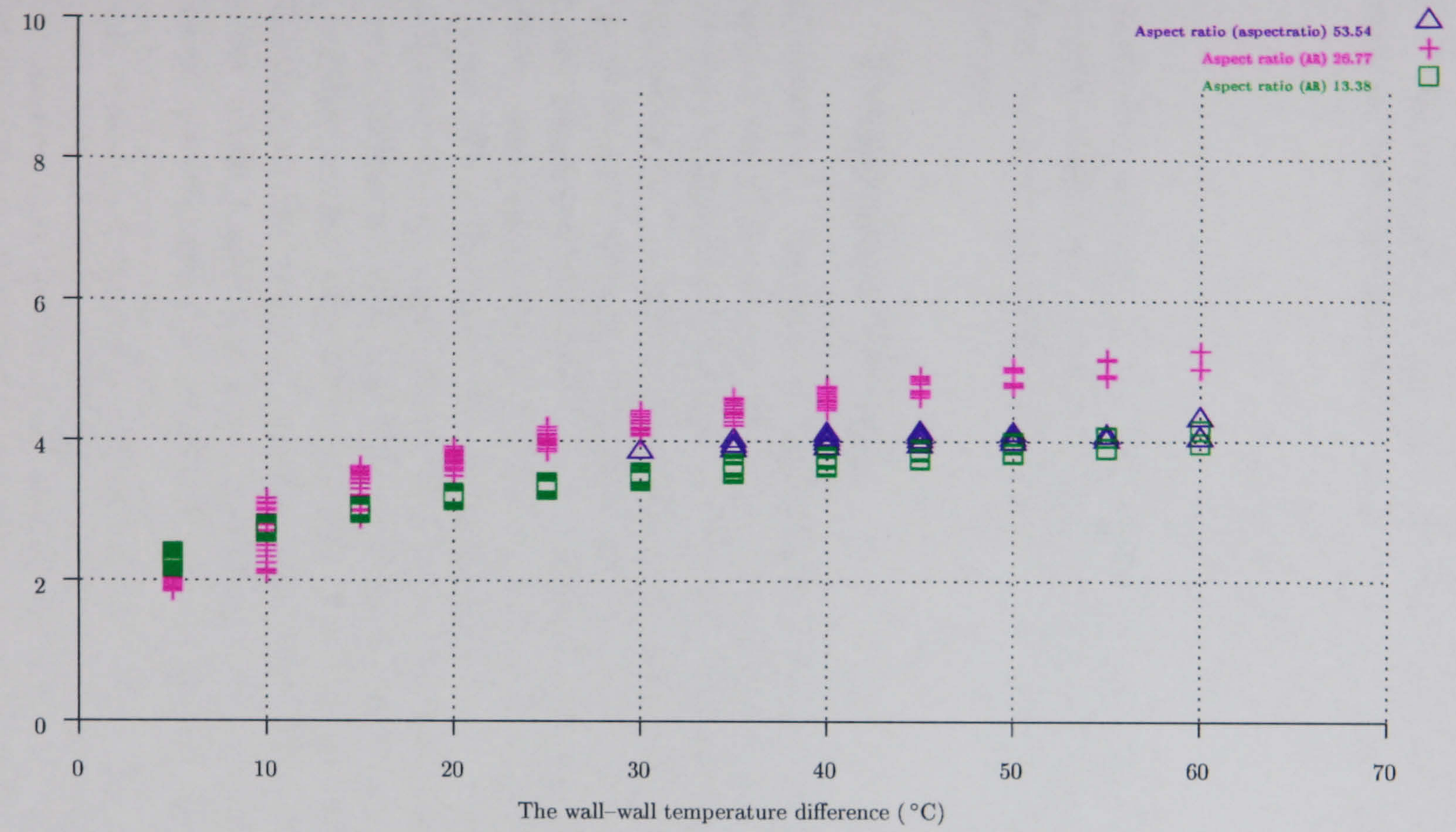


Figure 4.15: The effect of temperature difference on the buoyancy–driven heat transfer coefficient within a horizontal enclosure.

The effect of temperature difference ($\triangle T$) on the buoyancy–driven heat transfer coefficient (h) within a horizontal enclosure over a range of temperature and aspect ratios; culled from Vliet (1969), Fuji and Imura (1972). The data used is taken from equations given by ASHRAE (1976).

PhD Thesis © 1999 Cranfield University —Refrigeration Appliances: Performance enhancements via novel Thermal - Energy Storage—

(a) a vertical surface, (b) horizontal surfaces and (c) within an enclosure of specified aspect ratios, in the temperature range -10 °C $\leq (T_{air}, T_{surface}) \leq$+50 °C. In these three cases the value of h is virtually independent of the mean (surface–air and wall–wall) temperature ($\overline{T}$) and the maximum heat transfer coefficient (h) at a 60 °C temperature difference lies within the range $2.5 \leq h \leq 7.5$[1]. Therefore, with the aid of the correlations given, it is thus possible to define mean heat transfer coefficients for the DRA exterior and interior using the relation

$$\overline{h} = \frac{\sum_{j=1}^{6} (hA\triangle T)_j}{\sum_{j=1}^{6} (A\triangle T)_j}$$

Of particular interest is the fact that for moderate temperature differences the heat transfer coefficient, over the ranges considered, does not depart too markédly from 4W/m² °C and, as such, this value is to be used in subsequent heat transfer computations.

4.5.4 Evaporator Design

Insufficiencies in the heat transfer to the TES may arise on account either of the limitations of the thermal conductivity of the TES medium or the relatively low heat heat transfer coefficients obtaining at the TES–DRA interface[2]. It may thus be necessary (depending on the heat fluxes required) to increase the DRA–TES heat exchange surface area by providing an extended the surface[3]. In order to provide such a surface for the proposed PCM–LHTES it is necessary to interpose the TES between two metal plates, one planer and the other with the required extended surface geometry. Two of these TES units are to be subsequently
placed adjacent to the evaporator see Figure 4.16 on page 146. This initial concept presupposes sufficient TES material will be available to totally enclose the evaporating surface within the TES. Strictures in the production process necessitated a modification to the original concept and the TES was repositioned between the evaporating surface and one such extended heat transfer surface[4] in a concertina arrangement see Figures 4.17 and 4.18, *qv.* pages 146 and 148 respectively

[1] (a) For vertical and horizontal surfaces $3.5 \leq h \leq 7.5$, (b) within 'vertical' 90° enclosures $2.5 \leq h \leq 4.5$ and (c) within 'horizontal' 0° enclosures $3.75 \leq h \leq 5.5$

[2] As it is assumed that the TES would be thin, the latter is more likely.

[3] See the discussion in section 2.4.2 on page 59, for reasons why heat transfer area enhancement is the chosen method of solution.

[4] With hindsight, this may have been a better arrangement as the magnitude of the direct heat transmission to the TES via the evaporator would have been potentially doubled were the original design adhered to.

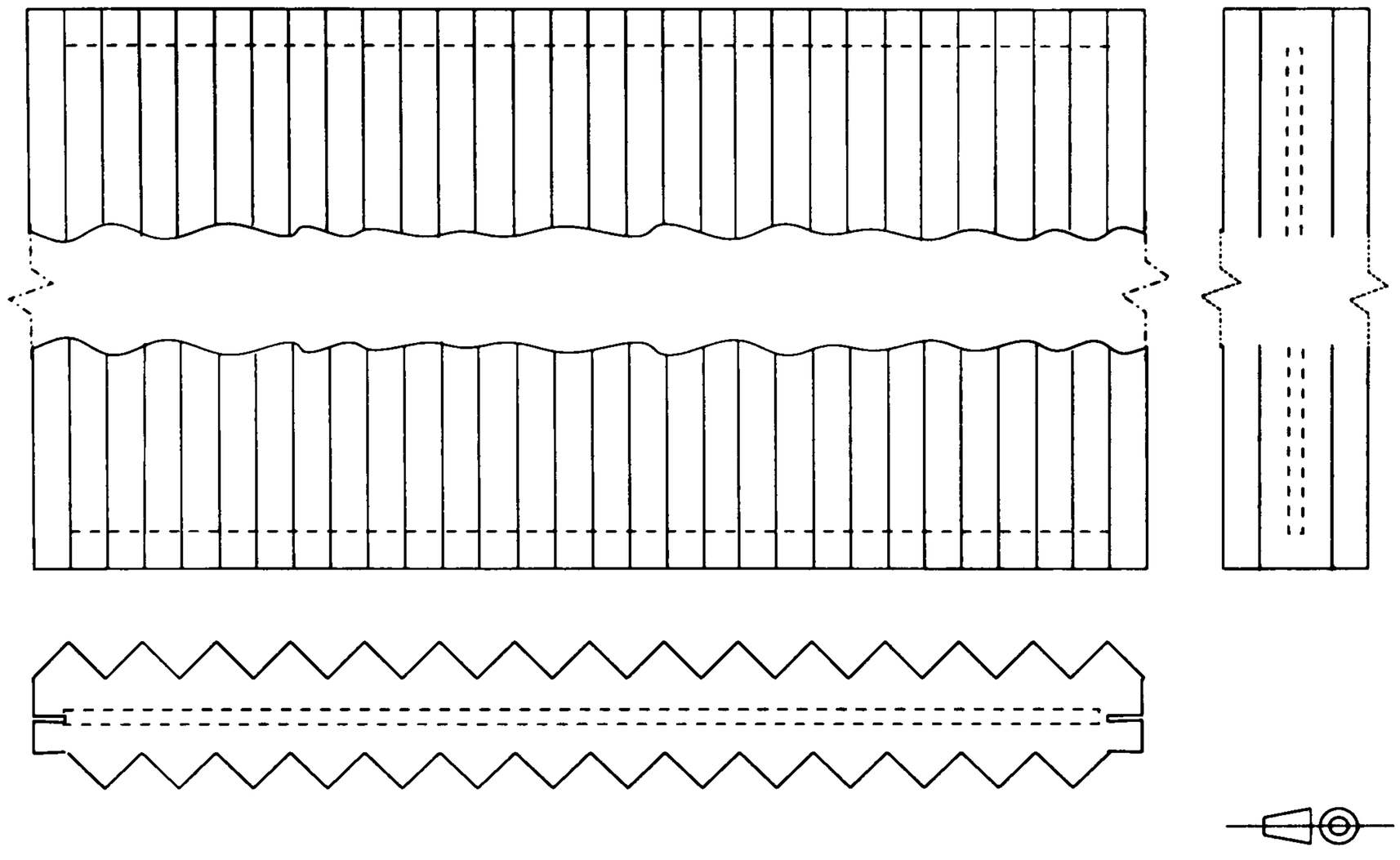


Figure 4.16: Initial evaporator–TES design sketch.

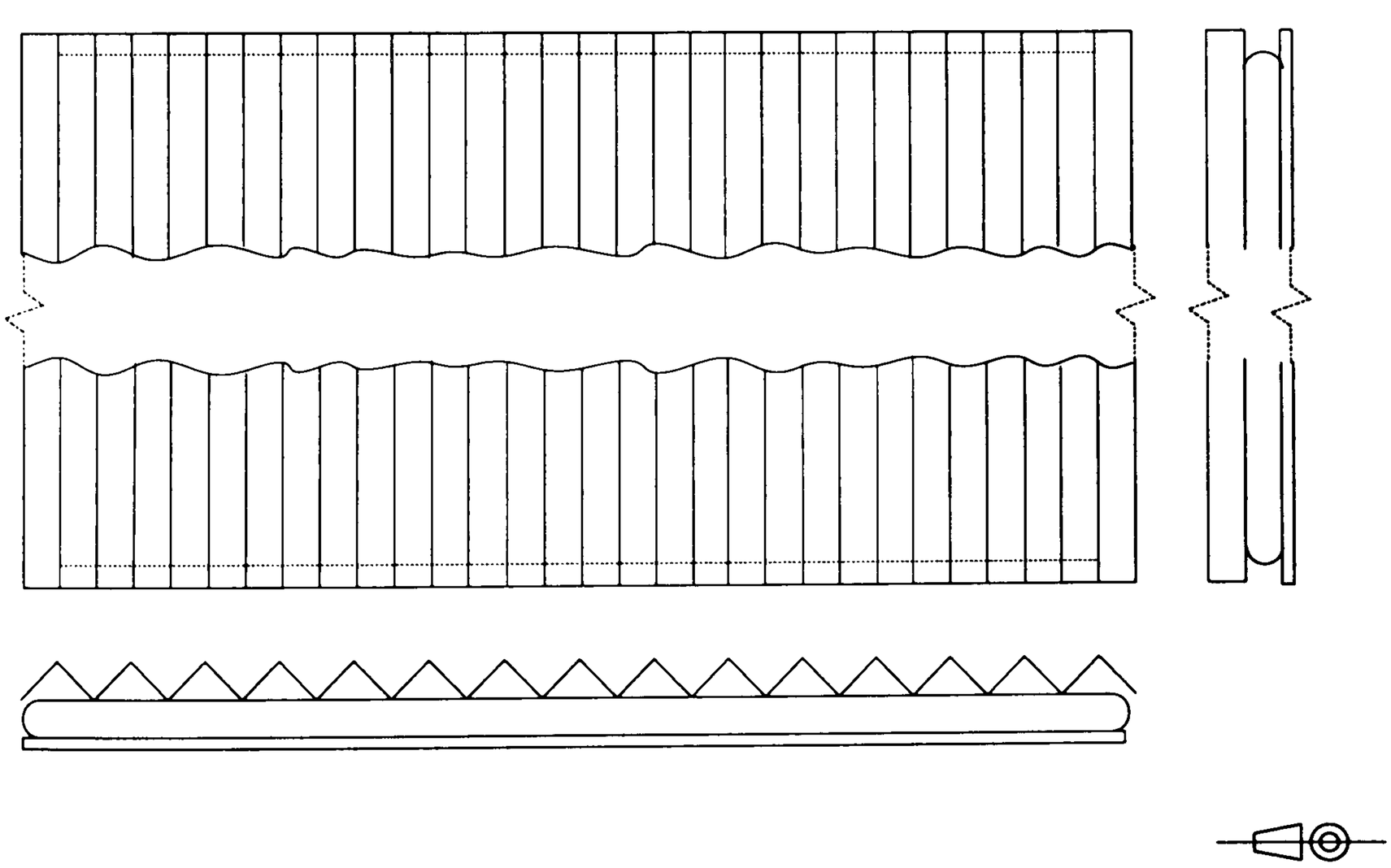


Figure 4.17: Revised (concertina) evaporator–TES design sketch.

4.5.5 Food Load

The assumption, rife in the literature [Guldbrandsen et al., 1986; Nørgård, 1989; March Consulting Group, 1990; Boardman, 1995b; ASHRAE, 1994]), that upwards of 80% of the energy consumption in a DRA is due to cabinet–associated heat ingress (see Table 1.3 on page 12 for the ASHRAE breakdown) is indeed an unfortunate one, for it conveys the impression that this is about all there is to the cooling load of a DRA[1]. In reality there are other loads which bear significantly on the coolth burden of a DRA in service; these include the actual utilisation load and the load due to human interaction[2]. In truth, there is no way in which the utilisation load of a DRA may be estimated *a priori*, as utilisation patterns are very application dependent. However, it is reasonable to assume that in the worst case, a fixed proportion of the volume will always be used, and to estimate a base utilisation load on that assumption. The WHO adopt a similar strategy in the specification of vaccine refrigeration units (see Footnote 1 on page 106, for pertinent references) reckoning on a mean utilisation load of 30%.

4.5.6 Thermal Energy Storage analysis

Introduction

This section deals with the physical dimensioning of the thermal store (TES). This is done based on the thermal storage requirement E_{TES}, the minimum discharge (and/or charge) time ($t_{TES_{\Delta+}}$ and $t_{TES_{\Delta-}}$ respectively) and the rates of heat transfer to the TES ($\dot{Q}_{TES_{\Delta+}} = \dot{Q}_{HP}$) and to the DRA compartment ($\dot{Q}_D$ and $\dot{Q}_N$) respectively[3]. The aim here is to determine (a) the minimum volume of storage material adequate for storing the requisite amount of thermal energy, (b) the maximum evaporator temperature to effect the storage process and (c) the linear dimensions of both the evaporator and the thermal store.

The TES volume ($V_{TES(1)}$), given E_{TES} and the thermo–physical properties of the storage medium, may be computed thus: the (solid–liquid latent–heat) energy–density (kJ/m^3)[4] of the TES medium is defined as

$$(\rho_E)_{TES(1)} = (\rho_m)_{TES(1)} \cdot \Delta H_{LH}$$

---

[1]This is probably one reason for the abysmal (empty appliance) testing standards.

[2]See also section 2.2.2 on page 46.

[3]These requirements are computed in section 4.4 on page 111.

[4]Referred to the liquid phase. The ratio $\frac{\rho_{m(s)}}{\rho_{m(1)}}$ may be used to refer the value to the solid ('charged') phase.

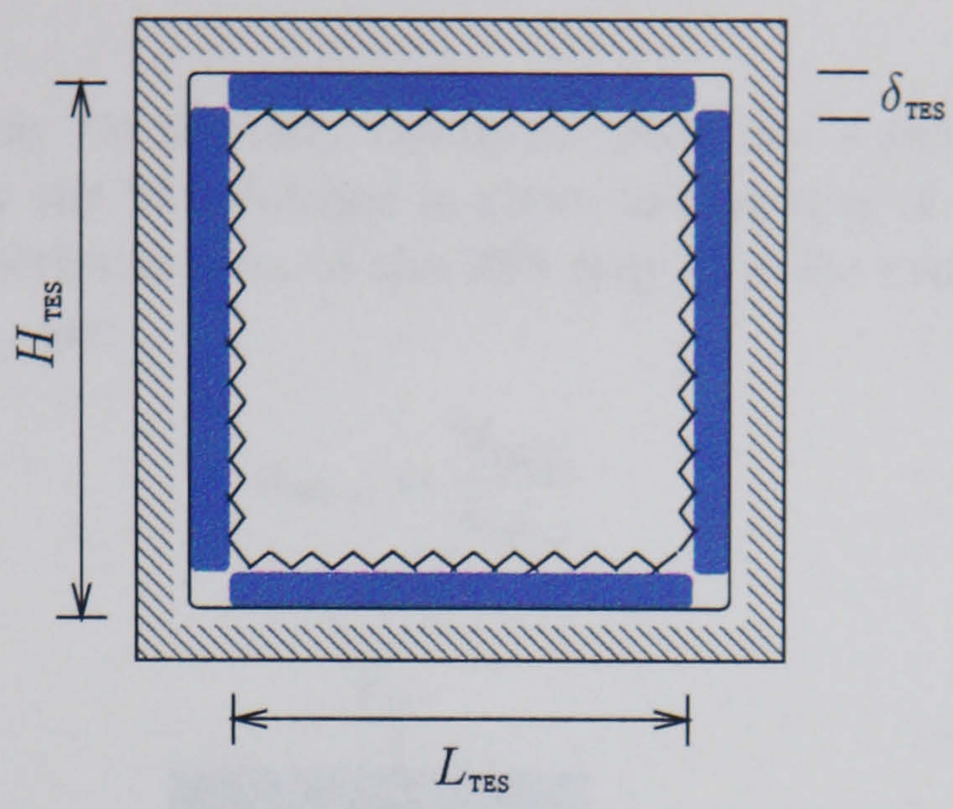


Figure 4.18: Schematic diagram of the actual TES layout

Thus the minimum storage volume is

$$V_{TES(1)} = \frac{E_{TES}}{(\rho_E)_{TES(1)}} \tag{4.54}$$

Given the estimates for the required charge/discharge[1] times of the TES, it remains to compute the distribution of the storage medium about the DRA interior. For this purpose, it is assumed that (a) the TES medium is evenly distributed on all the four vertical sides of the DRA interior, (b) there is to be some clearance between the DRA wall and the TES medium (the same clearance existing between the top and bottom of the DRA and the TES) and (c) the TES parcels are located between the evaporator (rear) and a restraining grid which may be used as a means of enhancing the heat transfer between the TES and the DRA interior. The height of each TES parcel is taken to be H_{TES}[2], the width to be L_{TES}[3] (see Figure 4.18 on page 148) and the thickness to be δ_{TES}, say. These can be related to the volume of each TES parcel as

$$\begin{aligned} \frac{V_{TES(1)}}{4} &= (H_{TES} \times L_{TES} \times \delta_{TES})_{(1)} \\ &= H_{TES} \times (H_{TES} - 2.0 \cdot \delta_{TES}) \times \delta_{TES} \\ &= (H_{TES})^2 \cdot \delta_{TES} - 2.0 \cdot (\delta_{TES})^2 \times H_{TES} \end{aligned} \tag{4.55}$$

[1]The melting times will differ from this for several reasons. The principal source of discrepancy in *this* case is the heat gain through the evaporator surface as discussed earlier. For this reason, the use of exact solutions to the 'melting problem' is considered unwarranted.

[2]Which is equivalent to the internal height of the DRA less clearances at the top and the bottom.

[3]Equivalent to the width of the TES less twice the thickness of each parcel (δ_{TES}).

From this $\delta_{\text{TES}(1)}$ may be trivially obtained using the quadratic formula[1]. The worst case scenario for the TES volume is given as the case of the TES–only configuration[2]. The cross–sectional area of the TES may thus be computed from $\delta_{\text{TES}(1)}$ in conjunction with $V_{\text{TES}(1)}$ *viz*:

$$A_{\text{TES}(1)} = \frac{V_{\text{TES}(1)}}{\delta_{\text{TES}(1)}} \tag{4.56}$$

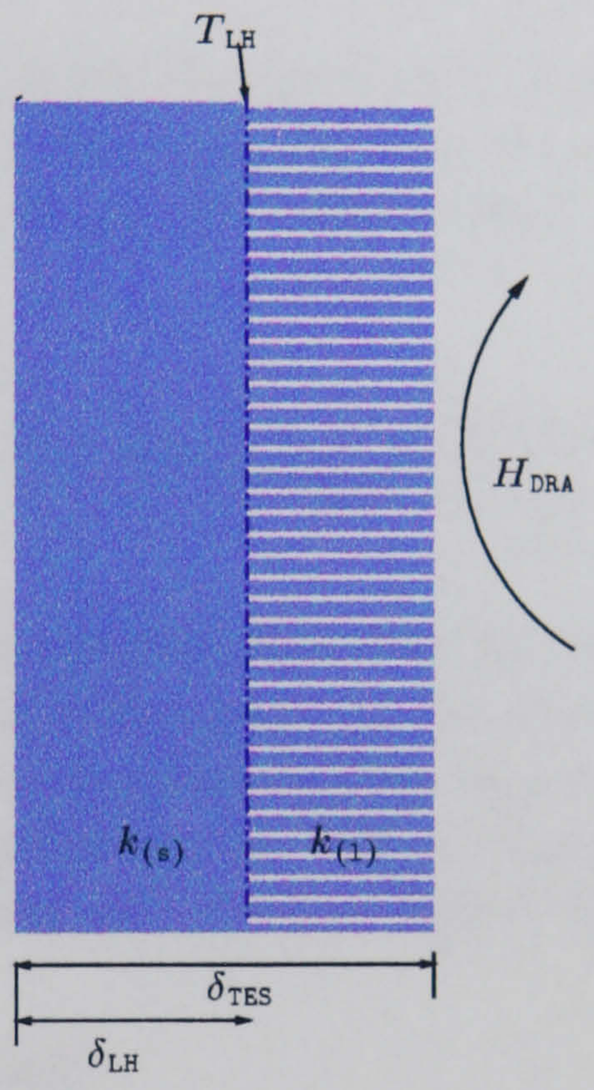


Figure 4.19: Schematic diagram of the TES charge–discharge process.

The maximum rate of heat transfer from the TES surface is dictated by the requirement to extract the required heat from the DRA during the night period (when the appliance has been recharged for the next day). The observation is made that although the mass densities across the phases differ, due to the nature of the containment matrix there will be virtually no vortices set up in the fluid phase as a result of these differences. The implication is that, conduction will be the predominant heat transfer mechanism in both phases. In addition, given the following simplifying assumptions: (a) the thickness of the TES is at least an order of magnitude smaller

[1]The 'solid' length $\delta_{\text{TES}(s)}$ is related to the 'liquid' length by the relation $\delta_{\text{TES}(s)} = \frac{\delta_{\text{TES}(l)}}{3}\left(\frac{\rho_{m(s)}}{\rho_{m(l)}} + 2\right)$.

[2]A similar requirement to the $(n+1)^{th}$ night–time for the multi–day HES configuration.

than its lateral dimensions[1], (b) on account of (a) the temperature across the TES is effectively constant (at the phase transition temperature, T_{LH}) and (c) any temperature variations which may otherwise exist will be more appreciable in the liquid phase as it possesses the lower thermal diffusivity, then the mean heat transfer rate from the TES surface[2] may be represented, based on a heat balance across the liquid phase of the DRA during discharge as[3]

$$\overline{\dot{Q}}_{TES_{\Delta-}} = \frac{h_{DRA} \cdot \zeta_f A \cdot k_{TES(1)} \cdot (T_{DRA} - T_{LH})}{\delta_{TES}} \int_{\delta_{TES}}^{0} \frac{\delta_{LH}}{h_{TES} \cdot (\delta_{TES(1)} - X_{LH}) + k_{TES(1)}} \tag{4.57}$$

Where ζ_f is the extent to which the area normal to the TES thickness has to be extended in order to cater for the requisite heat transfer. On substitution for the store thickness δ_{TES} and integrating, the result is then solved for the (TES–DRA heat transfer) area to yield

$$\zeta_f = \frac{k_{TES(1)}}{h_{DRA} \cdot \delta_{TES}} \cdot \left| 1 - \exp\left(- \frac{\dot{Q} \cdot \delta_{TES(1)}}{k_{TES} \cdot A \cdot \delta_{TES} \cdot \Delta T_{LH,DRA}} \right) \right| \tag{4.58}$$

The preceding analysis has assumed that the TES charging will take place over the entire night–time period. This will seldom be the case and will only occur after an '*inclement period*'; as such the extended surface factor (ζ_f) solved for here is for the worst case. During normal operation, the TES re–charge will be accomplished much earlier on during the night–time and thereon higher heat fluxes may be expected.

4.5.7 Solar Cell Sizing

In deducing the required solar cell surface area, account must be taken of the location where the DRA is to be used[4]. If that has been determined, depending on the solar collection/conversion efficiency of the solar cells required, the size of the solar cell can be trivially computed given the computed values for the solar cell power (P_{SPV}).

---

[1] In essence it is very thin, reducing the analysis to that of a one–dimensional problem.

[2] $\dot{Q}_{DRA} = \max\left(\dot{Q}_D, \dot{Q}_N\right)$

[3] On the understanding that T_{LH} is the solid–liquid phase transition temperature, and δ_{LH} the phase front.

[4] In fact, if the appliance is to be adapted to use mains electricity (or generated power), such an analysis will be unnecessary.

Closure

This chapter presents formal equations for assessing the energy requirements in the design of a passive–TES DRA under three different prime–mover control options. It initially identifies stringent operating requirements, conditions and energy limitations under which such a system may be employed. The chapter goes on to discuss various energy storage types and options, as well as energy management strategies which may facilitate the design of an energy efficient system. Finally the various system assessment/design equations are presented. These equations are to form the basis for a computer–based model (Chapter 4 on page 105) for predicting the outcome (in terms of energy consumption) of implementation of the different energy management technologies in DRA design.

Chapter Five

Active Thermal Storage Systems

We did then what we knew how to do ... Now we know better, we *might* do different.

–M. Angelu

Introduction

The passive TES system previously designed in Chapter 4 on page 105 is thermal–conduction limited. This limitation, on account of the low values of the thermal transport properties of typical PCM used for LHTES, restricts the number and type of applications to which such a design can be put. For large–scale commercial/industrial systems, in terms of output capacity and cooling power, such heat–flux limitations are untenable. Thus the engineering design of such systems requires an alternative, more effective, method/mechanism of heat transmission to and from the TES. There are several methods by which the transmission of heat may be enhanced, (each with it's own unique set of merits and demerits); this chapter documents the procedure for substituting the passive TES with an alternative (active) high heat–flux TES system[1].

[1]Only the hybrid (battery–TES) configuration will be considered in the following analyses.

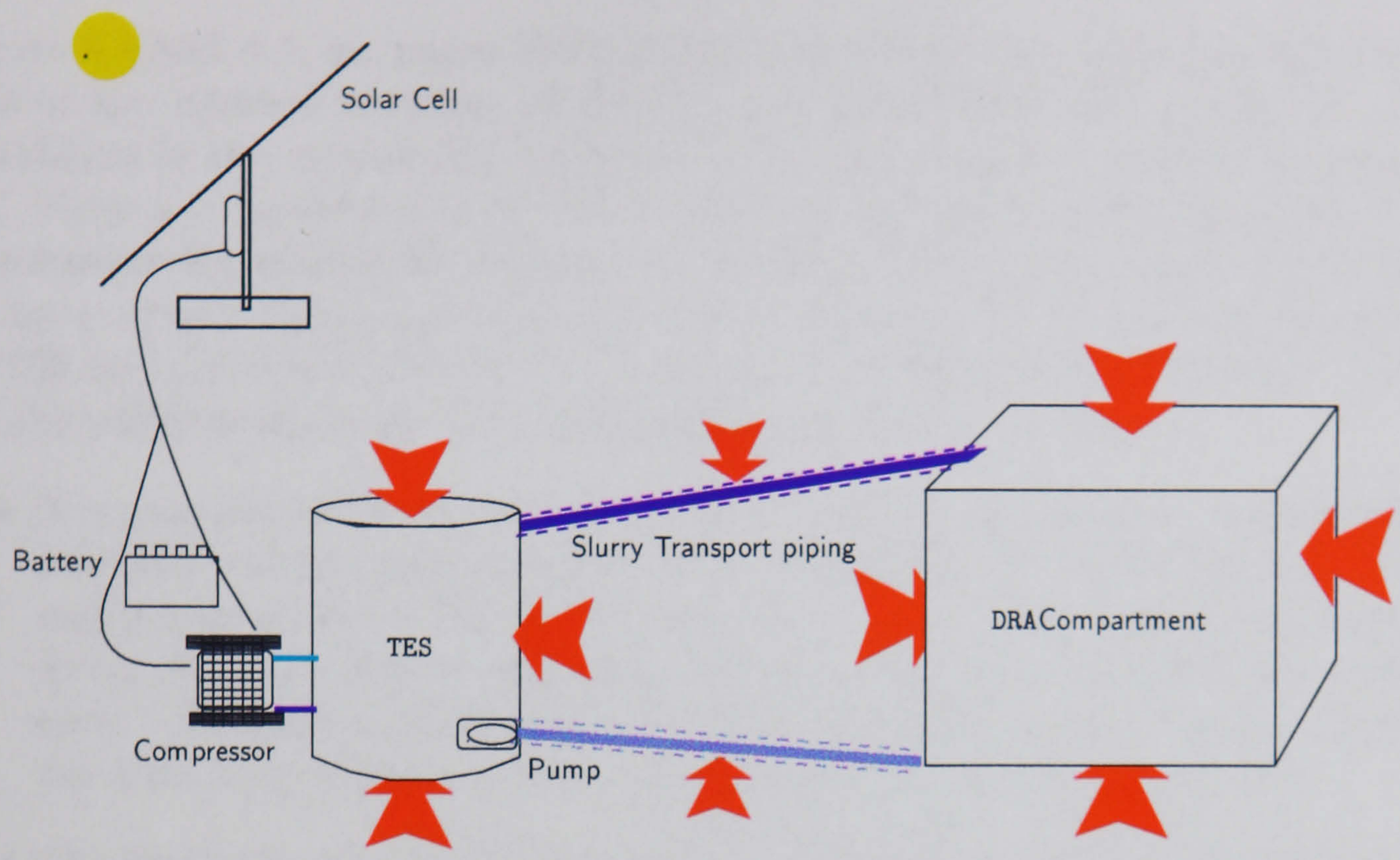


Figure 5.1: Schematic diagram of integrated TES's

5.1 General Discussion on the Application

5.1.1 Brief Description

The chosen (test case) method is the use of a slurry–based, secondary-cooling circuit fed from a TES (remotely located from the refrigerating appliance) of well–agitated[1] phase–change particles in fluid suspension; the prime–mover is thus used to charge the TES *via* a heat exchanger (the evaporator).

The term slurry as used here implies a *fluidised* (liquid in this case) particulate system consisting of a base–fluid conveying a PCM, designed for the specific purpose of high heat–flux thermal transport. The slurry is designed to use (a) the high specific energy capacity attending the phase–change process and (b) eliminate the effects of poor thermal conductivity by the particulate sizing and/or changing the fluidisation conditions[2].

The slurry is to be pumped through the system from the TES *via* a conduit through a heat exchanger located within the refrigerating appliance[3] and then back to the TES; Figure 4.2 on page 109 is a schematic diagram of one such layout (while

[1]For heat transfer enhancement.

[2]For a strong rationale and the benefits of using slurries consisting of phase–change particles see Highgate (1977), Kasza and Chen (1982), Charunyakorn et al. (1991), Augood (1997).

[3]This heat exchanger is akin to the heat exchanger within a normal DRA.

Figures 4.3 and 4.4, *qv.* pages 109 and 109 respectively are more detailed illustrations of the internal workings of the TES and the ES–DRA compartment). Thus, in addition to the normal DRA inventory (*i.e.* prime–mover, condenser, evaporator *etc.*), there are requirements for (a) at least one pump for slurry circulation, (b) a mechanism for mixing the contents of the TES[1]; in this case a mechanical stirrer has been chosen, (c) a mechanically–strong, thermally–insulated containment for the TES and (d) thermally–insulated piping to convey the slurry between the TES and the refrigerating appliance. Important observations are that:

- It is imperative that the insulation applied to the TES (and the conduits) be *at least* of the same quality as (preferably superior to) that of the DRA, as the thermal potential of the TES will be lower than that of the refrigerating appliance giving rise to a higher propensity for heat ingress within the same environment. Thermal insulation/heat isolation is highly essential and is probably the most critical issue which is to be considered for this application.

- The fluid pump(s) should be such that the amount of heat injected into the system on account of either its functioning, or due to its exposure to the ambient, is minimised.

- The geometry of the TES should be such as to minimise its volume to external surface-area ratio. The considerations here are similar to those for the DRA geometry, see section 4.4.1 on page 111. However in this case cylindrical geometries are more appropriate.

- The TES should be located as close as possible to the refrigerating appliance to minimise, (a) the heat gains to the conduits from the ambient and (b) the head–losses associated with the transport of the slurry through the system.

- As with most slurry–based applications, the most important issue is the prevention of stasis (hold–up) along the slurry transport route (conduit). If adequate consideration is not given to this issue, an unacceptable level of particle deposition will occur which will ultimately lead to clogging and eventually stasis, grinding the implementation to a halt and possibly damaging the pumping equipment. Deposition tends to increase the mean (dynamic) pressure within conduits and consequently the power (and ultimately energy) requirements in instances where the head is provided by a fixed mass–flow pump (*e.g.* a reciprocating device). In some instances this increase in dynamic pressure (and thus flow velocity) is sufficient to re–entrain previously deposited particles. In such cases the mass transport appears to be between 'dunes' on a haltingly

[1]It is conceivable that (a) may be the same as (b), depending on the design.

moving slurry bed, a condition known as 'saltation flow'. This (deposition) impairs heat transfer when it occurs in regions where heat transfer is to take place; also the power consumption curve of the pumping device may exhibit a periodic character which might be detrimental to the device. It is important to note that the pressure within the moving slurry (equivalent to the pumping power) is at a minimum at the onset of non–saltation flow when no bed exists. Transition between these two flow regimes is characterised, in addition to this minimum fluid pressure, by a critical mass transit velocity.

- The control of the slurry–flow may necessitate the installation of valves. Valves used in such applications are particularly prone to wear (corrosive and erosive) and, as such, the selection of such valves is a highly specialised process; in most slurry transport applications, clogging tends to take place first within the valves; see Tyson (1982) for a detailed account.

- Size degradation of the particulates within the slurry occurs due to attrition during transport. This can be reduced by the inclusion of finer particulates along with the larger ones. Incidentally, this helps to increase the maximum (volume) fraction of the particulates to fluid ratio which the slurry can contain [Shook and Roco, 1991, *pp.* 9], as well as the maximum concentration of the slurry which can be successfully pumped [Lam, 1980].

- In laminar flow of slurries (and possibly within the laminar sub–layer of turbulent flows) micro–convective thermal conductivity enhancements take place as a consequence of the motion of the smaller fines within the slurry [Sohn and Chen, 1981].

5.1.2 Flow Characterisation

Slurry (liquid–solid) flow regimes can be characterised roughly into three or four different classes, see Table 4.1 on page 111. The homogenous–Bingham flow is the limiting ideal–flow condition for slurries. The boundaries between each of these flow regimes are not distinct and as with most flow transitions in fluids, are accompanied by a transition region where neither regime can be said to solely exist. The transition between a fully–moving bed and heterogeneous flow is characterised by the slurry flow velocity and it occurs when the flow velocity reaches what is known as the 'critical deposit velocity'. The characterisation between homogenous and heterogenous is based on the manner and extent to which the solid–load is dispersed within the base–liquid. In reality, with the exception of the situation when the solid–load consists *solely* of very finely divided particles, homogeneity is

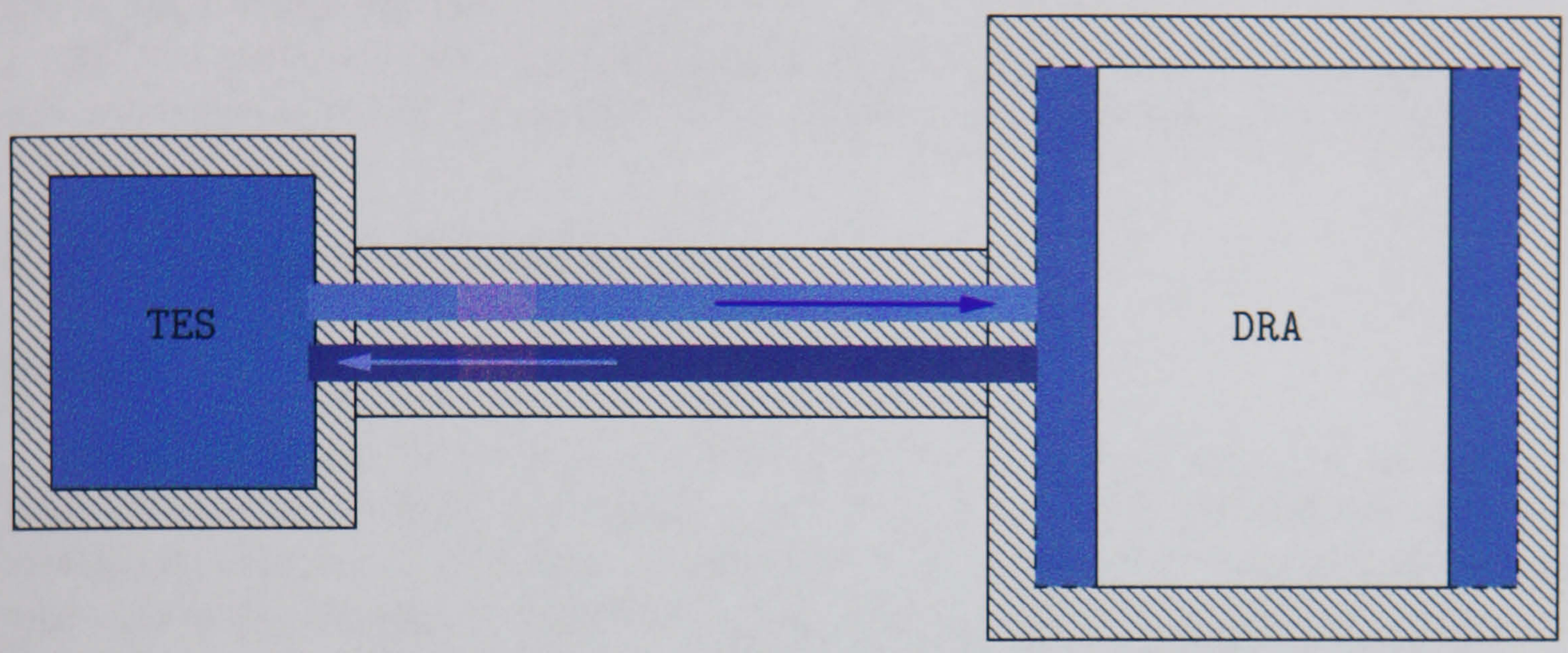


Figure 5.2: Schematic diagram of ES–DRA, with remotely–located TES's.

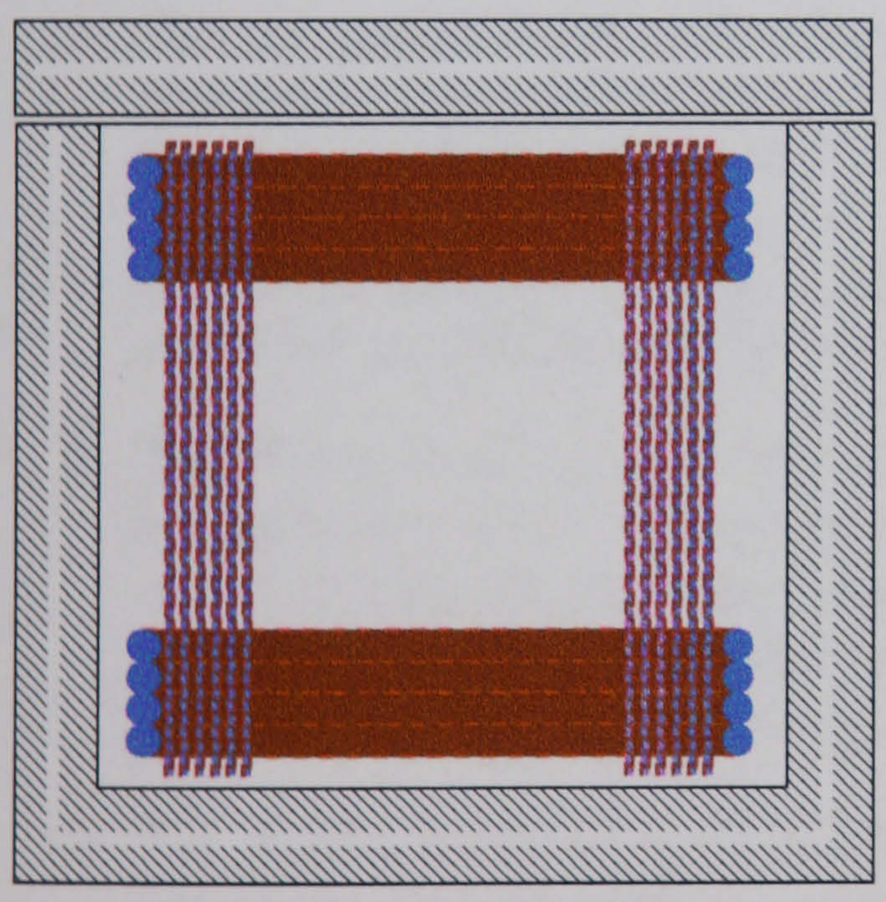


Figure 5.3: Schematic diagram of ES–DRA compartment, indicating the heat transfer surfaces.

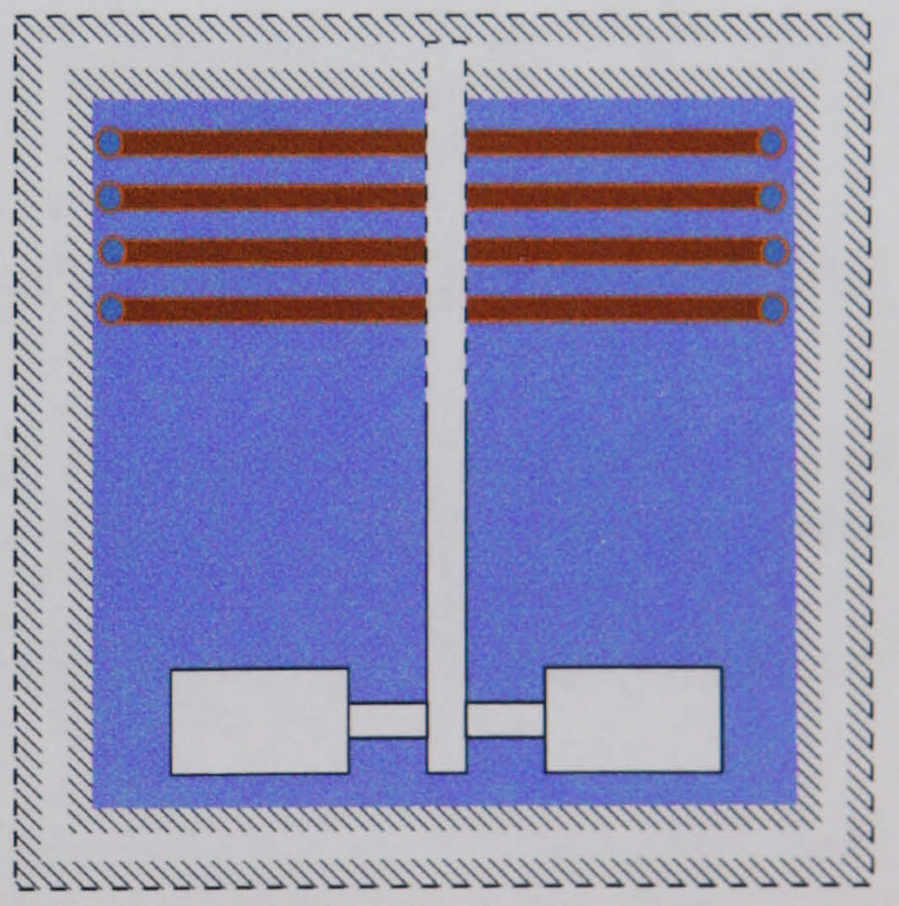


Figure 5.4: Schematic diagram of external storage TES indicating the stirrer and the internal pipe–work.

never reached; see Hunt (1969) and, Shook and Roco (1991), Chapters 2, 3 and 5, for discussions on the subject.

For the purpose of this analysis, it will be assumed that the flow regimes will be (a) heterogenous or non–homogenous, (b) fully–developed and (c) turbulent.

5.2 Design Parameters

Scope

Much of systems analysis of this design is akin to that given in section 4.4.4 on page 118 and as such the principal concern here is to assess the differences in the coolth requirements and identify any additional electrical energy requirements which arise due to the difference in thermal storage and transport requirements. These are then fed into the model devised in Chapter 4 on page 105 for a further analysis.

The following are the design parameters to be used in this design analysis:

5.2.1 Basic Assumptions

The following basic assumptions have been made:

1. The secondary fluid shall consist of a slurry of phase–change (hydrophilic) 'particles', hereinafter referred to as the '*solid–load*', carried in an inert oil stream (*e.g.* Paraffin).

2. The flow regime is to be such that no settling/sedimentation of the hydrophilic particles (*i.e.* solid–load) occurs[1].

3. The slurry is to be such that during normal operation, no agglomeration of the particles occur. This places restrictions on the maximum proportion of the (volume) ratio of the solid–load to the carrier fluid for a given flow velocity, see Augood (1997). This and the preceding assumption (2) place restrictions as to the minimum particle size.

4. The characteristic diameter of the average particle size shall be significantly less than[2] the conduit characteristic diameter (hydraulic mean bore). The particle diameter has a bearing on the extent of the heat transfer enhancement which may be achieved. If the (slurry) flow is assumed to be turbulent,

[1] Ideally, the particles should be neutrally–buoyant *at the stream velocity* and the latent heat transition temperature of the solid–load. This is to prevent either settling or the case where the solid–load aggregates on the upper surface of the conveying conduit.

[2] In the order of magnitude sense; in the present case, assumed to be one order of magnitude.

Bed exists			→	*No bed exists*
			Two–phase behaviour →	Flow behaves as single phase
			Settling Mixtures →	Non and slow settling Mixtures
Stationary bed	→	Fully–moving bed		
No solid movement	↘			
Rolling and Rippling movement				
Saltation				
Fully suspended flow				
Heterogenous flow →		Pseudo–homogenous flow	→	Homogenous flow
Newtonian →				Non–Newtonian
Pseudo–plastic →				Bingham Plastic

Table 5.1: Comparative characterisation of two–phase solid–liquid flow. Culled from Lam (1980); originally from Lazarus and Faddick (1980).

then micro–convective thermal conductivity enhancement within the *laminar* boundary layer would occur, *if* the solid–load particle diameters are considerably less than the boundary layer thickness [Goel et al., 1994]. The particle diameter can be a key factor in determining the minimum slurry flow velocity and also, from the point of view of bulk transport there is less likelihood of particle damage due to attrition, the smaller the mean particle size *op. cit.*

5. No significant spatial variations in either the particle, or fluid temperatures and no temperature gradients exist either within the pipe[1], or between the piping and its contents. The justification for this goes thus:

   - Given that due to the *two–phase* nature of the fluid, (a) the flow is turbulent and (b) consists of fluid particles (solid–load) with average diameters sufficiently smaller than the pipe diameter, then:

     (i) Irrespective of the enhanced particle–fluid heat transfer (due to (a))[2] and in consequence of the geometrical implications inherent in (b) above, the magnitude of the particle Biot numbers may be sufficiently small (< 0.1) to justify the approximate uniform particle cross–sectional temperature (lumped parameter) criterion for individual particles, and

     (ii) For small pipe diameters, turbulent–mixing as a consequence of (a) above, may suffice for the approximation of uniform cross–sectional temperature to hold within the *fluid*, for regions not too near the pipe wall.

     Based on these considerations, the slurry (particles and fluid bulk) may be essentially characterised by one temperature.

   - If the (effective) thermal resistance on the pipe exterior is higher than that on the interior surface[3] and the thermal resistance of the pipe is comparatively low[4], then the temperature of the pipe would be practically indistinguishable from that characterising its interior boundary layer, which in turn would not differ markédly from that of the bulk fluid.

[1] *i.e.* the contents are thermally mixed.

[2] Which presumably will be restricted to the laminar boundary layer, if the flow is turbulent.

[3] This would be expected in situations where the pipe surface is insulated and/or the exterior heat transfer mechanism is due to buoyancy *i.e.* the heat transfer coefficient exterior to the pipe is much less than that on the interior surface.

[4] Presumably as a consequence of a high thermal conductivity of the pipe material and/or small pipe wall thickness.

6. The solid–load is the principal thermal energy carrier from the TES. Thus the mass–flow rate required for heat transfer from the slurry to the refrigerating compartment can be reckoned on the premise that the transferable energy in the stream is entirely due to the solid–load latent heat storage capacity. This constant temperature stream assumption has several implications. In addition to those laid out commencing on page 88, it can help to minimise the energy loss on account of the heat gain to the slurry during transport to the refrigerating appliance and it can provide an isothermal heat exchange surface for the heat transfer from the refrigerating appliance. This consideration gives rise to the condition that the maximum temperature of the heat transfer fluid (slurry) entering or exiting the refrigerating appliance is T_{LH} (the slurry solid–load phase transition temperature).

7. The heat pump sizing shall be done on the basis of the maximum heat transfer rates.

8. The thermal store shall be situated at a proximity $L_{TES,DRA}$ away from the refrigerator[1].

5.2.2 Physical Property Estimates

In order to characterise the slurry behaviour under working conditions, it is necessary to obtain reliable estimates for the values of parameters to be used in correlating the relevant phenomena. In general, the estimates for the apparent values of the various thermo–physical properties tend to be higher for slurries than for the base–liquid. This effect is the result of several different phenomena occurring on account of the nature of suspensions and the additional effects of the motion (and relative motion) of the base–liquid and the solid–load (see Legal (1973), Sohn and Chen (1981) for discussions as to these effects). In some instances, the effect of these increases in apparent fluid–property values may counteract, attenuating rather than enhancing derived fluid transport parameters. An instance of this (pertinent to these analyses) is the determination of the heat transfer coefficient. Consider the well known Sider and Tate (1936) correlation[2] for the Nusselt number for turbulent flow in pipes.

$$Nu \sim Re^{0.8} Pr^{1/3}$$

[1]This is particularly crucial for the flow between the TES and the refrigerating appliance, as concerns about heat gains to the slurry return line can be addressed, in part, by cooling the condenser coolant with this return slurry stream.

[2]The same conclusion can be reached using the Dittus–Boelter correlation [Chapman, 1984, *pp.* 281].

This may be represented as:

$$h \sim k^{2/3} C_p{}^{1/3} v^{0.8} \mu^{-0.467}$$

Clearly the magnitude of the improvements of the thermo–physical properties are attenuated in the carry–through to the heat transfer coefficient. This is true for other (physical–property based) characterising parameters, particularly in situations where quotients are involved, as with the viscosity in the illustration. Illustrative of this are reports in the literature where claims of up to thirty–fold improvements in the resultant thermal conductivity [Kasza and Chen, 1982; Choi et al., 1994] are only met with claims of *circa* three–fold increases in heat transfer coefficient [Choi et al., 1994; Goel et al., 1994].

The following relations are given on the basis that the slurry can be assumed to be homogenous (or at least approaches this ideal condition). In line with the isothermal heat transfer assumption, only property values at the phase transition temperature T_{LH} will be considered.

The solid volume ratio, $(\zeta_V)_{(s)-load\,slur.}$, of the slurry is defined as the *average*[1], of the *in situ*, volume ratio (ζ_V) of the particulates (solid–load) to the fluid content of the slurry. For the purpose of the ensuing analysis, the magnitude of these two quantities shall be assumed equal, *i.e.* that the slurry is completely mixed.

The ratio of the density of the suspended particles (solid–load) in the flow to the density of the suspending fluid is known as the slurry mass density ratio, $(\zeta_{\rho m})_{slur.}$, and is defined as:

$$(\zeta_{\rho m})_{slur.} = \frac{(\rho_m)_{(s)-load}}{(\rho_m)_{base-(1)}}$$

The solid–load mass density, $(\rho_m)_{(s)-load}$, may be obtained from the relative volume proportions of the mass densities of water and TES (PVA) contents in the solid–load.

$$(\rho_m)_{(s)-load} = (\rho_m)_{PVA} + (\zeta_{V[H_2O]})_{(s)-load} \times [(\rho_{m[H_2O]}) - (\rho_m)_{PVA}]$$

As the degree of hydration of the PVA approaches 100%, $(\rho_m)_{(s)-load} \rightarrow (\rho_m)_{[H_2O]}$. The slurry density, $(\rho_m)_{slur.}$, in turn may be computed from the volume proportions of the mass densities of the solid–load and slurry base–liquid.

$$(\rho_m)_{slur.} = (\rho_m)_{base-(1)} [1.0 + (\zeta_V)_{(s)-load} \cdot ((\zeta_{\rho m})_{slur.} - 1.0)]$$

[1] A definition necessitated because of the radial variations in the distribution of the solids within the carrying fluid, a greater proportion being close to the bottom of the conduit, see Shook and Roco (1991), *pp.* 29.

The resultant viscosity of the slurry, $\mu_{slur.}$, may be obtained from the Einstein (1906)–Thomas (1965) relation. This relation is best for mono–sized spheres in a homogeneous suspension and is used here as an approximation. Ideally the viscosity of the resultant *'fluid'* should be experimentally determined.

$$\frac{\mu_{slur.}}{\mu_{base-(1)}} = \left[1.0 + 2.5\cdot(\zeta_v)_{(s)-load} + 10.05\cdot(\zeta_v)_{(s)-load}{}^{2.0} + 0.00273\exp\left(16.6\cdot(\zeta_v)_{(s)-load}\right)\right]$$

The mass fraction of water $(\zeta_{m[H_2O]})$ in the slurry may be computed from

$$(\zeta_{m[H_2O]})_{slur.} = (\zeta_m)_{(s)-load} \times (\zeta_{m[H_2O]})_{(s)-load}$$

The apparent latent heat capacity of the slurry, $(Q_{LH})_{slur.}$, may be computed from the relation

$$(Q_{LH})_{slur.} = (\zeta_{m[H_2O]})_{slur.} \times (Q_{LH})_{[H_2O]}$$

The thermal conductivity of the hydrated solids may be computed on the assumption that each individual particle may be modelled assuming parallel conduction paths exist within the lattice. The resultant conductivity is thus

$$k_{(s)-load} = k_{PVA} + (k_{[H_2O]} - k_{PVA}) \times (\zeta_{m[H_2O]})_{(s)-load}$$

The evaluation of $k_{[H_2O]}$ will be made depending on whether the contained water is in the solid or liquid state (*i.e.* $H_2O_{(s)}$ or $H_2O_{(1)}$). As with most other thermo–physical properties of slurries, the evaluation of the bulk mean conductivity for the slurry poses several difficulties, particularly at high solid–load content. Most of the available correlations and theoretical equations for slurry thermal conductivity estimates are for 'dilute' suspensions. In such fluids the assumption is usually made that each particle of the solid–load is free of interaction with other particles to the extent that uniform conditions are assumed to exist about each particle. There is also the assumption that the slurry behaves like a homogenous material on the macro–scale. The problem of determining the effective thermal conductivity of a (dilute) suspension was first posed by [Maxwell, 1892, *pp.* 440] who presented a formal analysis and arrived at the following correlation.

$$\frac{k_{slur.}}{k_{base-(1)}} = \frac{2.0\cdot\frac{k_{(s)-load}}{k_{base-(1)}} + 1.0 + (\zeta_v)_{(s)-load}\left(\frac{k_{(s)-load}}{k_{base-(1)}} - 1.0\right)}{2.0\cdot\frac{k_{(s)-load}}{k_{base-(1)}} + 1.0 - 2.0\cdot(\zeta_v)_{(s)-load}\left(\frac{k_{(s)-load}}{k_{base-(1)}} - 1.0\right)} \tag{5.1}$$

Maxwell's result (the most widely used in the literature) has been extended by a number of investigators notably Rocha and Acrivos (1973), who gave results for arbitrarily–shaped particulates in suspension. Legal (1973) first investigated the case

of a slurry in motion[1], where he indicated that thermal conductivity enhancements occur on account of relative motion between the base–liquid and the solid–load (see also Nir and Acrivos (1976)). Charunyakorn et al. (1991) took cognisance of previously published theoretical estimates and arrived at a more complicated correlation for flow in circular ducts limited to concentrations of not exceeding 15% solids by volume. However, evidence from the literature [Goel et al., 1994] tends to suggest that the Maxwell correlation may be used for slurries of concentrations of up to 22%. There is a lot of confusion in the literature as to the appropriate correlation for the thermal conductivity of slurries exceeding 30% solids content (by volume) and most authors only make cursory reference to it, if any at all, (see for instance Govier and Aziz (1972), Shook and Roco (1991), Cheremisinoff (1986)). The consensus though, is that the value predicted by the Maxwell correlation will be a conservative estimate. In the current undertaking, eqn (4.1) will be used for estimating the effective thermal conductivity of the slurry.

5.3 Energy Requirement Assessment

In order to compute the system's total energy requirement it is necessary to compute the head–losses that would be incurred in the pumping and the mixing of the slurry. In addition to the (pump) energy required to cater for these head–losses, there are thermal energy burdens:

1. Associated with the intrinsic viscous dissipation of 'head–loss work', the magnitudes of the converted energy (work to heat) being entirely equivalent in consequence of the first law[2].

2. Accruing on account of pump efficiency, whereby, power consumption in excess of the electrical energy equivalent of the total head requirement is converted to heat; a good proportion of which may be admitted to the system.

The ensemble of these heat loads will be hereinafter referred to as the heat gains due to the slurry pumping process, Q_{pump}. In the light of the foregoing it is highly expedient to attempt to keep mechanical work inputs to the system minimal, as (generally) each unit of mechanical work input to the system places at least an additional equivalent thermal burden on the system.

[1]Because of the enhancement created by the particle–fluid interactions, the effective conductivity of flow slurries is higher than that predicted by eqn (4.1).

[2]An exception to this is any work done against gravity; this work is not converted to heat.

5.3.1 Slurry Bulk Velocity

The rate at which the slurry flows in the pipe is a key factor in these analyses and it is thus necessary to determine a bulk velocity at which the slurry will be conveyed to and from the TES. This is because the mass–flow rate (or mass–velocity), $\dot{m}$, determines the mean flow velocity, which is inextricably linked to other system parameters such as, the flow heat transfer coefficient and the line head–losses. In the present application, there are several factors that influence the determination of the mass–velocity. Two key factors are the need (a) for the transport fluid to contain sufficient (coolth) energy for transfer (*i.e.* the cooling mass–flow rate requirement) and (b) to ensure that the flow is homogenous (or at least pseudo-homogenous) to prevent deposition (*i.e.* that its flow velocity exceeds the critical resuspension/deposition velocity, v_{m0}, for the continuous suspension of its constituent solid–load).

5.3.1.1 Coolth Capacity

In the determination of the mass–velocity, which is here based on the heat transfer rate required to compensate for the heat gains to the refrigerating appliance (inclusive of the gains associated with slurry transport), account has to be taken of both the heat addition to the (slurry) transport lines due to viscous dissipation of work and other heat gains to the conveying conduit incurred during transport. The following analysis is cast to determine the minimum mass–flow rate necessary to cater for the thermal gains to the refrigerating compartment and the gains associated with the process.

If in addition to the initial assumption that the slurry transport-pipe (and contents) remain isothermal throughout the process, the consistent assumption is made that all the *latent* heat available for transfer in any element of fluid would be completely transfered out of the slurry as it makes its way from and back to the TES, then

$$\dot{m}_{slur.} = \max\left(\frac{(\rho_m)_{slur.} \times \sum^{N,pump,pipe} Q}{(\rho_E)_{slur.}}, \frac{(\rho_m)_{slur.} \times \sum^{D,pump,pipe} Q}{(\rho_E)_{slur.}}\right) \tag{5.2}$$

The mass continuity[1] equation can be rearranged to make the velocity the subject term *viz*

$$(v_{slur.})_Q = \frac{4.0 \cdot \dot{m}_{slur.}}{\pi \rho_m \cdot D_{pipe}{}^2} \tag{5.3}$$

The mass–flow rate relation eqn (4.2) and the slurry density suffice to determine one value for the flow velocity.

[1]The understanding here is for full-bore pipe flow.

5.3.1.2 Critical Velocity Analysis

The process of settling during slurry flow is characterised by a great many individual phenomena. While it is sufficient to assume that if the particles are 'neutrally–buoyant' in suspension, deposition will not occur, factors like the particle drag coefficient, the mean slurry velocity, the relative velocity between each particle and the suspending fluid *etc.* also play key roles in dictating whether settling will or will not occur and if so to what extent. As mentioned earlier one defining parameter with regard to this is the critical (resuspension) velocity, v_{m0}.

Thus a second criteria for the determination of the mass–velocity of the flow is the condition that the flow velocity is not less than the critical resuspension velocity. This will ensure that settling does not occur in the flow, adversely affecting heat transfer and ultimately causing blockage/hold–up. This critical resuspension velocity is a function of the mean settling velocity (v_0) of the particles within the slurry and other flow characterising parameters (*e.g.* viscosity, density, *etc.*). In turn, the settling velocity is a function of the resultant drag coefficient on each individual particle, interaction between particles, the properties of the ensuing fluid *etc.* There are several correlations in the literature for the determination of the settling velocity, drag coefficient and their interdependence. However several of the correlations neither take into account the stream velocity nor the viscosity of the resultant slurry or that of the base fluid. In many cases the correlations are cast in terms of the resultant coefficient of drag of the suspended particles, for which there is no satisfactory correlation. Unsurprisingly, there does not seem to be much consistency amongst them, [Govier and Aziz, 1972; Wani, 1986][1]. In view of the necessity to determine some value for these parameters, the following need to be considered.

The particle settling velocity

The settling velocity of a particle depends on the resistance to flow the particle experiences in free fall. It is dependent on the physical properties of the fluid in which the motion occurs, on the geometric shape and surface roughness of the particle. The geometric and surface roughness dependence is characterised by the coefficient of drag of the particle. Generally, the smoother a body and the closer its geometric shape approaches that of a sphere, the lower its coefficient of drag and the higher its settling velocity. In situations where there is relative motion between the surrounding fluid and the particle's normal to the direction of settling, the settling velocity is also affected by the various forces of lift ([Shook and Roco, 1991, *pp.* 15–

[1] Wani (1986), gives six different tables each cataloguing 16 correlations for estimates for the critical velocity from different studies, each correlation in each table yielding a different result! See also Oroskar and Turian (1980), for a discussion on this.

17]) and the critical diameter of the smallest settling particle will differ considerably from that for a stagnant fluid [Atapattu et al., 1988]. Also, the settling velocity of a *single* particle in a fluid differs greatly from that of the mean settling velocity of particles in the same fluid *ceteris parabus*. The reason for this is the (direct and indirect) interaction between particles, in particular the increased resistance to flow as a result of the interference of the boundary layers of each particle and from inter–particle collusions. Observation reveals a tendency for the particles in a moving slurry to agglomerate; for slurries of diverse particle sizes, the smaller 'fines' tend to form 'homogeneous' suspensions with the carrier fluid increasing its viscosity and thus its flow resistance (as well as the mean heat transfer coefficient within the slurry [Goel et al., 1994]). It thus stands to reason that, if the settling velocity is computed on the basis of a single spherical particle, predicted velocities would exceed observed values. This would result in critical velocities that are also higher than observed, guaranteeing that sedimentation would not occur. On this understanding, the settling velocity can be computed based on the recommendation of Govier and Aziz (1972), *pp.* 6, using Allen (1900):

$$v_0 = 0.20\left[g\frac{\rho_{m\,(s)-load} - \rho_{m\,base-(1)}}{\rho_{m\,base-(1)}}\right]^{0.72}\frac{D_{(s)-load}{}^{1.18}}{(\mu/\rho_m)_{base-(1)}{}^{0.45}} \qquad (5.4)$$

$$1.0 < \frac{D_{(s)-load}\,v_0\,\rho_{m\,base-(1)}}{\mu_{base-(1)}} < 1000$$

$D_{(s)-load}$ in this case being the mean particle diameter.

The particle critical velocity

The mean critical resuspension velocity (v_{m0}) can be computed from the correlation of Oroskar and Turian (1980) [1]

$$\frac{v_{m0}}{[g \cdot D_{pipe}\,((\rho_m)_{slur.} - (\rho_m)_{(1)})]^{0.5}} = 1.85 \cdot (\zeta_v)_{(s)-load}{}^{0.1536}(1 - (\zeta_v)_{(s)-load})^{0.3564}\left(\frac{D_{pipe}}{D_{(s)-load}}\right) \times \left(\frac{D_{pipe} \cdot (\rho_m)_{(1)} \cdot [gD_{(s)-load} \cdot (\zeta_{\rho m} - 1)]^{0.5}}{\mu_{(1)}}\right)^{0.09} \qquad (5.5)$$

In determining the mass–flow rate of the slurry, the maximum of the slurry velocity based on either the heat transfer requirements, $(v_{slur.})_Q$, eqn (4.3) or the critical resuspension velocity, v_{m0}, eqn (4.5) is used to determine the slurry bulk velocity

$$v_{slur.} = \max\left((v_{slur.})_Q, v_{m0}\right) \qquad (5.6)$$

[1] Here the assumption is that the ratio $\frac{v_0}{v_{m0}} < 0.5$; see Shook and Roco (1991), *pp.* 98, for an explanation.

and from this the mass–flow rate of the slurry can be obtained.

5.3.2 Head–Loss Assessment

In assessing the *fluid* pumping requirements for the application, the total length of the piping is added to estimates for *equivalent*[1] pipe-loss lengths. The values for the head–losses are dependent on the mean friction factor obtaining over each length; the Darcy–Weisbach equation is generally used for estimating head–losses in pipe flow

$$\triangle H = 64 \cdot \left(\frac{f}{2}\right)\left(\frac{L}{\mathrm{D_{pipe}}}\right)\left(\frac{v^2}{\mathrm{g}}\right)$$

The correction for slurry flow is then applied to this resultant equivalent length and finally, the total head–loss is computed as the sum of the different head–losses. The velocity used in the computation of the head is the slurry mean flow velocity (as computed from eqn (4.6)); were f is the non–dimensional frictional coefficient, (this differs from the so called Fanning friction factor by a factor of 4). For turbulent flows this can be obtained from either the Moody (1944) plot, or from correlations[2]. The length of the piping comprises:

- The length of pipe work within the heat exchanger positioned inside the refrigerating compartment.
- The length of pipe work conveying the slurry between the refrigerating compartment and the TES.
- The length of any pipe work within the thermal sink.

The equivalent lengths consists of:

- Length losses associated with changes in elevation.
- Length losses associated with bends.
- Length losses associated with entry into and exit from the TES.

[1]These are additions to the length of say, a bend, to cater for the increases in head–losses due to the bend.

[2]See Schlichting (1968), *Chapter XX*, for a comprehensive exposition, with references, on friction factors.

5.3.2.1 Elevation Losses

The head–loss analysis is to be undertaken on the assumption that the bulk of the piping is to be mounted horizontally. In order to accommodate this assumption, it is necessary to account for the pressure head required to move the slurry against the maximum vertical distance it travels, in addition to the gravity head. This distance is either the height of the appliance, or the height of the TES[1] depending on which is larger. The pertinent head–loss relation is simply:

$$\triangle H_{\uparrow} = \sum \triangle \text{height} \cdot \left(1.0 + \left(\frac{f}{2}\right) \frac{v_{\text{slur.}}{}^{2}}{\text{g} \cdot \text{D}_{\text{pipe}}}\right)$$

The value of the friction coefficient, f, is to be computed as in the case for the normal pipe run (see eqn (4.12)). Also note that the first term in the outer parenthesis is representative of the work done against gravity and is *not* converted to heat by viscous dissipation.

5.3.3 Bend Losses

The head–losses associated with each bend in the pipeline are necessarily greater than those for straight–runs. Slurry flow head–losses are usually correlated in relation to the head–losses of the base carrier fluid under a similar set of circumstances. The nature of the liquid flow alters markédly in passing through a bend, due to the usual occurrence of twin centrifugally–induced vortices normal to the flow direction, see Goldstein et al. (1950), *pp.* 314, and Schlichting (1968), *pp.* 589. For slurries, the flow pattern is much more complex, [Wildman et al., 1984], as there is a tendency for centrifugally–induced segregation to occur at sharp bends, with the coarser particles migrating to the 'outer' wall and the fines concentrating on the suction wall.

For the present application, the limitations of space in the refrigerating compartment necessitate the use of low bend radii (principally for the corners). A value of 1.5 has been chosen for r_r/D_{pipe}. Based on the forgoing considerations, the head–losses of the carrier fluid under similar conditions shall be deemed to be a *reasonable approximation* to those occurring in the slurry. The friction factor for head–losses in single–phase fluids through bends can be computed from the correlations of It-

[1]The value of the slurry storage height is dependent on, amongst other things, this gravity–associated work.

o (1959, 1960, 1987), who gives the following correlations for f

$$f = \frac{0.029 + 0.304 \cdot \mathrm{De}^{-0.25}}{\left(2 \cdot \frac{r_r}{D_{pipe}}\right)^{0.5}} \tag{5.7}$$

$$300 > \mathrm{De} > 0.034$$

where De is the flow Dean number[1], defined ([Schlichting, 1968, *pp.* 589]) as

$$\mathrm{De} = \left(\frac{D_{pipe} \cdot (v_{slur.} \times \rho_m)_{(1)}}{\mu_{(1)}}\right)\left(\frac{D_{pipe}}{2 \cdot r_r}\right)^{2.0}$$

Thus the head–loss due to all the corners is

$$\triangle H_r = \left(\frac{f}{2}\right)\frac{{v_{slur.}}^2 \times \sum L_r}{g \cdot D_{pipe}} \tag{5.8}$$

where $\sum L_r$ is the total length of all the pipe bends (90 ° elbows), each representable as

$$L_r = \frac{2\pi \cdot r_r}{4}$$

5.3.3.1 End Losses

On the assumption that there is no piping within the thermal sink (TES), the additional head–losses are due to the sudden expansion and contraction at the reservoir–pipe exit and entrance. These can be estimated from the correlations given by Duncan et al. (1981), *pp. pp.* 411 *ff.* For the entry flow into the reservoir, the losses may be assumed to be those due to sudden expansion (assuming that there would be some pressure recovery). In this case, the approximate equation for the head–loss (length) is

$$\triangle H_\prec = \left(\frac{{v_{slur.}}^2}{2 \cdot g}\right)\left(1 - \frac{A_{pipe}}{A_{TES}}\right)^2 \tag{5.9}$$

If the available reservoir expansion area perpendicular to the pipe is much larger than the pipe area, then the head–loss may be modified to omit the area ratio term. Thus, this head–loss is reduced to the quotient of the dynamic pressure within the pipe before entry and the corresponding fluid density.

[1] Below a value of 0.034 the friction factor of a curved pipe practically coincides with that of a straight pipe.

For the slurry transfer from the reservoir into the conduit, the losses may be approximated as that of sudden contraction *op. cit.*

$$\triangle H_{\succ} \sim \left(\frac{v_{slur.}{}^2}{2.0 \cdot g} \right) \tag{5.10}$$

Where the relevant constant of proportionality is dependent on the ratio of the two diameters (the conduit, A_{pipe}, and the reservoir, A_{TES}) and on the Reynolds number of the downstream flow. From the table given in that reference, the maximum approaches 0.51. If this is applied to the current design, the value of the head–loss due to this contraction is seen to be half that of the case of the inlet.

$$\triangle H_{end} \sim \sum \triangle H_{\prec} + \sum \triangle H_{\succ}$$

5.3.3.2 Length Losses

The (straight–run) line losses can be estimated from (see page 120)

$$\triangle H_{\rightarrow} = f \frac{L_{pipe} \cdot v_{slur.}{}^2}{2 \cdot D_{pipe} \cdot g} \tag{5.11}$$

For laminar pipe flow it is demonstrable that the value of this coefficient is

$$f = \frac{64}{Re_D} \tag{5.12}$$

Where Re_D is the pipe diameter Reynolds number.

$$Re_D = \frac{\rho_m \cdot v \cdot D_{pipe}}{\mu}$$

It is expected that the Reynolds number (Re_D) for the base fluid (paraffin), with the same flow velocity as the slurry, will be well within the laminar regime[1]. In the unlikely event that the base flow is turbulent, the relation given by Schlichting (1968) will be used:

$$\frac{1}{f} = 0.817 \cdot \log(Re_D \sqrt{f}) - 0.8 \tag{5.13}$$

It is to be noted that this relation should only be used for 'smooth' pipes, *i.e.* smooth in the sense that typical pipe rugosities lie within the laminar sub–layer. If this is not the case, then the Moody, *op. cit.*, plot *must* be used.

[1] O. Reynolds characterises the onset of the laminar–turbulence transition, for pipe flow, as occurring at around 2,100, while at Reynolds numbers in excess of 2,500 flows may be characterised as fully turbulent. However, due to solid–load activity within the flow, there is little likelihood that laminar behaviour would persist over any appreciable length. This notwithstanding, the correlation is used as recommended as the consideration here is for the *base–liquid*.

5.3.3.3 Slurry Head–Loss Correction

The slurry head–losses are typically correlated as a linear function of the head–losses of the carrier fluid [Shook and Roco, 1991, *pp.* 102] in terms of a non–dimensional excess head–loss coefficient Φ

$$\Phi = \frac{H_{\text{slur.}} - H_{(1)}}{(\zeta_V)_{(s)-\text{load}} \cdot H_{(1)}}$$

or

$$H_{\text{slur.}} = H_{(1)} \cdot (1.0 + (\zeta_V)_{(s)-\text{load}} \cdot \Phi) \tag{5.14}$$

Typically the computation of this Φ coefficient is by some variant of the generalised Durand and Condolis (1952), non–dimensional head–loss correlation

$$\Phi = \frac{v^2 \sqrt{C_D}}{g \cdot D_{\text{pipe}} \cdot ((\zeta_{\rho m})_{\text{slur.}} - 1)} \tag{5.15}$$

Vertical runs The slurry correction for vertical flows can be represented as

$$\Phi_{\uparrow} = ((\zeta_{\rho m})_{\text{slur.}} - 1) \tag{5.16}$$

However for slurries of low–moderate (up to 30% $(\zeta_V)_{(s)-\text{load}}$) concentration *and* for coarse particles ($D_{(s)-\text{load}} > 0.5\,\text{mm}$), the wall friction has been observed to approach that of the carrier fluid *i.e.* $\Phi \to 0$, [Newitt et al., 1961]

Ends Little research has been done to assess the slurry head–loss correction for sudden changes in section. The evidence tends to suggest that the correction is negligible within regions of practical significance (see Weltmann and Keller (1956)) hence $(\Phi_{\succ}, \Phi_{\prec}) = 0$.

Bends Toda et al. (1972, 1973) determined that for bends in the horizontal *and* for ratios of bend radius to pipe diameter (r_r/D_{pipe}) of less than *eight*, the difference in water and slurry flow pressure drops are virtually undetectable ([Shook and Roco, 1991, *pp.* 241]). Thus for the present application, $\Phi_{r} = 0$.

Horizontal runs Newitt et al. (1955) give the following correlation for the *upper* limit of Φ in horizontal pipe flow

$$\Phi_{\rightarrow} = \frac{66 \cdot g \cdot D_{\text{pipe}} \cdot [(\zeta_{\rho m})_{\text{slur.}} - 1]}{v_0} \tag{5.17}$$

Total Head–Loss

The total head–loss is the sum of all the other subsidiary head–losses (elevation losses, bend losses, end losses, length losses); from the foregoing, the total head is:

$$\triangle H_{\text{tot.}} = \sum_{j}^{\uparrow,\text{end},\curvearrowright,\rightarrow} \triangle H_j \cdot (1.0 + (\zeta_v)_{(s)-\text{load}} \cdot \Phi_j) \tag{5.18}$$

The head–loss in terms of pressure can be computed from the relation

$$\triangle \mathrm{P} = (\rho_{\mathrm{m}})_{\text{slur.}} \cdot \mathrm{g} \cdot \triangle H_{\text{slur.}} \tag{5.19}$$

Pump Capacity and Electrical Energy Requirements

In considering the issue of pump selection, the intended application, efficiency and cost must also be taken into account. For most slurry conveyance applications centrifugal pumps[1] are the usual choice, see Walker (1980) and Ando et al. (1986), *pp.* 772. The volumetric capacity of the selected pump is given by

$$\dot{\mathrm{V}}_{\text{slur.}} = (\dot{\mathrm{m}} \cdot \rho_{\mathrm{m}})_{\text{slur.}} \tag{5.20}$$

and required pressure head is given by eqn (4.19)

The efficiencies of such pumps (η_{pump}) are characteristically in the region of (65–80)%. Taking into account the variations in loading conditions, an efficiency estimate of about 50% has been chosen here. The electrical power requirements for the delivery of a given mass–flow ($\dot{\mathrm{m}}$) of a fluid of density (ρ_{m}) at a specified pressure head ($\triangle$P) may be obtained from:

$$P_{\text{pump}(e)} = \left(\frac{\triangle \mathrm{P} \cdot \dot{\mathrm{m}}}{\rho_{\mathrm{m}} \times \eta_{\text{pump}}} \right)_{\text{slur.}} \tag{5.21}$$

5.3.4 Reservoir agitation requirements

It may be necessary to stir the slurry within the reservoir for the following reasons

- To inhibit sedimentation.

[1]There are other more efficient pumps which have been developed for the movement of slurries, most notably, the pulsating pump which is highly desirable for pumping large concentration slurries. Investigation into such technologies may become more appropriate at the prototype–design stage of the design process.

- To enhance heat transfer at the slurry–evaporator interface.
- To ensure the rapid cooling of the spent, returned slurry.

A full analysis of the mixing of slurries in vessels is a very involved and complex process and a detailed treatment will not be attempted here. From a design perspective, it is instructive to consider the conclusions of various workers in the field.

The mixing in stirred vessels is usually dominated by a process called back–mixing [Ando et al., 1986]. This phenomenon is characterised by adjacent regions of 'contra–flow' within the vessel. Oldshue (1986) states important considerations to be given with regard to mixing impellers *viz*[1]:

- Impeller size.
- Impeller speed.
- Impeller geometry (width, blade angle, pitch, *etc.*).

That author further indicates that a (highly application–specific) optimum design can be achieved taking these into consideration. In general, however the most efficient impellers are the so called axial 3–blade impellers [Oldshue, 1986, *pp.* 817] (see also Zwietering (1958) where the power numbers obtained in a series of experiments are given). The design of any such impeller must be done in conjunction with the design of the tank geometry. It is expedient to avoid non–cylindrical vessels, *op. cit.*, as this tends to engender stagnation or secondary flow regions close to the corners. For most applications the best tank geometry is a (cylindrical) '*square batch*'. As an absolute minimum, the vessel diameter–to–fluid height must not be less than 0.3, whilst for ratios in excess of 1.0 a multi–impeller design is desirable. Thus the volume of the TES is

$$V_{TES} = \pi \frac{D_{TES}^{\ 3}}{4} \tag{5.22}$$

In order to ensure efficient stirring, special attention should be paid to the ensuing flow pattern. Generally, for most applications, baffles are required. This is to ensure that swirling and poor blending do not result. Typically, unbaffled systems have virtually no vertical currents or velocity gradients, both of which are essential for mixing. There is evidence to suggest that for efficiency purposes the impeller shaft should be inclined to the vertical in the absence of baffles, the exact tilt angle being

[1]Other techniques may be used for this stirring process *e.g.* fluid injection. The decision here was, as with elsewhere in this work, to use the simplest technique.

dependent on the application and the impeller blade angle (Oldshue, *loc. cit.*. *pp.* 816). Extreme care must be taken in the baffle design, as baffle design insufficiency can greatly inhibit the system's overall performance. The most important parameter to be borne in mind in this instance is the viscosity of the mix. Generally, for viscosities in excess of 0.50 $\mathrm{N\,s/m^2}$ (500 cP), baffles are usually not necessary as the viscous drag of the fluid acts as a dynamic baffle. Oldshue, *loc. cit. pp.* 281, gives the following correlations for the power required for mixing[1]

$$P = \mathrm{Po}_N\,(\ldots) \cdot (\rho_m)_{\mathrm{slur.}} \cdot \omega^3 \cdot \mathrm{D_{imp.}}^5 \tag{5.23}$$

alternatively,

$$\mathrm{Po}_N = \frac{P}{(\rho_m)_{\mathrm{slur.}} \cdot \omega^3 \cdot \mathrm{D_{imp.}}^5} \tag{5.24}$$

where

ω is the angular velocity of the impeller,

$\mathrm{D_{imp.}}$ the diameter of the impeller and

$\mathrm{Po}_N\,(\ldots)$ is the non–dimensional power number, Po_N, and is a function of the impeller flow Reynolds number $\mathrm{Re_{imp.}}$.

The definition of $\mathrm{Re_{imp.}}\,(\ldots)$ is given in a footnote at the bottom of page 127[2].

---

[1]The density term (ρ_m) was added by the present author, as the correlation given in the reference is dimensionally inconsistent. If the power is resolved dimensionally in terms of the mass density ρ_m, viscosity μ, impeller diameter, $\mathrm{D_{imp.}}$, and the angular velocity, ω, the following results

$$P \sim \left[\left(\frac{\rho_m}{\mu}\right)_{\mathrm{slur.}} \cdot (\omega \cdot \mathrm{D_{imp.}}) \cdot \mathrm{D_{imp.}}\right]^b \cdot \left(\frac{\mu_{\mathrm{TES}}}{\mathrm{D_{imp.}}}\right)^2$$

$$\sim \mathrm{Re_{imp.}}\,(\ldots)^{b-2} \times \rho_m \cdot \mathrm{D_{imp.}}^5 \cdot \omega^3$$

where $\mathrm{Re_{imp.}}$ is a characterising Reynolds-type number with the impeller diameter as characteristic length.

$$\mathrm{Re_{imp.}}\,(\ldots) = \mathrm{Re}\,(\omega, \mathrm{D_{imp.}}, (\rho_m)_{\mathrm{slur.}}, \mu_{\mathrm{slur.}})$$

$$= \left[\frac{(\rho_m)_{\mathrm{slur.}} \cdot \mathrm{D_{imp.}}^2 \cdot \omega}{\mu_{\mathrm{slur.}}}\right]$$

As this is a dimensional analysis, some constant (in this case $\mathrm{Po}_N\,(\ldots)$) serves to relate this expression to experimental observation.

[2]A figure plotting the dependence of Po_N on $\mathrm{Re_{imp.}}$ is given on *pp.* 820 of the said reference where the author erroneously writes

$$\mathrm{Po}_N = \frac{\mathrm{g} \cdot P}{\rho_m \cdot \omega^3 \cdot \mathrm{D_{imp.}}^5}$$

The minimum rate of stirring required is that which would curtail the onset of sedimentation, *i.e.* the slurry should be stirred at a rate commensurate with compensating for the particle settling velocity [Oldshue, 1986, *pp.* 817]. Conti and Gianetto (1986) give criteria for the classification of different types of solid–liquid systems in vessels. Heterogeneous 'fully–suspended' systems are identified by the so called '*one second* criterion' *op. cit. pp.* 887; [Zwietering, 1958]. This is simply the mean time in which any particle can remain at rest at the base of the vessel before it is resuspended. These authors state a correlation (initially given by Zwietering, *loc. cit.*,)[1] for the critical speed (ω_0) for which this condition is realised

$$\omega_0 = S_Z \frac{\left(\frac{\mu}{\rho_m}\right)_{(1)}^{0.1} \cdot D_{(s)-load}^{0.2} \cdot [g \cdot ((\zeta_{\rho m})_{slur.} - 1)]^{0.45} \cdot [100 \cdot (\zeta_{\rho m})_{slur.} \cdot (\zeta_V)_{(s)-load}]^{0.13}}{D_{imp.}^{0.85}} \tag{5.25}$$

$$\begin{aligned} 0.31 &< \mu_{(1)} < 9.3 \quad (\times 10^{-3} N\,s/m^2) \\ 125 &< D_{(s)-load} < 850 \quad (\times 10^{-6} m) \\ 720 &< \|\rho_{(1)} - \rho_{(s)-load}\| < 1,810 \quad (kg\,m^{-3}) \\ 0.5 &< 100 \cdot (\zeta_{\rho m})_{slur.} \cdot (\zeta_V)_{(s)-load} < 20 \\ 0.05 &< D_{imp.} < 0.22 \quad (m) \end{aligned}$$

S_Z is a dimensionless constant characterised, in part, by the ratios of the impeller to vessel diameter and the impeller diameter to impeller–vessel base clearance. The evidence tends to suggest that lower values of S_Z may be utilised with decreasing impeller–vessel base clearance, [Conti and Gianetto, 1986, *pp.* 890]. Several correlations are available for the determination of this parameter (S_Z), predictions of which are in close agreement. The following correlation is taken from Zwietering, *loc. cit.*[2].

$$S_Z = 1.33 \left(\frac{D_{TES}}{D_{imp.}}\right)^{1.55} \tag{5.26}$$

The given data correlates as:

$$g \times Po_N = 0.36 + 57.39 \cdot Re_{imp.}(\ldots)^{-3.81} + 25.89 \cdot Re_{imp.}(\ldots)^{-0.735}$$
$$1.0 \leq Re_{imp.}(\ldots) \leq 10^6$$

[1]Baffles are requisite in this case.

[2]This is for a two–blade paddle, with a paddle diameter–to–height ratio of 4 and vessel height to impeller–base clearance of 20; the quoted power number, Po_N, was 2.5.

Electrical Energy Requirements

The determination of the diameter of the impeller is subject to the prevention of impairment of impeller motion. For this analysis the clearance between the TES walls and the impeller tips will be *circa* four mean particle diameters. Thus the stirrer mechanical power requirements can be determined, and assuming a stirrer efficiency of 80%, the electrical power requirements for the stirrer can also be determined

$$P_{\text{imp.}(e)} = \frac{P_{\text{imp.}}}{\eta_{\text{imp.}}} \tag{5.27}$$

5.3.5 Heat Gains

The additional thermal gains[1] to the system consist of (a) heat ingress to the conduits and TES on account of the ambient temperature and (b) the heat generated on account of viscous dissipation of the mechanical work used for the TES mixing and for pumping the slurry, taking into cognisance the various process mechanical efficiencies.

5.3.6 Conductive Heat Gains

5.3.6.1 Conduit Heat Ingress

The thermal energy gains (to the slurry in transit) due to the ambient temperature can be computed from the heat equation. On the assumption that (a) the pipe is clad with a thermal insulant of known thickness (L_k) and conductivity ($k_{\text{insul.}}$)[2], (b) the ambient heat transfer coefficient is known and (c) that the conduit can be classed as isothermal, then the conduit heat gain per unit run of the conduit can be estimated from

$$\frac{Q_{\text{pipe}}}{L_{\text{pipe}}} = \frac{2\pi \cdot (T_{\text{pipe}} - T_{\text{amb.}})}{\frac{\log\left(\frac{(r_{\text{insul.}})_{\text{ext.}}}{(r_{\text{pipe}})_{\text{ext.}}}\right)}{k_{\text{insul.}}} + \frac{1}{(r_{\text{insul.}})_{\text{ext.}} \cdot h_{\text{amb.}}}} \tag{5.28}$$

5.3.6.2 Heat Gains to the Thermal Store

It is assumed that an insulant of the same insulating capability as for the refrigerating compartment (k_{VPSI}), with a thickness of L_k, is to be used for the TES, under

[1] *i.e.* the additional cooling requirements.

[2] As mentioned earlier, the thickness and quality of the insulant, as well as the length of the conduits, are central considerations to this design.

the same heat transfer conditions and on the understanding that the TES fluid bulk is at temperature T_{LH}. The heat gains to the TES may be computed from the equation of conduction of heat to an infinite cylinder, with provision made for the ends. Here, as elsewhere, no provision is made for edge effects, which serve to increase heat ingress into the system. Defining the exterior and interior diameters of the clad vessel as $(D_{TES})_{ext.}$ and $(D_{TES})_{int.}$, respectively, the pertinent approximate equation is

$$Q_{TES} = \frac{\pi \cdot (D_{TES})_{int.} \cdot (T_{TES} - T_{amb.})}{\frac{\log\left(\frac{(D_{TES})_{ext.}}{(D_{TES})_{int.}}\right)}{2 \cdot k_{VPSI}} + \frac{1}{(D_{TES})_{ext.} \cdot h_{amb.}}} + \frac{\pi \cdot k_{VPSI} \cdot (D_{TES})_{ext.}{}^{2} \cdot (T_{TES} - T_{amb.})}{2 \cdot k_L} \tag{5.29}$$

Thus the additional *direct* sensible heat gains to the system are:

$$Q_{(T)} = Q_{TES} + Q_{pipe} \tag{5.30}$$

5.3.7 Viscous Dissipation

On account of the viscous dissipation of the work used to overcome the wall friction (the principal part of the head–losses), heat $Q_{mech.}$ is generated *within* the slurry. In addition to this, inefficiencies within the pumping mechanism give rise to the heat equivalent of the unavailable proportion of the energy input which is lost in conversion. For conventional pumps (where the vanes are not thermally isolated from the pump rotor) the bulk of the heat generated will find its way into the slurry stream. The agitation of the TES also gives rise to heat generation due to the viscous dissipation of the work used in stirring; the proportion of this mechanical work which is converted to heat would vary depending on the stirrer design. Also, as in the case of the slurry pump, the greater part of the heat generated due to the inefficient conversion of electrical to mechanical work would tend to ingress the TES. For the purpose of estimating an upper bound, it is assumed that all the non–gravity associated electrical energy is converted to heat. Thus for the pump

$$(Q_{mech.})_{pump} = \frac{\dot{m}_{slur.} \cdot g \cdot [\sum_j^{\uparrow,end,\curvearrowright,\rightarrow} (\triangle H + \triangle H \cdot \Phi)_j - \triangle height_{TES}]}{\eta_{pump}} \tag{5.31}$$

For the mechanical agitator the heat generated is given by eqn (4.27)

$$(Q_{mech.})_{imp.} = \frac{(P_{imp.})_{(e)}}{\eta_{imp.}} \tag{5.32}$$

Thus the additional heat generated on account of mechanical work done on the system is

$$Q_{\text{mech.}} = (Q_{\text{mech.}})_{\text{pump}} + (Q_{\text{mech.}})_{\text{imp.}} \tag{5.33}$$

5.3.8 Summary

This sub–section collects the results of the analyses presented in the earlier part of this section. As mentioned earlier the relations developed in the forgone part of this section are for active–TES design the requirenemts *in addition to* the basic energy demands outlined in the previous chapter (Chapter 4 on page 105) for the passive–TES case. The information is classified into two categories by energy type and subsequently the relation for the total energy requirements is present.

5.3.8.1 Thermal Storage Requirements

The additional heat gain (*i.e.* the cooling load) has been assessed from the heat gains to the TES, conduits and the thermal equivalent of the mechanical work required to pump the slurry round the system and to keep the TES constantly agitated.

$$\mathsf{E}_{(T)} = Q_{(T)} + Q_{\text{mech.}}$$

(*i.e.* eqn (4.30) and eqn (4.33)) and comprises

- The energy requirement to cater for the thermal gains for one day.
- The energy gains associated with conveying the slurry to and from the thermal sink. This includes the heat gains from the pump, the heat gains from the ambient to the conduit and the heat gains due to viscous dissipation (head–loss equivalent).
- The energy gains to the thermal sink.
- The energy gains due to the electrical–to–mechanical work conversion inefficiency of the pump.
- The energy gains as a result of the mixing.

5.3.8.2 Electrical Energy Requirements

The additional electrical energy requirements have been assessed from

$$\mathsf{E}_{(e)} = P_{\mathsf{pump}(e)} + P_{\mathsf{imp.}(e)}$$

i.e. eqn (4.21) and eqn (4.27) and comprise

- The energy requirements to cater for the continuous movement of the slurry through the system.
- The energy requirements to keep the solid–load within the TES in constant suspension.

5.3.8.3 Total Energy Requirements

The total energy input into the *entire* system for each day must equal the sum of the total heat gain to the system and the total work input into the system.

$$\begin{aligned} \mathsf{E}_{\mathsf{tot.}} &= \mathsf{E}_{(T)} + \mathsf{E}_{(e)} \\ &= \sum^{\mathsf{D,N}} Q_{\mathsf{DRA}} + \sum Q_{\mathsf{pipe}} + \sum Q_{\mathsf{mech.}} + \sum \mathsf{E}_{\mathsf{mech.}} \end{aligned} \tag{5.34}$$

where

$$Q_{\mathsf{mech.}} = Q_{\mathsf{pump}} + Q_{\mathsf{imp.}}$$

$$\mathsf{E}_{\mathsf{mech.}} = \mathsf{E}_{\mathsf{pump}} + \mathsf{E}_{\mathsf{imp.}}$$

5.4 Thermal Energy Store Sizing

In order to compute the heat gains to the thermal sink, the dimensions of the thermal sink need to be determined. It is justifiable to use a cylindrical cross–section of diameter equal to vertical height[1]. These internal dimensions are determined by the required storage capacity. This is determined by the energy gains accrued over one day–time period, Q_{D}, say. Thus the containment height (and diameter) are defined

$$\mathsf{D}_{\mathsf{TES}} = \sqrt[3]{\frac{4 \cdot Q_{\mathsf{D}}}{\pi \cdot (\rho_{\mathsf{E}})_{\mathsf{slur.}}}} \tag{5.35}$$

[1] *i.e.* a '*square batch*'; this can be deduced from both heat transfer and agitation power requirement perspectives, see section 4.3.4 on page 125.

Implicit in the value of Q_D is the heat gain to the TES due to the ambient temperature and the heat gain due to viscous dissipation of the stirrer work, both being dependent the TES geometry *i.e.* D_{TES}, estimates for which have been previously given. The computation of D_{TES} would necessarily involve some iteration.

5.5 Closure

This chapter has presented a subset of the thermal design analysis of a slurry–based external storage refrigerating appliance, which can be used as an alternate system to that discussed previously in Chapter 4 on page 105. It focused on the additional energy requirements such a system will have in comparison to its passive storage counterpart (see Chapter 4 on page 105) which result from the remote location of the TES from the ES–DRA. The (additional) requisite energy requirements identified in this chapter have been integrated into the model devised in Chapter 4 on page 105 and the results, with discussions, are presented alongside the results of that chapter.

As mentioned in the introduction to this chapter, mechanical agitation is just one method of designing such a system. Fluidisation is another method by which the TES agitation may be achieved and in which some of the heat gains/energy requirements to the system can be reduced. Conceivably, this may be integrated within the prime–mover circuit, with the refrigerant acting as the particle fluidising[1] and entraining agent, ex prime–mover. Figure 4.1 on page 106 illustrates a few 'integrated' options within which the fluidisation concept may be implemented. This (fluidisation) has the advantages of:

(a) Negating the need for a separate slurry pump and the heat gains and head–losses associated with it.

(b) Reducing the heat heat transfer process from a two–stage process (primary circuit → secondary circuit → refrigeration appliance heat exchanger) to a single stage (primary compressor circuit → refrigeration appliance heat exchanger). This implies less complexity, less inventory and fewer avenues for coolth losses and thus prime–mover associated irreversibilities.

(c) Considerably better heat transfer as (i) the particles may (depending on design) release their latent heat at the same time as the refrigerant is expanding within the evaporator, (ii) greater turbulence and better mixing within the refrigerating appliance heat exchange inventory.

[1] *i.e.* a rotating/circulating fluidised bed.

(d) Greater leeway in the choice/optimisation of particle size as the boundary layers will be thinner, on account of the fluid properties and faster (expansion) gas–phase velocities.

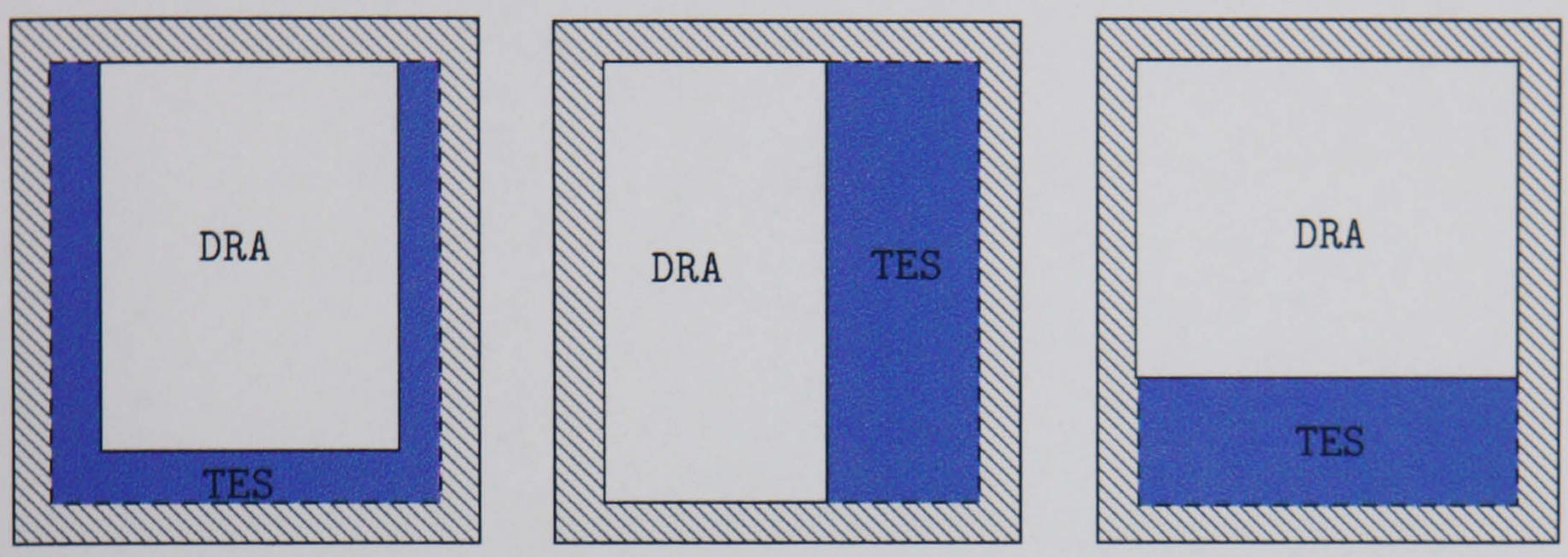


Figure 5.5: Schematic diagram of integrated TES's

Foreseeably, problems which need to be primarily addressed have to do with (a) ensuring inertness between the chosen PCM and the refrigerant and (b) devising a method to avoid the PCM particles interfering with the workings of the prime–mover, possibly using some kind of filtration technique.

The transmission of slurries through heat exchange inventory in refrigeration systems is a technology still well in its infancy and while the heat transfer potential is clear, there is little else which is certain about the behaviour of such systems. This makes the analytic design process difficult (and probably inefficient). In order to harness the potential inherent in such designs, much research into the underlying phenomena of the technology will need to be undertaken. It is the view of the author that, whatever resources are expended on such research will be at least commensurate with the benefits which are to be obtained from such systems over their passive TES counterparts.

Chapter Six

Model Results

We did then what we knew how to do ... Now we know better, we *might* do different.

–M. Angelu

6.1 Introduction

This chapter documents the predictions of the computer–model which was written to facilitate the (thermal) design specification of the prototype energy storage domestic refrigerating appliance (ES–DRA). This preliminary assessment–prediction model was developed, in the 'C' computer programming language from the analyses presented in Chapters 4 and 5, *qv.* pages 105 and 153 respectively, about the commercial ambitions of a refrigeration manufacturing company (Quest Refrigeration Manufacturing Ltd., Aber park, Flint, Clwyd, North Wales, CH6 5EX UK.) and enables the design calculation of both passive– and active–TES ES–DRA applications. The results were used to help guide the design of, principally, a 391 fridge for developing–world applications within the expertise of the sponsoring company. Subsequent to presentation of the findings of the model, the company implemented

a detailed design[1], manufactured and supplied a DRA unit which formed the basis of an experimental rig. The experimental test procedure, results, and illustration of which are discussed in Chapter 6 on page 181.

6.2 A Brief Description of the Application

The modelling process was essentially undertaken in three stages *viz* (a) an assessment of the heat gains into the system, including gains due to utilisation, under a given set of conditions, (b) the prediction of the energy storage requirements to effectively operate the ES–DRA under these conditions using different energy management strategies, taking into consideration the expected performance of the different components and (c), finally, the sizing of the individual components for the appliance.

The computational procedure is based on the concept of 'temperature–time' zones, where each 24–hour period is discretised into two distinct time–zones[2], *viz* day–time and night–time; associated with each is a distinct average temperature. The assessment of the total appliance's (coolth and electrical) energy requirements was thus computed as the sum of the requirements for each time–zone. A second feature of the model is that it is a 'component–based' model, as it deals individually with each component as if it were in isolation and does not consider the effects of the behaviour of each component on the workings of other components. Specifically, it does not 'numerically–model' the DRA compartment in the finite–difference or finite–element sense.

In implementing this model certain simplifying assumptions (consistent with those laid out in section 4.2 on page 106) were made regarding the computation of the (a) compartment heat gains to the DRA and (b) energy (electrical and thermal) requirements of the appliance. Principally, the compartment was idealised as a single 'quasi–steady' component[3] and the heat gains were computed based on the steady–state equation of Langmuir et al. (see eqn (B.I)) over the two distinct temperature periods *i.e.* the 'day' and 'night' times. The sensible and latent heat gains (accounting for the gains due to coolth loss on account of user interaction) for each period were computed based on an estimated number of air changes for each period and the appliance's (thermal) utilisation load, assumed to be water initially at the

[1]The different (minimum) size/capacity requirements for the components (evaporator, TES *etc.*) were then specified using the predictions of the model, taking into account the different approximations/assumptions made during the analytical phase of the design process and the available industry–standard sizes of the required components.

[2]The use of two time–zones was entirely arbitrary and the number may be extended as desired.

[3]The multiplicity of the number of variables was influential in the decision to model the system as a collection of components.

day–time temperature, modelled as a fixed percentage of the internal volume. In computing the heat gain through the compartment walls, the assumption is made that the super–insulant (VPSI) is located within the composite insulation adjacent to the useful cooling space; this is on account of the findings of section 2.5.2 on page 64[1].

The 'passive' storage section of the model investigates the three different configurations, as given in section 4.4.2 on page 112, *viz* the 'battery–only' scenario, the 'TES–only' scenario and the *hybrid* energy storage, HES (battery and TES), scenario. Within the HES scenario, one DRA control mode was investigated, *viz* the situation where the heat–pump is used only during the night–time.

The 'active' storage section of the model only investigates the scenario whereby the heat–pump is utilised solely during the night–time for the HES case. The decision to proceed only with the night–time prime–mover operation for the HES in the case of the active–TES was based on the results of the passive TES (given in section 5.3.2 on page 143).

With respect to the active–TES, the model was used to compute the energy consumption and the requisite energy storage capacities for the ES–DRA for (a) a nominal day, (b) a three–day *inclement* period[2] and (c) a five–day inclement period. Depending on the TES and DRA operating temperatures, the daily utilisation–load cooling requirements and the thermal resistance at the DRA–TES interface, it might be necessary to extend the DRA interior heat–transfer surface area to meet the cooling requirements. This has also been taken into account in the model implementation[3].

6.3 Model Findings

Introduction

This section presents the results of the computer model; in all cases the computational work was carried out in relation to a 'base–case' set of conditions and system parameters. These conditions were drawn up in part from the specifications laid out in section 4.2 on page 106 and partly from other considerations *e.g.* size,

[1] Hereinafter, the phrase 'latent heat gain' will refer to the total heat gains due to the volume–air changes, while the term 'sensible heat gain' will refer to the heat gains through the DRA compartment walls.

[2] Essentially this is a period during which the energy supply to the appliance is some fraction of that nominally expected; see section 4.4.4.2 on page 129 for a fuller description of this and the length of time implied.

[3] Note that this is only applicable to cases where a TES is in existence and is assumed to operate at a fixed temperature. In other cases *i.e.* the battery–only scenario, the evaporating temperature may be reduced (in theory) without limit negating the use of a surface area extender.

flexibility during experimentation *etc.* Many of these conditions may be varied[1] depending on the intention of the modelling exercise. These include (a) the lengths of the day–, night– and solar insolation–time and the inclement period, (b) the day– and night–time temperatures, relative humidities, compartment volume air changes, mean COP, (c) the DRA operating temperature, the TES operating temperature, the TES properties (type, degree of hydration, operating temperature *etc.*), the slurry properties (concentration, base fluid *etc.*), the daily utilisation–load, the insulant characteristics (number of layers, layer properties *etc.*), the daily utilisation (load, pull–down time *etc.*), (d) the daily top–up period, the energy recovery fraction of that nominally expected during an inclement period, the night–time prime–mover operation early–start period, the component efficiencies (battery, TES, pump, agitator) *etc.* The choice of the appliance internal volumes modeled was to a great extent to satisfy the production requirements of the affiliated company and to some extent for the ease of experimentation. In modelling the active–TES the sponsors requirement was only for results of the large volume (110 litre) appliance; but to facilitate a direct comparison a 39 litre appliance was also modelled.

Initially the predictions for the base–case conditions are presented followed by an investigation of the effect of the utilisation load.

6.3.1 Base Case Results

This section documents the results of the computer model applied to a 'base–case' set of conditions. The results presented here include both the passive– and active–TES cases as indicated earlier in section 5.2 on page 137. In the interest of clarity, these will be presented in tabular form. The initial set of tables contain general descriptive information of the 'base' conditions *e.g.* ambient conditions, TES properties *etc.* The results of the analyses for the passive– and active–TES cases are then presented in subsequent subsections.

[1] A few of the default parameters are application specific and changes would require slight modifications and recompilation of the sources.

Compartment specifications.

DRA casing material	: PVC	
DRA geometry	: Cubic	
Insulation type	: Composite (polyurethane foam+VPSI)	
Layer position (relative)	Internal	External
Insulation	VPSI	polyurethane foam
Thickness (mm)	25.4	40.0
Conductivity (W/mK)	0.002	0.022

Component efficiencies.

Efficiencies[a] (%)	Charge	Dwell	Discharge
TES	100	100	100
Battery	90	100	90
Solar Cell	15[b]		

Period sensitive data.

	Day–time	Night–time
Temperature (°C)	35	20
Relative Humidity (%)	85	65
Period (hours)	12	12
Volume air–changes	51	4
Heat–Pump COP	1.67	2.07

Table 6.1: Model input data

[a]The qualifying term 'dwell' characterises the degradation/loss of energy during storage.

[b]This represents the conversion efficiency of solar energy to electricity. The stated value was arrived at after lengthy discussions with solar cell manufacturers and is used throughout the modelling process.

Energy related base–conditions.

Internal temperature (°C)	:	4 ± 1
Utilisation load (% total capacity)	:	60 at day–time temperature (T_D)[a]
Principal load cooling period	:	18:00 – 06:00
Internal heat transfer coefficient (W/m°C)	:	6.0
External heat transfer coefficient (W/m°C)	:	6.0
Nominal daily insolation length (hours)	:	10
Mean (harvestable) daily insolation (kWh/m^2)[b]	:	3.5
Mean daily insolation strength (W/m^2)	:	52.5[c]

Inclement Period.

Daily recoverable fraction of nominal solar insolation[d]	:	0.2
Daily (fractional) recovery of total (battery/TES) capacity pursuant to period[1]	:	0.25

Night–time prime–mover operating regime.

Day–time top–up requirements (fraction of Q_D)	:	0.00
Fraction of non–solar active period ($t_D - t_{sol}$) when the prime–mover is active	:	1.00

Table 6.2: Application characteristics.

[a] Day–time utilisation.
[b] See section 4.2 on page 108.
[c] $3.5\,kWh/m^2 \div 10$ hours $\times$ 15%
[d] See section 4.4.4 on page 118.

Thermal Stores				
	Passive–TES	Active–TES		
		solid–load	base–liquid	Slurry
Material	Cross–linked (aqueous) PVA		Paraffin	base–liquid + solid–load
Concentration (w/w)	95% H_2O	90% H_2O	–	30% (v/v) solid–load
Thermal conductivity (W/mK)	2.46	2.92	0.138	0.22
Heat capacity (kJ/kgK)	4.203	2.006	1.83	1.89
Latent heat capacity (kJ/kg)	286.035	272.13	–	86.03
Latent energy density (MJ/m^3)	261.19	247.45	–	74.23
Density (kg/m^3)	913.15	909.3	843	863
Viscosity (kg/m-s)	–	–	0.0088	0.027
Mean solid–load particle diameter (mm)	–	2.5	–	2.5
Mean solid–load ($< 74\,\mu m$) fines (%)	–	–	–	0.00
DRA wall — TES/conduit clearance (mm)	25.4			
Operating temperature (°C)	0.0			

Table 6.3: Thermal energy store/carrier data.

PhD Thesis © 1999 Cranfield University

6.3.2 Passive–TES

The results for 39, 85 and 110 litre DRA's are presented here as computed for the preceding base–case conditions. The calculated energy requirements are presented first, followed by a more detailed specification of the different parts of the appliance. In the passive–TES design, the TES–DRA interior interface area is the primary heat exchange surface, with the evaporator assumed to be completely enclosed within the TES.

Internal Capacity (l)		39	85	110
Internal dimensions (mm)		340×340×340	440×440×440	493×493×493
DRA wall conductance (W/K)		0.05	0.08	0.10
DRA–TES heat exchange area (m^2)		0.66	1.21	8.23
Extended surface area factor[a]		4.02	4.8	5.3
Daily coolth requirements				
Latent heat gains ($Wh_{(T)}$)[b]	Day	0.014	0.030	0.042
	Night	0.000[c]	0.001	0.001
	Total	0.014	0.031	0.043
Sensible heat gains ($kWh_{(T)}$)	Day	0.016	0.027	0.034
	Night	0.010	0.016	0.020
	Total	0.026	0.043	0.054
Utilisation heat load ($kWh_{(T)}$)[a]	Day	0.00	0.00	0.00
	Night	0.764	1.67	2.35
	Total	0.764	1.67	2.35
Total heat burden ($kWh_{(T)}$)	Day	0.016	0.027	0.034
	Night	0.769	1.67	2.37
	Total	0.791	1.71	2.40

[a]60% day–load utilisation. By day–load utilisation the implication is a thermal load equivalent to the given percentage of the DRA capacity, at the mean day–time temperature (T_D), is placed into the ES–DRA at the commencement of the night–time period, with the expectation that this load will be brought to the appliance regulation temperature (T_{DRA}) at the end of the night–time period.

[b]Note that the unit in this row is three orders of magnitude less than the norm in the rest of the table.

[c]Less than half of one part in the fourth decimal place.

Table 6.4: Base–case dimensions, heat energy burden and heat exchange requirements for 39, 85 and 110 litre ES–DRA's.

In gaining an insight to the results presented in the following tables, it is helpful to note the comparative sizes of the required compressor ratings across the three

Systems Configuration			39 litre capacity DRA			85 litre capacity DRA			110 litre capacity DRA		
			Battery	TES	HES	Battery	TES	HES	Battery	TES	HES
Energy storage requirements	Thermal ($kWh_{(T)}$)		–	0.777	–	–	1.69	–	–	2.18	–
	Electrical ($kWh_{(e)}$)		0.375	–	0.382	0.815	–	0.826	1.05	–	1.07
Battery	Capacity ($kWh_{(e)}$)		0.417	–	0.424	0.905	–	0.918	1.17	–	1.19
	Charge rate ($W_{(e)}$)		42	–	43	91	–	92	117	–	119
	Discharge rate ($W_{(e)}$)		27	–	28	59	–	59	76	–	77
TES	Capacity ($kWh_{(T)}$)		–	0.777	0.014	–	1.69	0.023	–	2.18	0.027
	Charge rate ($W_{(T)}$)		–	78	1.0	–	169	2.0	–	218	2.0
	Discharge rate ($W_{(T)}$)		–	56	1.5	–	121	2.5	–	156	3.0
	Volume (l)		–	11.3	0.2	–	24.5	0.33	–	31.7	0.39
	Dimensions (mm)	Height	–	288	288	–	389	389	–	428	428
		Width	–	288	288	–	389	389	–	428	428
		Thickness	–	34	1	–	40	1	–	43	1
Compressor rating	Thermal ($W_{(T)}$)		65	80	57	140	171	122	181	221	157
	Electrical ($W_{(e)}$)		32	50	28	68	107	59	88	138	76
Solar cell	Rating ($W_{(e)}$)		48	50	48	102	107	102	132	138	132
	Size (m^2)		0.90	0.94	0.90	1.94	2.03	1.94	2.51	2.63	2.51

Table 6.5: Single–day requirements 60% (day–load) utilisation capacity (night–time cooled).

PhD Thesis © 1999 Cranfield University

control regimes. The thermal rating of the compressor is least for the HES configuration and most for the TES–only configuration. As is expected, the ratings remain constant irrespective of either weather clemence or the duration thereof.

The single–day electrical rating (size) of the solar cells (Table 5.5 on page 144) are the same for the battery–only and HES type configurations. This rating is slightly lower than the corresponding rating of the TES–only configuration. However, the inclement period rating (Table 5.6 on page 146) of the solar cell is highest for the battery–only design and least for the HES control regime.

In all cases the *electrical* energy *storage* requirement for the battery–only configuration is less than for the HES–design under corresponding conditions. The converse is true in comparing the TES requirements for the TES–only and HES control configurations, where the TES–only configuration requires greater TES capabilities.

In observing the TES (energy storage) capacity trends, the comparative volumes which are required to fulfil the storage requirements may be placed in perspective in relation to the useful volume of the appliance. For the HES configuration, in *all* cases, the volume of the TES amounted to less than 1% of the appliance–volume (a proportion which decreases with increasing capacity). This is in contrast to the TES–only configuration which requires increasingly greater proportions of the appliance–volume for the TES as the duration of the inclement weather period increases (29%, 86% and 117% for single–day, three–day and five–day 39 litre energy storage applications respectively). As a result, for the five–day inclement weather applications, the TES–only configuration is infeasible as the volume of the TES exceeds the appliance volume.

As is expected the energy storage requirements are linear with the increasing length of the inclement period. However, the single–day requirement will not conicide with any trend–line extraplated from the inclement period energy requirements for reasons given in section 4.4.4.2 on page 129.

Another interesting implication of the difference of the TES–only and HES applications is that over an inclement weather period there are more (TES) charge/discharge cycles associated with the HES–only configuration. This, as mentioned earlier (see section 3.3 on page 77), is desirable for increased rate of return on TES capital investment. The charge and discharge rates of the TES under the HES configuration are significantly less than that of the TES–only configuration. However the electrical energy storage charge/discharge requirements are *smaller* for the battery–only configuration than for the HES–only configuration. This is discussed in further detail later on in this chapter, along with the reason for the trend, how this can be overcome and the implications for a non–storage application.

Systems Configuration			39 litre capacity DRA			85 litre capacity DRA			110 litre capacity DRA		
			Battery	TES	HES	Battery	TES	HES	Battery	TES	HES
Energy storage requirements	Thermal ($kWh_{(T)}$)		–	2.32	–	–	5.03	–	–	6.5	–
	Electrical ($kWh_{(e)}$)		0.961	–	1.04	2.08	–	2.26	2.68	–	2.92
Battery	Capacity ($kWh_{(e)}$)		1.07	–	1.16	2.31	–	2.51	2.98	–	3.25
	Charge rate ($W_{(e)}$)		72	–	75	155	–	161	200	–	208
	Discharge rate ($W_{(e)}$)		32	–	32	68	–	69	88	–	89
TES	Capacity ($kWh_{(T)}$)		–	2.32	0.014	–	5.03	0.023	–	6.5	0.027
	Charge rate ($W_{(T)}$)		–	136	1.0	–	294	2.0	–	380	2.0
	Discharge rate ($W_{(T)}$)		–	65	1.5	–	140	2.5	–	181	3.0
	Volume (l)		–	33.7	0.2	–	73.0	0.33	–	94.3	0.39
	Dimensions (mm)	Height	–	288	288	–	389	389	–	428	428
		Width	–	288	288	–	389	389	–	428	428
		Thickness	–	101	1	–	121	1	–	128	1
Compressor rating	Thermal ($W_{(T)}$)		65	137	57	140	297	122	181	383	157
	Electrical ($W_{(e)}$)		32	86	28	68	185	59	88	239	76
Solar cell	Rating ($W_{(e)}$)		95	86	80	204	185	172	263	239	222
	Size (m^2)		1.8	1.63	1.51	3.89	3.53	3.27	5.01	4.56	4.23

Table 6.6: Three–day inclement period 60% (day–load) utilisation capacity (night–time cooled).

PhD Thesis © 1999 Cranfield University

Systems Configuration			39 litre capacity DRA			85 litre capacity DRA			110 litre capacity DRA		
			Battery	TES	HES	Battery	TES	HES	Battery	TES	HES
Energy storage requirements	Thermal ($kWh_{(T)}$)		–	3.15	–	–	6.82	–	–	8.81	–
	Electrical ($kWh_{(e)}$)		1.11	–	1.38	2.41	–	3.00	3.11	–	3.87
Battery	Capacity ($kWh_{(e)}$)		1.24	–	1.54	2.68	–	3.33	3.46	–	4.30
	Charge rate ($W_{(e)}$)		77	–	85	165	–	184	213	–	238
	Discharge rate ($W_{(e)}$)		32	–	32	68	–	69	88	–	89
TES	Capacity ($kWh_{(T)}$)		–	3.15	0.014	–	6.82	0.023	–	8.81	0.027
	Charge rate ($W_{(T)}$)		–	156	1.0	–	339	2.0	–	438	2.0
	Discharge rate ($W_{(T)}$)		–	65	1.5	–	140	2.5	–	181	3.0
	Volume (l)		–	45.7	0.2	–	98.9	0.33	–	128	0.39
	Dimensions (mm)	Height	–	288	288	–	389	389	–	428	428
		Width	–	288	288	–	389	389	–	428	428
		Thickness	–	137	1	–	163	1	–	174	1
Compressor rating	Thermal ($W_{(T)}$)		65	158	57	140	341	122	181	441	157
	Electrical ($W_{(e)}$)		32	99	23	68	213	59	88	275	76
Solar cell	Rating ($W_{(e)}$)		118	99	90	255	213	195	329	275	251
	Size (m^2)		2.25	1.88	1.71	4.86	4.06	3.71	6.27	5.25	4.79

Table 6.7: Five–day inclement period 60% (day–load) utilisation capacity (night–time cooled).

6.3.3 Active Storage

One major difference between the active– and passive–storage ES–DRA's is the location of the TES. Whereas in the passive–storage case the TES is internally located, the TES is externally located in the active–storage scheme. As a direct consequence of this, there are several components (and modifications) needed for an active–storage ES–DRA in addition to the requirements for passive–storage ES–DRA *e.g.* conduits, pumps *etc.*

This section will initially present general information about the active–storage ES–DRA (see also Table 5.3 on page 142); this will be followed by the additional energy burdens (thermal and electrical) accrued due to these modifications, then by the performance requirements of the various components and finally, by the gross energy requirements of the system. These predictions are presented only for the HES case and are restricted to the 39 and 110 litre ES–DRA's. As in the passive–TES case the utilisation capacity is assumed to be 60% of the DRA volume, with the charging load being water at the day–time temperature at the commencement of the night–time period *i.e.* the load–cooling period.

DRA–TES conduit (circular pipe)	
Material	Copper[a]
Schedule	40
Nominal size	1 inch (25 mm)
Inside diameter (mm)	26.6
Outside diameter (mm)	33.4
Total length (m)	2.0
Insulation type	Polyurethane foam
Insulant thickness (mm)	25.4
Insulant value (W/mK)	0.022

[a]Data taken from [Chapman, 1984]

Table 6.8: DRA compartment properties.

Unlike the passive–TES case, a separate heat exchanger has to be provided within the DRA for the active–TES implementation. This consists of several turns[1] of the (bare) slurry–carrying conduit within the DRA, with sufficient clearance between the DRA walls and the coiled conduit to permit air movement. As in the passive–TES

[1]Typically, the maximum number of turns will depend on the internal height of the appliance, the external diameter of the conduit and the various 'clearances' between the DRA–wall and the conduit.

Dynamic TES	
Geometry	Cylindrical (square–batch)
Insulation type	Polyurethane foam
Insulant thickness (mm)	25.4
Insulant value (W/mK)	0.022
Slurry return	Base
Pump location	Base

Table 6.9: Active–TES layout description.

case, at high utilisation loads, there is the need to extend this heat transfer surface area to augment the (DRA air–side) heat transfer.

Slurry pump	Type	Impeller
	Efficiency (%)	50
TES (dynamic) agitator	Type	3–blade propeller
	Efficiency (%)	70

Table 6.10: Slurry pump and agitator description.

Within the active–TES there is the need to continuously agitate the slurry to ensure that the solid–load remains in suspension (see section 5.3.4 on page 173). For this purpose an 3–blade propeller has been used[1] and the clearance between the propeller–edge and the TES wall has been set at four solid–load diameters.

For the case where no daily utilisation is expected[2], the additional system requirements remain largely unchanged. The only modifications which need to be made to Table 5.11 on page 150 on account of this are the (mass and linear) velocity requirements needed to satisfy the maximum cooling demand and, the internal heat transfer surface requirements (see Table 5.13 on page 152). The slurry transport (mass and linear) velocities have been based on the 'critical resuspension' criteria and hence much of the additional system requirements remain the same[3].

[1]This was chosen based on the recommendations of Zwietering (1958); arguably, other more appropriate technologies may be employed to perform this function, see also Augood (1997), Augood et al. (1999).

[2]For instance when the appliance and its contents have been cooled previously, and as such the ES–DRA's function is just to maintain the temperature of its contents.

[3]The same is true for other utilisation–load schemes used in the parametric study, see section 5.4.1 on page 154.

Active–storage HES			39 litre	110 litre
Flow (velocities)	Solid–load settling (m/s)		0.012	0.012
	Slurry critical resuspension (linear, m/s)		0.222	0.222
	Slurry critical resuspension (mass, kg/s)		0.107	0.107
	Coolth requirement (linear, m/s)		0.004	0.009
	Coolth requirement (mass, kg/s)		0.002	0.004
	Minimum slurry transport (linear, m/s)		0.222	0.222
	Minimum slurry transport (mass, kg/s)		0.107	0.107
Pump	Volume flow rating (l/s)		0.124	0.124
	Power consumption $W_{(e)}$		2.5	3.5
	Minimum pressure drop (kPa)		9.8	13.6
	Heat generated (24–hourly, $kWh_{(T)}$)		0.042	0.057
Agitator	Diameter (m)		0.22	0.23
	Critical angular resuspension velocity (r.p.m)		79	75
	Power consumption ($W_{(e)}$)		3.5	4.0
	Heat generated (24–hourly, $kWh_{(T)}$)		0.08	0.09
TES	Heat gains (direct, $kWh_{(T)}$)	day–time	0.113	0.122
		night–time	0.074	0.08
	Total heat gain (24–hourly, $kWh_{(T)}$)		0.187	0.202
conduit	Heat gains (direct, $kWh_{(T)}$)	day–time	0.086	0.086
		night–time	0.056	0.056
	Total heat gain (24–hourly, $kWh_{(T)}$)		0.142	0.142
	Number of turns within DRA		9	13
	Available heat exchange area (m^2)		1.16	2.44
	Required heat exchange area (m^2)		2.69	7.56
	Extended surface area factor		2.4	3.1
Additional daily cooling requirements				
($kWh_{(T)}$)	Day–time		0.260	0.280
	Night–time		0.192	0.209
	Total		0.452	0.489
Additional daily electrical energy requirements				
($kWh_{(e)}$)	Day–time		0.099	0.124
	Night–time		0.099	0.124
	Total		0.197	0.249

Table 6.11: Active–TES ES–DRA additional requirements/modifications, 60% (day–load) utilisation capacity (night–time cooled).

Systems Configuration			39 litre capacity DRA		110 litre capacity DRA	
			Single–day	Three–day	Single–day	Three–day
Energy storage requirements	Thermal ($kWh_{(T)}$)		–	–	–	–
	Electrical ($kWh_{(e)}$)		0.80	2.17	1.55	4.25
Battery	Capacity ($kWh_{(e)}$)		0.89	2.41	1.72	4.72
	Charge rate ($W_{(e)}$)		112	155	202	303
	Discharge rate ($W_{(e)}$)		66	49	121	106
TES	Capacity ($kWh_{(T)}$)		0.23	0.23	0.026	0.026
	Charge rate ($W_{(T)}$)		17	17	19	19
	Discharge rate ($W_{(T)}$)		23	23	26	26
	Volume (l)		11.2	11.2	12.6	12.6
	Dimensions (mm)	Height	242	242	252	252
		Diameter	242	242	252	252
Compressor rating	Thermal ($W_{(T)}$)		86	86	189	189
	Electrical ($W_{(e)}$)		42	42	92	92
Solar cell	Rating ($W_{(e)}$)		111	134	207	284
	Size (m^2)		2.11	2.56	3.94	5.4

Table 6.12: Active–TES ES–DRA energy requirements, 60% (night–time cooling) utilisation capacity.

PhD Thesis © 1999 Cranfield University

Active–storage HES		39 litre	110 litre
Flow (velocities)	Solid–load settling (m/s)	0.012	0.012
	Slurry critical resuspension (linear, m/s)	0.222	0.222
	Slurry critical resuspension (mass, kg/s)	0.107	0.107
	Coolth requirement (linear, m/s)	0.001	0.001
	Coolth requirement (mass, kg/s)	0.000[a]	0.000
	Minimum slurry transport (linear, m/s)	0.222	0.222
	Minimum slurry transport (mass, kg/s)	0.107	0.107
conduit	Number of turns within DRA	9	13
	Available heat exchange area (m^2)	1.16	2.44
	Required heat exchange area (m^2)	0.06	0.11
	Extended surface area factor	0.05	0.05

Table 6.13: Active–TES ES–DRA additional system requirements, 0% utilisation capacity.

[a]Less than half of one part of the fourth decimal place.

PhD Thesis © 1999 Cranfield University

Systems Configuration			39 litre capacity DRA		110 litre capacity DRA	
			Single–day	Three–day	Single–day	Three–day
Energy storage requirements	Thermal ($kWh_{(T)}$)		–	–	–	–
	Electrical ($kWh_{(e)}$)		0.352	0.968	0.413	1.15
Battery	Capacity ($kWh_{(e)}$)		0.392	1.08	0.459	1.28
	Charge rate ($W_{(e)}$)		40	80	46	96
	Discharge rate ($W_{(e)}$)		26	26	30	30
TES	Capacity ($kWh_{(T)}$)		0.23	0.23	0.026	0.026
	Charge rate ($W_{(T)}$)		23	23	26	26
	Discharge rate ($W_{(T)}$)		17	17	19	19
	Volume (l)		11.2	11.2	12.6	12.6
	Dimensions (mm)	Height	0.242	0.242	0.252	0.252
		Diameter	0.242	0.242	0.252	0.252
Compressor rating	Thermal ($W_{(T)}$)		31	31	35	35
	Electrical ($W_{(e)}$)		15	15	17	17
Solar cell	Rating ($W_{(e)}$)		56	89	67	106
	Size (m^2)		1.06	1.69	1.27	2.01

Table 6.14: Active–TES ES–DRA energy requirements, 0% utilisation capacity.

PhD Thesis © 1999 Cranfield University

6.4 Parametric Study

6.4.1 Load Dependence

Introduction

The model was run to examine the effect variations in the loading pattern can have on the size of various components of the designed ES–DRA. The investigation was carried out for variations in the utilisation load capacity ranging from no–utilisation to 60% day–time utilisation. The results of this study are presented here initially in tabular form and then subsequently the variation in the solar cell capacities (which gives an indication of the procurement and running cost of the system) is charted.

Heat Loads – 39 litre internal capacity							
% Utilisation[a], night–time : day–time		0:0	50:50	40:20	30:30	20:40	60:0
Daily coolth requirements							
Utilisation heat load ($kWh_{(T)}$)	Day	0.000	0.386	0.309	0.232	0.155	0.464
	Night	0.000	0.636	0.255	0.382	0.509	0.000
	Total	0.000	1.023	0.564	0.614	0.664	0.464
Total heat burden ($kWh_{(T)}$)	Day	0.016	0.402	0.325	0.249	0.171	0.480
	Night	0.010	0.646	0.264	0.392	0.519	0.010
	Total	0.026	1.049	0.590	0.641	0.690	0.490
Extended Surface Area Factor		0.09	3.4	1.7	2.1	2.7	2.5

[a]It should be remembered that night–time utilisation denotes the charging of the appliance with the indicated fraction of the appliance volume, at the night–time temperature, over the day–time period.

Table 6.15: Base–case dimensions, heat energy burden and heat exchange requirements for a 39 litre ES–DRA under different utilisation patterns.

Systems Configuration			Single–day			Three–day		
			Battery	TES	HES	Battery	TES	HES
Energy storage requirements	Thermal ($kWh_{(T)}$)		–	0.013	–	–	0.064	–
	Electrical ($kWh_{(e)}$)		0.006	–	0.013	0.031	–	0.029
Battery	Capacity ($kWh_{(e)}$)		0.007	–	0.015	0.034	–	0.032
	Charge rate ($W_{(e)}$)		1.0	–	1.5	2.0	–	2.5
	Discharge rate ($W_{(e)}$)		0.5	–	1.0	1.0	–	1.0
TES	Capacity ($kWh_{(T)}$)		–	0.013	0.014	–	0.064	0.014
	Charge rate ($W_{(T)}$)		–	1.5	1.0	–	3.0	1.0
	Discharge rate ($W_{(T)}$)		–	1.0	1.5	–	1.5	1.5
	Volume (l)		–	0.183	0.197	–	0.918	0.197
	Dimensions (mm)	Height	–	288	288	–	288	288
		Width	–	288	288	–	288	288
		Thickness	–	1	1	–	3	1
Compressor rating	Thermal ($W_{(T)}$)		1.5	3.0	2.0	1.5	4.5	2.0
	Electrical ($W_{(e)}$)		1.0	2.0	1.0	1.0	3.0	1.0
Solar cell	Rating ($W_{(e)}$)		2.0	2.0	2.0	3.5	3.0	2.5
	Size (m^2)		0.030	0.031	0.030	0.061	0.050	0.047

Table 6.16: 39 litre DRA requirements for no–utilisation capacity.

PhD Thesis © 1999 Cranfield University

Systems Configuration			Single–day			Three–day		
			Battery	TES	HES	Battery	TES	HES
Energy storage requirements	Thermal ($kWh_{(T)}$)		–	0.714	–	–	2.75	–
	Electrical ($kWh_{(e)}$)		0.345	–	0.517	1.25	–	1.25
Battery	Capacity ($kWh_{(e)}$)		0.383	–	0.574	1.38	–	1.39
	Charge rate ($W_{(e)}$)		39	–	58	78	–	92
	Discharge rate ($W_{(e)}$)		25	–	37	26	–	40
TES	Capacity ($kWh_{(T)}$)		–	0.714	0.336	–	2.75	0.336
	Charge rate ($W_{(T)}$)		–	72	24	–	140	24
	Discharge rate ($W_{(T)}$)		–	51	34	–	54	34
	Volume (l)		–	10.36	4.87	–	39.95	4.87
	Dimensions (mm)	Height	–	288	288	–	288	288
		Width	–	288	288	–	288	288
		Thickness	–	31	15	–	120	15
Compressor rating	Thermal ($W_{(T)}$)		54	105	71	54	174	71
	Electrical ($W_{(e)}$)		26	66	34	26	109	34
Solar cell	Rating ($W_{(e)}$)		64	66	64	127	109	102
	Size (m^2)		1.21	1.25	1.21	2.41	2.07	1.93

Table 6.17: 39 litre DRA requirements for 50% night–time and 50% day–time utilisation capacity.

PhD Thesis © 1999 Cranfield University

Systems Configuration			Single–day			Three–day		
			Battery	TES	HES	Battery	TES	HES
Energy storage requirements	Thermal ($kWh_{(T)}$)		–	0.319	–	–	1.46	–
	Electrical ($kWh_{(e)}$)		0.154	–	0.293	0.693	–	0.67
Battery	Capacity ($kWh_{(e)}$)		0.171	–	0.325	0.770	–	0.745
	Charge rate ($W_{(e)}$)		18	–	33	40	–	50
	Discharge rate ($W_{(e)}$)		11	–	21	17	–	22
TES	Capacity ($kWh_{(T)}$)		–	0.319	0.271	–	1.46	0.271
	Charge rate ($W_{(T)}$)		–	32	20	–	69	20
	Discharge rate ($W_{(T)}$)		–	23	28	–	28	28
	Volume (l)		–	4.63	3.94	–	21.22	3.94
	Dimensions (mm)	Height	–	288	288	–	288	288
		Width	–	288	288	–	288	288
		Thickness	–	14	12	–	64	12
Compressor rating	Thermal ($W_{(T)}$)		28	59	39	28	96	39
	Electrical ($W_{(e)}$)		17	37	19	17	60	19
Solar cell	Rating ($W_{(e)}$)		36	37	37	72	60	57
	Size (m^2)		0.69	0.70	0.69	1.36	1.14	1.07

Table 6.18: 39 litre DRA requirements for 40% night–time and 20% day–time utilisation capacity.

PhD Thesis © 1999 Cranfield University

Systems Configuration			Single–day			Three–day		
			Battery	TES	HES	Battery	TES	HES
Energy storage requirements	Thermal ($kWh_{(T)}$)		–	0.433	–	–	1.68	–
	Electrical ($kWh_{(e)}$)		0.209	–	0.315	0.760	–	0.764
Battery	Capacity ($kWh_{(e)}$)		0.233	–	0.350	0.844	–	0.849
	Charge rate ($W_{(e)}$)		24	–	35	48	–	56
	Discharge rate ($W_{(e)}$)		15	–	23	16	–	25
TES	Capacity ($kWh_{(T)}$)		–	0.433	0.207	–	1.68	0.207
	Charge rate ($W_{(T)}$)		–	44	15	–	86	15
	Discharge rate ($W_{(T)}$)		–	31	21	–	33	21
	Volume (l)		–	6.29	3.00	–	24.34	3.00
	Dimensions (mm)	Height	–	288	288	–	288	288
		Width	–	288	288	–	288	288
		Thickness	–	19	9	–	73	9
Compressor rating	Thermal ($W_{(T)}$)		33	64	43	33	106	43
	Electrical ($W_{(e)}$)		16	40	21	16	67	21
Solar cell	Rating ($W_{(e)}$)		39	40	39	74	67	62
	Size (m^2)		0.74	0.77	0.74	1.47	1.26	1.18

Table 6.19: 39 litre DRA requirements for 30% night–time and 30% day–time utilisation capacity.

PhD Thesis © 1999 Cranfield University

Systems Configuration			Single–day			Three–day		
			Battery	TES	HES	Battery	TES	HES
Energy storage requirements	Thermal ($kWh_{(T)}$)		–	0.548	–	–	1.89	–
	Electrical ($kWh_{(e)}$)		0.265	–	0.338	0.827	–	0.857
Battery	Capacity ($kWh_{(e)}$)		0.294	–	0.375	0.919	–	0.953
	Charge rate ($W_{(e)}$)		30	–	38	56	–	62
	Discharge rate ($W_{(e)}$)		19	–	25	21	–	27
TES	Capacity ($kWh_{(T)}$)		–	0.548	0.142	–	1.89	0.142
	Charge rate ($W_{(T)}$)		–	55	11	–	102	11
	Discharge rate ($W_{(T)}$)		–	40	15	–	43	15
	Volume (l)		–	7.95	2.07	–	27.46	2.07
	Dimensions (mm)	Height	–	288	288	–	288	288
		Width	–	288	288	–	288	288
		Thickness	–	24	6	–	83	6
Compressor rating	Thermal ($W_{(T)}$)		44	69	48	44	116	48
	Electrical ($W_{(e)}$)		21	44	23	21	73	23
Solar cell	Rating ($W_{(e)}$)		42	44	42	83	73	68
	Size (m^2)		0.79	0.82	0.79	1.58	1.38	1.29

Table 6.20: 39 litre DRA requirements for 20% night–time and 40% day–time utilisation capacity.

PhD Thesis © 1999 Cranfield University

Systems Configuration			Single–day			Three–day		
			Battery	TES	HES	Battery	TES	HES
Energy storage requirements	Thermal ($kWh_{(T)}$)		–	0.09	–	–	1.03	–
	Electrical ($kWh_{(e)}$)		0.044	–	0.248	0.559	–	0.483
Battery	Capacity ($kWh_{(e)}$)		0.048	–	0.276	0.621	–	0.537
	Charge rate ($W_{(e)}$)		5.0	–	28	24	–	37
	Discharge rate ($W_{(e)}$)		3.5	–	18	25	–	18
TES	Capacity ($kWh_{(T)}$)		–	0.09	0.4	–	1.03	0.4
	Charge rate ($W_{(T)}$)		–	9	29	–	35	29
	Discharge rate ($W_{(T)}$)		–	7	40	–	40	40
	Volume (l)		–	1.31	5.78	–	14.97	5.78
	Dimensions (mm)	Height	–	288	288	–	288	288
		Width	–	288	288	–	288	288
		Thickness	–	4	17	–	50	17
Compressor rating	Thermal ($W_{(T)}$)		40	49	30	40	75	30
	Electrical ($W_{(e)}$)		25	31	15	25	47	15
Solar cell	Rating ($W_{(e)}$)		31	31	31	61	47	45
	Size (m^2)		0.58	0.58	0.58	1.15	0.89	0.85

Table 6.21: 39 litre DRA requirements for a 60% night–time utilisation capacity (day–time cooled).

PhD Thesis © 1999 Cranfield University

One issue of particular interest is the effect of employing a 'no–loss' electrical energy storage system. Such a scenario will be realised in the event that the ES–DRA is connected to 'mains electricity'. The results of such a case for a 39 litre ES–DRA with 60% day–load utilisation is given in Table 5.22 on page 162; the principal heat gains are as in Table 5.4 on page 143. A similar analysis may be performed for the case of no–utilisation load, see Table 5.23 on page 163; the principal heat gains in this case are as given in Table 5.15 on page 154.

6.5 Discussion

The indices of merit used to assess the predicted performance of the ES–DRA are the solar cell surface area (equivalently, the solar cell watt rating) and the electrical rating of the prime–mover. These two indices were chosen as they give a clear indication as to the total energy consumption and the maximum power requirements of the appliance. Another important consideration is that the (financial) cost of the solar–cell will comprise a large proportion of the capital outlay of the appliance.

In interpreting these results it is instructive to take into consideration certain limitations of the model. As noted earlier in section 5.2 on page 137, the model makes no allowance for heat ingress from the surrounding environment via the evaporator[1]. This will create discrepancies between the model–predicted component sizes (particular the TES size and the actual component size. The extent of these will depend on the exact manner in which the DRA heat exchange inventory is designed and interfaces with the prime–mover and condenser. An attempt will be made to compensate for this, in part, by the large utilisation capacities allowed for; this should permit the successful testing of the appliance, at least under low–load conditions. Another important issue is that the effect of the (thermal) loading on the performance of the prime–mover has been neglected. section 2.4.1 on page 50 discusses the possible effect the loading conditions can have on the performance of the prime–mover.

In presenting the data, all watt–ratings have been rounded *up* to the nearest whole number, except in cases where the ratings are less than 10 watts, in which case the values have been rounded *up* to the nearest half watt. Other data have been approximated to three significant figures or decimal places where less than unity, or to two decimal places otherwise.

The proportion of the heat–gains accrued on account of 'user–interaction' *i.e.* door–openings in relation to the base–load is such that the effects of varying this number of door openings over the day– and night– times is negligible[2] (see the

[1]This was as not satisfactory estimates of the magnitude of these heat gains were available or could be arrived at without recourse to experimental investigation.

[2]This is, of course, within reason *e.g. circa* four volume air–changes (door–openings) have been

Systems Configuration			Single–day			Three–day		
			Battery	TES	HES	Battery	TES	HES
Energy storage requirements	Thermal ($kWh_{(T)}$)		–	0.777	–	–	2.32	–
	Electrical ($kWh_{(e)}$)		0.375	–	0.382	1.07	–	1.12
Battery	Capacity ($kWh_{(e)}$)		0.375	–	0.382	1.07	–	1.12
	Charge rate ($W_{(e)}$)		38	–	39	65	–	67
	Discharge rate ($W_{(e)}$)		27	–	28	32	–	32
TES	Capacity ($kWh_{(T)}$)		–	0.777	0.014	–	2.32	0.014
	Charge rate ($W_{(T)}$)		–	78	1	–	136	1
	Discharge rate ($W_{(T)}$)		–	56	1.5	–	65	1.5
	Volume (l)		–	11.3	0.2	–	33.7	0.2
	Dimensions (mm)	Height	–	288	288	–	288	288
		Width	–	288	288	–	288	288
		Thickness	–	34	1	–	101	1
Compressor rating	Thermal ($W_{(T)}$)		65	80	57	65	137	57
	Electrical ($W_{(e)}$)		32	50	28	32	86	28
Solar cell	Rating ($W_{(e)}$)		39	50	39	77	86	67
	Size (m^2)		0.73	0.94	0.73	1.46	1.63	1.26

Table 6.22: 39 litre DRA requirements for 60% day–time utilisation capacity and 100% (electrical) energy transfer efficiency.

PhD Thesis © 1999 Cranfield University

Systems Configuration			Single–day			Three–day		
			Battery	TES	HES	Battery	TES	HES
Energy storage requirements	Thermal ($kWh_{(T)}$)		–	0.013	–	–	0.064	–
	Electrical ($kWh_{(e)}$)		0.006	–	0.013	0.034	–	0.032
Battery	Capacity ($kWh_{(e)}$)		0.006	–	0.013	0.034	–	0.032
	Charge rate ($W_{(e)}$)		1	–	1.5	1.5	–	2.0
	Discharge rate ($W_{(e)}$)		0.5	–	1.0	1.0	–	1.0
TES	Capacity ($kWh_{(T)}$)		–	0.013	0.014	–	0.064	0.014
	Charge rate ($W_{(T)}$)		–	1.5	1.0	–	3.0	1.0
	Discharge rate ($W_{(T)}$)		–	1.0	1.5	–	1.5	1.5
	Volume (l)		–	0.183	0.197	–	0.918	0.197
	Dimensions (mm)	Height	–	288	288	–	288	288
		Width	–	288	288	–	288	288
		Thickness	–	1	1	–	3	1
Compressor rating	Thermal ($W_{(T)}$)		1.5	3.0	2.0	1.5	4.5	2.0
	Electrical ($W_{(e)}$)		1.0	2.0	1.0	1.0	3.0	1.0
Solar cell	Rating ($W_{(e)}$)		1.5	2.0	1.5	3.0	3.0	2.5
	Size (m^2)		0.028	0.031	0.025	0.052	0.050	0.040

Table 6.23: 39 litre DRA requirements for no–utilisation capacity and 100% (electrical) energy transfer efficiency.

PhD Thesis © 1999 Cranfield University

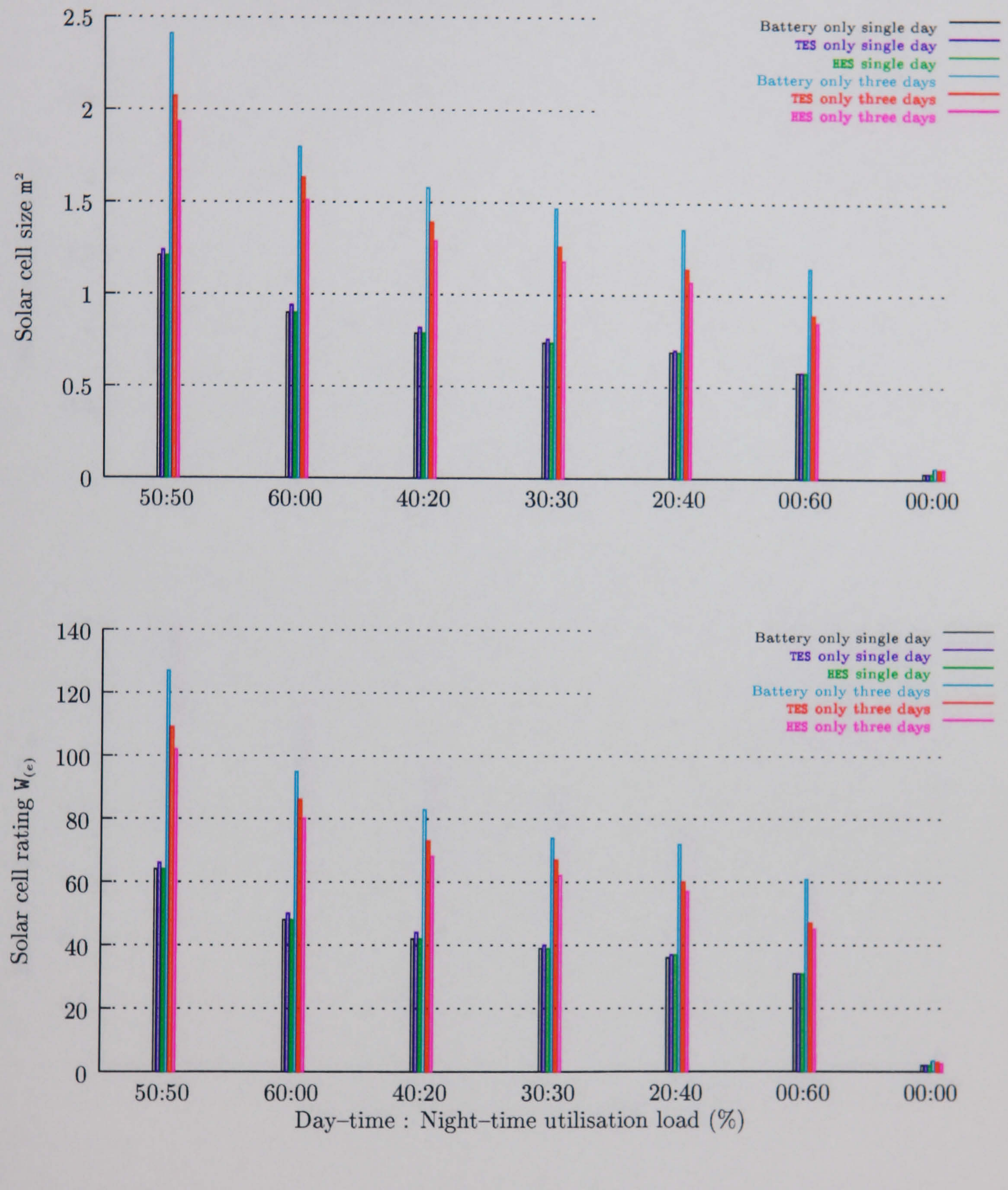


Figure 6.1: Plot of the solar–cell specifications against utilisation ratio

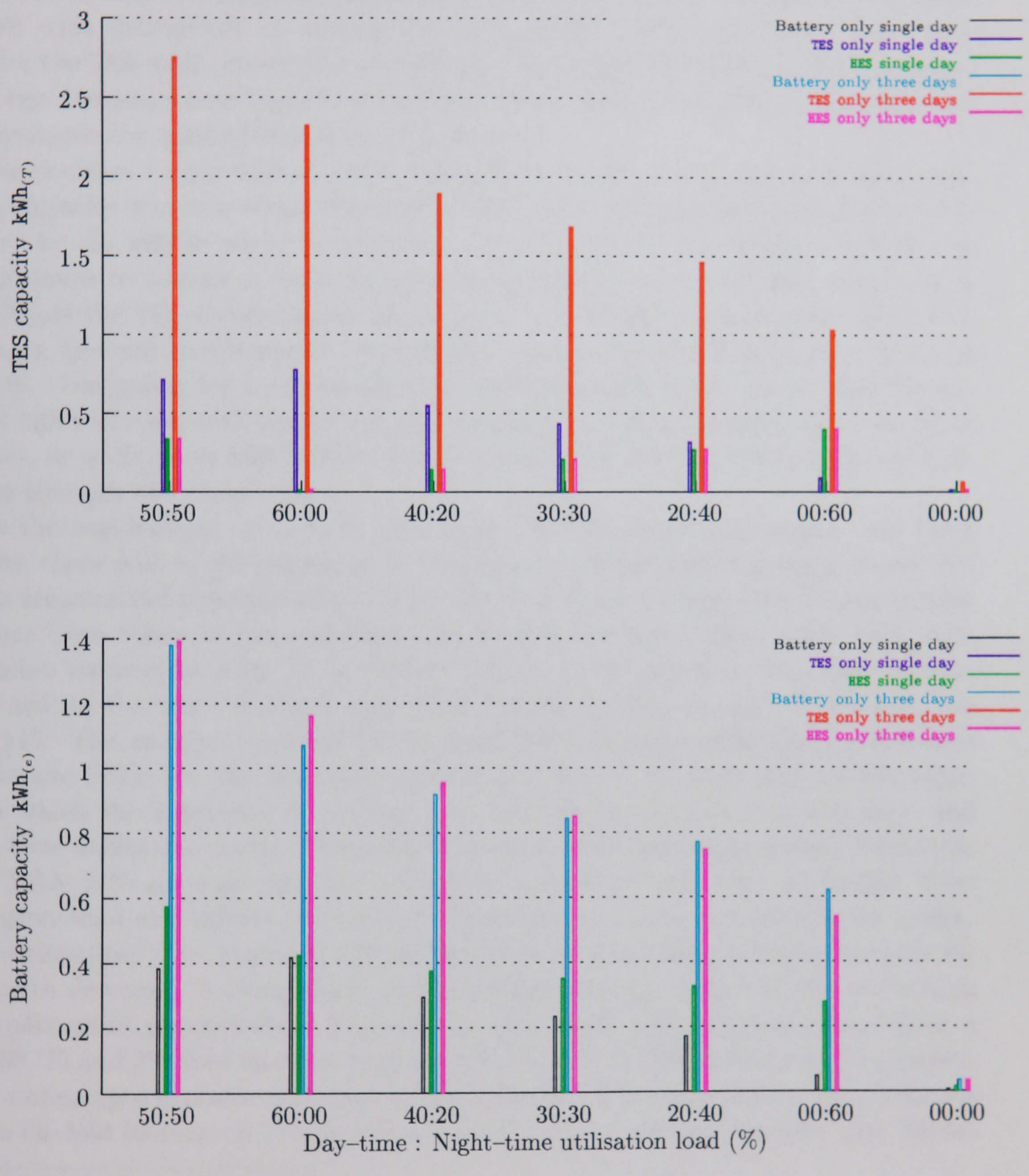


Figure 6.2: Plot of the battery and TES capacities against utilisation ratios

portion of Table 5.4 on page 143 marked 'latent heat gains').

The effect of the variation in the thermal conductivity of the composite insulation is dealt with extensively in section 2.5 on page 61. However the analyses only consider the DRA–wall conduction in isolation. In reality, the wall conduction ceases to be the dominant heat ingress mechanism below some critical K_{DRA} value as other heat transmission paths become more prominent.

The decision to use 60% of the total appliance capacity as the base–load utilisation capacity was in a sense arbitrary[1]. This value is higher than the 30% recommended by the WHO as noted in section 4.5.5 on page 147. The decision was driven by the desire to impose a very stringent requirement on the ES–DRA, particularly to facilitate the TES design and in an attempt to forestall problems associated with appliance thermal performance under heavy load as discussed in section 2.2.2 on page 46. Designing for a severe loading utilisation will help ensure that the designed DRA will cope with widely varying user habits which are expected to occur in practice; in addition to this it will serve to compensate for the aforementioned heat ingress through the evaporator.

As the requirement to remove heat from the DRA interior increases over fixed periods, there will be the necessity to increase the surface area through which this heat is transmitted from the DRA interior. For the passive–TES case the base surface area has been taken as the equivalent of the four vertical surface areas with each dimension reduced by 5 cm. In the active–TES case the base heat–exchange surface is defined on the basis of slurry–transport conduit diameters, see section 5.3.3 on page 148. The required increase to the available base heat–exchange surface area (within the DRA), *i.e.* the extended surface area factor, is dependent on the manner in which the appliance is 'utilised', *i.e.* the totality and ratio of the day– and night–time utilisation–loads. Generally increasing with increasing (total) utilisation load, Table 5.15 on page 154, the relative proportion of the day– and night–time utilisation–load also affects the surface extension requirements. Of interest is that at no–utilisation[2], the available TES surface area is more than sufficient to cater for the coolth demand. A comparison of the (single–day) predicted effects of running the appliance at no utilisation–load and at 60% of the day utilisation–load gives a *circa* 30, 25 and 23 –fold increase in the solar cell area, output rating and compressor power consumption across all regimes, while for the TES– and battery–only regimes a *circa* 60–fold increase is seen in the required relevant storage capacity (see Tables

allowed for each hour during the day–time.

[1]The choice was made after considering various crystal packing factors and optimal packing strategies, see Scott (1960) and Bernal and Mason (1960).

[2]The no–utilisation scenario represents the *status quo* operation, where the performance demand on the ES–DRA is to simply maintain its (already cooled) contents at its design temperature. Presumably, this is the basis of the current EU testing standards.

5.5 and 5.16, *qv.* pages 144 and 155 respectively). Thus the highly subjective. design utilisation–load (inclusive of the load distribution and cooling profile) will decidedly influence the definition of the extended surface factor. The foregoing raises the question as to whether it is at all practicable to provide the requisite surface extension (required by both the active and passive –TES applications) which in some cases can have a factor as high as four. While it is conceivable that this may be achieved, the issue as to the practicality of the design and whether or not the desired effect will be achieved is doubtful as the requirement is based on the fin–base temperature; as such it might be necessary to provide some additional means of heat transfer enhancement.

The loading pattern of the appliance plays a major role in the energy–use performance of the DRA, particularly in HES–mode. The base–case loading pattern, *viz* 60% of the total capacity (assumed water) at the mean day–time temperature, to be cooled over the night–time period, is slightly biased against the HES ES–DRA. This is due to energy losses incurred on account of the battery charge/discharge process. These battery efficiencies play a major role in the relative energy consumption of the devices. Tables 5.22 and 5.23, *qv.* pages 162 and 163 respectively, give an indication of the expected results when the battery charge and discharge efficiencies are increased to 100% from the 70% used for the computation of the base–case results. These show a marked improvement in the performance of the HES configuration (compare the results with those of Tables 5.5 and 5.16, *qv.* pages 144 and 155 respectively), changing the single–day performance ranking of the different ES–DRA implementations. These results have a bearing on non–mobile applications *e.g.* domestic or commercial environments where there is no need for an electric battery and the implementation intent is to conform to some set energy–consumption profile. A more optimal implementation will need to weigh the actual efficiency losses against the use of the heat–pump during the day/night–time and effect a strategy as appropriate.

The presence of the TES within the ES–DRA reduces the available utilisation space within the appliance and the use of a large (in this case 60% of the total volume) utilisation load poses some problems with respect to the TES requirements for operation during multiple–day inclement periods. As the energy storage requirement increases, the TES–volume can become untenably large[1], in some cases larger than the volume of the ES–DRA (see Tables 5.6 and 5.7, *qv.* pages 146 and 147 respectively). For passive–TES implementations which are restricted by this, the active–TES configuration may present a viable alternative. Even for applications where the TES

[1]For a TES–only application to cater for a three–day inclement period, it requires *circa* 85% (which increases with increasing DRA capacity) of its internal volume — 60% of which has already been taken up by the utilisation load.

volume may not pose an installation problem, the proportion of the interior volume taken up by the TES may present a sales problem. The issue is of more relevance to the TES–only ES–DRA implementation than to the HES ES–DRA.

While, comparatively, the energy consumption requirements are higher for the active–TES ES–DRA than for its passive–TES counterpart (compare Tables 5.5 and 5.12, *qv.* pages 144 and 151 respectively), the active–TES design exhibits several advantages over the corresponding passive–TES ES–DRA. One such advantage is the unintrusive nature of the thermal store; thus the volume limitations which attend the passive–TES ES–DRA design are absent in the active–TES implementation. One of the major constrictions of the (active) design is the higher energy requirements necessary for operation[1]. The extra energy requirement accrues on account of the need to transport the slurry through the system and to ensure the continual suspension of the solid–load within the TES storage–tank. The additional (coolth) energy requirement for the active–TES case is *circa* one order of magnitude greater than the base–load energy requirements in the case of the 39 litre ES–DRA under a 60% single–day day–utilisation load regime[2], compare Tables 5.4 and 5.11, *qv.* pages 143 and 150 respectively. This (coolth energy requirement) is in addition to the accompanying electrical energy requirements, *circa* 50% of the (60% utilisation–load) requirements, for the same regime[3].

In defining the flow velocity of the slurry, two different criteria must be taken into consideration (see section 5.3.1 on page 165) *viz* (a) the minimum flow–velocity to ensure that the slurry remains 'quasi–homogenous' and (b) the minimum slurry mass–flow rate to ensure that sufficient coolth is delivered to the DRA. The respective linear velocity requirements to meet these two criteria may not necessarily be coincident depending on the cooling requirements and the solid–load concentration within the slurry; in the current design, the maximum of these two requirements (the critical resuspension velocity) has been selected. A better design might consider the 'design' of the slurry (essentially varying the solid–loading or the energy density of the solid–load) in order to synchronise the critical coolth requirement and resuspension velocities. This will permit better matching of the prime–mover and the flow–pump to the systems requirements and possibly decrease the energy required for transport on account of the reduced slurry solid–loading.

Comparing the results of the four different ES–DRA implementations, the active–TES implementation performed worst in terms of energy consumption (solar cell area)

---

[1]While the active–TES design requires a higher capital outlay in comparison to the passive–TES implementation, the cost of energy may well be the deciding factor in choosing between the two applications.

[2]Night–time prime–mover operation.

[3]This proportion reduces as the capacity of the ES–DRA increases, dropping to *circa* 20% for a 110 litre appliance under the same regime.

and power consumption[1] (compressor rating). This was expected and the merit of such a system is its applicability to situations where large storage is required and possibly higher coolth flux rates desired[2]. The TES–only ES–DRA performed much worse than the battery–only and HES implementations, irrespective of the fact that the TES was assumed to have 100% charge and discharge efficiencies. The reason for this poorer performance is the projected difference in the COP of the prime mover between the night–time and the day–time. This poor performance was consistent over single– and multiple–day design criteria. The battery–only ES–DRA fared better than the HES ES–DRA in terms of energy consumption (solar cell area) for the single–day design applications. However on the basis of maximum power demand (prime–mover rating) the HES implementation performed much better. For multiple–day inclement periods, the HES ES–DRA's performance superseded the performance of the battery–only application in all aspects. The differences in the performance of all these systems was much less at no utilisation–load and became more apparent as the utilisation–load increased and varied with the distribution of the utilisation load. The discrepancies were also greater with increased length of the inclement period. The apparent (single–day) superior performance of the battery–only ES–DRA over the HES implementation is attributed to the battery charge/discharge efficiency losses. When these losses are assumed to be non–existent the performance of the HES ES–DRA surpasses that of the battery–only implementation in single–day mode as well, see also Figures 5.1 and 5.2, *qv.* pages 164 and 165 respectively.

6.5.1 Further Parametric Analysis

Introduction

This section looks further into the effects of varying some of the parameters which might have a bearing on the thermal and energy performance of the system. The effect of the assumed loading condition has been investigated earlier section 5.4.1 on page 154 and the following parametric analysis will is applied to an *empty* appliance[3]

Variations of 20% were studied in general, excepting certain cases where such a basis is unattainable or some other variation better suits the parameter (these cases will be highlighted prior to the presentation of the relevant results). Typically, the effect of a 20% (or pertinent other) change above *and* below the base–case condition has been examined. The results for each computed variation are then considered

[1] A lower power rating would indicate a less–peaky demand profile.

[2] Subject to the availability of an appropriate mechanism of coolth transmission.

[3] This will (a) enable the effect of these variations with respect to the steady–state operation of the system be investigated in conformance to the current EU and USA DRA testing standards and (b) factor–out the uncertainties due to variations in appliance utilisation.

in relation to the results for an *empty* appliance running at otherwise base–case conditions[1].

The analysis was performed for the three different modes of operation (*i.e.* electro–chemical (battery–only) energy storage, TES–only storage and HES). A total 43 different parameters were investigated for these three different modes and the analysis undertaken with respect to both categories, *i.e.* single–day operation and the three–day inclement period contingency. For each category, the following (eleven) variables were considered *viz* the number of daily door openings, the length of the day–time period, the length of the daily insolation period, the mean intensity of the (expected nominal) daily insolation, the length of the inclement period, the systems post inclement–period recovery time, the amount of solar insolation recoverable during an inclement period, the daily relative humidity, the mean COP of the prime–mover over the day– and night–time periods, the mean daily temperature and the mean effectiveness of the battery charge/discharge process. In performing this sensitivity analysis, it was necessary to cluster certain variables together to make the analysis slightly more wieldy[2]. Affected variables were the number of day– and night–time door openings, mean day– and night–time ambient relative humidities, mean day– and night–time prime–mover COP's, mean day– and night–time ambient temperatures and the charge and discharge efficiencies of the electro–chemical energy store.

In interpreting these results, several cautionary issues must be borne in mind *viz* the clustering the variation of the various day– and night–time parameters may have the effect of not fully unravelling the implication of the variation of each individual parameter on the system's performance. In addition to this, as the model has been written only to consider mean parameter values, these results only serve as indicative of the trend which may be expected with the variation of the different parameter. Finally, as will be mentioned in a later chapter, the model is based on the assumption that the heat ingress into the system through the DRA compartment wall is sufficiently inhibited by the use of the super–insulant (VPSI). In truth, there are other thermal conduction paths which compromise this assumption (see page 209) and for this reason it is reiterated that the results presented here may only be used as an indication of the *type* and at best upper performance bounds, in *relative* percentage terms, of the changes which may result as a consequence of the variations indicated. In presenting the results, the data has been rounded to the nearest five percent; thus limiting the sensitivity interpretable into the data.

Two instances exist where the stipulated 20% *increase* about the base–case con-

[1]Which in turn has been compared to the modelled results of the appliance running *strictly* at the base–case conditions).

[2]The net effect of this was to reduce the total number of inspected variables from 3784 to 2064; a reduction of 83%.

dition could not be attained. These were for the battery charge/discharge capacities (both initially specified at 90%) and for the night–time relative humidity (initially specified at 85%). These were assigned their maximum values *i.e.* 100% as the upper bounds for the analysis, with the lower bounds kept consistent with the overall −20% requirement below the base–case value. Other departures from the stipulated 20% variation are (a) the variation in the inclement period, which was set at one and five day(s) for the lower and upper bounds of the variation test (*i.e.* a two day variation about the base–case) (b) the length of the recovery period after an inclement period. This was set as an additional ±2 days to the length of the inclement period (*i.e.* one and five days *cf:* the four days stipulated as the base–case).

6.5.2 General Discussion

The first stage in the analysis comprises a comparison between the results of the "no–load" appliance to the "fully–laden" system[1]. The analysis was undertaken in two stages, for the single– and three–day inclement period scenarios, and the results will be presented in relation to these two conditions. The discussion within each of these two sub categories will dwell (in some instances comparatively) on the three different system implementation scenarios *viz* battery (electro–chemical) only, TES–only and the HES system configurations. In cases where a change in a certain parameter is not mentioned, it is to be understood that the predicted changes in that parameter are below 2.5 percent[2] in relation to the reference case. Beyond the initial comparison of the no–load condition to the fully–laden base–case appliance, all further analysis will be in comparison to the no–load condition.

6.5.2.1 The Load to No–Load Comparison

The single–day case : A previous analysis has investigated the effect of the variation in the loading condition on the appliance performance and highlighted the sensitivity of the application to the loading condition (see section 5.5 on page 161). Here the analysis will be restricted to a comparison between the fully–laden and the no–load conditions otherwise operating at the base case. Of the three different scenario's the HES configuration energy (storage) requirements[3] show the least sen-

[1] With the exception of the loading conditions (no–load and a 60% day–time utilisation capacity, charged at the commencement of the night–time period, see the base–case specifications in section 4.2 on page 106.) all other system settings were at the stipulated base–case conditions.

[2] As is consistent with the pre–stipulated rounding scheme.

[3] The reader is here again reminded that the energy (storage) requirements refer to the stored energy required by the DRA for cooling and thus the type (electrical or thermal) is dependent on the systems layout; expressly, the energy (storage) requirements for the battery–only and HES configurations are expressed in $W_{(e)}$ while that of the TES–only layout is in $W_{(T)}$. The overall energy

sitivity to the transition from the fully–laden to the no–load scenario. For both the battery– and TES–only layouts, the ratio of the energy (storage) requirements is *circa* 62, with similar *proportions* observed in the required relevant energy storage capacities (and in the case of the TES–only scenario, TES dimensions). Both configurations exhibit a factor decrease in solar cell rating of *circa* 30. However, the TES–only layout exhibited lower (30) factor decrease in heat–pump[1] ratings as opposed to the 48 and 38 factor decreases respectively experienced by the battery–only configuration. The required extension to the evaporator/DRA–interior interface surface–area fell 48 fold for both the TES and the HES implementation. In comparison to the other two systems, the HES exhibited a 30 fold decrease in the energy (storage) requirements, solar cell ratings and the battery ratings. The heat–pump rating for the HES fell by a factor of 34 where no appreciable change was observed in the TES ratings for the no–load HES case when compared with the fully–laden base–case system

The three–day inclement period case : In terms of the effect of the changes over the three–days, the battery–only layout tended to exhibit higher percentage changes in the component sizes. In this case the changes in the energy, requirements, solar cell rating and the battery capacity were all in the range of 30–32 fold. The battery discharge and the heat–pump *electrical* ratings showed a 38 fold decrease while the battery charge and the heat–pump thermal ratings were diminished by factors of 44 and 48 respectively. For the TES–only case the energy (storage) requirements and the TES capacities depreciated by a factor of 37 in the transition from the fully–laden configuration to the no–load configuration. In this (TES) case the required TES thickness, solar cell ratings[2] and the heat–pump electrical rating were diminished *circa* 37 fold; with the charge and discharge capacities decreasing by a factor of *circa* 49. The extensions to the available evaporator/DRA–interior surface area is decreased 48 fold; the same being true for the HES system. This HES system exhibits no appreciable change in the TES dimensions *per se*. However, the solar cell ratings and the battery charge capacity were decreased by factors of 33 and 35 respectively and while the energy (storage) requirements and the energy requirements and the the battery capacity ratings fell 36 fold, the battery discharge rating and the heat–pump rating decreased by a factor of 34.

---

demand for each system can only be deduced, comparatively, in terms of the ratings of the solar panels.

[1]Unless explicitly stated, references to the rating of the heat pump will refer to the both the thermal and electrical ratings.

[2]Comprising the solar cell electrical rating $W_{(e)}$ and area m^2.

6.5.2.2 Variation in the Number of Door Openings

No appreciable changes in the systems parameter specifications were observed with the ±20% variation in the *total* number of day– and night–time door openings[1] in both the single and three day scenarios across the three different system types.

6.5.2.3 Variation in the Ambient Relative Humidity

As with the number of door openings, the stipulated variations in the relative humidity during both the day– and night–time did not produce any significant effects in the sizing of the systems components.

6.5.2.4 Changes in the Length of the Day Period

The single–day case : In both the battery– and TES–only cases, a ±20% change in the length of the day–time period[2] yielded a ±15% change in the energy (storage) requirements and the energy storage capacities. While the decrease in the day–time period failed to institute any appreciable change in the TES dimensions, the converse increase required a TES thickness which was insignificant in comparison to the no–load base–case scenario. In both the (battery– and TES–only) layouts, the storage *charge* rates were decreased (30%) and increased (50%) with the stipulated ±20% change in the day–time period respectively. No noticeable changes were observed in the discharge rates of the energy stores. In all cases the solar cell ratings decreased (15%) and increased (25%) with the relative 20% increase and decrease in the length of the day–time period respectively. While in the case of the battery–only configuration no significant change in the heat–pump sizing was observed, the TES–only layout required a 15% reduction and a 25% increase in the heat–pump rating for ± 20 changes in the day–time period respectively. In the case of the HES the changes in the TES capacity varied by ±25% and the battery *discharge* capacity by ±5% with ±20% respective variations in the length in the day–time period; however, the energy requirements for this system layout only varied by ±5% with the changes in the day length. In contrast to the TES–only system, for the HES system, no appreciable changes were discerned in the thickness of the TES. Apart from the TES discharge rate, for which no significant changes were observed, all other energy transfer ratings exhibited some degree of change (battery charge −15/+25%, battery discharge −25/+20% and TES charge +50/−35%) with respect to the stipulated ±20% changes in the length of the day–time. The (±20%) variation was also reflected in the sizing of the heat–pump which varied +25/−20%.

[1] Each one equivalent to a volume air change.

[2] The daily insolation period being typically two hours short of the day–time length.

The three–day inclement period case : For the three–day inclement period scenario, with respect to the HES layout, the results are virtually identical to those for the single–day case, with one exception *viz* the changes in the battery capacity is in this case insignificant as compared to the no–load base–case reference model. For the battery–only implementation there was an observed variation of ±5% in the energy (storage) requirements and battery capacity, while the variation in the solar cell rating was −15/+25% (a result coincident with that of the single–day case). Regarding the battery–only configuration, the charge rating of the energy store varied −25/+35% in relation to the ±20% change in the day–length period. This may be compared to the −20/+35% change required for the TES charge rating in the TES–only configuration for the same change. In the case of the TES–only layout, the heat–pump requirements varied −15/+25% with the given change in the day–time length (*cf:* single–day results).

6.5.2.5 Changes in the Length of the Daily Insolation Period

The single–day case : The variation of the length of the daily insolation period (nominally two hours less than the length of the day–time period) appears to produce very consistent results (in percentage terms) across the three systems configuration. For the single–day case, virtually all the affected parameter changes are *circa* ±5%. Notable exceptions are the energy storage discharge ratings for the battery–only configuration and the TES–only configuration which vary by ±10% with the required ±20% variation in the length of the inclement period. The affected variables are: in all the relevant cases, the solar cell requirements and the TES dimensions, for the battery– and TES–only configurations the energy requirements and energy storage capacities, for the HES and TES–only system configurations the heat–pump rating and for the HES configuration the battery charge rates. However it should be noted that due to the nature of the HES application, the sign of the extent of the changes in the heat–pump, TES charge and capacity ratings are reversed *i.e.* ∓5% for the ±20% change in the length of the daily insolation period.

The three–day case : For the three–day inclement period scenario, similar trends to the single–day cases are observed with the following exceptions. In all cases the changes to the required energy consumption is relatively insignificant as are the required energy storage capacities in both the battery–only and TES configurations; however for the HES case only the changes in the battery capacity are negligible. Furthermore for the battery– and TES–only layouts, the required energy storage and charge rates are reduced by 5%.

6.5.2.6 Changes in the Length of the Inclement Period

The three–day case : Changes in the length of the inclement period have no bearing on the single–day operation of the system and as such only the multiple day scenario will be investigated here. The model was run to consider the comparative effects of a five– and single–day inclement period in relation to the three–day inclement period for the the no–load base–case scenario. For the battery–only configuration, the 5/1 day inclement period induced a $+10/-30\%$ change in the energy storage requirements of the system, a similar change was observed with respect to the battery storage capacity. The solar cell ratings changed by $-15/+50\%$ and the battery charge ratings by $-15/+25\%$ for the 5/1 day inclement periods as compared with the three–day case. Considering the TES–only layout, the energy (storage) requirements, TES capacity and size varied $+5/-10\%$ while the solar cell and heat pump ratings varied $-10/+30\%$. The TES thickness only changed appreciably (-35%) for the case of the single–day inclement period. The nature of the HES configuration and energy management strategy implied that the size and capacity of the TES would remain unchanged. There was however, a $+5/-15\%$ change in the energy storage requirements and the battery capacity, a $-10/+25\%$ change in the solar cell ratings and a $-10/+30\%$ change in the predicted charge rating of the battery for the five– and single–day cases when compared with the three–day case (see also Tables 5.6 and 5.7, *qv.* pages 146 and 147 respectively).

6.5.2.7 Changes in the Length of the Recovery Period

The three–day case : The time allowed for systems recovery after an inclement period (stated in relation to the length of the inclement period) was varied $\pm$ two days about the length of the inclement period (*i.e.* one and five days). As expected, these changes had no bearing on the single–day case. The greatest range of effects was seen in the TES–only configuration in which a $+5/-30\%$ change was observed in the energy and storage requirements of the system. Increasing the recovery length to five days brought about no significant change in the thickness of the TES, while the single–day recovery period warranted a 35% decrease in the TES thickness. The charge rating of the TES varied $-10/+105\%$ with respect to the five– and single–day recovery periods, while the changes in the heat–pump and the solar cell ratings changed $-5/+70\%$ with respect to same changes. For the battery–only layout the changes in energy storage and charge requirements were *circa* $+5/-9\%$; the solar cell ratings changed by $-10/+145\%$ and the charge capacity of the energy storage by $-10/-35\%$ for the one and five day recovery cases respectively. For the HES configuration, changes of $+5/-30\%$ in the systems energy and battery storage requirements, $-35/+65\%$ in the solar cell ratings were observed along with a

−5/+70% change in the charge ratings of the battery for the five– and single–day recovery period scenarios.

6.5.2.8 Changes in the Energy Recovered During an Inclement Period

The three–day case : In this case the quantity of energy harvestable *each* day *during* an inclement period (expressible as a fraction of the nominally expected daily insolation) was varied ±20% about the base–case assumption. As with the previous cases, this did not effect any changes in the component sizes for the single–day case. For the battery–only case the variation manifested as a −15/+10% change in the systems energy and storage requirements as well as a −5/+5% change in the rating of storage charge. In the case of the TES–only system the bulk of the effected parameters (energy requirements, TES size and thickness, store charge and discharge ratings and heat–pump *thermal* rating) required a −5/+5% change with respect to the ±20% in the relevant parameter. While the solar cell and heat–pump electrical ratings appeared to engender no size changes for the increase in the quantity of harvestable solar insolation, a 5% increase in component sizes is necessary for a 20% decrease. The HES layout required a ∓10% change in the energy storage requirements and the battery capacity, while the solar cell and the battery charge ratings varied by ∓5% for the stipulated ±20% change in the recoverable portion of the incident solar insolation during an inclement period.

6.5.2.9 Variations in the COP of the Prime–Mover

The single–day case : The model was run in order to ascertain the effect of the variation in the COP of the system on sizes of the various parameters. The majority of the changes in the affected parameters, across the three different system configurations, were consistently −15/+25% for a ±20% variation in the mean day– and night–time COP. Regarding the battery–only configuration, with the exception of the thermal rating of the prime mover which exhibited no change, all the affected parameters exhibited the said variation. The affected parameters in the case of the TES–only configuration were the solar cell and heat pump (thermal) ratings. In the case of the HES layout, the changes observed were the totality of those apparent in in both the battery–only and TES–only layouts.

The three–day case : The changes here were *exactly* the same as in the single–day case.

6.5.2.10 Changes in The Mean Daily Temperatures

The single–day case : The mean daily (day– and night–time) temperatures were varied between ±20% with markéd effects on almost all the parameters in the three layouts. For the battery–only configuration, the energy (storage) requirements, store capacity, charge and discharge ratings changed by +35/−30% with response to the stated increase and decrease to the mean daily temperatures. The solar cell rating varied +40/−30% and the heat pump (electrical) rating by +45/−35%. The effect of the greater thermal dependence on the COP in comparison to the thermal dependence on DRA cooling load, is patent in the observation that the (thermal) rating of the heat pump varied by +20/−25% for the same changes. For the TES–only case, changes of ±25% were observed with respect to the heat pump thermal rating, required extension to the evaporator/DRA–interior heat exchange area and the TES sizing and ratings, with the exception of TES thickness which exhibited no variation as a result of the increase and became insignificantly small with the 20% decrease in the mean daily temperature when compared with the no–load reference case. The highest changes of +45/−35% were evident in the heat pump (electrical) and solar cell ratings. For the HES system layout, again ±25% changes were observed with respect to the heat pump thermal rating, the required extension to the evaporator/DRA–interior heat transfer surface, the TES size and ratings, with the exceptions of the TES thickness (as in the TES–only case) and TES discharge ratings which varied +20/−25%. All other changes to the parameter sizes were +35/−30%; theses were the energy (storage) requirements, the heat pump (electrical) and solar cell ratings as well as the battery capacity and energy transfer ratings.

The three–day case : The changes here were *exactly* the same as in the single–day case.

6.5.2.11 Changes in The Daily Mean Solar Insolation Intensity

The single–day case : The the daily mean solar insolation intensity was varied ±20% about the base–case value. In all configurations, the only affected parameter was the required area of the solar cell which varied ±20%.

The three–day case : The effects here were identical to those for the single–day case.

6.5.2.12 Changes in The Efficiency of the Battery Charge and Discharge Processes

The single–day case : The charge and discharge efficiencies of the battery were changed +11/−20% and the effect of this variation on the model results obtained. As would be expected this brought about no effect in the TES–only systems layout. For the battery–only configuration, this manifested as a −45/+25% change in the solar cell requirements and the battery capacity and ratings also varied by −90/+25%. When the same changes are applied to the HES configuration, no changes in the solar cell rating are evident for the 11% increase in each of the efficiencies but, a 55% increase was observed in the efficiencies were decreased by 20%. The battery capacity and charge rating in comparison to the reference case varied by −90/+25% for the examined +11/−20% changes in the efficiencies, see also Tables 5.22 and 5.23, *qv.* pages 162 and 163 respectively.

The three–day case : For the battery–only configuration greater changes were observed in the affected systems parameters than for the single–day case. The energy (storage) requirements varied by +45/−11% for the same +11/−20% change. The solar cell rating changed by −75/+40%, the battery capacity by −85/−5%[1] and the battery charge rating by +95/−20%. For the HES layout, the changes in the energy (storage) requirements were smaller than obtained for the single–day case. The energy (storage) requirement changed by +45/−20%, the solar cell rating by −90/+40% and the battery charge rating by −95/+25% (for the +11/−20% changes in the battery charge and discharge efficiencies). The battery capacity in this case decreased by 85% for the 11% increase in both efficiencies, with no appreciable changes observed in with the 20% decrease in the battery charge and discharge efficiencies.

6.5.2.13 Conclusion

The actual performance of the DRA will depend on the system's configuration utilised in the final design. A brief perusal of the results obtained indicate that the HES configuration has advantages in terms of energy consumption and component sizing over the battery– and TES–only configurations. In considering the relative weight of the each of the variable used in the design of the system, it is to be noted that the effect of the battery charge and discharge rates play the most significant role in determining the systems parameter sizes. In descending ranking order, the next set of variables are the mean day– and night–time temperatures, the mean day–

[1]This −85/−5% appears to be indicative of an underlying optimal condition within the +11/−20% range explored.

and night–time COP, the length of the day–time period and the length of the daily insolation period. If the system is to be designed for inclement period contingencies, then the length of the inclement period, the time allowed for the system to recover after such a period and the amount of the energy recoverable during each inclement weather day would, in that order, displace the length of the daily insolation period in the order of rankings. However, it must be stressed that the results obtained are specific to the configurations used and have only taken into account the cooling load incurred as a result of the use of the VPSI[1]. A further ranking criteria could be based on an analysis of the economic implication of variations in the individual parameter ratings.

In specifying the sizes for the prototype passive–TES, HES–DRA the decision was made to base the component specification around the 50:50 day/night–time utilisation–load capacity design.

6.5.3 Closure

The foregoing presented the results of the computer–model predictions of the prototype ES–DRA in four different modes. The results indicate that the HES ES–DRA operating the prime–mover only during the night–time performs better than the other (active–TES, passive–TES and battery–only) ES–DRAs. This preliminary assessment–prediction model may be further optimised around the HES ES–DRA in order to investigate other possible energy–management schemes, *e.g.* constant prime–mover power consumption, constant prime–mover coolth delivery, minimum energy consumption *etc.* Based on the results of the experimental testing of the specified prototype, an assessment can be made of the heat leak via the evaporator as well as a more accurate (load–temperature) profile of the prime–mover COP. These can then be fed back into the model during the next stage of the iterative research–implement–experiment procedure.

[1]See the discussion on page 209.

Chapter Seven

Experimental Results

– A few good experiments are better than a multitude of faulty ones, as far as it is possible that the errors of all the faulty ones are in the same direction.

–E. H. Griffiths (The Thermal Movement of Energy; 1901)

Introduction

Based on the results of Chapter 6 on page 184 a passive thermal energy storage refrigeration test rig (ES–DRA) was built. This chapter documents the experimental procedures, with results, carried out *vis–a–vis* the current research. The principal objective of this chapter is to experimentally assess the designed ES–DRA under a number of criteria and to adduce the results in proof of the energy–efficient advantages of the (energy storage) concept relative to a normal DRA.

Several preliminary experiments/processes were carried out to facilitate the main experimental procedure:

(a) The calibration of the instrumentation used for the main experiment, documented in Appendix A on page A-240.

(b) The experimental determination of a pragmatic estimate for the *effective* thermal resistance of the composite thermal insulant. The composite (polyurethane foam–VPSI) insulant used for that test consisted of (25.4 mm) VPSI panels held *in situ* with (*circa* 4.0 mm) polyurethane foam. The experiment yielded an effective thermal conductivity value of *circa* 0.012W/mK. The experiment is described in detail in Appendix B on page B-253.

(c) The manufacturing of the thermal stores (with a few observations as to the TES behaviour); this is documented in Appendix C on page C-266 and section 6.1.3.1 on page 191.

(d) The estimation of the mass–flow rate across the condensing unit (documented *qv.* page 193). 6.1)

The main experiment was conducted with the aim of determining practical values for various performance indicators of the prototype ES–DRA and thus to attest to the veracity of the underlying design rationale. It sets out to assess the:

- 'Pull–down' behaviour[1] of the ES–DRA in comparison to the DRA without TES facilities.
- Thermal behaviour of the ES–DRA under thermal cycling.
- The 24–hour energy consumption of the ES–DRA.
- Conformance of the ES–DRA to the current regulatory standards, specifically to the GEA short– and long– term standards.

In order to characterise the behaviour of the ES–DRA, it is necessary to define explicitly a set of performance indicators and also the desired levels of these indicators which can reasonably be expected to constitute an acceptable level of performance. Thus, based on this, if at any time the ES–DRA fails to deliver the said performance, it may be adjudged to have failed *on that account.* To this end, the following is set forth; the refrigerator would be deemed acceptable if:

- It at least conforms to the most severe standards set out for *any* category of appliance as set out in the EN–153[2] standards as proposed for the EU on DRA's.

[1]The time it takes for the appliance to 'come to temperature' at initial start up. This is indicative of the time required for the appliance to recover from thermal disturbances which cause (higher temperature) thermal excursions from the appliance's intended set–point, see also section 2.2.2 on page 46.

[2]see Buhl-Pedersen et al. (1993), *pp.* 20 *ff.* and *pp.* 211 *ff.*.

- It continues to operate within the stipulated internal air temperature range in excess of 90% of its operational time in an ambient environment of no more than 35 °C.

Specific indicators of performance to be considered in this are:

1. The Coeficient Of Performance (COP) of the appliance.
2. The on–time of the compressor.
3. The energy consumption of the appliance.
4. The ability of the appliance to function *effectively* for protracted periods in the absence of functional energy input.

A comparison of these indices for the TES applications and the non–TES application is undertaken in assessing the measure of improvement obtained from incorporating the TES within the DRA.

7.1 The Experimental Apparatus

Introduction

This section describes the experimental set–up used for the testing of the ES–DRA design outlined in Chapter 6 on page 184. It discusses the different aspects of the 'rig'[1] highlighting the various modifications which have had to be made to the ES–DRA during prototype manufacture, the underlying reasons for this and possible implications thereof.

7.1.1 Rig Description

The main components of the rig are as follows:

1. A temperature–controllable (environmental) chamber (Dimensions 2.7m × 3.6m × 4.5m) insulated internally with polystyrene and fitted with a rail of hollow fins mounted on two parallel conduits to permit fluid circulation through the fins.
2. The manufactured ES–DRA[2] prototype.

[1]Comprising of the ES–DRA, the test environment and allied equipment *e.g.* controller, circuits *et hoc*.

[2]Manufactured by Quest Refrigeration Manufacturing Ltd., Aber park, Flint, Clwyd, North Wales, CH6 5EX UK.

3. A MICROLINK (3000)[1] data–logger *cum* controller with 2 × 3054 (32 channel), 1 × 3050 (16 channel) temperature/analogue modules with cold junction compensators and 1 × 3030 control module, amongst others. The main interface module was the 3042, 16 bit analogue–to–digital converter. This was employed to switch various devices (compressor, chamber heaters and cooler) as well as collect data from thermocouples and the other instrumentation devices.

4. Three 3903 isothermal boxes with cold junction compensation[2].

5. A Philips PE 1646 (75V @ 6 amp max) dc power supply (PSU) used as the primary power supply to the ES–DRA (a dc device). The device was fitted with electrical current/voltage limiting facilities and thus enabled the restriction of the maximum power drawn from the mains.

6. Four 12V batteries (2× 36 ah and 2× 60 ah), for start–up as the power requirements of the (24 V) ES–DRA compressor[3] exceeded that which could be met by the dc power supply.

7. A Viglen 80486 DX-33 computer loaded with the Linux[4] operating system. This was used to control the MICROLINK, typically issuing instructions as to when and which device to switch on/off as well as to collect data. All the control was effected using a set of in-house computer programs written in the 'C' programming language[5].

8. 48 T–type thermocouples.

9. Two 13 amp fuses (used as shunts) for determing the electrical current drawn within the compressor–battery loop of the circuit and that drawn within the PSU–battery loop.

10. Three 3.6 kΩ resistors connected as a 3:1 voltage divider (see Figure 6.2 on page 187) used for stepping down the voltage across the batteries, to within the (0 – 12) V range acceptable to the MICROLINK.

11. Two electric heaters ([750+2000] W in total) used for increasing the environmental chamber temperature.

---

[1]Equipment suppliers: Biodata Ltd., 10 Stocks Street, Manchester M8 8QG, UK. See also the user manual [Biodata Ltd., 1994].

[2]Equipment suppliers Biodata Ltd. *loc. cit.*

[3]Model GE3 manufactured and supplied by INDEL "B" (gruppo Berloni) 61019 S. Agarta Felrita (localitá Ca'. Baldone), Pesaro, Italy.

[4]Version 2.0.0. This software (© (1991) Linus Torvalds <torvalds@transmeta.com>) is available free on the Internet at http://www.linux.org amongst other mirrors.

[5]The control software is listed in Appendix D on page D–275

12. A Conair Churchill 05/CTCV ($1.4\,\mathrm{kW}_{(T)}$ @ 10 °C) cooler[1] used for decreasing the environmental chamber temperature. This was attached to a set of cooling fins fixed to one of the walls of the environmental chamber for cooling.

13. A large fan (built in–house) used for moving air past the heaters and the cooler to ensure rapid removal of heat or coolth from the heater and cooling fin surfaces. The fan also served to even out the temperature distribution within the main environmental chamber.

14. A large piece of gauze netting used to partition the environmental chamber into two parts and to ensure that no appreciable air currents were set up within the partition of the environmental chamber housing the ES–DRA, in spite of the operation of the fan in the other.

15. An assortment of voltmeters (digital and analogue), electro–mechanical timers, electronic relays, connectors, stands, oil, ethelyne glycol (a 50% aqueous solution), pipes, foam insulation and connecting wires.

The environmental chamber was partitioned into two with the gauze netting. The batteries, heaters, fans and calibration equipment were placed within the partition adjoining the wall with the rail of cooling fins, whilst the ES–DRA and environmental chamber temperature stand were placed in the other partition. The general layout is illustrated by Figure 6.1 on page 186.

7.1.1.1 The Electrical Circuit Connections

The electrical circuits were connected up as illustrated in Figure 6.2 on page 187. The main primary circuit consisted of two secondary sub–circuits. The first secondary circuit is the parallel connection between the voltage divider and the dc PSU terminals. The input to the dc PSU was permanently connected to live mains. Connected in series within the first secondary circuit, were:

- An electro–mechanical timer to enable the on–off regulation of (dc) power into the ES–DRA system.
- A shunt to facilitate the determination of the electrical current within the dc PSU–dc battery section of the first secondary circuit loop.
- A protective diode (50V) to inhibit a back emf from the battery to the PSU.

[1]Equipment suppliers: Beta Tech. Controls Ltd. 104, Tanners Drive, Blakeheads, Milton Keynes MK14 5BP.

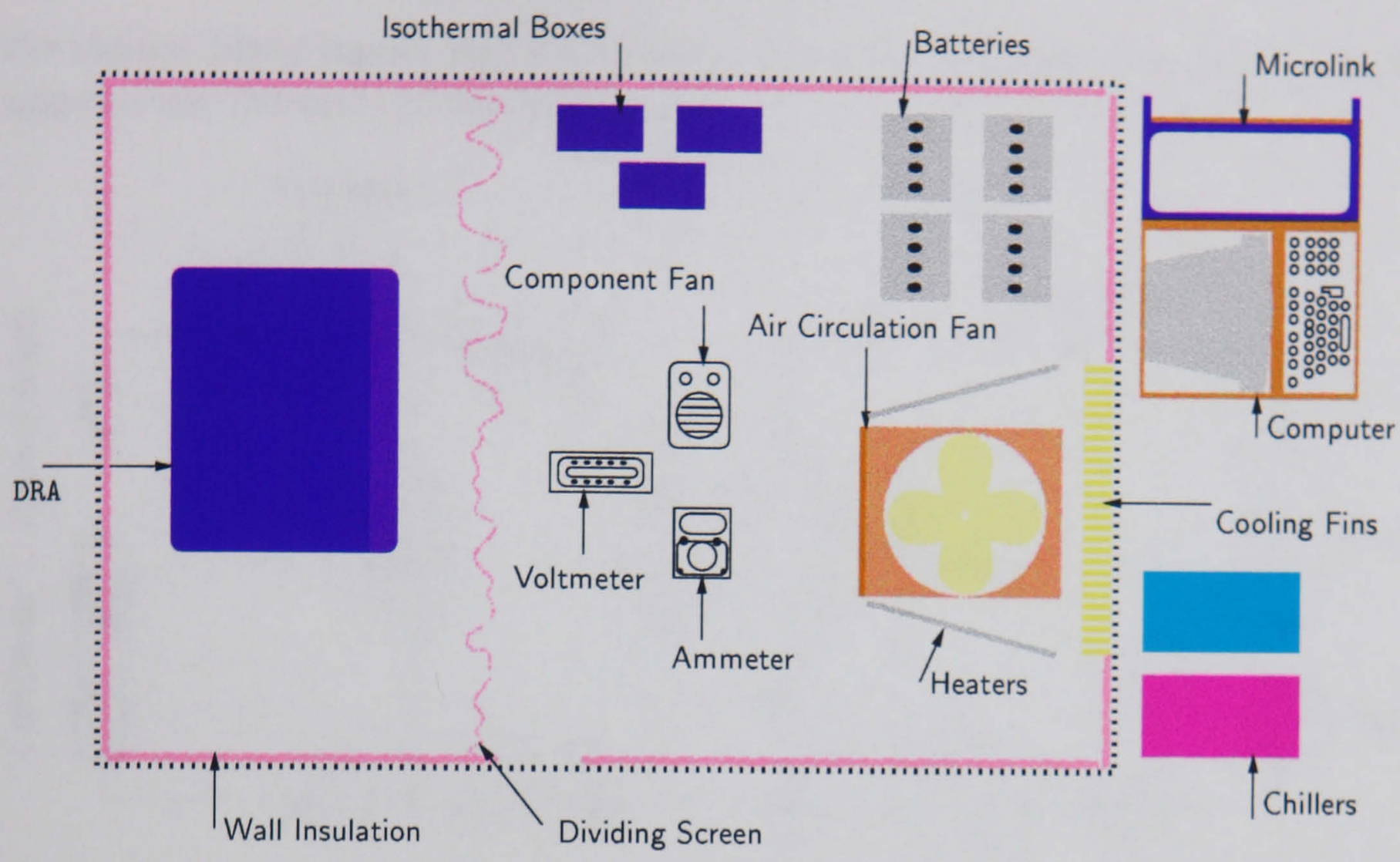


Figure 7.1: Schematic plan–view illustration of the entire experimental 'rig' indicating the main component parts.

- A circuit breaker to ensure that no discharge (from the battery) took place across the resistive elements within the dc PSU while it was off.

In parallel with the dc PSU output terminals were:

- A series–connected pair of parallel–connected twin batteries (24V output) connected across the terminals.
- The high–voltage side of the resistor (voltage–divider) arrangement. This was tapped to enable the determination of the voltage across either the dc PSU (or the battery arrangement when the dc PSU is off).

The second secondary circuit loop was a parallel connection between the power terminals to the DRA compressor and the low–voltage side of the voltage dividers. Connected within this circuit in series were:

- A shunt, connected in series within the electrical current loop between the batteries and the ES–DRA inputs to facilitate the determination of the electrical current drawn by the ES–DRA.
- A switching relay to enable the on–off switching of the ES–DRA compressor[1].

[1]The original control circuit of the ES–DRA did not offer the type of flexibility required for the testing of the appliance and so it was dispensed with.

All the shunts (data input) and switching relays (signal output) were connected to the appropriate channels of the MICROLINK.

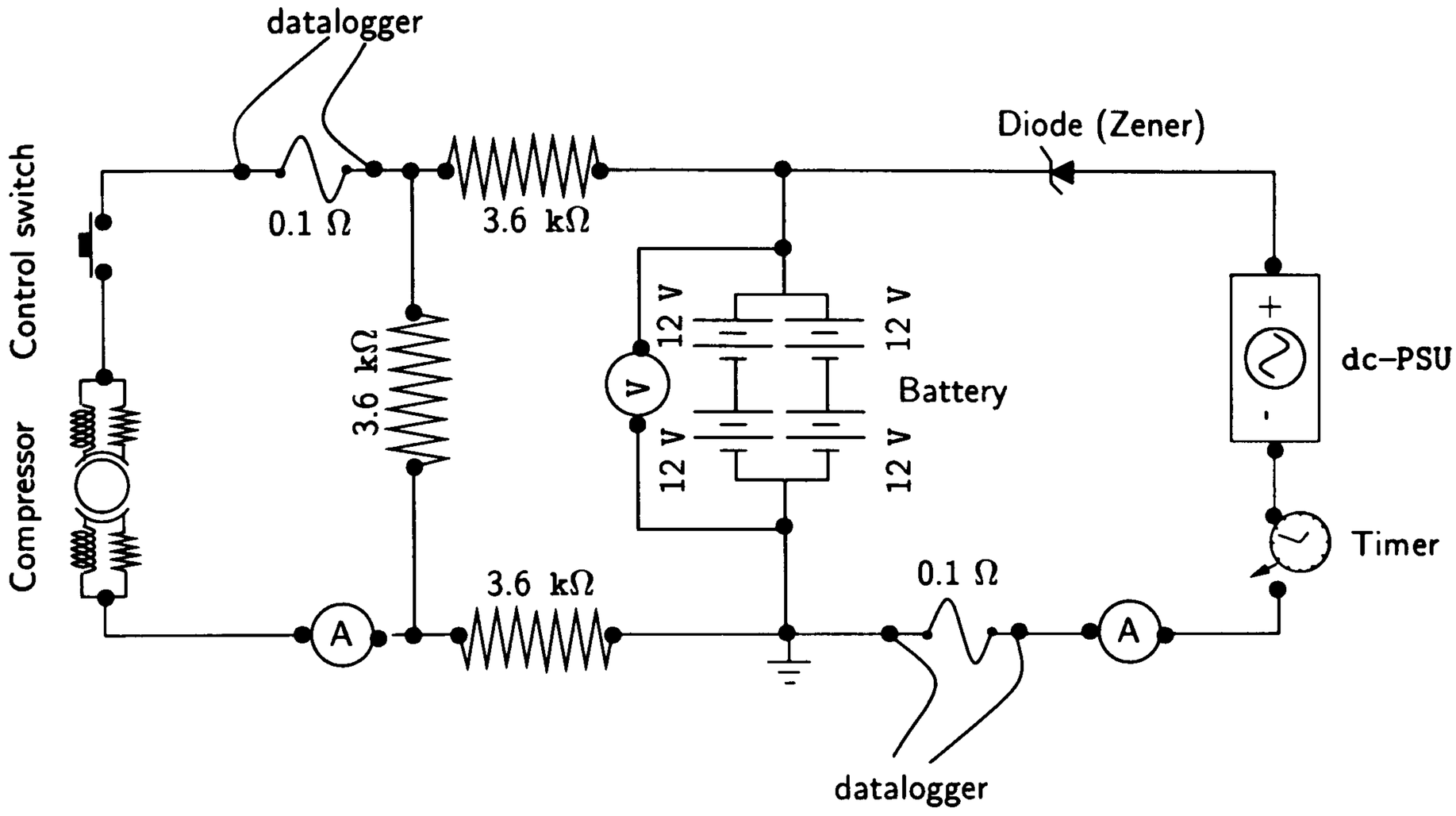


Figure 7.2: Diagrammatic representation of experimental circuit.

The two heaters were plugged into a junction box which was fitted with a 30 amp relay and plugged into the mains. The cooler was likewise plugged into the mains with a relay in series within the (cooler–mains) loop. The power into these devices was permanently on and the relays, used to control the switching on/off of the devices, were connected to the MICROLINK. The fan was left permanently on with no controls.

7.1.2 Thermocouples

A total of forty–eight T–type thermocouples were utilised for the experiments, each connected to a separate channel on the MICROLINK. Of these:

- Two were used to monitor changes in the (thermal) ambiance of the environmental chamber.
- Three were used to monitor the ES–DRA internal air temperature. These were shielded with aluminium foil and mounted equi–spaced on a stand in the centre of the cold compartment.

- One was used to monitor the compressor temperature (located on the top of the compressor).
- Two were used to determine the temperature of the air flowing through the condenser heat exchanger (in and out).
- Four were utilised for measuring the vertical temperature distribution within one of the thermal stores (the TES closest to the evaporator exit was chosen as the reference as it will have the highest temperature of the four).
- Four were used for monitoring the temperature of the evaporator (one on the middle of the top of the evaporator section adjacent to each vertical wall).
- The remaining thirty–two were placed at various locations on the inside and outside of the ES–DRA storage compartment. The exact locations can be seen from Figures 6.4 and 6.3, *qv.* pages 189 and 188 respectively.

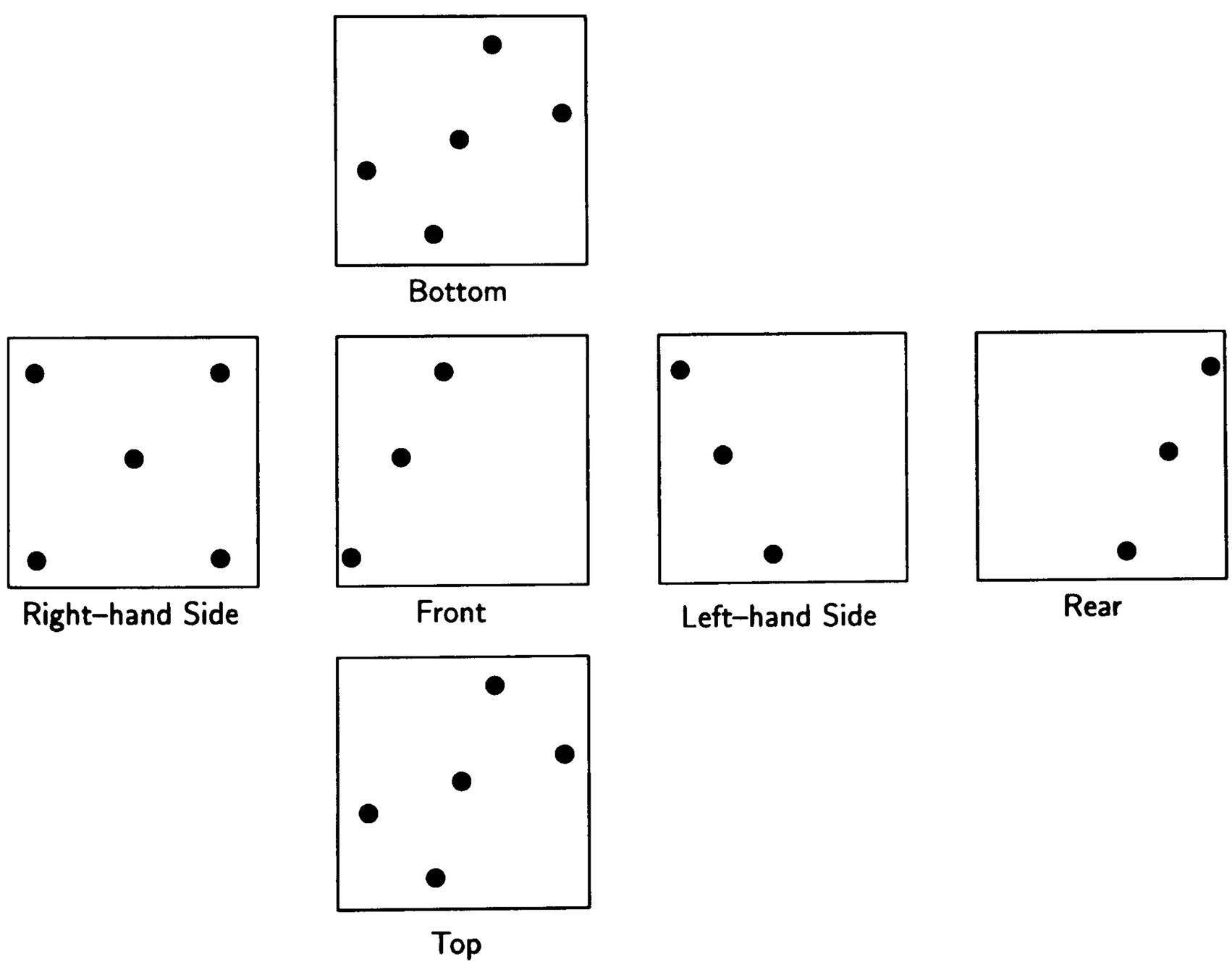


Figure 7.3: Location of thermocouples on the ES–DRA rig exterior.

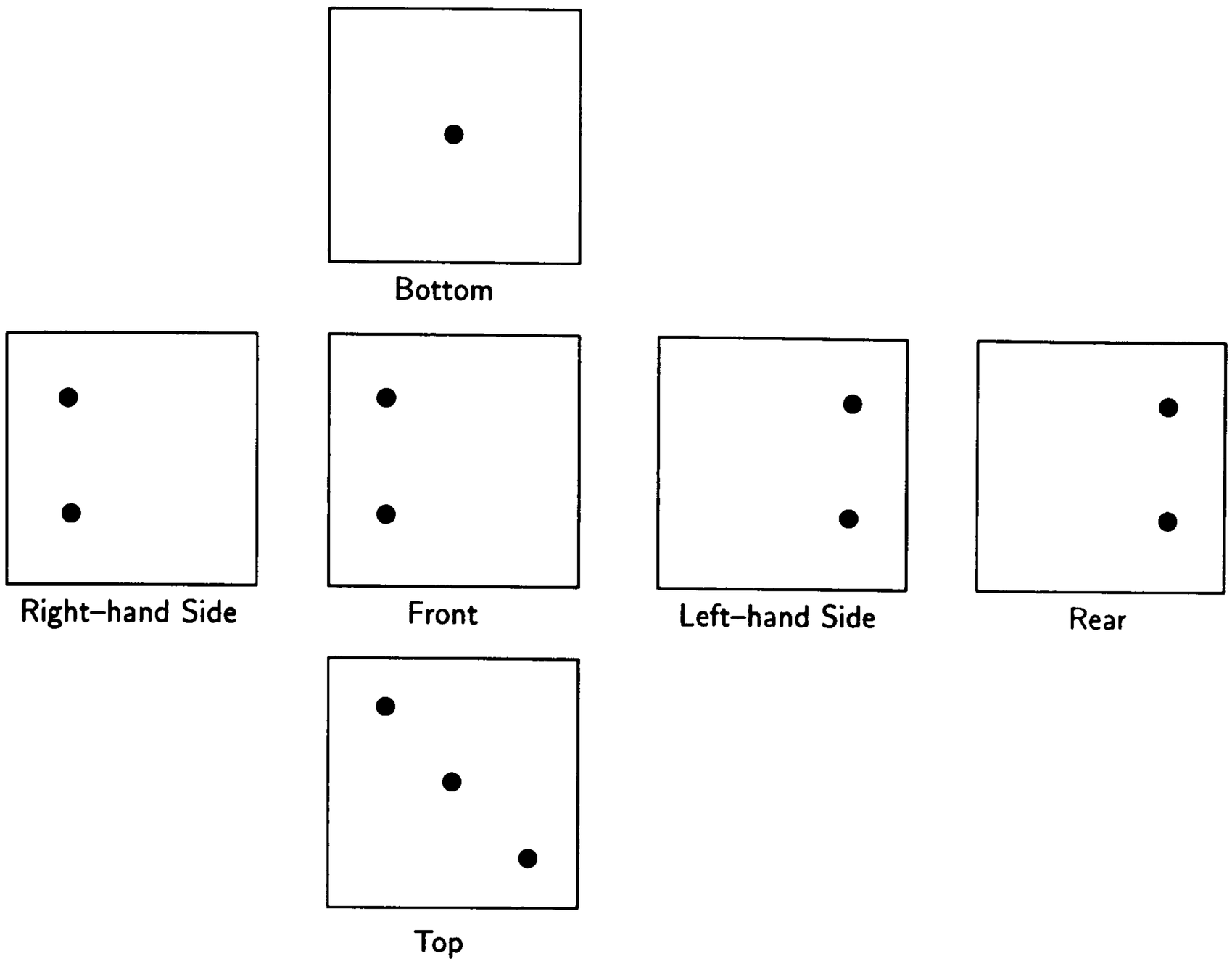


Figure 7.4: Location of thermocouples in the ES–DRA rig interior.

7.1.3 General Observations

In this section, several observations and comments are made as to modifications which had to be made to the ES–DRA and the suitability of the different instruments to their application.

7.1.3.1 The DRA

The design of the rig had to be modified for manufacturing purposes; this was necessary as the design outlined in Chapters 4 and 6, *qv.* pages 105 and 184 respectively was done strictly on a heat transfer basis with no reference to the principles of design for manufacture. These modifications are listed hereunder and discussed.

1. On the basis of energy management and thermal control, the most significant modification made was that to the evaporator–thermal store configuration. The initial design stipulated that an evaporator surface be provided adjacent to each vertical surface, each encased within a quarter of the total amount of LH–PCM used for the TES. (a) The prototype consists of one continuous evaporator

surface bent in the form of a hollow parallelepiped. (b) The TES material is located only on the internal side of the plane surfaces of the evaporator. This leaves the other side (adjacent to the ES–DRA wall) of the evaporator exposed to the air in the refrigeration compartment. This will tend to reduce the ES–DRA compartment temperatures to below desired levels during store charging.

2. The construction of the evaporator from a single continuous plate has resulted in (observed) differential rates of store charging between the different thermal stores, the TES adjacent to the refrigerant entry to the evaporator section charging first and the TES closest to the evaporator exit charging last. The observed times between the (sequential) initiation (and termination) of charge of the thermal stores is of the order of 2 hours and 15 minutes during tests in a 25 °C environment (see Figure 6.13 on page 204).

3. The TES material remained contained in polythene bags (see Appendix C on page C-266). This may have some bearing on the heat transfer between the ambient air and the storage medium. Substituting the containment material may serve (in addition to altering storage containment geometry) as a means for effecting control on the rate of heat transfer into the refrigerating compartment.

4. The thermal stores were relocated between the (aluminium) evaporator and the (steel) corrugated sheeting which defines the useful storage space of the appliance. This provided little, if any, room for expansion and thus it is envisaged that the energy required to fully charge the store (*i.e.* cross the phase–transition temperature) may be increased on account of increased pressure due to the resistance to expansion.

5. The compressor was located adjacent to the refrigerating compartment. However, this (from the thermal store charging sequence) did not appear to have a significant effect on the charging sequence of the thermal stores. This is probably due to the use of the VPSI.

6. The total thickness of the insulation used was 480 mm, as opposed to the 650 mm stipulated in the initial design. The effect of this is deemed to be insignificant as the principal (VPSI) insulant was present.

7. The door seals were made of insulating polyurethane foam; this appears to be sub–standard when compared, on the basis of the amount of air ingress which it permits, to what is used commercially.

The Thermal Energy Stores

The thermal stores were made from the irradiation of *circa* 95% PVA–H_2O solution. The manner of preparation along with some general observations are documented in Appendix C on page C–266. Due to the nature of the preparation/manufacturing process, there were differences (deviations less than 50g in 1.3 kg, a maximum of *circa* 4%) in the weights of the individual bags. These were distributed in a manner as to attempt to compensate for the delay between initiation and termination of store charge (*i.e.* the heaviest placed adjacent to the evaporator section where charging was first noticed to occur). This did not appear to have any discernable effect on the order or manner in which the store charging occurred. The observation of the rate of dessication of the TES material mandates that the hydrated PVA must be kept isolated from the ambient to prevent moisture loss, amongst other reasons (see also Appendix C.6 on page C–271).

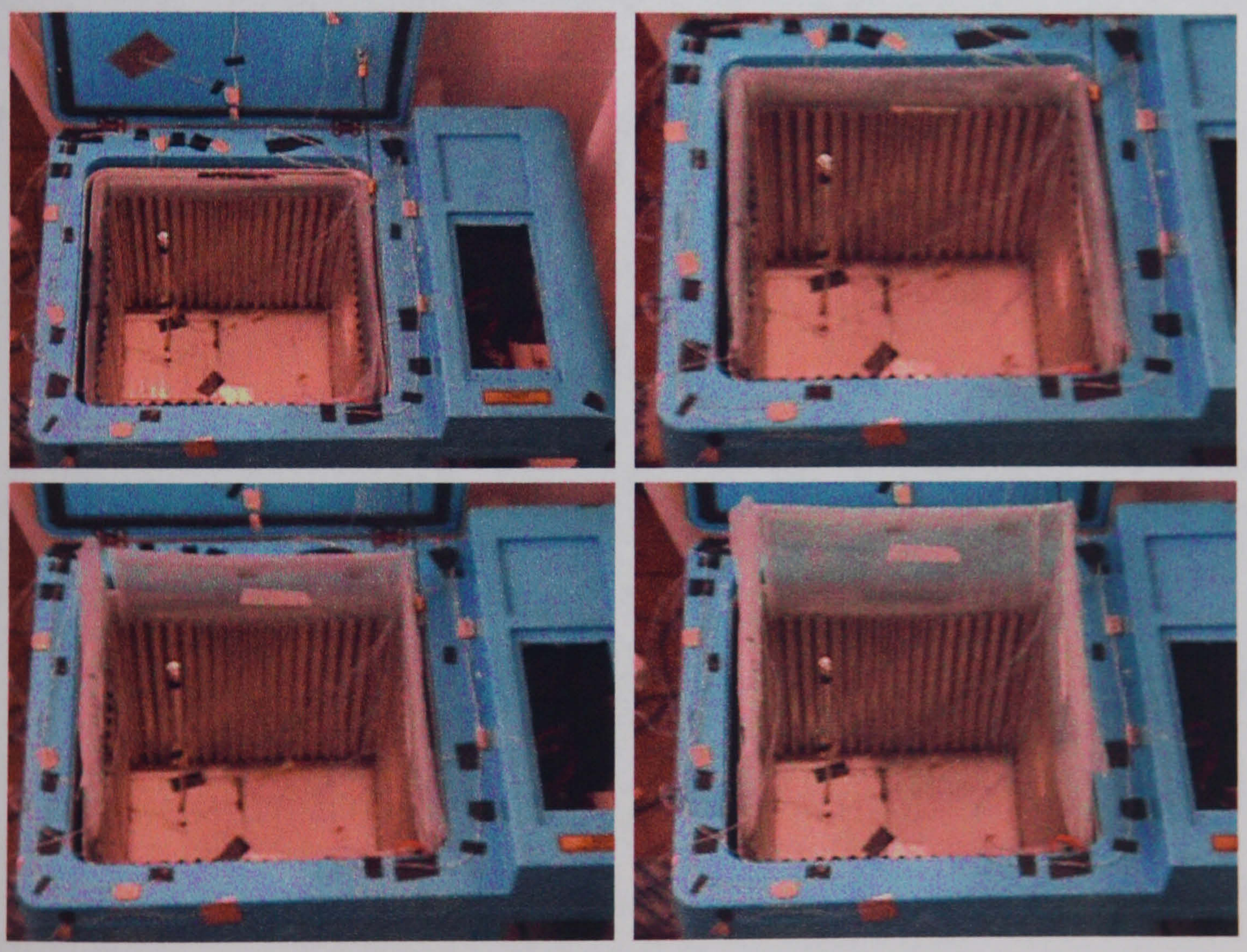


Figure 7.5: Images indicating the location of the TES's within the DRA

Two parameters which play an important role in the manner in which the TES will respond to temperature changes in the ambient ES–DRA temperature and changes

in the contacting evaporator temperature are (a) the characterising TES—air–side Biot number (Bi_{TES}), with the TES thickness as the characteristic thickness and (b) the Fourier number (Fo_{TES}) of the TES as time progresses, with the TES length as the characteristic thickness (*cf:* (a)).

The Bi_{TES} gives an indication of the thermal response behaviour of the TES. Small values of this parameter ($Bi_{TES} < 0.1$) imply that conductive effects within the TES dominate air–side convective effects, resulting in the TES effectively behaving as if it had a uniform temperature.

The implication of a small Bi_{TES} on the air–side is that in comparison to heat transfer taking place at the evaporator–TES interface, the TES air–side interface can be considered adiabatic. On this assumption, the TES can be modelled one–dimensionally as an infinite slab with one end at temperature $T_{evap.}$ and the other end adiabatic. The solutions to problems of this type can be represented by an infinite series. On the assumption[1] that $Fo > 0.2$, only the first term need be used for a fairly accurate approximate result.

Representing the uniform temperature of the TES with its bulk mean temperature $\overline{T}_{TES}$, initially assuming a constant $T_{evap.}$, the T_{TES} can be approximated, assuming a uniform initial temperature $(T_{TES})_{initial}$, as:

$$\frac{T_{TES}(0) - \overline{T}_{TES}(t)}{T_{TES}(0) - T_{evap.}} = 1.0 - \sum_{n}^{1\cdots\infty} \frac{2 \cdot \exp\left(\left[\frac{(2\cdot n+1)\pi}{2}\right]^2 Fo_{TES}\right)}{\left[\frac{(2\cdot n+1)\pi}{2}\right]^2} \cdot \left[1 - \cos\left(\frac{(2 \cdot n + 1)\pi}{2}\right)\right]^2 \quad (7.1)$$

The effect of a varying evaporator temperature can be obtained by applying the Duhamel integral to eqn (6.1), given a knowledge of the temperature profile of the TES. The maximum TES–bulk (mean) temperature change per second, $\dot{T}_{evap.}$ (°C/s), can be estimated, ignoring the thermal capacity of the evaporator, from

$$\dot{T}_{TES} \approxeq \frac{\dot{Q}_{evap.}}{(mC_p)_{TES}} \quad (7.2)$$

For the GE3, the maximum output capacity is $78W_{(T)}$ (coolth) which is divided between the four thermal stores, neglecting the heat transfer to the ES–DRA compartment. In applying the preceding arguments to the TES within the ES–DRA the following Table 6.2 on page 193 is presented:

The implications are that for *each* degree change in the evaporator temperature there will be *circa* 0.3 °C change in $\overline{T}_{TES}$ *above* the phase change temperature T_{LH} and approximately a 0.6 °C change in $\overline{T}_{TES}$ *below* T_{LH}, after sixty seconds respectively.

[1] See Incropera and DeWitt (1990), *pp.* 239 *ff.*.

Material[a]	Bi_{TES}[b]	Fo_{TES}[c]	$\dot{T}_{TES} \times 60s$ (°C)	$\frac{\Delta T_{initial,TES}}{\Delta T_{initial,evap.}}$
$H_2O_{(s)}$[d]	0.03	0.278	0.466[e]	0.591
$H_2O_{(l)}$[f]	0.1	0.0351	0.214[g]	0.278[h]

[a]Property values at $(T_{LH})_{[H_2O]} = 0\,°C$.
[b]$h = 4.0\ W/m^2\,°C$.
[c]Characteristic time 60s.
[d]Characteristic length 0.0165m.
[e]Based on $\dot{T}_{evap.} = \frac{78}{4\times1.3\times1.93\times10^3} = 7.8 \times 10^{-3}\ °C/s$.
[f]Characteristic length 0.015m.
[g]Based on $\dot{T}_{evap.} = \frac{78}{4\times1.3\times4.2\times10^3} = 3.6 \times 10^{-3}\ °C/s$.
[h]Two terms of the series expansion are needed in this case.

Table 7.2: Table of non–dimensional parameters Bi and Fo for the TES using the properties of H_2O.

This can be observed from the experimental data, see Figure 6.15 on page 206. Incidentally, the estimated $\dot{T}_{evap.}$ above T_{LH} indicates a pull–down time, from 25 °C to 4 °C, of $21 \div (3.6 \times 10^{-3} \times 3600) \approxeq 1.62$ hours; this is in agreement with the observed time of *circa* 1.5 hours.

Condenser In order to assess the heat rejected from the condenser (of the fan–assisted type, see Figure 6.7 on page 194) during operation, it was necessary to calculate average values for the fan mass–flow throughput. For this reason, a brief experiment was carried out using an anemometer[1] to assess the magnitude and direction of the air velocities on either side of the condenser. Figure 6.6 on page 194 is a diagrammatic representation, giving an indication of the approximate velocity distribution fore and aft (with respect to the air–flow direction), of the condenser[2]. The mean air temperature in the laboratory was *circa* 20 °C.

From the fan and condenser geometries, the air flow areas are estimated as:

$$A_{inlet} = 3.27 \times 10^{-2} m^2$$
$$A_{exit} = 8.47 \times 10^{-3} m^2$$

[1]Solomat MPM 500e; manufacturers Solomat Mig Ltd., Devon EX11 1BP. UK.
[2]The fan is attached to the condenser, with air flow moving initially across the condenser to and then through the fan *i.e.* the air inlet adjacent to the condenser and the air outlet adjacent to the fan.

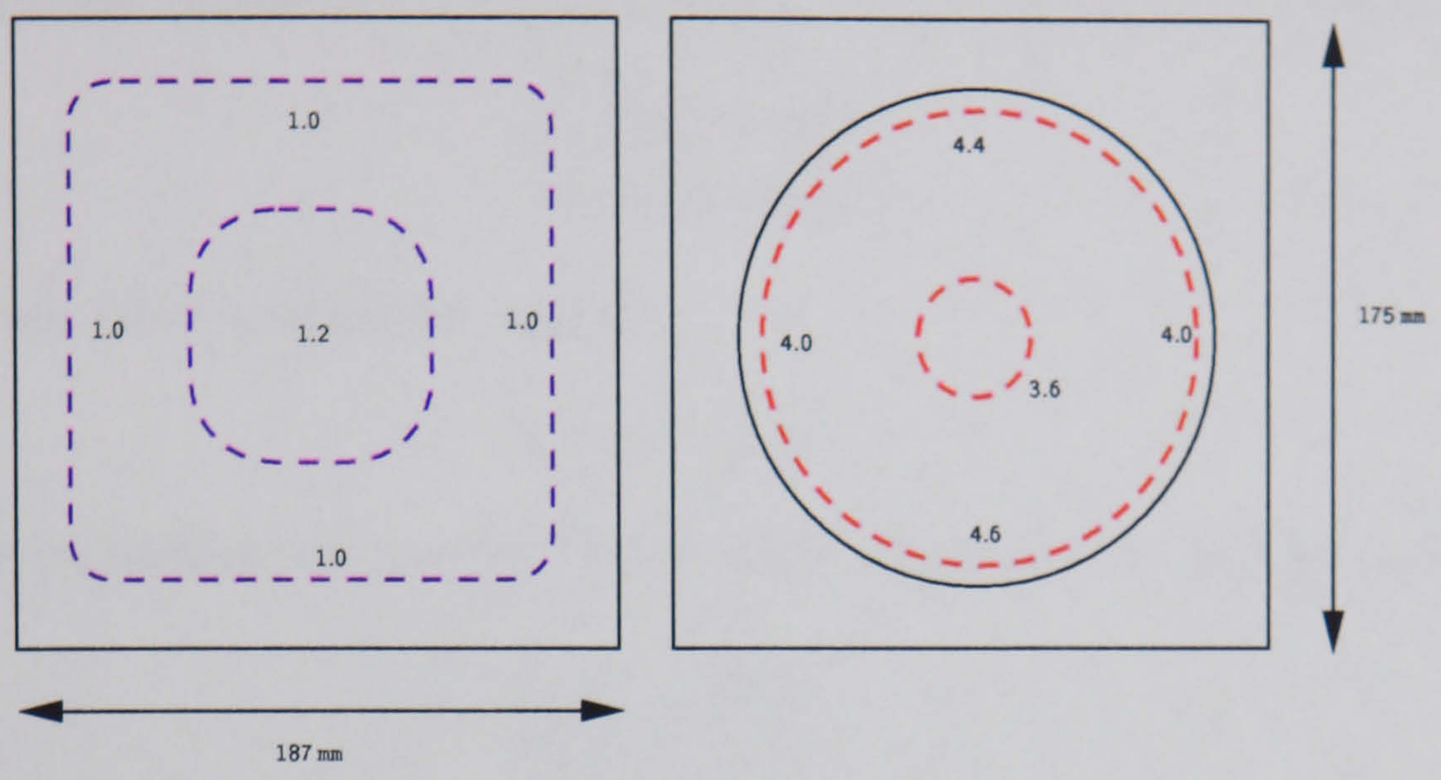


Figure 7.6: Diagrammatic representation of the velocity flow (m/s) across the condenser; air intake (left) and air exit (right)

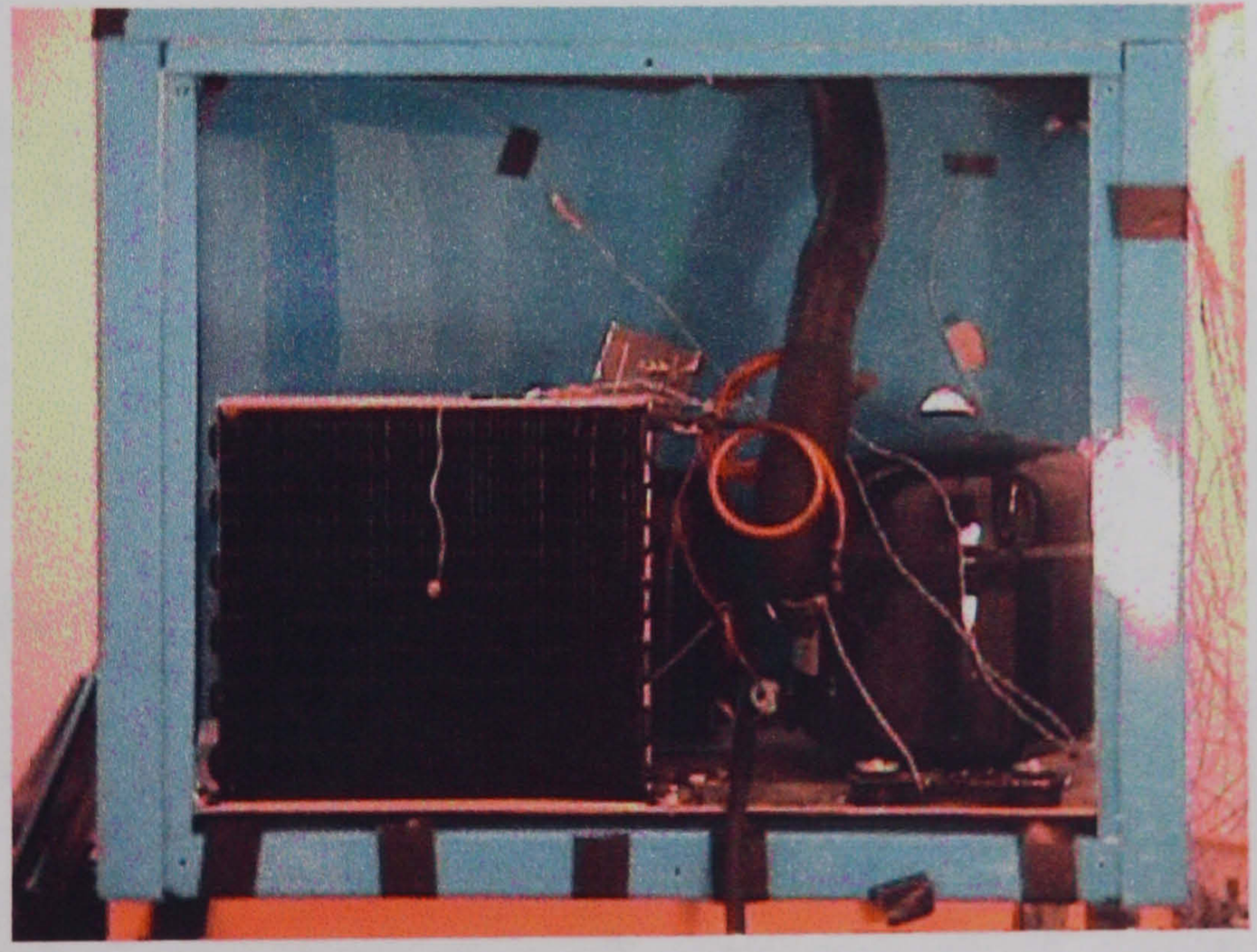


Figure 7.7: End view of the DRA indicating the condenser (air intake, left) and compressor (right).

From the data collected, the mean air flow on either side is computed[1] as the arithmetic average of the velocity distribution. Thus, the mean velocities are:

$$\overline{v}_{inlet} \approxeq 1.05\mathrm{m/s}$$
$$\overline{v}_{exit} \approxeq 3.925\mathrm{m/s}$$

From the basic mass continuity relation

$$\dot{\mathrm{m}} = \rho_{\mathrm{m}} \cdot A \cdot v \tag{7.3}$$

it is possible to deduce the relation (for a fixed mass–flow at a given mass density):

$$\frac{A_{inlet}}{A_{exit}} = \frac{v_{exit}}{v_{inlet}} \tag{7.4}$$

From the geometric dimensions of the air–flow path

$$\frac{A_{inlet}}{A_{exit}} = 3.86$$

and the velocity ratio

$$\frac{v_{exit}}{v_{inlet}} = 3.74$$

This validates eqn (6.4) to within 3%. From the mass continuity relation, eqn (6.3), the mass–flow rate can be computed (air density $1.2\,\mathrm{kg/m^3}$ @ 20 °C):

$$\dot{\mathrm{m}}_{inlet} \approxeq 0.041\,\mathrm{kg/s}$$
$$\dot{\mathrm{m}}_{exit} \approxeq 0.040\,\mathrm{kg/s}$$

Thus the mean mass–flow rate across the condenser is estimated at $0.04\,\mathrm{kg/s}$.

7.1.4 The Compressor

Figure 6.6 on page 194 is a photographic image illustrating the GE 3 compressor (rated at $78\mathrm{W}_{(T)}$ @ 32 °C). As noted in section 2.4.1 on page 50[2], the benefit gained from the compressor *i.e.* the coefficient of the system's performance, will be dependent on the (a) loading conditions (heat lifted from the system), (b) the fraction of that load which results from heat leaks into the system and (c) the required rate of

[1]The assumption in this case is that the velocity profiles are 'full' and as such the displacement thickness of the boundary layer (adjacent to the flow channel walls) is thin [Duncan et al., 1981, *pp.* 250].

[2]In particular see eqn (2.14).

cooling. Thus the temperatures of the ambient, compressor, condenser. evaporator and DRA will affect the resultant COP of the compressor; this will be illustrated later.

Another important factor is the behaviour of the cooling circuit under thermal cycling. Figures 6.8 and 6.9, *qv.* pages 197 and 198 respectively, are plots of the temperatures at various locations of one of the TES's and of the evaporator during compressor cycling. Apart from the heat gain into the system on account of ingress through the evaporator–TES interface there are also the effects of (a) the equilibration of the refrigerant pressure across the system when the compressor goes off–line; this manifests as a sharp drop in the temperature of the system immediately after the compressor is switched off (particularly the initial dip in the compressor temperature)[1] and, (b) the heat injected into the system by the compressor on start–up, generated in the process of overcoming inertial forces, restoring the system's pressure differential and ohmic losses. This heat generated is manifest in both the initial rise (to a maximum) of the compressor temperature[2] and the rapid rise in the TES and evaporator temperatures at the onset of each compressor on–cycle. The rise in the compressor temperature peaks a few minutes after start–up and drops until it reaches an equilibrium temperature, probably on account of heat transmission between the evaporator and the compressor.

7.1.5 Other Observations

One problem faced with the environmental chamber was the control of its temperature–time characteristics. Ideally, the chamber temperatures should be controllable to provide a uniform sinusoidal temperature distribution when desired; however, the differences in and limitations of the effective heating and cooling powers in the 'air conditioning' apparatus made this difficult. The heat transfer rate, between the chamber air and the cooling fins, was such as not to permit a reduction in the air temperature within the chamber below 20 – 21 °C in reasonable time whilst the ambient laboratory temperature was 25 °C. This was in contrast to the heating equipment which could effect chamber temperatures of *circa* 35 – 37 °C within a reasonable timescale. These limitations were definitive as to the extent of the temperature range over which the experiments could be conducted. The chamber was also susceptible to the variations in the ambient laboratory temperature.

[1] This trend has been observed with data from other tests within this work and from other sources.

[2] This is in evidence in *all* instances of compressor start–up.

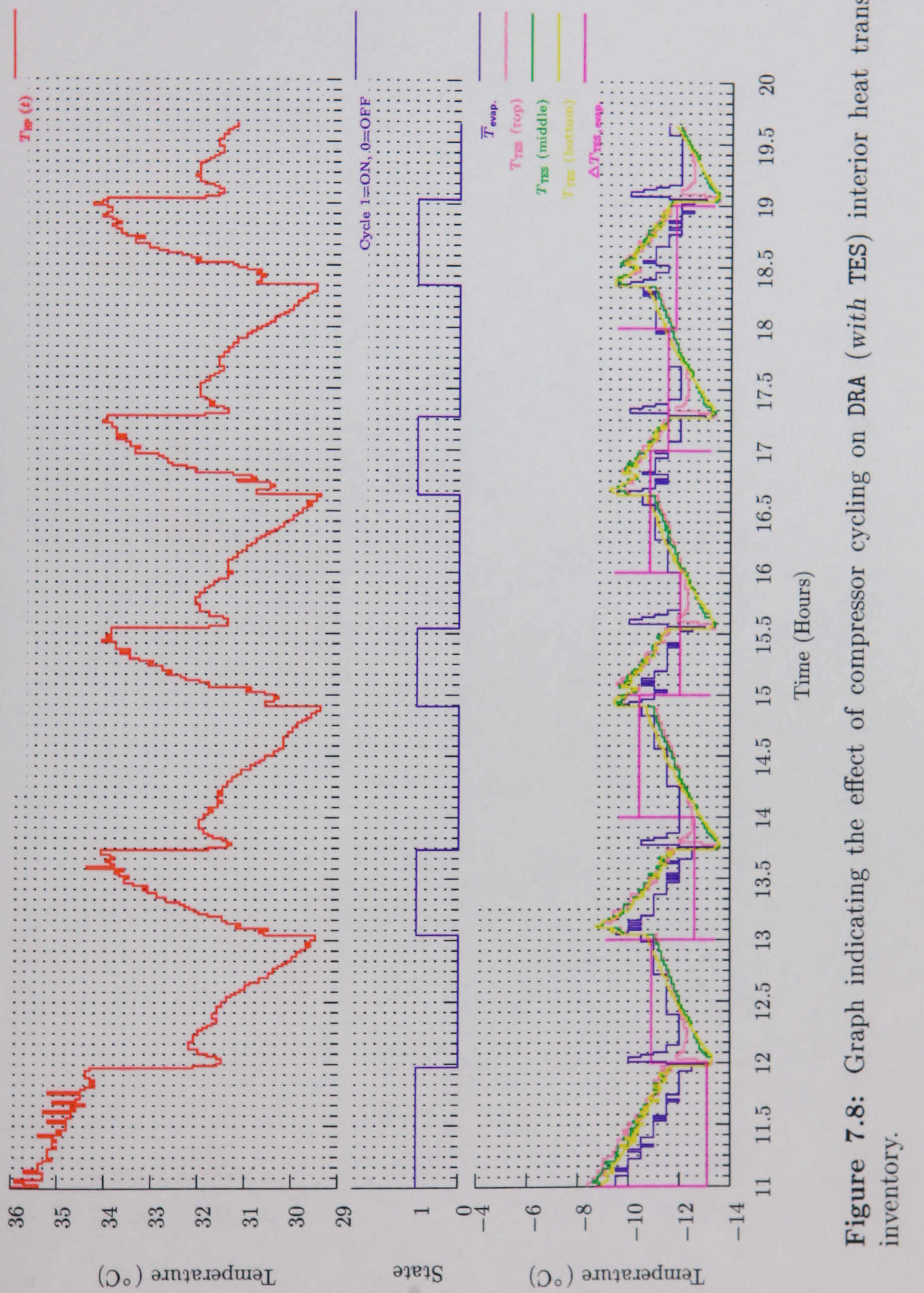


Figure 7.8: Graph indicating the effect of compressor cycling on DRA (*with* TES) interior heat transfer inventory.

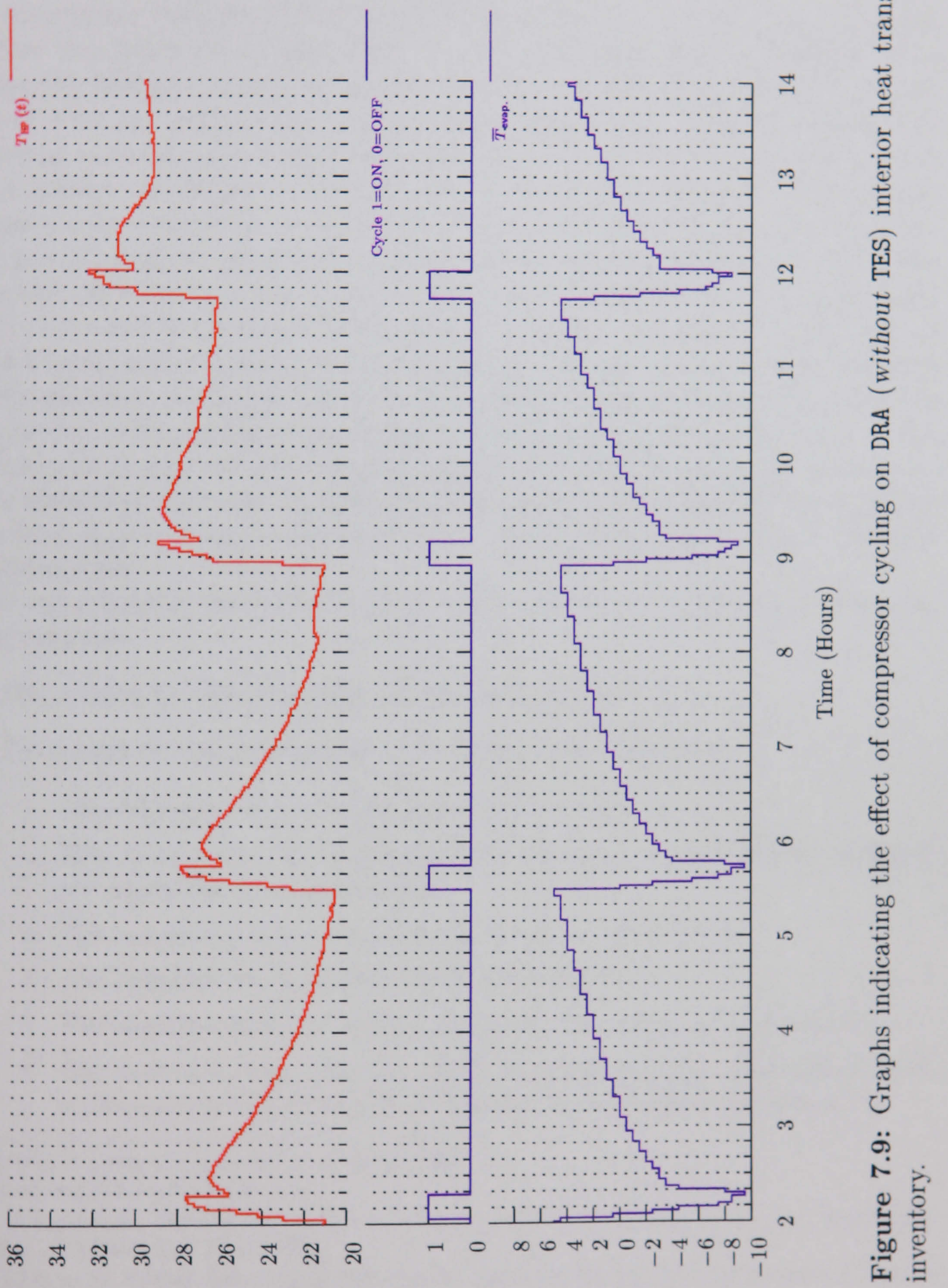


Figure 7.9: Graphs indicating the effect of compressor cycling on DRA (*without* TES) interior heat transfer inventory.

7.2 The experimental procedure

In comparison with the setting up of the experiment, the actual data gathering procedure was relatively straightforward. The main difficulties encountered were effecting the desired control on (a) the environmental chamber and (b) the ES–DRA, and with the development and implementation of the control software[1]. In considering the controller design/implementation for the ES–DRA, several options were examined, *viz* simple on–off control, PID[2] control and fuzzy (logic) control[3]. Amongst issues which were considered were: the ease of manipulation of the controller and the need for (past and current) data to implement the control logic. One particularly relevant issue was the need for a reliable indicator for the thermal energy content of the TES, for instance how does one determine whether or not say, 30% of the TES's initial energy content remains within it? Perhaps this could be determined from the thickness of the TES[4]; however this would require several additional levels of complexity, other auxiliary experiments, additional equipment *etc.* The final decision to implement an on–off controller was on the basis of its simplicity and ease of design, implementation and manipulation during experimentation. However, closer to the final stages of large–scale production, other control types *may* be deemed more appropriate.

The experimental procedure consisted of stipulating the following within the control program:

- The number of experiments to (sequentially) perform.
- The length of each experiment, and within each experiment:
  1. The temperature and voltage channels to log.
  2. How to calibrate the instrumentation (the data for this already obtained, see Appendix A on page A-240).
  3. The required mean environmental chamber temperature.
  4. The required mean ES–DRA internal temperature.
  5. The required control regime (on and off times) for the compressor.
  6. The minimum time between which temperatures (ES–DRA internal, environmental chamber) should be checked for set–point compliance.

[1] A listing is given in Appendix D on page D–275.

[2] Proportional–Integral–Derivative.

[3] Some implementations of this technique in refrigeration control are given in Cheung and Kamal (1996), Robinson and Mort (1996).

[4] Another is to simply guess depending on the previous charge time, duration and loading conditions, see Mithal and Yang (1994).

Experiments were run to determine:

1. The temperature–time characterisation phase.
   - The pull–down and charge time of the ES–DRA.
   - The discharge time of the ES–DRA.
   - The time response of the ES–DRA.
2. Energy consumption values for the different control regimes.
   - Data for the night–time only operation of the ES–DRA compressor.
   - Data for the day–time only operation of the ES–DRA compressor.
   - Data for the ES–DRA running without TES facilities.

As with all experiments, the data is determined within a given accuracy. The accuracy of the data collected has been estimated in Appendix A on page A-240. Except where otherwise stated, the following scheme has been used to rationalise the data presented here. The thermocouple readings are quoted to the nearest half degree, voltages, currents and COP's are quoted to 25% of the unit (*i.e.* to 0.25), powers are quoted to the the nearest 5W and energy to the nearest 10J.

Further consideration as to the limits of the presented information will be given, where necessary, as the results are deduced from the data. It is also noted that the computer timer tended to lose a few seconds each day. However, this is considered insignificant compared to the time scale of the experiment[1]. The precautions laid out in Appendices A and B, *qv.* pages A-240 and B-253 respectively also apply here, along with the measure that the ES–DRA was taped shut to prevent accidental opening and to inhibit air ingress which would otherwise occur on account of sealing insufficiencies.

7.3 The Pull–Down and Charge–Discharge Times

Introduction

This section presents and discusses the data obtained in the pull–down and charge–discharge tests during the temperature–time characterisation phase of experiments. A further (theoretical) discussion as to the estimates for the pull–down time along with estimates for the maximum temperature deviations between the

[1] A typical data gathering and set–point verification cycle could take up to two minutes depending on the number of channels used for the experiment.

evaporating surface and the mean TES temperature (on either side of the phase–transition temperature) is given in Appendix 6.1.3.1 on page 191. The test was performed at different ambient air temperatures in order to give an indication of the relative merits of TES charging at different ambient temperatures. The measured (TES) data was taken from the TES packet mounted on the evaporator section, closest to the refrigerant exit[1].

7.3.1 The Pull–Down Times

The pull–down times for 25 °C and 44 °C *starting* points were observed for the ES–DRA with the TES's in place (Figures 6.10 and 6.11, *qv.* pages 201 and 202 respectively). The data collected clearly indicates the (time) benefits of store–charging during periods of lower ambient temperature, with 0 °C pull–down occurring at 2.75 hours and 5 hours for the 25 °C and 44 °C[2] ambients respectively. The ambient

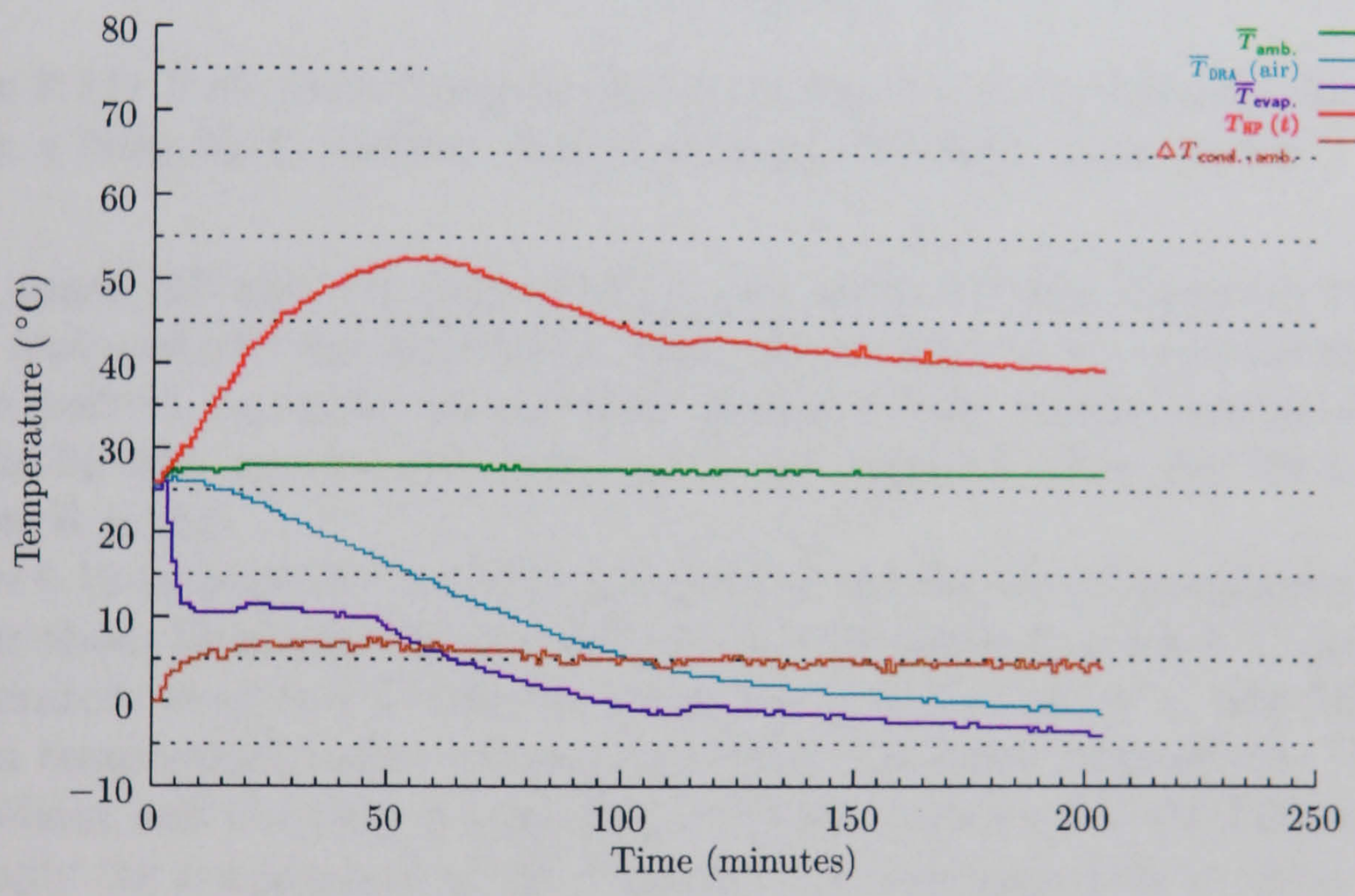


Figure 7.10: Pull–down Temperature–Time history of the DRA with the TES in place in a *circa* 25 °C ambient.

(initial ES–DRA temperature) effects on the pull–down times (see Figures 6.10 and

[1]This location was selected as it would give the worst possible state of the TES's in general.

[2]Due to problems with maintaining ambient air temperatures in excess of 40 °C in the environmental chamber, the room temperature had to be readjusted from 44 to 32 °C. The kink in the data curve (Figure 6.11 on page 202) coincides with a drop in the current drawn by the compressor; this is consistent with the appliance having been momentarily tripped off, probably on account of a thermal cut out.

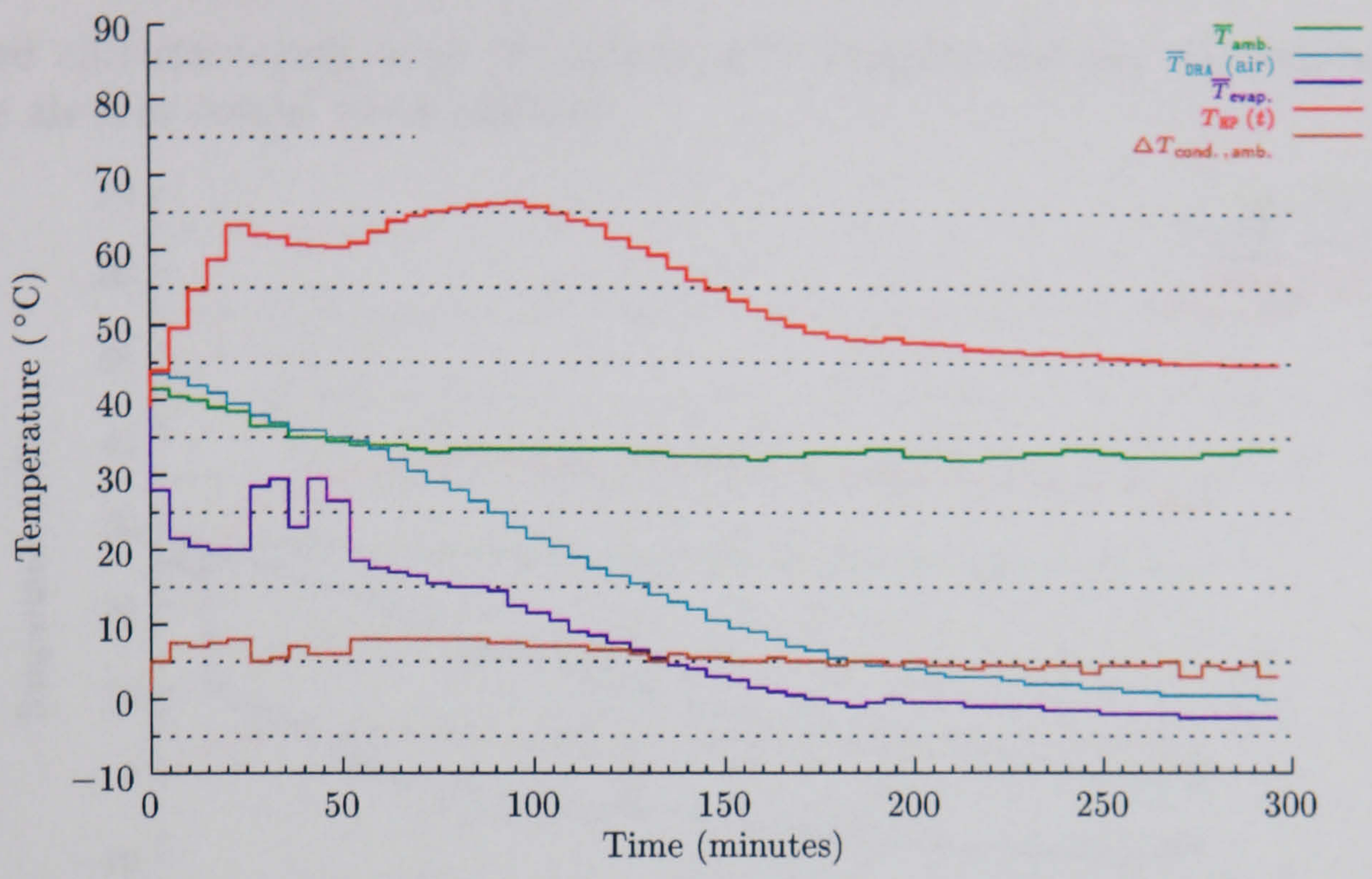


Figure 7.11: Pull–down Temperature–Time history of the DRA with the TES in place in a *circa* 32 °C ambient (initial starting air temperature 44 °C).

6.11, *qv.* pages 201 and 202 respectively) are patent in their indication that lower ambient temperatures are favourable when shorter pull–down (and initial charge) times are desired. As would be expected, because of the thermal inertia of the TES within the ES–DRA, greater pull–down times are required when the TES is in place than when it is not.

Figure 6.12 on page 203 (no TES) is presented here by way of comparison. It indicates that about 15 minutes is required for the evaporator to reach 0 °C (ie T_{LH}); the air temperature reaches 4 °C (the set–point temperature) and 0 °C (the TES phase–transition temperature) after about 1 hour and 1.25 hours respectively. This (one hour) is about half the time it takes for (4 °C) pull–down when the TES is in place. Interestingly the temperature of the evaporator at this stage falls to *circa* -10 °C in that period; this would not normally occur when the TES is present[1]. Notice that the *evaporator* temperatures gradually approach -8 °C as the TES charge processes traverses *on account of the under–cooling taking place* (see also section 6.3.2 on page 203). Also interesting to note is the effect of the compressor temperature on the evaporator temperature, where the rise in the compressor temperature serves to arrest the progressive decrease of the evaporator temperature. In steady–state, this

[1]Figure 6.14 on page 205 indicates that the evaporator and TES temperatures drop to *circa* -8 °C during the sub–cooling phases of the charge process. In the event that the charging is effected without sub–cooling (either by the use of a nucleation initiator or slower cooling rates) the evaporator will operate at a higher temperature with attendant COP benefits.

is achieved simultaneously with the compressor temperature and the temperature lift in the air flow across the condenser.

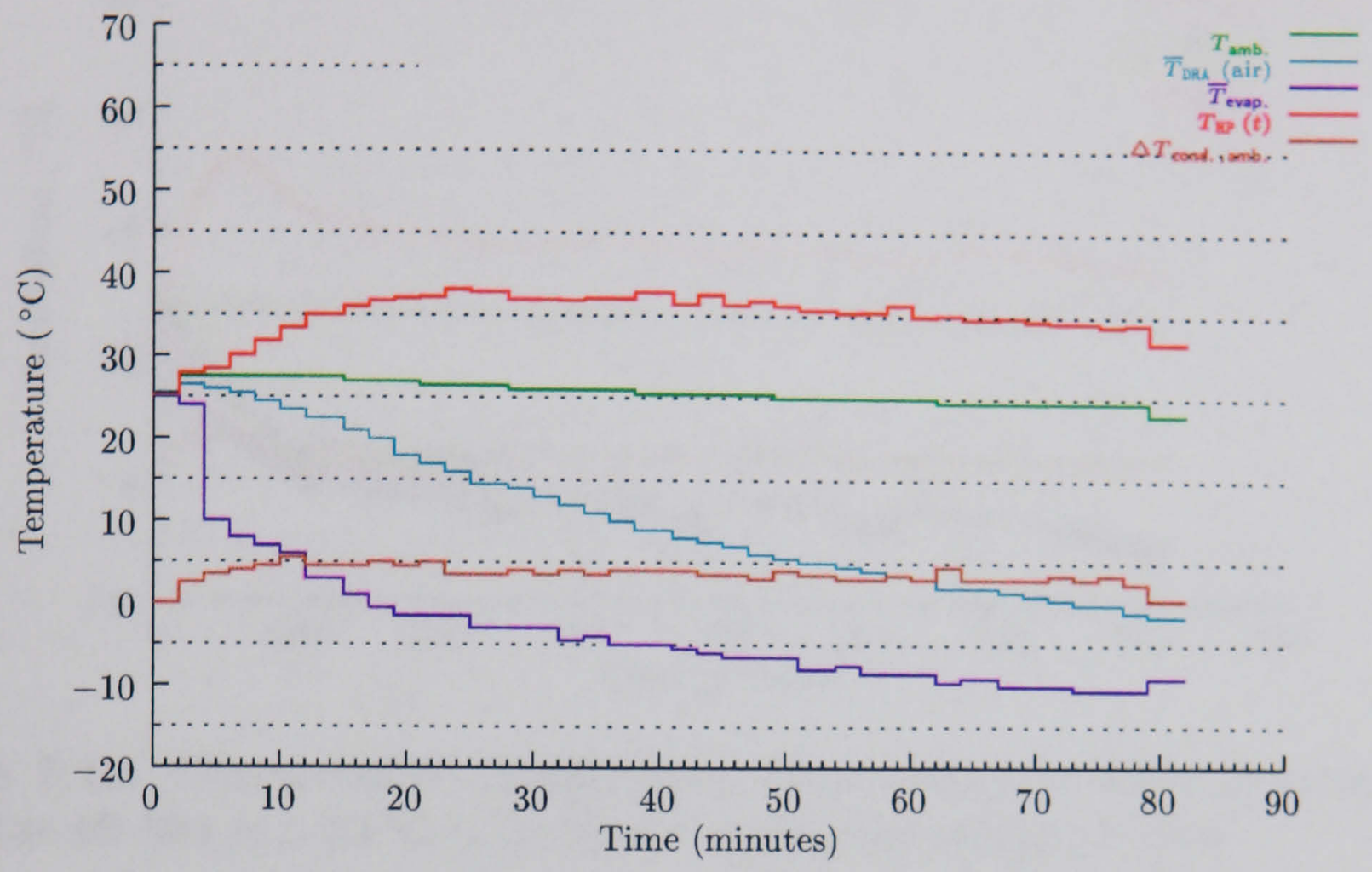


Figure 7.12: Pull–down Temperature–Time history of the DRA without the TES in place (25 °C environment).

7.3.2 The Thermal Store Charge Time

Similar tests were performed to determine the period for TES charging at different ambient temperatures. Figure 6.13 on page 204 is given to indicate the characteristic profile of the results of these tests (25 °C ambient) while Figure 6.15 on page 206 is the result for TES charging in a 35 °C ambient, with the enlargements of various portions of Figure 6.15 given in Figure 6.16 on page 207. The overall results indicate transition times (alone) of *circa* 9.2 and 13 hours for 25 and 35 °C ambients respectively. One implication of this is that lower charge powers[1] could be used to charge the TES in lower temperature environments.

For a 25 °C ambient (see Figures 6.13 and 6.14, *qv.* pages 204 and 205 respectively), the initiation time for the first phase change was just under two hours and the time between each phase–transition was in the region of 2.25 hours. On the other hand, for a 35 °C ambient (see Figure 6.15 on page 206), the cooling initiation time was approximately 2.5 hours with a lag of *circa* 3 hours between the onset of the initiation of successive phase–transitions in the TES parcels.

[1] *i.e.* a smaller design compressor–capacity.

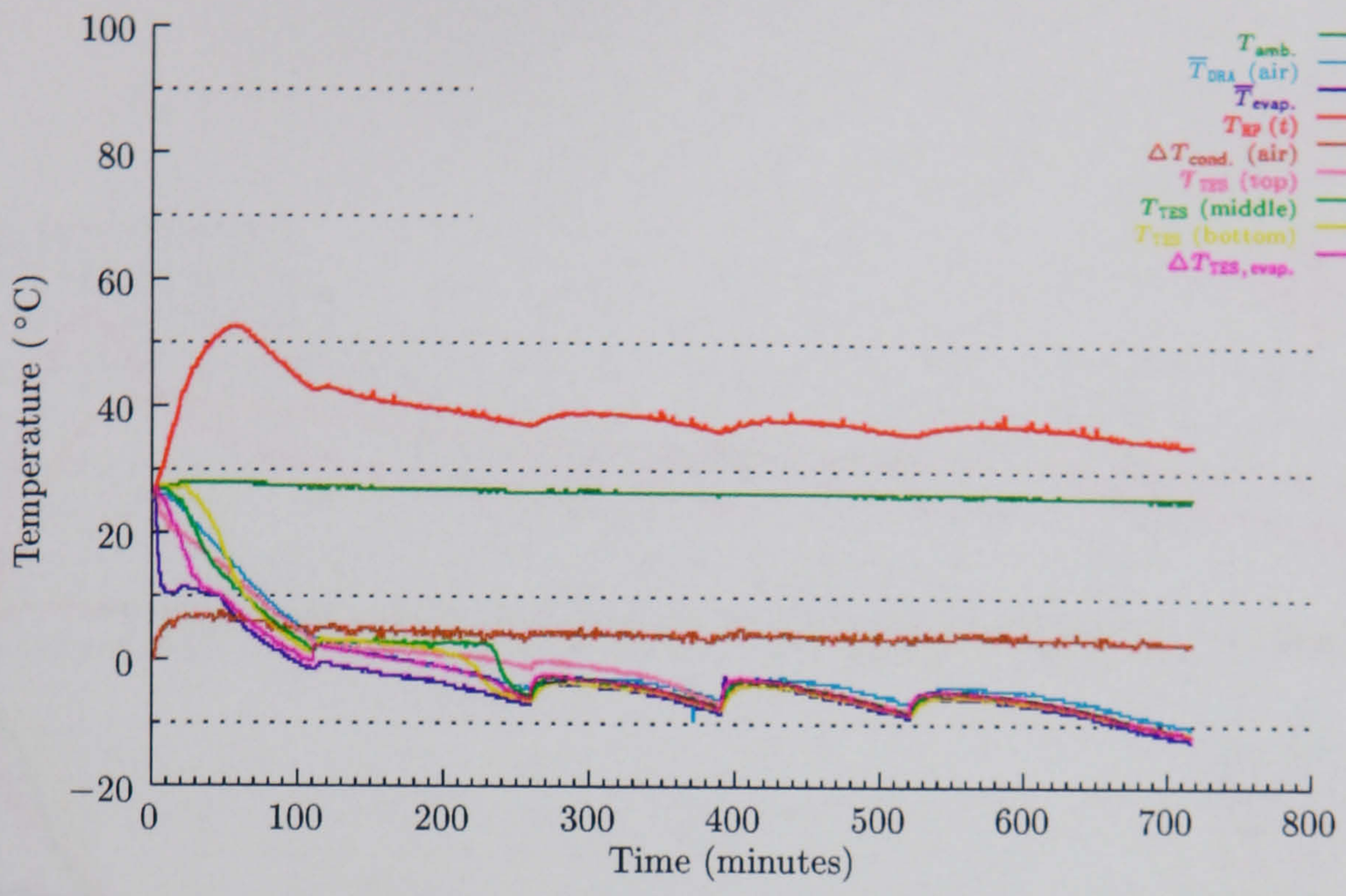


Figure 7.13: Characteristic Temperature–Time history of different locations about the ES–DRA in a 25 °C environment during the charge process.

Qualitative assessment within the limits of the accuracy of the data, tends to indicate a *consistent* inversion of the expected temperature ranking order (within each category[1]) during the onset of the phase–transition process (post sub–cooling). Thus the thermocouples which would be expected to measure the lowest temperatures during the charge process (*e.g.* TES bottom, l.h.s[2]) consistently exhibit the greatest temperature swings (within their category) during the phase–transition process. The result is that these thermocouples indicate the highest temperatures during the phase–transition process. As at yet, no reason has been found for this and further research will be required to illuminate the issue.

The data (see Figures 6.14 and 6.16, *qv.* pages 205 and 207 respectively) is indicative of a sub–cooling effect taking place[3]. The phenomenon is also evident in the compressor temperature and power consumption which rise on the onset of phase–transition in each TES packet. The phenomenon is not observed during TES charge–discharge cycles outside the ES–DRA see Figure C.1 on page C–272.

The phenomenon of undercooling will be almost invariably present in the absence of (heterogenous) nucleating centres, see Winegard (1964)[4]. Given the matrix

[1] *i.e.* When the comparison is between evaporating temperatures or between TES temperatures.

[2] The expansion sequence in the evaporator sections is l.h.s., rear, r.h.s., front.

[3] A similar behaviour was observed by Augood (1997) in ground–up hydrophilic particles used as the solid–load in slurries designed for PCM–TES applications.

[4] Chapter 2.

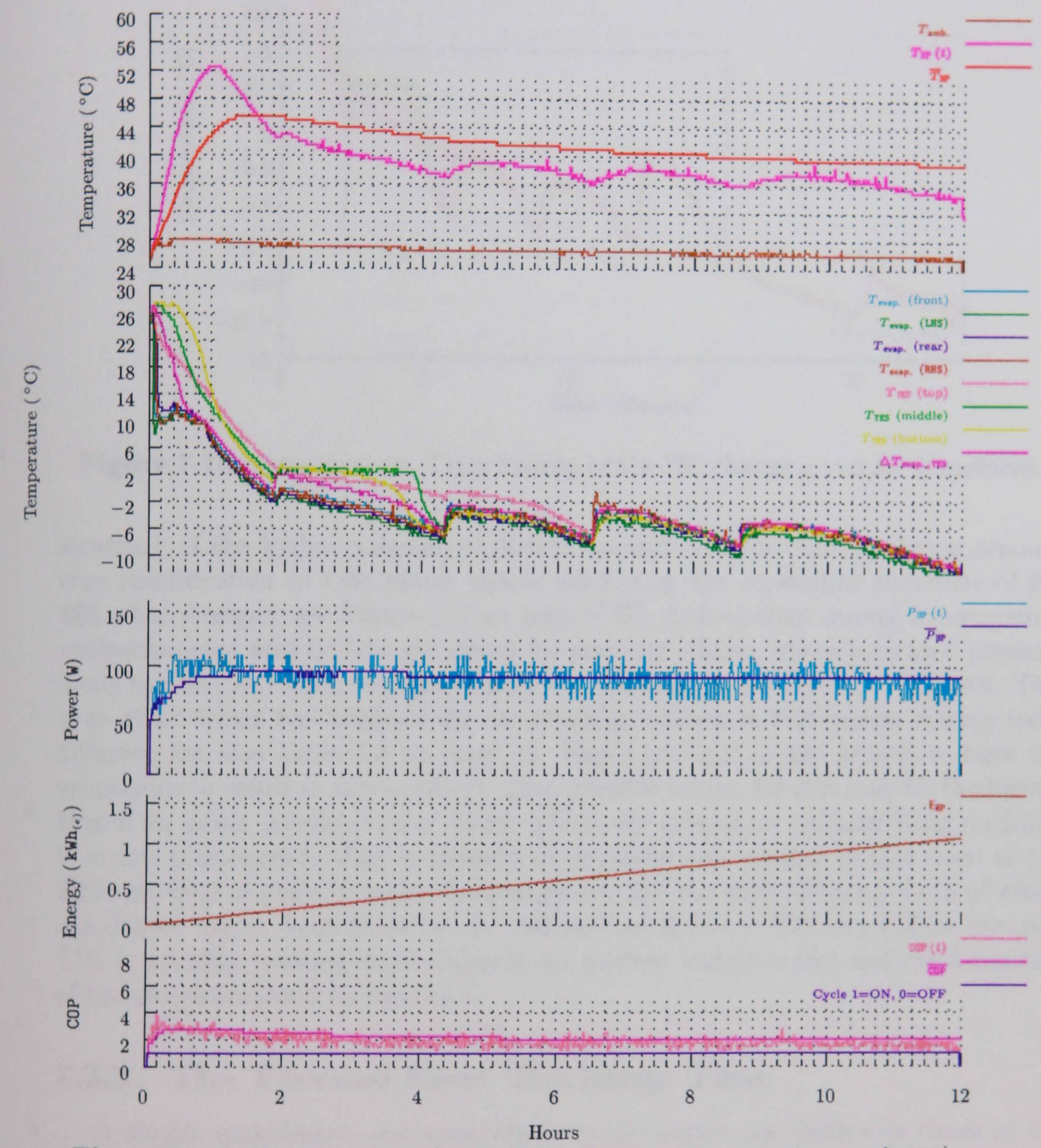


Figure 7.14: Temperatures (ambient, compressor, evaporator and TES), power consumption (compressor), energy consumption (compressor) and COP attending the TES charge process in a 25 °C ambient.

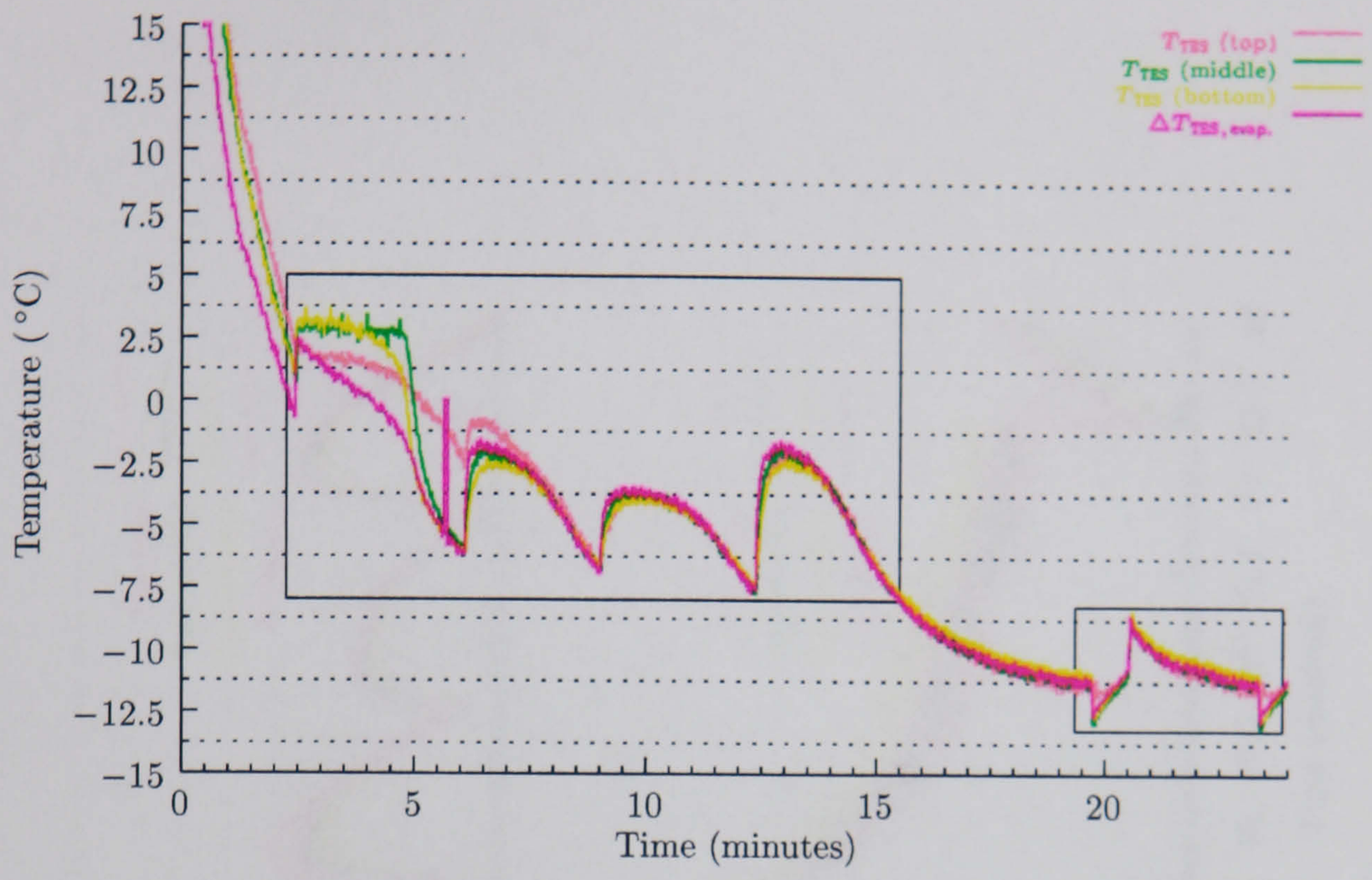


Figure 7.15: Temperature–Time history of the TES charging in a 35 °C ambient.

structure of the hydro–polymer, sufficient nucleation sites exist for heterogenous–type solidification to take place; this is evident in the crystalline structure of the TES when charged, see Figure C.3 on page C–272. Sub–cooling during heterogenous nucleation may also be brought about by pressure effects, where increased pressure tends to delay the onset of phase–transition, see also Callen (1960), Chapter 9. This is an effect which has blighted the use of encapsulation in PCM energy storage technologies, see also Table 3.3 on page 95. Rapid cooling[1] is also known to have the propensity to result in sub–cooling[2]. One possible reason for this may be the formation of an outer, solidified layer which effectively acts as an encapsulating medium. It is this phenomenon that is thought to engender sub–cooling in this case, as the TES's are held in place between the evaporator and the steel restraint, both of which can deliver higher heat fluxes to the TES surface than the PCM can diffuse inwards. This is possibly creating depressions in the surface temperatures and the formation of the aforementioned surface layer.

7.3.3 The Thermal Store Discharge Time

A simple experiment was undertaken to determine the discharge times of the TES *within* the ES–DRA (see Appendix C.4.2 on page C–270 for a brief discussion

[1]The cooling rate in this case is *circa* $78 \div (4 \times 2 \times 0.3^2) \sim 108\,\mathrm{W/m^2}$.
[2]See for instance Rochester (1981).

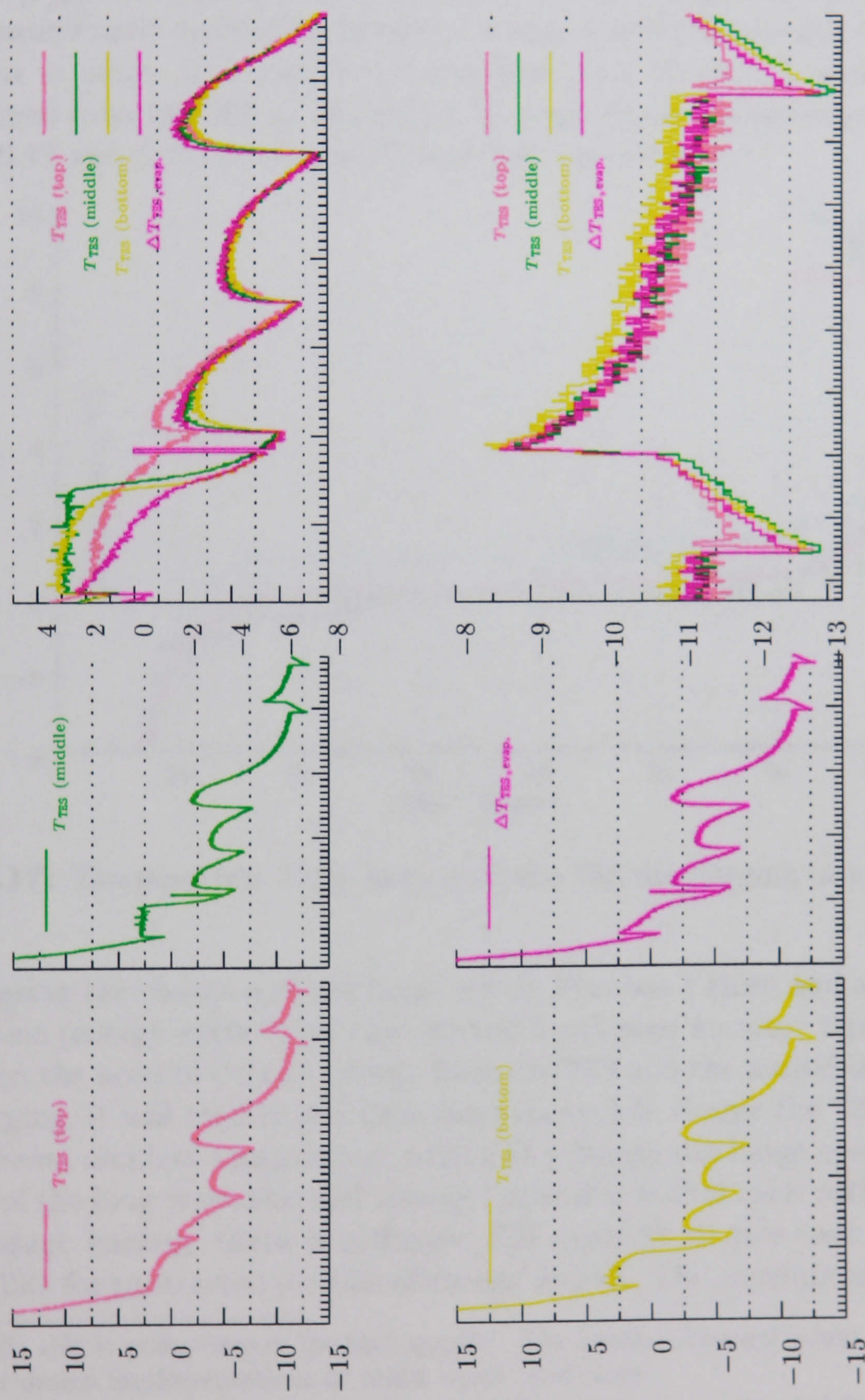


Figure 7.16: Enlargements of indicated portions of Figure 6.15.

on preliminary TES charge–discharge tests outside the ES–DRA). Beginning with a charged TES within the ES–DRA (see earlier on in this section 6.3 on page 200), the procedure was to regulate the ambient temperature to one degree about a fixed temperature and monitor the TES temperature until it rose above its transition temperature (T_{LH}). As expected the temperature–time history curves were smooth, with the characteristic transition–phase plateaux normally associated with first–order changes in state. The results indicate that *circa* 52 and 40 hours of cooling can be obtained from the TES at 25 and 32 °C respectively for an empty appliance, see Figures 6.17 and 6.18, *qv.* pages 208 and 209 respectively.

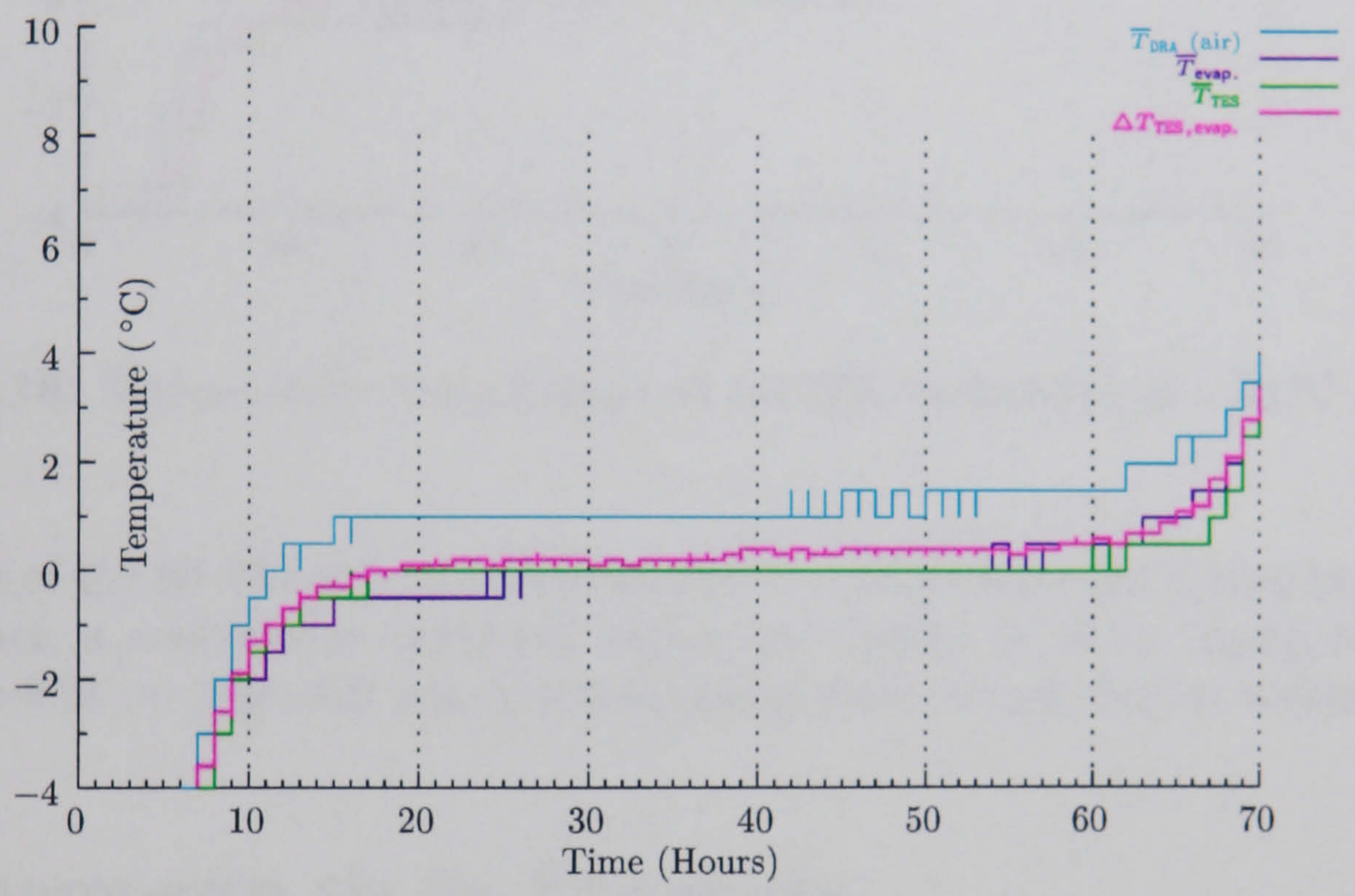


Figure 7.17: Temperature–Time history of the TES discharging in a 25 °C ambient.

In comparing the charge and discharge times, between a third and a sixth of the TES utillisation (energy extraction) time should be allowed for store replenishment[1]. Depending on the need to extract energy from the TES and the availability of energy for TES charging, it will require less time (and energy) to charge the TES during the periods of lowest ambient temperature within the charge–discharge cycle[2]. Another implication of the long–term thermal storage capability is that even *without* electro–chemical storage backup, there is sufficient TES capacity to tide–over an *already–charged* ES–DRA for protracted periods of energy dearth. The constant mean internal

[1] Admittedly, this is prime–mover (power) specific. The results obtained would most certainly differ for other design implementations or under other conditions.

[2] One immediate consequence of this is that lower charge powers can be used for store chaging for a given TES charge–time.

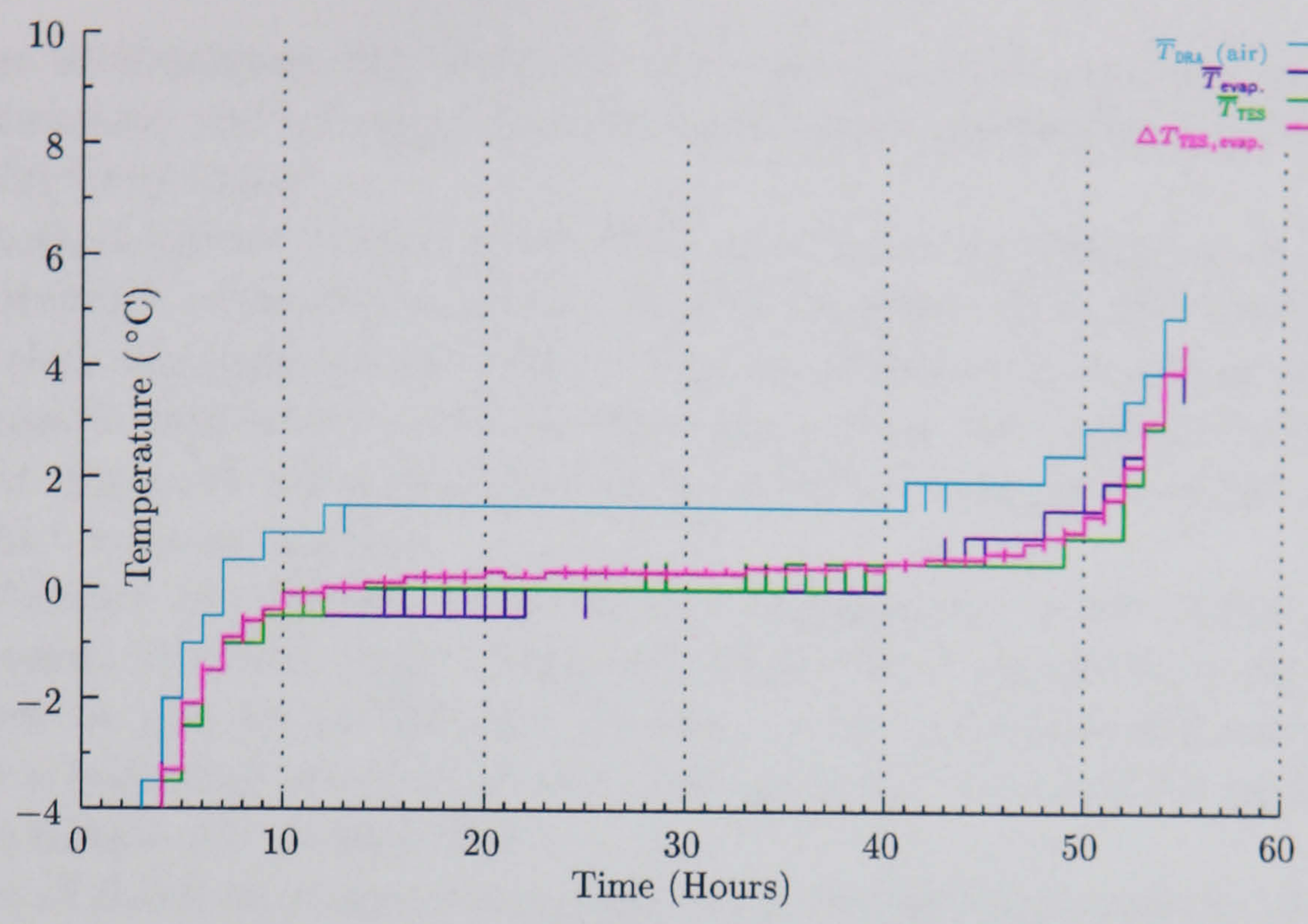


Figure 7.18: Temperature–Time history of the TES discharging in a 32 °C ambient.

temperature of the ES–DRA is further evidence of the temperature stabilising impact–potential such a contrivance can have within the design of DRA's (compare this with Figure 6.31 on page 223 which characterises what occurs during normal DRA operation).

Heat Transmission via the Evaporator

The behaviour of the compressor is discussed briefly in section 6.1.4 on page 195. As can be seen from Figure 6.14 on page 205 the effect of the initial compressor start–up power is to inject heat *into* the ES–DRA. This effect persists in the TES's long[1] after the initial effect on other evaporator surfaces has abated and is observed with every compressor on–off cycle (see also Figure 6.8 on page 197).

Figures 6.19 and 6.20, *qv.* pages 211 and 211 respectively are representations of the temperatures at the mid–points of either side of one of the TES's during discharge cycles at 25 and 32 °C respectively. Of interest are the relatively higher temperatures at the TES–evaporator interface in comparison to those at the TES–ES–DRA air interface. As can be seem from the figures, prior to the commencement of the latent heat absorption phase of the discharge cycle the temperature difference across the TES mid–plane is very small. However, as the TES discharges across the

[1] *circa* 30 minutes.

phase–change temperature, the observed difference increases until the latent heat plateau is traversed and subsequently the temperature difference diminishes with increasing TES temperature.

Although the observed temperature difference across the TES is small, it is particularly remarkable as the expectation is that the presence of the TES would smooth out any interface temperature variations. This establishes the existence of a direct heat transmission path between the ES–DRA interior and the ambient; further, that cognisance of this path must be taken in defining the manner in which the heat ingress to DRA's is to be assessed.

The implication of reducing the number of compressor on–off (initially a heat injection process) cycles is clear. Such reductions[1] in compressor cycling can be brought about by the use of TES and the DRA energy–utilisation efficiency further enhanced by a judicious selection of the control regime employed for energy management, see section 6.5 on page 214.

The effect of this heat transmission path of particular detrimental to the ES–DRA application due to (a) the increased surface area of the evaporator and (b) the fact that the heat exchange temperature is that of the TES, which is $(T_{\text{DRA}} - T_{\text{TES}})$ lower than it would have otherwise been in the absence of the TES's.

While there are considerations which mitigate the use of large evaporators in DRA design (see section 2.4.2 on page 59), from the foregoing it is clear that the larger the evaporator area, the greater the heat transmission into the system; this is clearly definitive of a criterion for the optimisation of the evaporator design. However, it may be more advantageous to seek avenues of curtailing this heat leak prior to proceeding with the search for this optimum.

7.4 Response to Thermal Cycling

In section 2.5.3 on page 66, eqn (2.31) was deduced as a theoretical estimate of the expected lag for the ES–DRA compartment interior relative to changes in the ambient temperature. The existence of this time lag can have a bearing on the optimal energy management strategy for the ES–DRA. In order to quantify this lag, an experiment was set up where the temperature of the environmental chamber was cycled and the response of the air temperature within the appliance monitored. The ES–DRA had previously been switched off and allowed to equilibrate with the chamber ambient temperature. Figures 6.21 and 6.22, *qv.* pages 212 and 213 respectively,

[1] A six–fold reduction is estimated by Michael and Yang (1991), Mithal and Yang (1994); however there is no reason for adherence to this value as the number of on–off cycles is (ES–DRA) controller dependent.

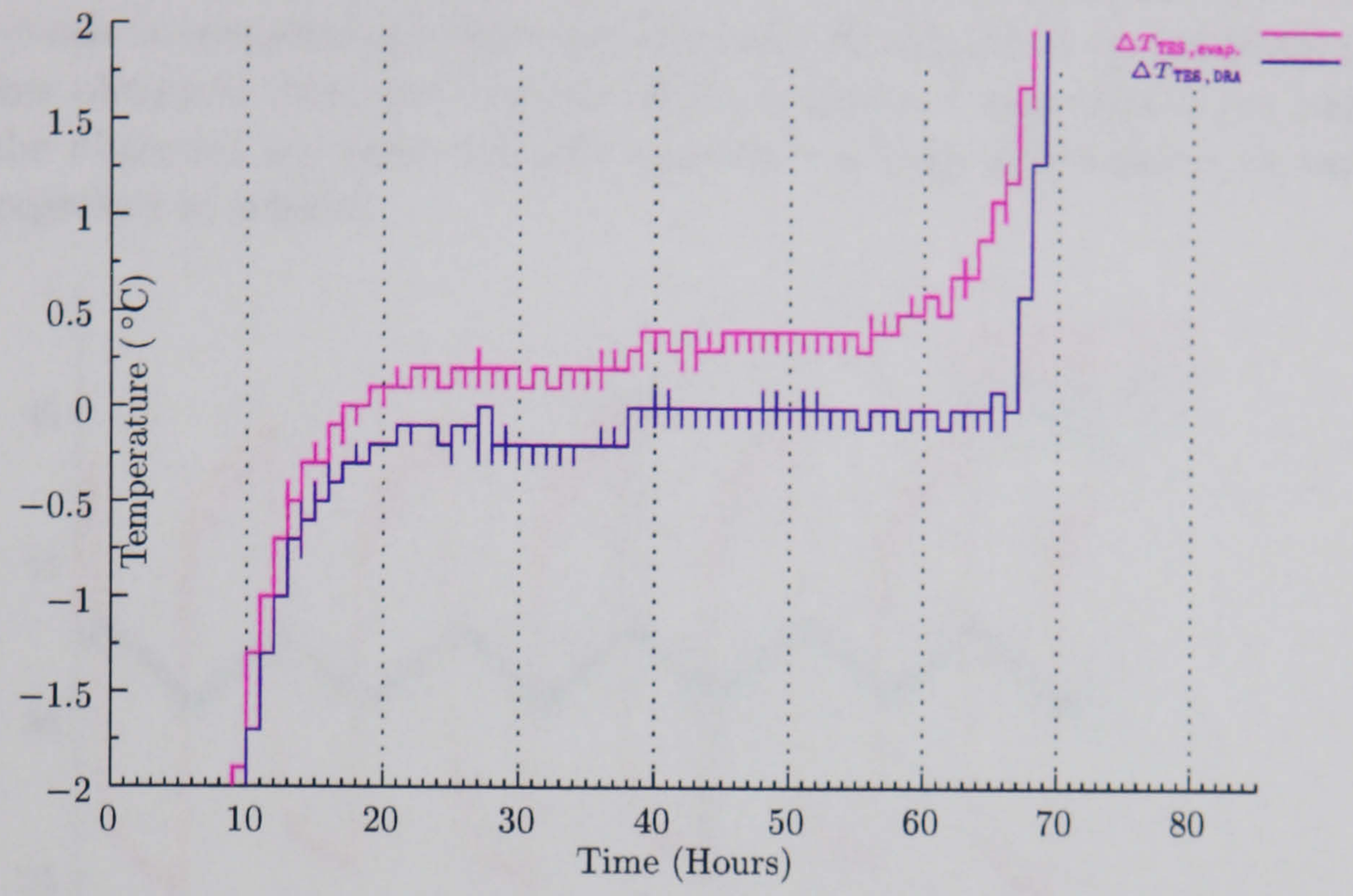


Figure 7.19: Temperatures across the TES mid–plane during discharge at 25 °C.

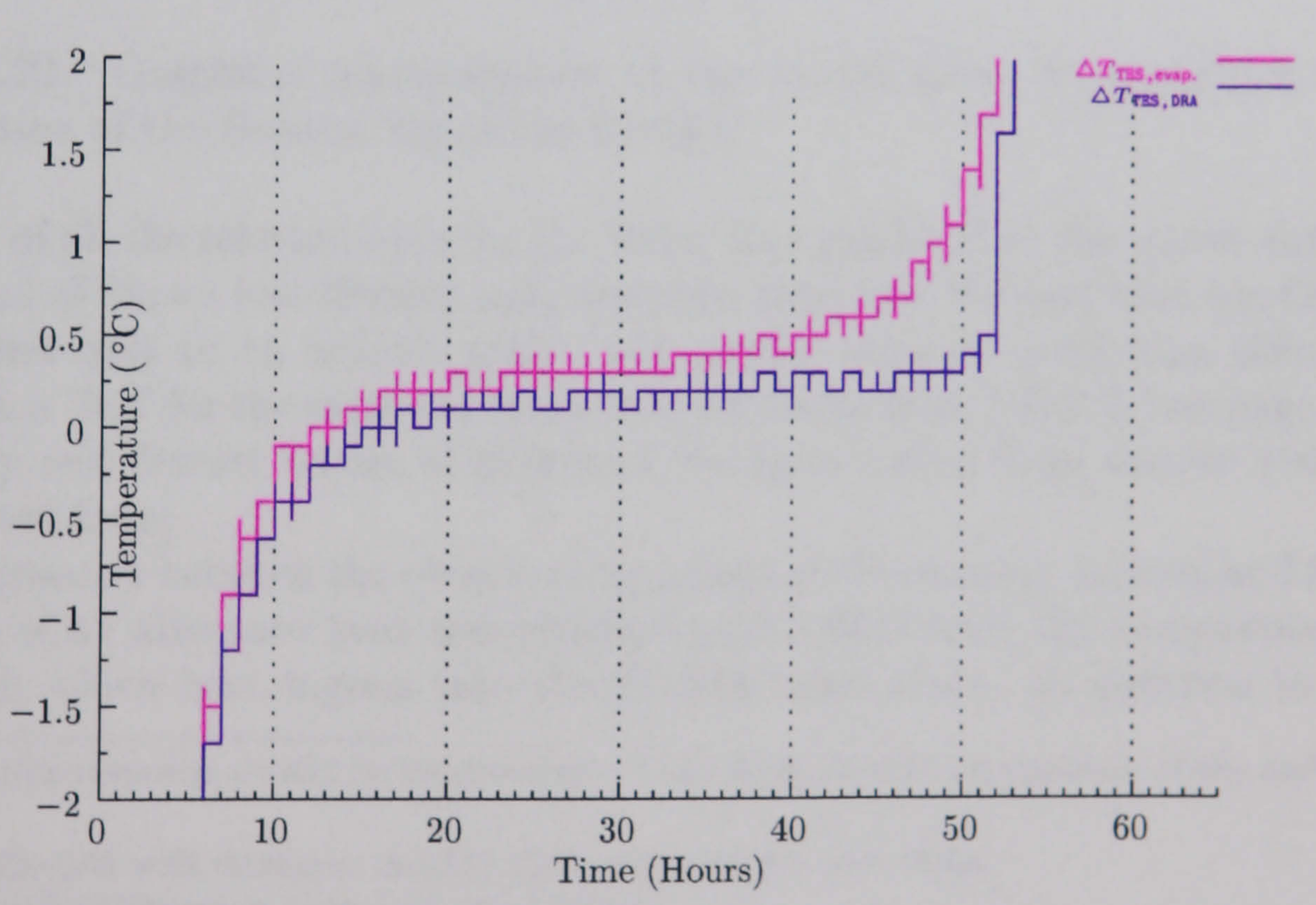


Figure 7.20: Temperatures across the TES mid–plane during discharge at 32 °C.

are graphical representations of the results of one such experimental run[1]. Close inspection reveals a temperature–time lag of about 28 minutes[2]; in comparing this with the value obtained from the first set of experiments (Appendix B on page B-253) where the observed lag time was 240 minutes[3], a large discrepancy in what is intuitively expected is evident.

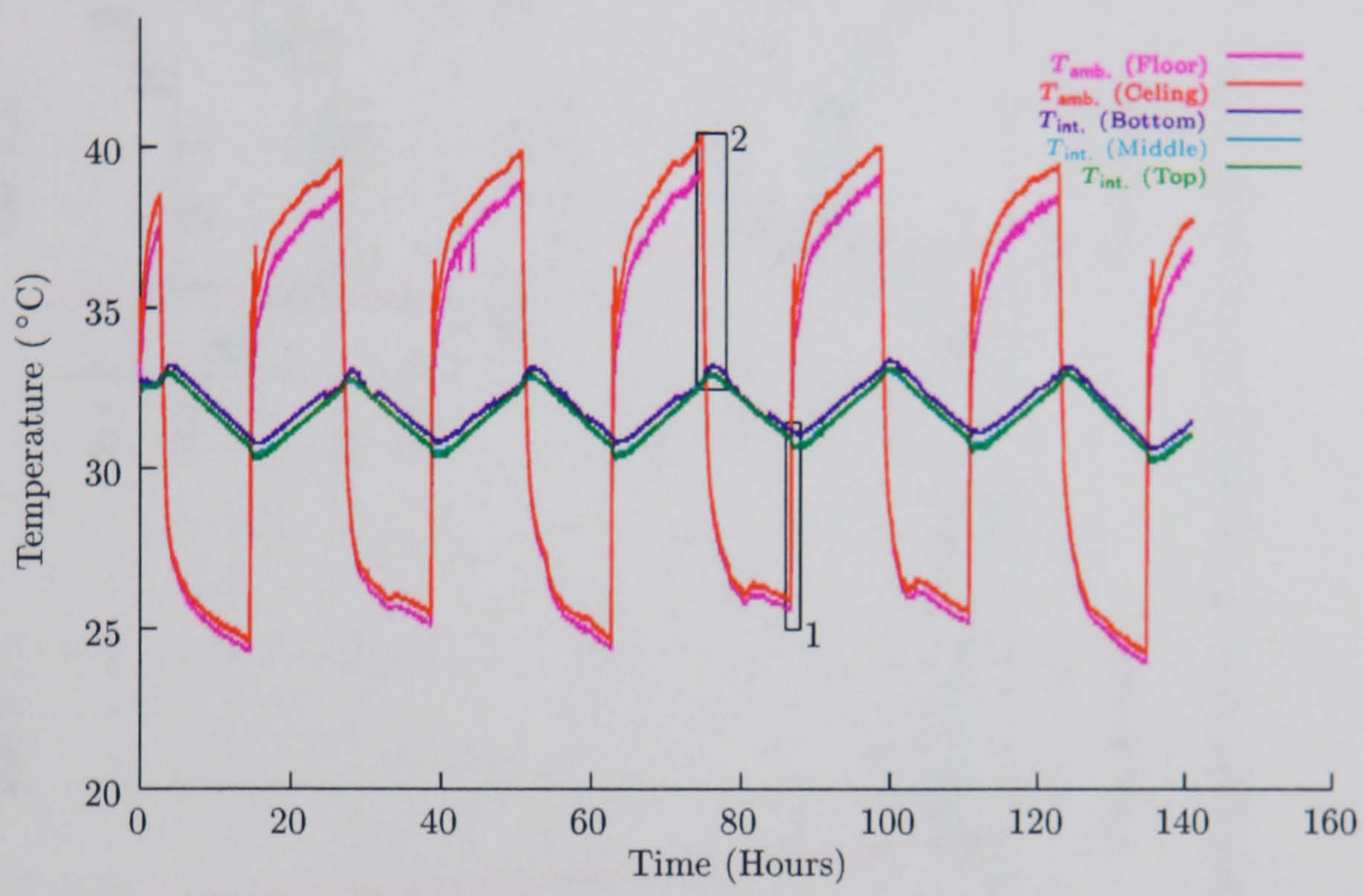


Figure 7.21: Graphical representation of the results from the experimental determination of the thermal lag of the ES–DRA.

The lack of all the relevant data for the VPSI, the variation[4] in the sparse data of the properties of blown low–density polyurethane foam and the fact that eqn (2.31) strictly applies only to an infinite plane wall, makes accurate prediction difficult. Nevertheless, a 'feel' for the expected times may be drawn from Table 6.3 on page 214 (conductivity and density values of polyurethane foam drawn from various sources have been used here).

The discrepancy between the observed lag times (of the insulant–test rig and DRA) is indicative of an alternate heat transmission path, other than the compartment–wall, through which heat ingress into the ES–DRA takes place. In addition to the

[1]In theory, this response should be independent of the changes in the magnitude of the ambient temperature.

[2]The total ES–DRA wall thickness used in these experiments was 48 mm.

[3]The total wall thickness in that case was 57.5 mm.

[4]Two of the several possible reasons for this are (a) the variation in manner and agent employed in blowing the insulant and (b) the tendency for the blown insulant to settle with time.

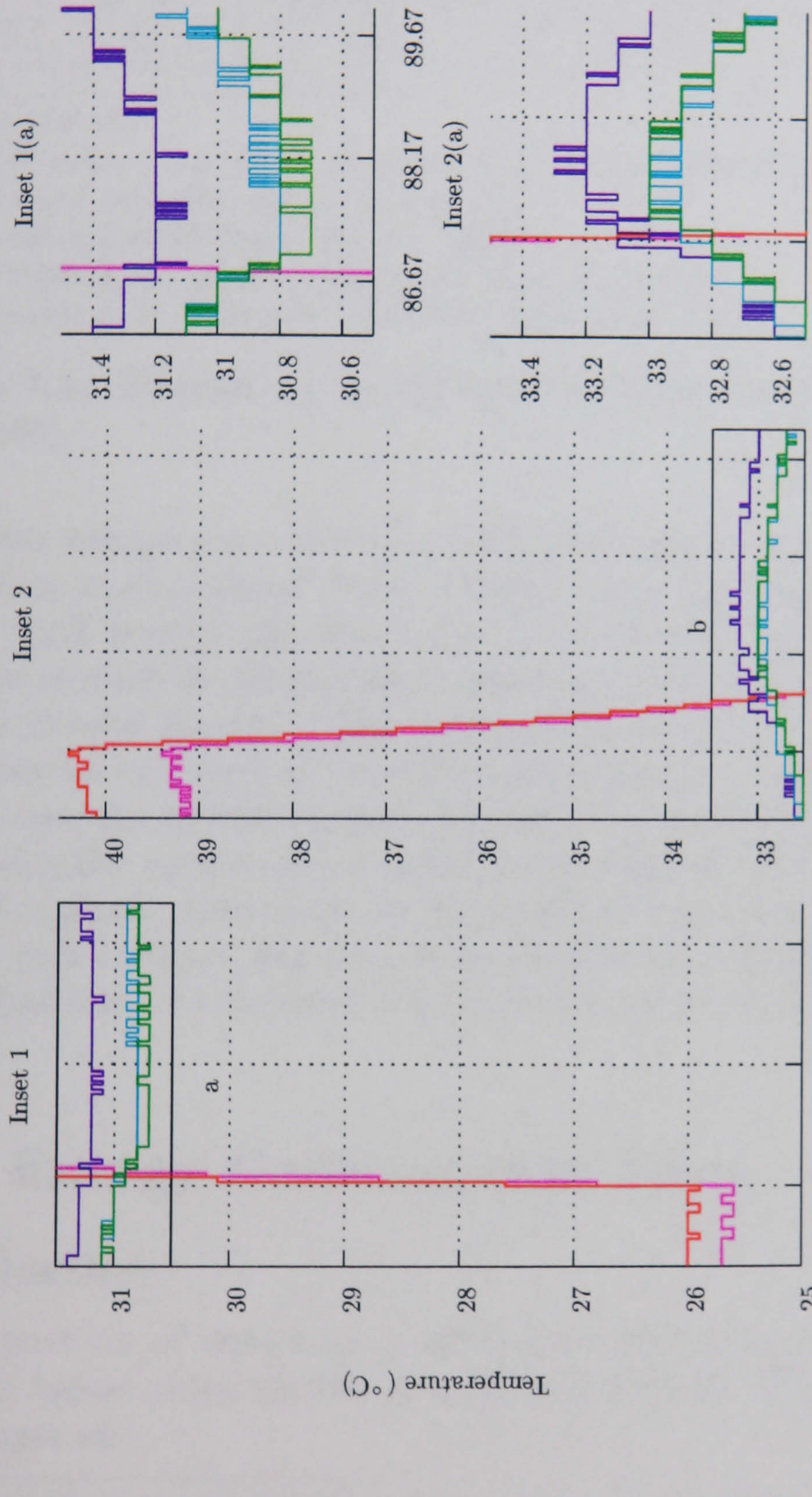


Figure 7.22: Enlargements of various portions of Figure 6.21 on page 212.

	ρ_m $(\mathrm{kgm^{-3}})$	C_p (kJ/kg–K)	k (W/mK)	Lag time (hours)[a]	Lag time (hours)[b]
1.[c]	20	1.400	0.034	0.36	2.46
2.[d]	24	1.59	0.023	0.66	3.18
3.[e]	27–48	0.838–1.046	0.019–0.026	0.46–0.78	2.34–3.92
4.[f]	70	1.045	0.026	1.13	5.03

[a] $h = 4$ W/m²–K.
[b] Ditto h and k = 3.5 mW/mK estimated as in section B.5 on page B–258 using rig dimensions.
[c] Data taken from [Drysdale, 1999, *pp.* 33].
[d] Data taken from [ASHRAE, 1985, *pp.* 23.8].
[e] Data taken from [Guyer and Brownell, 1988, *pp.* 3-13 *ff.*].
[f] Data taken from [Incropera and DeWitt, 1990, App. A3].

Table 7.3: Thermal lag estimates across a polyurethane foam wall based on eqn (2.31).

evaporator–compressor conduction path identified in section 6.3.3 on page 209, the door seal is another likely avenue through which this might take place.

The (half hourly) response time of the ES–DRA to (twelve hourly) changes in ambiance is small in comparison to the mean fluctuation time of the ambient temperature (twelve hourly). This places some restrictions on the available options which may be exercised in developing an intelligent control regime for the ES–DRA and the quantity of PCM required for TES[1]. In the future, attention should be paid to resolving this issue as it not only has implications on the heat gain to the ES–DRA but it also places restrictions on the kernel of control strategies which may be applied to such a device. For the current application, barring COP degradation due to load magnitude, TES charging is best done at times when the ambient temperature is lowest.

7.5 Energy Consumption Tests

Introduction

The next set of tests were performed to determine the (no–load[2]) energy consumption values of the ES–DRA over 24–hour periods. The tests were carried out in three stages *viz*:

[1] For instance, a four–hour lag would mean that, say, the noon–day heat would be 'felt' by the appliance in the early evening, when the ambient temperature was lower and by comparison better COP's were obtainable from the appliance's prime–mover.
[2] This is the current standard test for non–freezing appliances.

- Tests to determine the energy consumption based on a night–time TES charge regime.
- Tests to determine the energy consumption based on a day–time TES charge regime.
- Tests to determine the energy consumption in the absence of TES, where control was effected to ensure that the temperature of the appliance was within normal limits.

In all these tests the environment temperature was varied between (+20 and +32)±1 °C on a twelve–hourly basis to mimic the normal 'diurnal' cycle. Due to the difference in the heating and cooling capacity of the environment control equipment, the thermal control regime for the environmental chamber had to be carefully controlled during the heating periods. For all the experiments assessing energy consumption the following environmental chamber control regime was used:

Period	Temperature (±1) °C.
Morning (06.00am–10.00am)	+26
Midday (10.00am–14.00pm)	+32
Evening (14.00pm–18.00pm)	+25
Night (18.00pm–06.00am)	+20

Table 7.4: Daily ambient–temperature set–points used during the experiments.

The principal problems which were encountered with the data collection process during this stage had to do with (a) the 40 Hz ripple introduced into the system by the compressor, discussed in item A.4 of Appendix A.4 on page A-251 and (b) the occasional spurious reading in the acquired data. This ripple tended to affect the current readings to a greater extent than the voltage readings, with variations in adjacent data of up to a maximum of 20% as compared with only 0.3% for the latter; the issue as to how the data is to be interpreted is dealt with in Appendix A.2.5 on page A-243. While these fluctuations had varying effects on the computation of the instantaneous values of the power consumption and COP of the prime mover, the mean and cumulative values remained within what are considered as normal limits.

Except where otherwise stated, the control set–point temperature for the ES–DRA interior was +4 ± 2 °C. The criteria for *recharging* the TES was based on the assumption that recharging will commence *prior* to full discharge of the TES. This will negate the need to re–initiate the phase transition process and avoid the accompanying sub–cooling effect.

In the relevant cases, the TES charge process was continued until the mean temperature of the TES fell two degrees below the phase–transition temperature. This

was to ensure that there could be no question as to energy saved during partial TES charging augmenting the energy consumption figures of the ES–DRA. Thus the TES will be assumed to be fully recharged each day if the mean TES temperature[1] lies below -2.5 °C. Due to the nature of the TES charge control process, some degree of compressor cycling was inevitable. However, this served only to compromise the various indices of energy performance for this control regime and the extent of the benefits therein. Preliminary tests indicate that this cycling is unnecessary and should be one area which is examined carefully in the quest to further improve appliance performance.

7.5.1 Night–Time Only Prime–Mover Operation

The ES–DRA was run in a simulated diurnal thermal environment (20 °C night–time and 32 °C day–time) and the appliance response logged over several days. TES charging was done during the time window of 21:00–02:00 hours each day and the charge criterion was to ensure that the mean TES temperature at the end of each charge cycle was between (1–2) °C[2]. In spite of the compressor cycling mentioned in the last paragraph of the previous section, the results obtained are sufficient to indicate the potential advantages of the concept. Several experimental runs were made, each lasting a number of days, and the data analysed. Tables 6.5 and 6.6, *qv.* pages 217 and 219 respectively, presented below provide a summary of two such set of results (for different minimum TES charge temperatures); agreement of the data (within each table) is within normal (*circa* 10%) limits.

A more extensive graphical representation of these results is presented in Figure 6.23 on page 217 (COP values), Figure 6.24 on page 218 (Voltage and Current values), Figure 6.24 on page 218 (Energy throughput) and Figure 6.25 on page 218 (Temperature profiles).

[1]Measured at the top, (air–side) middle and bottom.

[2]Other preliminary tests were run using lower control temperatures *e.g.* between (-3 and -2.5) °C. These indicated that no benefit was obtained by charging the TES to temperatures lower than just below the phase change temperature (T_{LH}), as the energy stored in those cases will be sensible heat energy (see Tables 6.5 and 6.5, on page 217).

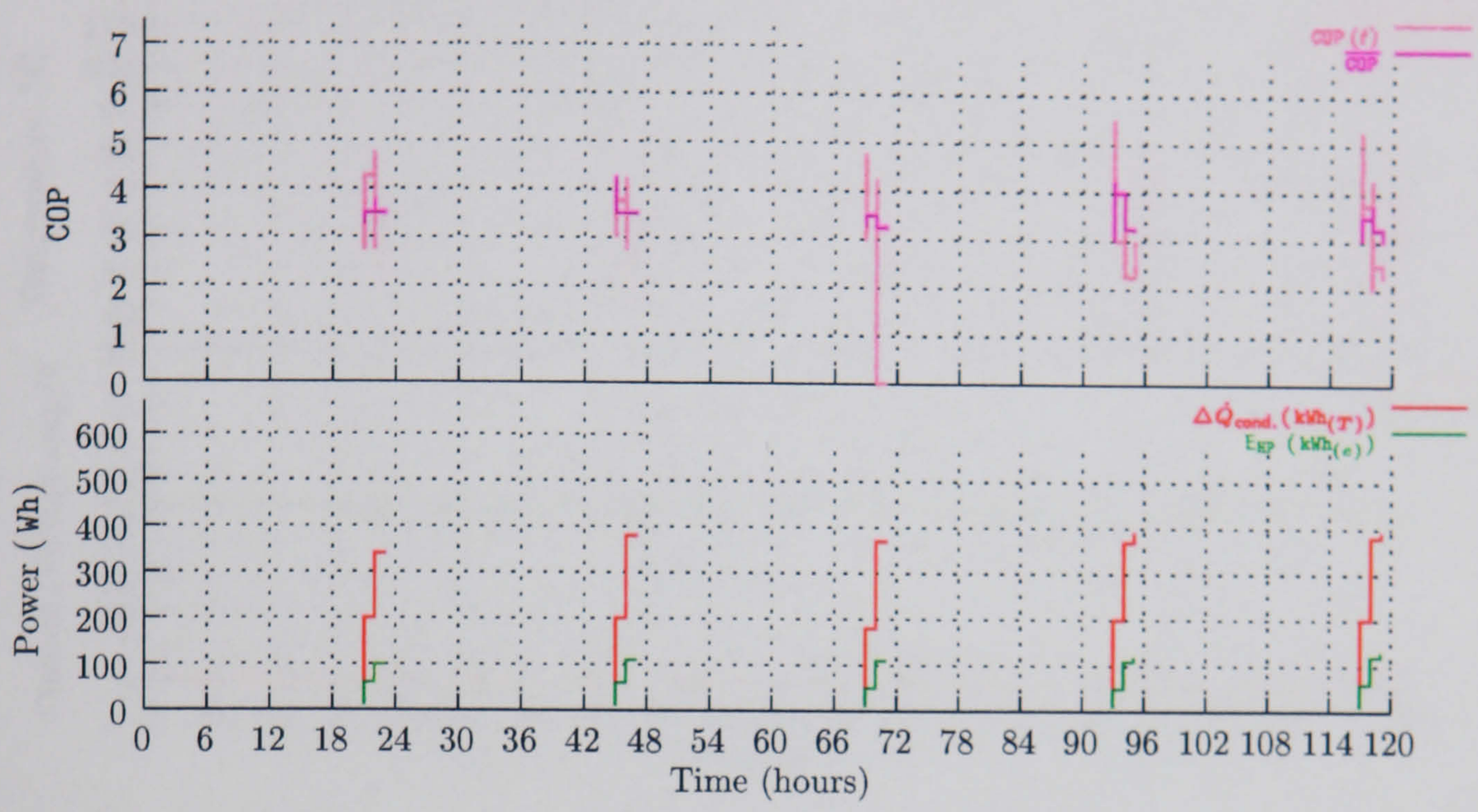


Figure 7.23: Instantaneous and mean coefficient of performance COP (top), condenser heat ejected, $Q_{condenser}$ ($\mathtt{kWh}_{(T)}$), and compressor energy consumption, $\mathtt{E}_{HP}$ ($\mathtt{kWh}_{(e)}$, bottom), during compressor 'on' periods for the night–time control regime.

Day	Compressor					DRA	TES	Evap.
	COP	Consumed		On–time		Temperature		
		E ($\mathtt{Wh}_{(e)}$)	P ($\mathtt{W}_{(e)}$)	(hours:mins)	cycles	°C		
1	3.50	100	55	1:49	1	36.5	0.5	-0.5	-2.0
2	3.50	110	55	1:59	1	37.0	1.0	-0.5	-2.0
3	3.25	110	55	1:53	1	37.0	0.5	-0.5	-2.0
4	3.25	120	55	2:04	1	37.5	1.0	-0.5	-2.0
5	3.00	130	60	2:04	1	38.0	1.0	-0.5	-1.5

Table 7.5: Summary of experimental results for the night–time prime–mover control regime. TES control temperature $(-2 - -1)$ °C. The values displayed in this table are 24–hourly mean values.

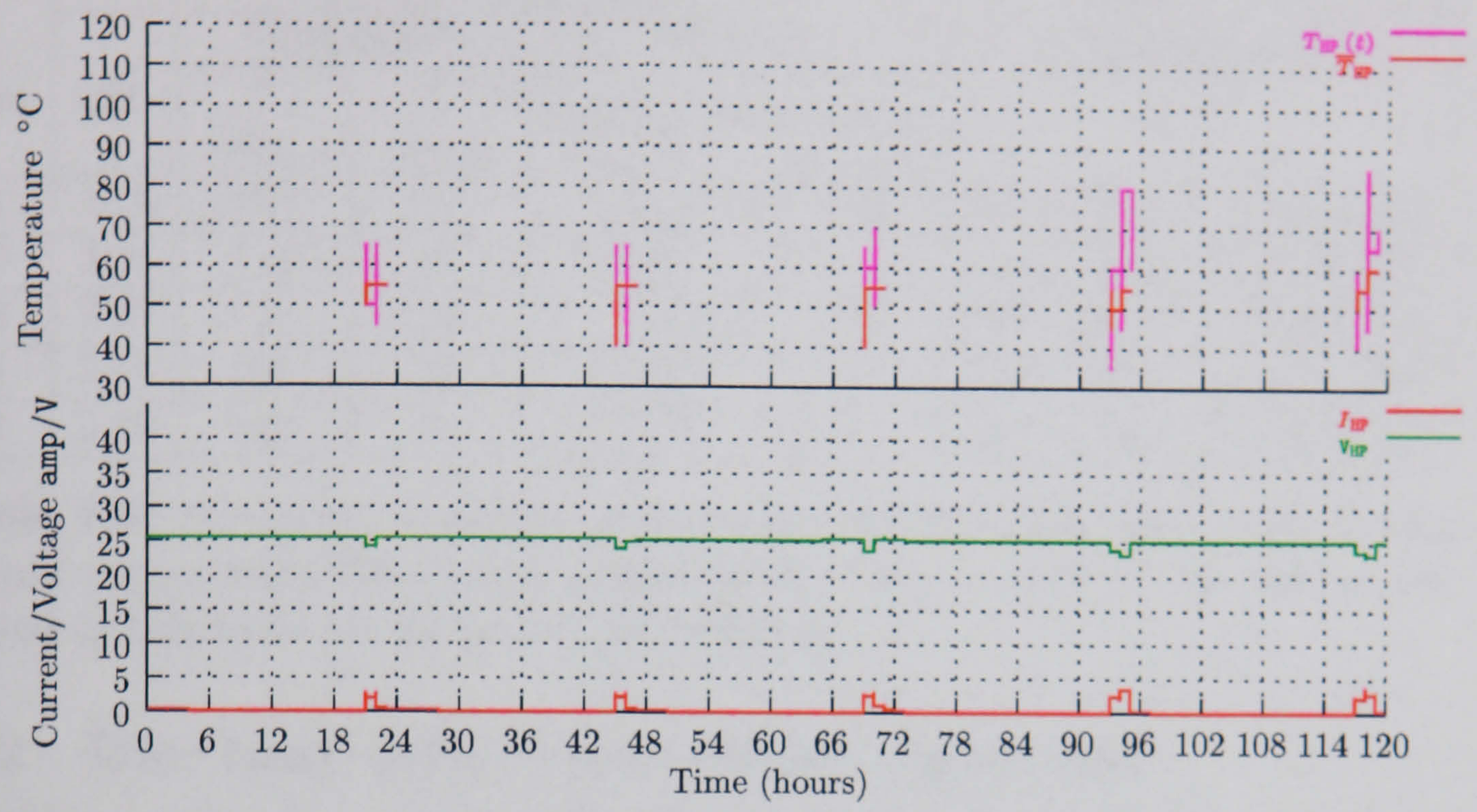


Figure 7.24: Compressor Temperature profile T_{HP} (top), Voltage V_{HP} and Current drawn (bottom) during compressor 'on' periods for the night–time control regime.

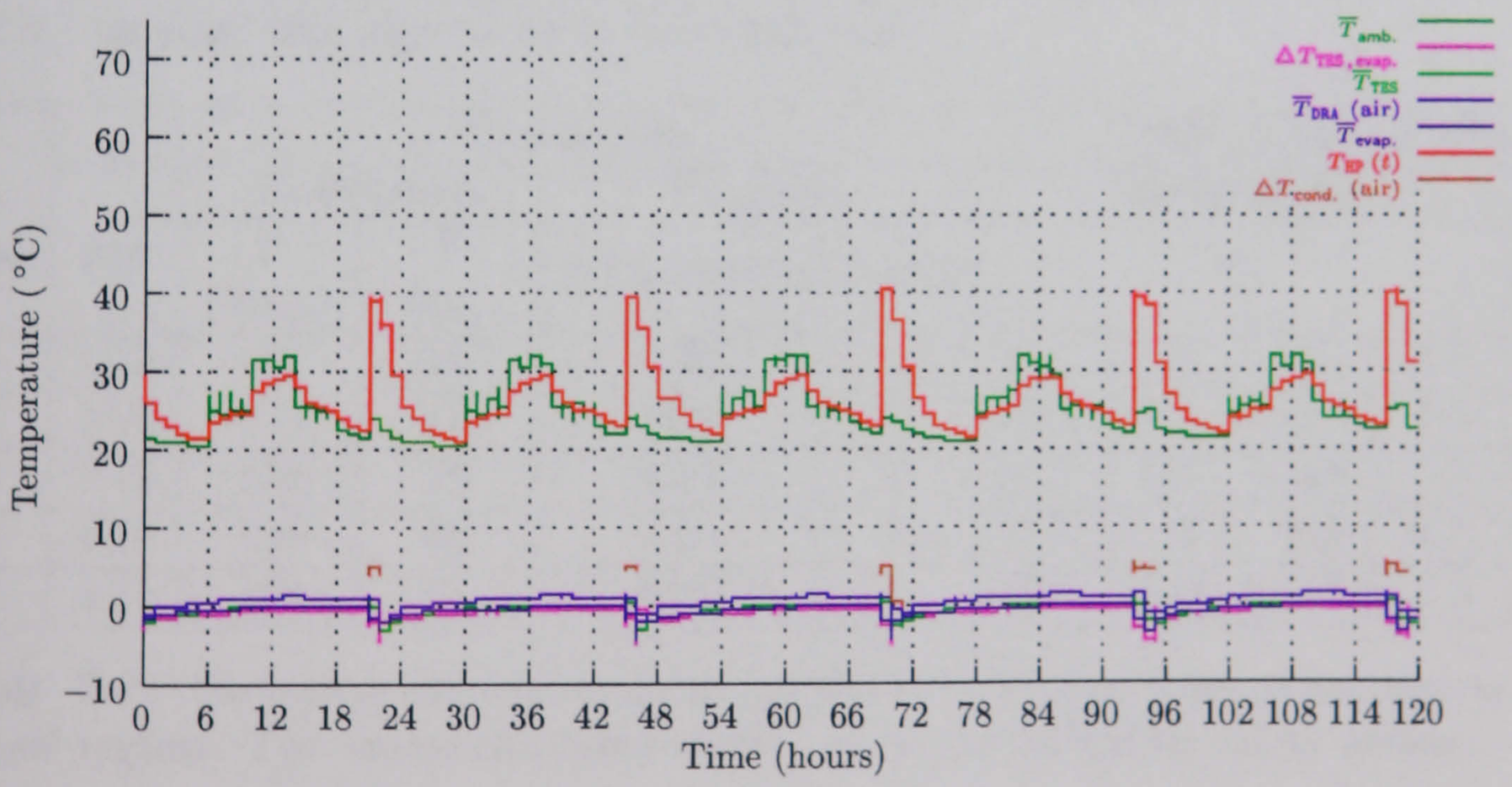


Figure 7.25: Mean temperature profile at various locations on the experimental rig (bottom) during compressor 'on' periods for the night–time control regime.

Day	Compressor					DRA	TES	Evap.
	COP	Consumed		On–time		Temperature		
		E ($Wh_{(e)}$)	P ($W_{(e)}$)	(hours:mins)	cycles	°C		
1	3.25	100	55	1:53	2	35.5	0.5	-1.0	-2.5
2	3.25	120	55	2:04	2	35.0	0.0	-1.0	-3.0
3	3.25	110	55	1:59	2	35.0	0.0	-1.0	-2.5
4	3.50	100	50	1:59	2	36.0	0.0	-1.0	-2.5
5	3.25	110	55	1:59	2	36.0	0.5	-1.0	-2.5

Table 7.6: Summary of experimental results for the night–time prime–mover control regime with TES control temperature $(-3.0 - -2.5)\,°C$. The values displayed in this table are 24–hourly mean values.

7.5.2 Day–time only Prime–Mover Operation

Similar energy consumption tests (day–time TES–charge regime), were run to establish the energy–use profile of the ES–DRA when the compressor was operated only during the day. The ES–DRA was run in a simulated diurnal thermal environment (20 °C night–time and 32 °C day–time) and the appliance response logged over several days. Charging was done typically between the period 10:00 – 15:00 hours each day (the simulated 'heat of the day'). Several experimental runs were made over a number of days each, and data analysed. One set of results is summarised in Table 6.7 on page 219; agreement is to within 10%.

Day	Compressor					DRA	TES	Evap.
	COP	Consumed		On–time		Temperature		
		E ($Wh_{(e)}$)	P ($W_{(e)}$)	(hours:mins)	cycles	°C		
1	2.75	170	70	2:29	1	41.5	1.0	-0.5	-1.5
2	3.00	150	65	2:19	1	41.5	1.0	-0.5	-1.5
3	2.75	170	70	2:25	1	41.5	1.0	-0.5	-1.5
4	2.75	160	65	2:25	1	41.5	1.0	-0.5	-1.5
5	2.75	160	65	2:25	1	42.0	1.0	-0.5	-1.5

Table 7.7: Summary of experimental results for the day–time prime–mover control regime. The values displayed in this table are 24–hourly mean values.

The results are presented graphically in greater detail in Figure 6.26 on page 220 (COP values), Figure 6.27 on page 220 (Voltage and Current values), Figure 6.27 on

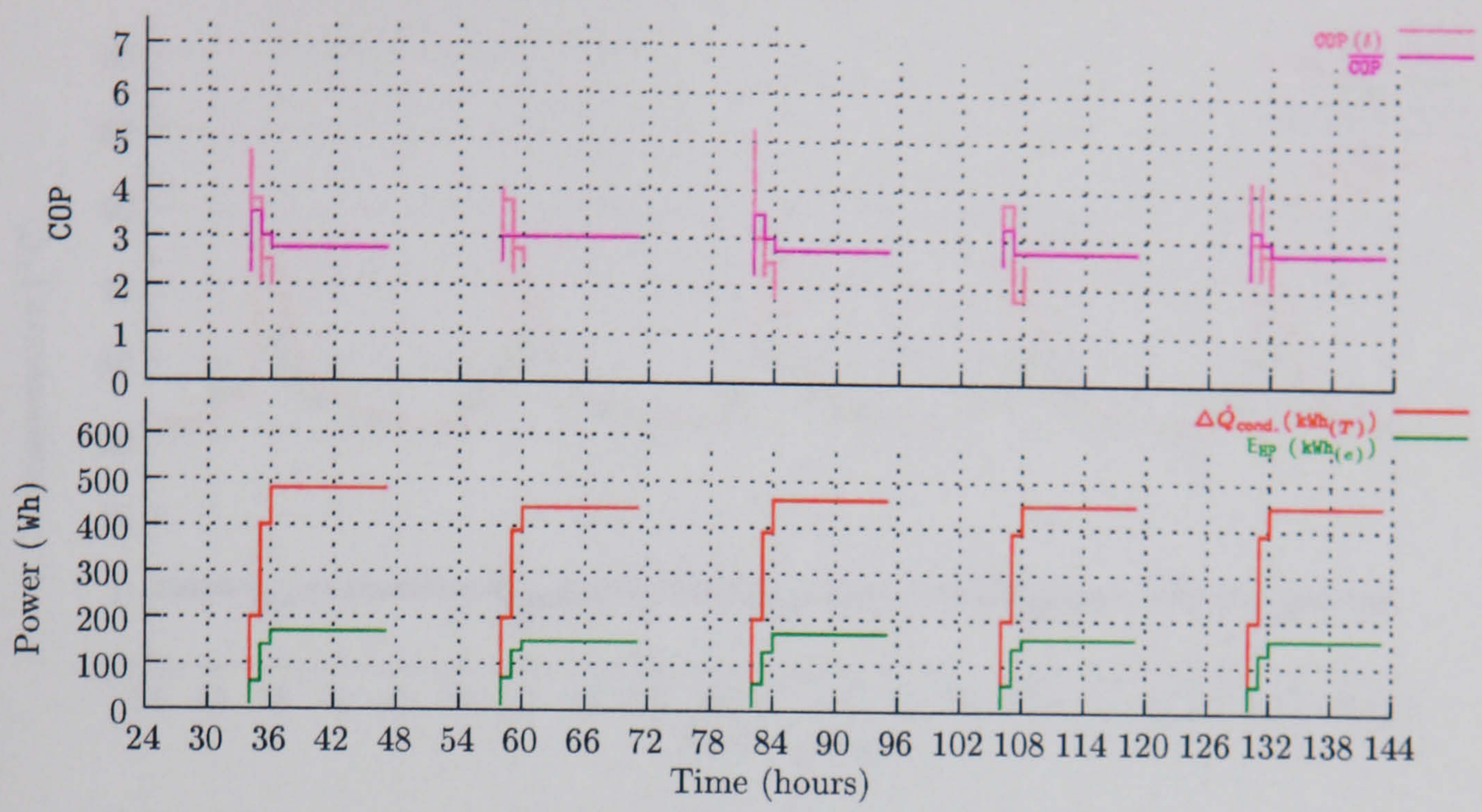


Figure 7.26: Instantaneous and mean coefficient of performance COP (top), condenser heat ejected, $Q_{condenser}$ ($\mathtt{kWh}_{(T)}$), and compressor energy consumption, $\mathtt{E}_{\mathtt{HP}}$ ($\mathtt{kWh}_{(e)}$, bottom), during compressor 'on' periods for the day–time control regime.

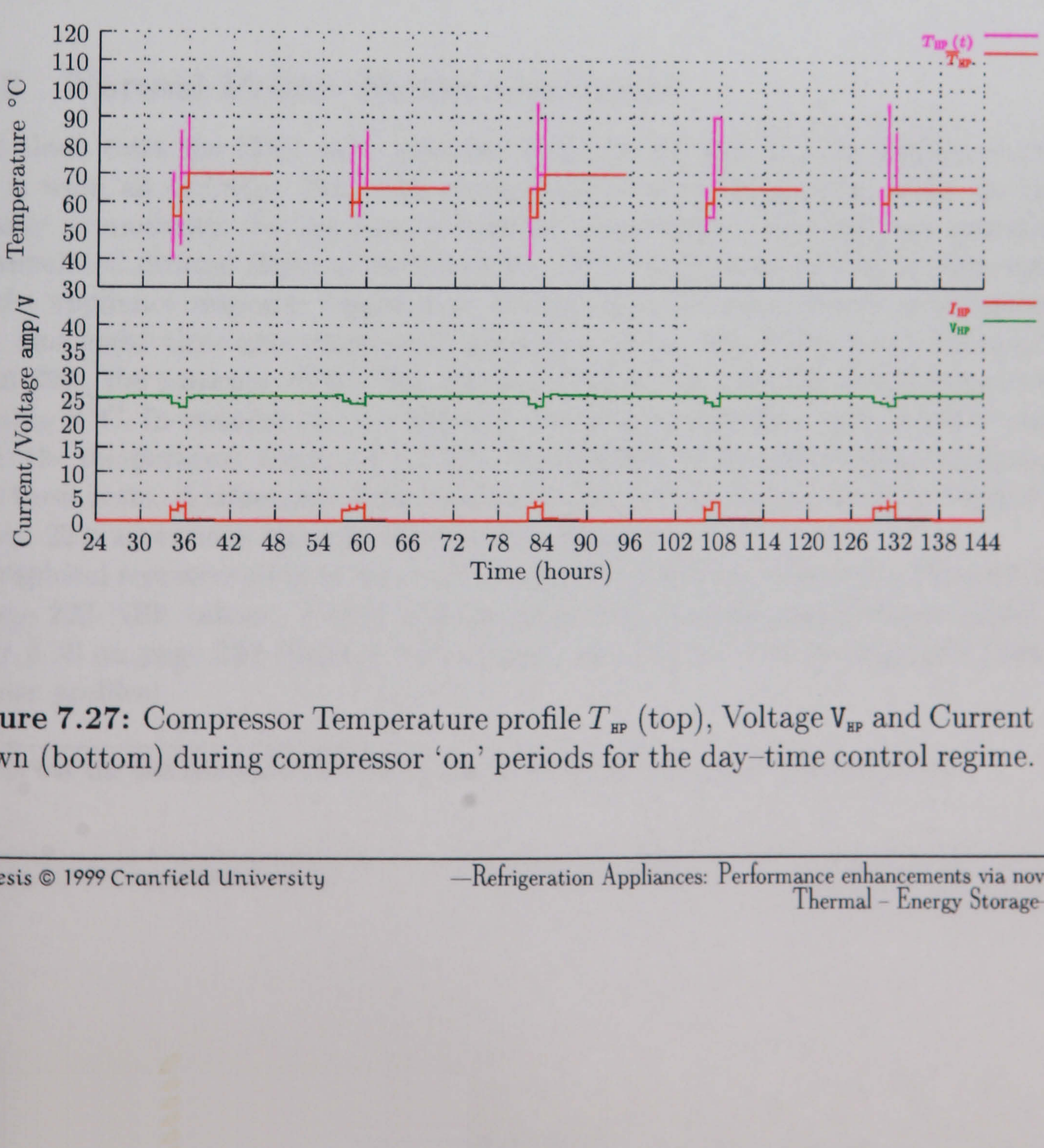


Figure 7.27: Compressor Temperature profile $T_{\mathtt{HP}}$ (top), Voltage $\mathtt{V}_{\mathtt{HP}}$ and Current drawn (bottom) during compressor 'on' periods for the day–time control regime.

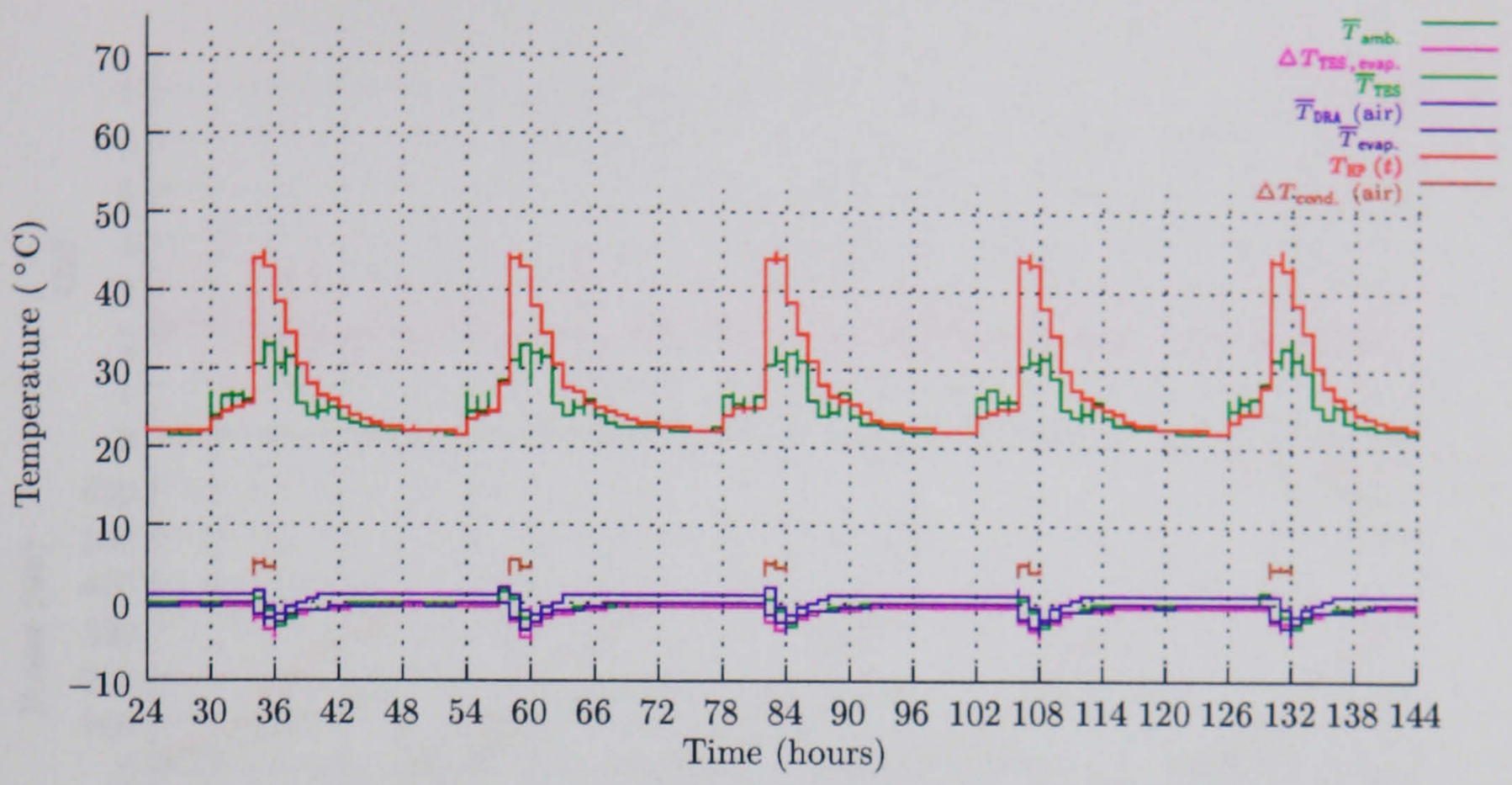


Figure 7.28: Mean temperature profile at various locations on the experimental rig (bottom) during compressor 'on' periods for the day–time control regime.

page 220 (Energy throughput) and Figure 6.28 on page 221 (Temperature profiles).

7.5.3 Normal Prime–Mover Operation

In these tests the TES's were removed from the ES–DRA and the appliance run as if it were an ordinary DRA, with compressor activity dependent solely on the necessity to moderate the appliance's internal temperature. The DRA was operated in a simulated diurnal thermal environment (20 °C night–time and 32 °C day–time and the appliance response logged over several days. In the previous experiments (day– and night–time only compressor operation tests), due to the small volume of the ES–DRA, the presence of the TES ensured that at all times the air temperature was *circa* 0 °C. In running the no–TES test, the DRA temperature was found to stay within the temperature range $+4 \pm 2$ °C[1]; this is likely to bias the findings in favour of the these tests. A summary of the analysis of the results are presented in Table 6.8 on page 222; agreement again is within normal limits.

Graphical representation of the results in greater detail is presented in Figure 6.29 on page 222 (COP values), Figure 6.30 on page 223 (Voltage and Current values), Figure 6.30 on page 223 (Energy throughput) and Figure 6.31 on page 223 (Temperature profiles).

[1]This was the DRA internal temperature control set–point used for all the experiments.

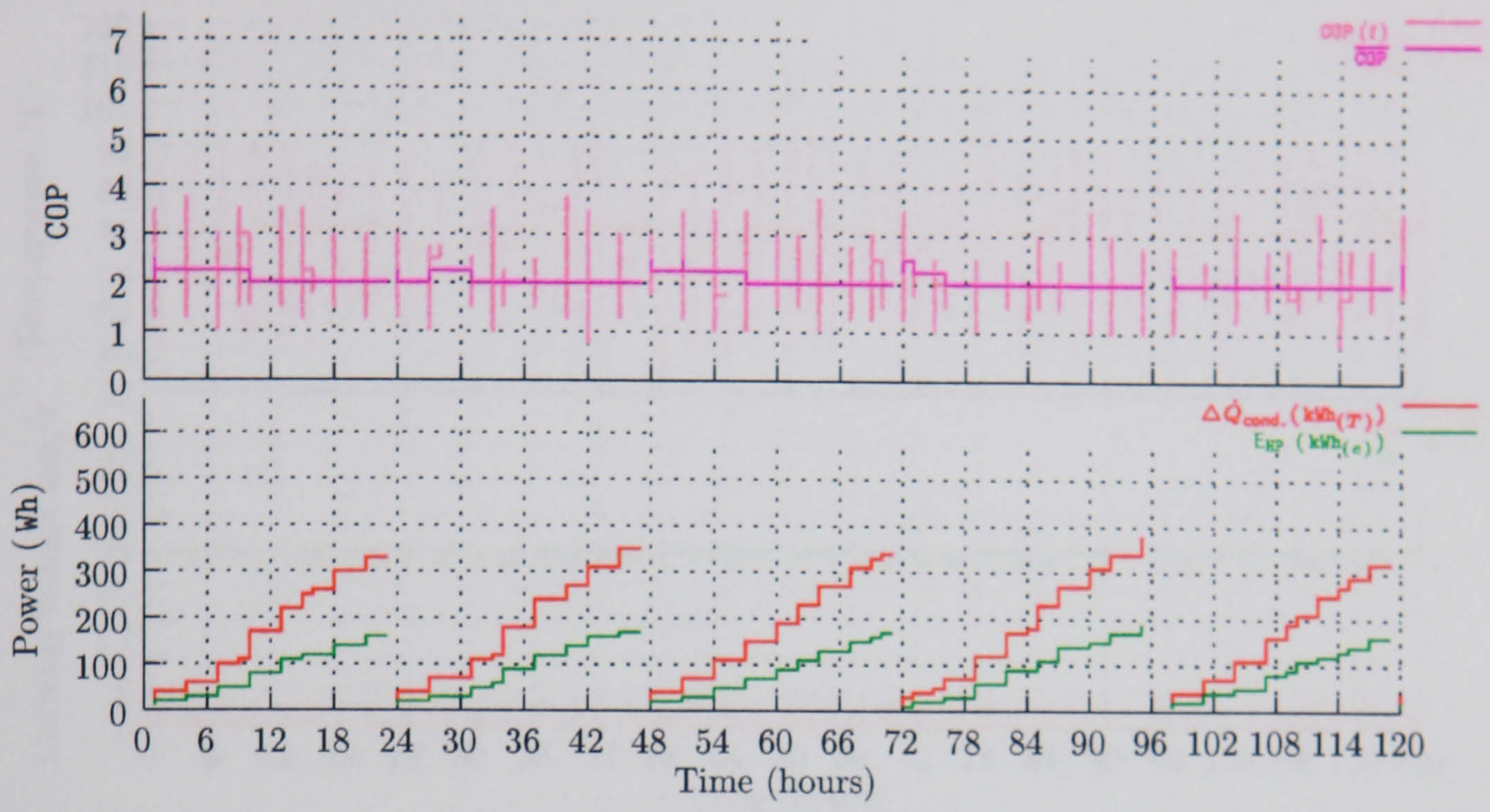


Figure 7.29: Instantaneous and mean coefficient of performance COP (top), condenser heat ejected, $Q_{condenser}$ (kWh$_{(T)}$) and compressor energy consumption, E_{HP} (kWh$_{(e)}$, bottom), during compressor 'on' periods for the normal–operation mode scenario.

Day	Compressor					DRA	TES	Evap.
		Consumed		On–time		Temperature		
	COP[a]	E (Wh$_{(e)}$)	P (W$_{(e)}$)	(hours:mins)	cycles	°C		
1	2.0	160	70	2:17	8	31.5	3.5	–	-4.5
2	2.0	170	70	2:23	8	32.0	3.5	–	-4.5
3	2.0	170	70	2:21	9	32.0	3.5	–	-3.5
4	2.0	190	75	2:35	9	32.0	3.5	–	-4.0
5	2.0	160	70	2:12	8	32.5	3.5	–	-3.5

Table 7.8: Summary of experimental results for the 'normal mode' prime–mover control regime. The values displayed in this table are 24–hourly mean values.

[a]The *compressor* manufacturer quotes a value of 1.15@32 °C ambient and a -10 °C evaporating temperature. However, the DRA manufacturer's tests indicate values of *circa* 1.5 and 1.6 @32 °C without and with a (sensible–heat) TES in place respectively, a discrepancy attributed to the relatively large surface area of the evaporator (*circa* 0.44m²) which is *circa* four times what would be expected in a conventional 1101 DRA.

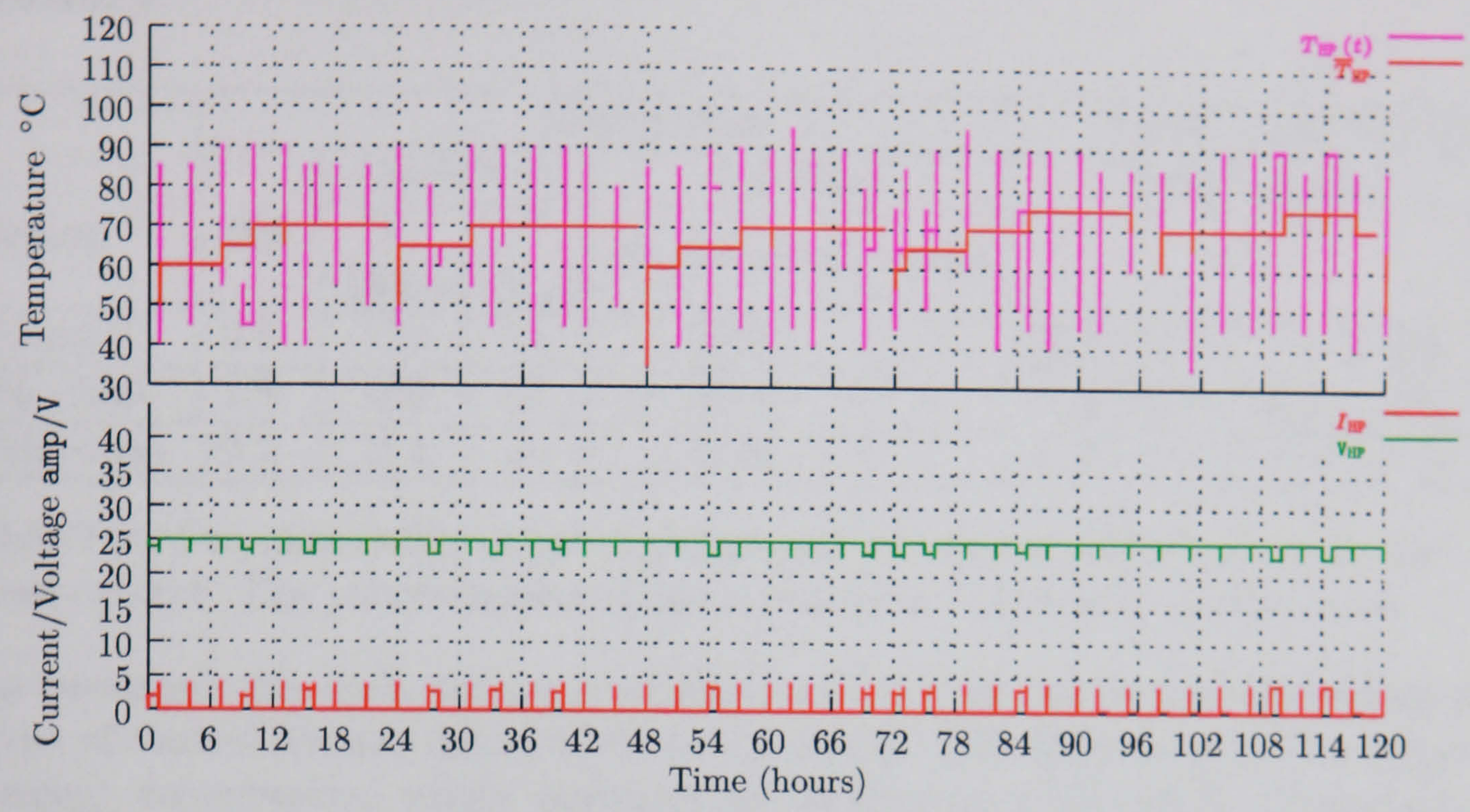


Figure 7.30: Compressor temperature profile T_{HP} (top), Voltage V_{HP} and Current drawn (bottom) during compressor 'on' periods for the normal–operation mode scenario.

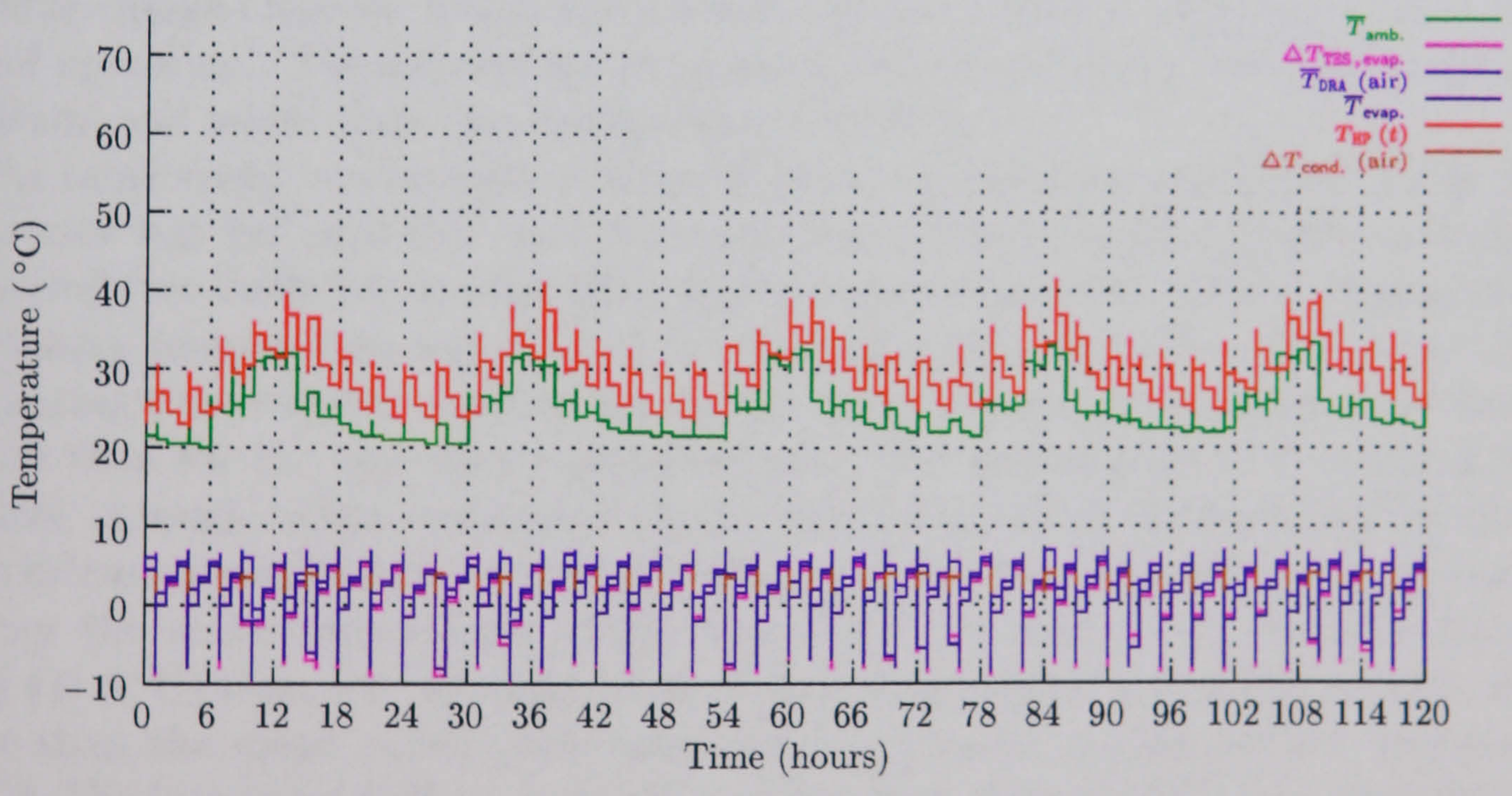


Figure 7.31: Mean temperature profile at various locations on the experimental rig (bottom) during compressor 'on' periods for the normal operation mode scenario.

Summary

Regime	Compressor					DRA	TES	Evap.
		Consumed		On–time		Temperature		
	COP	E ($Wh_{(e)}$)	P ($W_{(e)}$)	(hours:mins)	cycles	°C		
Normal	2.0	170	71	2:22	8	32.0	3.5	–	-4.0
Day–time	2.8	162	67	2:25	1	41.5	1.0	-0.5	-2.0
Night–time	3.3	114	56	1:58	1	37.0	1.0	-0.5	-1.5

Table 7.9: Summary table of the experimental results for all regimes of prime–mover control. The values displayed in this table are 24–hourly mean values.

As envisaged, the daily energy consumption of the ES–DRA varied depending on the type of control regime employed for its operation. The differences in the respective energy consumption values indicate the superiority of the night–time control regime over the day–time control regime (42%) which in turn was superior (6%) to what would be obtained under normal operation. The percentage improvement in the energy consumption between the 'normal–operation' and night–time only regime was *circa* 52%.

A similar trend is observed with respect to the COP values, where the night–time charge regimen offers superior performance (18%) over that achieved with the day–time charge regimen, which in turn was superior (40%) to that delivered under normal operation. The percentage improvement in the COP between the 'normal–operation' and night–time only regime was *circa* 65%.

The same trend can be seen in other indices *e.g.* the total period for which the compressor was 'on' each day[1] and the mean power drawn by the compressor during this period (see Table 6.9 on page 224). In both cases where the TES was in place, the evaporating temperature was *circa* 2–2.5 °C *higher* than for the no–TES case. The evaporating temperatures reached during the night–time control regime were lower (0.5 °C) than for the day–time control regime. This is probably as a result of the heat leak through to the evaporator via its connections to the ambient (compressor and condenser) establishing a slightly higher equilibrium evaporating temperature. However the mean temperature of the compressor was higher for day–time charge cycles (41.5 °C) than for the night–time charge cycles (35.5 °C), which in turn was higher than the mean compressor temperature observed during normal operation (32 °C). The former probably occurs on account of the lower night–time temperature while the latter is due to the intermittent nature of the 'normal operation' process allowing the compressor temperature to drop.

[1] This can have far reaching implications in situations where energy supply is infrequent.

In evidence (see Figure 6.31 on page 223 and section 6.3.2 on page 203) is the effect of the intermittent start–up energy consumption on the temperature of the compressor and the TES in the relevant cases (this heat will *also* be ejected into the system during normal operation).

7.5.4 Conformance to the Regulatory Standards

In 1996 the EU essentially adopted the GEA long–term standards for DRA energy consumption as the targets for appliances manufactured or acceptable within its member states (see EU (1996)). In confirming that the energy performance of the designed ES–DRA conforms to that standard, the energy consumption values obtained here are to be compared with the estimates given in the following table, which was drawn up based on research done by Waide (1993) for the proposed 1997 standards. Except where otherwise stated, the values are for 32 °C day–time and 25 °C night–time ambients:

	Daily Energy Consumption $kWh_{(e)}$	
Standard	Short–term (up to 1997)	long–term
Following 1992 trend	0.698	
GEA[a]	0.678	0.313
Greenpeace[b]	0.621	0.382
Vacuum panel insulant (Waide, *loc. cit.*) estimate[c]		0.140
Polyurethane foam–VPSI estimate (*qv.* section 6.3.2 on page 191)		0.026
ES–DRA measured value ('normal–operation' mode *qv.*)		0.170[d]
ES–DRA measured value (night–time regime *qv.*)		0.114[e]

[a]For a 32 °C ambient.
[b]For a 32 °C ambient.
[c]For a 25 °C ambient.
[d]Five–day average.
[e]Five–day average.

Table 7.10: Comparion of the energy consumption of the ES–DRA with different standards and projected estimates.

7.6 Discussion

This section discusses the observations made during the process of obtaining the results presented in this chapter, and the implications of the use of such an ES–DRA in harsh thermal environments and for applications with erratic or impoverished energy

supply. In commencing this discussion, the observation is made that the results furnished here support the preliminary results given by Michael and Yang (1991) and Mithal and Yang (1994).

As with most experimental prototypes, a few quirks will exist within the system which will need to be resolved during the reiterative phases of the development stage. There are one or two issues not covered in the main discussion on which a cursory note will be made prior to a summary analysis of the material presented here. However, on no account was the ES–DRA adjudged to have failed in any of aspect of the stipulated criteria.

The first is the observation that a slight amount of frost formation appeared on the surface of the TES–DRA (corrugated steel) interface. This was due to the sub–zero degree Celsius transition–temperature required for charging the TES, an issue compounded by the sub–cooling effect observed during the charge phase. It is probable that the use of a polymer as a replacement for this interface may have alleviated this problem, but this might have deleterious effects on the heat transfer performance of the interface[1]. However, this might not necessarily be inhibiting to the efficient working of the system, considering that the temperature of the ES–DRA remained well below the lower limit of the set–point.

A second issue is the propensity of the evaporator temperature to drop sharply each time the compressor is turned off. This is due to a combination of the effect of the equilibration of the pressure across the compressor (which amounts to an expansion in the evaporator) and the loss of the heating effect of the compressor. The equilibration of the pressure across the compressor is undesirable as the work required to reinstate the working pressure differential on compressor start–up is essentially lost, *in addition to* the detrimental effect of the heat generated in the process of this pressure build up. Clearly, reducing the number of times this occurs would help address the problem to some extent. This not withstanding, it might be of some benefit to also investigate the advantages of preserving this pressure head during the compressor off–cycle.

In much of the preceding sections and much of what is to follow, mention is made of the detrimental effect of the conduction path across the heat transfer inventory of the appliance from the ambient to the DRA interior. While discussions in those sections are valid and relevant in highlighting the problem at hand, it is to be unequivocally understood that the TES's are located *at the appropriate places i.e.* close to the positions of thermal ingress into the system. The effect of placing the TES's as close to the system's boundary as possible is to act as the low temperature equivalent of guard heaters.

In the interest of brevity and clarity the annotated review of the results will be

[1] *e.g.* it might reduce the rate of heat transfer from the DRA to the TES.

presented in list form:

- The pull–down times were greater in 'ES–DRA mode' than in 'normal DRA mode'.
- The charge times were ambient–temperature dependent. The recorded times for two of the tests were 9.2 hours @ 25 °C and 13 hours @ 35 °C. This is probably as much a result of the improvements in the mean COP values attainable at lower ambient temperatures as it is due to the relative magnitudes of the heat ingressing the compartment on account of the differences in the ambient temperatures. This highlights the need to ensure that, as much as it is possible, TES charging is done during the lower temperature periods of the charge–discharge cycle.
- Sub–cooling may be a problem during the initial charging of the TES's and this has to be looked into. The submission here is that the concertina–type evaporator–restraint used to hem in the TES may be participant to the orchestration of the sub–cooling. Apart from the deterioration in compressor performance due to the necessarily low temperatures required to bring about the phase–transition, losses in thermodynamic availability (one of the reasons latent heat storage was selected above sensible heat storage) of the order (see Winegard (1964), Chapter 2):

$$W_{unavail} \sim Q_{LH} \cdot \frac{T_{LH} - T_{evap.}}{T_{evap.}}$$

  will attend in the process[1]. This can be considerable on account of the large values Q_{LH} tends to assume and is additional to any losses which occur on account of the thermal capacity of the material.
- The TES discharge times varied according to the prevailing ambient temperature and will do so further, depending on the nature of the interaction it is subjected to in service. However, for an empty device or one which is infrequently interacted with, in excess of two days coolth energy delivery can be expected without recourse to backup batteries, in the event of electrical energy supply failure.
- A clear indication of an evaporator–compressor thermal conduction path was illustrated with the aid of the TES's[2]. Apparent was the evidence of heat

[1] Where $T_{evap.}$ is the minimum sub–cooling temperature, occurring immediately prior to phase transition.

[2] No doubt a similar path exists between the condenser and the evaporator.

injected into the system on account of the 'start–up' power drawn by the compressor (irrespective of whether the TES's were in place or not).

The effect of this thermal conduction path is felt not only in terms of the heat ejected into the system on compressor start–up but also in terms of the thermal response time of the DRA compartment to the diurnal fluctuations in the ambient temperature. The nett effect of this (apart from the heat–gain implications in harsh thermal environments) is the loss of a considerable proportion of the thermal lag, which effectively limits the kernel of energy management strategies available for ES–DRA controller design.

The recommendations here are to (a) limit the number of compressor switching 'events' and (b) undertake further research into the thermal isolation of the internal heat transfer inventory (evaporator) from the external heat transfer inventory (condenser and compressor).

- There were marked improvements in the calculated COP of the compressor when the appliance was operated as an ES–DRA (as opposed to the operation in 'normal DRA mode'). In quantitative terms, these tests indicate that the night–time TES charge operation consistently delivers superior COP's and consumes less energy (18% and 30% respectively) in comparison to the day–time TES charge regime, which in turn performed better than the DRA functioning in normal mode (40%,6%), using the same indices. This was in–spite of certain biases which favoured the 'normal DRA mode' tests.

- In both day–time and night–time operation modes of the ES–DRA, more stable internal temperatures were observed in comparison with the 'normal DRA mode' of operation.

- Invariably, higher power consumption was observed with the appliance operating in 'ES–DRA mode' than with the 'normal DRA mode'. The implication of this is that comparatively large capacity devices (*e.g.* prime–movers) have to be employed in 'ES–DRA mode'; these tend to be more efficient on account of the higher relative proportion of work output to inertial loads for a given amount of energy transfer.

- The mean temperature of the compressor in 'ES–DRA mode' was higher when compared to the temperatures observed in 'normal DRA mode'.

- The results of a comparison with the current EU standards indicate that the basic, no–TES DRA design is far superior (*circa* 100%) in energy consumption efficiency terms to what is required by the standards. This is due to the presence of the VPSI used in its construction. With the incorporation of a TES

and implementation of an appropriate energy management strategy further improvements of 52% on that superiority can be obtained.

7.7 Closure

The results presented herein have proven the viability of the concept of thermal energy storage (based on hydrophilic polymers) within domestic refrigeration appliances. The results conclusively illustrate that there are several advantages of an **ES–DRA** over its non–energy–storing counterpart in terms of (a) energy–use flexibility, (b) energy use (and conversion) efficiency, (c) the devolution of energy use from conversion, (d) appliance robustness to lacuna in energy supply and fluctuations in the ambient temperature, (e) reduction in compressor cycling and (f) thermal performance (particularly in relation to the fluctuations in the appliance's internal temperature about the set–point). The comparisons with the battery–only energy storage implementation demonstrate that the **HES DRA** design approach is much better than the traditional battery storage technique used for solar–powered refrigeration.

Certain aspects of the results highlight areas where further development is required in order to reap the full potential of the appliance; in particular these include, the development of an intelligent controller, the need to dispense with the heat conduction path between the interior (evaporator) and the exterior (compressor and condenser) heat transfer inventory and the issue of sub–cooling of the **TES** during the initial charge phase.

Chapter Eight

Conclusions and Recommendations

8.1 Introduction

This chapter, in concluding this research undertaking, summarises the previous seven chapters, identifies opportunities for further research and goes on to briefly discuss the findings of the scope for commercially exploiting the proposed DRA design.

8.2 Research Rationale

The manner in which man has hitherto utilised the earth's natural resources has been unfortunate in as much as it is potentially threatening to his long–term existence on earth. In recent years, there has been much socio–political, academic and commercial activity addressing this issue. Whilst much governmental expenditure has been directed at driving and assisting the development of mechanisms, identifying practices and disseminating information which might help to ameliorate the energy/environmental situation, issues of consumer attitudes and behavioural practices need to be addressed with greater vigour. Indeed environmental concern needs to be an integral part of the educational curriculum 'at all levels' and governmental practices/policies should be patently consistent with the theme of 'environmental

conservation' across the board.

From a socio–technological point of view, there is the need for a continual, critical review into the various currently–undertaken tasks (*e.g.* energy conversion, transportation, *etc.*) regarding their necessity and the current methods utilised to achieve the desired objectives. Concomitantly, there is the need to ensure that, *within the limits of the current understanding* of each process, only the best possible appliances are available and universally affordable 'on the market'[1]. As user practices and demands do and will vary unpredictably, it is expedient to ensure that the appliances placed in the public domain, for consumption, are robust to variations in user practices and are as simple to use as they are efficient. Indeed the best devices will tend to be those which, whilst exhibiting a high level of energy utilisation efficiency with probably low energy consumption and minimum (embodied) environmental impact, remain easy to use (particularly in the sense of minimum consumer attention), are unintrusive and have minimum maintenance cost.

The current research investigated domestic refrigeration appliances (including appliances used for small–scale non–domestic applications *e.g.* public houses, corner shops, mobile vaccination or recreational units) with the view of devising a methodology for enhancing the (energy and thermal) performance of these appliances. Essentially the aim was to design a super–efficient (in terms of both energy consumption and energy utilisation), intelligent DRA which is robust to the energy–supply profile whilst still delivering superior thermal regulation and cooling performance to a comparable DRA. The result was a 'hybrid energy storage domestic refrigeration appliance' (HES–DRA) which incorporated vacuum panel super insulation (VPSI), thermal and electro–chemical (electric battery) energy storage technologies and an energy management system as an integral part of the DRA design.

8.3 Results

The work was carried out in five stages namely (a) the identification of the research area (state of the art, potential benefits *etc.*) and the analysis of the basic technological requirements (b) the formulation of the solution methodologies, the identification of the relevant and appropriate technologies and the analysis of the various energy–management strategic–options, (c) the modeling of the entire scheme to facilitate the design of the DRA, (d) the modification of the DRA prototype for experimentation, the writing of the appliance control software and the data ac-

[1]It is questionable why it is permissible for an energy–inefficient device to be sold alongside an efficient one (*e.g.* an A and D rated refrigerator) when the sale of a mechanically– or electrically–unsafe device is expressly prohibited. This discrepancy sets energy use apart from the other product requirements where there is one standard which has to be met by all *e.g.* safety.

quisition process and (e) the actual experimental proceedures, the consequent data analysis and finally the prototype evaluation.

The research exercise included making certain changes to the basic DRA design, these were to (a) replace the outer steel shell with a plastic one (this negates the need of the use of 'anti–sweat' heaters), (b) use appropriate energy storage technologies to enhance systems energy consumption performance based on a well–defined control routine, rather than permit ambient criteria to determine the energy consumption pattern of the DRA, (c) utilise the best commercially–available thermal insulation and (d) employ a high performance compressor.

The rationale behind the energy management strategies employed was to provide a means by which (a) the appliance's energy–use profile can be decoupled from the energy supply profile of the system, (b) more rapid thermal energy transfer to the DRA interior may be obtained while at the same time preserving the COP of the prime–mover, (c) temperature fluctuations within the DRA interior compartment may be stabilised and (d) energy consumption may be minimised.

Three basic appliance management strategies were tested: (a) the appliance without thermal energy storage, to act as a control experiment, (b) the appliance utilising thermal energy storage with the prime–mover functioning only during the day–time and (c) the appliance utilising thermal energy storage with night–time prime mover operation. The results of these tests indicate that the *appliance's* measured COP, energy utilisation efficiency and the stability of the DRA's internal temperature markédly improved when the appliance was fitted with a TES and run with either energy management protocol. With the appliance fitted with TES's, higher evaporating temperatures and less prime–mover cycling[1] were required. Other test results indicated that the appliance could function (with the TES alone) without any energy input in a *circa* 25 °C environment for approaching 54 hours.

As expected, significantly longer appliance temperature 'pull–down' times were observed with the TES in place, these being *circa* two– to three–fold longer than for tests in the absence of the TES. In running the DRA in energy storage modes it is necessary to initially charge and then to recharge the stores at periodic intervals. The TES tended to undergo sub–cooling during the initial charge phase, usually to a temperature of *circa* -5 – -8 °C; however thereafter the charge process took place at *circa* -2 °C, which was higher than the *mean* evaporating temperature observed during 'normal' operation.

The performance indicators (energy consumption, COP, *etc.*) of the designed ES–DRA varied depending on the control regime employed for its operation. However, in all cases the performace of the ES–DRA was superior to the performance of the

[1]This presumably may increase the longevity of the device and have a beneficial impact on the acoustic comfort of the home.

same appliance operated without the benefit of the TES (and energy management strategy).

The results otained indicate that an improvement in the measured (appliance) COP of 65% may be realised by the use of a TES and an appropriate control regime in the design of a DRA. As a result of this improvement, a reduction in the appliances energy consumption of much as 52% may be achieved. This was accompanied by a 15W (21%) decrease in the mean power consumption of the compressor[1] The presence of the TES (adjacent to the evaporator) in the DRA permitted higher evaporating temperatures under the same loading condition for an ES–DRA when compared to its no–TES counterpart. The mean appliance air–temperature for the ES–DRA did not vary more than one degree during duration of operation as compared to the no–TES appliance which varied as much as 6 °C[2][3]. The employed technologies afforded user defined control on the load–demand shape of the ES–DRA, the energy management strategies employed in this implementation afforded as much as an eight–fold reduction in compressor cycling during operation. This was accompanied by as much as a 24–minute reduction in the compressor on–time.

A comparison of the energy consumption of the designed ES–DRA to the requirements of the EU standards indicates that the basic, no–TES DRA can offer *circa* 100% improvement in terms of energy consumption. With the incorporation of an appropriate TES *and* the implementation of an appropriate energy management strategy further improvements of up to 52% may be achieved.

8.4 Recommendations For Further Research

The work documented herein consists of the principal stage of the research process into implementing the concept of *improving energy consumption efficiency by careful energy management via appropriate energy storage and control technologies.* In demonstrating the viability of the concept, several of the current thinking/practices in the DRA manufacturing industry have been challenged. Notably, the appliance is devoid of heaters, has been designed specifically with the environment in mind (particularly in the sense that it is efficient in terms of both energy conversion and energy utilisation), is robust to variations in energy supply, provides a constant temperature internal compartment during periods of 'non–interactive' use and is 'intelligent' in as much as it possesses the ability to be programmed to respond to a myriad of different energy supply or utilisation demand scenarios. As

[1] Averaged over the compressor on–time.

[2] The maximum permitted by controller

[3] These comparisons do not include the compressor on–times which consistently depress the temperature of the appliance.

with all proof–of–concept devices, several passes of the design–implementation iteration loop will have to be undergone to produce a state–of–the–art device. The following is a brief list of tasks which forseeably should form the basis of the next stage of the process:

- During the course of the experimental process, it became apparent that the existence of a thermal transmission path between evaporator and the 'external inventory' (compressor and condenser)[1], would compromise the thermal isolation of the system. This is in fact the case, albeit that the exact mechanism needs to be identified. However, one modification which could be made is to replace the aluminium evaporator with a plastic–based alternative[2]. This will eliminate the issue of heat transmission, by direct conduction, from the TES to the exterior (not to mention reducing the evaporator cost). The gas–phase and heat pipe type heat–transmission issues (see Footnote 1 on page 235) may be tentatively addressed by the insertion of one–way valves at the appropriate places in the refrigerant conduit. This is classed as essential work, as much of the benefits of utilising a super–insulant is lost on account of this, and it will serve to improve the utilisation capacity of the TES in long–term storage.

- The initial design stipulated that the evaporator be completely enclosed within the TES. However, in this experimental run this was not implemented. Such an implementation will enable the thorough investigation of the extent to which the heat transfer to the DRA interior is impeded on account of the presence of the TES as well as serve as an encasing protection for the plastic evaporator suggested earlier.

- The work done remains incomplete in the sense that much more data collection/analysis is required in order to comprehensively charactersise the HES–DRA behaviour. Advancing the research will principally involve experimenting with the 'rig' at various settings and charting the various indices of merit alongside the chosen energy management regime. These results should then be fed back into a modified version of the computer model and the process reiterated until sufficient data is obtained to fine–tune the appliance design and subsequently reprogram some type of complex adaptive controller.

[1]Thermal transmission would be of several forms (i) by direct conduction, (ii) gas–phase convective transmission and (iii) by a heat–pipe type effect between the condenser/compressor and the evaporator.

[2]The reader is reminded that the controlling resistance is either the DRA–air side thermal resistance or the TES thermal resistance. In fact, at least one manufacturer (MENERGA Ltd. Unit D, Princes Drive, Kenilworth CV8 2FD, UK) is already producing plastic radiators/heat exchange surfaces.

- The compressor used was a fixed speed (dc) compressor[1]; in spite of its single speed specification, it was discovered that running the compressor at turned–down voltages (66% of the rated) reduced its power output as well as the maximum compressor temperature. The ability to run the compressor at variable speeds and power outputs would be invaluable to the appliance's energy management system, as it would permit optimum utilisation of the time available for TES charging. One design which may be looked into regarding this is the use of multiple individually–wound stators placed serially along the device's rotor and/or a mechanism for isolating particular compression chambers based on coolth demand.

- The use of an electric battery as a backup is unlikely to gain wide range acceptance in the current domestic sector as the electricity supply is, apart from a few exceptional circumstances, fairly constant in much of western Europe. However for remote applications and in developing regions, the choice may be born of necessity. It may be worth investigating the use of possibly lighter and greener alternative electricity generation technologies *e.g.* fuel cells, to replace electric batteries.

- Due to the nature of the design of the system, TES charging occurs sequentially (as was evident from the TES charge tests); it might be worth investigating the use of 'thermo–glide' refrigerants[2] in an attempt to alleviate the problem. This might also be useful in applications where large evaporators are in use to ensure uniform energy transfer occurs as the refrigerant traverses the refrigerator.

8.5 Opportunities for Commercial Exploitation

Much of the recommendations for further work reside in the realm of applied–research development and can be carried out either in the further research or development of the DRA. In its current guise, the DRA has all the necessary requirements to make it fit for commercial sale, with one or two modifications. Principally, the basic energy management facilitating mechanism (the TES's) may be retro–fitted into commercially–sold refrigeration appliances. In doing so, two main issues have to be addressed; the first is the need to modify the surface area of the evaporating surface in order to provide a sufficient heat transfer area for the required heat

[1]While this is seldom seen in domestic devices, it was chosen because of its relevance to other related applications.

[2]A blend of several immiscible refrigerants each with different phase–transition thermo–physical properties.

transmission from the TES to the DRA interior at the TES operating temperature[1]. The second issue is the need to ensure the integrity of the store at all times[2] and thus, a more rigid form of encasing is recommended. The only other modification which will need to be made to the system is the insertion of the chip containing the compressor control mechanism and the necessary relays into the compressor's electric circuit. These modifications are all that are needed to give a *circa* 30–60 % improvement in the *system's* COP.

While the use of the 'vacuum panel super insulation' would significantly reduce the overall energy consumption of the appliances[3], the current author is of the opinion that due to the cost of these panels[4], it is imperative that all the thermal transmission paths are detected and adequately dealt with prior to their adoption. A cost estimate of these addended components is:

Component	Cost (£)
(VPSI) insulation	59.00
Thermal stores	12.50
Intelligent control system (estimated)	30.00

Table 8.1: Cost of various addended components to the basic DRA.

If this is compared to the cost of a new 200 litre refrigerator (*circa* £250), the estimated material cost of retrofitting the TES and energy management mechanism alone is *circa* 20%.

8.6 Closure

It is difficult to make a quantitative assessment of the immediate (or indeed long–term) energy and cost impact of the implementation of this mechanism on

[1]This is estimated at around a four– to five–fold increase in surface area *i.e.* essentially doubling the evaporator dimensions.

[2]This protection is simply to prevent the TES from structural damage and to protect it from fungal attack. The TES material is relatively inert and non–toxic and may be viewed as environmentally friendly in the sense that it is biodegradable (can be 'eaten' by fungi) or (being a hydrocarbon) can be combusted as fuel.

[3]Indeed some manufacturers claim that just the use of *one* panel foamed in place on the rear side of a standard DRA gives up to a 30% (measured) improvement in energy consumption. This is strategically located to increase the thermal resistance in the heat transmission path between, both, the air rising past the compressor and the heat ejected from the condenser and the DRA interior.

[4]At the time of purchase the cost was *circa* £10.00 per panel.

the UK (or OECD) economies or the environment at large. Suffice it to say that the potential impact of this technology when introduced into a new environment is to reduce appliance energy consumption by between 30–60 %. More important is the potential of such a cheap robust appliance to the developing world, and the medical[1]/recreational sectors in general. However, the greatest application is bound to be in developing world countries where energy supply may be intermittent. In one sense, the research presented herein provides the appliance designer (or user) with the flexibility to respond to different energy supply or demand scenarios efficiently. With the imminent maturity of solar/wind energy conversion technologies it may well be that in some regions of the world the burden of refrigeration carried by the environment may be reduced to that of a standby role.

[1]Similar appliances for vaccine storage are supplied to the WHO at *circa* $US 5,000.00 and rely solely on electric batteries to cope with discontinuities energy supply.

Appendices

Appendix A

The calibration of the instrumentation

Introduction

In any experimental procedure it is imperative, in order to prove the instrumentation and to attest the veracity of the data collected, to calibrate *all* the instrumentation used in the experiment. This section briefly outlines the method by which the thermocouples, voltage and electrical current measurement devices were calibrated. For more information about the measurement of temperature the interested reader is referred to Keenan (1941) and on their calibration to Barber (1971). The measurement of voltages was achieved using the voltage divider principle, whilst the measurement of electrical current utilised Ohms law (see for instance Nelkon (1981) and Resnick et al. (1993)).

A.1 General Procedure

The calibration technique used in this exercise is based on the assumption that, within the ranges considered[1], the relationships between actual and observed values of the measured quantities are sufficiently linear. On this understanding, two fiducial points (lower and higher) in the quantity measurement space are selected. The lower point serves as a reference *zero* datum for all subsequent measurements, whilst the higher point was used to determine the necessary scaling factors.

In order to preserve the integrity of the calibration and ensure its applicability within the experimental setup, it was deemed necessary to calibrate as many of the measuring devices as possible *in situ*, preferably with as much, if not all[2], the other instrumentation and reference instruments for calibration in place. Where possible these reference instrumentation were left in place during the actual experiments. Practicality excluded the calibration of thermocouples being done *in situ*; however the electrical current and voltage measuring devices were calibrated *in situ*.

The specific procedures employed in the calibration of the thermocouples is documented in Appendix A.2 on page A-241, whilst that for the calibration of the voltage

[1] For temperatures, -15–$+50\,^{\circ}C$, for voltages 14–30V and for currents 0–4amp.

[2] To reduce the possibility of the inclusion of additional instrumentation causing deviations in the measured fiducial states of already installed instrumentation.

and electrical current measuring devices is documented in Appendix A.3 on page A-244. These contain the relevant diagrammatic layouts with subsequent discussions considering the issue of accuracy and possible lacunae which may result from the use of the devices. The discussion further attempts to offer an insight into possible methods of interpreting observations in-spite of these.

A.2 The Calibration of the Thermocouples

Introduction

This section deals with the general technique used to calibrate the thermocouples used for the different experiments undertaken during the course of this work. Unless otherwise stated, the thermocouples used were of the Copper–Constantan T–type.

A.2.1 Aim

The aim of this experiment is to determine, for any particular thermocouple, a reliable estimate for the zero offset and a scaling factor within the region of the triple point and boiling point of water. These values are then used to correct any readings that are taken with the said thermocouple to obtain a closer estimate of the actual values from measured values.

A.2.2 Apparatus

The following apparatus were routinely employed in this procedure (see the figures for further details).

- The thermocouple(s) to be calibrated.
- An isothermal box with the cold junction compensator configured to enable direct reading of centigrade temperatures from the thermocouples.
- The MICROLINK data–logger with an appropriate data acquisition card.
- A standard calibrated thermometer.
- A zero degree (triple-point) reference thermal potential. This was typically an oil bath immersed in melting ice and left to stand for a few hours to equilibrate.
- A boiling/high temperature reference thermal potential. An aluminium isothermal block was used for his purpose.
- The computer and calibration software as given in Appendix D on page D-275

A.2.3 Procedure

The thermocouples were connected to the channels on the MICROLINK on which they would be ultimately used. The thermo–junctions were then placed in the cold (oil) baths along with the thermometer. After the values on the thermometer had stabilised, the channels were sampled repeatedly and the average and standard deviations for each channel reading were recorded. The value indicated by the reference thermometer was also noted and recorded.

The thermometer and thermocouple thermo-junctions were then placed in oil baths within the isothermal block, the target temperature was set and the device switched on. After the reference thermometer temperature stabilised, its reading was recorded and again the relevant data–logger channels were sampled repeatedly and the average and standard deviations for each channel reading computed and recorded. The experiment was repeated to ensure the repeatability of the results.

A.2.4 Precautions

In the calibration of thermocouples, several issues have to be considered, such as: (a) the accuracy of the calibration, (b) the repeatability of the results, (c) whether changes in the location of the device would affect the applicability of the results within the intended experimental setting *etc.* Extreme care has to be exercised in the connection of thermocouples to electronic data–loggers, particularly when other electrical analogue signals are being monitored by the same equipment. This is as to ensure that across the data logging device, only one reference voltage is defined as the earth. The failure to do this can lead to errors in the data collected during run–time which may go unnoticed. Other precautions which must be taken have to do with: (a) verifying the integrity of the connections and the thermo-junctions, (b) ensuring that both the thermocouple and the thermo-junction heads remain fully immersed in the oil bath to guarantee the temperature of the contacting medium, (c) ensuring continuity within the thermocouple wires, (d) care to avoid parallax errors and (e) in selecting the fiducial points, care to ensure that they spanned close to the anticipated measurement range.

A.2.5 Discussion

The results of the experiment demonstrate the need for calibration. For the lower 0.2 °C reference point, temperature excesses (in the raw data) of 2 °C were routinely measured with modal standard deviation of less than 0.1. Similarly for the upper 94–95 °C reference point temperature excesses of 3 °C, with a modal standard deviation of less than 0.2, were consistently observed. The low coefficient of variation observed across the experiments indicates the consistency across the experiments.

The variation observed for each individual thermocouple in repeated sampling tends to indicate that the accuracy of the sampling process is $\pm 0.5\,^{\circ}\mathrm{C}$ *i.e.* to the nearest half a degree. Figures A.1 and A.2, *qv.* pages A–243 and A–244 respectively are graphs of the measured deviations in individual thermocouple temperatures, the length of the accompanying error bar indicates the uncertainty in the data.

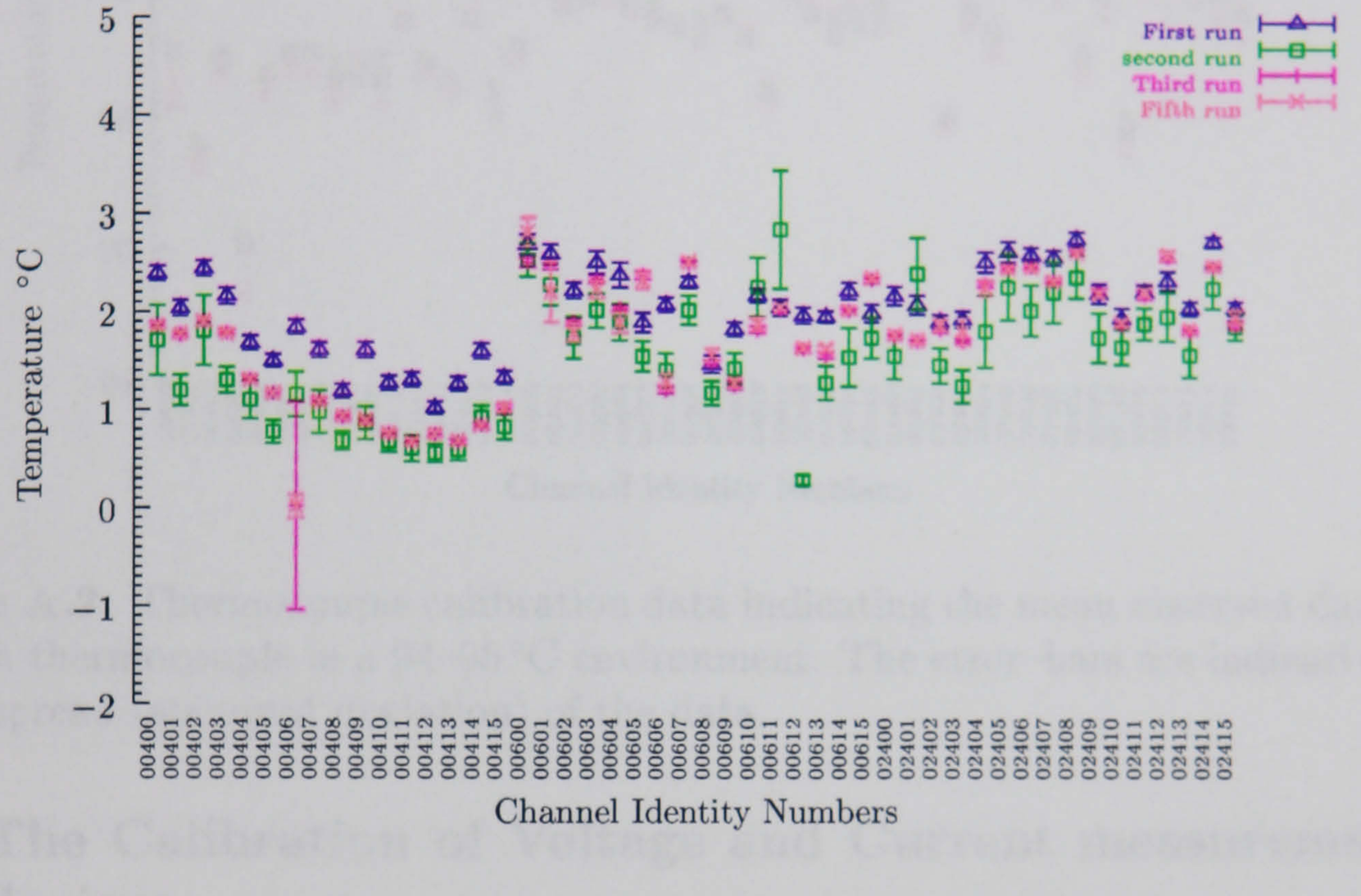


Figure A.1: Thermocouple calibration data indicating the mean observed data for each thermocouple in a $0.2\,^{\circ}\mathrm{C}$ environment. The error–bars are indicative of the spread (standard deviation) of the data.

Accuracy and sources of errors Several avenues exist wherefrom errors may arise, apart from the 'spurious' errors which may occur due to say, failure to heed any of the caveats given in section A.2.4 on page A–242. There are also systematic errors which may be introduced into the calibration procedure. These range from inaccuracies in the reference thermometer calibration, voltage offsets on the data acquisition cards to an improperly calibrated or configured cold junction compensator in the isothermal box.

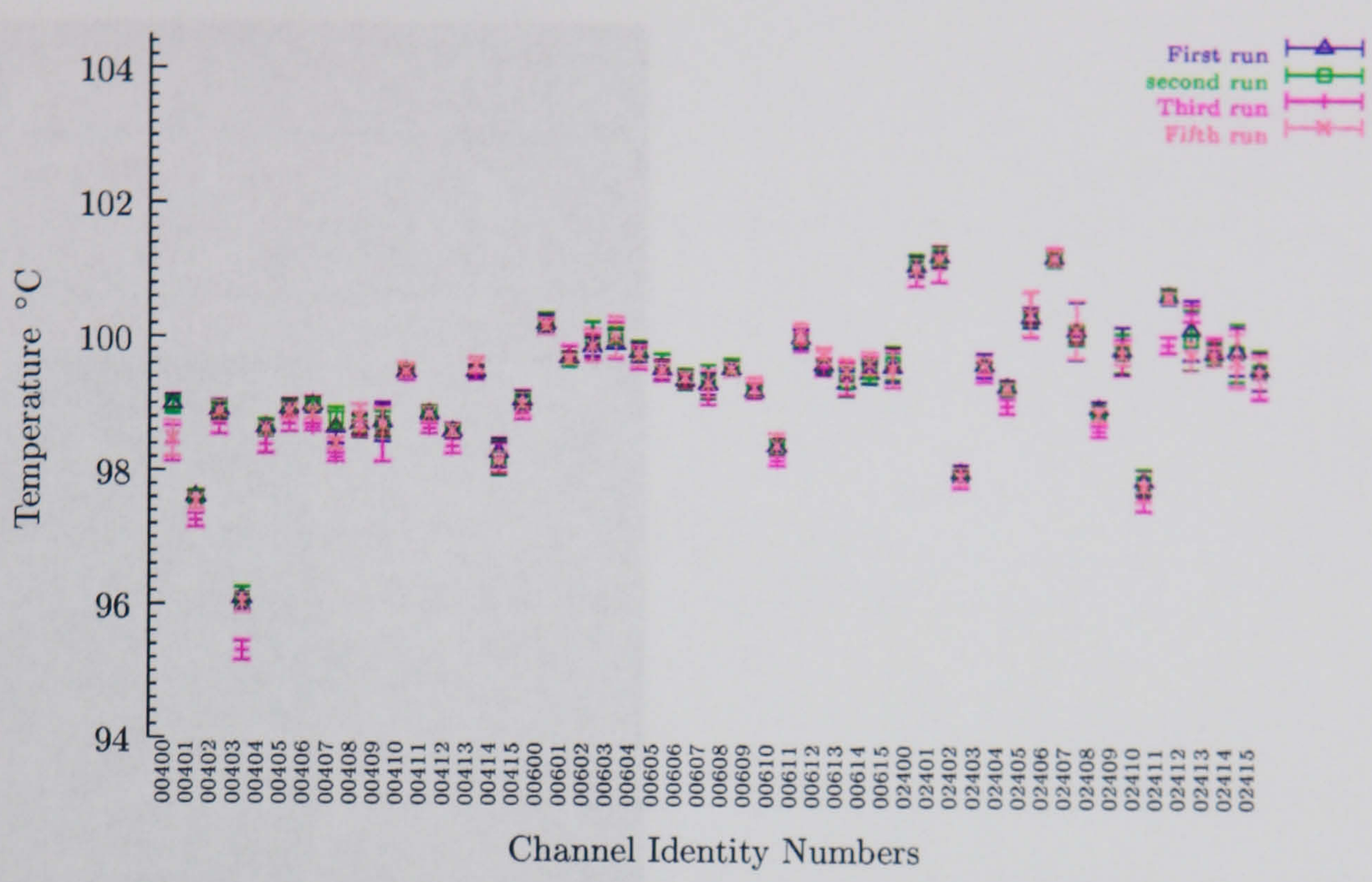


Figure A.2: Thermocouple calibration data indicating the mean observed data for each thermocouple in a 94–95 °C environment. The error–bars are indicative of the spread (standard deviation) of the data.

A.3 The Calibration of Voltage and Current measurement devices

A.3.1 Introduction

This section details the technique used for calibrating the voltage (voltage dividers) and current (shunts) measurement devices used during the remainder of the experimental works.

A.3.2 Aim

The aim of this experiment is to determine for each voltage divide or current shunt, a reliable zero offset and scaling factor within the intended operational range of the device. The obtained values are to be used to (linearly) relate measured potential differences to the actual value of the measured quantity.

A.3.3 Apparatus

The following apparatus were routinely employed in this procedure.

- The shunts and voltage divider to be calibrated.



Figure A.3: Thermometer in dewar flask

- Standard calibrated voltage and current measurement devices (ammeter and voltmeters).
- The `MICROLINK` data–logger with an appropriate data acquisition card.
- The intended experimental setup.
- The computer and calibration software as listed in Appendix D on page D–275.

A.3.4 Procedure

The intended experimental circuits were wired up and the necessary voltage taps (across the current shunts and the voltage dividers) connected to the relevant channels of the data acquisition apparatus. Ammeters were then connected next to the current shunts and voltmeters in parallel with the voltage divider, see Figure A.4 on page A–246 for a detailed diagram of the circuit.

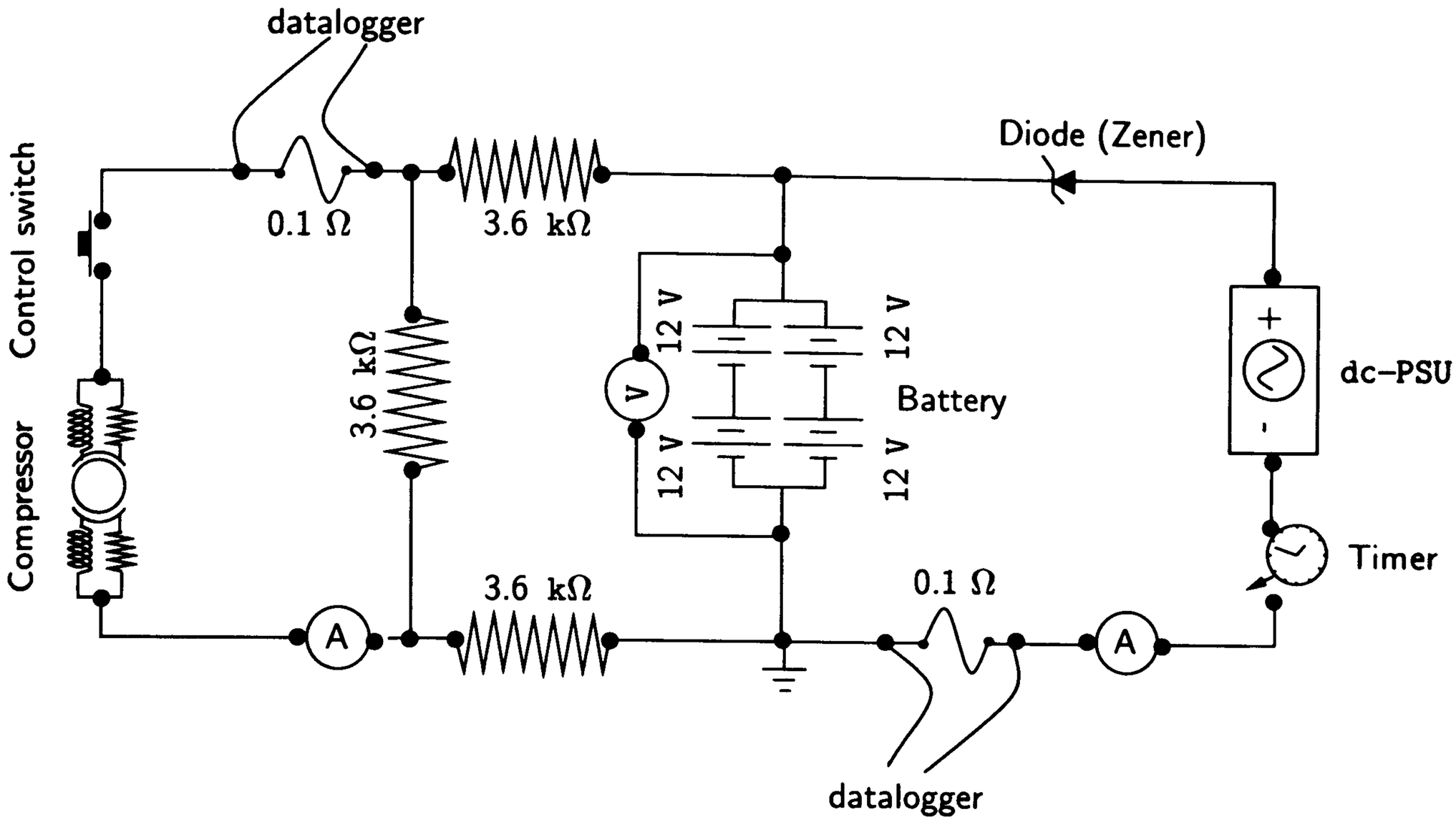


Figure A.4: Circuit diagram for the voltage divider and shuts calibration.

With the circuit 'opened', potential differences across each of the measuring devices (shunts and voltage dividers) were then scanned repeatedly by the data–logger and the average and standard deviations of the recorded values were computed and recorded. The values indicated by the reference instruments were also noted and recorded.

Power was then applied to the circuit and after the initial fluctuations on the instruments had settled the data–logger was again used to gather the relevant information and the average and standard deviation of the readings were computed. The readings of the reference instruments were again recorded. The entire experiment was repeated to confirm the results.

A.3.5 Precautions

Just as in the case of the calibration of the thermocouples, issues of calibration accuracy, result repeatability *etc.* have to be addressed. For the case of the voltage and current measuring devices the issue of relocating the measuring devices is not relevant. Again, care had to be exercised to ensure that all the terminal connections were ohmic and in reading the instrumentation. For reasons given in item A.4 of Appendix A.4 on page A-251 it was necessary to use analogue reference ammeters.

This was because these instruments tend to compensate for high frequency ripples in the measured signal due to their mechanical inertia.

A.3.6 Discussion

The results of the experiment indicate good and fair (due in part to the fluctuations mentioned in section A.3.5 on page A-246) reproducibility of the data for the open and closed circuit measurement respectively. Another feature which affected the closed circuit data was the constantly changing value of the power drawn from the device. This was as the power requirements of the experimental setup *decreased* exponentially with time and for this reason several trial runs were required to establish a pattern prior to the actual data collection process. For the open circuit case there were no variations in the reference data (shunts 00416,00417 0amp and voltage divider 00418 25V), while for the closed circuit case the following variations in the reference data was observed: Observed values: shunts 00416 −3.15−−3.0 amp and 00417 3.0–3.05 amp and voltage divider 00418 24.49–24.58V. In both cases, *i.e.* closed and open circuit runs, the (rms) deviation of the data within each experimental run was *circa* 5–8% and 9% respectively. Figures A.5 and A.6, *qv.* pages A-248 and A-249 respectively are graphs of the measured deviations in shunts (00416,00417) and voltage divider (00418); as before the length of the accompanying error bar indicates the uncertainty in the data *circa* 0.3%.

Accuracy and sources of errors As previously mentioned, failure to take the basic necessary precautions as outlined earlier will lead to corruption of the results. This is particularly true in relation to the fixity of the connectors. Poor non–ohmic connections will, as time progresses, induce non–systematic errors into the data causing random corruption of the results. The fluctuations of the closed circuit results may be a cause for concern in situations where the observed values are to be used in sensitive calculations and it is for this reason that a large number of sequential samples of the data was taken for *each* reading. Also due to the magnitudes of the voltages measured across the shunts in particular (units and fractions of millivolts), small deviations in the measurements will be magnified in the translation to the values measured.

In view of limitations in the resolution of the corrected data collected, it is necessary to define error–bounds within which the data may be interpreted. If proper care has been taken in collecting the data, the principal source of error will be random errors (*i.e.* in repeatability of the data). The standard deviation for successive observation gives and indication of the scatter of the observed values about the observed mean and can be used to obtain an indication of the expected error in subsequently acquired data. Assuming the errors are normally distributed and a sufficiently large

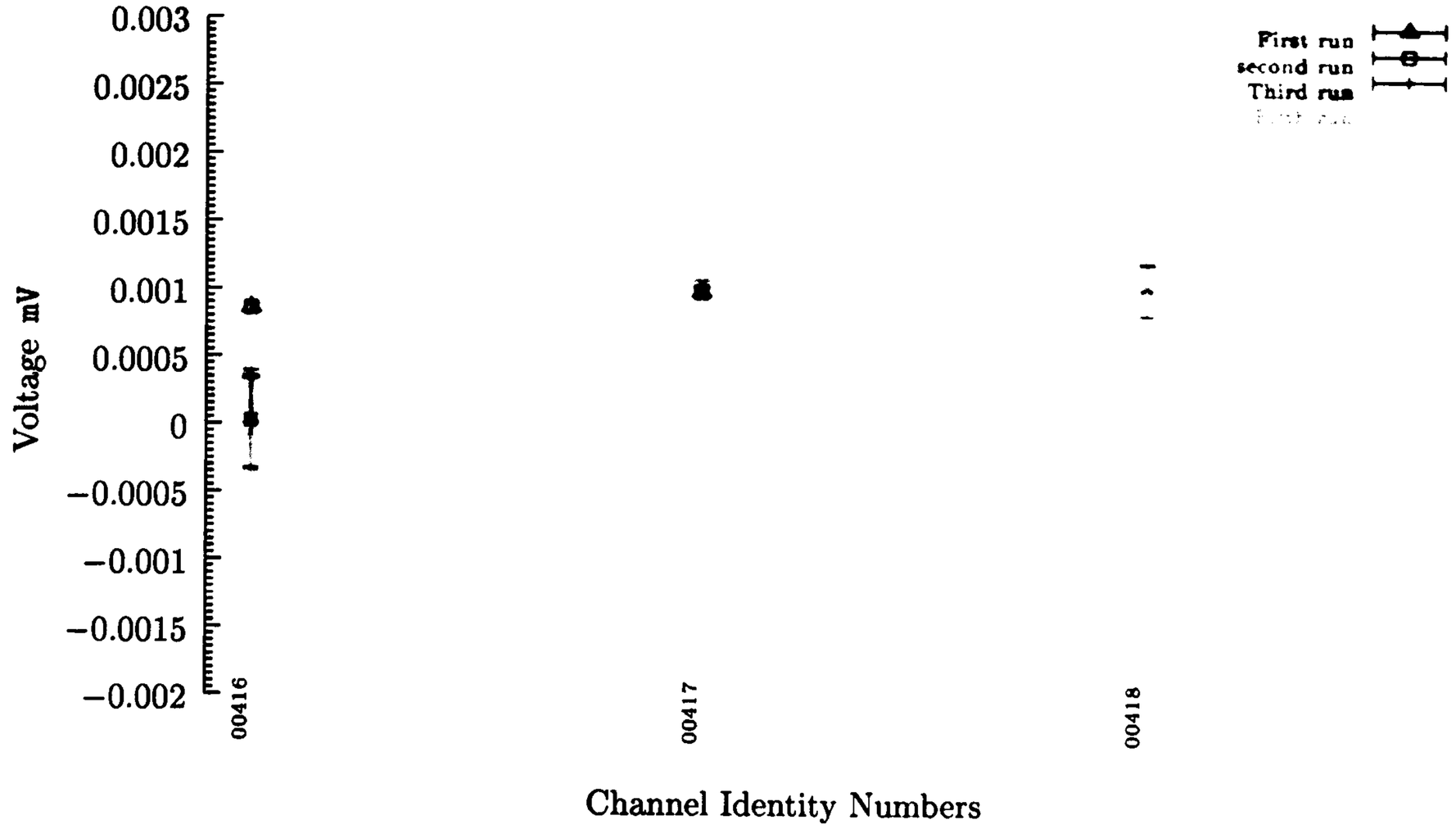


Figure A.5: Open circuit voltage and current calibration data indicating the mean observed data for each instrument. Observed values: shunts 00416,00417 0amp and voltage divider 00418 25V. The error–bars are indicative of the spread (standard deviation) of the data.

amount of data has been sampled, then probability of the collected data lying within one–, two– or three–standard deviations about the observed mean will be *circa* 68, 95.5 and 99.7%, respectively [Kreyszig, 1983]. In other words the accuracy inherent defining the resolution of observed data to $\pm\sigma$ is 68%. Unfortunately, the greater this error bounds are (*i.e.* increasing the confidence in approximating the data) the worse the resolution is. For instance, data with error–bounds represented by $\pm 3\sigma$ can only represent measurements that are at least 6σ apart. Thus while it is desirable to use higher σ limits for defining the error bounds it may be impracticable and lower levels of confidence will have to be accepted in order to make use of the data. The data collected in this calibration exercise will be resolved in terms of the multiples of the σ and irrespective of the number of significant figures of the collected and corrected data, the following data resolution scheme will be adhered to (see Table A.1 on page A-249).

(a) For the current shunts (00416,00417) the measured standard deviation was between six and ten percent of the measured quantity and as such the data resolution will be based on σ for practical reasons. Thus, the collected data will be quoted to the nearest 0.25amp. This is a convenience measure and from the Table A.1 on page A-249 it is clear that the preferred resolution would be

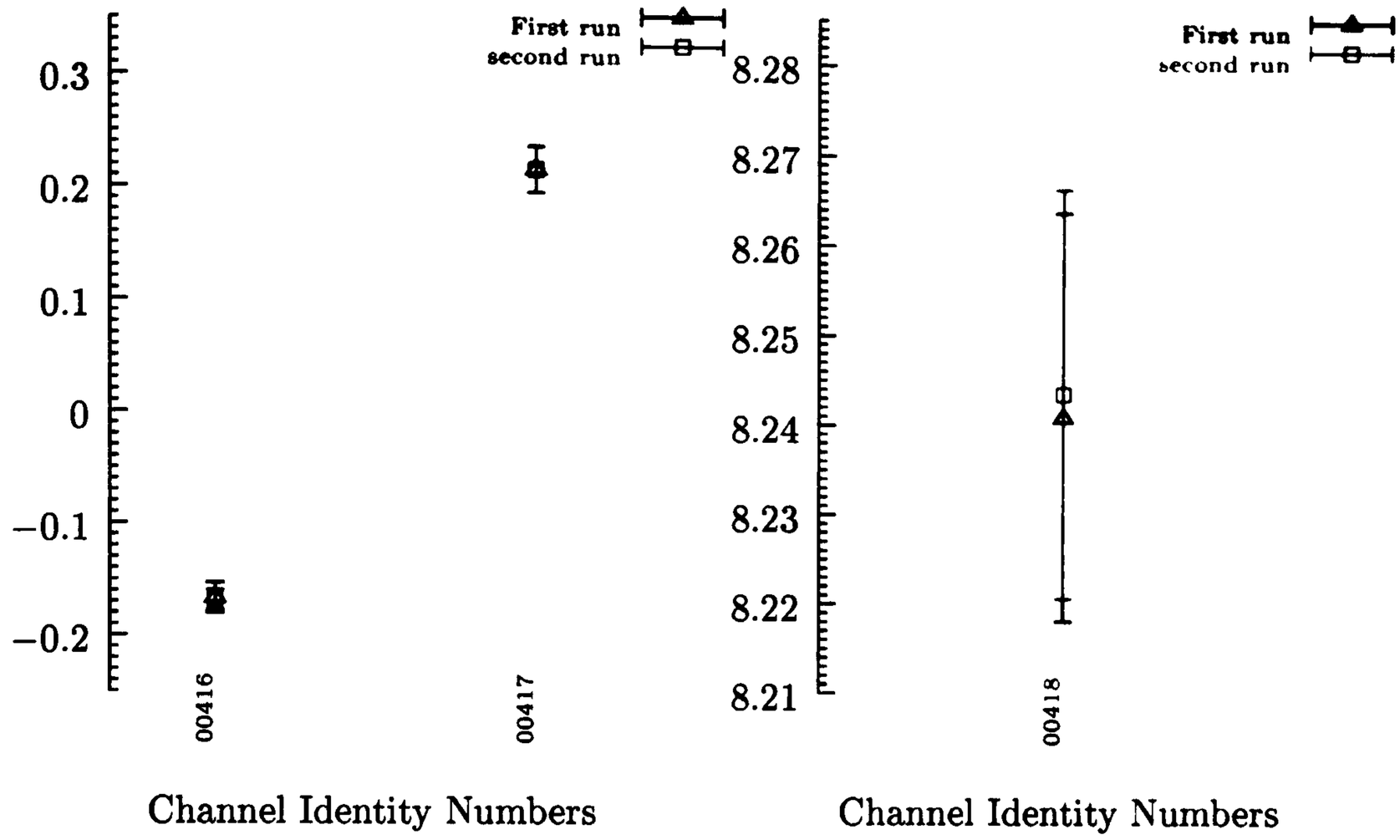


Figure A.6: Full load current and voltage calibration data indicating the mean observed data for each instrument. Observed values: shunts 00416 −3.15−−3.0 amp and 00417 (3.0–3.05) amp and voltage divider 00418 24.49–24.58V. The error-bars are indicative of the spread (standard deviation) of the data.

	Channel	Datum[a]	Data size	values ($\times 10^3$)				S[b]	R[c]
				$(\sigma_{400})_{max}$	$\overline{\sigma}_{400}$	$2\times\overline{\sigma}_{400}$	$3\times\overline{\sigma}_{400}$		
T	00400-15	lo	192	1058	980	196	295	1	0.3[c]
	00600-15	hi		452	163	325	488	1	0.5[c]
	02400-15	Total	384	1058	131	261	392	1	0.4[c]
I	00416	lo	4	3.73	1.93	3.86	5.79	0	–
		hi	2	13.6	11.2	22.5	33.7	18	0.2[d]
I	00417	lo	4	0.045	0.042	0.084	0.125	0	–
		hi	2	20.1	20.0	40.0	60.1	14	0.28[d]
V	00418	lo	4	0.194	0.180	0.36	0.539	0	–
		hi	2	22.9	28.2	45.7	68.5	3	0.2[c]

Table A.1:

[a] hi and lo indicate the high and low end of the calibration points.
[b] The ratio between the measured quantity and the observed data.
[c] The data resolution
[c] Based on $3\times\overline{\sigma}_{400}$
[d] Based on $\overline{\sigma}_{400}$

to the nearest 0.3amp. The implication of this is that the level of confidence of the data will be about one in three.

(b) For the voltage divider channel (00418) the data displayed less fluctuation in comparison to the value of the measured voltage (8.24V) and 3σ limits can be used to define the error bounds on the data to greater resolution than for the current shunts. In this case the mean square deviation in the data was less than 0.3% of the mean observed voltage. Thus, the voltages quoted are done to the nearest 0.25V.

(c) The size of the average σ of the measured temperatures also permit the use of the 3σ limits for resolving the data. Here the data is to be quoted to the nearest 0.5 °C, which is higher than the indicated 99% confidence limits in the table.

(d) From the measured data it will be necessary to derive power and energy consumption values; thus the following discussion on the *minimum* accuracy of derived data is undertaken with this in mind.

Given measured voltage (V) and current (I) values, the power consumption can be derived from ohms law *viz* $P_{(e)} = \mathtt{V} \times I$. Assuming the respective voltage and current errors are represented by $e_{\mathtt{V}} \times 10^{-1}$ and $e_I \times 10^{-1}$ respectively, then an accurate representation of the computed power would be

$$\begin{aligned} P_{(e)} &= (\mathtt{V} \pm e_{\mathtt{V}} \times 10^{-1}) \times (I \pm e_I \times 10^{-1}) \\ &= \mathtt{V} \cdot I + (\pm \mathtt{V} \cdot e_I \pm I \cdot e_{\mathtt{V}}) \times 10^{-1} \pm e_I \cdot e_{\mathtt{V}} \times 10^{-2} \end{aligned}$$

Where the sign on each of the terms will be dictated by the sense on the errors. Clearly, the worst case is when the errors all have the same sense *i.e.*

$$P_{(e)} = \mathtt{V} \cdot I \pm \left((\mathtt{V} \cdot (e_{\max})_I + I \cdot (e_{\max})_{\mathtt{V}}) \times 10^{-1} + ((e_{\max})_I (e_{\max})_{\mathtt{V}}) \times 10^{-2} \right)$$

Thus the *principal* part of the maximum error (e_{max}) is seen to be[1]

$$\triangle P_{(e)} \sim (\mathtt{V} \cdot (e_{\max})_I + I \cdot (e_{\max})_{\mathtt{V}}) \times 10^{-1}$$

[1]The likelihood of the error being consistently at its maximum is remote; a more realistic estimate of the error may be based on the *expectations* of the respective errors *i.e.* the first central moment of the probability density function ($F_{PDF}(3\sigma)$) of the error *e.g.*

$$E_{PDF}(e) = \int_{\bar{e}}^{3\sigma_e + \bar{e}} e \cdot F_{PDF}(3\sigma) \cdot .de$$

Using the values in the Table A.1 on page A-249 the principal error may be seen to be ±5.26, ±10.52 and ±15.78 for one–, two– and three–sigma limits (assuming 25V and 3amp for the maximum voltage and current) respectively. The data for the currents is to be quoted to $\pm\sigma$ and so the decision is here adopted to use the one–σ result for displaying the computed power values *i.e.* powers will be approximated to the nearest 5W

(e) The energy consumption data is effectively a cumulation of the power consumption and for this reason the resolution of the derived data will be half the resolution on the power consumption data *i.e.*, the energy consumption data will quoted to the nearest 10J.

A.4 General discussion

In order to gather the information required for the specific purpose of calibrating the instrumentation, a small module was put together drawing on the routines of the main control program (given in Appendix D on page D-275). The routine reads a given set of instrument channels on the MICROLINK[1] a user defined number of times and consequently computes the mean and standard deviation of the results as indicators of central tendency. In principle the implementation of this is (and was) fairly straightforward; however, within the data collection setting a number of difficulties, hereunder discussed, were encountered:

- In determining the values for each calibration point, it is necessary to repeatedly sample each device channel and with the information obtained, determine acceptable representative values using measures of central tendency[2]. This is as to reduce the impact of spurious results within the data collected on the consequent device calibration process. Thus there is the requirement to ensure that the number of repeated samples is sufficient for meaningful statistical inference. For these experiments, initially a sample size for each channel reading of 800 was decided upon. However, as the data points increased, there was

Therefore the expected error in this case is representable by

$$E_{\text{PDF}}\left(\triangle P_{(e)}\right) \sim \left(\mathrm{V}\cdot E_{\text{PDF}}\left(e_I\right) + I\cdot E_{\text{PDF}}\left(e_{\mathrm{V}}\right)\right)\times 10^{-1}$$

This can then be subsequently evaluated to compute the probable errors.

[1]A data acquisition and programmable controller, supplied by Biodata Ltd. see section 7.1.1 on page 231 for more details.

[2]In this case, the mean and standard deviation, with each sample value assigned the same 'statistical weight'.

an increased tendency for data to arrive at the input port whilst the CPU was still processing data from a previous request and thus for the port buffer to fill up. Whenever this happened an *'input overrun'* error warning was issued by the operating–system and the final data was compromised. For this reason the number of sequential samples for each reading was decreased to 400.

- During the calibration of the shunts and the voltmeter with the compressor running, there was a noticeable variation in the value of consecutive readings of each channel. Closer investigation on an oscilloscope revealed this to be caused by a 40Hz ripple introduced by the normal operation of the dc compressor as the (rotor) windings 'cut' through the magnetic flux. The Nyquist[1] criterion [Strang, 1986, *pp.* 325], [Franklin et al., 1990, *pp.* 193,197 *ff.*] stipulates that in such an event, data sampling should be done at twice this frequency. The attempt to adhere to this criterion was curtailed by the inability of the MICROLINK to sample data at that rate[2]. In fact for maximum wait times below 70 ms a *'device not responding'* error message returned by the control program, indicative of a failure for data to arrive at the input port before the device's response–failure time lapsed.

In computing the 'running' mean $\bar{x}$ and standard deviation σ the following algorithms were used:

$$\bar{x}_n = \bar{x}_{n-1} + \frac{x_n - \bar{x}_{n-1}}{n} \tag{A.I}$$

$$\sigma_n^2 = \frac{n-1}{n}\left[\sigma_{n-1}^2 + \frac{(x_n - \bar{x}_{n-1})^2}{n}\right] \tag{A.II}$$

Equation (A.I) was deduced in Strang (1986) whilst eqn (A.II) can be derived in the same manner in which eqn (A.I) was arrived at in the said reference. σ was based on n rather than n-1; the error in this value for $n > 100$ is less than one percent. This was considered sufficiently accurate for the present purpose of indicating the scatter of the data.

---

[13]

[2]A fact later confirmed by the equipment manufacturer (Biodata Ltd.).

Appendix B

Determination of the *in situ* thermal resistance of the composite insulant

Introduction

The effectiveness of thermal insulants in real systems may depend as much on the manner in which they are applied, as on the values of the thermal conductivities of the insulants. In some cases the geometry in and to which they are applied may also have as substantial a consequence on the thermal resistance of the resulting insulation as the thicknesses of the insulants applied. One well know case in point is the use of insulants on curved geometries where the ratio's of the insulants internal and external radii (and thus the ratio of the insulant thickness and mean radius) is significant in estimating the thermal resistance of the applied insulant. For this reason, particularly in non–simple geometries and composite[1] insulant arrangements, it is expedient where possible to obtain experimental estimates of the thermal resistance *in situ*. The current DRA application possesses a non–simple geometry and also utilises a composite insulant.

B.1 Aim

This appendix documents the experimental procedure utilised to determine the actual thermal resistance of a compartment similarly insulated to the proposed DRA.

B.2 Apparatus and Set up

The following apparatus were used for the current experiment:

- A cabinet of similar type as to be used in the construction of the DRA, fitted with the VPSI, see Figures B.1 and B.2, *qv.* pages B–254 and B–254 respectively; dimensional details are given in Figure B.3 on page B–255.
- Sixteen T–type thermocouples.
- A 15 Watt heat source (an incandescent bulb).

[1]Composite in the sense that more than one insulant (or insulation technique) contributes significantly to the resulting thermal resistance.

- A Fluke[1] data–logger.
- A power stabiliser.
- A watt meter.
- A variac.
- A standardised thermometer.
- A Thermos flask.
- Melting ice.
- Boiling hot water.
- Aluminium adhesive tape.

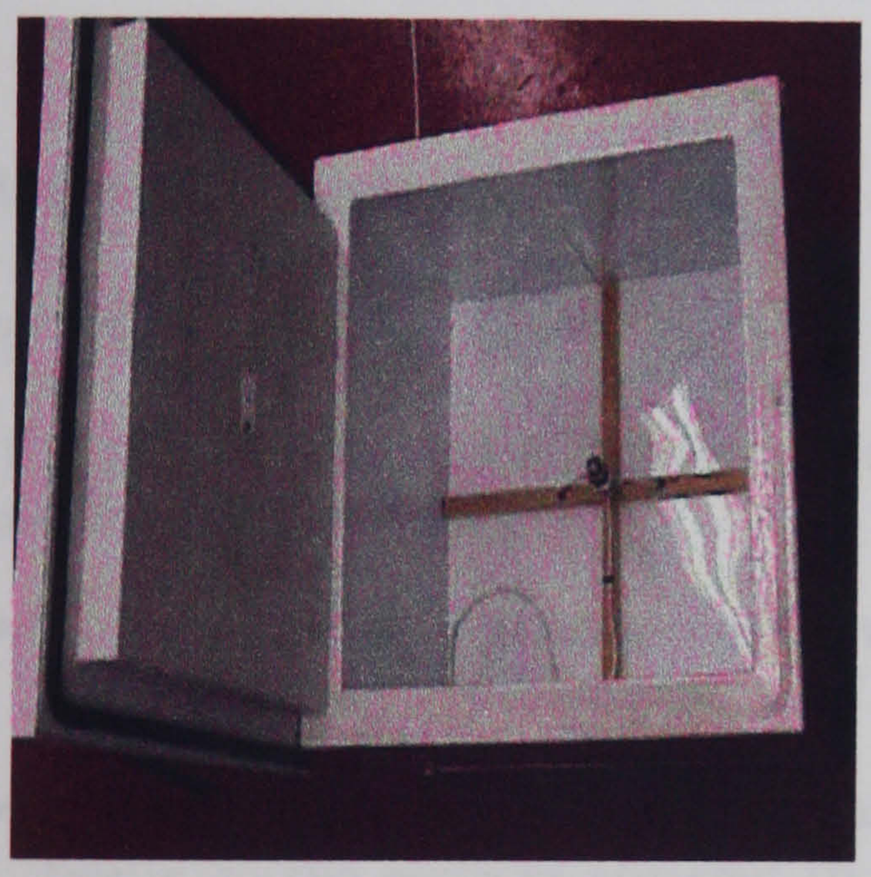


Figure B.1: Plan view of (open) experimental rig used for composite insulant conductivity determination.

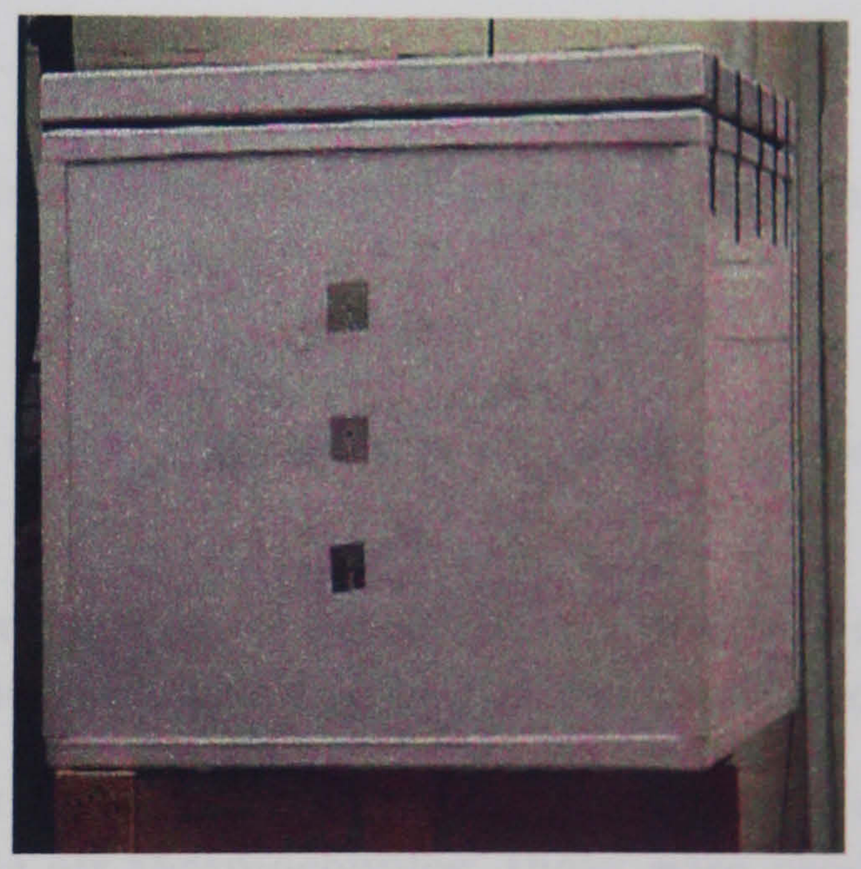


Figure B.2: End view of experimental rig used for composite insulant conductivity determination.

[1] John Fluke Manufacturing Co. Inc. USA

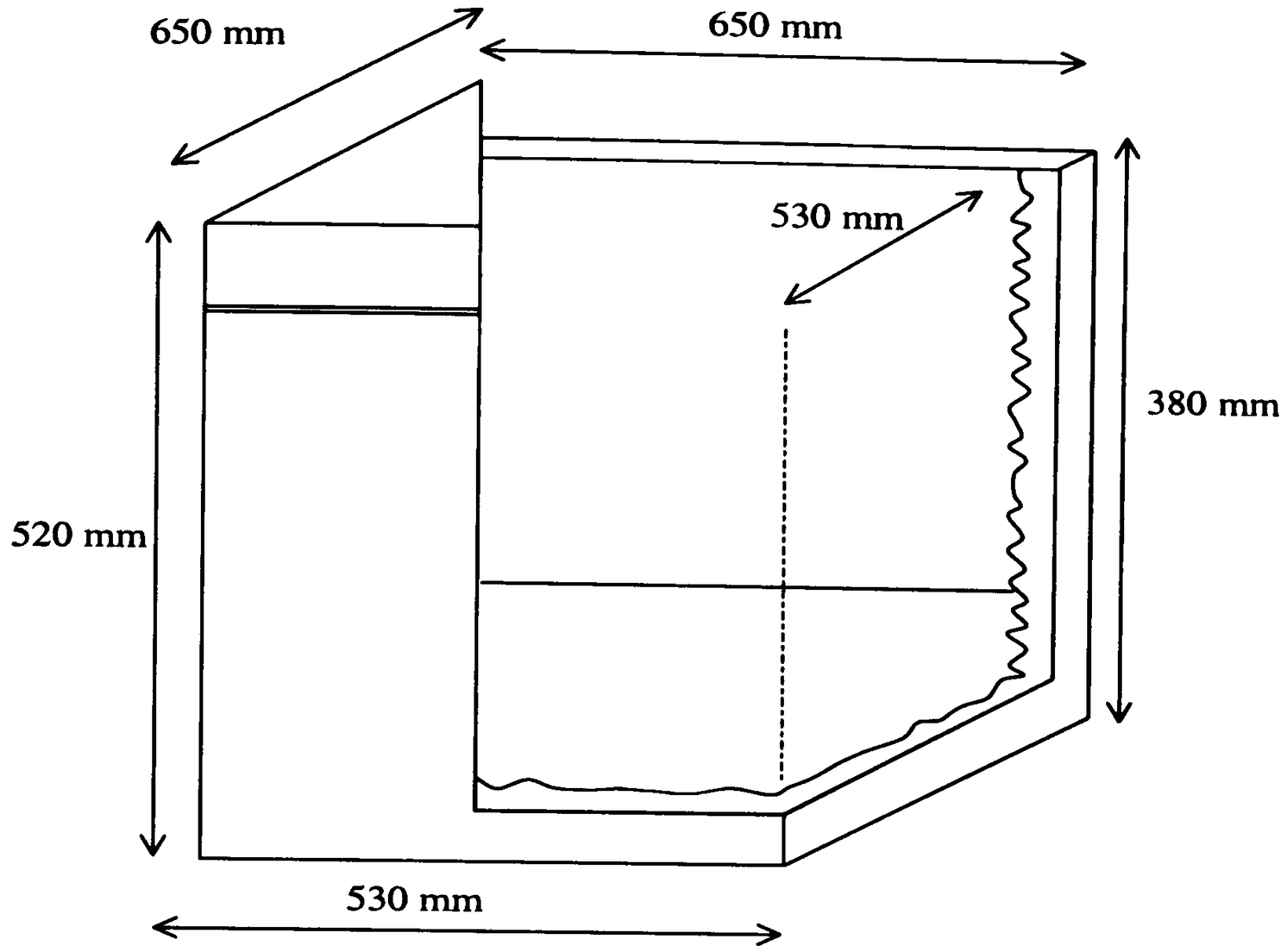


Figure B.3: Cut–away sketch of insulated compartment indicating dimensions.

B.3 The setup

The main experimental layout of the thermocouples was as follows (see also Figure B.4 on page B–256):

- Three equidistant thermocouples were placed vertically within the box and were used for the determination of the internal air temperature distribution.
- Seven thermocouples (four internally and three externally) were placed vertically on the surfaces adjacent to the air thermocouples; these were used to determine the temperature difference across the walls of the box. One thermocouple was placed adjacent to the thermocouple on the middle internal surface to check for temperature deviations along the horizontal.
- Two pairs of thermocouples were adjacently placed on either side of the lid, one pair at the centre and the other pair midway between the centre and an edge. These were to determine the temperature difference across the centre of the lid and to determine if there was a significant difference between the values across the centre and midway between the centre and an edge.
- One thermocouple was used to determine the ambient air temperature.

- One thermocouple was used to determine the air–heat source interface temperature.
- The heat source was connected to the mains via the variac. This was to facilitate the variation of the energy input to the system.
- All the thermocouples were attached at their thermo-junctions by means of the aluminium tape and connected to the data–logger.

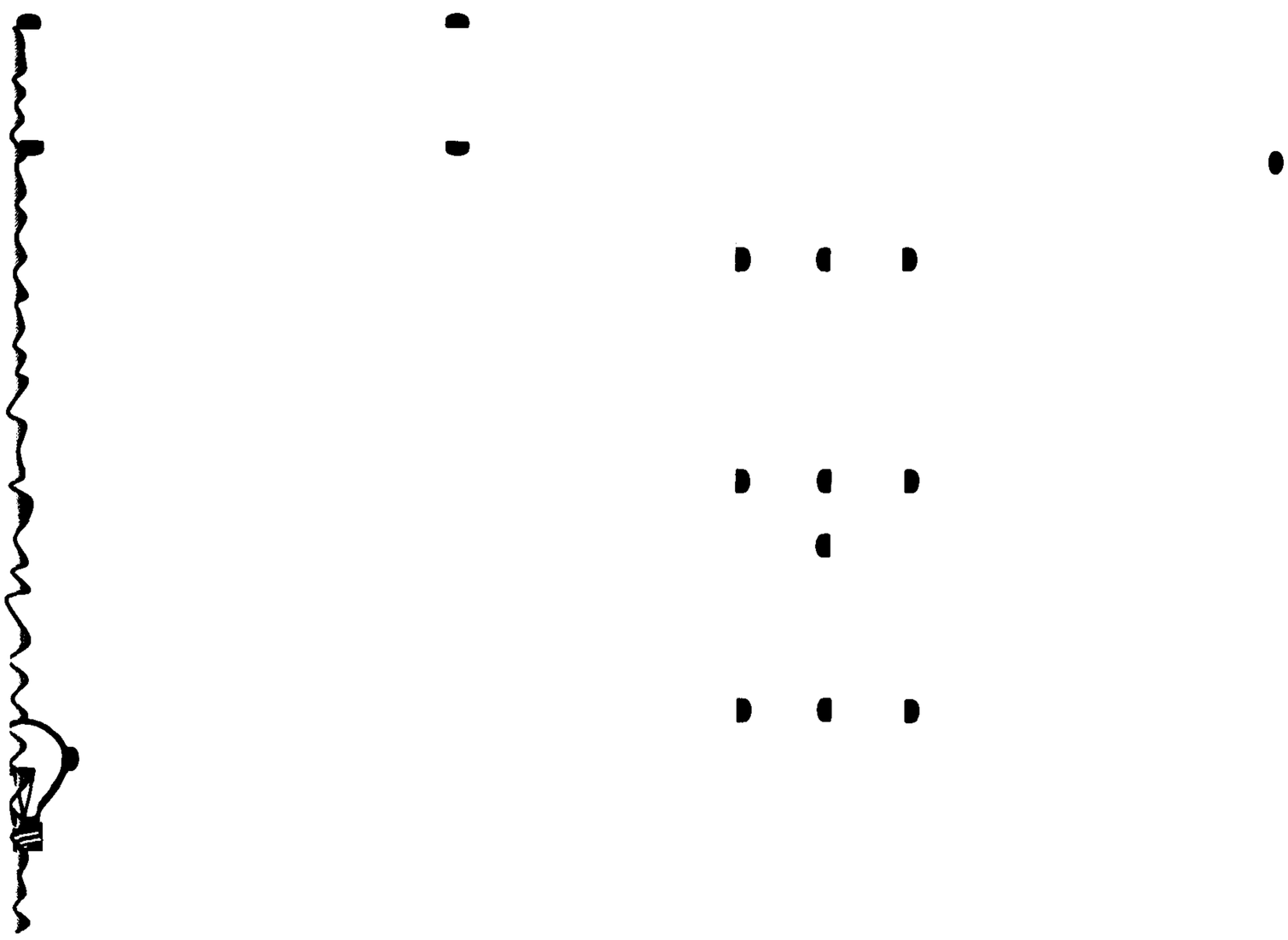


Figure B.4: Diagrammatic location of thermocouples.

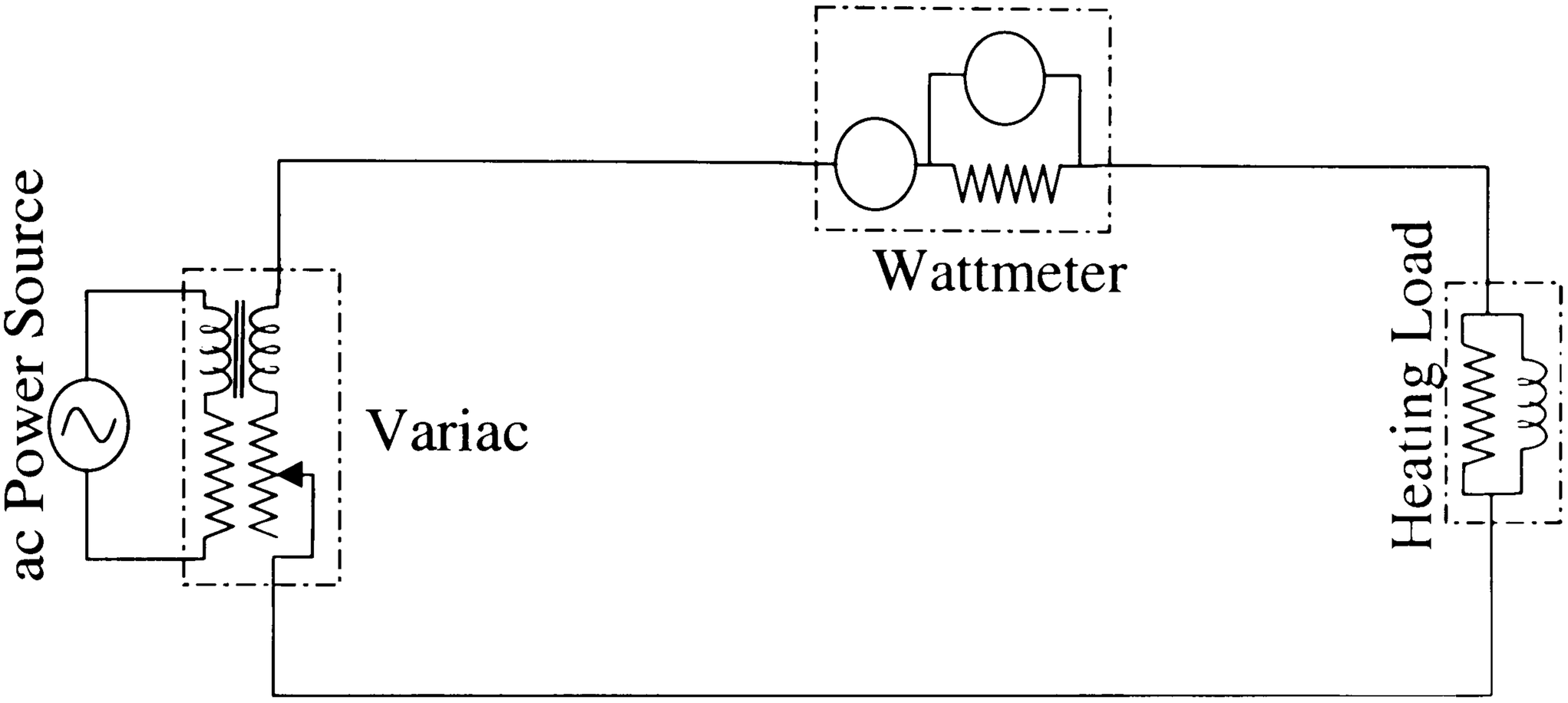


Figure B.5: Circuit diagram of experimental control layout

B.4 Procedure

Prior to the set up of the main experiment, the thermocouples were calibrated against a standard thermometer. The technique used is exactly as described in Appendix A on page A-288, excepting the following modifications:

- Boiling water held in the thermos flask was used in place of the isothermal heating block.
- The Fluke data–logger was used in place of the computer–MICROLINK arrangement.

- Fewer readings were used to determine the average values of the observed temperature[1] *i.e.* 3 as opposed to 400.

The results obtained in this pre–experiment were used to calibrate for accuracy. For information as to the algorithm for computing the offset and scaling factors and how appropriate corrections are made see Appendix A.2.5 on page A-290.

The rig was then set-up as described in Appendix B.2 on page B-253 and the access hole completely sealed off. The power source was switched on and the power input to the rig set. Readings were taken at four–hourly intervals until the readings from the data–logger at given locations became 'steady'. The experiment was repeated for three other input power settings. The average length of time for each experiment was four days and each experiment achieved a relevant temperature difference.

B.5 Theory

The underlying theory behind the experiment is relatively simple and draws on the basic (*Fourier*) law of conduction to determine an *effective* thermal conductance (K_{eff}) of the compartment. Schneider (1985) gives the following correlation (originally from Langmuir et al. (1913)) for the steady–state heat transfer *conductance*[2] into a parallelepiped shell:

$$\mathsf{K} = k\left[\frac{4ac}{\delta_{si}} + ab\cdot\left(\frac{1}{\delta_{fl}}+\frac{1}{\delta_{ce}}\right) + 1.08\cdot(a+b) + 2.16\cdot(a+c) + 0.4\cdot(4\delta_{si}+\delta_{fl}+\delta_{ce})\right] \tag{B.I}$$

$$\forall a,b,c > \frac{\delta_{max}}{5}$$

δ in this case represents the thickness of the enclosing wall, {a,b,c} being geometric internal dimensions. The exact representation of {a,b,c} as well as the subscripting notation for δ can be understood from the Figure B.6 on page B-259.

Due to the nature of the implementation of the composite insulation, it is necessary to consider the effect of parts of the VPSI layer which consists of polyurethane foam insulation. The shape factor S correlation given in Incropera and De-

[1] The system was much simpler than that of the main experiment, with a reduced propensity for data corruption from within the system.

[2] *cf:* $\dot{q} = \mathsf{K}\,\Delta\,T$

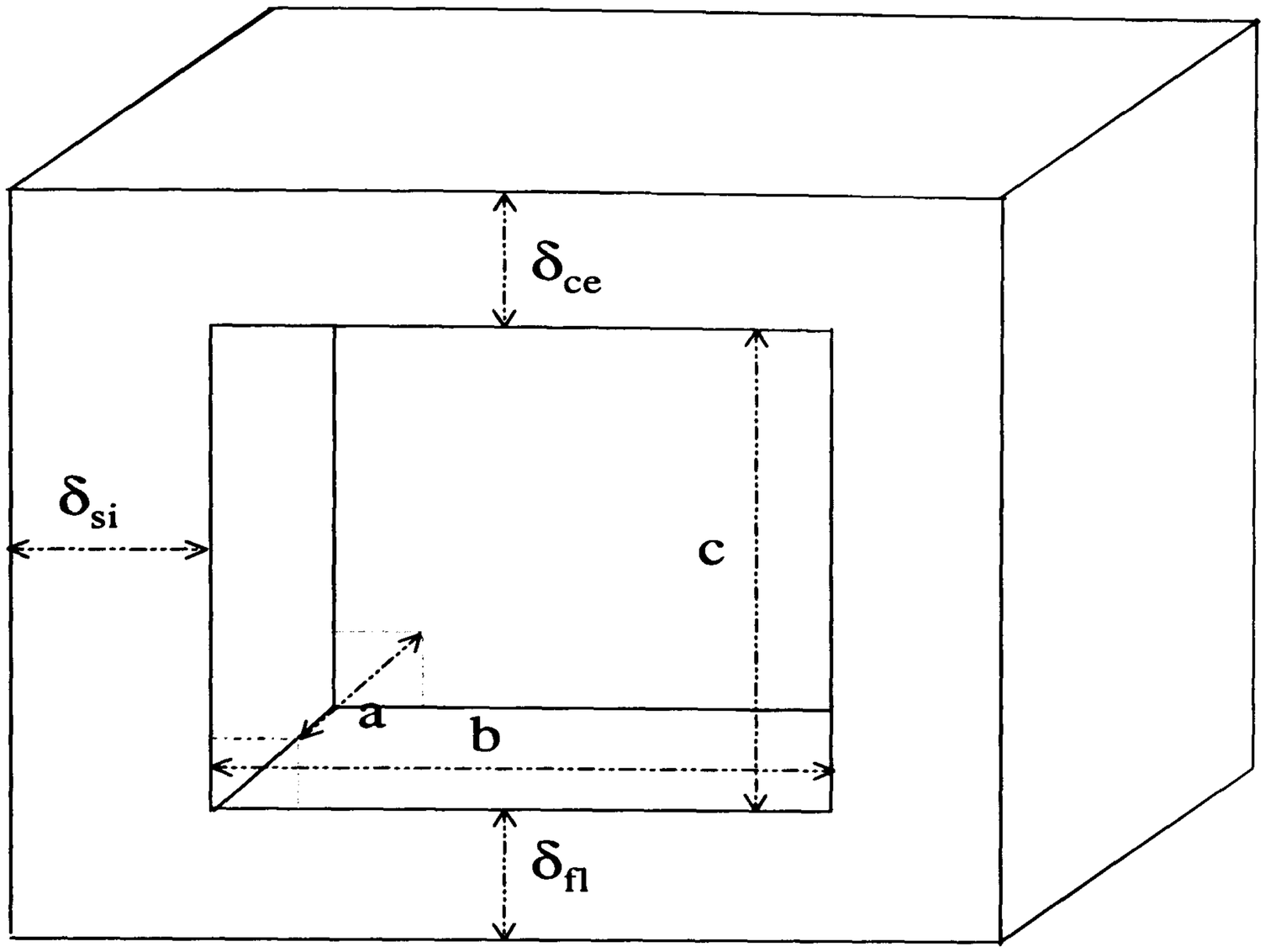


Figure B.6: Supporting figure for eqn (B.I)

Witt (1990), *pp.* 88, was used for this purpose.

$$S_{wall} = \sum_j \left(k \, \frac{A}{\delta} \right)_j , \quad S_{edge} = 0.54D, \quad S_{corner} = 0.15\delta$$
$$\mathsf{K} = \sum_j S_j \qquad \& \qquad D = \{a, b, c\} \tag{B.II}$$

In this case A is the area of each wall, δ the corresponding wall thickness and D the height of each edge[1].

In the event where the shell consists of several different layers of material *e.g.* as in the case of a composite insulant, the effective resultant conductance can be deduced as:

$$\mathsf{K}_{res.} = \frac{\prod_{j=1}^{n} k_j}{\sum_{i=1}^{n} \frac{\prod_{j=1}^{n} k_j}{k_i}} \tag{B.III}$$

The cabinet wall construction was of composite type, comprising 25.4 mm of VPSI ($k_1 \approxeq 0.0019$W/mK [Babyak, 1994][2]) sandwiched between 16.05 mm (sides). 12.3 mm

[1] see indicated reference for further clarification.

[2] Manufacturer's (OWENS-CORNING) quoted figures.

(bottom), 42.3 mm (inside top) and 12.3 mm (outside top) layers[1] of blown rigid low-density polyurethane foam $k_2 \approxeq 0.022$W/mK) [Woods, 1987]. Table B.1 on page B-260 charts the distribution of the various layers of thermal insulation making up the composite box. Using eqn (B.I) and eqn (B.II) with the aid of eqn (B.III) and the

Layer Conductivity (W/mK)	0.022	0.0019	0.022
depth (a) (mm)	535	567	618
width (b) (mm)	535	567	618
height (c) (mm)	380	445	495
δ_{si} (mm)	52	25	12
δ_{fl} (mm)	12	25	12
δ_{ce} (mm)	16	25	16

Table B.1: Distribution of composite insulation around compartment.

data in Table B.1 on page B-260, it is possible to deduce estimates for (a) the effective thermal conductance for each layer, (b) the resultant effective conductance for the compartment and (c) an apparent thermal conductivity for the composite insulant. Table B.2 on page B-260 tabulates the 'theoretical' conductances of various layers of the compartment's composite insulant, the total resulting conductance and the apparent thermal conductivity of the compostite insulant using two different correlations.

	layer conductance (W/°C)				Conductivity (W/mK)
Layer	0.022	0.0019	0.022	resultant	
eqn (B.I)	1.824	0.131	3.133	0.117	0.0044
eqn (B.II)	1.816	0.130	3.126	0.117	0.0045

Table B.2: Computed values for the thermal conductances and apparent conductivity

Applying eqn (B.III) to these results yields a value of $\approxeq 0.12$W/K as the theroretical conductance of the box containing the polyurethane foam–VPSI composite insulation. Similarly, eqn (B.II) may be applied to a box of similar geometry insulated with *only* polyurethane foam (the current practice since its introduction in the LER 2001 refrigerator which employed 65 mm of polyurethane foam, double the 30 mm thickness in common use at that time (1986) [Guldbrandsen et al., 1986]) the results yield

[1] Due to the method employed in manufacturing the box there was a 40 mm polyurethane foam protusion extending into the cabinet

$\approx 0.59\mathrm{W/K}$. Thus, in theory, a *circa* five–fold increase in the compartment thermal resistance may be expected with the change to the composite insulation.

From the data obtained from the experiment, the temperature differences between adjacent wall thermocouples (interior-exterior pairs) were computed. If *each* of these values are assumed, in turn, to be representative temperature differences either side (adjacent) of the cabinet wall, an apparent thermal conductance for the box may be computed, *viz*:

$$\mathrm{K}_{apparent} = \frac{\dot{q}}{\Delta T} \tag{B.IV}$$

B.6 Experimental Results

From the data–logger output, quiescent data[1] was taken over a 24–hour period and the apparent thermal conductance for the cabinet based on each adjacent wall thermocouple pair (internal and external) computed as described in Appendix B.5 on page B–258. The average value for each thermocouple pair was then computed (in an attempt to cancel out the diurnal fluctuations of the ambient) and the results, grouped by region, are presented in Figures B.7 and B.8, *qv.* pages B–261 and B–262 respectively

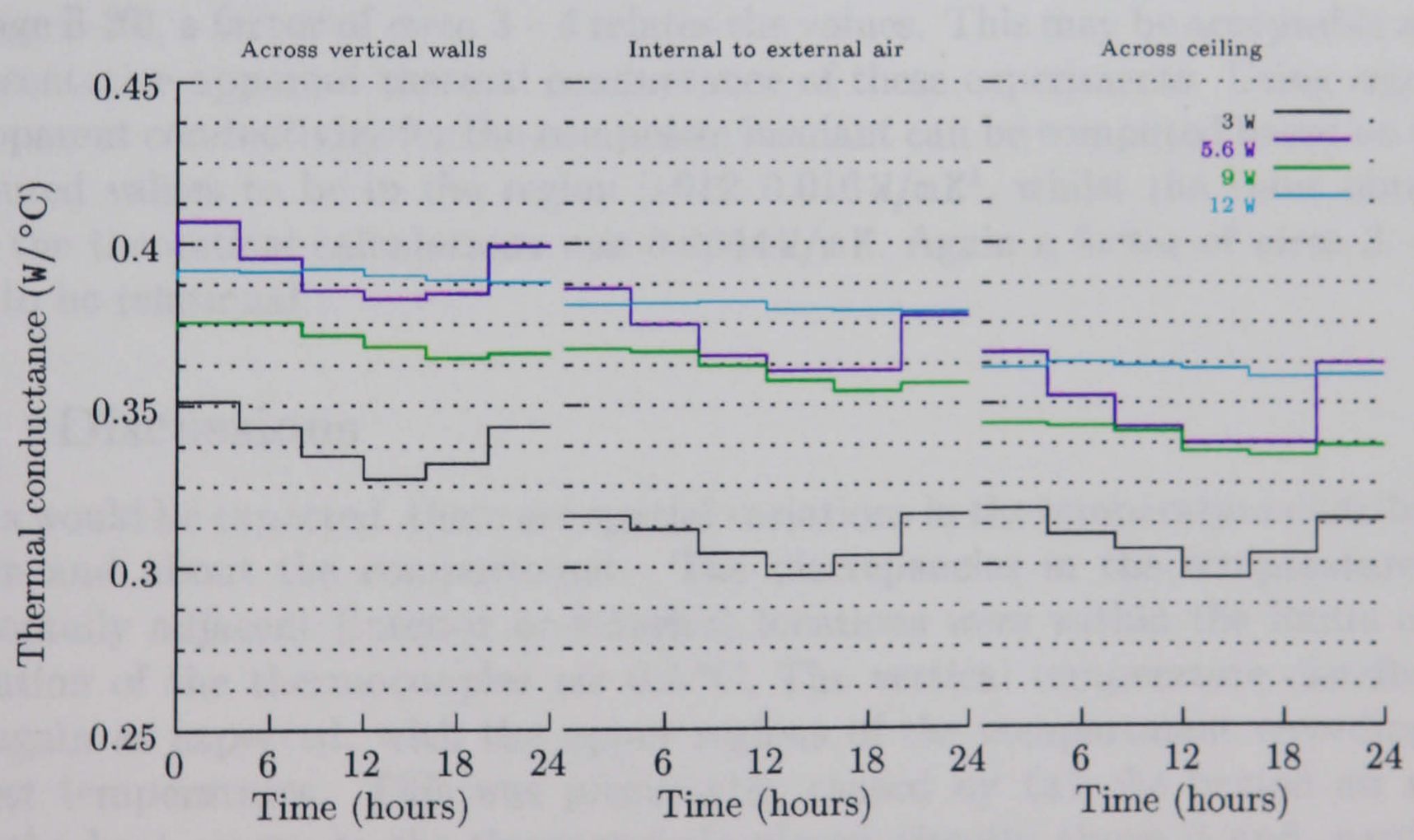


Figure B.7: Thermal conductance charts

[1] In the quasi steady–state sense, due to the diurnal fluctuations of the ambient temperature

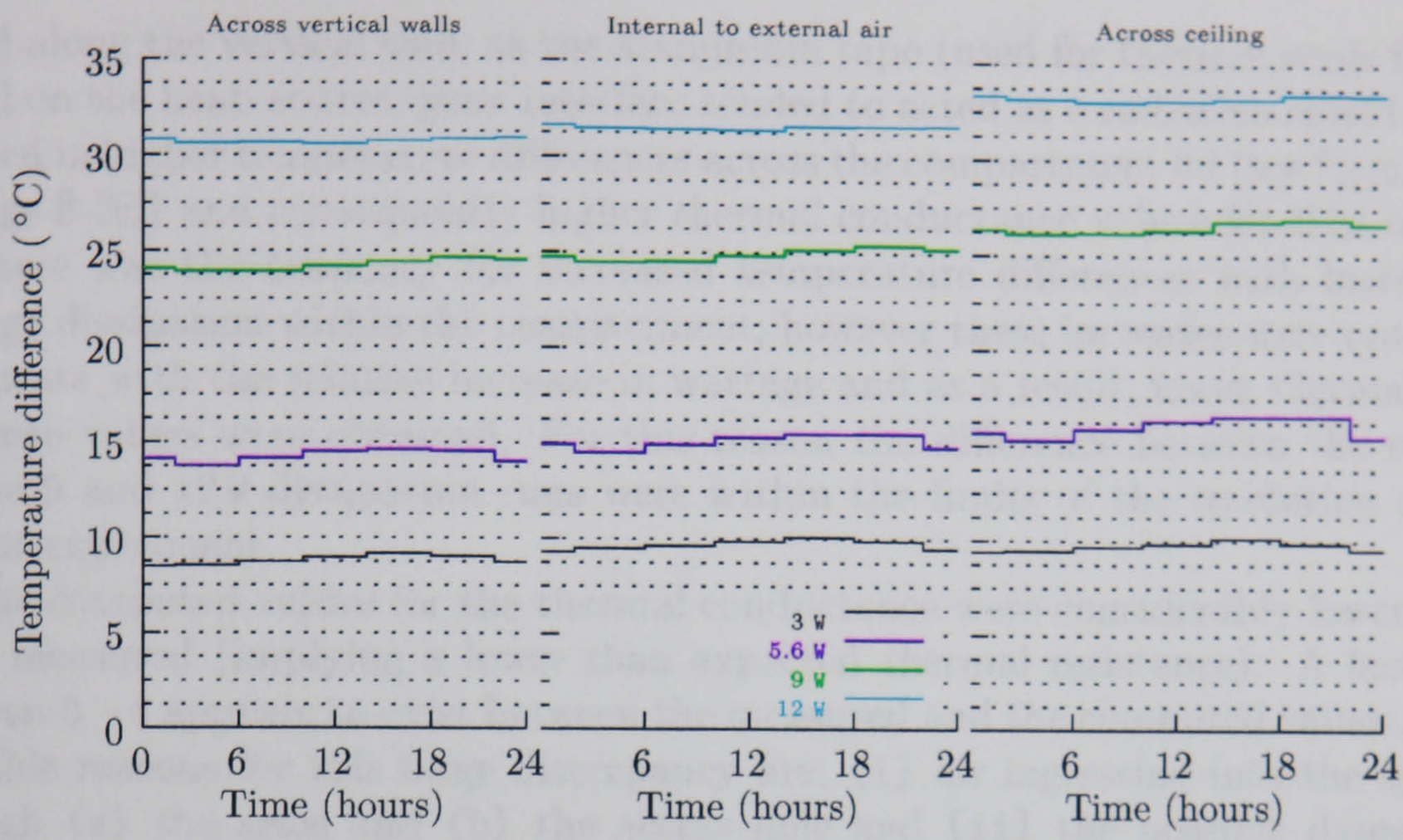


Figure B.8: Temperature difference charts

The range of the thermal conductance values obtained was between 0.33–0.40 W/K. In comparison with the theoretical estimates (0.117 W/K) given in Table B.2 on page B–260, a factor of *circa* 3 – 4 relates the values. This may be acceptable as the representative apparent thermal conductance of these experiments. Using eqn (B.I) an apparent conductivity for the composite insulant can be computed based on these measured values to be in the region 0.012–0.016 W/mK[1], whilst the value obtained from the theoretical calculations was 0.0044 W/mK. Again a factor of *circa* 3 – 4 is seen to be relational.

B.7 Discussions

As would be expected, there are spatial variations in the temperature distribution within and about the compartment. The discrepancies in the temperatures for horizontally adjacent (interior *or* exterior) locations were within the limits of the resolution of the thermocouples *viz* 0.5 °C. The vertical temperature distribution was again as expected, with the upper regions of the compartment recording the highest temperatures. This was presumably caused by (a) the heated air rising from the heat source to the thermocouple placed directly above it and, partly by (b) the effects of radiation from the heat source to that surface. The effect of this radiative component was deemed to be comparatively less on the thermocouples

[1]Similar values are obtained with the use of eqn (B.II).

placed along the vertical wall, as the aluminium tape (used for thermocouple fixing) placed on the heat–source/glass interface tended to acted as a radiation shield. This resulted in higher temperature differences across the compartment lid (see Figure B.8 on page B-262) and consequently higher thermal conductance values for that region.

There was the tendency for increased temperature differences with increasing wattage dissipation within the compartment; however these increases were not commensurate with the relative increase in wattage and as a result, lower thermal conductance values were obtained. For this reason the difference between the results for the 9 and 12 W dissipation runs were within the limits of the resolution of the current experiment.

The computed values for the thermal conductance were considerably lower than those measured (implying a lower than expected thermal resistance). A factor of between 3 – 4 appears to exist between the measured and the computed values. Two probable reasons for this large discrepancy are, [i] air ingressing into the system through (a) the seals and (b) the access hole and [ii] the possible damage of one of the panels during handling. That not withstanding, the apparent thermal conductivity of the composite insulant (estimated at 0.012–0.016 W/mK) is a marked improvement (50 – 70%) on the 0.022 W/mK which would otherwise be obtained from the polyurethane foam alone. It is thus clear that the polyurethane foam–VPSI composite insulation system is far superior as a thermal insulant to the polyurethane foam alone.

Incidentally, [i-(a)] above has far–reaching implications in the application of 'super insulants' in DRA's, in that currently some 32% of the total heat leak into DRA's is through the door gaskets [ASHRAE, 1994, *pp.* 48.3]. If the compartment wall insulation is improved, without due attention given to the door seals and other avenues of heat leak, much of the effort and expense might well be in vain.

Another interesting observation is the lag response time across the cabinet wall. If the data for the temperatures at various locations is plotted over time, a distinct lag between the cabinet internal temperatures behind the external ambient temperature is observed. In this case the lag is 240 minutes (four hours), see Figure B.9 on page B-264, which can have implications in the design of an effective thermal control strategy for a DRA utilising such an insulant.

B.8 The sources of errors

There are several avenues from which errors might have arisen in this experiment; these include:

- Fluctuations in the ambient temperatures made the ideal attaining of fixed steady–state temperatures impractical. Thus quasi–steady temperatures had

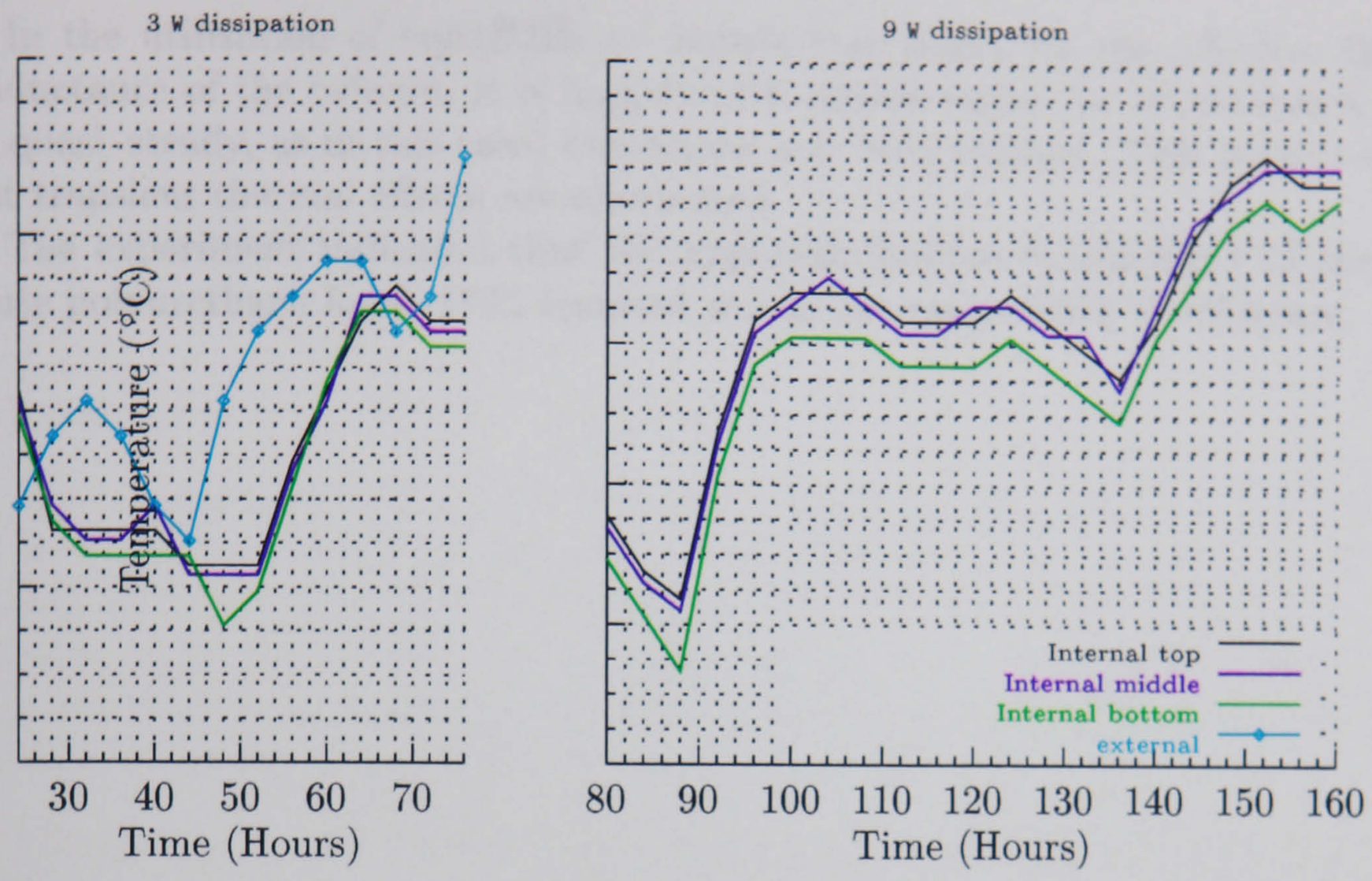


Figure B.9: Graphs indicating thermal lag during experiment.

to suffice.

- Despite of the fact that the power supply was connected to a stabiliser there were still noticeable fluctuations in the power input to the rig. The effects of these were more significant at lower power settings.

- The calibration of the thermocouples against the standard thermometer. Errors here may include those due to inaccuracies in the 'standard' (systematic) and errors due parallax (random).

B.9 Summary

The basis of these experiments was to deduce real estimates for the resultant thermal conductance (and apparent thermal conductivity) of the proposed composite insulant. In the utilisation of these results, it must be borne in mind that the calculations have been based on eqn (B.I) which is geometrically, as well as dimensionally, dependent. Thus the values obtained here should in no wise be applied to systems which are geometrically or markédly dimensionally different from the current one. Similar restrictions apply to temperature ranges within which these values are useful (*e.g.* such as temperature regions where the linearity approximation of the thermal conductivities breaks down) even within the current dimensional context.

In the utilisation of eqn (B.III) to deduce real values for the *effective* thermal conductance of the cabinet, it is important to utilise values for which steady-state (or quasi-steady, as in this case) conditions had been reached. This is as to ensure that transient thermal effects are eliminated.

The experiment indicated that the apparent thermal conductivity of the composite polyurethane foam-VPSI insulant was in the range 0.012-0.016 W/mK.

Appendix C

The Production of Hydrophilic PVA LHTES Samples

Introduction

This appendix documents the preparation process of a cross–linked hydrophilic (water retentive, polymeric) material used as LHTES. The polymer used was polyvinyl alcohol (PVA) and the chosen method of cross–linking was the use of *gamma*–radiation (from a Cobalt 60 source). The technique has been applied extensively to the production of hydro–polymers, particularly those used in medicine[1]. Radiation polymerisation has the advantages that:

- The very nature of the process (gamma–ray irradiation) yields a sterile product.
- The process is relatively simple compared with other polymerisation processes (*e.g.* chemical) and allows the use of polymer solutions which are less hazardous than monomers. There are no other residual chemicals (initiators or reagents left in the product) which are often poisonous.
- The process is comparatively cheap. This is because, the dosage of radiation required for the purpose is similar to that which is commercially used for other purposes (*e.g.* waste sterilisation).

Some disadvantages of the technique are:

- Whilst the process is not extremely sensitive to the *intensity* of the irradiation, some attention has to be payed to the dosage of radiation being supplied, as radiation damage may result. This usually takes the form of dissociation of water molecules producing hydrogen molecules which are then trapped in the rigid structure.
- The method is not particularly suited to the production of thick (in excess of 500 mm) as differential cross–linking may result, with cross–linking of the regions furthest from the radiation source less likely to proceed to full extent. This problem may partially be alleviated by rotation of the samples; however this is to within a limit. Increasing the dosage intensity of the radiation does

[1] For the manufacture of contact lenses, as a prosthetic aid *etc.* see [Holly and Refojo, 1976].

not appear to be the solution, as damage may result in regions closest to the radiation source which may yield samples which are not suited to the intended application.

- The process cannot be applied to the production of all types of cross–linkable hydro–polymers.

The process has been extensively studied and documented and the interested reader may consult any of the many standard texts which deal with polymers and their polymerisation, for instance [Buchholz and Peppas, 1994]. The use of radiation cross–linking for the preparation of cross–linked polymers has been applied here at Cranfield university within different projects [Leguay, 1994; Birkett, 1996] where it was reported to have performed satisfactorily. It was based on this and the foregoing that the process was chosen in this application.

After the preparation, preliminary experiments were carried out to assess the overall suitability of the resulting polymers for the thermal storage function. This appendix deals only with the manner in which the TES's were produced for use within this project and the various tests/observations made on the resulting product.

C.1 Aim

The aim of this exercise was to produce sufficient numbers[1] of well contained, inert portions of cross–linked hydrophilic PVA for the ES–DRA experiments. These are to have *circa* 95% water content and not weigh less than 1.26 kg[2], with a view to producing a total thermal storage capacity in excess of $0.4\,\mathrm{kWh}_{(T)}$ see section 6.5 on page 209 and Tables 6.17 and C.2, *qv.* pages 204 and C-321 respectively.

C.2 Apparatus

The following were used in the production of the storage medium:

1. Polyvinyl alcohol (500g), molecular weight 115,000[3].
2. Several gallons of distilled water, produced in the laboratory.
3. Several thick–walled polyethene bags 340 mm × 480 mm[4].

[1] At least four.

[2] Based on the computed estimates given in Chapter 6 on page 184.

[3] Suppliers: BDH Laboratory supplies, Poole, BH15 1TD, England.

[4] Suppliers: Flectalon Ltd.; Thermal insulation manufacturers, Treforest Industrial Estate. Pontypridd, Mid-Glamorgan CF37 5UA, England.

4. A Dapper bar–type impulse heat sealer[1].
5. A weighing balance.
6. A large bucket.
7. A stirrer.
8. A roll of thin polyethene sheeting '*cling film*'.

C.3 Procedure

The bucket was weighed and then tarred on the scales and 1.5 litres of *hot* water added to it[2]. Approximately 0.253 kg of PVA (for a 5% solution) was then weighed out and slowly added to the water as it was stirred vigorously. On contact with the water the PVA powder agglomerated into clumps due to the rapid partial dissolution (inadequate dispersion) of the material. When all the PVA had been added to the solution, the contents of the bucket were made up to 2.0 litres by the addition of more hot water. The bucket was then covered with the cling film and left for the gradual dissolution of the clumps to take place. Every six to eight hours the mixture was stirred to aid the process and after seventy–two hours, all the solid had passed into solution, the solution was then divided equally between four of the polythene bags and each bag made up to a weight slightly in excess of 1.2632 kg[3]. An attempt was then made to expel the air from the bags and they were then sealed.

The process was repeated to make up spare bags and for two other weight categories (0.65 kg and 0.33 kg). Subsequently, the bags were packaged (as flat as possible[4]) in cartons, between wood–chip board and sent off for irradiation[5]. Unfortunately, some of the bags burst during handling in transit and the package had to be returned. The process had to be repeated and was successful on the second attempt. The dosage used was 2.5 M*rads* which may be slightly more than is necessary for cross–linking; this was as the installation where the irradiation was carried out was set up for processing hospital/commercial waste where higher doses are routinely employed.

---

[1] Manufacturers: The Thames Packaging Equipment Company, Senate House, Tyssen Str., London E8 2ND, UK.

[2] There was no need to use distilled water as any living organisms would be destroyed during the irradiation process; *hot* water was used to aid the dissolution process.

[3] *circa* 1.3 kg; this excess is to accommodate any spillage that would occur during the bag sealing process.

[4] As this will define the geometry of the ensuing product

[5] This was done *gratis*, courtesy of Isotron PLC., Unit 2 Marcus Clo. Tilehurst, Reading, Berkshire RG3 4BJ. UK

Visual examination of the samples returned revealed the following:

- There was some variation in the degree of cross–linking across the bags. This variation bore some correlation to the position of the bag in the packaged stack. The PVA in the bags on the top of the stack were fully cross–linked, with the degree of cross linking diminishing with depth (as evidenced by the proportion of the fluid content in the bags). Some of the bags at the bottom of the stack did *not* cross–link at all. This may possibly be as a result of the manner in which the bags were irradiated or the location of the radiation source.

- In the uppermost PVA bags, there were a substantial amount of bubbles within the cross–linked matrix. This was probably as a result of the decomposition of water molecules due to the high dose of radiation, thermal heating due to the dose rate and/or the exothermic nature of the polymerisation process. These bubbles in themselves are not perceived to constitute a major compromise in the suitability of the particular bag to the given application. The immersion of bags with such defects in water was sufficient to fill the voids. The implication of filling the voids in the samples with water (particularly those with a high void content) is that the percentage of water (by mass) in the matrix may be slightly increased. As mentioned earlier this would not affect the suitability of such samples to the intended application.

- The bags which did not 'take' were discarded as they would probably change phase at temperatures removed from zero (foreseeably at the phase–change temperature of 5% PVA). This would not be suitable for the present application. There was no need to employ any of the bags with voids, as four of the bags returned were of sufficiently high quality. The weights of these bags were: (1347.8, 1313.1,1317.0 and 1301.3) kg respectively. These relatively higher quality bags were used in the experiments.

C.4 Other tests

Two short tests were carried out on samples of the returned cross–linked PVA product. The first was to ascertain whether the water content of the samples was about or in excess of 95%. The second was to ensure that the phase–change point of the resulting PVA–H_2O matrix was in the region of 0 °C and that the hysteresis effect reported by [Highgate et al., 1989; Okoroafor et al., 998a; Okoroafor et al., 998b] did not occur.

C.4.1 Estimation of the water content

Samples of the acceptable finished product were taken and dried at different temperatures in a fan–assisted oven. An attempt was then made to rehydrate the samples. Several similar runs were observed at differing temperatures. The experiments yielded somewhat varying results; in all cases the results indicated water–uptake values in excess of 94%. Typical sample results are tabulated in Table C.1 on page C-319. One apparent characteristic of the PVA samples was that the rate of initial dessication was high. On initial exposure to the ambient, surface dry–out occurred rapidly with the result that the polymer surface became sticky to touch.

Typically attempts to rehydrate the material resulted in rehydration weights which were less than the immediately preceding hydrated weight. In all cases the structure of the rehydrated polymer was markédly distorted in comparison with the original material; this was evident from the surface texture of the material. This was probably as a result of surface dry out and caking inhibiting the further desiccation of the material as well as possible damage to the material structure[1].

The changes in weight may have been the result of polymer loss and failure of the material to fully rehydrate, possibly as a consequence of structural changes/damage to the structure due to the thermal dessication process. Large changes in the initial dessication–rehydration run may have been due to the fact that the initial drying phase may have driven off any uncross–linked material from within the matrix. Lower rehydration weights and more surface damage were evident at higher temperatures, which tends to indicate greater degradation of the matrix structure.

A different technique was deployed in an attempt to obtain more consistent results across runs. This involved placing the sample in a vacuum chamber and waiting for a sufficient length of time for the weight to equilibrate. Several problems were encountered with this method. Principally it was not possible to remove the sample from the chamber without (a) the rapid rehydration of the sample and (b) the freezing of the water contained within the sample. Similar surface degradation as was observed using the oven technique was also observed in this attempt.

C.4.2 Estimation of Freezing point

In order to observe the thermal behaviour of the PCM, a sample of the accepted finished product was subjected to several freeze–thaw cycles[2]. The freeze/thaw characteristics of the material was as expected, the material changing phase at *circa* -1 °C on both the decent and accent stages of the cycle. The Figure C.1 on page C-

[1]The hydrated PVA samples were made from solution with the water present and 'as made' structure is likely to collapse on drying and may not rehydrate with the same morphology.

[2]Between a -25 °C freezer and a 21 °C ambient.

Drying temperature (°C)	Mass of hydrated sample (g)	Mass of dry sample (g)	$(\%)_{[H_2O]}$ in initial sample	Mass of rehydrated sample (g)	$(\%)_{[H_2O]}$ in rehydrated sample
110–120	48.5	1.4	(%w)	42.0	(%w)
90–100	24.1	1.5	94	16.5	91
60–70	41.2	1.9	95	18.5	90

Table C.1: Data obtained during the dessication–rehydration experiments during the estimation of the water content in the cross–linked PVA.

320 is one such map of the temperature–time curve of the material. It is interesting to note the manner in which the water within the polymer undergoes transition forming fine crystalline sub–structures within the cross–linked PVA matrix. This tends to indicate that the matrix structure serves to provide nucleating centres for ice growth.

C.5 Basic calculations and observations

The TES medium is to consist of 95% water; hence the latent energy content of the store will be 0.95 of what would be available if the water was the medium used. If an assumption is made that only 90% of the stored energy will be recoverable[1], this will reduce the energy storage density of the TES to 86% of its water equivalent. The latent heat of fusion of ice is in the region of 335 kJ/kg this gives an apparent heat of fusion of *circa* 286 kJ/kg for the 95% water–uptake TES. The following Table C.2 on page C-321, illustrates this (apparent latent heat concept) for different degrees of hydration of cross–linked PVA; with the information presented to give an indication of the TES weight and volumes which would be required per $kWh_{(T)}$. The Table was used as a means of assessing the LHTES material requirements for the current application and contains the required weights and volumes for the 0.4 $kWh_{(T)}$ TES used for the main experimental work Chapter 7 on page 229.

C.6 Discussions

In order to reduce the effect of the material conductivity on the rate of heat transfer into and from the store, LHTES medium containment dimensions of *circa* 9 mm × 300 mm × 300 mm has been specified. This also serves to reduce the impact on

[1]This is based on the quantity of free water likely to be in the 95% samples see Highgate et al. (1989).

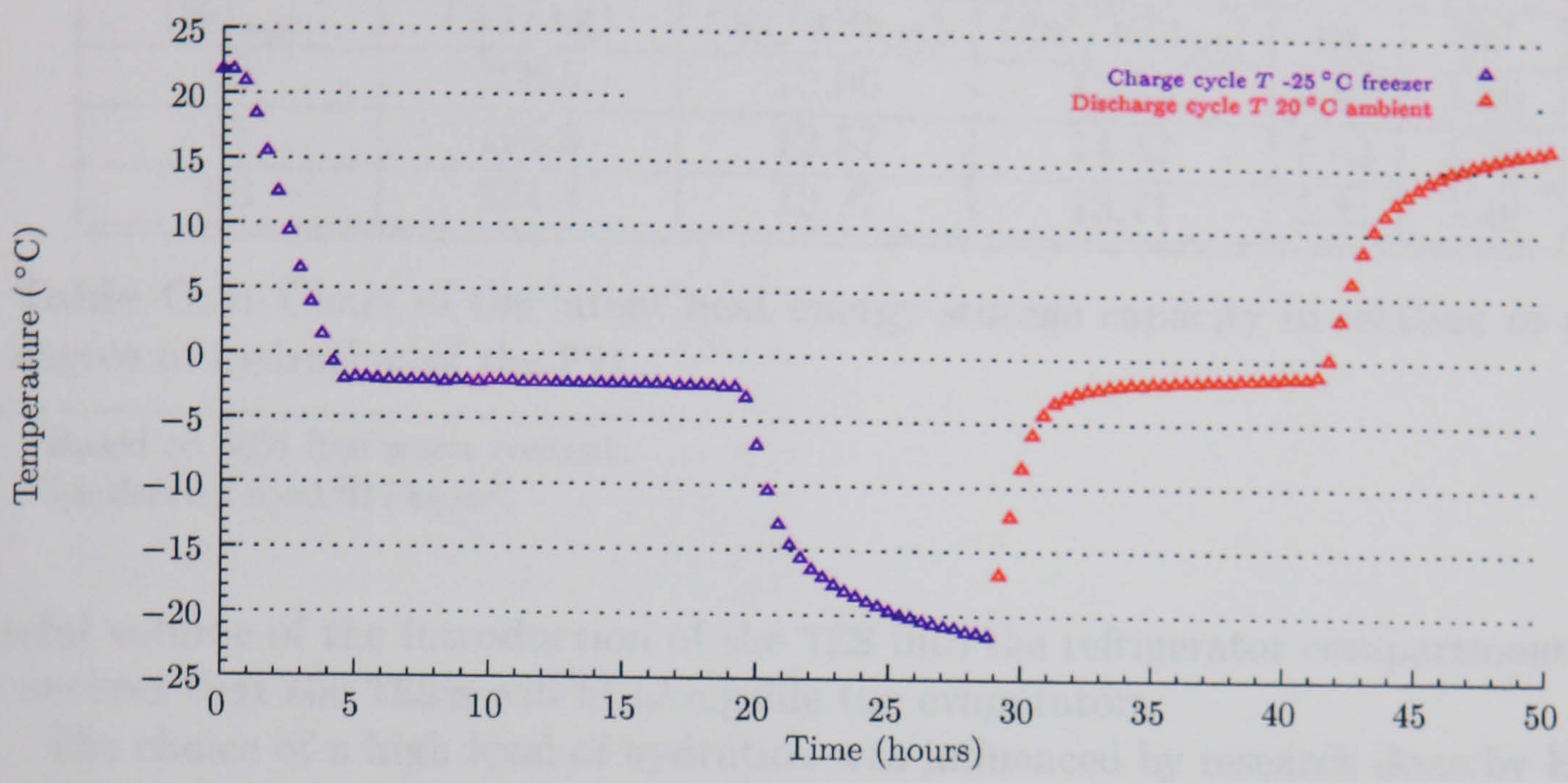


Figure C.1: Temperature–time history of a (95% w/w H_2O) cross–linked PVA TES (*circa* 305 mm × 305 mm × 14 mm) during a charge (−25 °C) – discharge (+20 °C) cycle.

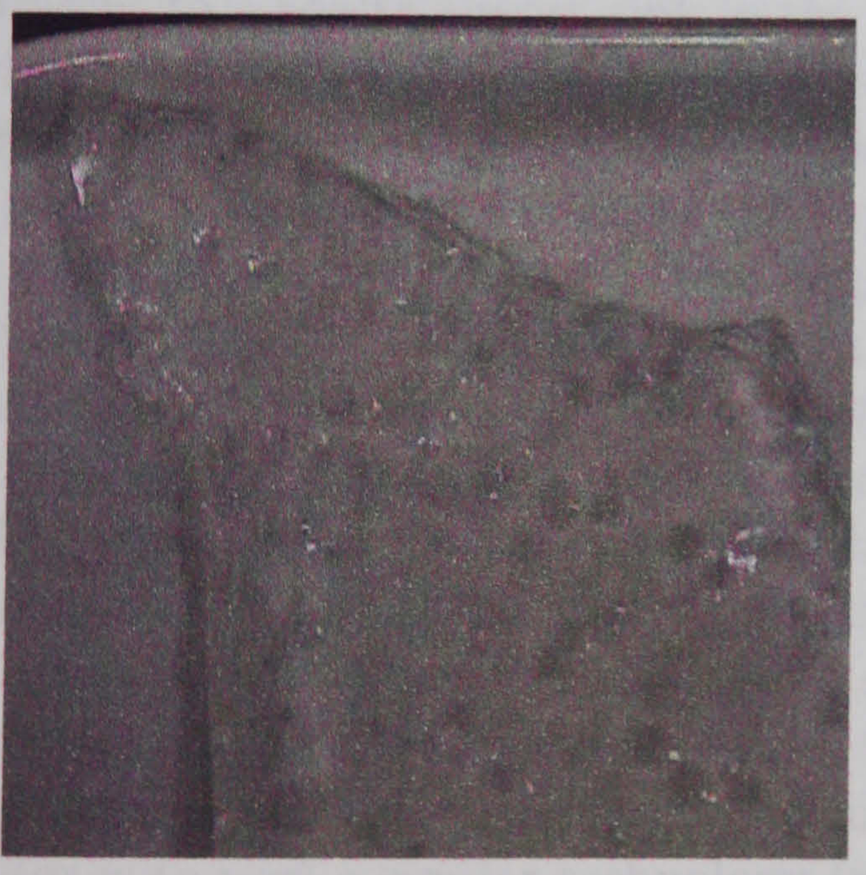


Figure C.2: PVA (cross–linked *circa* 95% w/w) *above* the phase–change temperature (T_{LH}) of water.



Figure C.3: PVA (cross–linked *circa* 95% w/w) *below* the phase–change temperature (T_{LH}) of water.

Degree of hydration	Apparent latent Heat[a]	Energy Content [b]		0.4 $kWh_{(T)}$ equivalent	
$(\%)_{[H_2O]}$	(kJ/kg)	$(kg/kWh_{(T)})$	$(dm^3/kWh_{(T)})$	kg	dm^3
99	298.5	12.06	13.15	4.82	5.26
95	196.5	12.57	14.47	5.03	5.79
90	271.4	13.27	13.71	5.31	5.48

Table C.2: Chart of the latent heat energy storage capacity in relation to the degree of hydration of the PVA.

[a]Based on 90% free water content.
[b]Ice density used 917 kg/m^3.

useful volume of the introduction of the TES into the refrigerator compartment and it ensures that the TES's will fit alongside the evaporators.

The choice of a high level of hydration was influenced by research done by Highgate et al. (1989), Okoroafor et al. (998a), Okoroafor et al. (998b) which demonstrates large hysteresis loops in the thermal path of low water content hydro–polymers under initial thermal cycling across the solid–liquid phase transition of water. This indicates a thermal energy transfer differential between the two paths, equivalent to a coolth energy sink in the freezing cycle, a behaviour which decreases markédly with increasing degree of hydration. This is possibly attributable, in part, to the cooling required to overcome the heat generated due to stresses building up in the hydro–polymer matrix during the expansion of the water molecules on freezing. The main inference from this is that higher water content hydro–polymers (hydro–gels) tend to act as better thermal stores. They have the disadvantage, as hydration approaches 100%, of loosing their rigidity and as such require increasingly delicate handling if physical damage is not to occur.

The PVA solution is easily degraded by fungal attach which tend to break down the longer chains and thus destroy its propensity for cross–linking. For this reason care was taken to ensure that the PVA solution was covered at all times prior to irradiation. The ensuing hydro–polymer (on irradiation) also has a tendency to grow fungi when exposed to unsterile conditions[1]. In view of this in any application which uses (or is to use) a similar technology (particularly in environments where hygiene is of some concern), the hydro–polymers have to remain isolated from any but inert environments (at least pending the identification of a suitable (aqueous) fungicide). This is another reason why the radiation method of hydro–polymerisation lends itself to the current application.

[1]Several specimens (of different types) which were left open in the labs tended to have been



Figure C.4: PVA (cross–linked *circa* 95% w/w) with fungal growth after a few months immersed in a sealed container of tap water.

colonised by what have the appearance of brown and/or green algae, see Figure C.4.

Appendix D

Computer Code Listing

Thermal Analysis and Experiment Controller Computer Code.

Due to the length of a hard copy code listing. the computer codes are provided on diskette.

References

UL and CAN/CSA (1998). Household Refrigerators and Freezers, UL 250 and CAN/CSA C 22.2 # 63-69 (1997).

UK-ISES (1976). Solar Energy:a UK assessment. Technical report, International Solar Energy Society, 21 Albemarle Street, London W1X 4BS.

ASHRAE (1976). *Thermodynamic Properties of Refrigerants* (Second ed.). 345 East 47th Street, New York: ASHRAE.

WHO (1979). Expanded Programme on Immunisation EPI. WHO Chronicle # 33.

EC (1979). On the Indication of Labelling the Energy Consumptions of Household Appliances. EC *Council Directive* (79/530/531).

ASHRAE (1985). ASHRAE *Handbook (Fundamentals)* (SI ed.). ASHRAE refrigeration handbooks. http://www.ASHRAE.org: MacGraw Hill Book Company.

WHO (1986a). A Guide to Estimating the Capacity Required for Storage and Transportation of EPI Vaccines. WHO *communique* # WHO/EPI/CCI1/86.3.

WHO (1986b). Guide on Implementation of Solar Energy for EPI. WHO *communique* # WHO/UNICEF/EPI.TS/86.3.

WHO (1988). EPI *Technical series: Standard Equipment and Test Proceedure* E3RF *(3–5)*. UN–WHO.

ANSI/AHAM (1988). Household Freezers, combined Fridge, Freezers and household refrigerators, ANSI/AHAM HRF-1-1988.

WHO (1990a). EPI Logistics and the Cold Improving Improving Quality. WHO *communique* # WHO/EPI/LHIS/90.5.

WHO (1990b). WHO/UNICEF Standard Performance Specifications for Solar (Photo–Voltaic) Refrigerators. WHO Performance specifications.

CAN/CSA (1991). Capacity measurement and energy consumption test methods for Household Freezers, combined Fridge, Freezers and household refrigerators, CAN/CSA C300-M91.

WHO/UNICEF (1991/1992). Logistics and Cold Chain Series: Module 26 (Users Handbook for photovoltaic refrigerators). WHO–EPI series.

UN (1993). *Report of the United Nations conference on environment and development : Rio de Janeiro, 3-14 June 1992*, United Nations conference on environment and development (1992 : Rio de Janeiro). UN.

WHO (1993/1994). WHO/UNICEF Product Information Sheets. WHO supplier reference release.

ASHRAE (1994). ASHRAE *Handbook (Refrigeration)* (SI ed.). ASHRAE refrigeration handbooks. http://www.ASHRAE.org: MacGraw Hill Book Company.

CADDET (1994). Household end–use consumption of energy and expenditures for that energy (1993). (World Wide Web (**INTER**national **NET**work) site http://www.cadet.ee.org.

EU (1996, 27th March). Directive 96/EC of the European Parliament and of the council of the European Union *On Energy Efficiency requirements for Household Electric Refrigerators, Freezers and combinations thereof.* document # 4507/2/96.

UN (1996). WORLD POPULATION INFORMATION. United Nations publication, (ST/ESA/SER.A/159) from the UN Population Division, Department of Economic and Social Affairs (World Wide Web (**INTER**national **NET**work) site http://www.undp.org/popin/.

ASHRAE (1998). ASHRAE *Handbook (Refrigeration)* (SI ed.). ASHRAE refrigeration handbooks. http://www.ASHRAE.org: MacGraw Hill Book Company.

IEA (for OECD) (1996, July). *Electricity Information 1995*, OECD Electricity Information, Paris. IEA (for OECD): OECD.

Abarbanel, S. (1960). Time Dependent Temperature Distribution in Radiating Solids. *Journal of Mathematical Physics 39*, 246–257.

Adebiyi, G. A. and L. D. Russell (1987). A Second Law Analysis of Phase–Change Thermal Energy Storge Systems. *ASME-HTD 80*, 9–20.

Al-Hinai, H. A. Z. (1991–1992, September). *Natural Cooling Techniques for Buildings in Hot Climates*. Doctoral thesis, School of Mechanical Engineering, Cranfield institute of Technology, Cranfield, Bedford MK43 0AL.

Al-Muslahi, S. (1979). Experimental and theoretical analysis of novel thermal stratification devices. Master's thesis, Cranfield Institute of Technology, School of Mechanical Engineering.

Allen, H. S. (1900). . [See also Govier and Aziz (1972)], pp. 323.

Ando, K., T. Fukuda, and K. Endoh (1986). *Dynamics of Single-Fluid Flows and Mixing*, Volume 2 of *Encyclopaedia of Fluid Mechanics*, Chapter [28] "Back-mixing in Stirred Vessels", pp. 773–802. London: Gulf Publishing Company.

Anon (1992). *Earth summit - (Financial Times survey)*. London: Financial Times, London.

Anon. (1995, April). Global Warming and Cooling Enthusiasm. *The Economist*, 33–34.

Argana, C. P. (1962). *Water Soluble Resins*. Reinhold Publishing Corp.

Atapattu, D. D., R. P. Chhabra, and P. H. T. Uhlherr (1988). Particle drag and equilibrum in viscoplastic fluids. See Shook and Roco [1991], pp. 253–260.

Atwood, L. (1991, February). Refrigerants of the Future:Facts and Fallacies. *J.* ASHRAE, 30–35.

Augood, P. C. (1997, April). *Low–Temperature Thermal–Energy Storage and Transmission Systems Employing Hydrophilic Polymeric Materials*. Doctoral thesis, School of Mechanical Engineering, Cranfield University, Bedford MK43 0AL.

Augood, P. C., N. M[arcus], and H. D. J. (1999). Thermal Behaviour of Phase–Change Slurries Incorporating Hydrated Hydrophilic Polymeric Particles. *International Journal of Experimental Thermal and Fluid Science*.

Aziz, A. (1983). Comments on "Critical thickness of a square section" by C. K. Hsieh . *J. Solar Energy 30*(5), 491–492. Letter to the editor.

Aziz, A. (1997). The Critical Thickness of Insulation. *Heat transfer engineering 18*(2), 61–91.

Babyak, Richard, J. (1994, June). Inside insulation. *Appliance Manufacturer*.

Bahar, S. J. (1980). Thermal Energy Storage Using Encapsulated Phase Change Materials. Master's thesis, Cranfield Institute of Technology, School of Mechanical Engineering.

Balcerzak, M. J. and S. Raynor (1961). Steady state temperature distribution and heat flow in prismatic bars with isothermal boundary conditions. *Int. J. of Heat and Mass Transfer 3*, 113–125.

Bar-Cohen, A. and W. M. Rohsenow (1984). Thermally Optimum spacing of vertical, natural convection cooled, parallel plates. *Trans. Amer. Soc. Mech. Engrs. J. Heat transfer 106*, 116–123.

Barber, C. R. (1971). *The Calibration of thermometers*. National Physical Laboratory, DTI: HMSO.

Barnhart, J. M. (1974). Economic thickness of thermal insulation. *Chemical Engineering Progress 70*(8), 50–54.

Bejan, A. (1978). Two Thermodynamic Optima in the Design of Sensible Heat Units for Energy Storage. *Trans. Amer. Soc. Mech. Engrs. J. Heat transfer 100*, 708–712.

Bejan, A. (1979). A general variational principle for thermal insulation system design. *Int. J. of Heat and Mass Transfer 22*(2), 219–226.

Bejan, A. (1982a). *Advances in Heat Transfer*, Volume 15 of *Advances in heat transfer*, Chapter "Second–law Analysis in Heat Transfer and Thermal Design", pp. 1–58. Academic Press.

Bejan, A. (1982b). *Entropy generation through heat and fluid flow*. John Wiley & Sons Inc..

Bejan, A. (1988). Theory of heat transfer–irreversible power plants. *Int. J. of Heat and Mass Transfer 31*(6), 1211–1219.

Bejan, A. (1989). Theory of heat transfer–irreversible refrigeration plants. *Int. J. of Heat and Mass Transfer 32*(9), 1631–1939.

Bejan, A. (1993). How to distribute a finite amount of insulation on a wall with non-uniform temperature. *Int. J. Heat Mass Transfer 36*(1), 49–56.

Bell, M. A. (1991). *Thermal energy storage using saturated aqueous solutions*. Doctoral thesis, Cranfield Institute of Technology, School of Mechanical Engineering.

Benson, D. K. and T. F. Potter (1992). *The effect of new priorities and new materials on residential refrigerator design*. ACEEE: National Renewable Energy Laboratory, ACEEE.

Benson, D. K., J. D. Webb, R. W. Barrows, J. D. O. McFadden, and C. Christensen (1985, March). Materials Research for Passive Solar Systems:*Solid–Solid Phase Change Materials*. Contractor report SERI/TR–255-1828, US-DoE, Solar Energy Research Institute.

Bernal, J. D. and J. Mason (1960, 10^{th}December). Co-ordination of Randomly Packed Spheres. *Nature 188*, 910–911.

Bianchi, P. and L. Forlai (1988). *The Structure of European Industry*, Chapter [**XI**] "The European Domestic Appliance Industry, 1945-1987", pp. 269–296. Acadamic Press.

Biodata Ltd. (1994). MICROLINK *Hardware User Manual (*M3000-2.07*)*. 10, Stocks Street, Manchester M8 8QG. UK (Tel: (0161) 834 6688): **Biodata Ltd**..

Birkett, G. A. (1996). Investigation of Hydrophilic Polymeric Coatings for Heat Exchanger Surfaces. Master's thesis, Department of Applied Energy, school of mechanical Engineering, Cranfield University, Cranfield, Bedford. U.K.

Boardman, B. (1995a, March). DECADE *(Domestic Equipment and Carbon Dioxide Emissions) -:- First year report*. University of Oxford: Environmental Change Unit.

Boardman, B. (1995b, November). DECADE *(Domestic Equipment and Carbon Dioxide Emissions) -:- Second year report*. University of Oxford: Environmental Change Unit.

Boardman, B., K. Lane, M. Hinnels, B. N., G. Milne, A. Goodwin, and T. Fawcett (1997, May). DECADE *(Domestic Equipment and Carbon Dioxide Emissions) -:- Transforming the UK Cold Market*. University of Oxford: Environmental Change Unit.

Boelter, L. K. M., V. H. Cherry, H. A. Johnson, and R. C. Martinelli (1965). *Heat Transfer Notes* (Second ed.). University of California, Berkeley: MacGraw Hill Book Company.

Buchholz, F. L. and N. A. Peppas (Eds.) (1994). *Super Absorbent Polymers: Science and Technology*, American Chemical Society (ACS) Symposium Series: Proc. 206th Nat. Meet., Chicago, Ill. USA. American Chemical Society (ACS): ACS Division of polymeric materials:science and engineering.

Buhl-Pedersen, P., B. Lebot, P. Michel, C. Nascimento, V. Østergaard, A. Szabo, R. Trines, and S. Van der Sluis (1993, March). Study on Energy Efficiency Standards for Domestic Refrigeration Appliances:FINAL REPORT. Contractor report GEA/92, Commission of the European Communities, Group for Efficient Appliances, ADEME, Danish Energy Agency, Novem.

Burke, M. (1990). *The Most Energy–Efficient Appliances* (1989-90 ed.). 1001 Connecticut Ave., N.W., Suit 535 Washington, DC 20036 U.S.A.: ACEEE.

Callen, H. B. (1960). *Thermodynamics* (First ed.). In Tiza [1977].

Carslaw, H. S. (1945). *Introduction to the mathematical theory of the conduction of heat in solids* (Second ed.). Dover Publications.

Carslaw, H. S. and J. C. Jaeger (1959). *Conduction of heat in solids* (Second ed.). Oxford: Clarendon Press.

Chambré, P. L. (1959, November). Nonlinear Heat Transfer Problem. *Journal of Applied Physics 30*(11), 1683–1688.

Chapman, A. J. (1984). *Heat Transfer* (Fourth ed.). New York: MacMillan Publishing Company.

Charunyakorn, P., S. Sengupta, and S. K. Roy (1991). Forced convection heat transfer in microencapsulated phase change material slurries: flow in circular ducts. *Int. J. of Heat and Mass Transfer 34*(3), 819–833.

Chen, J. (1981). Pelletization and roll encapsulation of thermal energy storage materials. In *Proceedings of the 16th Intersociety Energy Conversion Engineering Conference*, Volume 1. Amer. Soc. Mech. Engrs.

Cheremisinoff, N. P. (Ed.) (1986). *Slurry Flow Technology*, Volume 5 of *Encyclopaedia of Fluid Mechanics*. London: Gulf Publishing Company.

Cheung, J. Y. M. and A. S. Kamal (1996, September). Fuzzy Logic Control of Refrigerant Flow. In UKACC *Intern. Conf. on Control 1996*, Number Conf. Publication number 427, pp. 125–130. IEE: IEE.

Choi, E., Y. I. Cho, and H. G. Lorsch (1994). Forced convection heat transfer with phase-change-material slurries: turbulent flow in a circular tube. *Int. J. of Heat and Mass Transfer 37*(2), 207–215.

Churchill, S. W. and H. H. S. Chu (1975). Correlating Equations for Laminar and Turbulent Free Convection from a Vertical Plate. *Int. J. of Heat and Mass Transfer 18*, 1323.

Cohen, R. R. (1986). *Thermal energy accumulation in stratified hot water stores*. Doctoral thesis, Cranfield Institute of Technology, School of Mechanical Engineering, Bedford MK43 0AL UK.

Cohen, R. R., R. J. Wood, and S. D. Probert (1983, May). Thermal Energy Storage in Fossil-Fired Central-Heating Systems. In *Papers presented at the 2nd* BHRA*Fluid Engineering International Conference on Energy Storage for Energy Management*, Cranfield University, Cranfield, Bedford MK43 0AL, UK, pp. 85–104. BHRA Fluid Engineering Group.

UK Consumers' Association (1982, August). Improving the Energy Efficiency of Electrical Domestic Appliances:A Survey of Development work in the UK. Technical report, Electricity Consumers' Council (UK), Brook House 2/16 Torrington Place London WC1E 7LL.

Conti, R. and A. Gianetto (1986). *Dynamics of Single-Fluid Flows and Mixing*, Volume 2 of *Encyclopaedia of Fluid Mechanics*, Chapter [31] "Solid Agitation and Mixing in Aqueous Systems", pp. 886–900. London: Gulf Publishing Company.

De Nevers, N. (1994, December). *Air Pollution Control Engineering*. UK: Whitaker.

Dinter, F., M. Geyer, and R. Tammne (1991). A Feasibility Study on Economic Storage Systems. Technical report, Deutsche Forschungsanstalt Für Luft-Und Raumfahrt E.V (DLR).

Douglass, G. (1980, September). Development of a Thermal Energy Storage Test Facility. Master's thesis, School of Mechanical Engineering, Cranfield University.

Drysdale, D. (1999). *An Introduction to Fire Dynamics* (Second ed.). John Wiley & Sons Inc..

Duguid, T. P. and C. A. Mee (1994, October). The Drivers behind the UK experience of DSM. *Power Engineering*, 225–228.

Duhamel, Jean Baptiste. (1833). Mémoire sur la méthode générale relative au mouvement de la chaleur dans les corps solides plongés dans les milieux dont la température varie avec le temps. [See also Carslaw (1945)], pp. 20. Cah. 22.

Duncan, W. J., A. S. Thom, and A. D. Young (1970 (reprinted 1981)). *Mechanics of fluids* (Second ed.). Pitman Press, Bath, Great Britain: Edward Arnold.

Durand, R. and E. Condolis (1952). Hydraulic transport of coal and solid materials in pipes. In *Proceedings of a colloquium on the hydraulic transport of coal*, pp. 39–52. National coal board.

Eckert, E. R. G. and R. M. Drake, Jr. (1972). *Analysis of heat and mass transfer*. McGraw-Hill series in mechanical engineering. MacGraw Hill Book Company.

Edwards, A. (1984). A high temperature, self-contained phase change thermal energy store. Master's thesis, Cranfield Institute of Technology, School of Mechanical Engineering.

Eissenberg, D. and C. Wyman (1980, May). What is in store for phase change? *Solar Age*, 12.

Elliott, D. E. and T. Stephens (1976, 1st–5th March). High Temperature Thermal Energy Storage. In G. K. Eugene (Ed.), *Thermal Energy Storage*, Report of a NATO science committee conference, Headington Hill Hall, pp. 11–26. NATO: Pergamon Press Ltd..

Fearon, D. J. (1984). Internal combustion engine pre-heater using stored thermal energy. Master's thesis, Cranfield Institute of Technology, School of Mechanical Engineering.

FICHTNER, C. E. (1988). The Potential for Energy Saving in the Applications of Electrical Energy. Technical Report 06-410/4818P03/T4/823 D, FICHTNER, Consulting Engineers. Study for the Commission of the European Communities Directorate General for Energy : Contract # 87-B-7080-11-1-17.

Formby, J. R. (1994, October). Communications Technologies for Demand-Side Management. *Power Engineering*, 214–215.

Frachet, Y. (Ed.) (1995). *"Energy" Yearly statistics;* 1993, EUROSTAT: Thermie Energy and Industry series year books and yearly statistics, Luxembourg. Office for official Publications of the European Communities: EU, Italy.

Franklin, G. F., J. D. Powell, and M. L. Workman (1990). *Digital Control of Dynamic Systems* (Second ed.). Addison Wesley.

Freedman, S. I. and J. C. Dudley (1974). Off Peak Air–Conditioning using Thermal Energy Storage. Technical report, University of Pennsylvania, Philadelphia, USA.

Freeman, A. (1955). Analytical theory of heat (Eng. trans. of "Fourier, J. B. Théorie analytique de la chaleur"). Dover Publications.

Fuji, T. and H. Imura (1972). Natural Convection from a Plate with Arbitrary Inclination. *Int. J. of Heat and Mass Transfer 15*, 755.

Geller, H. (1995, November). *National Appliance Efficiency Standards: Cost Effective Federal Regulations.* 1001 Connecticut Avenue, Washington DC, USA.: ACEEE.

Geller, H. S. (1988, May). Residential Equipment Efficiency:A STATE-OF-THE-ART OVERVIEW. Technical report, ACEEE, 1001 Connecticut Ave., NW Suite 535 Washington, DC 20036. Prepared for: Energy and Materials Program, Office of Technology Assessment, U.S. Congress, Washington, DC 20510.

Gladwell, D. S. (1979). Thermal energy storage using encapsulated phase change materials. Master's thesis, Cranfield Institute of Technology, School of Mechanical Engineering.

Goel, M., S. K. Roy, and S. Sengupta (1994). Laminar forced convection heat transfer in microcapsulated phase change material suspensions. *Int. J. of Heat and Mass Transfer 37*(4), 593–604.

Goldstein, R. R., E. M. Sparrow, and D. C. Jones (1973). Natural Convection Mass Transfer Adjacent to Horizontal Plates. *Int. J. of Heat and Mass Transfer 16*, 1025.

Goldstein, S., L. Bairstow, A. Fage, M. Jones, A. R. Low, E. F. Relf, L. F. G. Simmons, R. V. Southwell, H. B. Squire, and G. I. Taylor (1950). *Modern Developments is Fluid Dynamics:*AN ACCOUNT OF THEORY AND EXPERIMENT RELATING TO BOUNDARY LAYERS, TURBULENT MOTION AND WAKES, Volume 1 of *The Oxford Engineering Science Series.* Oxford University Press.

Golibersuch, D. C. (1977). Cool Storage Assessment Study. Technical Report EPRI EM-468, General Electric Co., Schenectady, New York.

Goodman, T. R. (1958, February). The Heat Balance Integral and Its Application to Problems Involving a Change of Phase. *Trans. Amer. Soc. Mech. Engrs. 80*, 335–342.

Goodman, T. R. (1961, February). The Heat Balance Integral–Further Considerations and Refinements. [See also Goodman (1958)], pp. 83–85.

Goodman, T. R. (1964). *Advances in Heat Transfer*, Volume 1 of *Advances in heat transfer*, Chapter "Application of Integral Methods to Transient Nonlinear Heat Transfer", pp. 51–122.

Govier, G. W. and K. Aziz (1972). *The flow of complex mixtures in pipes.* 645 New York avenue, Huntington, New York 11743: Robert E. Kriger publishing company inc.

Gröber, H., S. Erk, and U. Grigull (1961). *Fundamentals of heat transfer* (Third ed.). New York: MacGraw Hill Book Company.

Grubb, M. (1993). *The 'Earth Summit' agreements : A guide and assessment - an analysis of the Rio '92 UN Conference on environment and development.* Earthscan.

Guldbrandsen, T., J. Heebøll, K. Mehlsen, and Nørgård (1986). Development of Energy Efficient Electrical Household Appliances Part One: Refrigerators. Technical report, Technical University of Denmark, Technical University of Denmark, DK-2800 Lyngby, Denmark. Directorate–General Science, Research and Development, Commission of the European Communities, EUR 10449 EN, Final Report # : EUR 10449 EN Contracts # 's EE-A-3-025-DK () and EE-A-3-068-DK (SD).

Guldbrandsen, T. and J. Nørgård (1986). Achieving substantially reduced energy consumption in European type refrigerator. In *Proceedings of the 37th Annual International Appliance Technical Conference.*

Guyer, E. C. and D. L. Brownell (Eds.) (1988). *Handbook of Applied Thermal Design* (First ed.). MacGraw Hill Book Company.

Hale, D. V., M. J. Hoover, and M. J. O'Neil (1971). Phase Change Materials Handbook. Contractor Report : *Microfiche* NASA CR 61363, NASA, Lockheed Missiles and Space Company.

Hardcastle, R. (Ed.) (1984). *The Pattern of Energy in the* UK; (1980), Energy Efficiency Series II, Energy Technical Division, Aere, Harwell UK. Energy Efficiency Office of the United Kingdom Department of Energy: HMSO.

Harvey, B. (1980, Spring). Acid Rain from Man and Nature. *Quest 14*(4).

Heisler, M. P. (1947). Temperature Charts for Induction and Constant-Temperature Heating. *Trans. Amer. Soc. Mech. Engrs. 69*(3), 227–236.

Her Majesty's Government (1990, September). *This common inheritance :Britain's environmental strategy*. Parliament, House of Commons, Great Britain: HMSO.

Herring, H. (1994). Is Britain a Third World Country? : The case of German refrigerators. *Energy Policy 22*(9), 779–787.

Hersh, D. H. (1994, March). DDC and Ice Thermal Storage Systems Provide Comfort and Energy Efficiency. *J.* ASHRAE *36*(3), 35.

Highgate, D. J. (1977). Thermal storage :UK Patent # Great Britain 1,587,725. London Patent Office.

Highgate, D. J., C. Knight, and S. D. Probert (1989). Anomalous 'Freezing' of Water in Hydrophilic Polymeric Structures. *Applied Energy 34*, 243–259.

Holly, F. J. and M. F. Refojo (1976). Water Wettability of Hydrogels. In J. D. Andrade (Ed.), *Hydrogels for Medical Related Applications in Chemistry*, Number 31 in symposium, pp. 253–266. Am. Chem. Soc.

Hsieh, C. K. (1980). Critical thickness of insulation of a square cross section. *Solar Energy 25*, 569–570. *Technical Note.*

Hsieh, C. K. and L. Yang (1984). A New Theory on the Critical Thickness of Insulation. *Trans. Amer. Soc. Mech. Engrs.J. of Heat Transfer 106*, 648–651.

Humphries, W. R. and E. I. Griggs (1977, November). A Design Handbook for Phase Change Thermal Control and Energy Storage Devices. Contractor Report N78 15434 NASA TP–1074, NASA.

Hunt, J. N. (1969). On the turbulent transport of heterogenous sediment. *Quart. J. Mech. Appl. Math 22*(2), 235–246.

Incropera, F. P. and D. P. DeWitt (1990). *Fundamentals of heat and mass transfer* (Third ed.). Singapore: John Wiley & Sons Inc..

Ito, H. (1959, June). Friction factors for turbulent flow in curved pipes. *Trans. Amer. Soc. Mech. Engrs. J. Basic Engineering series D 81-D*, 123–35.

Ito, H. (1960). Pressure losses in smooth pipe bends. *Trans. Amer. Soc. Mech. Engrs. J. Basic Engineering series D 82-D*, 131–139.

Ito, H. (1987). Flow in Curved Pipes. *Int. Jour. Jap. Soc. Mech. Eng. 30*(262), 543–552.

James, S. J. and J. A. Evans (1990, December). Performance of Domestic Refrigeration. In *Proceedings of the Institute of Refrigeration*. Institute of Refrigeration.

Jensen, J. and B. Sørenden (1984). *Fundamentals of Energy Storage*. Denmark: John Wiley & Sons Inc., Wiley-Interscience.

Kaelble, D. H., E. H. Cirlin, and P. J. Dynes (1975). Crystalline Polymers as Heat Storage Materials in Passive Thermal Protection Systems. [See also Lane (1983)], pp. 673.

Kasza, K. E. and M. M. Chen (1982, June). Development of enhanced heat transfer/trasport/storage slurries for thermal-system improvement. Technical Report ANL–82-50, Argonne national laboratory, 9700 South Cass Avenue, Argonne, Illinois 60439 USA.

Kauffman, K. W., H. G. Lorsch, and D. M. Kyllonen (1977). Thermal Energy Storage by means of Saturated Aqueous Solution. Technical report, Franklin Institute Research Labs., Philadelphia, Pennsylvania, USA.

Keenan, J. H. (1941). *Thermodynamics*. John Wiley & sons Inc..

Keener, J. P. (1988). *Principles of Applied Mathematics : transformation and approximation*. Addison-Wesley Publishing Company.

Kent, P. J. C. and J. K. R. Page (1980a). European Patent Application # 0,011,411. London Patent Office.

Kent, P. J. C. and J. K. R. Page (1980b). US Patent # 4,209,413. US Patent Office.

Kreyszig, E. (1983). *Advanced Engineering Mathematics* (Fifth ed.). Wiley.

Lam, K.-W. (1980). The hydraulic transport of large coal particles. Master's thesis, BHRA Fluid Engineering Unit, Cranfield Institute of Technology, Cranfield, Beds MK43 0AL.

Lane, G. A. (1983). *Solar Heat Storage: Latent Heat Material*, Volume 1. Florida, USA: CRC Press.

Langmuir, I., E. Q. Adams, and F. S. Meikle (1913). Flow of Heat through Furnace Walls. *Trans. Amer. Electrochem. Soc. 24*, 53–84.

Lazarus, J. H. and R. R. Faddick (1980). Short course notes for slurry pipelining.

Lebot, B. and A. Szabo (1992, June). Preparing Minimum Efficiency Standards for European Appliances. In *Proceedings of the International Energy Conference, Use of Efficiency Standards in Energy*, pp. 55–66. International Energy Agency.

Legal, L. G. (1973). On the effective conductivity of a dilute suspension of spherical drops in the limit of low particle peclet number. *Chem. Eng. Commun 1*, 21–33.

Leguay, C. (1994). Hydrophilic materials for use in a fluidised bed energy storage system. Master's thesis, Department of Applied Energy, school of mechanical Engineering, Cranfield University, Cranfield, Bedford, U.K.

Lim, J., A. Bejan, and J. H. Kim (1992). The Optimal thickness of a wall with convection on one side. *Int. J. of Heat and Mass Transfer 35*(7), 1673–1679.

Lim, J. S. and A. Bejan (1994). Two fundamental problems of refrigerator thermal insulation design. *Heat transfer engineering 15*(3), 35–41.

Lloyd, J. A. (1998, October). *Novel Heat Treatment in Fluidised Beds of Particles.* EngD., Cranfield University, School of Mechanical Engineering, Cranfield, Bedford MK43 0AL.

Lloyd, J. R. and W. R. Moran (1974). Natural Convection Adjacent to Horizontal Surfaces of Various Planforms. *Amer. Soc. Mech. Engrs. 74-WA/HT-66.*

Lorsch, H., K. W. Kauffman, and J. C. Denton (1976). Thermal Energy Storage for Solar Heating and Air–Conditioning. *Energy Conversion 16*, 23–33.

Lovins, A. B. (1988). Energy Savings Resulting from the Adoption of More Efficient Appliances: Another Review. *Energy Journal 5*(2), 155–162.

Lovins, A. B. (1990, September). The Efficient Use of Electricity. *Scientific American*, 28–36.

Lovins, A. B. (1996, April). NegaWatts Twelve Transitions, Eight Improvements and One Distraction. *Energy Policy 24*(4), 331–334.

Lumb, D. (1996, April). Pumped Storage. In *Energy Storage Technologies for Utility Network Optimisation*, First Hydro Pumped Storage, Gwynedd, pp. Session 7. EA Technology, Capenhurst, Chester, UK: EA Technology Ltd..

Malin, A., A. Reisbacka, and A. Rytkönen (1993). On the Location of Household Appliances in Kitchen Furnishings. *TTS-Institutes Household Bulletin Series 4* (22).

Malloy, J. F. (1969). *Thermal Insulation.* Van Nostrand Reinhold environmental engineering series. New York: Van Nostrand-Reinhold.

Manley, B. J. W. and I. E. Smith (1983, May). Thermal Energy Storage using Encapsulated Phase Change Materials. In *Papers presented at the 2nd BHRA Fluid Engineering International Conference on Energy Storage for Energy Management*, Cranfield University, Cranfield, Bedford MK43 0AL, UK, pp. 151–160. BHRA Fluid Engineering Group.

Manning, R. E. (1985). *An investigation of thermal energy storage and its applications to industrial systems.* Doctoral thesis, Cranfield Institute of Technology, School of Mechanical Engineering.

Mansouri-Azar, I. (1996, April). *Energy Consumption and Environmental Impacts of Household Electrical Appliances.* Doctoral thesis, Mechanical Engineering, Cranfield University, Cranfield, Bedford MK43 0AL.

Marshall, R. (1981, May). Experimental Experience with the **ASHRAE/NBS** Procedures for Testing a Phase Change Thermal Storage Device. In *Papers presented at the International Conference on Energy Storage*, Volume 1, Cranfield University, Cranfield, Bedford MK43 0AL, UK, pp. 129–143. BHRA Fluid Engineering Group, ETSU & SRC.

Maxwell, J. C. (1892). *A treatise on electricity and magnetisim* (Third ed.), Volume One, Chapter [IX] "Conduction through heterogenous media", pp. 435. London, UK: Oxford University Press.

March Consulting Group (1990). Energy Efficiency in Domestic Electric Appliances:Energy Efficiency Series 13. Technical report, The United Kingdom, Department of Energy, Energy Efficiency Office.

McElroy, D. L., D. W. Yarborough, G. L. Copeland, F. I. Weaver, R. S. Graves, T. W. Long, and H. A. Fine (1984, July). Development of Advanced Thermal Insulation for Appliances. Technical Report ORNL/CON-159, Oak Ridge National Laboratory, Oak Ridge. AT-90-22-1.

Merler, S. (1968). *Thermal Insulation*, Chapter [II] "Superinsulation in Cryogenic Engineering", pp. p. 15*ff*. London: Elsevier, publishing **Co**..

Michael, Y. C. and K. T. Yang (1991). The Use of Cold Storage in Household Refrigerators. *Amer. Soc. Mech. Engrs./Jap. Soc. Mech. Engrs. Thermal Engineering Proceedings 3*, 283–288.

Mithal, P. and K. T. Yang (1994). A Phase Change Material–based Thermal Energy Storage ion for Household Refrigerators. *Amer. Soc. Mech. Engrs.* (94-WA/HT-5), 1–8.

Moody, L. F. (1944). Friction factors for pipe flow. *Trans. Amer. Soc. Mech. Engrs. 66*, 671.

Nadel, S. M. (1994, April). Using Utility *Demand Side Management* Programmes to Spur the Development of More Efficient Appliances. [See also Mansouri-Azar (1996)], pp. 877–882.

Nagengast, B. A. (1996). History of Sealed Refrigeration Systems **Part I**. **ASHRAE** *magazine 38*(1), S37–S48.

Nagengast, B. A. (1997). History of Sealed Refrigeration Systems **Part II**. **ASHRAE** *magazine 39*(1), S44–S52.

Nagengast, B. A. (1998, January). History of Refrigeration Systems **Part III**. **ASHRAE** *magazine 40*(1), 43–47.

Nelkon, M. (1981). *Principles of Physics* (IIXth ed.). Longman.

Newitt, D. M., J. F. Richardson, M. Abbot, and R. B. Turtle (1955). Hydraulic conveying of solids in horizontal pipes. *Trans. Inst. Chem. Engrs. 33*(2), 93–113.

Newitt, D. M., J. F. Richardson, and B. J. Gliddon (1961). Hydraulic conveying of solids in vertical pipes. *Trans. Inst. Chem. Engrs. 39*, 93–100.

Nilsson, H. (1994, October). The many faces of Demand–Side management. *Power Engineering*, 207–210.

Nir, A. and A. Acrivos (1976). The effective thermal conductivity of sheared suspensions. [See also Rocha and Acrivos (1973)], pp. 33–48.

Nissen, M. J. (1979). Re–saturation of Salt Solutions for Application to Thermal Energy Storage. Master's thesis, Cranfield Institute of Technology, School of Mechanical Engineering.

Nørgård, J. S. (1989). Low Electricity Appliances – Options for the future. In J. B. Johansson (Ed.), *Electricity Efficient End–Use and New Generation Technologies and their Planning Implications*, pp. 125–172. London University Press.

Okoroafor, E. U., M. Newborough, and D. Highgate (1998b, July). Effects of thermal cycling on the crystallisation characteristics of water within cross–linked hydro–active polymeric structures. *J. of Phys. D: App. Phys 31*, 3130–3138.

Okoroafor, E. U., M. Newborough, D. Highgate, and P. Augood (1998a, June). The thermal behaviour of water in cross–linked hydro–active polymeric structures: crystallisation of water. *J. of Phys. D: App. Phys 31*, 3120–3129.

Oldshue, J. Y. (1986). *Dynamics of Single-Fluid Flows and Mixing*, Volume 2 of *Encyclopaedia of Fluid Mechanics*, Chapter [29] "Industrial Mixing Equipment", pp. 803–850. London: Gulf Publishing Company.

O'Neil, P. (1993). *Environmental Chemistry* (2nd Rev. ed.). Chapman & Hall.

Oroskar, A. R. and R. M. Turian (1980, July). The critical velocity of pipeline flow of slurries. *J. Amer. Inst. Chem. Eng. 26*(4), 550–558.

OSS (1996, October). Advanced Refrigerator/Freezer Technology Development, Technology Assessment. Contractor Report (Phase I) 198484, **NASA**, Oceaneering Space Systems, Inc. **OSS**.

Owens Coring (July 1994). **AURA™** SUPERINSULATION ... technology for imagination. Manufacturers preliminary technical data/fact sheet.

Peube, J. L. and G. F. Hewitt (1976, 1st–5th March). Heat Transfer and Thermal Energy Transport. In G. K. Eugene (Ed.), *Thermal Energy Storage*, Report of a NATO science committee conference, Headington Hill Hall, pp. 35–48. NATO: Pergamon Press Ltd..

Pickering, K. T. and L. A. Owen (1994). *An Introduction to Global Environmental Issues*. 11, New Fetter Lane London: Rutledge.

Potter, T. F. and D. K. Benson (1990). Performance Tests of Compact Vacuum Insulation for Refrigerators. In *Proceedings of* ACEEE *1990 summer study on Energy Efficiency in Buildings*, Volume 1, pp. 177–184. ACEEE.

Priestnall, M. A. (1985). Phase-Change Thermal Energy Storage for Domestic Space Heating. Master's thesis, Cranfield Institute of Technology, School of Mechanical Engineering.

Pritchard, J. C. (1970). *Polyvinyl Alcohol: Basic properties and uses*. Number 4 in Polymer Monographs. New York: Gordon and Beach, science publishers Ltd..

Probert, S. D. (1967). Thermal Insulation in Relation to Cryogenics. Technical Report TRG (report) 1455 ($^{R}/_{x}$), UK Atomic Energy Authority, The reactor Group Headquarters, Risley, Warrington Lancashire UK.

Probert, S. D. (1993). Course Notes (Thermal Insulation). unpublished.

Probert, S. D. and S. Giani (1976). Economics of Thermal Insulation. *Applied Energy 2*, 189–204.

Rarid, M. F., Y. Kim, and A. Kansawa (1990, May). Thermal Performance of a Heat Storage Module Using PCM's with Different Melting Temperature: Experimental. *Trans. Amer. Soc. Mech. Engrs. J. Energy Engineering 112*(2), 125–131.

Redford, S. J. (1994, October). The Rationale for Demand–Side Management. *Power Engineering*, 211–217.

Redford, S. J. and M. Fry (1993). *Energy Efficiency Yearbook*, Chapter "Demand Side Management and its Implications on Commerce and Industry", pp. 42–43. DTI.

Reis, A. S. (1975). Design of an Intermittent Solar Powered Refrigeration System. Master's thesis, School of Mechanical Engineering, Cranfield University, Cranfield, Bedford MK43 0AL,UK.

Resnick, R., D. Haliday, and J. Walker (1993). *Fundamentals of Physics* (IVth ed.). John Wiley and Sons Inc..

Robinson, C. and M. Mort (1996, September). A Neural Network Solution to the Problem of Frost Prediction. In UKACC *Intern. Conf. on Control 1996*, Number Conf. Publication number 427, pp. 136–139. IEE: IEE.

Rocha, A. and A. Acrivos (1973). On the effective thermal conductivity of dilute disperses: General theory for inclusions of arbitrary shape. *Quart. J. Mech. Appl. Math 26*, 217–233.

Rochester, D. C. (1981). Delayed Nucleation of Super–cooled Salt Hydrates and its Significance in Thermal Storage Applications. Master's thesis, Cranfield Institute of Technology, School of Mechanical Engineering.

Saberi, R. (1991, September). Concept and Design of a Portable Solar Refrigerator for Vaccine Loads. Master's thesis, College of Aeronautics, Cranfield Institute of Technology., Cranfield, Beds MK43 0AL UK.

Saler, I. O. (1979, 3-4 December). Development of an Optimum Process for Electron Beam Cross–linking of High Density Polyethylene Thermal Energy Storage Pellets. In *Thermal Energy Storage, Fourth Annual Review Meeting*, Volume CONF-791232, Tysons Corner, Va. USA, pp. 315. US-DoE: US-DoE.

Sathaye, J. (1988, November). Urbanisation and Modern lifestyles: Implications for Fuel Use. *Proceedings of the Chinese–American Symposium on energy Markets and the Future of Energy Demand, Bejing, China. 22-24 June 1988.* Technical Report LBL-26260, Lawrence Berkeley National Laboratory.

Scarinage, R. P. (1979). A Variable Capacity Thermal Storage Device. In M. B. McCarthy (Ed.), *Proceedings of solar energy storage Options*, Volume 1 (Part 2), Trinity University, San Antonio, Texas USA, pp. 609 *ff*..

Schlichting, H. (1968). *Boundary–Layer Theory* (Sixth ed.). McGraw Hill. Tr. Kestin, J.

Schneider, P. J. (1985). *Handbook of Heat Transfer Fundamentals*, Chapter [4] "Conduction", pp. 4–169,4–170. MacGraw Hill Book Company.

Sciubba, E. and A. Bejan (1992). The Optimal spacing of parallel plates cooled by forced convection. *Int. J. Heat Mass Transfer 35*(12), 3259–3264.

Scott, D. G. (1960, 10thDecember). Packing of Equal Spheres. *Nature 188*, 908–909.

Service, E. I. (1996, February). Business Brief:Energy Efficiency–Hot Tempers in the Refrigeration Business. Eur. Report; European Information Service Archive (Q1:110).

Shook, C. A. and M. C. Roco (1991). *Slurry Flow: Principle and practice* (First ed.). Butterworth–Heinemann series in chemical engineering. 80 Montvale Avenue, stoneham, MA 02180: Butterworth–Heinemann.

Sider, E. N. and E. G. Tate (1936). Heat transfer and pressure drop of liquids in tubes. *Ind. Eng. Chem. 28*, 1429.

Silla, S. M. (1989, September). Optimisation of the Design of Vaccine Carriers for Transportation in Immunisation Programmes. Master's thesis, School of Mechanical Engineering, Cranfield Institute of Technology, Cranfield, Beds MK43 0AL UK.

Sillanpää, L. (1997). Private Communication.

Sillanpää, L., P. de Bruin, and H.-G. Hloch (1996). Optimising Energy–Efficiency Conditions for Household Appliances: A project plan. Technical Report 3/1996 (45), TTS Institute. Commission of the European Communities, contract No:XVII/4.1031/Z/95-128.

Smith, L. K. and T. F. Porter (1990). Assessment of the Cost-Effective Energy Conservation Potential of Advanced Refrigerator Insulation. *Transactions,* ASHRAE *(Part 1)*, 1341–1348. AT-90-22-1.

Soderstrom, M. F. and T. R. Johansson (1983, May). The Use of Thermal Energy Storage in Industry: *Potential in Sweden.* In *Papers presented at the 2nd* BHRA *Fluid Engineering International Conference on Energy Storage for Energy Management*, Cranfield University, Cranfield, Bedford MK43 0AL, UK, pp. 61–84. BHRA Fluid Engineering Group.

Sohn, C. W. and M. M. Chen (1981, February). Microconvective Thermal Conductivity in Disperse Two-Phase Mixtures as Observed in a Low Velocity Couette Flow Experiment. *Int. J. of Heat and Mass Transfer 103*, 47–50.

Sousa, J. (1989). Design and Evaluation of Ice Thermal Storage systems for Air–Conditioning Purposes. Master's thesis, School of Mechanical Engineering, Cranfield University, Cranfield, Bedford, UK.

Sparrow, E. M. (1970). Reexamination and correction of the critical radius for radial heat conduction. *AICHE 16*(1), 149.

Strang, G. (1986). *Introduction to Applied Mathematics.* Massachusetts Institute of Technology: Wellesley-Cambridge Press.

Sudhakar, P. (1995, January 01). An Introduction To Quality Improvement Through Taguchi Methods. *Industrial engineering. 27*(1), 53–.

Tabassum, S. A. (1989, September). *Solar Refrigeration: Evaluation of the Technical ions and Design of a Solar–Gererator–Absopber for a Normal Absorption*

Refrigerator. Doctoral thesis, School of Mechanical Engineering, Cranfield Institute of Technology., Cranfield, Beds MK43 0AL, UK.

Telkes, M. (1949). A Review of Solar House Heating. *Heating Ventilation and Air–Conditioning 46*(68).

Telkes, M. (1975, August). Thermal energy storage. In *Record of the 10th annual Intersociety Energy Conversion Engineering Conference*, pp. 111 *ff.*.

Telkes, M. (1977). *Applications of solar energy for heating and cooling of buildings*, Chapter [7] "Solar energy storage". New York: American Society of Heating, Refrigeration and Air–Conditioning Engineers.

Telkes, M. (1980). US Patent # 4,187,189. Patent Office.

Telkes, M. and P. T. Kondo (1980). *Phase Change Thermal Storage, a Comprehensive Look at Developments and Prospects.* Monegon.

Thomas, D. G. (1965). Transport characteristics of suspensions: VII. A note on the viscosity of Newtonian suspensions of uniform spherical particles. *J. Colloid. Sci. 20*, 267–277.

Thompson, W. A. R. (Ed.) (1984). *Blakes Medical Dictionary* (33rd ed.). Adam & Charles Blake.

Tiza, L. (1977). *Generalized Thermodynamics.* Massachuesetts Institute of Technology, Cambridge, Massachuetts USA: M.I.T Press.

Toda, M., N. Komori, S. Saito, and S. Maeda (1972). Hydraulic conveying of solids through pipe bends. *J. Chem. Engrs. Japan 5*, 4–13.

Toda, M., N. Komori, S. Saito, and S. Maeda (1973). Hydraulic conveying of solids through a bend in the vertical plane. *Bull. Jap. Soc. Mech. Engrs. 12*(54), 1388–1396.

Turiel, I. and M. D. Levine (1989). Energy–Efficient Refrigeration and Reduction of Chloroflorocarbon Use. *Annual Review of Energy 14*, 173–204.

Tyson, J. K. (1982, September). The design of a reliable relief valve for use in particulate and/or highly viscous non-Newtonian fluids. Master's thesis, School of mechanical engineering, Cranfield Insitute of Technology, Cranfield, Bedford MK43 0AL.

Valencia, L. J. (1991, September). Improving the Efficiency of Domestic Refrigeration Appliances. Master's thesis, School of Mechanical Engineering, Cranfield University, Cranfield, Bedford, MK43 0AL, UK.

Vliet, G. C. (1969). Natural Convection Local Heat Transfer on Constant-Heat-Flux Inclined Surfaces. *Amer. Soc. Mech. Engrs. J. of Heat Transfer 91*, 511.

Waide, P. (1993, September). *Mandatory Energy Efficiency Standards for domestic Refrigeration Units in the European Community: Analysis of the draft EC directive and Alternative Proposals for a standard.* Cannonbury villas, London N1 2PN, U.K.: Greenpeace International.

Walker, C. I. (1980, September). Pumping solid-liquid mixtures:perfomance characteristics of centrifugal pumps when handling fine granular solids in suspension and a computer aided pump selection procedure for slurry applications. Master's thesis, School of mechanical engineering,, Cranfield Institute Technology Cranfield, Bedford MK43 0AL.

Wani, G. A. (1986). *Slurry Flow Technology*, Volume 5 of *Encyclopaedia of Fluid Mechanics*, Chapter [4] "Critical velocity in multisize particle transport through pipes", pp. 155–187. London: Gulf Publishing Company.

Ward, M. (Ed.) (1997). *Digest of United Kingdom Energy Statistics;* 1997, Digest of United Kingdom Energy Statistics, London. The United Kingdom Department of Trade and Industry: United Kingdom Government Statistical Service, HMSO.

Wells, G. L. (1971, November). Calculation of Economic Thickness of Insulation. *Jour. Inst. of Fuel 44*, 606–609.

Weltmann, R. N. and T. A. Keller (1956, September). Pressure Losses of Titania and Magnisum Slurries. Technical Report NACA TN-3889, Nat. Advis. Comm. for Aero. (NACA), USA.

Weston, E. (1983, May). Energy Storage and Storage effects in Industry. In *Papers presented at the 2nd BHRA Fluid Engineering International Conference on Energy Storage for Energy Management*, Cranfield University, Cranfield, Bedford MK43 0AL, UK, pp. 1–18. BHRA Fluid Engineering Group.

Wildman, D, J., J. M. Ekmann, and G. F. Klinzing (1984). Flow Studies of Highly Loaded Coal-water Mixtures Around Bends and Across Horizontal Sections. See Shook and Roco [1991], pp. 209–216.

Wilson, J. E. and I. Glendenning (1976, 1st–5th March). The Impact of TES on Energy Structures. In G. K. Eugene (Ed.), *Thermal Energy Storage*, Report of a NATO science committee conference, Headington Hill Hall, pp. 49–72. NATO: Pergamon Press Ltd..

Winegard, W. C. (1964). An Introduction to the Solidification of Metals. Number 29 in Institute on Metals Monograph and Report series. 17, Belgrave Sq., London SW1, UK.

Wood, R. J., D. T. Baldwin, P. O. O'Callaghan, and S. D. Probert (1983, May). Survey of 'The Industrial Potential' for Thermal Energy Storage Systems. In

Papers presented at the 2nd BHRA *Fluid Engineering International Conference on Energy Storage for Energy Management*, Cranfield University, Cranfield, Bedford MK43 0AL, UK, pp. 29–44. BHRA Fluid Engineering Group.

Woods, G. (1987). *The* ICI *Polyurethanes book*. John Wiley and Sons Inc..

Zegers, P. (1983, May). Overview of Energy Storage; *Work carried out in the framework of the* EC*'s Energy R, D & D programme*. In *Papers presented at the 2nd* BHRA *Fluid Engineering International Conference on Energy Storage for Energy Management*, Cranfield University, Cranfield, Bedford MK43 0AL, UK, pp. 19–28. BHRA Fluid Engineering Group.

Zwietering, T. N. (1958). Suspending of Solid Particles in Liquid by Agitators. *Chem. Eng. Sci. 8*, 244–253.

Epilogue

Lord Jesus, I love Thee, I know Thou art mine;
For Thee all the pleasures of sin I resign:
My gracious Redeemer, my Saviour art Thou,
If ever I lov'd Thee, Lord Jesus, 'its now.

I love Thee, because Thou has first loved me,
And purchased my pardon on Calvary's tree:
I love Thee for wearing the thorns on Thy brow;
If ever I loved Thee, Lord Jesus, 'tis now.

I'll love Thee in life, I will love Thee in death,
And praise Thee as long as Thou lendest me breath:
And say when the death-dew lies cold on my brow,
If ever I loved Thee, Lord Jesus, 'tis now.

In ages eternal of endless delight
I'll ever adore Thee in glory so bright;
I'll sing with the glittering crown on my brow,
If ever I loved Thee, Lord Jesus, 'tis now.

-William R. Featherstone